The Faculty of Civil and Environmental Engineering

The Stephen and Nancy Grand Water Research Institute

The 11th Dahlia Greidinger Memorial Symposium -2013

Advanced methods for investigating nutrient dynamics in soil and ecosystems

4-7 March, 2013
Technion-IIT, Haifa, Israel

Symposium
Proceedings

Organized and Supported by:

The Dahlia Greidinger Memorial Fund

and

BARD, The United States – Israel
Bi-national Agricultural Research and Development Fund

Edited by: Uta Cheruti, David Myrold, Avi Shaviv

The 11th Dahlia Greidinger Memorial Symposium -2013

Advanced methods for investigating nutrient dynamics in soil and ecosystems

4-7 March, 2013
Technion-IIT, Haifa, Israel

Symposium
Proceedings

Organized and Supported by:

The Dahlia Greidinger Memorial Fund

and

BARD, The United States – Israel
Bi-national Agricultural Research and Development Fund

Edited by: Uta Cheruti, David Myrold, Avi Shaviv

The 11th Dahlia Greidinger Memorial Symposium -2013

Advanced methods for investigating nutrient dynamics in soil and ecosystems

Local Organizing Committee

Chair- Dr. A. Shaviv, Technion-IIT; Prof. Emeritus J. Hagin, Technion-IIT;

Dr. S. Avrahami, Ruppin Academic Center; Dr. Yael Dubovski, Technion-IIT;

Dr. V. Alchanatis, ARO, Volcani Center; Dr. A. Angert, Hebrew Uni., Jerusalem;

Dr. Paricia Imas, ICL Fertilizers.

Scientific Committee

In addition to the scientists listed above, the scientific committee included:

Co-Chair Dr. David Myrold, OSU, USA; Dr. Peter Bottomley, OSU, USA;

Dr. Barbara Cade-Menun, Agriculture and Agri-Food Canada.

Symposium coordinator

Dr. Uta Cherui, CEE, IIT-Technion

Symposium link - http://dgsymp13.technion.ac.il/

Table of Contents

PREFACE

The symposium on *Advanced Methods for Investigating Nutrient Dynamics in Soils and Ecosystems* addressed knowledge gaps and R&D priorities related to the need to quantify nutrient dynamics and reaction mechanisms, particularly those of nitrogen and phosphorus in crop/food production systems. Special emphasis was placed on interactions with organic loads/wastes and under possible global changes (warming and/or rainfall/water scarcities), and the urgent need to assure sustainable crop/food production with minimal environmental threats. There was a focus on advanced and novel tools and approaches (including those developed in other disciplines) that enable real time investigation and quantification of processes and options to observe and model changes at various scales (from nano/micro up to field scale). Tools and methods leading to improved and sustainable utilization of nutrients were discussed as well.

Four themes were explored during nine oral sessions and one poster session that were held over the course of four days: *Global Aspects of Food Security*, *Advanced Tools/Approaches to Investigate N or P Dynamics in Soil*, *Soil Organic Matter Dynamics*, and *Advanced Sensors for Sustainable Utilization of Nutrients in Soil Systems*. Presentations about the importance of sustainable soils to food security provided the foundation for the symposium and were followed by two overview presentation that introduced the three scientific and technical themes. Four sessions were devoted to new approaches for understanding N and P cycling in soils, two sessions focused on organic matter and interactions between C and N, and two sessions reported on advances in measurement methods at multiple scales. The proceedings contains reports based mainly on the symposium talks and selected posters presented at the conference. A selection of manuscripts was also be published as a special section in the *Soil Science Society of America Journal (*Volume 78, Issue 1, January-February 2014; open access). Abstracts of the manuscripts in Volume 78 of *SSSAJ* are placed in the proceedings book followed by a link to their open access in *SSSAJ*.

At the end of this book there is a summary of the final panel discussion highlighting several of the important findings and main points stressed in the presentations, as well as subjects that require further investigation or issues that should serve as key topics for

future research. This is followed by a brief introduction of the selected manuscripts, which were published by *SSSAJ*.

The symposium generously supported by **BARD** and the **Dahlia Greidinger Memorial Fund**, which for the 11th time made this important scientific meeting possible. Thanks are also due to the Grand Water Research Institute – GWRI and the Faculty of Civil and Environmental Engineering at the Technion, ICL Fertilizers Ltd. and Fertilizers and Chemicals Ltd., who contributed time, effort and resources to support this event. Special thanks are given to members of the Scientific Committee, the staff of the Department of Environmental Engineering, Water and Agriculture, and particularly to Dr. Uta Cheruti, who efficiently coordinated all the administrative arrangements and took responsibility over editing and publishing the Calls, The Book of Abstracts, and finally these Proceedings.

In the name of the organizing committee,

Avi Shaviv and David Myrold

Session 1: Global Aspects of Food Security Soils and Sustainability & Approaches for Better Understating Nutrient Processes in Terrestrial Ecosystems – Overviews

WHAT WILL FUTURE FOOD SYSTEMS LOOK LIKE?

Achim Dobermann

International Rice Research Institute (IRRI), Los Baños, Philippines.

The demand for food will greatly increase due to rising incomes and an additional two or three billion people to feed. Investing in agriculture is also one of the most effective strategies for achieving critical post-2015 development goals related to poverty and hunger, nutrition and health, education, economic and social growth, peace and security, and preserving the world's environment. To achieve the new post-2015 global development goals, rising food yields must be decoupled from unsustainable utilization of water, energy, fertilizers, chemicals and land. This can only be done through a multi-faceted agro-ecological intensification of agriculture and food systems. The specific policies, business models and technologies for implementing such an agro-ecological intensification depend on the social and biophysical contexts in which farmers operate. Different solutions are required for large farms with good market access and high input use, small farms with good market access and high input use, or small farms with low market access and low input use. The domestic private sector – composed of millions of farmers and other local business – is by far the biggest investor in agriculture. It must be central to any investment and policy strategy that enables the development and widespread adoption of new solutions for more efficient, sustainable food production systems.

Structural transformations in the agricultural sector are already emerging that will change the way food will be grown in the future. Many of these changes are driven by

processes such as a declining share of agriculture in gross domestic product and employment, rural to urban migration, the rise of an industrial and service economy, and demographic transitions from high rates of birth and death to low rates. Land is scarce and input costs are rising, requiring further increases in productivity as well as greater efficiency of labor, water, fertilizer and energy. This also provides an incentive for more skilful, more precise agriculture through which one can also better adapt to the environment, or even control parts of it. Traditional smallholder farm management will more and more be supplemented or replaced with outsourcing of farming operations or the formation of small and medium-size agribusiness enterprises, including contract farming. Value chains for major agricultural commodities will become more tightly integrated because processors and consumers demand more information and control over how food is being produced, with supermarket chains playing a particularly important role. Farmers will increasingly turn to the private sector as a source of new technologies and information, but also as a direct buyer of their produce, requiring agricultural raw materials with higher standards. Access to interactive, locally tailored information will be increasing, leading to much wider rural communication networks than ever before.

These mega trends will provide new opportunities for the development, adaptation and adoption of technologies that could enable an ecological intensification of cropping systems, a more eco-efficient way of food production at high levels of productivity and resource use efficiency and with lower risk. Agricultural science needs to be re-oriented towards that. We need to anticipate what is needed by farmers and others in the value chain 10 or 20 years from now, and we need to take full advantage of such new opportunities for agronomic research. Increasing complexity in the demand and supply of food, feed and fuel at local, regional and global scales asks for tailor-made solutions. Agronomists must lead such efforts and thus help shaping a new image for modern agriculture. The grand challenge for agronomists lies in developing cropping systems and crop management technologies that allow operating at the upper limits of yield and resource efficiency, yet are stable in yields, sustainable and environmentally sound. We have already seen some amazing success stories for large yield and efficiency increases in recent years that demonstrate what can be achieved. Hence, agronomists should critically re-evaluate their research and extension strategies and approaches. They should look ahead and focus their efforts on new technology solutions for tactical management of crops and crop rotations at greater precision than ever before. Foresight

is needed to avoid that the world runs into another food crisis. Hence, in addition to investing in early solutions or technologies that are likely to become available in the next 5-10 years, strategic investments in groundbreaking research are needed to potentially make quantum leaps in the performance of agricultural systems beyond that.

FUTURE POTASH AND FERTILIZER CONSUMPTION TO SUSTAIN AGRICULTURAL PRODUCTION: POSSIBLE TRENDS AND CHARACTERISTICS

Hillel Magen[1] and Patricia Imas[2]

[1]International Potash Institute (IPI), Horgen, Switzerland;
[2]ICL Fertilizers, Beer Sheeva, Israel.

Abstract

During the last 50 years, global production of oil crops, vegetables, sugarcane, fruit and cereals increased by 6.5, 4.3, 3.8, 3.5 and 2.8 times respectively, the additional production achieved mainly via intensification. Nitrogen (N), phosphorus (P_2O_5) and potassium (K_2O), played a major role in this intensification process and their use (from 1961-2010) increased by 8.7, 3.7 and 3 times respectively. In China, increases in productivity over the last few decades have resulted primarily from increases in fertilizer use, mechanization and irrigation. By contrast, limited use of fertilizers in sub-Saharan Africa, (less than 10 percent of the world average), is a major cause for low yields in this region. Nutrient deficiencies are widespread. However, in some regions there is an overuse of N and P, which does not contribute to crop productivity and leads to nutrient imbalances, inefficiency and environmental damage. Mueller et al. (2012) estimate that globally, for farmers to achieve 75 percent attainable yield (current level is approximately 50 percent), consumption of N, P and K will need to be adapted by +9, -2 and +34 percent respectively. Clearly, according to this analysis, low K application is a serious limiting factor for increased productivity.

Estimates of additional crop production required by 2050 vary from 50 to 110 percent. Accordingly, nutrient demand is projected to increase at the same level, yet respond to efficiency and improved management practices as well as environmental stewardship. Relatively little research has estimated how the demand for nutrients will change by 2050. While the future demand of N varies between 40 to 100 percent, that of P and K is similar to the overall nutrient demand increase, projected at about 50 percent. A more detailed analysis using partial nutrient balance (PNB) for K, show that K use is projected to increase by 47-55 percent. The continued increase in the production of

vegetables, sugarcane, oil crops (e.g. soybean) and maize, will account for much of this projected increased.

Nutrient use 1960-today and levels of deficiency:

Driven by population growth and improved diets, global crop production has steadily increased. Over the last 50 years (1960-today) global population has about doubled and cereal production has increased by almost three-fold. This was achieved with little increase in the arable land under cultivation, but with a doubling of land under irrigation (Fig. 1; FAOSTAT). During the same time period, fertilizer use increased: N consumption increased dramatically by more than eight-fold, while that of P and K increased by about three-fold (FAOSTAT). In addition to increased fertilizers use, the use of other agro inputs, such as irrigation water and pesticides, contributed to the marked increase in global production of food crops (Tilman et al., 2002).

The link between fertilizer use and agricultural production is well established. Smil (2002) estimated that during the last 50 years N fertilizers enabled a 40 percent increase in per capita consumption. Stewart et al., (2005) estimated that the average percentage of yield attributable to fertilizer ranged from about 40 to 60 percent in the USA and UK, but tended to be even higher in the tropics. Mineral fertilizers as well as manures and leguminous crops have played a key role in increasing agricultural intensification globally (Foley et al., 2011). In China, increases in productivity have been mainly a consequence of an increase in fertilizer use (Dyson, 1999) and fertilization, mechanization and irrigation (Jingzhu Zhao et al., 2008).

Shortages of fertilizer, deficiency of N fertilizer and depletion of soil fertility have been identified as major production constraints in major farming systems in Asia and Africa (Waddington, 2010). Nutrient deficiencies which limit yield potential are widespread (The Royal Society, 2009; Mueller et al., 2012), but at the same time overuse of N and P leads to nutrient imbalances and inefficiencies in regions such as China (Mueller et al., 2012).

The stagnation of some productive cropping systems in Asia is related to unbalanced application of fertilizers, especially that of K (Ladha et al., 2003). Globally, it is estimated that in order to increase the level of yields of the major grain crops from their

current level (approx. 50 percent of attainable yield) to reach a level of 75 percent of attainable yield potential, the application of N, P and K will need to be adapted by +9, -2 and +34 percent, respectively (Mueller et al., 2012). According to this analysis, the current low K application rate is a serious limiting factor for increased productivity, which if increased will boost yields. Increasing K applications will also improve the balance between N and K which will improve the capacity of the plant to exploit N, leading to a higher yield benefit from applied N (Milford and Johnston, 2007; The Royal Society, 2009).

Global nutrient consumption has increased from approximately 10 million mt for N, P_2O_5 and K_2O in 1961, to more than 100, 40 and 25 million mt in 2010 (Fig. 2). This increase was disrupted severely by the fall of the Soviet Union (USSR) in the late 1980s early 1990s. Two other events have impacted the growth of nutrient consumption: the energy crises of the early 1970s and the 2008 financial crisis. Measuring the average consumption growth rates of N, P and K over 13 years (1994-2007) - a period of steady growth starting after the recovery from the fall of the USSR until the financial crisis of 2008 - offers a better entry point to understanding the growth process of the industry than measuring growth rates from 1961 to 2010. From 1994-2007, the growth rate of K consumption (3.1 percent pa) was much higher than that of N and P (2.4 and 2.1 percent, respectively). We believe that this is explained by the large increase in the production of crops, such as oil seeds (mostly soybean and oil palm) and horticultural crops (vegetables and fruits), that have a higher K demand than cereals, reflecting a shift in changing global diets. China has seen a shift in cropping patterns and a large increase in vegetable production, in Brazil soybean production has increased significantly, and growth of oil palm production has been strong in Indonesia and Malaysia. However, the increase in vegetable and fruit production in India has had a lesser impact (Magen and Imas, 2007).

Gaps in crop productivity:

Agricultural production varies greatly between regions. The gap between developing and developed regions is particularly large (Table 1). For example, maize production in Africa reaches only 7 percent yield potential, compared to 47 percent in the US. These gaps are mainly the result of better management practices used by farmers in developed countries.

The gap between attainable yield - which is achieved using current technology and management techniques (Mueller et al., 2012) - and actual productivity for various crops is significant (Table 2). Mozambique, for example, achieves only 28 percent of attainable yield, while in countries with well managed systems, such as the US and Brazil, average productivity is similar to attainable yield. In countries like China, India and Ukraine, there is a large scope for improvement in productivity (Table 2) if current technologies and management techniques are more widely adopted.

Another factor affecting productivity is irrigation. Rosegrant et al. (2002) show that while total rainfed cereal production on average is about 30 percent higher than irrigated production, irrigated land is twice as productive. In China, for example, it is estimated that 30 percent of the land (which is irrigated), provides 70 percent of the food (Fusuo, personal communication). Lobell et al. (2009) have calculated the gap to yield potential in rainfed crops to be 50 percent, suggesting significant potential for improvement.

Mueller et al. (2012) identified fertilizer use, irrigation and climate as the major causes for yield variability, with high fertilizer application rates typically occurring in high-income regions as well as in some rapidly developing countries. While 'attainable yield' is lower than the biophysical 'potential yield', it has the advantage of benchmarking realistic, achievable yield goals. Improvements in productivity can be achieved through plant breeding, and improved crop management, tillage, fertilization, weed and pest control, harvesting, and water use (Borlaug, 2007). Improving soil fertility and breeding crops with better tolerance for stresses (St. Clair and Lynch, 2010) will also help. But while there are ample of ways for improvement, many of these are closely related to farmers' knowledge. If high commodity prices prevail, providing incentive to farmers, better and more affordable agro inputs are made available and more effective extension tools are used - all these enable farmers to produce more effectively and raise productivity.

Future needs for food:

Estimations for the amount of additional crop production that will be required in the future vary. Dyson (1995), at a time when the impact of biofuels on cereal production was unclear, assumed that population growth would be the main determinant for cereal demand to 2020. Tilman et al. (2011) projected a 100-110 percent increase (2005-

2050), driven mostly by the increase in GDP per capita and consequently the per capita caloric demand. This is much higher than FAO's prediction (Alexandratos, 2009) of 70 percent for the same period, who also emphasize that any change in biofuel production may change the figure significantly.

The agricultural sector will be required to produce more food for more people, which will require food production to double within 40 years to meet this demand. If the global population was to remain at approximately 9 billion people, and a reasonable per capita calorie intake was achieved by 2050, the period until 2050 would likely be the last period that dramatic food production increases were seen. However, the next phase of growth will need to increase sustainable crop and animal production practices (including land, water and nutrient use efficiency), maintain and restore soil fertility, and provide ecosystem services (Tilman et al., 2002).

With limited land expansions forecast (from 1.592 billion ha in 2005/07 to 1.661 billion ha in 2050; Alexandratos and Bruinsma, 2012), increased crop productivity will have to emerge from increases in production in regions with low yields and where there is ample scope for improvements. Mueller et al. (2012) revealed that on average world productivity in 2008 (data of Monfreda et al., 2008) for many crops is only 50 percent of attainable yield (Table 3). The authors refer to 'attainable yields' as those that can be achieved using 'current technology and management techniques', thus comparing these with regions that have a similar climate may provide a more accurate estimate of achievable yield increases.

When comparing FAO projections for 2050 production levels (Alexandratos and Bruinsma, 2012), and attainable yield (Mueller et al., 2012) of various crops (Table 3), it appears that in most cases reaching 50 to 100 percent attainable yield will meet the target. This suggests that a significant portion of future demand of food can be met by simply adopting better management practices in low productivity regions.

Future nutrient demand:

Assessments

Estimations of future nutrient demand have been assessed by various researchers, with reference to meeting population and crop demand (Tenkorang and Lowenberg-DeBoer, 2009; Alexandratos and Bruinsma, 2012), to efficiency and improved management practices (Dobermann and Cassman, 2005; Tilman et al., 2011) and environmental stewardship (Tilman et al., 2001). In these assessments, N captures most of the attention, for a few reasons: 1) N is the yield builder of food crops, especially of crops that provide protein (excluding leguminous crops), and insufficient amounts will jeopardize plant performance, and consequently food security; 2) when not efficiently used, the effect of reactive N on the environment is negative; and 3) properly managed N application at farm level offers a significant improvement in efficiency of use, as compared to the application management of P and K, where the degrees of efficiency that can be improved is less.

Current (2012) and future nutrient consumption is summarized in Table 4. The various projections differ significantly from each other: according to Alexandratos and Bruinsma (2012), the increase in N consumption by 2050 will be ~40 percent, while others (Tilman et al., 2001; 2011) project an increase of ~100 percent (Table 4). Alexandratos and Bruinsma (2012) project that by 2050 P and K consumption will increase by ~40 percent while the total amount of $N+P_2O_5+K_2O$ being used will be 262.9 million mt, representing an increase by 2050 of 47.5 percent over 2012 consumption levels. Tenkorang and Lowenberg-DeBoer (2009), in their assessment for 2030, however, project a lower amount of 223.1 million mt, which represents a 25 percent increase over 2012 levels. Clearly, the basis for these calculations is different, and hence results deviate significantly.

Potassium partial nutrient balance (PNB_K)

Nutrient balance or audit calculations are commonly used to assess nutrient requirement and fertilization rates (Sheldrick et al., 2002 and 2003; Roy et al., 2003; Buresh et al., 2010; Spiess, 2011) as well as its effect on sustainability and impact on the environment (Eltun et al., 2002; Vitousek et al., 2009). Nutrient balance is another way to look at future requirements of nutrients, by assessing the 'takeoff' of nutrients through the removal of the harvested part from the field and adjusting fertilizer rates accordingly

(Witt et al., 2007). Partial nutrient balance (PNB) only takes into account easily measured inputs and outputs, for example mineral and organic fertilizers as inputs, and harvested products and crop residues as outputs (Roy et al., 2003). In this manner, PNB = 1 is when offtake is fully compensated by nutrient input, and PNB<1 is when fertilization is not sufficient to compensate for nutrient offtake. In this paper, we make use of the PNB approach to assess K balance (PNB_K), using mineral fertilizers only as the input, and the harvested products as the output.

IPI (2012) has calculated K offtake by major crop groups, and estimated that with 2011 crop production levels 28.9 million mt of K_2O was removed from fields. This calculation assumes that only the harvested part is removed and all crop residues are left in the field. Hence, when crop residues are removed (for feed, fuel or any other purpose), offtake is much higher, and can be even doubled. The calculated level of K_2O removal is identical to the amount of K_2O that was consumed in 2012 (28.9 million mt K_2O; IFA 2012), which implies that additional K removal through crop residues caused a highly negative balance between application of fertilizers and the removal by crops. Mueller et al. (2012) indirectly supports this assumption by indicating that K application could be increased by 34 percent to reach attainable yield on a global level (equivalent to 9 million mt K_2O).

To assess future K requirements, IPI calculated K offtake for crop production in 2050, as projected by FAO (2012) and Kearney (2010) (Table 5). The biggest projected increase in K offtake in 2050 is for vegetables (4 to 10.5 million mt K_2O), reflecting the growing demand for this crop group, followed by sugarcane (4.7 to 7.9 million mt K_2O). The projected increase in production of cereals is lower. Fruit, other oil crops and other crops appear under “Others”. In total, K_2O offtake in 2050 is projected to reach 44.8 million mt K_2O, which is similar 47.3 million mt estimated by Alexandratos and Bruinsma (2012; Table 4), representing a 55 percent increase over 2012 levels.

IPI calculated global PNB_K for selected crops, using fertilization rates (Heffer, 2009) and removal rates (IPI, 2012), in order to assess the degree to which each is fertilized with K (Fig. 3). According to this, rice farmers appear to apply more K to their crops than maize farmers, and considerably more than is used in wheat crops. It is important

though to point out that if offtake by crop residues is considered, then both maize and rice are at PNBK<1.

Oilseeds and sugar crops are also at PNBK<1, meaning that on a global basis, they are under fertilized with K. The only crop group in this comparison to be well fertilized with K is fruit and vegetables. With no crop residues to be accounted for, it is clear that this group receives more K than is removed, reflecting farmers' desire to achieve high quality and reduce biotic and a biotic stresses. It also reflects a lower sensitivity to the cost of fertilizer, as these are considered 'cash crops'.

In conclusion, global or national PNB calculations provide an assessment of nutrient use requirements. When used for K, this calculation is very sensitive to crop residue management in cereals, and is more accurate in crops with less crop residues. Moreover, in order to achieve more accuracy, the inclusion of organic and other sources of nutrients (e.g. from irrigation water and deposition) is required.

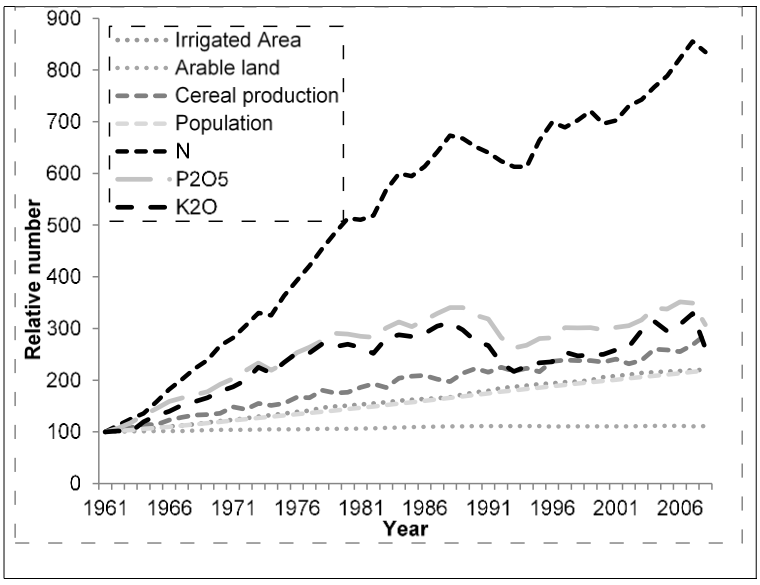

Fig. 1. Relative growth 1961-2008 in population, arable and irrigated land, N, P and K nutrients and cereal production (data from FAOSTAT).

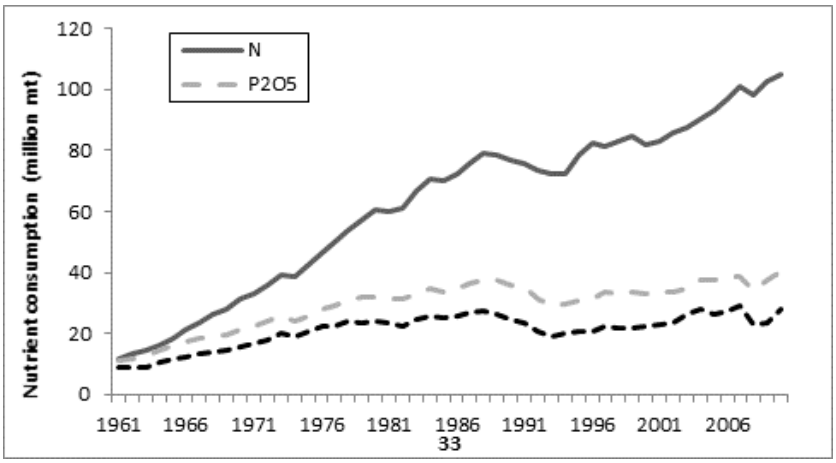

Fig. 2. Global nutrient consumption 1961-2008 (data from FAOSTAT and IFA).

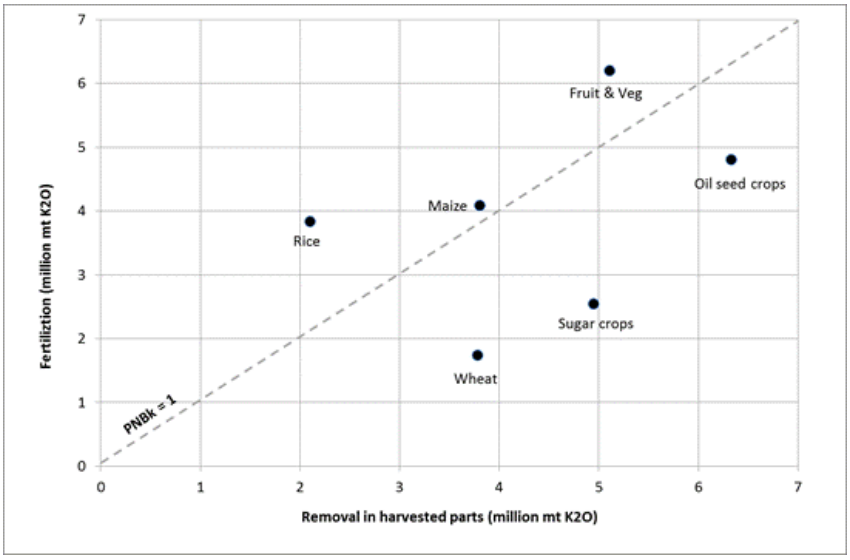

Fig. 3. Global PNB_K for selected crop groups. Note: Fertilization by crop group from Heffer, 2009.

Table 1. Average yield of staple crops as a percentage of yield potential. Adapted from St. Clair and Lynch, 2010.

Region	Crop and production (2003-2005)			
	Maize	Rice (paddy)	Wheat	Millet
Yield potential(†) (mt ha^{-1})	20	10	10	4.3
	Percent of yield potential			
Africa, developing	7.0	20.0	22.0	16.3
Asia, developing	20.0	40.0	29.0	23.3
Latin America (developing) and Caribbean	16.5	39.0	26.0	39.5
Asia, developed	79.5	63.0	36.0	23.3
Latin America, developed	54.0	48.0	44.0	
United States	47.0	75.0	29.0	30.2
Developed countries	20.0	40.0	29.0	23.3

(†)With high water and nutrient input; from various sources cited by St. Clair and Lynch, 2010.

Table 2. Attainable yield (Mueller at al., 2012) and average maize yields (FAOSTAT; 2009-2011) in selected countries.

Country	Attainable yield	Average yield (2009-2011)	Percent of yield potential
	mt ha^{-1}		*%*
Brazil	4.9	4.10	84
China, mainland	8.8	5.49	62
Ethiopia	5.7	2.32	41
India	3.2	2.35	73
Mozambique	3.9	1.10	28
Ukraine	9.3	5.37	58
United States of America	9.8	9.72	99

Table 3. Average, attainable and projected production of major crops

Crop	Average productivity 2005-07(†)	Attainable yield(β)		Projected productivity 2050(‡)
		50%	100%	
	----------*mt ha^{-1}*----------			
Wheat	2.8	2.87	4.41	3.8
Maize	4.7	4.76	6.98	6.1
Rice (paddy)	4.1	3.78	5.3	5.3
Barley	2.4	2.6	3.86	2.9
Soybean	2.3	2.16	2.66	3.2
Sunflower	1.3	1.25	1.73	1.7
Sorghum	1.3	1.46	2.17	1.9
Groundnut	1.5	1.46	2.15	2.0
Millet	0.9	0.78	1.16	1.4
Rapeseed	1.6	1.49	1.99	2.8
Sugarcane	68	61.66	85.37	104

(†)Alexandratos and Bruinsma, 2012; (‡) Mueller et al., 2012

Table 4. Projections and estimations of required levels of nutrients, from present to 2050

Source	Year	Projected consumption			Total
		N	P_2O_5	K_2O	
		Million mt			
IFA, 2013	2012	108	41.3	28.9	178.2
Tilman et al., 2001	2050	236	83.7	-	
Dobermann and Cassman, 2005†	2025	114-140	-	-	
Tenkorang and Lowenberg-DeBoer, 2009‡	2030	137.4	52.9	32.8	223.1
Tilman et al., 2011§	2050	200-280	-	-	
Alexandratos and Bruinsma, 2012¶	2050	149.9	65.7	47.3	262.9
IPI, 2012#	2012	-	-	28.9	
IPI, 2012#	2050	-	-	44.8	

†Varies with the degree of improved management, ‡ Total is +25% over 2012 levels
§ Varies with the degree of improved management, Total is +47.5% over 2012 levels. N is projected, while P and K are calculated by ratio to N, assuming same nutrient ratio in 2050 as in 2012, #Offtake calculation

Table 5. 2010 and 2050 (projected) crop production and estimated K removal.

Crop	2010 global production(†)	2010 estimated quantity of K_2O in products†	2050 global production‡	2050 estimated quantity of K_2O in products
	million mt			
Soybean	261.6	5.0	390	7.5
Sugarcane	1,685.4	4.7	2,822	7.9
Maize, grain	844.4	4.2	1,178	5.9
Vegetables, fresh	1,036.3	4.0	2,723§	10.5
Wheat, grain	650.9	3.6	858	4.7
Rice, paddy, grain	672.0	2.2	827	2.7
Others		5.2		5.6
Total (in harvested products)		28.9		44.8

Sources: †IPI, 2012 (http://www.ipipotash.org/udocs/388-ipi-booklet-potassium-a-nutrient-for-life.pdf.pdf), ‡Alexandratos and Bruinsma, 2012 (FAO), §Kearney, 2010

References

Burger, M., and Jackson, L. E., 2004, Plant and microbial use and turnover: rapid conversion of nitrate to ammonium in soil with roots, Plant and Soil, 266: 289-301.

Galloway, J. N., and Cowling, E. B., 2002, Reactive nitrogen and the world: 200 years of change, Ambio, 31: 64-71.

Hall, E. K., Maixner, F., Franklin, O., Daims, H., Richter, A., and Battin, T., 2011, Linking microbial and ecosystem ecology using ecological stoichiometry: a synthesis of conceptual and empirical approaches, Ecosystems, 14: 261-273.

Inselsbacher, E., Öhlund, J., Jämtgard, S., Huss-Danell, K., and Näsholm, T., 2011, The potential of microdialysis to monitor organic and inorganic nitrogen compounds in soil, Soil Biology & Biochemistry, 43: 1321-1332.

Inselsbacher, E., Wanek, W., Strauss, J., Zechmeister-Boltenstern, S., and Müller, C., 2013, A novel ^{15}N tracer model reveals: Plant nitrate uptake governs nitrogen transformation rates in agricultural soils, Soil Biology & Biochemistry, 57: 301-310.

Jørgensen, J. C., Struwe, S., and Elberling, B., 2012, Temporal trends in N_2O flux dynamics in a Danish wetland – effects of plant-mediated gas transport of N_2O and O_2 following changes in water level and soil mineral-N availability, Global Change Biology, 18: 210-222.

Parkin, T. B., 1987, Soil microsite as a source of denitrification variabilitiy, Soil Science Society of America Journal, 51: 1194-1199.

Robertson, L. A., and Kuenen, J. G., 1990, Physiological and ecological aspects of aerobic denitrification, In "Denitrification in soil and sediment" (N. P. Revsbech and J. Sørensen, eds.), pp. 91-104. Plenum Press, New York.

Alexandratos, N. 2009. World food and agriculture to 2030/2050. Highlights and views from mid-2009. FAO In: How to feed the world in 2050. Expert Meeting on How to feed the World in 2050. FAO, Economic and Social Development Department.

Alexandratos, N. and J. Bruinsma. 2012. World agriculture towards 2030/2050: the 2012 revision. ESA Working paper No. 12-03. FAO, Rome. Available at http://www.fao.org/docrep/016/ap106e/ap106e.pdf.

Borlaug, N. 2007. Feeding a Hungry World. Science, 318(5849): 359.

Dobermann, A. and K.G. Cassman. 2005. Cereal area and nitrogen use efficiency are drivers of future nitrogen fertilizer consumption. Science in China Series C Life Sciences, 48: 745–758.

Dyson, T. 1995. World food demand and supply prospects. The International Fertiliser Society (IFS), UK.

Dyson, T. 1999. World food trends and prospects to 2025. Proc. Natl. Acad. Sci. USA, 96(11): 5929–5936.

Eltun, R., A. Korsæth and O. Nordheim. 2002. A comparison of environmental, soil fertility, yield, and economical effects in six cropping systems based on an 8-year experiment in Norway. Agriculture, Ecosystems and Environment, 90(2): 155–168.

FAOSTAT. http://faostat.fao.org/. Accessed 2/2013.

Foley, J.A., N Ramankutty, K.A. Brauman, E.S. Cassidy, J.S. Gerber, M. Johnson, N.D. Mueller, C. O'Connell, D.K. Ray, P.C. West, C. Balzer, E.M. Bennett, S.R. Carpenter, J. Hill, C. Monfreda, S. Polasky, J. Rockstrom, J. Sheehan, S. Siebert, D. Tilman and D.P.M. Zaks. 2011. Solutions for a cultivated planet. Nature, 478: 337–342.

Heffer, P. 2009. Assessment of Fertilizer Use by Crop at the Global Level 2006/07 – 2007/08. International Fertilizer Industry Association, Paris.

Heffer, P. and M Prud'homme. 2013. Fertilizer Outlook 2013-2017, International Fertilizer Industry Association, Paris. http://www.fertilizer.org/ifa/HomePage/LIBRARY/Publication-database.html/Fertilizer-Outlook-2013-2017.html

International Fertilizer Industry Association (IFA). http://www.fertilizer.org/ifa/ifadata/search. Accessed 3/2013.

International Potash Institute (IPI). 2012. Potassium - a Nutrient Essential for Life. IPI, Horgen. http://www.ipipotash.org/en/publications/detail.php?i=388

Jingzhu Zhao, Qishan Luo, Hongbing Deng and Yan Yan. 2008. Opportunities and challenges of sustainable agricultural development in China. Phil. Trans. R. Soc. B, 363, 893–904.

Junfang Niu, Weifeng Zhang, Xinping Chen, Chunjian Li, Fusuo Zhang, Lihua Jiang, Zhaohui Liu, Kai Yiao, M. Assaraf, and P. Imas. 2011. Potassium Fertilization on Maize under Different Production Practices in the North China Plain. Agronomy J., 103(3): 823–829.

Kearney, J. 2010. Food consumption trends and drivers. Phil. Trans. R. Soc. B, 365: 2793-2801.

Ladha, J.K., D. Dawe, H. Pathak, A.T. Padre, R.L. Yadav, Bijay Singh, Yadvinder Singh, Y. Singh, P. Singh, A.L. Kundu, R. Sakal, N. Ram, A.P. Regmi, S.K. Gami, A.L. Bhadari, R. Amin, C.R. Yadav, E.M. Bhattarai, S. Das, H.P. Aggarwal, R.K. Gupta,. and P.R. Hobbs. 2003. How extensive are yield declines in long-term rice-wheat experiments in Asia? Field Crops Research, 81: 159-180.

Lobell, D.B., K.G. Cassman and C.B. Field. 2009. Crop Yield Gaps: Their Importance, Magnitudes, and Causes. Annu. Rev. Environ. Resour. 34:179–204

Magen, H. and P. Imas. 2007. Characteristics of potassium fertilization and demand. In: Balanced Fertilization for Sustaining Crop Productivity. Eds. Benbi, D.K., M.S. Brar, and S.K. Bansal. 22-25 November, Ludhiana, India. International Potash Institute (IPI), Horgen, Switzerland.

http://www.ipipotash.org/udocs/BALANCED_FERTILIZATION_FOR_SUSTAINING_CROP_PRODUCTIVITY.pdf

Milford,G.F.J and A.E. Johnston. 2007. Potassium and nitrogen interactions in crop production. Proceedings No. 615. International Fertiliser Society, York.

Mueller, N.D., J.S. Gerber, M. Johnston, D.K. Ray, N. Ramankutty and J.A. Foley. 2012. Closing yield gaps through nutrient and water management. Nature, 490: 254-257.

Monfreda, C., N. Ramankutty, and J.A. Foley. Farming the planet: 2. Geographic distribution of crop areas, yields, physiological types, and net primary production in the year 2000. Glob. Biogeochem. Cycles, 22(1).

The Royal Society. 2009. Reaping the benefits: science and the sustainable intensification of global agriculture. 2009. The Royal Society, London.

Rosegrant, M., X. Cai, S. Cline, and N. Nakagawa. 2002. The Role of Rainfed Agriculture in the Future of Global Food Production. EPTD Discussion Paper No. 90. International Food Policy Research Institute, Washington, D.C.

Roy, R.N., R.V. Misra, J.P. Lesschen, and E.M. Smaling. 2003. Assessment of soil nutrient balance; approaches and methodologies. FAO, Rome.

Sheldick,W.F., J.K. Syers and J. Lingard. 2002. A conceptual model for conducting nutrient audits at national, regional and global scales. Nutrient Cycling in Agroecosystems, 62: 61-67.

Sheldick,W.F., J.K. Syers and J. Lingard. 2003. Soil nutrient audits for China to estimate nutrient balances and output/input relationships. Agriculture, Ecosystems and Environment, 94: 341–354.

St. Clair, S.B. and J.P. Lynch. 2010. The Opening of Pandora's Box: Climate Change Impacts on Soil Fertility and Crop Nutrition in Developing Countries. Plant and Soil. 335 (1-2): 101-115.

Smil, V. 2002. Nitrogen and Food Production: Proteins for Human Diets. Ambio, 31 (2): 126-31.

Spiess, E. 2011. Nitrogen, phosphorus and potassium balances and cycles of Swiss agriculture from 1975 to 2008. Nutrient Cycling in Agroecosystems, 91: 351-365.

Stewart, W.M., D.W. Dibb, A.E. Johnston and T.J. Smyth. 2005. The Contribution of Commercial Fertilizer Nutrients to Food Production. Agron. J., 97:1–6.

Tenkorang, F. and J. Lowenberg-DeBoer. 2009. Forecasting long-term global fertilizer demand. Nutr Cycl Agroecosyst, 83:233–247.

Tilman, D., K.G. Cassman, P.A. Matson, R. Naylor and S. Polasky. 2002. Agricultural sustainability and intensive production practices. Nature, 418: 671-677.

Tilman, D., J. Fargione, B. Wolff, C. DAntonio, A. Dobson, R.W. Howarth, D. Schindler, W.H. Schlesinger, D. Simberloff and D. Swackhamer. 2001. Forecasting Agriculturally Driven Global Environmental Change. Science, 292: 281-284.

Tilman, D., C. Balzer, J. Hill, and B.L. Befort. 2011. Global food demand and the sustainable intensification of agriculture. Proceedings of the National Academy of Sciences, 108 (50): 20260-20264.

Waddington, S.R., X. Li, J. Dixon, G. Hyman and M.C. de Vicente. 2010. Getting the focus right: production constraints for six major food crops in Asian and African farming systems Food Sec., 2:27–48.

Witt, C., R.J. Buresh, S. Peng, V. Balasubramanian and A. Dobermann. 2007. Nutrient management. In: Fairhurst, T., C. Witt, R. Buresh and A Dobermann. (eds) Rice: a practical guide to nutrient management. International Rice Research Institute (IRRI), Los Baños and International Plant Nutrition Institute and International Potash Institute, Singapore.

ADVANCES IN UNDERSTANDING NITROGEN TRANSFORMATIONS IN TERRESTRIAL ECOSYSTEMS

Christoph Müller[1,2] and Timothy Clough[3]

[1] Institute of Plant Ecology, Giessen University, Germany
[2] School of Biology and Environmental Science, University College Dublin, Ireland
[3] Department of Soil and Physical Sciences, Faculty of Agriculture and Life Sciences, Lincoln University, New Zealand

Abstract

The nitrogen (N) cycle is one of the best studied elemental cycles. However, the N flows and transformations, in particular in aggregated soils, at small scales and in plant-soil systems are not yet fully understood. Analytical and molecular techniques are now available to address N dynamics at small scales. The methodological advances should go hand in hand with the development of suitable mathematical models addressing the small scale and the full complexity of the many interacting effects. The importance of denitrification within the N cycle is highlighted and used as an example of the progress achieved in recent times. Research gaps and possible research pathways are outlined.

Introduction

The world population is rapidly increasing and is expected to reach approx. 9 billion in the middle of this century with projected associated effects on all terrestrial ecosystems (Barnosky et al., 2012). To feed an increasing world population and enhance agricultural production a parallel increase in N consumption has been observed. The increasing amount of N, predominantly originating from industrial N fixation, has contributed to an increase in N availability in terrestrial ecosystems and in particular has enhanced the speed with which N is cycled in the environment, i.e. both the rate at which N has been added to but also lost from the environment has increased (Figure 1). This increase of available N in the environment is also responsible for enhanced N deposition in all agriculturally dominated landscapes since the mid-19th century and will further increase till the mid- 21st Century (Galloway et al., 2008; Galloway et al., 2004). Thus, anthropogenically generated reactive N cascades throughout the global environment (Galloway and Cowling, 2002) and the increasing N availability affects the N flows and transformations, in particular the relative dynamics of mineral and

organic N which are important indicators of the extent of human interference with ecosystem N dynamics (Schimel and Bennett, 2004). Reactive N may be lost from ecosystems as nitrate (NO_3^-), via leaching, or in of gaseous N form such as, nitric oxide (NO), nitrous oxide (N_2O) or dinitrogen (N_2). These N losses are of significant importance both economically and environmentally. Despite more than 150 years of N cycling research, starting with studies by well known scientists such as Liebig (van der Ploeg et al., 1999), Bausingault (Aulie, 1970), Winogradsky (Ackert, 2006) and others, there are still significant questions to be addressed with respect to N transformations and losses from terrestrial ecosystems. In particular the interactions and impact of plants with the N cycle (Knops et al., 2002), the key processes for the N cycle: in particular denitrification (Davidson and Seitzinger, 2006) and the small scale variability and microsite N dynamics and interactions are to a great extent unresolved and not adequately understood. This paper attempts to present a brief overview of some current thinking in these areas and also attempts to review and suggest modelling concepts and new analytical approaches that might help to elucidate N flows and pathways in terrestrial ecosystems.

Interactions of plants with the N cycle

Plant-soil interactions are an area of research attracting increasing interest with respect to N cycling. They are predominantly governed by interactions between the carbon (C) and N cycles. The microbial loop in soil is driven by recent plant C inputs (e.g. rhizodeposition), which influences the microbial activity in soils, while ecosystem N availability is controlled by the initial chemical composition and litter N concentrations (Manzoni et al., 2008; Parton et al., 2007). In the rhizosphere, potential N transformations such as denitrification decrease rapidly in the first few millimetres of roots (Beauchamp et al., 1989). Thus soil aggregate-microsite reactions and the influence of roots are likely to cause small-scale variations in substrate availability and environmental regulators and prompt a diverse reaction of the microbial community (Barnard et al., 2005).

Nitrogen cycling is closely associated with plant productivity and factors affecting it. For instance, conditions that favour plant C assimilation may also enhance rhizodeposition and subsequently alter microbial community composition and function

with subsequent effects on N dynamics. Conversely, a higher demand for N by plants, that may occur as a result of environmental change, (e.g. favourable growth temperatures), increases competition for N between plants and microbes, potentially affecting microbial community structures and subsequent N transformations in the soil (Zak et al., 2003). However, few studies have examined the links between the N cycle, plant activity and associated changes in microbial form and function that affect N transformations and fluxes. In N-limited systems, the gross N transformation rates and not the sizes of the soil N pools govern the availability of N for plants and microbes (Rastetter et al., 1997).

Plants utilise mineral N (e.g. NH_4^+ or NO_3^-) and low molecular organic N compounds (Schimel and Bennett, 2004). The latter enter the soil via rhizodeposition (e.g. amino acids) or are made available following microbial mineralization of organic material. Organic N (dissolved organic N, DON) uptake is reported to be more significant under conditions of N limitation and low pH (Jones et al., 2004). Despite the significance of DON as a loss pathway in agricultural ecosystems (Van Kessel et al., 2009) current knowledge of the organic N forms utilized by plants, with respect to soil DON dynamics over time and space, and their rates of production and utilization is still limited (Cabrera et al., 2005). Similarly, the role DON plays in gaseous N loss pathways is also under researched. A recent review indicates that nitrosation reactions may be an important loss pathway for gaseous N (Spott et al., 2011).

Rhizodeposition stimulates microbial biomass growth and N turnover (Knops et al., 2002), which further stimulates the growth of predating organisms such as protozoa and nematodes (Osler and Sommerkorn, 2007; Sanderman and Amundson, 2003) (Figure 2). Thus soil organic matter (SOM) is mineralized/decomposed and may even be accelerated via priming processes (Stockmann et al., 2013). So far a quantitative evaluation of the various simultaneously occurring N transformations in plant-soil systems (Figure 2), that lead to mineralization and immobilization of N in the rhizosphere, is lacking. Can plants actively control exudation to create conditions in the rhizosphere to maximize the availability of N? Do plants actively produce compounds that deter non-beneficial organisms/pathogens directly or indirectly via relationships along trophic levels that in turn affect N cycling? Rhizodeposition of C compounds can directly influence N cycling, for instance enhancing N_2O emissions in the presence of

an N substrate (Uchida et al., 2011). But relatively little is known about the forms and rates of C released. Research between cell densities and exoenzyme production in the rhizosphere (quorum sensing) are likely to contribute to a quantitative understanding of N dynamics in the rhizosphere. DeAngelis et al. (2008) showed that the activity of extracellular enzymes and N mineralization are closely associated and the production of exoenzymes is likely to be controlled by quorum sensing.

N loss from ecosystems – the importance of denitrification

A key process in the N cycle is denitrification which is a heterotrophic process performed by facultative anaerobic organisms that utilize various C substrates as electron donors (Beauchamp et al., 1989; Davidson and Seitzinger, 2006). Therefore a better understanding of this process and the dynamics of associated N transformations is pivotal. Nitrate (NO_3^-) is the key N species for N losses and is affected by numerous N flows that produce (e.g. nitrification) and consume (e.g. leaching) NO_3^- (Figure 3). To be rendered environmentally benign NO_3^- must be reduced to a non-reactive form (e.g. dinitrogen, N_2). Three major biological pathways of NO_3^- reduction are known (Figure 3): i) assimilatory NO_3^- reduction into biomass, ii) dissimilatory NO_3^- reduction to NH_4^+ (DNRA) and iii) dissimilatory NO_3^- reduction to N_2 (denitrification) (Burger and Jackson, 2004; Robertson and Kuenen, 1990). DNRA may outcompete denitrification under conditions where electron acceptors are limited and it provides an energetically favourable alternative to denitrification (Rütting et al., 2011; Tiedje, 1988). However, further research is still required to understand the importance of DNRA in terrestrial systems and to perfect methods for studying the process (Rütting et al., 2011).

Denitrification is a key transformation process in soils with adverse and beneficial roles, since it impairs N use efficiency of agricultural crops, is both a source and sink for N_2O, and lowers the potential for NO_3^- leaching to aquatic systems (Davidson and Seitzinger, 2006). In aquatic systems, autotrophic denitrification may also occur in the presence of inorganic electron donors like sulphides or ferrous iron (Clément et al., 2005; Knowles, 1982).

The reductases involved in denitrification are well recognized. The membrane bound nitrate reductase (*Nar*) is the first in the denitrification sequence and occurs in very diverse microbial communities including a, b, g, and e proteobacteria , gram positive bacteria and archaea while the periplasmic NO_3^- reductase (*Nap*) occurs only in gram-negative bacteria (Philippot, 2005). The key enzyme and key precursor for gaseous N emissions in the denitrification sequence is nitrite reductase which is encoded by either *nirS*, a cytochrome cd1 containing gene, or *nirK*, a copper containing gene. The two nitrite reductases provide a functional marker for the diversity of denitrifying bacteria (Braker and Conrad, 2011; Braker et al., 2000). The genes *norB* and *nosZ* encode the NO and N_2O reductase respectively (Groffman et al., 2006) and it is the dynamics of these two reductases in relationship to substrate and environmental regulators and in particular the balance between *nar*/*nir* and *nos* which controls the net production and release of N_2O. Philippot et al. (2011) showed that denitrifiers with and without *nosZ* encoding can co-exist and that higher N_2O/N_2 ratios can be related to the proportions of bacteria with and without *nosZ* encoding. Differential encoding may also be related to soil pH which may differ in distinct niches (Philippot et al., 2009). This highlights the fact that the observed overall denitrification dynamic is governed by the sum of the individual dynamics of co-existing microbes, possibly living in different niches (Philippot et al., 2011) and/or soil aggregates (Miller et al., 2009). Moreover, aggregation affects diffusive exchange of mineral (e.g. NO_3^-) and gaseous N species (e.g. N_2O) and O_2 between denitrifying microsite and inter-aggregate pores, which affects both, total denitrification (Sexstone et al., 1985) and the product ratio of denitrification (Arah and Smith, 1989).

While available organic C and O_2 have a major impact on total denitrification, soil pH mainly influences the ratio of N_2O/N_2 (Šimek and Cooper, 2002). Maximum denitrification occurs usually at relatively highe pH values and a linear relationship is often observed between dentrification and pH (Focht, 1974). There is a tendency for the N_2O/N_2 ratio to increase with decreasing pH (Burford and Bremner, 1975; Liu et al., 2010; Šimek and Cooper, 2002) and a more complete reduction towards N_2 is found at higher pH values (Nõmmik, 1956). The effect of pH may be due to an impact on substrate availability which influences membrane permeability or speciation of chemical species (Dassonville and Renault, 2002). N_2O reductase is more sensitive to pH than other reductases in the denitrification sequence and therefore low pH may

increase the lag phase of de novo synthesis of this enzyme (Liu et al., 2010; Šimek and Cooper, 2002). Apparently the detrimental effect of low pH on N_2O reductase occurs at the post-transcriptional level by interfering with translation, protein assembly or an effect on the activity of functional enzymes (Liu et al., 2010). Microsite variations in soil pH may support a diverse microbial community which exhibits a different sensitivity to pH (Cavigelli and Robertson, 2000; Šimek and Cooper, 2002). Also chemodenitrification may play a role for N_2O and N_2 production in acidic microsites (Chalk and Smith, 1983; Stevens et al., 1998). At pH below 3 chemical decomposition of NO_2^- is most likely the dominant process for N_2 production and may account for up 50% of N losses in tropical soils (Laudelout et al., 1977). Denitrifiers adapt to low pH over long periods of time, thus experimental setups including ad hoc pH manipulations are not conducive to evaluating natural soil conditions (Šimek and Cooper, 2002). However, one of the key unknowns is the lack of suitable field methods to quantify the N_2O/N_2 ratio *in situ*. Techniques based on the inhibition of acetylene are no longer appropriate (Bollmann and Conrad, 1997) and easy-to-use ^{15}N labelling techniques are still lacking and can be prohibitively expensive.

In general, it is the relationship between microbial communities in diverse ecosystems, the numerous proximal and distal factors and ecosystem functioning which are not completely understood yet (Braker and Conrad, 2011). In particular the activities of microbial communities under various conditions and how these contribute to soil N dynamics is a very important area of research. Studies such as the one by Jørgensen et al. (2012) who investigated in detail the spatio-temporal dynamics of factors and gaseous N losses in natural soil-plant systems provide an important contribution to elucidate in detail the processes and pathways of N dynamics in intact ecosystems.

Understanding N dynamics and the associated microbial communities

Microbial community dynamics are influenced by the interacting effects of environmental conditions together with the substrate relationships (carbon substrates) and the availability of electron acceptors (N-oxides). For instance, the most important environmental regulators for denitrification are: oxygen > pH > temperature (1974). Mineralisation activity provides substrates and is closely related to moisture/oxygen-temperature conditions (Focht and Verstraete, 1977; Morley and Baggs, 2010; Myrold

and Tiedje, 1985b). A high rate of C mineralisation favours O_2 consumption. However, in fertilized soils, C rather than NO_3^- availability limits total denitrification, but NO_3^- has a pronounced effect on the ratio of N_2O/N_2 (Beauchamp et al., 1989; Dendooven and Anderson, 1994; McCarty and Bremner, 1993; Myrold and Tiedje, 1985a; Myrold and Tiedje, 1985b; Nõmmik, 1956). Many studies have focused on either proximal or distal factors, as described by Groffman et al. (1988), but only a few studies so far have tried to link these factors. The C substrate determines the efficiency with which N oxides (NO_3^-, NO_2^-) are reduced (Beauchamp et al., 1989). Denitrifiers are able to compete successfully for C with other heterotorophs (Myrold and Tiedje, 1985b). Thus specific microbe-substrate relationships exist that may explain the link between decomposition products and microbial populations (Beauchamp et al., 1989). However, these relationships are still not well understood. The availability and identity of the C substrates and in particular the ratio between C substrate to e^--acceptor also governs whether denitrification or DNRA occurs in soils. While the need for C is universally acknowledged there is still a need to identify assays that can predict forms of C substrate utilised by various microbial groups (Rütting et al., 2011) in various soil niches. Thus, to advance the mechanistic understanding of microbial N cycling in terrestrial ecosystems there is a need to link microsite and not only bulk soil conditions to microbial activities.

In natural environments diverse microbial populations are observed (Tiedje, 1988). The greatest spatial aggregation is generally observed in the top soil (Nunan et al., 2002) and is most likely a response to the patchy distribution of organic material (Parkin, 1987) and environmental conditions (Tiedje, 1988) such as aerobic-anaerobic microsites. The need to better understand the microenvironment where N transformations occur was emphasised more than 40 years ago (McLaren, 1970) but progress in this area has been slow. Microbial processes are affected by substrate availability, thermodynamic regulation and inhibition, pH, and redox potential (Brock, 1967; Dassonville and Renault, 2002; Firestone and Davidson, 1989). Interactions between these factors are not fully understood. Cavigelli and Robertson (2000) investigated for instance the effect of pH and oxygen on the N_2O/N_2 ratio in both an arable and a non-disturbed successional field and observed that differences were most likely governed by the prevailing microbial community.

New conceptual frameworks and modelling concepts for soil N dynamics

There is a need for new theoretical and conceptual frameworks to understand how microorganisms influence ecosystem processes (Hall et al., 2011). Two aspects need to be taken into account to understand the relationships between environmental regulators and microbial activity. First, there needs to be an acknowledgement that different *microsites* exist in the soil, which to date have been considered as homogenous spaces with respect to environmental regulators. Secondly, there is a requirement to identify the *units* that represent physiologically similar microbial entities that live in mutualistic or antagonistic relationships within these *microsites*. For instance while anaerobic conditions are required for denitrification to procede, aerobic denitrification (NO_3^- reduction under microaerophyillic conditions) has been observed (Bréal, 1892) and this later process seems to be related to heterotrophic nitrification, and presents most likely a detoxifying mechanism to reduce high NO_2^- concentrations (Robertson and Kuenen, 1990).

Thus, to understand gaseous N dynamics from terrestrial ecosystems it is essential to understand the individual potential production processes. For instance N_2O is produced by nitrifiers and denitrifiers and also via groups that combine the two processes via nitrifier-denitrification (Wrage et al., 2001). Kool et al. (2011) showed that the nitrifier-denitrification pathway can be a major source for N_2O if conditions for denitrification are suboptimal and therefore it should not be ignored as a source of N_2O from soil (Wrage et al., 2001).

Furthermore chemical transformations may also contribute to N dynamics. Chemodenitrification may occur in low pH soils, including the van Slyke reaction where organic N together with NO_2^- reacts to N_2 (Tiedje, 1988). However, our understanding of the potential contribution of chemodenitrification to gaseous N losses as NO and N_2O is far from complete as demonstrated by recent studies. Further studies on chemodenitrification are warranted, especially under high N input agricultural systems (Spott et al., 2011). Besides bacteria, fungi and archaea are capable of N transformations such as NO_3^- assimilation and denitrification when NH_4^+ is depleted (Laughlin and Stevens, 2002; Zumft, 1997). The quantitative understanding of fungal denitrification (Morozkina and Kurakov, 2007) and also archaeal related N transformations are still in its infancy.

Modelling concepts

An important tool to simultaneously consider all N cycling processes is mathematical modelling. Betlach and Tiedje (1981) concluded that kinetic models can provide a useful guide to evaluate the physiology of microbial N transformations. Various kinetic expressions such as zero-order, first-order or Michaelis-Menten kinetics can easily be tested as well as dual substrate relationsships (Betlach and Tiedje, 1981; Bowman and Focht, 1974; Focht, 1974). In kinetic chain reactions such as denitrification the N dynamics can be governed by the dynamics of electron donors and N oxides for each reduction step and competition between organisms for NO_3^- which is governed by C availability (Dendooven et al., 1994).

Diffusion and conditions in aggregated soil

Kinetic parameters in N cycling models that are applied to field situations are most likely not representative of the true kinetic reaction at the reaction sites because heterogenic distribution and diffusion of N oxides and electron donors has to be taken into account (Betlach and Tiedje, 1981; Focht, 1974). In aggregated soils it is important to consider diffusion to the centre of aggregates where denitrification predominantly occurs (a kind of “hot spot” for denitrification) (Arah, 1990b). Therefore microsite specific conditions and microbial interactions need to be taken into account (Arah, 1990b; Myrold and Tiedje, 1985a). In particular the distribution of microbes and their activity should be included across the range of soil aggregates (Miller et al., 2009). In diffusion-reaction models which take into account the aeration status, the diffusion of oxygen (Greenwood and Goodman, 1964; McElwain, 1978) and of the various N species are required to predict N cycling in structured soils (Arah, 1990a; Burford and Stefanson, 1973).

General model development

Models for microbial N dynamics should be embedded in larger models that predict microbial process and their link to nutrient cycling and take into account the high spatial and temporal nature of the processes (Groffman, 1991). Not only a single relationship but also the complexity of microbial reactions that reflect the high spatial and temporal variability needs to be considered to adequately connect ecological theory with molecular-microbial composition and function (Groffman, 1991). Thus spatial and

temporal explicit relationships between the e.g. denitrifier community and environmental regulators should be taken into account. Furthermore, a bottom-up approach should be considered where spatial and temporal variability of microbial dynamics at the microsite level will be used to predict N flows and transformations at the field and regional scale. Furthermore, modelling concepts should be embedded in models that simulate the interactions among the various elemental cycles such as C-N-(P) (e.g. DNDC,Li et al., 1992; NCSOIL, Molina et al., 1983; CENTURY, Parton et al., 1987). Currently no model exists that takes into account all these aspects, in particular the high spatial and temporal nature of microbial processes.

Advances in analytical approaches – resolution of small scales

Mathematical models are only as good as the dataset addressing the various model components for model development and validation. While mathematical concepts regarding small scale diffusion processes were already well advanced more than 20 years ago (Arah, 1990a; Bouldin, 1961; McConnaughey and Bouldin, 1985; Misra et al., 1974) it is only now possible to validate them with appropriate techniques that are able to resolve the small-physical scales (Herrmann et al., 2007; Vogel et al., 2010).

Stable isotope techniques (^{13}C, ^{15}N) in combination with suitable mathematical analysis tools are available to quantify simultaneously occurring N transformations dynamics in soil. With the latest ^{15}N tracing models it is possible to identify more than 14 simultaneously occurring N transformations including nitrite dynamics (Rütting and Müller, 2008) and plant uptake dynamics (Inselsbacher et al., 2013). Together with the latest analytical techniques based on nanoSIMS it should be possible to resolve processes at µm or nm scales and the gross N dynamics at these fine spatial scales (Clode et al., 2009; Herrmann et al., 2007). This will most likely alter our view of soil N dynamics because of the non linearity among microsites (i.e. a linear relationship between microsites is inherently assumed with bulk soil determinations).

At the µm and mm scale advanced microsensor techniques are available for a range of gaseous and mineral N species (Andersen et al., 2001; Meyer et al., 2002; Neumann et al., 2009) which were recently applied in field studies (Jørgensen et al., 2012). Non-invasive techniques, such as X-ray computed tomography (CT), allow three-

dimensional visualization of soil structures and pore geometry at µm scales (Vogel et al., 2010; Wildenschild et al., 2002). Together with techniques such as microdialysis (Inselsbacher et al., 2011) it will be possible to resolve N transformations at small scales in the field, which will without doubt generate data that reflect much more realistically the N transformation processes in structured soils.

Conclusions

The advancement of our knowledge of N flows and transformations hinges on the identification of the N dynamics at small scales. A combination of suitable analytical techniques with appropriate modelling will help to understand the spatial heterogeneity in soil-plant and aggregated systems.

Acknowledgements

We thank the organisers of the Greidinger Symposium who made this presentation possible.

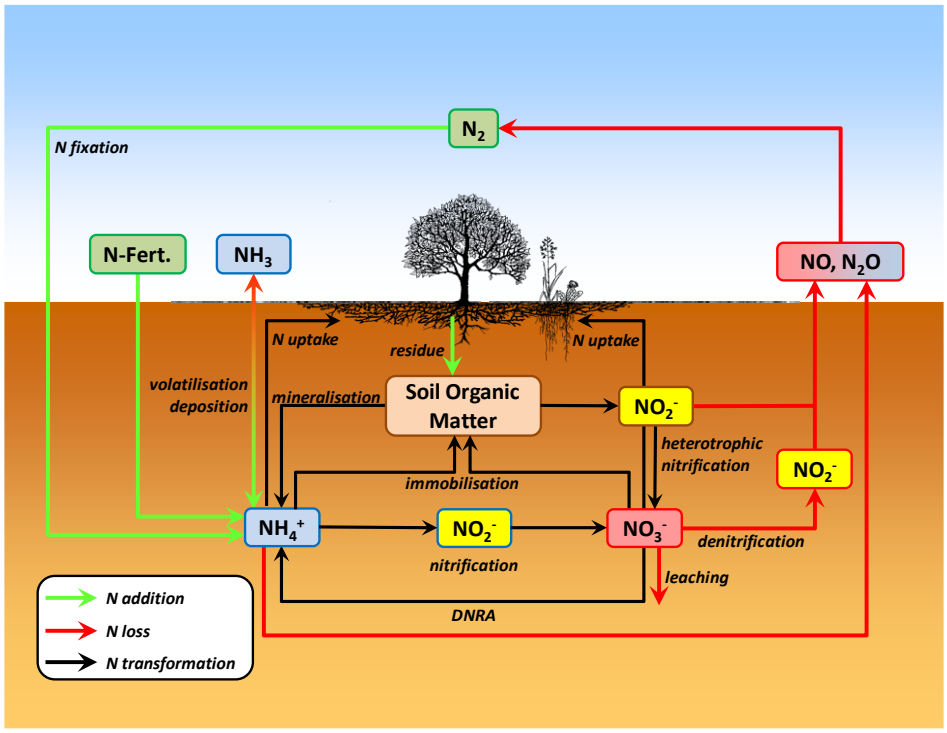

Fig. 1. Terrestrial N cycle with the major N additions (green) and N losses (red) and internal N transformations (black).

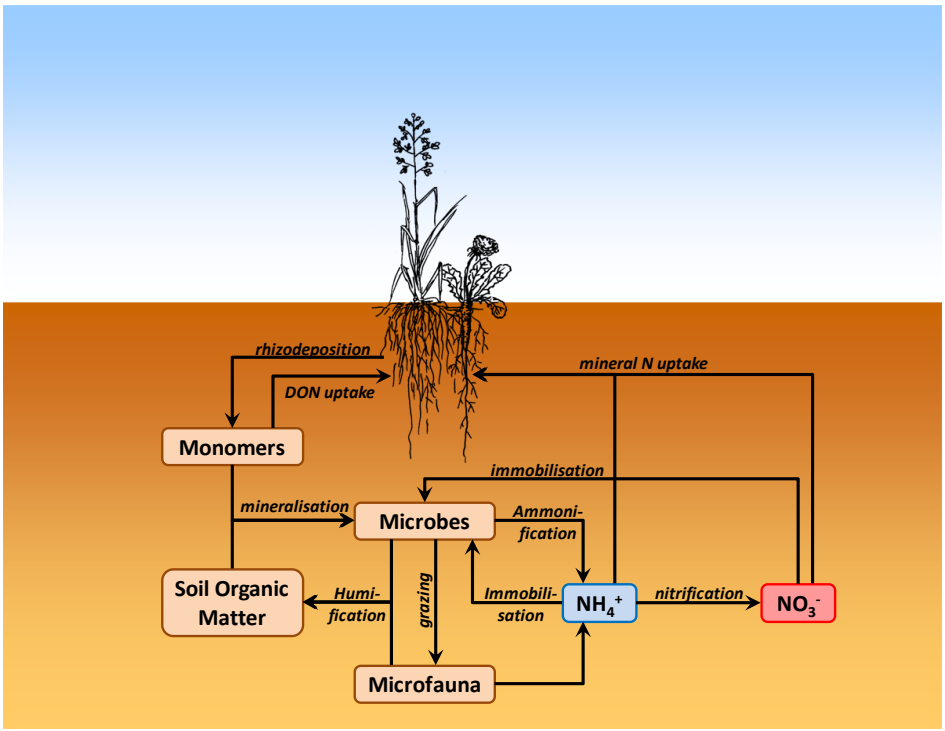

Fig. 2. Major N flows in the rhizosphere.

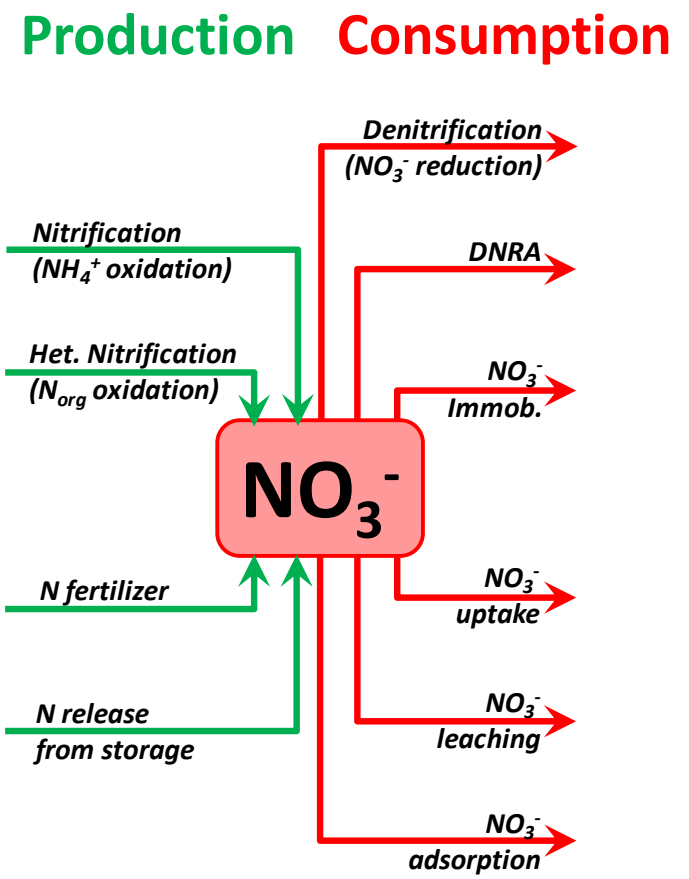

Fig. 3. Major production and consumption processes affecting the size of the soil NO_3^- pool size (note the interactions of NO_3^- with a hypothetical storage component follows the ideas of Müller et al. (2002).

References

Ackert, L.T., Jr. 2006. The role of microbes in agriculture: Sergei Vinogradskii's discovery and investigation of chemosynthesis, 1880-1910. Journal of the History of Biology 39:373-406.

Andersen, K., T. Kjær, and N.P. Revsbech. 2001. An oxygen insensitive microsensor for nitrous oxide. Sensors and Actuators B81:42-48.

Arah, J., and K.A. Smith. 1989. Steady-state denitrification in aggregated soils: a mathematical model. Journal of Soil Science 40:139-149.

Arah, J.R.M. 1990a. Diffusion-reaction models of denitrification in soil microsites, p. 245-258, *In* N. P. Revsbech and J. Sørensen, eds. Denitrification in soil and sediment. Plenum Press, New York.

Arah, J.R.M. 1990b. Modelling spatial and temporal variability of dentrification. Biology and Fertility of Soils 9:71-77.

Aulie, R.P. 1970. Boussingault and the nitrogen cycle. Proceedings of the American Philosophical Society 114:435-479.

Barnard, R., P.W. Leadley, R. Lensi, and L. Barthes. 2005. Plant, soil microbial and soil inorganic nitrogen responses to elevated CO_2: a study in microcosms of *Holcus lanatus*. Acta Oecologica 27:171-178.

Barnosky, A.D., E.A. Hadly, J. Bascompte, E.L. Berlow, J.H. Brown, M. Fortelius, W.M. Getz, J. Harte, A. Hastings, P.A. Marquet, N.D. Martinez, A. Mooers, P. Roopnarine, G. Vermeij, J.W. Williams, R. Gillespie, J. Kitzes, C. Marshall, N. Matzke, D.P. Mindell, E. Revilla, and A.B. Smith. 2012. Approaching a state shift in Earth's biosphere. Nature 486:52-58.

Beauchamp, E.G., J.T. Trevors, and J.W. Paul. 1989. Carbon sources for bacterial denitrification. Advances in Soil Science 10:113-142.

Betlach, M.R., and J.M. Tiedje. 1981. Kinetic explanation for accumulation of nitrite, nitric oxide, and nitrous oxide during bacterial denitrification. Applied and Environmental Microbiology 42:1074-1084.

Bollmann, A., and R. Conrad. 1997. Acetylene blockage technique leads to underestimation of denitrification rates in oxic soils due to scavenging of intermediate nitric oxide. Soil Biology & Biochemistry 29:1067-1077.

Bouldin, D.R. 1961. Mathematical description of diffusion processes in the soil-plant system. Soil Science Society of America Proceedings 25:476-480.

Bowman, R.A., and D.D. Focht. 1974. The influence of glucose and nitrate concentrations upon denitrification rates in sandy soils. Soil Biology & Biochemistry 6:297-301.

Braker, G., and R. Conrad. 2011. Diversity, structure, and size of N_2O-producing microbial communities in soils—What matters for their functioning? Advances in Applied Microbiology 75:33-70.

Braker, G., J. Zhou, L. Wu, A.H. Devol, and J.M. Tiedje. 2000. Nitrite reductase genes (*nirK* and *nirS*) as functional markers to investigate diversity of denitrifying bacteria in pacific northwest marine sediment communities. Applied and Environmental Microbiology 66:2096-2104.

Bréal, E. 1892. De la prèsence, dans la paille, d'un ferment aérobie, réducteur des nitrates. Comptes Rendus hebdomadaires des Séance de l'Academie des Sciences (Paris) 114:681-684.

Brock, T.D. 1967. The ecosystem and the steady state. BioScience 17:166-169.

Burford, J.R., and R.C. Stefanson. 1973. Measurements of gaseous losses of nitrogen from soils. Soil Biology & Biochemistry 5:133-141.

Burford, J.R., and J.M. Bremner. 1975. Relationships between the denitrification capacities of soils and total, water-soluble and readily decomposable soil organic matter. Soil Biology & Biochemistry 7:389-394.

Burger, M., and L.E. Jackson. 2004. Plant and microbial use and turnover: rapid conversion of nitrate to ammonium in soil with roots. Plant and Soil 266:289-301.

Cabrera, M.L., D.E. Kissel, and M.F. Vigil. 2005. Nitrogen mineralization from organic residues: research opportunities. Journal of Environmental Quality 34:75-79.

Cavigelli, M.A., and G.P. Robertson. 2000. The functional significance of denitrifier community composition in a terrestrial ecosystem. Ecology 81:1402-1414.

Chalk, P.M., and C.J. Smith. 1983. Chemodenitrification, p. 65-89, *In* J. R. Freney and J. R. Simpson, eds. Gaseous loss of nitrogen from plant soil systems. Martinus Nijhoff and Dr W Junk, Dordrecht.

Clément, J.-C., J. Shrestha, J.G. Ehrenfeld, and P.R. Jaffé. 2005. Ammonium oxidation coupled to dissimilatory reduction of iron under anaerobic conditions in wetland soils. Soil Biology & Biochemistry 37:2323-2328.

Clode, P.L., M.R. Kilburn, D.L. Jones, E.A. Stockdale, J.B. Cliff, III, A.M. Herrmann, and D.V. Murphy. 2009. In situ mapping of nutrient uptake in the rhizosphere using nanoscale secondary ion mass spectrometry. Plant Physiology 151:1751-1757.

Dassonville, F., and P. Renault. 2002. Interactions between microbial processes and geochemical transformations under anaerobic conditions: a review. Agronomie 22:51-68.

Davidson, E.A., and S. Seitzinger. 2006. The enigma of progress in dentrification research. Ecological Applications 16:2057-2063.

DeAngelis, K.M., S.E. Lindow, and M.K. Firestone. 2008. Bacterial quorum sensing and nitrogen cycling in rhizosphere soil. FEMS Microbiology Ecology 66:197-207.

Dendooven, L., and J.M. Anderson. 1994. Dynamics of reduction enzymes involved in the denitrification process in pasture soil. Soil Biology & Biochemistry 26:1501-1506.

Dendooven, L., P. Splatt, J.M. Anderson, and D. Scholefield. 1994. Kinetics of the denitrification process in a soil under permanent pasture. Soil Biology & Biochemistry 26:361-370.

Firestone, M.K., and E.A. Davidson. 1989. Microbiological basis of NO and N_2O production and consumption in soil, p. 7-21, *In* M. O. Andreae and D. S. Schimel, eds. Exchange of trace gases between terrestrial ecosystems and the atmosphere. John Wiley & Sons, New York.

Focht, D.D. 1974. The effect of temperature, pH, and aeration on the production of nitrous oxide and gaseous nitrogen - a zero order kinetic model. Soil Science 118:173-179.

Focht, D.D., and E. Verstraete. 1977. Biochemical ecology of nitrification and denitrification, p. 135-214, *In* M. Alexander, ed. Advances in Microbial Ecology, Vol. 1. Plenum Press, New York.

Galloway, J.N., and E.B. Cowling. 2002. Reactive nitrogen and the world: 200 years of change. Ambio 31:64-71.

Galloway, J.N., A.R. Townsend, J.W. erisman, M. Bekunda, Z. Cai, J.R. Freney, L.A. Martinelli, S.P. Seitzinger, and M.A. Sutton. 2008. Transformation of the Nitrogen Cycle: Recent Trends, Questions, and Potential Solutions. Science 320:889-893.

Galloway, J.N., F.J. Dentener, D.G. Capone, E.W. Boyer, R.W. Howarth, S.P. Seitzinger, G.P. Asner, C.C. Cleveland, P.A. Green, E.A. Holland, D.M. Karl, A.F. Michaels, J.H. Porter, A.R. Townsend, and C.J. Vörösmarty. 2004. Nitrogen cycles: past, present, and future. Biogeochemistry 70:153-226.

Greenwood, D.J., and D. Goodman. 1964. Oxygen diffusion and aerobic respiration in soil spheres. Journal of the Science of Food and Agriculture 15:579-588.

Groffman, P.M. 1991. Ecology of nitrification and denitrification in soil evaluated at scales relevant to atmospheric chemistry, p. 201-217, *In* J. E. Rogers and W. B. Whitman, eds. Microbial production and consumption of greenhouse gases: methane, nitrogen oxides and halomethanes. American Society for Microbiology, Washington, D.C.

Groffman, P.M., J.M. Tiedje, G.P. Robertson, and S. Christensen. 1988. Denitrification at different temporal and geographical scales: proximal and distal controls, p. 174-192, *In* J. R. Wilson, ed. Advances in nitrogen cycling in agricultural ecosystems. CAB International, Wallingford.

Groffman, P.M., M.A. Altabet, J.K. Böhlke, K. Butterbach-Bahl, M.B. David, M.K. Firestone, A.E. Giblin, T.M. Kana, L.P. Nielsen, and M.A. Voytek. 2006. Methods for measuring denitrification diverse approaches to a difficult problem. Ecological Applications 16:2091-2122.

Hall, E.K., F. Maixner, O. Franklin, H. Daims, A. Richter, and T. Battin. 2011. Linking microbial and ecosystem ecology using ecological stoichiometry: a synthesis of conceptual and empirical approaches. Ecosystems 14:261-273.

Herrmann, A.M., K. Ritz, N. Nunan, P.L. Clode, J. Pett-Ridge, M.R. Kilburn, D.V. Murphy, A.G. O'Donnell, and E.A. Stockdale. 2007. Nano-scale secondary mass sprectrometry - a new analytical tool in biogeochemistry and soil ecology: a review article. Soil Biology & Biochemistry 39:1835-1850.

Inselsbacher, E., J. Öhlund, S. Jämtgard, K. Huss-Danell, and T. Näsholm. 2011. The potential of microdialysis to monitor organic and inorganic nitrogen compounds in soil. Soil Biology & Biochemistry 43:1321-1332.

Inselsbacher, E., W. Wanek, J. Strauss, S. Zechmeister-Boltenstern, and C. Müller. 2013. A novel ^{15}N tracer model reveals: Plant nitrate uptake governs nitrogen transformation rates in agricultural soils. Soil Biology & Biochemistry 57:301-310.

Jones, D.L., D. Shannon, D.V. Murphy, and J. Farrar. 2004. Role of dissolved organic nitrogen (DON) in soil N cycling in grassland soils. Soil Biology & Biochemistry 36:749-756.

Jørgensen, J.C., S. Struwe, and B. Elberling. 2012. Temporal trends in N_2O flux dynamics in a Danish wetland – effects of plant-mediated gas transport of N_2O and O_2 following changes in water level and soil mineral-N availability. Global Change Biology 18:210-222.

Knops, J.M.H., K.L. Bradley, and D.A. Wedin. 2002. Mechanisms of plant-species impacts on ecosystem nitrogen cycling. Ecology Letters 5:454-466.

Knowles, R. 1982. Denitrification. Microbiological Reviews 46:43-70.

Kool, D.M., J. Dolfing, N. Wrage, and J.W. van Groenigen. 2011. Nitrifier denitrification as a distinct and significant source of nitrous oxide from soil. Soil Biology & Biochemistry 43:174-178.

Laudelout, H., L. Germain, P.F. Chabalier, and C.N. Chiang. 1977. Computer simulation of loss of fertilizer nitrogen through chemical decomposition of nitrite. Journal of Soil Science 28:329-339.

Laughlin, R.J., and R.J. Stevens. 2002. Evidence for fungal dominance of denitrification and codenitrification in a grassland soil. Soil Science Society of America Journal 66:1540-1548.

Li, C., S. Frolking, and T.A. Frolking. 1992. A model of nitrous oxide evolution from soil driven by rainfall events: 1. model structure and sensitivity. Journal of Geophysical Research 97:9759-9776.

Liu, B., P.T. Mørkved, Å. Frostegård, and L.R. Bakken. 2010. Denitrification gene pools, transcriptionand kinetics of NO,N_2O and N_2 productionas affected bysoil pH. FEMS Microbiology Ecology 72:407-417.

Manzoni, S., R.B. Jackson, J.A. Trofymow, and A. Porporato. 2008. The global stoichiometery of litter nitrogen mineralization. Science 321:684-686.

McCarty, G.W., and J.M. Bremner. 1993. Factors affecting the availabiltiy of organic carbon for denitrification of nitrate in subsoils. Biology and Fertility of Soils 15:132-136.

McConnaughey, P.K., and D.R. Bouldin. 1985. Transient microsite models of denitrification: I. model development. Soil Science Society of America Journal 49:886-891.

McElwain, D.L.S. 1978. A re-examination of oxygen diffusion in a spherical cells with Michaelis-Menten oxygen uptake kinetics. Journal of Theoretical Biology 71:255-263.

McLaren, A.D. 1970. Temporal and vectorial reactions of nitrogen in soil: a review. Canadian Journal of Soil Science 50:97-109.

Meyer, R.L., T. Kjær, and N.P. Revsbech. 2002. Nitrification and denitrification near a soil-manure interface studied with a nitrate-nitrite biosensor. Soil Science Society of America Journal 66:498-506.

Miller, M.N., B.J. Zebarth, C.E. Dandie, D.L. Burton, C. Goyer, and J.T. Trevors. 2009. Denitrifier community dynamics in soil aggregates under permanent grassland and arable cropping systems. Soil Science Society of America Journal 73:1843-1851.

Misra, C., D.R. Nielsen, and J.W. Biggar. 1974. Nitrogen transformations in soil during leaching; I. theoretical considerations. Soil Science Society of America Proceedings 38:289-293.

Molina, J.A.E., C.E. Clapp, M.J. Shaffer, F.W. Chichester, and W.E. Larson. 1983. NCSOIL, A model of nitrogen and carbon transformations in soil: sescription, calibration, and behavior. Soil Science Society of America Journal 47:85-91.

Morley, N., and E.M. Baggs. 2010. Carbon and oxygen controls on N_2O and N_2 production during nitrate reduction. Soil Biology & Biochemistry 42:1864-1871.

Morozkina, E.V., and A.V. Kurakov. 2007. Dissimilatory nitrate reduction in fungi under conditions of hypoxia and anoxia: a review. Applied Biochemistry and Microbiology 43:544-549.

Müller, C., M. Martin, R.J. Stevens, R.J. Laughlin, C. Kammann, J.C.G. Ottow, and H.-J. Jäger. 2002. Processes leading to N_2O emissions in grassland soil during freezing and thawing. Soil Biology & Biochemistry 34:1325-1331.

Myrold, D.D., and J.M. Tiedje. 1985a. Diffusional constraints on denitrification in soil. Soil Science Society of America Journal 49:651-657.

Myrold, D.D., and J.M. Tiedje. 1985b. Establishment of denitrification capacity in soil: effects of carbon, nitrate and moisture. Soil Biology & Biochemistry 17:819-822.

Neumann, G., T.S. George, and C. Plassard. 2009. Strategies and methods for studying the rhizosphere—the plant science toolbox. Plant and Soil 321:431-456.

Nõmmik, H. 1956. Investigations on denitrification in soil. Acta Agriculturæ Scandinavica 6:195-228.

Nunan, N., K. Wu, I.M. Young, J.W. Crawford, and K. Ritz. 2002. In situ spatial patterns of soil bacterial poplulataions, mapped at multiple scales, in an arable land. Microbial Ecology 44:296-305.

Osler, G.H.R., and M. Sommerkorn. 2007. Toward a complete soil C and N cycle: incorporating the soil fauna. Ecology 88:1611-1621.

Parkin, T.B. 1987. Soil microsite as a source of denitrification variabilitiy. Soil Science Society of America Journal 51:1194-1199.

Parton, W., W.L. Silver, I.C. Burke, L. Grassens, M.E. Harmon, W.S. Currie, J.Y. King, E.C. Adair, L.A. Brandt, S.C. Hart, and B. Fasth. 2007. Global-scale similarities in nitrogen release patterns during long-term decomposition. Science 315:361-364.

Parton, W.J., D.S. Schimel, C.V. Cole, and D.S. Ojima. 1987. Analysis of factors controlling soil organic matter levels in great plains grasslands. Soil Science Society of America Journal 51:1173-1179.

Philippot, L. 2005. Tracking nitrate reducers and denitrifiers in the environment. Biochemical Society Transactions 33:200-204.

Philippot, L., J. Andert, C.M. Jones, D. Bru, and S. Hallin. 2011. Importance of denitrifiers lacking the genes encoding the nitrous oxide reductase for N_2O emissions from soil. Global Change Biology 17:1497-1504.

Philippot, L., J. Čuhel, P.A. Saby, D. Chèneby, A. Chroňáková, D. Bru, D. Arrouays, F. Martin-Laurent, and M. Šimek. 2009. Mapping field-scale spatial patterns of size and activity of the denitrifier community. Environmental Microbiology 11:1518-1526.

Rastetter, E.B., G.I. Ågren, and G.R. Shaver. 1997. Responses of N-limited ecosystems to increased CO_2:a balanced-nutrition, coupled-element-cycles model. Ecological Applications 7:444-460.

Robertson, L.A., and J.G. Kuenen. 1990. Physiological and ecological aspects of aerobic denitrification, p. 91-104, *In* N. P. Revsbech and J. Sørensen, eds. Denitrification in soil and sediment. Plenum Press, New York.

Rütting, T., and C. Müller. 2008. Process-specific analysis of nitrite dynamics in a permanent grassland soil by using a Monte Carlo sampling technique. European Journal of Soil Science 59:208-215.

Rütting, T., P. Boeckx, C. Müller, and L. Klemedtsson. 2011. Assessment of the importance of dissimilatory nitrate reduction to ammonium for the terrestrial nitrogen cycle. Biogeosciences 8:1779-1791.

Sanderman, J., and R. Amundson. 2003. Biogeochemistry of decomposition and detrital processing, p. 350-419, *In* W. H. Schlesinger, ed. Biogeochemistry, Vol. 8. Elsevier, Amsterdam.

Schimel, J.P., and J. Bennett. 2004. Nitrogen mineralization: challenges of a changing paradigm. Ecology 85:591-602.

Sexstone, A.J., N.P. Revsbech, T.B. Parkin, and J.M. Tiedje. 1985. Direct Measurement of Oxygen Profiles and Denitrification Rates in Soil Aggregates. Soil Science Society of America Journal 49:645-651.

Šimek, M., and J.E. Cooper. 2002. The influence of soil pH on denitrification: progress towards the understanding of this interaction over the last 50 years. European Journal of Soil Science 53:345-354.

Spott, O., R. Russow, and C.F. Stange. 2011. Formation of hybrid N_2O and hybrid N_2 due to codenitrification: First review of a barely considered process of microbially mediated N-nitrosation. Soil Biology & Biochemistry 43:1995-2011.

Stevens, R.J., R.J. Laughlin, and J.P. Malone. 1998. Soil pH affects the processes reducing nitrate to nitrous oxide and di-nitrogen. Soil Biology & Biochemistry 30:1119-1126.

Stockmann, U., M.A. Adams, J.W. Crawford, D.J. Field, N. Henakaarchchia, M. Jenkins, B. Minasny, A.B. McBratney, V. de Remy de Courcelles, K. Singh, I. Wheeler, L. Abbott, D.A. Angers, J. Baldock, M. Bird, B.C. Brookes, C. Chenug, J.D. Jastrow, R. Lal, J. Lehmann, A.G. O'Donnell, W.J. Parton, D. Whitehead, and M. Zimmermann. 2013. The knowns, known unknowns and unknowns of sequestration of soil organic carbon. Agriculture, Ecosystems and Environment 164:80-99.

Tiedje, J.M. 1988. Ecology of denitrification and dissimilatory nitrate reduction to ammonium, p. 179-244, *In* A. J. B. Zehnder, ed. Biology of anaerobic microorganisms. John Wiley & Sons, New York.

Uchida, Y., T.J. Clough, F.M. Kelliher, J.E. Hunt, and R.R. Sherlock. 2011. Effects of bovine urine, plants and temperature on N_2O and CO_2 emissions from a sub-tropical soil. Plant and Soil 345:171-186.

van der Ploeg, R.R., W. Böhm, and M.B. Kirkham. 1999. On the origin of the theory of mineral nutrition of plants and the law of the minimum. Soil Science Society of America Journal 63:1055-1062.

Van Kessel, C., T.J. Clough, and J.W. Van Groenigen. 2009. Dissolved organic nitrogen: an overlooked pathway of nitrogen loss from agricultural systems? Journal of Environmental Quality 38:393-401.

Vogel, H.-J., U. Weller, and S. Schlüter. 2010. Quantification of soil structure based on Minkowski functions. Computers & Geosciences 36:1236-1245.

Wildenschild, D., J.W. Hopmans, C.M.P. Vaz, M.L. Rivers, D. Rikard, and B.S.B. Christensen. 2002. Using X-ray computed tomography in hydrology: Systems, resolutions, and limitations. Journal of Hydrology 267:285-297.

Wrage, N., G.L. Velthof, M.L. van Beusichem, and O. Oenema. 2001. Role of nitrifier denitrification in the production of nitrous oxide. Soil Biology & Biochemistry 33:1723-1732.

Zak, D.R., W.E. Holmes, D.C. White, A.D. Peacock, and D. Tilman. 2003. Plant diversity, soil microbial communities, and ecosystem function: are there any links? Ecology 84:2042-2050.

Zumft, W.G. 1997. Cell biology and molecular basis of denitrification. Microbiology and Molecular Biology Reviews 61:533-616.

THE POTENTIAL OF METAGENOMIC APPROACHES FOR UNDERSTANDING SOIL MICROBIAL PROCESSES

David D. Myrold[1], Lydia H. Zeglin[1] and Janet K. Jansson[2]

[1]Dep. of Crop and Soil Science Oregon State Univ. Corvallis, OR 97331
[2]Earth Sciences Division Lawrence Berkeley National Lab. Berkeley, CA 94720

Abstract

Technological advances in sequencing technologies and bioinformatics analysis tools now enable the generation of a metagenome from soil, although the ultimate goal of obtaining the entire complement of all genes of all organisms in a given sample of soil still lies in the future. The rich information obtained from a soil metagenome will undoubtedly provide new insights into the taxonomic and functional diversity of soil microorganisms; the question is whether it will also yield greater understanding of how C, N, and other nutrients cycle in soil. The purpose of this review is to describe the steps involved in producing a soil metagenome, including some of the potential pitfalls associated with its production and annotation. Possible solutions to some of these challenges are presented. Selected examples from published soil metagenomic studies are discussed, with an emphasis on clues that they have provided about biogeochemical cycling.

https://www.soils.org/publications/sssaj/articles/78/1/3?highlight=&search-result=1

Session 2: Advanced Tools to Investigate N Processes in Soil

CHANGES IN RELATIVE DIFFUSIVITY EXPLAIN SOIL N_2O FLUX DYNAMICS

Nimlesh Balaine[1], Tim J. Clough[1], Mike H. Beare[2], Steve M. Thomas[2], Esther D. Meenken[2], James G. Ross[3]

[1]Dep. of Soil and Physical Sciences, Lincoln Univ., Lincoln 85084, Canterbury, New Zealand

[2]Soil Water and Environment Group, Canterbury Agriculture & Science Centre, Gerald St, Lincoln 7608, New Zealand

[3]Dep. of Ecology, Lincoln Univ., Lincoln 85084, Canterbury, New Zealand

Abstract

Nitrous oxide (N_2O) is a greenhouse gas and the main anthropogenic emission contributing to stratospheric ozone depletion. Agricultural soils dominate anthropogenic N_2O emissions but there is very limited information specifically relating relative soil gas diffusivity (*Dp/Do*) to N_2O emissions. This study was conducted to determine the effects of soil bulk density (ρ_b) and matric potential (ψ) on *Dp/Do* and the associated N_2O fluxes in the presence of unlimited denitrification substrate. The interaction between soil ρ_b and ψ on *Dp/Do* and N_2O fluxes was investigated using 880 repacked soil cores that were saturated with nitrate (NO_3^-) solution and placed on tension tables at 11 levels of ψ and 5 levels of soil ρ_b. After equilibration (4 days) N_2O fluxes, *Dp/Do*, inorganic-N concentrations, and soil physical characteristics were determined. Emissions of N_2O peaked at increasingly lower levels of ψ (-1.5 to -6.0 kPa) as soil ρ_b increased (1.1 to 1.5 Mg m^{-3}) due to increasing microporosity. Peak N_2O emissions occurred across a relatively wide range of WFPS and volumetric water content (θ_v). A Gaussian fit of N_2O-N fluxes against ψ showed maximum fluxes were related to the soil's air-entry potential (r^2 = 0.96). Maximum N_2O emissions occurred at a *Dp/Do* value of 0.006 that was independent of soil ρ_b. LogN_2O-N flux was a function of log *Dp/Do* (r^2 = 0.82) when *Dp/Do* was > 0.006. Soil *Dp/Do* is a key

indicator of N_2O emission potential and needs to be further explored as a predictor of N_2O emissions in a range of soil textures.

Abbreviations: WFPS, water-filled pore space; DOC, dissolved organic carbon; Dp/Do, relative gas diffusivity; ψ, matric potential; ρb, bulk density; ε, air-filled porosity; θ_v, volumetric soil water content.

Introduction

Nitrous oxide (N_2O) is a greenhouse gas and contributes to ozone depletion in the stratosphere (Ravishankara et al., 2009). The production and evolution of N_2O from a soil are determined by substrate supply and the soil's biological and physical properties. Soil compaction alters a soil's physical and water retention properties by increasing bulk density (ρ_b) and soil moisture, which is often expressed as water-filled pore space (WFPS) or soil matric potential (ψ) (Stepniewski, 1981). As soil ρ_b and soil water content increase, oxygen (O_2) diffusion into the soil decreases. This may lead to changes in the magnitude of N_2O fluxes since the dominant mechanisms of production are nitrification and denitrification, which are aerobic and anaerobic processes respectively, while nitrifier-denitrification occurs as O_2 becomes limiting and soils transition to an anaerobic status (Wrage et al., 2001).

Many studies have attempted to relate N_2O emissions with changes in soil WFPS (Beare et al., 2009; Dobbie and Smith, 2001; Dobbie et al., 1999). However, according to Farquharson and Baldock (2008) the use of total porosity in the calculation of WFPS makes it inadequate for describing processes in soils with different ρ_b, as it does not represent the fraction of the entire soil volume. Thus variation in a soil's ρ_b will result in different WFPS and air-filled porosities which will distort any relationship between WFPS and N_2O fluxes derived at a single soil ρ_b. Thus for compacted soils, the use of WFPS to predict N_2O emissions is questionable.

Other studies have explained variability in soil N_2O emissions using soil matric potential (ψ). For example, Dobbie and Smith (2006) showed that varying ψ from -3.5 to -4.5 kPa in N fertilised grassland resulted in a 30% reduction in N_2O emissions, while Smith et al. (1998) found that N_2O emissions from a soil treated with ammonium nitrate (NH_4NO_3) peaked at -5.0 kPa and ceased at -2.5 kPa as soil became wetter. Pilot and Patrick (1972) examined the effect of ψ on NO_3^- reduction in four soils with different textures and found that there was a critical value of ψ, specific for each soil type, above

which no NO_3^- reduction occurred. Castellano et al. (2010) suggested that ψ could be a more suitable predictor of relative N_2O emissions across different soils since ψ showed less variation than other variables in explaining N_2O emissions. A recent study by van der Weerden et al. (2012) also showed that ψ was a better variable than WFPS for explaining N_2O emissions emitted from NO_3^- fertilised intact soil cores of two different soil types. They also recommended that future studies should include soils with varying ρ_b values and pore size distributions when determining a suitable variable for predicting N_2O emissions. Currently there is a lack of such studies in the literature.

When soil ρ_b and water content are altered the relative gas diffusivity (*Dp*/*Do*) of a soil varies. However, there are very few studies where measurements of N_2O fluxes and *Dp*/*Do* have both been performed. Emissions of N_2O, *in situ*, increased when the diffusivity of freon-22 was reduced following compaction of N fertilized soil (Sitaula et al., 2000). McTaggart et al. (2002) demonstrated a linear relationship (r^2 =0.55) between *Dp*/*Do* and cumulative N_2O emissions from N fertilized intact soil cores maintained at three different moisture tensions. Andersen and Petersen (2009) also showed that calculated *Dp*/*Do* values were a better predictor of N_2O emissions than WFPS in a study using repacked soil, adjusted to three matric potential (ψ) levels (-1.5 to -10 kPa), however, no effect of variation in soil ρ_b was considered. Thus there is still a need for experiments where both *Dp*/*Do* and N_2O emissions are measured in order to further test the relationship between these variables (Andersen and Petersen, 2009).

There has been a call for greater emphasis to be put on examining the interaction between soil physical and biological processes in order to increase understanding of greenhouse gas emissions (Ball, 2013). Currently, there are no published studies examining the interaction between soil ρ_b and ψ on both *Dp*/*Do* and N_2O emissions resulting from denitrification. Such studies are needed in order to find better predictors of N_2O fluxes and in order to understand soil management effects on these fluxes. It was hypothesised that, in the presence of unlimited denitrification substrates, N_2O production would be explained by differences in *Dp*/*Do* that occurring as a result of varying ψ and soil ρ_b.

Materials and Methods

Soil Collection, Experimental Design and Setup

A silt loam soil (Templeton silt loam, Typic Immature Pallic, New Zealand Soil Classification (Hewitt, 1998), was randomly sampled (0-15 cm depth) from the Duncan Block, Lincoln University (43° 38' 0.7'' S, 172° 29' 40'' N). It was air-dried and sieved to ≤ 2 mm. Soil cores were made by compacting sieved soil to a depth of 4.1 cm into stainless steel rings (7.3 cm internal diameter, 7.4 cm deep) according to treatments as follows. A factorial experiment was arranged in a randomised block design. Treatments included five levels of ρ_b (1.1, 1.2, 1.3, 1.4, and 1.5 Mg m^{-3}), two levels of NO_3^- (±N) and 11 levels of ψ (-1.0, -1.5, -2.0, -3.0, -4.0, -5.0, -6.0, -7.0, -8.0, -9.0 and -10 kPa), replicated four times.

At each level of ψ, 2 sets of cores were made, 'Set A' and 'Set B', both of which contained 40 soil cores each, comprising all five levels of ρ_b with ±N treatments. Set A was used to measure N_2O fluxes and *Dp*/*Do* while set B was used to measure soil physical and chemical characteristics**.** Soil cores receiving N (+N) were pre-soaked in a KNO_3 (1800 µg mL^{-1} NO_3^--N) for 2 days. After this soil cores were placed on a tension table to equilibrate for another 4 days at designated ψ levels, whereupon *Dp*/*Do* and N_2O readings were taken as noted below. All the non-N cores (-N, controls) were treated in a similar way except DI water was used in place of the NO_3^- solution to saturate the cores. Tension tables were prepared as described by (Romano et al., 2002). Before placing soils cores on the tension tables, 10 mL of either KNO_3 or deionised water were poured evenly across the tension tables for +N and -N soil cores, respectively, to provide a good connection between the soil cores and the tension table.

Running all the 880 soil cores at once (5 levels of ρ_b x 11 levels of ψ x 4 replicates x 2 N levels x 2 sets i.e. A and B), was logistically impossible, so groups of 80 soil cores, 40 for 'Set A' (± N x 5 levels of ρ_b x 4 replicates) and 40 for 'Set B' (± N x 5 levels of ρ_b x 4 replicates) were made each time and then used to evaluate the effect of a given level of ψ. The process from soil core saturation to completion of the measurements including N_2O and *Dp*/*Do* and destructive analysis from 80 soil cores at each ψ level took 8 days. A new set of cores for each ψ level also ensured that the initial NO_3^- and dissolved organic carbon (DOC) concentrations were the same for each level of ψ level,

which would not have been possible if the same set of cores had been sequentially drained stepwise to different ψ levels.

In order to confirm the availability of sufficient substrate concentrations for denitrification, a preliminary test was performed to observe the changes in NO_3^--N and DOC levels over a period of 6 days following soil core saturation. Measurements were made of inorganic N and DOC on day 2 (2 days after soil core saturation), on day 4 (2 days after placing cores on tension tables), and on day 6 (4 days after placing cores on tension tables). For this test, 4 replicates soil cores at each level of ρ_b were made and soaked in the KNO_3 solution for 2 days, and then drained at -1.0 kPa for a further 4 days. After which NO_3^--N and DOC were measured by destructive analysis.

Soil water retention curves for each level of soil ρ_b over the matric range of 0 to -1500 kPa were performed, and pore size distributions were also determined, using a further separate set of cores (5 ρ_b x 4 replicates) which were sequentially drained, stepwise, at designated matric potential levels. Soil water retention curves (WRC) were then used to calculate the air entry value (ψ_a) using the Campbell equation (Campbell, 1974) and pore size distribution (Schjønning et al., 2003). The temperature of the room in which the tension tables and soil cores were housed was in the range of 21.8-24.2^{o}C (mean 23.1^{o}C) throughout the experimental period.

Measurements

Nitrous oxide fluxes and Dp/Do

Nitrous oxide fluxes were measured after soil cores had equilibrated on the tension tables (after 4 days), using 'Set A' soil cores, by placing each soil core in a 1 L tin container, which was then sealed with an air-tight lid equipped with a septa. Gas samples (10 mL) were taken at 0, 15 and 30 min after sealing the tin using a 20 mL glass syringe fitted with a 3-way stopcock and a 25G hypodermic needle. These gas samples were injected into pre-evacuated 6 mL Exetainer® vials (Labco, U.K), over pressurizing the vial. Immediately prior to analysis the gas samples were brought to ambient pressure and then analysed on a gas chromatograph (SRI- 8610, CA, USA) equipped with a ^{63}Ni electron capture detector, as described by Clough et al. (2006), with a configuration similar to that used by Mosier and Mack (1980). Nitrous oxide fluxes were calculated according to Hutchinson and Mosier (Hutchinson and Mosier,

1981). Entrapped N_2O in the soil cores at day 4 was determined by placing each soil core, from 'Set B', into a Ziploc® plastic bag and sealing it tight. Then, working rapidly, the soil core was extruded and broken open to release entrapped N_2O. Gas samples (10 mL) were then taken immediately, as described above, by inserting the hypodermic needle into the gas bag. The volume of N_2O inside the plastic bag was determined by immersing the still sealed plastic bag into a bucket of water and measuring the volume of displacement, while allowing for the volume of soil and ring. Concentrations of N_2O dissolved in the soil water were calculated according to Davidson and Firestone (Davidson and Firestone, 1988).

Measurements of *Dp*/*Do* were performed on 'Set A' cores, after N_2O flux measurements were performed, using the method of Rolston and Moldrup (2002). In brief, a chamber containing a calibrated O_2 sensor (KE-25, Figaro Engineering Inc., Osaka, Japan) was purged with a gas mixture (90% Ar and 10% N_2) while the base of the soil core was isolated from the chamber. Once the chamber O_2 concentration equalled 0% the base of the soil core was exposed to the O_2 free chamber atmosphere. As O_2 diffused through the soil core into the chamber the change in O_2 concentration was recorded as a function of time, over a period of 120-180 minutes. It was assumed that any error in the measured value of *Dp*, due to O_2 consumption was negligible (Moldrup et al., 2000). Regression analysis of the log-plot of relative O_2 concentration versus time enabled *Dp/Do* to be calculated according to Rolston and Moldrup (2002). All diffusivity calculations were performed at 25ºC and the value of *Do* at 25ºC was calculated to be 0.074 $m^2\ h^{-1}$ (Currie, 1960). An index of diffusion pore continuity (*C*) (dimensionless ratio) was also derived as the ratio of *Dp/Do*: air-filled porosity (ε) (Ball et al., 1988).

Soil analyses and calculations

Destructive soil analyses were performed on 'Set B' soil cores. Bulk soil pH was measured by adding 25 mL of deionized water to 10 g of air-dried soil (Blakemore et al., 1987). Soil inorganic-N concentrations were determined after extracting soil with 2M KCl (10 g soil: 100 mL KCl) and shaking on an end-over-end shaker for 1 hour, filtering (Whatman 42), followed by flow injection analysis (Blakemore et al., 1987). Cold water DOC extractions (Ghani et al., 2003) were performed by adding 30 mL of deionized water to the equivalent of 5 g of air-dried soil and shaking for 30 minutes,

centrifuging at 3500 rpm for 20 minutes, filtering (Avantec 5C), followed by analysis on a total organic carbon analyser (TOC 5000A, Shimadzu, Australia). Sub-samples of soil were oven-dried at 105ºC for 24 h to determine gravimetric water content. Air-filled porosity and WFPS were determined using calculated values of soil ρ_b, while assuming a particle density of 2.65 Mg m^{-3} (Hillel, 1998).

Statistical analyses

Statistical analyses were performed using Minitab® (Minitab, 2010). Data were tested for normality using the Anderson-Darling test (Anderson and Darling, 1952). The N_2O-N flux data were log-transformed (ln (value +1)) as were the *Dp*/*Do* data (log_{10}). One way ANOVA and Tukey's test were performed to detect the differences between treatment means with the level of significance specified as $p < 0.05$ unless otherwise stated. A general linear model was used to determine the effects of soil ρ_b on N_2O-N fluxes, inorganic N, bulk soil pH and DOC within each ψ level and also the interaction between soil ρ_b and ψ on these variables from ±N soil cores. Graphing and non-linear curve fitting were performed using Sigmaplot (version 12). A three-parameter Gaussian function, described by equation [1], was fitted to the N_2O-N fluxes and ψ data to identify ψ_{N2Omax}, i.e the value of ψ where maximum N_2O occurred for each level of soil ρ_b.

$$y = ae^{\left[-0.5\left(\frac{x-x_o}{b}\right)^2\right]} \qquad [1]$$

where, y = N_2O-N (mg m^2 h^{-1}), $x = \psi$ (-kPa), $x_o = \psi_{N2Omax}$(-kPa) while a and b are fitting parameters (dimensionless).

Results

Soil chemical and physical properties

Bulk soil pH in +N soil cores ranged from 6.60 to 6.97 at -1.0 kPa and decreased with further decreases in ψ, reaching values of 5.30 to 5.65 at -10 kPa. In +N soil cores, soil pH was higher ($p < 0.01$) at all levels of ψ in the 1.4 and 1.5 Mg m^{-3} treatments compared to soil ρ_b treatments $\leq$ 1.3 Mg m^{-3}. Averaged over all soil ρ_b treatments, the bulk soil pH in +N soil cores was higher ($p < 0.01$) than in -N soil cores at each ψ level from -1.0 to -7 kPa and ranged from 5.30 to 6.18. In -N soil cores, soil ρ_b generally had no consistent effect on bulk soil pH.

After 4 days of equilibration on tension tables, mean soil NO_3^--N concentrations in the +N soil cores ranged from 126 to 84 µg g^{-1} soil at 1.1 and 1.5 Mg m^{-3}, respectively, at -1.0 kPa. At -10 kPa, mean soil NO_3^--N concentrations at soil ρ_b values of 1.1 and 1.5 Mg m^{-3} were 389 and 286 µg g^{-1} soil, respectively (Fig. 1a). Mean soil NO_3^--N concentrations in -N soil cores were lower ($p < 0.01$) and ranged from 0.3 to 0.4 µg g^{-1} soil at -1.0 kPa and from 15.1 to 18.0 at -10 kPa, respectively. Increasing soil ρ_b caused soil NO_3^--N concentrations to decline ($p < 0.01$) in +N cores with an interaction ($p < 0.01$) between soil ρ_b and ψ, where at soil $\rho_b \leq 1.3$ Mg m^{-3}, the rate of decrease in NO_3^--N concentrations was greater as ψ increased (Fig. 1a). Mean soil NH_4^+-N concentrations in both the +N and -N cores declined with decreasing ψ ($p < 0.01$) with no soil ρ_b or N treatment effects and after 4 days at -1.0 kPa they averaged 19.4 (± 3.0 stdev) µg g^{-1} while at -10 kPa they averaged 1.0 (± 0.4 stdev) µg g^{-1} soil (Fig. 1b).

In the +N soil cores DOC concentrations declined as ψ and soil ρ_b increased and ranged from 38 to 15 µg C g^{-1} soil at 1.1 and 1.5 Mg m^{-3}, respectively at -1.0 kPa, while at -10 kPa they ranged from 94 to 68 µg C g^{-1} soil at 1.1 and 1.5 Mg m^{-3}, respectively (Fig. 2a). The DOC concentrations in -N soil cores were higher ($p < 0.01$) than in +N soil cores from -1.0 to -9.0 kPa decreasing as ψ went from -1.0 to -10.0 kPa (Fig. 2b). In -N soil cores at 1.1 and 1.5 Mg m^{-3} DOC concentrations ranged from 132 to 148 µg C g^{-1} soil at -1.0 kPa and from 95 and 82 µg C g^{-1} soil at -10 kPa at soil ρ_b values of 1.1 to 1.5 Mg m^{-3}, respectively (Fig. 2b). Soil ρ_b only influenced DOC concentrations in -N soil cores at -4.0, -7.0 and -8.0 kPa where mean DOC concentrations at 1.5 Mg m^{-3} were lower ($p < 0.01$) than at 1.1 Mg m^{-3}.

Total soil porosity and macroporosity declined with increasing soil ρ_b (Table 1). Mean ε ranged from 0.06 to 0.34 m^3 m^{-3} at 1.1 Mg m^{-3} and 0.05 to 0.16 m^3 m^{-3} at 1.5 Mg m^{-3} as ψ decreased from -1.0 to -10 kPa, respectively. Soil WFPS ranged from 89 to 41% at 1.1 Mg m^{-3} and 88 to 65% at 1.5 Mg m^{-3} with the decrease in ψ from -1.0 to -10 kPa, respectively. Values of Dp/Do were zero at -1.0 kPa at all levels of soil ρ_b. Mean values of Dp/Do ranged from 0 to 0.077 at 1.1 Mg m^{-3} and 0 to 0.015 for 1.5 Mg m^{-3} with the decrease in ψ from -1.0 to -10 kPa, respectively (Fig 3). Mean air-entry values (ψ_a) ranged from -1.3 kPa at 1.1 Mg m^{-3} to -6.0 kPa at 1.5 Mg^{-3} and decreased (becoming more negative) as soil ρ_b increased ($p < 0.01$). Soil pore continuity (C) was higher at low soil ρ_b ($p < 0.01$) with mean values ranging from 0 to 0.22 at 1.1 Mg m^{-3} and 0 to

0.09 at 1.5 Mg m^{-3} as ψ went from -1.0 to -10 kPa. Values of *C* correlated well with *Dp/Do* with a value of $r = 0.91$ when considering all soil ρ_b treatments together, and ranging from $r = 0.91$ to $r = 0.98$ when considering individual soil ρ_b treatments.

Soil N_2O-N fluxes and relationships with soil physical parameters

Nitrogen addition (+N) increased N_2O-N fluxes ($p < 0.01$) and they ranged from 0.01 to 71 mg m^{-2} h^{-1} (Fig. 4) and from < 0.01 to 0.03 mg m^{-2} h^{-1} without N addition. An interaction ($p < 0.01$) between ρ_b and ψ in the +N treatments resulted in N_2O-N fluxes peaking at different values of ψ depending on soil ρ_b (Fig. 4). Maximum N_2O-N fluxes occurred at -1.5 and -6.0 kPa for the 1.1 and 1.5 Mg m^{-3} ρ_b treatments, respectively (Fig. 4). Fitting a three-parameter Gaussian function (equation 1) to the data established a theoretical ψ value where maximum N_2O fluxes (ψ_{N2Omax}) occurred. A linear relationship between, ψ_{N2Omax} and the derived ψ_a values was observed ($r^2 = 0.96$, $p < 0.01$; Fig. 5). The measured N_2O-N flux values were at a maximum when a specific pore size was drained and these ranged from 197 to 57 µm for the 1.1 and 1.5 Mg m^{-3} treatments, corresponding to a ψ of approximately -1.5 and -6.0 kPa, respectively. The value of ψ_a declined exponentially with decreasing macroporosity ($p < 0.01$; $r^2 = 0.99$) and thus the value of ψ_{N2Omax} was also strongly influenced by macroporosity ($p < 0.01$; $r^2 = 0.96$; Fig. S2).

Plotting measured N_2O-N fluxes against WFPS and θ_v (Fig. 6a and 6b) showed that maximum measured N_2O fluxes occurred at WFPS and θ_v values ranging from, 67 to 80%, and 0.34 to 0.42 m^3 m^{-3}, respectively. Similarly the maximum measured N_2O-N fluxes occurred at ε values ranging from 0.09 to 0.16 m^3 air m^{-3} soil (Fig.7a). However, plotting measured N_2O-N fluxes versus *Dp*/*Do* showed a critical and narrow *Dp*/*Do* range, which did not trend or vary statistically with soil ρ_b (0.0060 ±0.0003 – 0.0067 ±0.0002), where all maximum measured N_2O-N fluxes occurred, regardless of the soil ρ_b and ψ treatments applied (Fig 7b). At *Dp/Do* values both less than and greater than this critical value (0.006), N_2O fluxes declined. A regression of log N_2O flux against log *Dp/Do*, for *Dp/Do* values > 0.006 resulted in a significant linear relationship ($p < 0.01$; $r^2 = 0.82$) (Fig. 8) which improved ($r^2 = 0.87$) if the very low N_2O fluxes measured at -9.0 and -10 kPa in the 1.1 Mg m^{-3} ρ_b treatment were removed. In the +N soil cores,

mean concentrations of entrapped N_2O were higher as soil ρ_b and ψ increased with a significant effect ($p < 0.01$) of soil ρ_b between -1.0 and -6.0 kPa and ψ treatments.

Discussion

Soil chemical and physical characteristics

Denitrification may be limited by low concentrations of NO_3^- (< 5 mg N kg^{-1} soil) (Ryden, 1983) while, conversely, high concentrations of NO_3^- increase the denitrification rate in the presence of a C substrate (Weier et al., 1993). Beauchamp et al. (1980) showed that a minimum of 40 µg C g^{-1} soil, as water extractable C, was required before denitrification could occur, while Burton and Beauchamp (1985) found that the concentration of soluble organic C required to promote and sustain denitrification was in the range of 60-80 µg C g^{-1} soil. Based upon these results the mean NO_3^--N (505-657 µg g^{-1} soil) and DOC (113-158 µg C g^{-1} soil) concentrations initially present were non-limiting for denitrification following saturation of the soil cores.

Evidence of denitrification proceeding was provided by the increase in soil pH and the decline in both the soil NO_3^--N and DOC concentrations as soil ρ_b and ψ, increased (Fig. 1a, 2a). Denitrification is a process which results in the net release of OH^- ions (Wrage et al., 2001). For example, Glinski et al. (1992) showed that denitrification was accompanied by an increase in pH of 2.5 units, in a soil amended with a 2% NO_3^- concentration. In contrast, the lack of any observed reduction in DOC concentrations in the -N soil cores with increasing soil ρ_b and ψ indicates that DOC utilisation was lower due to a lack of N substrate for denitrification.

Conditions became more anaerobic and conducive for denitrification because *Dp/Do* decreased as soil ρ_b and ψ, increased, due to the concurrent decline in ε. The fact that ε still ranged from 0.05-0.06 m^3 m^{-3} when *Dp*/*Do* values equalled zero at -1.0 kPa was most likely the result of blocked pores containing entrapped air which cannot contribute to gas exchange (Ball et al., 1988; Xu et al., 1992). Soil *Dp*/*Do* values were in the range expected based on previous soil core studies performed at different soil ρ_b (Fujikawa and Miyazaki, 2005; Hamamoto et al., 2011).

Relationship of N_2O-N fluxes with ψ, WFPS and *Dp*/*Do*

Fluxes of N_2O-N were stimulated by the addition of N and declining *Dp/Do*, a direct measure of the ability of O_2 to diffuse into the soil. Due to the interaction between soil ρ_b and ψ on *Dp/Do* the maximum N_2O-N fluxes occurred at varying combinations of soil ρ_b and ψ. As observed, maximum N_2O-N fluxes were higher with increasing soil ρ_b, however, they occurred at varying values of ψ. This was the result of soil compaction increasing the percentage of micropores, which in turn meant that increasingly more negative values of ψ were required to drain the soil and permit O_2 entry. Decreases in the N_2O-N fluxes at higher values of ψ within each soil ρ_b treatment, when *Dp/Do* was < 0.006, resulted from either the conversion of N_2O to N_2 and/or N_2O becoming entrapped in the soil cores (Clough et al., 2001; Letey et al., 1980). Stepniewski (1981) reported that when *Dp*/*Do* is within the range 0.005-0.02 soils become anaerobic and, using this classification, the soil cores in the current study, with *Dp*/*Do* values < 0.006, would be anaerobic. The N_2O reductase enzyme is inhibited by O_2 and N_2 production is favoured by anaerobicity (Firestone and Davidson, 1989). Thus given the abundance of denitrification substrate and the anaerobic conditions at *Dp/Do* < 0.006 it can be assumed N_2 production was occurring. Likewise the data show that entrapment of N_2O also contributed to reduced N_2O emissions as soil ρ_b and ψ increased. Differences in the maximum N_2O fluxes at the critical *Dp/Do* value (0.006) are not explained directly by *Dp/Do* but are indirectly the result of soil cores taking a longer time to reach the critical *Dp/Do* value, following saturation, as soil ρ_b increased, which allowed for more prolonged denitrification and greater use of substrate, as evidenced by the NO_3^--N concentrations measured. Upon reaching the critical *Dp/Do* gas exchange occurred rapidly due to macropores draining at the soil's air-entry value of ψ. Differences in the magnitude of the maximum N_2O fluxes may also be partially due to differing amounts of entrapped N_2O being released.

It has been previously shown that soil N_2O-N fluxes may be described by a Gaussian function of WFPS (Davidson, 1991; Jambert et al., 1997; Rafique et al., 2011; Veldkamp et al., 1998; Vilain et al., 2010) or be exponentially related to WFPS (Beare et al., 2009; Clough et al., 2004; Smith et al., 1998). However, the inconsistent relationship between N_2O-N flux and WFPS seen in the current study has been previously observed (Castellano et al., 2010; van der Weerden et al., 2012). The reason WFPS does not make a good predictor across soils varying in soil ρ_b is because WFPS

defines the fraction of the total pore space that is water-filled and thus it is not proportional to the actual diffusion of gases and thus is an inappropriate measure to use when comparing soils of varying ρ_b (Ball, 2013; Farquharson and Baldock, 2008).

Instead, Farquharson and Baldock (2008) suggested the use of θ_v and ε when estimating emissions of N_2O via denitrification and nitrification, across soils varying in ρ_b. However, this current study shows that when both ψ and soil ρ_b are varying, θ_v is also a poor predictor of maximum N_2O flux. The term, θ_v, is a measure of the volume of water in a given volume of soil (the m^3 of water per m^3 of soil) and thus while it is informative about the relative water content on a volume basis it still does not inform with respect to which pore size fractions are filled with water. Hence, it does not directly relate to the potential for gas exchange between soil and air, which is dependent on the pore size distribution and which of the soil pore classes are water-filled.

The strong relationship observed between the air entry value (ψ_a) and ψ_{N2Omax}, and also ψ_{N2Omax} and % macroporosity, demonstrates that the reason for the maximum N_2O-N fluxes occurring at the given values of ψ_{N2Omax} was that the first-drained pores were macropores. Once drained, these macropores facilitated the diffusion of N_2O out of the soil cores and O_2 into the soil cores. This is further supported by the strong correlations observed between *C* and *Dp/Do*, and work by McTaggart et al. (2002) who showed a strong relationship between air-filled porosity and measured *Dp/Do*.

In one of the few studies to assess the relationship between N_2O produced via denitrification and ψ, Castellano et al. (2010) took soils varying in soil ρ_b (0.69 Mg m^{-3} 1.20 Mg m^{-3}) and texture, injected NO_3^- into the soil profiles, and showed that maximum N_2O emissions occurred across a small range of ψ (-1.88 to -4.48 kPa) that was independent of the effect of soil texture, structure and soil ρ_b. It was concluded that ψ was a better predictor of the *timing* of maximum N_2O fluxes, for soils differing in texture and ρ_b because it influences water-filled pore *size* (Castellano et al., 2010). The mean pore size corresponding to the maximum N_2O fluxes measured by Castellano et al. (2010) was 39.6 μm and in the macropore pore-size range. In the current study the range in ψ where measured N_2O fluxes peaked in the current study (-1.5 to -6.0 kPa as soil ρ_b increased from 1.1 to 1.5 Mg m^{-3}) encompasses the range observed by Castellano et al. (2010) and the results show this peak N_2O flux was also related to drainage of macropores. Van der Weerden et al. (2012) also showed that ψ was a better measure of

denitrification derived N_2O fluxes, when compared to WFPS, θ_v and calculated *Dp/Do*, after a NO_3^- solution was surface applied to two soils of similar ρ_b (0.82 and 0.88 Mg m^{-3}) prior to draining to designated ψ levels in a stepwise fashion to -10 kPa (van der Weerden et al., 2012). Nitrous oxide emissions reduced with an increase in macroporosity and were sensitive to changes in calculated *Dp/Do* (van der Weerden et al., 2012).

We hypothesised that in the presence of unlimited denitrification substrates, N_2O fluxes would be explained by changes in *Dp*/*Do* as ψ and soil ρb increased. The production of N_2O was highly sensitive to changes in *Dp/Do* with increases in N_2O production occurring between 0.006 and 0.020 as soils became anaerobic. Importantly, the relationship between N_2O-N flux and *Dp/Do* was independent of soil ρ_b and able to be expressed in a linear fashion (Fig. 8). Thus a measure of *Dp/Do* could be used to predict potential for N_2O emissions to occur. We have shown that a critical value of *Dp/Do* occurs at specific value of ψ that corresponds to the air-entry point for the given soil conditions, and that as ψ becomes more negative enhanced gas exchange diminishes the denitrification rate. Future work now needs to focus on examining the relationship of *Dp/Do* and N_2O-N fluxes, using soils not only varying in soil ρ_b and ψ but also texture, while also examining cumulative fluxes over time.

Conclusions

Under non-limiting substrate conditions for denitrification soil ρ_b and ψ interact to affect the magnitude of N_2O-N fluxes with the value of ψ, where maximum fluxes occur, increasing with soil ρ_b. Maximum fluxes of N_2O-N occur at specific values of ψ that correspond to the air-entry potential. Relative gas diffusivity is soil variable that can identify soil conditions when maximum N_2O-N fluxes will occur, which in this study was a *Dp*/*Do* value equal to 0.006. Importantly, this variable was found to be independent of the effects of soil ρ_b on N_2O emissions and could potentially be used to predict N_2O fluxes in soils of varying soil ρ_b. Future studies under different soil textures and are now required to further explore the potential for *Dp/Do* to be a predictor of N_2O fluxes.

Table 1. Total porosity of soil cores and % of total soil volume occupied by each given pore size. Note the sum of macroporosity, mesoporosity and microporosity equals total porosity. (n = 4; stdev in brackets). Values in a row that do not share a common letter are significantly different ($p < 0.01$, Tukey's test).

% of soil volume	Matric potential (-kPa)	Soil bulk density (Mg m^{-3})					
		1.1	1.2	1.3	1.4	1.5	
Total Porosity		58.5a	54.7b	50.9c	47.1d	43.3e	**
Macroporosity	< 10	36.4a	26.1b	20.8c	16.6d	13.2e	**
> 30µm		(0.32)	(0.62)	(0.64)	(0.62)	(0.43)	
Mesoporosity	10-1500	20.4b	26.0a	26.8a	27.3a	26.6a	**
30-0.2 µm		(0.65)	(0.86)	(0.82)	(0.61)	(0.52)	
Microporosity	< 1500	1.6c	2.5b	3.2ab	3.3ab	3.6a	**
< 0.2 µm		(0.42)	(0.42)	(0.19)	(0.21)	(0.22)	

** $p < 0.01$

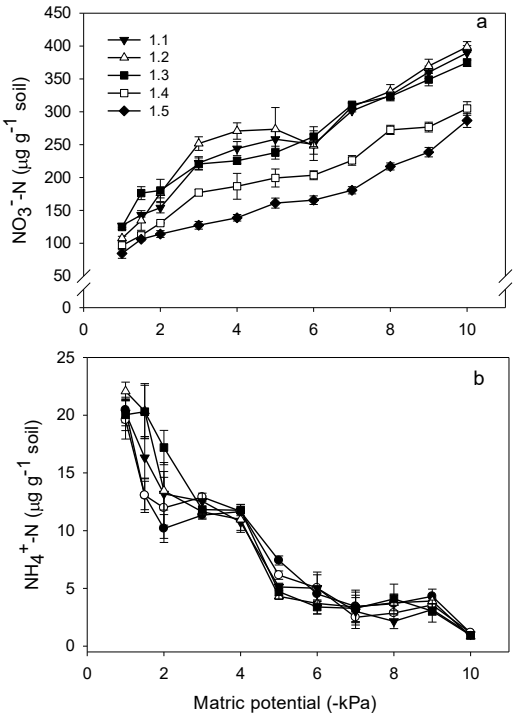

Fig. 1. Mean inorganic-N concentrations for the +N treatment at day 4; (a) NO_3^--N, (b) NH_4^+-N. Numerals in the legend indicate soil ρ_b treatments applied (Mg m^{-3}). Error bars = s.e.m, n = 3.

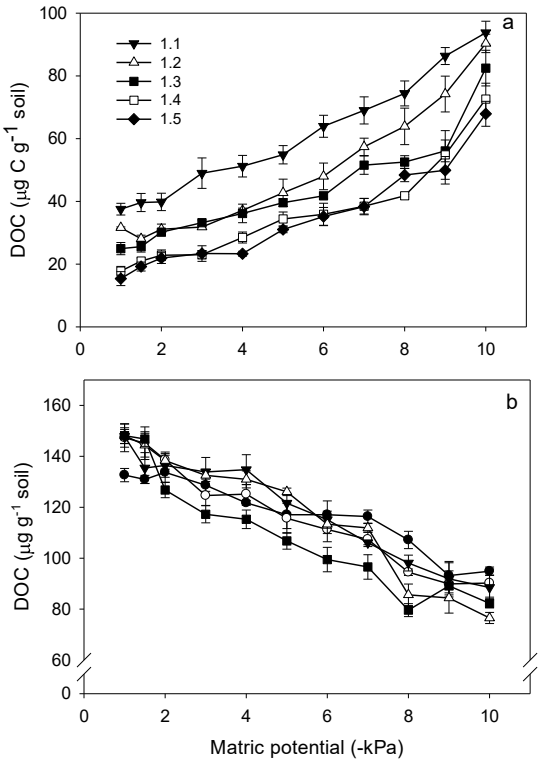

Fig. 2. Mean DOC concentrations in soil cores at day 4; (a) +N (b) -N soil cores. Numerals in the legend indicate soil ρ_b treatments applied (Mg m^{-3}). Error bars = s.e.m, n = 3.

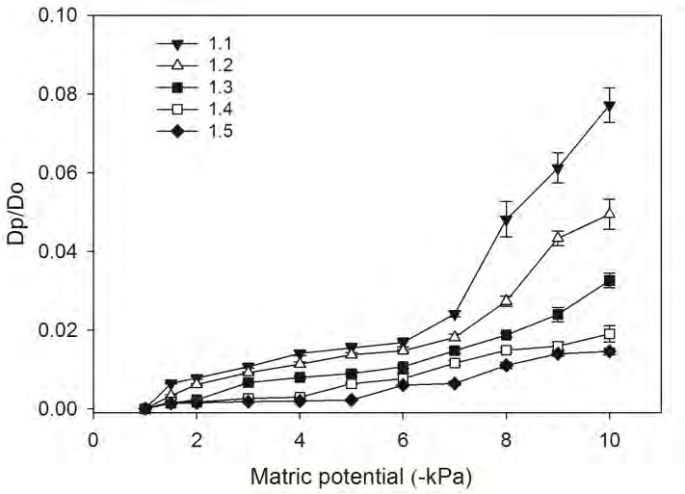

Fig. 3. Effect of soil ρ_b relative gas diffusivity (Dp/Do) for the 11 levels of matric potential (ψ) in the +N soil cores. Numerals in the legend indicate soil ρ_b applied (Mg m^{-3}). Error bars = s.e.m, n = 4.

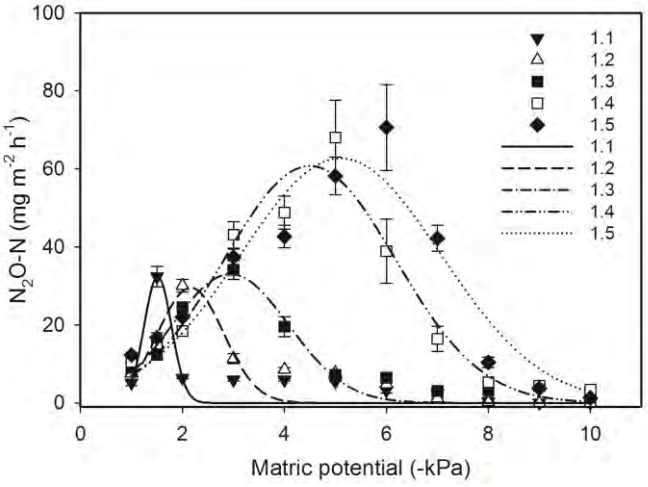

Fig. 4. Effect of soil ρ_b on mean N_2O-N fluxes for +N soil cores for the 11 levels of matric potential (ψ). Plotted lines are derived from a three-parameter Gaussian model fitted to the N_2O-N flux and ψ data. Numerals in the legend indicate soil ρ_b treatments applied (Mg m^{-3}). Error bars = s.e.m, n = 4.

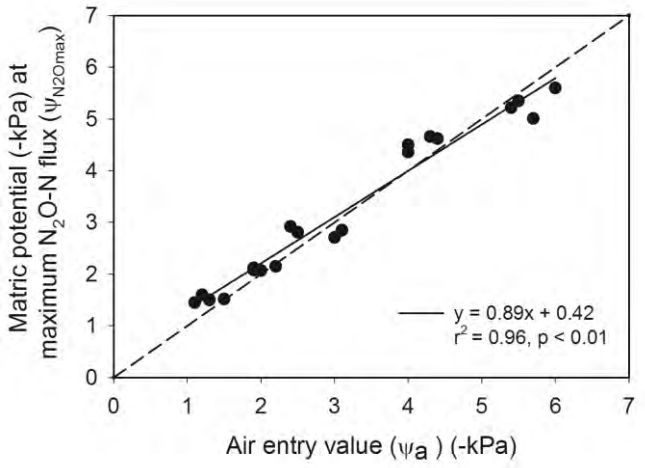

Fig. 5. Relationship between ψ_{N2Omax} (-kPa) and air entry value (ψ_a) (-kPa). Values represent individual replicates. The ψ_{N2Omax} variable was obtained by fitting a three parameter Gaussian function to the measured N_2O-N fluxes and ψ. The values of ψ_a were obtained by fitting linear regressions to the log-log plot of the water retention curves. The dashed line is a 1:1 line.

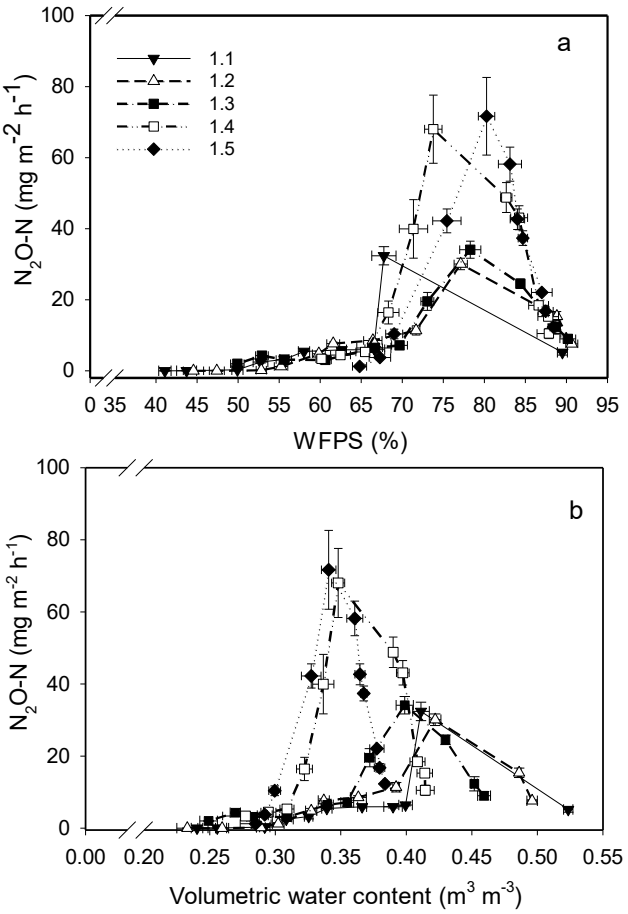

Fig. 6. Relationship between measured N_2O-N fluxes and (a) WFPS (%) (b) volumetric water content (m^3 m^{-3}) at varying soil ρ_b (Mg m^{-3}). Numerals in the legend indicate soil ρ_b treatments applied (Mg m^{-3}). Error bars = s.e.m, n = 4.

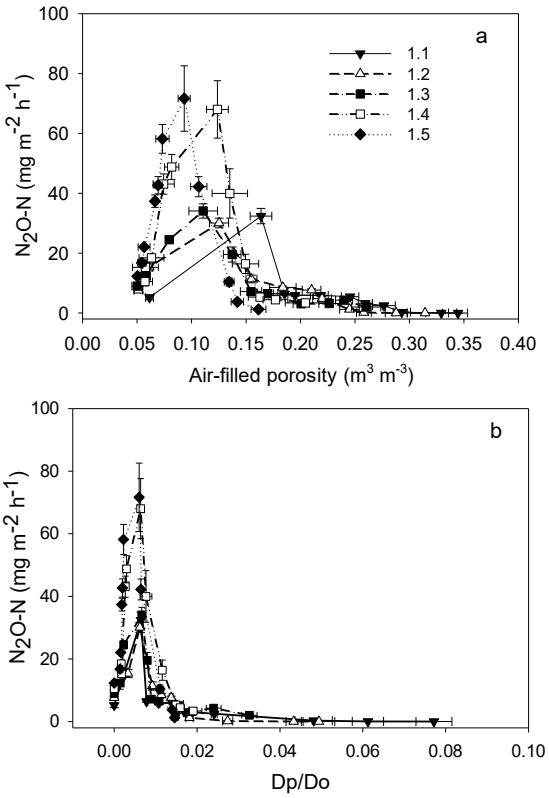

Fig. 7. Relationship of measured N_2O-N flux with (a) air-filled porosity (b) relative soil gas diffusivity (*Dp*/*Do*) (m^3 m^{-3}) at varying soil ρ_b (Mg m^{-3}). Numerals in the legend indicate ρ_b treatments applied (Mg m^{-3}). Error bars = s.e.m, n = 4.

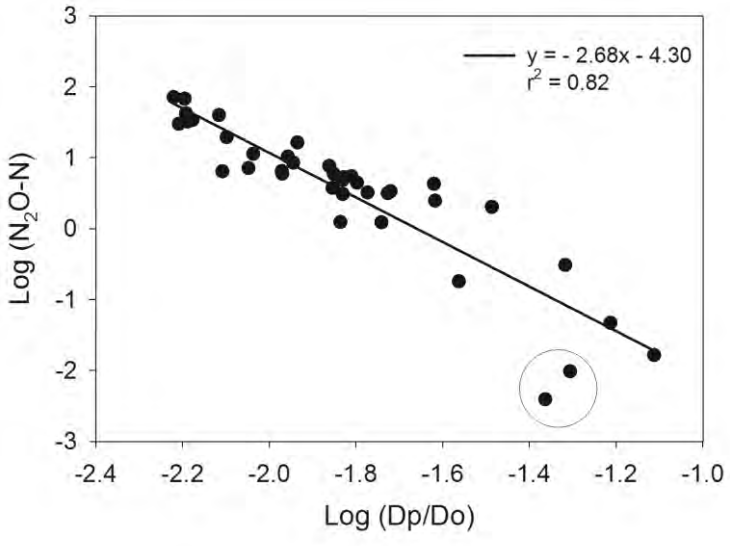

Fig. 8. Regression of mean N2O-N fluxes (n=4) expressed as Log N2O-N versus the Log of mean Dp/Do values (n=4). Circled data points are for the lowest N2O-N fluxes that occurred at a soil ρb of 1.1 (Mg m-3) and a values of ψ at -9 and -10 kPa. If these data points are excluded then r2 = 0.87.

References

Andersen A.J., Petersen S.O. (2009) Effects of C and N availability and soil-water potential interactions on N_2O evolution and PLFA composition. Soil Biol. & Biochem. 41:1726-1733.

Anderson T.W., Darling D.A. (1952) Asymptotic theory of certain "Goodness of Fit" criteria based on stochastic processes. Ann. Math. Stat. 23:193-212.

Ball B.C. (2013) Soil structure and greenhouse gas emissions: a synthesis of 20 years of experimentation. Eur. J. Soil Sci. DOI: 10.1111/ejss.12013.

Ball B.C., O'Sullivan M.F., Hunter R. (1988) Gas diffusion, fluid flow and derived pore continuity indices in relation to vehicle traffic and tillage. J. Soil Sci. 39:327-339.

Beare M.H., Gregorich E.G., St-Georges P. (2009) Compaction effects on CO_2 and N_2O production during drying and rewetting of soil. Soil Biol. & Biochem. 41:611-621.

Beauchamp E.G., Gale C., Yeomans J.C. (1980) Organic matter availability for denitrification in soils of different textures and drainage classes. Commun. Soil Sci. Plant Anal. 11:1221-1233.

Blakemore L.C., Searle P.L., Daly B.K. (1987) Methods for Chemical Analysis of Soils., NZ Soil Bureau Scientifica Report 80. , NZ Soil Bureau, Lower Hutt.

Burton D.L., Beauchamp E.G. (1985) Denitrification rate relationships with soil parameters in the field. Commun. Soil Sci. Plant Anal. 16:539-549.

Campbell G.S. (1974) A simple method for determining unsaturated conductivity from moisture retention data. Soil Sci. 117:311-314.

Castellano M.J., Schmidt J.P., Kaye J.P., Walker C., Graham C.B., Lin H., Dell C.J. (2010) Hydrological and biogeochemical controls on the timing and magnitude of nitrous oxide flux across an agricultural landscape. Global Change Biol. 16:2711-2720.

Clough T.J., Kelliher F.M., Sherlock R.R., Ford C.D. (2004) Lime and soil moisture effects on nitrous oxide emissions from a urine patch. Soil Sci. Soc. Am. J. 68:1600-1609.

Clough T.J., Kelliher F.M., Wang Y.P., Sherlock R.R. (2006) Diffusion of ^{15}N-labelled N_2O into soil columns: a promising method to examine the fate of N_2O in subsoils. Soil Biol. & Biochem. 38:1462-1468.

Clough T.J., Sherlock R.R., Cameron K.C., Stevens R.J., Laughlin R.J., Muller C. (2001) Resolution of the ^{15}N balance enigma? Aust. J. Soil Res. 39:1419-1431.

Currie J.A. (1960) Gaseous diffusion in porous media. Part1. A non-steady state method. Brit. J. Appl. Phys. 11:314-317.

Davidson E.A. (1991) Fluxes of nitrous oxide and nitric oxide from terrestrial ecosystems, in: J. E. Rojers, Whitman, W.B (Ed.), Microbial Production and Consumption of Greenhouse Gases: Methane, Nitrogen oxides and Halomethanes, American Society for Microbiology, Washington DC. pp. 219-236.

Davidson E.A., Firestone M.K. (1988) Measurement of nitrous oxide dissolved in soil solution. Soil Sci. Soc. Am. J. 52:1201-1203.

Dobbie K.E., Smith K.A. (2001) The effects of temperature, water-filled pore space and land use on N_2O emissions from an imperfectly drained gleysol. Eur. J. Soil Sci. 52:667-673.

Dobbie K.E., Smith K.A. (2006) The effect of water table depth on emissions of N2O from a grassland soil. Soil Use & Mgt. 22:22-28.

Dobbie K.E., McTaggart I.P., Smith K.A. (1999) Nitrous oxide emissions from intensive agricultural systems: Variations between crops and seasons, key driving variables, and mean emission factors. J. Geophys. Res. 104:26891-26899.

Farquharson R., Baldock J. (2008) Concepts in modelling N_2O emissions from land use. Plant and Soil 309:147-167.

Firestone M.K., Davidson E.A. (1989) Microbiological basis of NO and N_2O production and consumption in soil, in: M. O. Andreae and D. S. Schimel (Eds.), Exchange of Trace gases between terrestrial Ecosystems and the Atmosphere, John Wiley & Sons, Chichester. pp. 7-21.

Fujikawa T., Miyazaki T. (2005) Effects of bulk density and soil type on the gas diffusion coefficient in repacked and undisturbed soils. Soil Sci. 170:892-901

Ghani A., Dexter M., Perrott K.W. (2003) Hot-water extractable carbon in soils: a sensitive measurement for determining impacts of fertilisation, grazing and cultivation. Soil Biol. & Biochem. 35:1231-1243.

Glinski J., Stahr K., Stepniewska Z., Brzezinska M. (1992) Changes of redox and pH conditions in a flooded soil amended with glucose and nitrate under laboratory conditions. Z. Pflanzenernähr. Bodenkd. 155:13-17.

Hamamoto S., Moldrup P., Kawamoto K., Wickramarachchi P., Nagamori M., Komatsu T. (2011) Extreme compaction effects on gas transport parameters and estimated climate gas exchange for a landfill final cover soil. J. Geotech. Geoenviron. Eng. 137:653-662.

Hewitt A.E. (1998) New Zealand Soil Classification. Landcare Research Science Series No.1. 2nd ed. Manaaki Whenua Press, Lincoln, NZ.

Hillel D. (1998) Environmental Soil Physics Academic Press, San Diego, CA.

Hutchinson G.L., Mosier A.R. (1981) Improved soil cover method for field measurement of nitrous oxide fluxes. Soil Sci. Soc. Am. J. 45:311-316.

Jambert C., Delmas R., Serça D., Thouron L., Labroue L., Delprat L. (1997) N_2O and CH_4 emissions from fertilized agricultural soils in southwest France. Nutri. Cycl. Agroecosyst. 48:105-114.

Letey J., Jury W.A., Hadas A., Valoras N. (1980) Gas diffusion as a factor in laboratory incubation studies on denitrification. J. Environ. Qual. 9:223-227.

McTaggart I.P., Akiyama H., Tsuruta H., Ball B.C. (2002) Influence of soil physical properties, fertiliser type and moisture tension on N_2O and NO emissions from nearly saturated Japanese upland soils. Nutri. Cycl. Agroecosyst. 63:207-217.

Minitab. (2010) Minitab 16, Minitab, State college, PA.

Moldrup P., Olesen T., Gamst J., Schjønning P., Yamaguchi T., Rolston D.E. (2000) Predicting the gas diffusion coefficient in repacked soil water-induced linear reduction model. Soil Sci. Soc. Am. J. 64:1588-1594.

Mosier A.R., Mack L. (1980) Gas chromatographic system for precise, rapid analysis of nitrous oxide. Soil Sci. Soc. Am. J. 44:1121-1123.

Pilot L.U.C., Patrick W.H.J. (1972) Nitrate reduction in soils: effect of soil moisture tension. Soil Sci. 114:312-316.

Rafique R., Hennessy D., Kiely G. (2011) Nitrous oxide emission from grazed grassland under different management systems. Ecosystems 14:563-582.

Ravishankara A.R., Daniel J.S., Portmann R.W. (2009) Nitrous Oxide (N_2O): The dominant ozone-depleting substance emitted in the 21st century. Science 326:123-125.

Rolston D.E., Moldrup P. (2002) Gas diffusivity, in: G. C. Topp and J. H. Dane (Eds.), Methods of Soil Analysis, Part 4, Physical methods., Soil Science Society of America, Madison, WI. pp. 1113-1139.

Romano N., Hopmans J.W., Dane G.H. (2002) Water retention and storage, in: G. C. Topp and G. H. Dane (Eds.), Methods of Soil Analysis, Part 4, Physical methods, Soil Science Society of America, Madison, WI. pp. 692-698.

Ryden J.C. (1983) Denitrification loss from a grassland soil in the field receiving different rates of nitrogen as ammonium nitrate. J. Soil Sci. 34:355-365.

Schjønning P., Thomsen I.K., Moldrup P., Christensen B.T. (2003) Linking Soil Microbial Activity to Water- and Air-Phase Contents and Diffusivities. Soil Sci. Soc. Am. J. 67:156-165.

Sitaula B.K., Hansen S., Sitaula J.I.B., Bakken L.R. (2000) Effects of soil compaction on N_2O emission in agricultural soil. Chemosphere - Global Change Sci. 2:367-371.

Smith K.A., Thomson P.E., Clayton H., McTaggart I.P., Conen F. (1998) Effects of temperature, water content and nitrogen fertilisation on emissions of nitrous oxide by soils. Atmos. Environ. 32:3301-3309.

Stepniewski W. (1981) Oxygen diffusion and the strength as related to soil compaction. II Oxygen diffusion coefficient. Polish J. Soil Sci. 14:3-13.

van der Weerden T.J., Kelliher F.M., de Klein C.A.M. (2012) Influence of pore size distribution and soil water content on nitrous oxide emissions. Soil Res. 50:125-135.

Veldkamp E., Keller M., Nuñez M. (1998) Effects of pasture management on N_2O and NO emissions from soils in the humid tropics of Costa Rica. Global Biogeochem. Cycles 12:71-79.

Vilain G., Garnier J., Tallec G., Cellier P. (2010) Effect of slope position and land use on nitrous oxide (N_2O) emissions (Seine Basin, France). Agric. For. Meteorol. 150:1192-1202.

Weier K.L., Doran J.W., Power J.F., Walters D.T. (1993) Denitrification and the dinitrogen/nitrous oxide ratio as affected by soil water, available carbon, and nitrate. Soil Sci. Soc. Am. J. 57:66-72.

Wrage N., Velthof G.L., van Beusichem M.L., Oenema O. (2001) Role of nitrifier denitrification in the production of nitrous oxide. Soil Biol. & Biochem. 33:1723-1732.

Xu X., Nieber J.L., Gupta S.C. (1992) Compaction effect on the gas diffusion coefficient in soils. Soil Sci. Soc. Am. J. 56:1743-1750.

In Situ Measurement of Ammonia Content in Soil Headspace Using Mid-Infrared Photoacoustic Spectroscopy

Du Changwen*, Wang Jiao, Zhou Zijun, Shen Yazhen, Zhou Jianmin

The State Key Laboratory of Soil and Sustainable Agriculture, Institute of Soil Science, Chinese Academy of Sciences, Nanjing 210008, China
* Corresponding author: E-mail: chwdu@issas.ac.cn

Abstract

Ammonia (NH_3) volatilization is one of important pathway of nitrogen loss in alkaline soil, and the NH_3 content in soil headspace is directly linked with NH_3 volatilization. NH_3 was characterized by mid-infrared photoacoustic spectroscopy, two typical absorption bands around 2560-2660 cm^{-1} and 950-1200 cm^{-1} were observed, and both bands could be used for the prediction of NH_3 content in soil headspace. An alkaline soil from north of China was involved in soil incubation, pot and field experiments under different fertilization treatments, and NH_3 contents in soil headspace were determined in each experiment. In the soil incubation experiment the NH_3 emission was trigged by the N input, and it reached the highest content in the second day, then it took another 8 days to decrease to the level as control without N input; the NH_3 content in soil headspace in conventional urea treatment significantly increased comparing with coated urea treatment, especially in the first 4 days after N input. The NH_3 content in soil headspace in pot experiment showed the similar dynamics as that in incubation experiment; however, the NH_3 content in soil headspace in field experiment demonstrated significantly different emission pattern comparing with incubation and pot experiments, there were a 4 days' delay for NH_3 emission. Therefore, the NH_3 emission in incubation and pot experiments could not be directly used to model the real NH_3 emission in the field, and light irrigation in the second week after fertilization and involvement of controlled release coated urea could significantly decrease N loss from the perspective of NH_3 volatilization.

Abbreviations: FTIR-PAS, Fourier transform mid-infrared photoacoustic spectroscopy; N, nitrogen; NH_3, ammonia; PCA, principal component analysis; PCR, principal component regression; PCA1, the first principal component.

Introduction

A large number of studies on nitrogen (N) use efficiency have been conducting due to its important economic and environmental effects (Luis et al., 2005; Delin et al., 2008; Shi et al., 2012). N loss mainly resulted from leaching, running off and N-contained gases emission, and among N-contained gases ammonia (NH_3) volatilization is associated with a number of environmentally detrimental effects, including eutrophication of aquatic ecosystems, soil acidification problems, loss of biodiversity, formation of fine particulates (with associated human health risks) and secondary emissions of nitrous oxide from NH_3 deposition which contribute to global warming (Krupa, 2003; Erisman et al., 2007; Salazar, et al., 2012).

NH_3 volatilization after fertilizer application is an important pathway of nitrogen (N) movement from the soil, resulting in large losses of soil N (Harrison and Webb, 2001; Pacholski et al., 2008). The volatilized NH_3 represents a significant fraction of current emission inventories and is typically considered the second most important source of NH_3 in many countries. Anderson et al. (2003) reported that, in developed countries, 10-20% of the emissions may originate from applied fertilizer. In developing countries, NH_3 volatilization from nitrogen fertilizer ranges from 10% to 50% (Streets et al., 2003; Zhang et al., 2011). Ammonia emission contributed to the nitrogen loss, especially in paddy soil and alkaline soil (Salazar, et al., 2012), thus monitoring ammonia emission will enhance the understanding of the emission process, which will be useful for the improvement of nitrogen use efficiency (Kentaro et al., 2008; Luc et al., 2010; Singh et al., 2012 Cao et al., 2013).

The ammonia emission from soil was usually determined using chemical methods including a closed chamber to contain soil and fertilizer with an acid trap to capture volatilized NH_3 (Fenn and Kissel, 1973; Hargrove and Kissel, 1979; Cole et al., 2005; Ndegwa et al., 2009), then colorimetric or titration followed to determine the concentration of NH_3 in solution. However, the samples collection and pretreatment are relatively complicated, cost and time-consuming, and also, the results may deviate from the real one due to the influences of the sample collection and pretreatment styles (Helga et al., 2008). On the other hands, micrometeorological methods and wind-tunnel methods employed in field experiments were disadvantaged by the changeful climatic factors (Fox et al., 1996; Van et al., 1996; Loubet et al., 1999). For this reason, new techniques and methods for more efficient monitoring of ammonia are essential. The

determination of volatile organic compounds in near-surface soils (soil headspace) and vegetation is the foundation for a more efficient sampling strategy to improve understanding of environmental problems (Jorge et al., 2004; Serrano and Gallego, 2006; Minna, 2007), which provided option to characterize soil NH_3 volatilization. Since the gas exchange between soil and the space close to its surface, namely soil headspace, was directly linked with soil with minimum environmental effects at a time (Alvarado et al., 2004; Serrano and Gallego, 2006; Minna, 2007), and the NH_3 content in the headspace could be used to characterize NH_3 volatilization (Sims et al., 1991); then the point is how to determine the NH_3 content in the gas samples from soil headspace without pretreatment. Fortunately, the emergency of Fourier transfer photoacoustic spectroscopy (FTIR-PAS) combining the advanced detector of cantilevel-type microphone significantly improved the determination limit of gas (Kauppinen et al., 2004), and provides an alternative technique for gas measurements owing to high selectivity and sensitivity, real time and rapidity (Schilt et al., 2004; Besson et al., 2006; Iqbal et al., 2013; Du and Zhou, 2009)

In this study the technique of NH_3 determination using FTIR-PAS was firstly established, and was involved in the direct determination of NH_3 in the soil headspace gas samples collected from incubation, pot and field experiments, so that to better understand the NH_3 volatilization under different N fertilization treatments, which will benefit better management of N use efficiency.

Materials and Methods

Soils

The soil used in this research was Fluvo-aquic soil collected from surface layer (0-15 cm) in Fengqiu Ecological Experimental Station in Henan province, locating in north China. The basic agro-chemistry properties are demonstrated in Table 1. All the soils were air-dried, ground to pass through a 2 mm sieve for use in incubation and pot experiments.

Collecting of Gas Samples from Soil Headspace

Soil headspace is defined as the surface space of soil, i. e. the space about 1-2 cm height above solid soil surface (Fig. 1). Plastic syringe with the volume of 100 mL was used to slowly and carefully pump the gas samples from the soil headspace into 100 mL

PVDF gas sampling bag (Dalian Haide Inc., China), and the gas samples were immediately transferred to laboratory for analysis.

FTIR-PAS Spectra Recording of Gas Samples

Photoacoustic spectra were recorded for all standard NH_3 gas samples (Sigma, USA) and gas samples collected from soil headspace using a Fourier transform infrared spectroscopy (Nicolet 6700, USA) equipped with a photoacoustic gas accessory (PA101, Gasera, Finland). The scans were conducted for the standard NH_3 samples in the mid-infrared wavenumber range of 500-4000 cm^{-1} with a resolution of 4 cm^{-1}; the mirror velocities of 0.32 cm s^{-1}; The pure N gas (99.99%) was used to collect the responding reference spectrum for spectra-intensity normalization. 32 successive scans were recorded, and the average for each sample was used.

Spectral Data Processing

The obtained leaf spectra were pre-processed with a smoothing filter (first-order Savitzky-Golay filter with a 25-point window) (23) and standardized using the software Matlab 7.8 (MathWorks inc. MA, USA). The spectrum of NH_3 was characterized and the typical absorption band was selected for calibration and prediction using principal component analysis (PCA). Then the established model was used to predict the NH_3 content in soil headspace from incubation experiment, pot experiment and field experiment.

Soil Incubation Experiment

One kilogram of sieved soil were placed in 2000 mL lidless plastic jar, three treatments were set: CK (without N input), conventional urea treatment, coated urea treatment (20% conventional urea was replaced by coated urea), three replicates. The N application rate was 0.2 g N kg^{-1}, and the fertilizers were mixed with soils. Yizheng Waterborne Chemical Company made the coated urea. The N content was 42.7%, with a release time of 40 d in water at 25℃. The soils were wetted to 60% field capacity, then the jars were placed in 25℃ incubator, and the gas samples in soil headspace were collected at 3 o'clock in the afternoon every day for the determination of NH_3.

Pot Experiments

Pot experiment was conducted in a greenhouse with winter wheat (Xinong 979). 6 kg of air-dried soil was added to a pot (diameter, 18.5 cm; height, 23.5 cm). There were

three treatments: Ck (without N input), conventional urea treatment, coated urea treatment (20% conventional urea was replaced by coated urea), three replicates. The N, P (P_2O_5) and K (K_2O) application rates all were 0.2 g N kg^{-1}, and the fertilizers were mixed with upper one-third soil; P and K were incorporated in the form of superphosphate and K_2SO_4. The pot soils were wetted to 60% field capacity, and winter wheat was sowed in the pot. Gas samples in soil headspace were collected at 3 o'clock in the afternoon every day for the determination of NH_3.

Field Experiments

Field experiment was conducted Fengqiu ecological experimental station in Henan province, China. There were three treatments: Ck (without N input), conventional urea treatment, coated urea treatment (20% conventional urea was replaced by coated urea), 2 Hm^2 for each treatment. The N, P (P_2O_5) and K (K_2O) application rates were 225, 75, 75 kg hm^{-2}, respectively. P and K were incorporated in the form of superphosphate and K_2SO_4, the fertilizers were banding applied, and winter wheat (Xinong 979) was sowed, followed a conventional irrigation. Gas samples in soil headspace after irrigation were collected at 3 o'clock in the afternoon every day for the determination of NH_3.

Results and Discussion

Characterization and NH_3 Using FTIR-PAS

Figure 2 shows the FTIR-PAS spectra of standard ammonia with different content in the specific wavenumber region of 500-4000 cm^{-1}. There were mainly three absorption bands around 2560-2660 cm^{-1}, 1880-2180 cm^{-1} and 950-1200 cm^{-1}. The bands around 2560-2660 cm^{-1}, and 950-1200 cm^{-1} resulted from N-H vibration of NH_3 (Kyle and Et-touhamiEs-sebbar, 2013), and the absorption band around 2560-2660 cm^{-1} was due to CO_2 absorption from the air; though this band was strong there were little interferences on the other two absorption bands. The bands around 2560-2660 cm^{-1} was relatively higher and narrower, while the bands around 950-1200 cm^{-1} was relatively lower and broader. These two bands were visually observed to be linearly related with NH_3 concentration.

PCA was used to reduce dimensions of absorption bands. The explained variances of first principal components score (PCA1) from bands of 2560-2660 cm^{-1} and 950-1200 cm^{-1} were 99.66% and 99.75%, respectively; thereof the absorption bands could be perfectly presented by the PCA1, then principal components regressions were

conducted (Fig. 3). Both regression coefficients were more than 0.99, which showed the NH_3 content was perfectly related with PCA1. Since the bands around 2560-2660 cm^{-1} was higher and narrower it would be more sensitive to NH3, which was more suitable for low NH_3 content determination. Worthwhile, the band around 950-1200 cm^{-1} was more suitable for high NH_3 content determination. The NH_3 content in soil headspace is usually more than 30 mg L^{-1}, thus the band around 950-1200 cm^{-1} was involved in the determination of NH_3 content in soil headspace from different treatments and experiments.

NH_3 Release from Incubated Soil

Figure 4 shows the NH_3 content in soil headspace in the incubation experiment. The NH_3 content kept in a stable content around 50 mg L^{-1} in CK treatment, but the NH_3 content remarkably increased as around 300 mg L^{-1} in one day after fertilization in conventional urea treatment, reached highest content around 360 mg L^{-1} in two day, and the NH_3 content was decreased to that in CK treatment after 5 d. For the coated urea treatment, the dynamics of NH_3 content in soil headspace was similar as that of conventional urea treatment, but the absolute contents were significantly lower in first 5 d; the initial content in one day was around 80 mg L^{-1}, and the highest content in the second day was around 160 mg L^{-1}.

The NH_3 content in soil headspace was mainly influenced by the soil properties, such as soil texture, soil microbes, N status, etc. (Sims et al., 1991), and it could be consumed that the NH_3 volatilization was decided by both the soil properties and environmental factors, such as convection, therefore:

$$F_{NH_3} = f(S, E) \quad (1)$$

Where, F_{NH_3} represents NH_3 volatilization, S denotes soil properties and E denotes environmental factors.

Since NH_3 content in soil headspace was closely linked with soil properties, thus the F_{NH_3} could be alternatively expressed as:

$$F_{NH_3} = f(C_{headspace}, E) \quad (2)$$

Where, $C_{headspace}$ represents NH_3 content in soil headspace.

The environmental conditions would be approximately the same in a specific location, then:

$$F_{NH_3} = f(C_{headspace}) \quad (3)$$

From the equation, the NH_3 volatilization was positively related with NH_3 content in soil headspace in a specific location. For the soil incubation experiment, the ammonia volatilization occurred in less than one day after nitrogen input, and decreased to a stable level after the fifth days. N loss from NH_3 volatilization could be significantly decreased by coated urea. Therefore, for the alkaline soil the NH_3 volatilization occurred in the first 5 days after N input, and measures that effectively decrease ammonia volatilization should be strongly considered during this stage, such as spraying water in the second day after N application.

NH_3 Release from Pot Experiment

Figure 5 demonstrates the NH_3 content in soil headspace from pot experiment with winter wheat. The NH_3 content was slightly decreased to stable level (around 20-30 mg L^{-1}) from the first day to 15th day in CK treatment, but the NH_3 content significantly increased as around 60 mg L^{-1} in the first day after fertilization in conventional urea treatment, and in the third day the highest content around 75 mg L^{-1} was observed. The similar tendency of NH_3 dynamic was observed in coated urea treatment, and the absolute contents were lower comparing with that in conventional urea treatment.

The NH_3 content in soil headspace was significantly lower than that in soil incubation experiment, which resulted from the soil temperature (Zhen et al., 2003). In the soil incubation experiment the temperature kept at 25℃, and the balanced NH_3 content in soil headspace was around 50 mg L^{-1}. For the pot experiment the soil temperature showed a tendency to decrease (Fig. 6a), and the NH_3 content in headspace was positively related with temperature (Fig. 6b). The balanced NH_3 content in soil headspace was around 20-30 mg L^{-1}, which implied that the balanced NH_3 content in soil headspace was mainly influenced by soil temperature for a specific soil. Soil temperature is closely related with the activity of soil microbes, and soil microbes play a key role in N mineralization and urea hydrolysis, which is directly linked with NH_3 emission.

The increase of NH_3 volatilization after N input mainly occurred in first six days, which was almost the same as that in soil incubation experiment. Therefore, after N input both urea hydrolysis and soil N mineralization contributed to NH_3 emission, in the first six day the urea hydrolysis was the main factor, and thereafter the mineralization was the main factor (Schlesinger and Peterjohn, 1991). For the coated urea treatment the NH_3 emission was significantly lower in the first six days after N input, and the average

content of NH_3 content in soil headspace was 39.7 mg L^{-1} versus 52.4 mg L^{-1} in urea treatment; NH_3 emission decreased 24.3% which was because of 20% replacement with coated urea. However, the NH_3 emission in following days was similar as CK, which implied the controlled release of urea could significantly retard the NH_3 emission though decreasing the substrate dosage.

NH_3 Release from Field Experiment

Figure 7 shows the he NH_3 content in soil headspace from field experiment with winter wheat. In the first four days the NH_3 content in soil headspace was almost zero, and then kept increasing for all three treatments. The NH_3 content in soil headspace in CK treatment was significantly lower than that in urea and coated urea treatments from the sixth day, and the NH_3 content in soil headspace in coated urea treatment was significantly lower than that in conventional urea treatments. The average content of NH_3 content in soil headspace was 92.5 mg L^{-1} in coated urea treatment versus 120.6 mg L^{-1} in urea treatment, which implied 20% replacement of conventional urea with coated urea decreased NH_3 emission with 23.3%.

The dynamics of NH_3 content in this soil headspace was completely different from that in incubation experiment and pot experiment. In soil incubation experiment and pot experiment the NH_3 content started with a high value, and then decreased to a balanced level, which agreed with previous study (Martines et al., 2010). However, in the field experiment the NH_3 content started with a very low value, and then decreased to a high level. This difference in emission pattern might result from soil particle size and fertilizer input technique (Huijsmans et al., 2001). In the field experiment the soil particle was much larger, and fertilizer was band applied. In the incubation and pot experiments the soil was wetted and fertilizer was applied with good mixing thus accelerating nutrient diffusion and delivery to micro-sites, thus promoting urea hydrolysis and accordingly the NH_3 emission occurred in a relatively short time in the incubation and pot experiments, while it was delayed in the field experiment.

The NH_3 content in soil head space in the field experiment was relatively higher than that of the pot experiment, which mainly resulted from higher soil temperature (26 to 32 ℃ in field experiment versus 7 to 21℃) (Figure 6a, 8a) (Zhen et al., 2003; Huijsmans et al., 2003). The NH_3 content in soil headspace in the field experiment was also positively related with temperature (Figure 8b). However, the NH_3 content in soil headspace of field experiment was relatively lower than from the incubation experiment

with the soil temperature of 25℃, which resulted from significantly higher N application rate in the incubation experiment.

Conclusions

The FTIR-PAS spectra of NH_3 showed two typical absorption bands (2560-2660 cm^{-1} and 950-1200 cm^{-1}) without interferences, and these two bands could be applied for the prediction of NH_3 content. By applying this method, NH_3 in soil headspace could be rapidly determined. NH_3 in soil headspace was directly linked with NH_3 volatilization in the same location. The NH_3 emission from incubation experiment and pot experiment was similar, high emission of NH_3 occurred in a short time after N input, but it was significantly delayed in field experiment because of differences in soil particle size, soil temperature and fertilizer application mode. Replacement of conventional urea with coated urea could significantly decrease NH_3 emission because of lower available urea content and almost no emission was observed during the controlled release of coated urea. NH_3 emission in the incubation and pot experiments varied from that in field experiment, and could not be directly used in the modeling of NH_3 emission in field. A light irrigation in the second week after fertilization appears effective for increasing N use efficiency. Replacement of soluble urea with controlled release coated urea was another effective option to decrease NH_3 volatilization.

Acknowledgements

The National Natural Science Foundation of China (41130749) funded this research.

Table 1. Basic chemical properties of soil used in the experiments

Organic matter ($g\ kg^{-1}$)	pH	Available N ($mg\ kg^{-1}$)	Available P ($mg\ kg^{-1}$)	Available K ($mg\ kg^{-1}$)
5.83	8.65	9.51	1.93	78.8

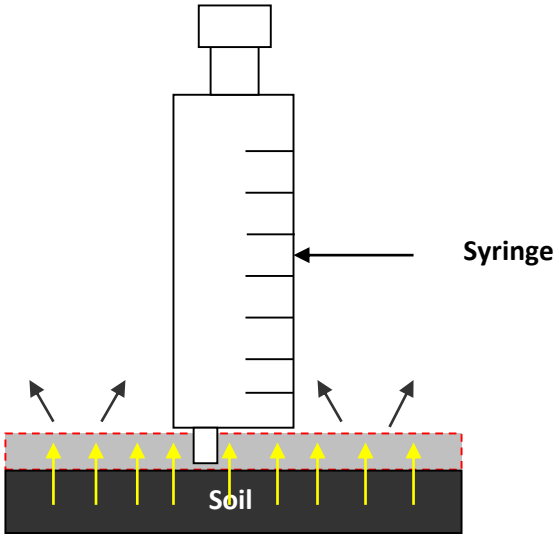

Fig. 1. Gas sample collection from headspace of soil

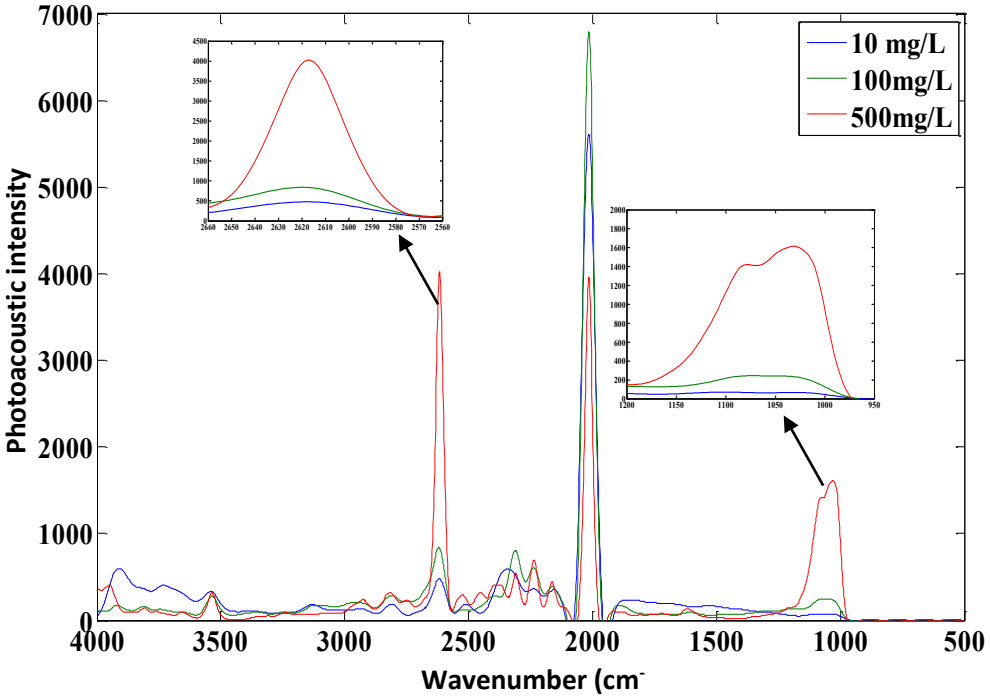

Fig. 2. FTIR-PAS spectra of standard ammonia with different concentrations in the wavenumber region of 500-4000 cm^{-1}. Two typical absorption bands (950-1200 cm^{-1} and 2560-2660 cm^{-1}) of NH_3 are demonstrated in the small subfigures.

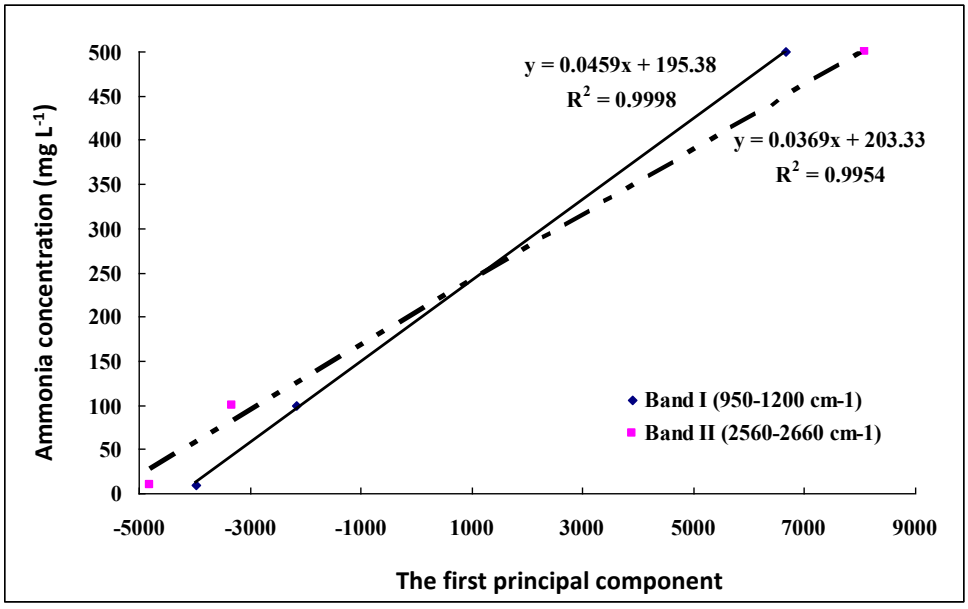

Fig. 3: Calibration of NH_3 using FTIR-PAS spectra based on principal components regressions.

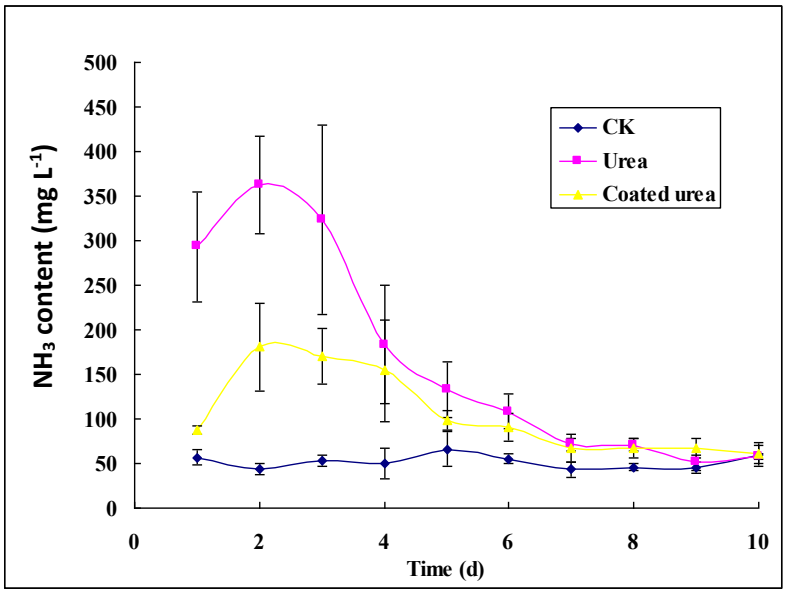

Fig. 4. NH_3 content in soil headspace in a incubation experiment (soil, alkaline Fluvo-aquic soil; temperature, 25℃; CK, no nitrogen input; urea, 0.2 g N (conventional urea) input per kilogram soil; coated urea, 0.2 g N input per kilogram soil in which 20% conventional urea was replaced by coated urea)

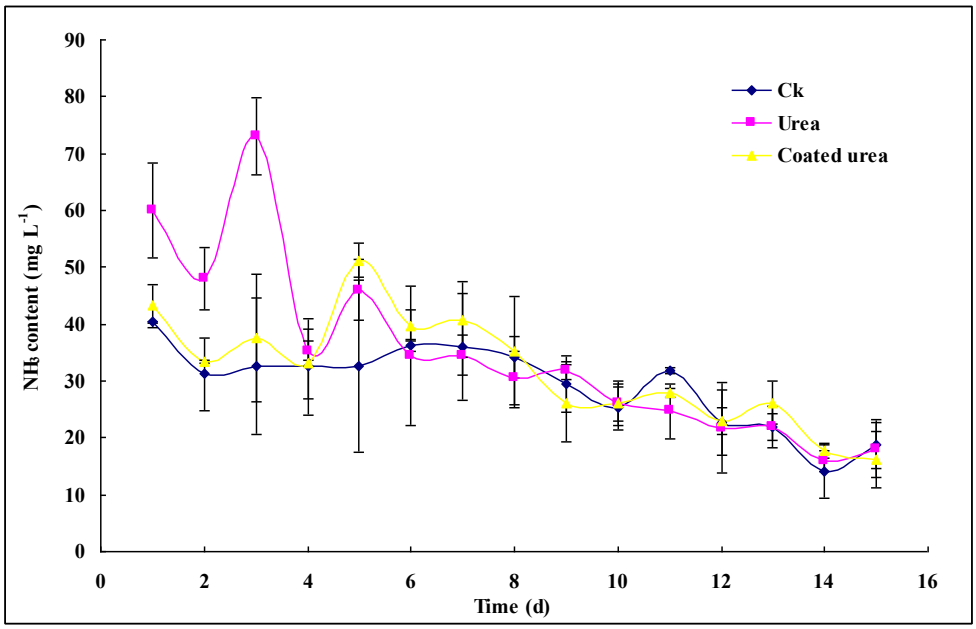

Fig. 5. NH_3 content in soil headspace from pot experiment with winter wheat. Soil, alkaline Fluvo-aquic soil; temperature, 25℃; CK, no nitrogen input; urea, 0.2 g N (conventional urea) input per kilogram soil; coated urea, 0.2 g N input per kilogram soil in which 20% conventional urea was replaced by coated urea.

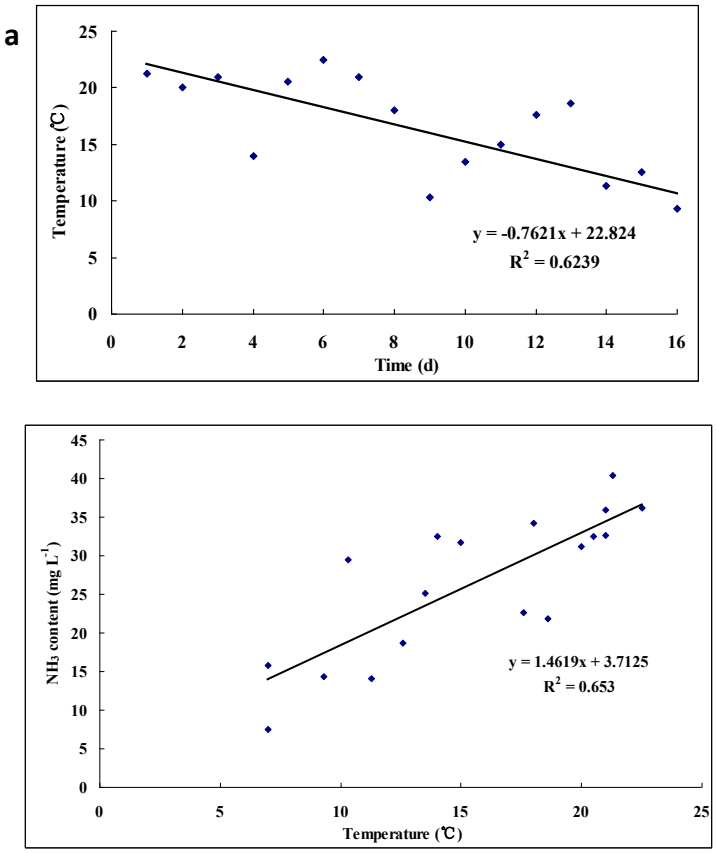

Fig. 6. Changes of temperature during the experiment (a) and the relationship between NH_3 content in soil headspace and temperature (b)

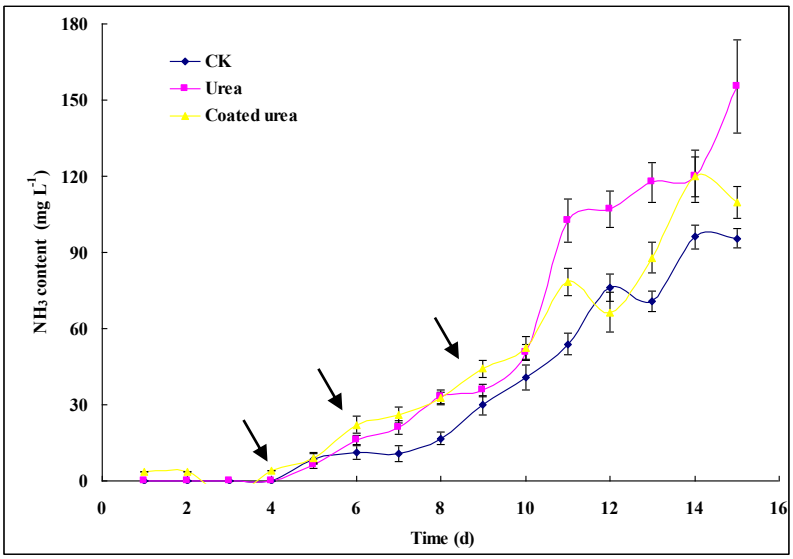

Fig. 7. NH_3 content in soil headspace in the field experiment under different fertilization treatments. Soil, alkaline Fluvo-aquic soil; temperature, 25℃; CK, no nitrogen input; urea, 0.2 g N (conventional urea) input per kilogram soil; coated urea, 0.2 g N input per kilogram soil in which 20% conventional urea was replaced by coated urea.

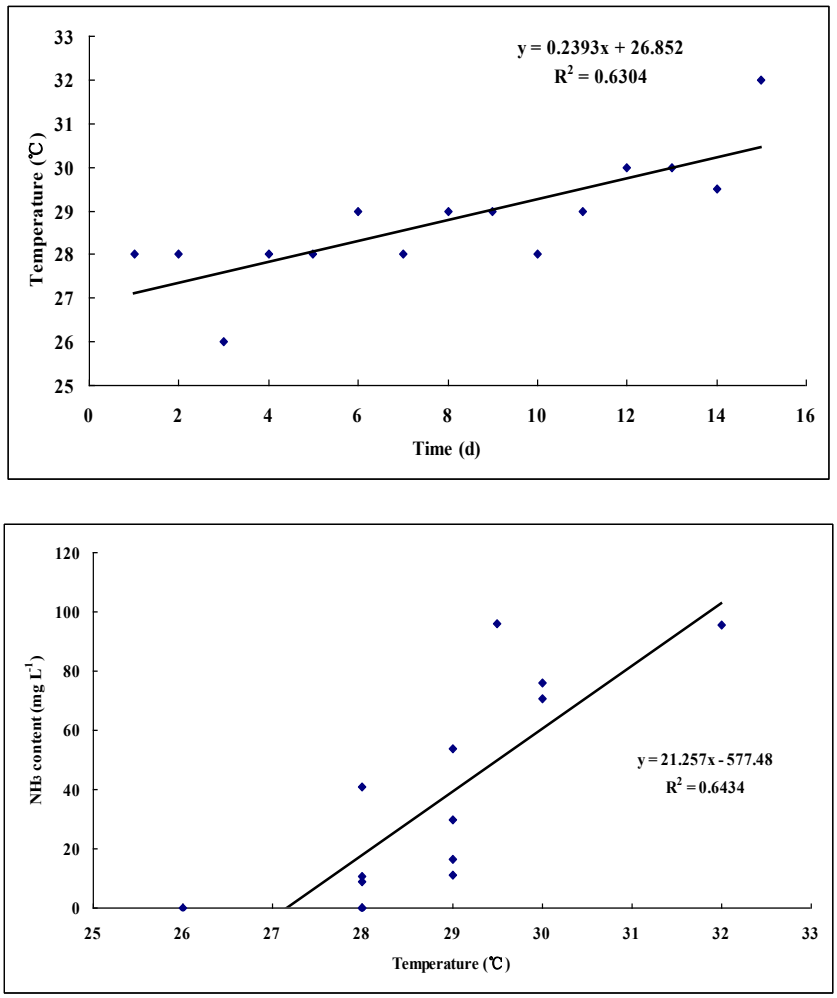

Fig. 8. Changes of temperature during the experiment (a) and the relationship between NH_3 content and temperature (b)

References

Alvarado, J.S., and C. Rose. 2004. Static headspace analysis of volatile organic compounds in soil and vegetation samples for site characterization. Talanta 62: 17-23.

Anderson, N., R. Strader, and C. Davidson. 2003. Airborne reduced nitrogen: ammonia emissions from agriculture and other sources. Environmental International 29: 277-286.

Besson, J.P., S. Schilt, E. Rochat, and L. Thevenaz. 2006. Ammonia trace measurements at ppb level based on near-IR photoacoustic spectroscopy. Appl. Phys. B: Lasers Opt 85: 323-328.

Cao, Y., Y. Tian, B. Yin, and Z. Zhu. 2013. Assessment of ammonia volatilization from paddy fields under crop management practices aimed to increase grain yield and N efficiency. Field Crops Research 147: 23-31.

Cole, N.A., R.N. Clark, R.W. Todd, C.R. Richardson, A. Gueye, L.W. Greene, and K. McBride. 2005. Influence of dietary crude protein concentration and source on potential ammonia emission from beef cattle manure. J. Anim. Sci. 83: 722-731.

Delin, S., A. Nyberg, B. Linden, M. Ferm, G. Torstensson, C. Lerenius, and I. Gruvaeus. 2008. Impact of crop protection on nitrogen utilisation and losses in winter wheat production. Eur. J. Agron. 28: 361-370.

Du, C., and J. Zhou. 2009. Evaluation of soil fertility using infrared spectroscopy: a review. Environ. Chem. Lett. 7: 97-113.

Erisman, J., A. Bleeker, J. Galloway, and M. Sutton. 2007. Reduced nitrogen in ecology and the environment. Environmental Pollution 150: 140-149.

Fenn, L.B., and D.E. Kissel. 1973. Ammonia volatilization from surface applications of ammonium compounds on calcareous soils: Ⅰ. General Theory. Soil Sci. Soc. Am. J. 37: 855-859.

Fox, R.H., W.P. Piekielek, and K.E. Macneal. 1996. Estimating ammonia volatilization losses from urea fertilizers using a simplified micrometeorological sampler. Soil Sci. Soc. Am. J. 60: 596-601.

Hargrove, W.L., and D.E. Kissel. 1979. Ammonia volatilization from surface application of urea in the field and laboratory. Soil Sci. Soc. Am. J. 43: 359-363.

Harrison, R., and J. Webb. 2001. A review of the effect on N fertilizer type on gaseous emissions. Advances in Agronomy 73: 65-108.

Hayashi, K., S. Nishimura, and K. Yagi. 2008. Ammonia volatilization from a paddy field following applications of urea: Rice plants are both an absorber and an emitter for atmospheric ammonia. Science of the Total Environment 390: 485-494.

Helga., A. Pogany, Z. Bozoki, A. Mohacsi, L. Horvath, and G. Azabo. 2008. Ammonia monitoring at ppb level using photoacoustic spectroscopy for environmental application". Sens. Actuators, B 134: 1027-1033.

Huijsmans, J.F.M., J.M.G. Holi, and G.D. Vermeulen. 2003. Effect of application method, manure characteristics, weather and field conditions on ammonia volatilization from manure applied to arable land. Atmospheric Environment 37: 3669-3680.

Huijsmans, IF.M., J.M.G. Holi, and M.M.W.B. Hendriks. 2001. Effect of application technique, manure characteristics, weather and field conditions on ammonia volatilization from manure applied to grassland. Netherlands Journal of Agricultural Science 49: 323-342.

Iqbal, J., M.J. Castellano, and T.B. Parkin. 2013. Evaluation of photoacoustic infrared spectroscopy for simultaneous measurement of N_2O and CO_2 gas concentrations and fluxes at the soil surface. GCB Bioenergy 19: 327-336.

Jorge, S. A., and Candace R. 2004. Static headspace analysis of volatile organic compounds in soil and vegetation samples for site characterization. Talanta 62: 17-23.

Kauppinen, J., K. Wilcken, I. Kauppinen, and V. Koskinen. 2004. High sensitivity in gas analysis with photoacoustic detection. Microchemical Journal 76: 151-159.

Krupa, S. 2003. Effects of atmospheric ammonia on terrestrial vegetation: a review. Environmental Pollution 124: 179-221.

Kyle, O., and A. Et-touhamiEs-sebbar. 2013. Measurements of NH3 linestrengths and collisional broadening coefficients in N2, O2, CO2, and H2O near 1103.46 cm^{-1}. Journal of Quantitative Spectroscopy & Radiative Transfer 121: 56-68.

Loubet, B., P. Cellier, D. Flura, and S. Genermont. 1999. An evaluation of the wind-tunnel technique for estimating ammonia volatilization from land: Part 1. analysis and improve of accuracy. J. Agric. Eng. Res. 72: 71-81.

Luc, D., J.A. Rocio, V. Cesar, L. Marco, F. Perez-Guevara, and M. Rodolfo. 2010. Dynamics of carbon and nitrogen in an extreme alkaline saline soil: A review. Soil Biology & Biochemistry 42: 865-877.

Luis, L., J.L. Rafael, and R. Ramon. 2005. Nitrogen efficiency in wheat under rainfed Mediterranean conditions as affected by split nitrogen application. Field Crops Research 941: 86-97.

Martines, A.M., M.A. Nogueira, C.A. Santos, A.S. Nakatani, C.A. Andrade, A.R. Coscione, H. Cantarella, J.P. Sousa, and E.J.B.N. Cardoso. 2010. Ammonia volatilization in soil treated with tannery sludge. Bioresource Technology 101: 4690-4696.

Minna, H. 2007. Developments in multiple headspace extraction. J. Biochem. Biophys. Methods 70: 229-233.

Ndegwa, P.M., V.K. Vaddella, A.N. Hriston, and H.S. Joo. 2009. Measuring concentration of ammonia in ambient air or exhaust air stream using acid traps. J. Environ. Qual. 38: 647-653.

Pacholski, A., G.X. Cai, X.H. Fan, H. Ding, D.L. Chen, R. Nieder, and M. Roelcke. 2008. Comparison of different methods for the measurement of ammonia volatilization after urea application in Henan Province, China. Journal of Plant Nutrition and Soil Science 171: 361-369.

Salazar, F., J. Martínez-Lagos , M. Alfaro, and T. Misselbrook. 2012. Ammonia emissions from urea application to permanent pasture on a volcanic soil. Atmospheric Environment 61: 395-399.

Schilt, S., L. Thevenaz, M. Nikles, L. Emmenegger, and C. Huglin. 2004. Ammonia monitoring at trace level using photoacoustic spectroscopy in industrial and environmental applications. Spectrochim. Acta, Part A 60: 3259-3268.

Schlesinger, W. H., and W.T. Peterjohn. 1991. Processes controlling ammonia volatilization from chihuahuan desert soils. Soil Biology and Biochemistry 23: 637-642.

Serrano, A., and Gallego, M. 2006. Sorption study of 25 volatile organic compounds in several Mediterranean soils using headspace–gas chromatography–mass spectrometry. Journal of Chromatography A 1118: 261-270.

Shi, Z., D. Li, Q. Jing, J. Cai, D. Jiang, W. Cao, and T. Dai. 2012. Effects of nitrogen applications on soil nitrogen balance and nitrogen utilization of winter wheat in a rice–wheat rotation. Field Crops Research 127: 241-247.

Sims, W.R., B.B. Looney, and C.A. Eddy. 1991. Evaluation of a rapid headspace analysis method for analysis of volatile constituents in soils and sediments. Ground Water Management 5: 655-668.

Singh, U., J. Sanabria, E.R. Austin, and S. Agyin-Birikorang. 2012. Nitrogen Transformation, ammonia volatilization Loss, and Nitrate Leaching in Organically Enhanced Nitrogen Fertilizers Relative to Urea. Soil Science Society of America Journal 76: 1842-1854.

Streets, D.G., T.C. Bond, G.R. Carmichael, S.D. Fernandes, Q. Fu, D. He, Z. Klimont, S. M. Nelson, N.Y. Tsai, M.Q. Wang, J.H. Woo, and K.F. Yarber. 2003. An inventory of gaseous and primary aerosol emissions in Asia in the year 2000. Journal of Geophysical Research 108 (D21), 8809. doi:10.1029/2002JD003093.

van der Weerden, T.J., J.F. Moal, J. Martinez, B.F. Pain, and F. Guiziou. 1996. Evaluation of the wind-tunnel method for measurement of ammonia volatilization from Land. J. Agric. Eng. Res. 64: 11-13.

Zhang, Y., S. Luan, L. Chen, and M. Shao. 2011. Estimating the volatilization of ammonia from synthetic nitrogenous fertilizers used in China. Journal of Environmental Management 92: 480-493.

Zhen, Y., N. Hirosh, K. Ken-ichi, and S. Yuko. 2003. Measurement of ammonia volatilization from a field in upland Japan, spread with cattle slurry. Environmental Pollution 121: 463-467.

EVALUATING THE LINKS AMONG CARBON AND NITROGEN SATURATION: THEORIES TO ADVANCE NUTRIENT CYCLING SCIENCE

Michael Castellano[1*] and Daniel Andersen[2]

[1]Department of Agronomy, Iowa State University, 2104 Agronomy Hall, Ames, Iowa 50011 USA.

[2]Department of Agricultural and Biosystems Engineering, Iowa State University, 3165 NSRIC, Ames, IA 50011 USA.

*Corresponding author: castelmj@iastate.edu

Abstract

The carbon and nitrogen contents of soil organic matter are well correlated with strong biological links and consistent stoichiometry. Over the past 25 years, carbon and nitrogen saturation theories have independently emerged to describe the ecosystem dynamics of these materials. We briefly summarize the development of each theory and then directly address three questions: 1) What is current state of C and N saturation concepts? 2) What are the important similarities and differences among these theories? 3) How can these theories be integrated to advance soil science and our understanding of nutrient cycling? Most of the similarities and differences among these theories are related to the initial concept: N saturation was developed to predict N losses from forests whereas C saturation was developed to predict the storage potential soil C. As a result, N saturation theory has focused on the factors affecting the kinetics of N mineralization and retention while C saturation has focused on the factors limiting C storage in stable soil organic fractions. We link these processes to improve nutrient cycling science, particularly as they relate to cultivated cropping systems.

Introduction

Over the past 25 years, development of carbon and nitrogen saturation theories has provided an important framework for understanding the response of soils and ecosystems to anthropogenic influence (Agren and Bosatta, 1988; Aber et al., 1989; Hassink, 1997). Both theories have been applied to improve the management of agricultural systems, (e.g., Gulde et al., 2008; McSwiney et al., 2010). Nevertheless,

direct links among these theories remain few despite the close relationship between C and N cycling in vegetation and soils (Castellano et al., 2012).

Explicit development of N saturation theory preceded that of C saturation by approximately 10 years. The theory emanated from research that was designed to understand the impact of increasing atmospheric N deposition on relatively unmanaged northeastern US and western European forest ecosystems. Environmental concerns included the potential for atmospheric N deposition to increase terrestrial ecosystem acidity and losses of N oxides. Ultimately, vegetation mortality was predicted (Aber et al., 1989). To evaluate these predictions, experiments added large amounts of inorganic N to forest ecosystems and measured the responses of vegetation, N dynamics, and downstream water quality (Wright and Breemen, 1995; Fenn et al., 1998).

Similar to N saturation theory, C saturation theory was at least partly developed due to environmental concerns; but in this case the concerns regarded rising atmospheric CO_2. Historical research demonstrated substantial reductions in soil C upon cultivation of untilled soils (up to 40%; Davidson and Ackerman, 1993). As a result, agricultural management practices that increase soil C were proposed as a potential approach to offset rising atmospheric CO_2 (Lal et al., 2007). This proposition led to research that added variable amounts of C inputs to cropping systems and measured the response of soil C storage. While some studies observed a positive linear relationship between C inputs and soil C storage (Paustian et al., 1997), other studies observed no increase in soil C despite large increases in C inputs (Huggins et al., 1998). Consequently, the concept of C saturation emerged (Six et al., 2002).

The goal of this paper is to integrate recent soil C and N saturation findings in the context of nutrient retention, nutrient mineralization, and net primary productivity. Although N saturation theory has focused on unmanaged systems (reviewed by Emmett, 2007), more recently N saturation concepts have been applied to agricultural systems (McSwiney et al. 2010). We focus on linking C and N saturation theories through interactions between crop and soil dynamics in agricultural systems. Three questions are addressed: 1) What is current state of C and N saturation concepts? 2) What are the important similarities and differences among these theories? 3) How can these theories be integrated to advance soil science and our understanding of nutrient cycling?

Current N Saturation Concepts

Initial N saturation hypotheses predicted that vegetation is the dominant sink for inorganic N; as vegetation sinks reach capacity, N saturation symptoms including N_2O and NO_3 losses will increase so that N inputs equal outputs (Aber et al., 1989). However, research quickly shifted focus to N retention within the soil due to the surprising results that soil, rather than vegetation, is typically the dominant sink for inorganic N and many ecosystems have a remarkable capacity to transfer inorganic N inputs to SOM sinks (Aber et al., 1995; Gundersen et al., 1998; Nadelhoffer et al., 1999). For example, over nine years, conifer and hardwood forests in MA, USA retained ~1107/1350 kg NH_4NO_3-N ha^{-1} inputs in the soil alone.

Based on these results, subsequent research investigated biotic and abiotic mechanisms of inorganic N retention in soil, with a particular focus on organic horizons (Currie, 1999). Biotic processes identified include competition between plants and microbes for mineral N, resulting in tight cycling with little mineral N loss (Kaye and Hart, 1997), especially when plant litter and soils have wide C/N ratios (Emmett et al., 1998; Lovett et al., 2002). Abiotic processes identified include the reaction of nitrite, ammonium and labile proteins with aromatic ring structures of SOM, resulting in the formation of potentially decomposition-resistant C-N compounds (Hättenschwiler and Vitousek, 2000; Davidson et al., 2003; Olk et al., 2009).

Both biotic and abiotic processes are dependent upon the quality of organic matter inputs (i.e., vegetation residues). The capacity of biotic mechanisms to immobilize inorganic N depends on a surplus of microbe-available C and a deficit of microbe-available N. As a result, low quality, high C/N ratio litters promote net N immobilization whereas high quality, low C/N ratio litters promote net nitrification (Emmett et al. 1998, Palm et al. 2001). The capacity of abiotic mechanisms to immobilize N depends on the availability of phenolic C substrates and nitrite (Fitzhugh et al., 2001; Davidson et al., 2003). Together, these results have directed research towards exploration of vegetation effects on N retention and mineralization (Lovett et al., 2004; Gundersen et al., 2009; Lewis and Kaye, 2011; Mueller et al., 2012; Gurmesa et al., 2013). However, no clear relationship between vegetation species or litter chemistry and N dynamics has emerged (Lovett et al. 2004; Mueller et al. 2012).

While the understanding of inorganic N sink identity has shifted from vegetation to soil, the understanding of soil N retention dynamics has recently shifted from a temporal, symptom-based process (Aber et al., 1998) to a mass balance process that includes capacity (i.e., thermodynamic) and kinetic saturation of N sinks (Lovett and Goodale, 2011). Capacity saturation occurs when N has accumulated in the vegetation and soils to the point that further net nitrogen retention in these sinks does not occur, while kinetic saturation occurs when the rate of N input exceeds the rate at which N can be retained before it is lost to the atmosphere or groundwater (i.e., sinks are still accumulating N, but not at a rate sufficient to prevent N losses from the ecosystem). Capacity saturation suggests that inputs and outputs are equal (i.e., equilibrium), while kinetic saturation suggests N losses will occur simultaneously with N retention.

From this evolution of research, three major points are particularly relevant to C saturation research: 1) Soil is typically the largest inorganic N sink 2) Most N saturation research focuses on organic soil horizons and SOM-rich surface mineral horizons 3) The explicit consideration of capacity and kinetic N saturation is a recent development.

Current C Saturation Concepts

Soil C equilibrium levels reflect the long-term balance of C inputs and losses from an ecosystem; thus current C levels are a function of both current and past environmental conditions and do not necessarily reflect an upper limit to the amount of C the soil could stabilize (i.e., a saturation limit; Six et al., 2002). Nevertheless, a growing body of evidence suggests soils have a finite capacity to store C (Hassink, 1997; Huggins et al., 1998; Six et al., 2002; Kong et al., 2005; Stewart et al., 2007, 2009; Chung et al., 2008; Gärdenäs et al., 2011; Heitkamp et al., 2012; Dungait et al., 2012). These experiments added different amounts of C to identically managed systems but did not observe differences in C storage among the different C input amounts. This pattern suggests C storage capacity is filled; soils have reached ‘C saturation’ (Six et al. 2002). At this point, C inputs and C mineralization are in equilibrium.

In contrast, to C-saturated soils, soils that are actively accumulating C in protected pools have an unsatisfied C storage potential that is referred to as the ‘saturation deficit’ (Stewart et al. 2007). For example, a soil with no SOC has a saturation deficit of 100% while a C-saturated soil has a saturation deficit of zero. Importantly, the C saturation concept is relative to management and environment: for example, a ‘C saturated’

system (i.e., no ΔSOC despite increasing C input) could experience a change in C saturation level with a change in management (e.g., tillage) or climate.

Two models have been developed to describe C saturation dynamics (Hassink and Whitmore 1997; Stewart et al. 2007; Fig 1). A one-pool whole-soil C saturation model suggests soils have a finite C storage capacity and the efficiency of C storage decreases with increasing input. Alternatively, a two-pool model suggests soils contain two distinct C pools: a stable pool that saturates and a labile pool that does not saturate. Most research with direct reference to soil C saturation has used physical fractionation of soil organic matter (SOM) to define labile and stable pools (Hassink, 1997; Chung et al., 2008; Gulde et al., 2008) although many other methods exist (Torn et al. 2009). Physical fractionation is particularly well suited to analyses of C saturation because it provides isolatable fractions of organic matter rather than hypothetical pools that are based on decomposition kinetics in the lab or field. In concept, the isolated pools differ in degree of physico-chemical protection from mineralization (e.g., Golchin et al. 1994). Stable pools include relatively stable mineral-associated organic matter (MAOM) that is chemically adsorbed to fine mineral particles such as silt and clay (Sollins et al., 1996) as well as particulate organic matter (POM) that is physically occluded within stable microaggregates (Jastrow et al., 1996). Labile pools include free POM that is not physically or chemically protected from mineralization.

Although a number of studies have either measured no change in total soil C with increasing C input or a saturation of total soil C pool with increasing input, recent research has begun to evaluate the two-pool model (Hassink and Whitmore 1997) by exploring saturation dynamics of stable and labile SOM pools. Using a combined dataset from 14 experimental sites, Stewart et al. (2008) found similar probability that data from C input addition experiments fit one-pool or two-pool saturation models. At individual sites, several C addition experiments have found positive relationships between C inputs and labile C pools, but no relationship between C inputs and stable C pools (Chung et al., 2008; Gulde et al., 2008; Castellano et al. 2012b). These data are consistent with the concept that only soil fractions with physico-chemical limitations on C stabilization should saturate.

Differences and Similarities among C and N Saturation Theories

Nitrogen saturation theory was developed by ecologists in temperate forests. In contrast, C saturation theory was developed by soil scientists in temperate cultivated agricultural systems. Although striking, this difference is only one of many.

From the perspective of soil and ecosystem management, perhaps the most striking difference between C and N saturation processes is that most agricultural ecosystems appear to simultaneously move away from C saturation and towards N saturation (i.e., the net loss of carbon from land to atmosphere occurs concurrently with a net gain in biologically available nitrogen in many ecosystems). This apparent disconnect made it easy for researchers to focus on each process individually. However, as suggested by Stewart et al.(2008) management changes could have lowered the ability soil to store C (i.e., the effective stabilization limit of the ecosystem), and thus moved the ecosystem closer to C saturation despite lower total C levels. Nevertheless, this important difference likely resulted in a lack of intuitive connections among the theories.

A second factor limiting connections among these theories is that different methodology was historically used to investigate each process. In C saturation studies, differing C-inputs levels were applied to field plots and then the response of C-stocks in the soil measured (often years apart so that the system could be considered to be in equilibrium). These studies typically occurred in agricultural systems that investigated the impacts of long-term rotations or manure inputs on agricultural productivity. Nitrogen saturation studies utilized a kinetic approach, often monitoring losses from the ecosystem (leaching losses and gaseous emissions) or changes in the amount of nitrogen in different sinks. However, in these cases researchers were typically interested in how an ecosystem responded to a perturbation (i.e., the path the ecosystem took to reach a new equilibrium rather than the relationship among equilibriums).

Compounding this difference, N saturation research focused on organic soil horizons (Currie, 1999) whereas C saturation research focused on mineral soils (Six et al. 2002). Recent research has highlighted that fundamental differences in microbial C and N cycling among organic and mineral soils (Schimel and Schaeffer, 2012). Whereas microbial community and vegetation chemistry is likely important in organic soils, environmental factors are likely more important in mineral soils. Moreover, organic soils would necessarily be classified as a labile pool in two-pool C saturation models.

As a result, methods for determining ecosystem responses to C and N additions differed at least partly because physico-chemical stabilization processes do not operate in the absence of mineral soils (Kleber and Johnson, 2010). Nevertheless, this difference does lead to an important similarity among C and N saturation theories that has resulted in significant recent debate: Both theories include considerable investigation into the role of biochemical stabilization mechanisms.

Historically, biochemical stabilization was thought to be the dominant SOM stabilization mechanism (Stevenson, 1982). Initial C saturation (Six et al. 2002) and later N saturation models (Johnson, 1992) include processes that account for long-term biochemical stabilization of C and N. However, recent evidences suggests: 1) biochemical stabilization (i.e., selective preservation of molecules that inherently resist decomposition) of SOM may be limited to molecules of pyrogenic origin (Kleber and Johnson, 2010; Schmidt et al., 2011) and 2) long-term SOM stabilization is dominated by organo-mineral interactions. Nevertheless, a lack of biochemical stabilization is somewhat inconsistent with N saturation research that has observed large long-term retention and stabilization of inorganic N inputs that far exceed microbial biomass (in O horizons). This result led researchers to explore the hypothesis that rapid biotic and abiotic chemical stabilization of inorganic N inputs is responsible for retention (Johnson, 1992). This hypothesis has received support from a number of studies that identify and evaluate specific mechanisms (Johnson et al., 2000; Davidson et al., 2003; Fitzhugh et al., 2003; Fricks et al., 2009) as well as observe long-term stability of retained N inorganic ecosystem studies (Lewis et al 2012). The apparent lack of biochemical stabilization in mineral soils and evidence supporting rapid stabilization of inorganic N inputs after transformation to insoluble organic N compounds in organic soils appears to be a significant area where C and N cycling theory can be linked.

A second common principle that has emerged among the theories is that saturation can occur via kinetic and capacity saturation. Although C saturation concepts are clearly based on capacity, they also include kinetic saturation via aggregate dynamics. Conceptual models and considerable empirical evidence suggest that macroaggregate turnover controls the formation of microaggregates and thus the capacity for occluded POM storage (Six et al., 2000, 2004; Plante and McGill, 2002). Rapid macroaggregate turnover inhibits POM occlusion because turnover is too fast to permit microaggregate formation. Slow macroaggregate turnover does not form microaggregates at a sufficient

pace to occlude POM before it is mineralized. Accordingly, macroaggregate turnover is likely to interact with the rate of organic matter inputs to affect SOM stabilization through the occlusion of POM in microaggregates. In contrast to the C saturation focus on storage capacity, N saturation theory has focused on measuring the response (i.e., kinetics) of N losses. Until recently (Lovett and Goodale, 2011), N saturation theory lacked a formal concept that the kinetics of N losses are a function of the capacity for N storage as well as kinetics of N retention in plant and soil sinks. This development is a major advance in N saturation research and provides a framework for linking C and N saturation theories through a common definition of saturation.

Recent focus on N saturation of mineral soils has advanced links among C and N saturation based on the common importance of physico-chemical stabilization mechanisms for C and N in mineral soils (Castellano et al., 2012). These links were developed from the observations that inorganic N inputs can be rapidly stabilized in mineral soils in addition to organic soils (Johnson et al., 2000) and the dominant mechanisms for rapid inorganic N stabilization in mineral soils appears to be rapid incorporation into microbial biomass and subsequent retention of microbial products in stable SOM pools (Norton and Firestone, 1996; Kaye et al., 2002). The process of rapid inorganic N immobilization into microbial biomass and subsequent transfer to SOM sinks is consistent with observations that vegetation (including fine roots) is not a major initial sink for inorganic N inputs (Zogg et al., 2000) and most SOM in stable mineral-associated pools has a microbial origin (Grandy and Neff, 2008; Sollins et al., 2009). Recent exploration of N retention in mineral subsoils is consistent with a strong link among C and N saturation theories: subsoils are often a more efficient N sink than organic matter-rich surface soils (Idol et al., 2003; Dittman et al., 2007; Castellano et al., 2012)

The extension of N saturation research from organic to mineral soils also allows direct links to be among the retention and mineralization of SOM. The balance between these processes should influence soil fertility. In the final section of the paper we review research that suggests C and N saturation theories can be applied to agricultural systems to advance nutrient cycling science.

Linking C and N Saturation Theories to Understand Nutrient Dynamics

Both C and N saturation theories describe soil processes that enhance N availability, which is one the primary goals in agricultural systems. Initial N saturation research on organic soil horizons and the factors affecting the kinetics of N losses determined that the C/N ratio of SOM and vegetation litter has a strong effect on N mineralization and nitrification (Emmett et al., 1998; Christenson et al., 2009). This concept is well known in agricultural systems where the C/N ratio of crop residues is a significant factor affecting N fertilizer requirement (Gentry et al., 2013). Even in systems where annual legumes are a net user of N from the soil, the un-harvested residue can have a positive effect on N availability despite an overall negative N balance (Christianson et al. 2012). In the developing world, the CN ratio of crop residues is commonly used to balance N retention and mineralization (Palm et al., 2001; Gentile et al., 2008).

Similar to N saturation theory, C saturation theory also includes mechanisms for enhanced SOM mineralization that result in greater N availability. However, the mechanisms focus on the mineral soil. In this case, as stable SOM pools become saturated, new organic matter inputs remain in the labile pool (Gulde et al., 2008). In other words, as stable pools accumulate organic matter, fewer nutrients from POM are ultimately stabilized in mineral-associated or microaggregate occluded SOM pools that resist mineralization. This process has recently been extended to show that saturation of the mineral-associated SOM pool is coincident with a decrease in the labile pool (POM) C/N ratio and an increase in N mineralization (Castellano et al., 2012; Fig 2). The decrease in POM C/N ratio likely occurs because SOM mineralization transforms organic C to gaseous CO_2 while the majority of mineralized organic N remains within the soil system.

Thus, independent of N fertilizer inputs, there are two paths to increased mineral N availability in the soil: 1) addition of high quality, low C/N residues (Palm et al. 2001) and 2) saturation of the capacity to store SOM in stable pools (Gulde et al. 2008; Castellano et al., 2012).

Most agricultural systems with access to N fertilizer maintain N saturation (McSwiney et al. 2010). This helps to alleviate N limitations the crop may encounter, and thus maximizes production, but leaves the system prone to N losses that are costly from economic and environmental perspectives (Raun and Johnson, 1999; Gruber and

Galloway, 2008). Importantly, N saturation in this case appears to be the result of kinetic saturation. Supporting evidence includes data that demonstrate agricultural soils, similar to forests, are a strong sink for inorganic N inputs (~30%; Stevens et al., 2005) and the fact that split N applications often increase crop yield (Jokela and Randall, 1989) and thus likely reduce N losses compared to a one-time application. Nevertheless, agricultural systems can be maintained at capacity saturation as well. Few, if any, data exist comparing N dynamics among agricultural with and without capacity C saturation. However, C saturation principles suggest that these systems would have high N mineralization potential from a labile, low C/N ratio POM pool. One might hypothesize that agricultural systems exhibiting capacity saturation could produce similar yields with greater fertilizer N use efficiency than systems that are not capacity saturated because the stable SOM sinks are not existent and the actively cycling labile pool is growing (Gulde et al., 2008).

The concept that stable SOM sinks, particularly mineral-associated, have rapid capacity to retain nutrients in sinks that preclude plant availability (Castellano et al., 2012) has potentially broad application for nutrients beyond N. Adsorption isotherms of nutrients such as P and S may be well correlated with the capacity for mineral-associated sinks to stabilize SOM. Indeed, sorption isotherms can be applied to dissolved organic C as well (Vance and David, 1992).

The major impediment to applying capacity C and N saturation to the management of agricultural systems is the difficulty of assessing saturation dynamics of soils. Annual net changes in C and N reflect at most 2% of the total soil pool. Moreover, samples across time and input rate of C and N are required to definitively show no gain over time despite differences in input rate. Nevertheless, there are clear benefits of managing soil organic C and N stocks at the highest levels possible: SOM is positively correlated with yield amount and stability as well as environmental metrics such as N retention.

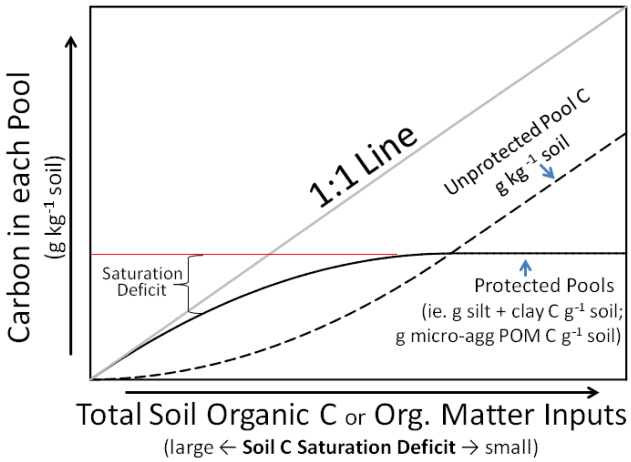

Fig. 1. Theoretical behavior of protected (stable) and unprotected (labile) SOC pools as a function of total SOC (x-axis); adapted from Stewart et al. 2007. Protection occurs through chemical mineral association, which is function of soil texture/mineralogy, and micro-aggregate formation, which is a function of macro-aggregate turnover. The capacity for C storage in protected pools is limited; as total SOC increases, storage of new C inputs in protected pools is initially rapid and efficient, but the storage efficiency (ΔSOC/ΔC input) declines in proportion to the amount of C already present in the pool (solid black curve). Carbon inputs not transferred to protected pools remain in unprotected pools (dashed curve) where they are subject to rapid mineralization. Protected and unprotected pools sum to the 1:1 line, which equals total SOC. The red line indicates the saturation level of the protected pools; unsatisfied storage capacity is referred to as the 'saturation deficit.'

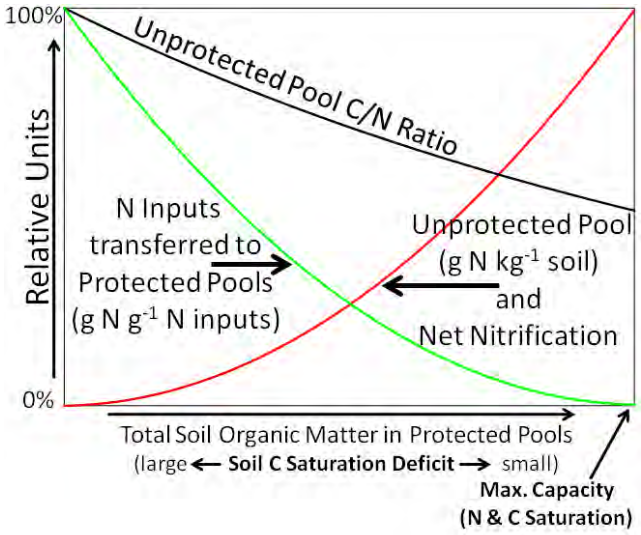

Fig. 2. Conceptual model for N retention and N mineralization are a function of the saturation deficit (i.e., the unsatisfied capacity for OM storage in protected pools). Note that the axes extend only to the point of saturation of protected pools (see Figure 1); unprotected pools and N mineralization could continue to increase beyond saturation of protected pools.

References

Aber, J.D., A. Magill, S.G. Mcnulty, R.D. Boone, K.J. Nadelhoffer, M. Downs, and R. Hallett. 1995. Forest biogeochemistry and primary production altered by nitrogen saturation. Water, Air, & Soil Pollution 85: 1665–1670.

Aber, J., W. Mcdowell, K. Nadelhoffer, and A. Magill. 1998. Nitrogen Saturation in Temperate Forest Ecosystems. Bioscience 48: 921–934.

Aber, J., K. Nadelhoffer, P. Steudler, and J.M. Melillo. 1989. Nitrogen saturation in northern forest ecosystems. BioScience 39: 378–386.

Agren, G.I., and E. Bosatta. 1988. Nitrogen saturation of terrestrial ecosystems. Environmental pollution (Barking, Essex : 1987) 54(3-4): 185–97Available at

Castellano, M.J., J.P. Kaye, H. Lin, and J.P. Schmidt. 2012. Linking Carbon Saturation Concepts to Nitrogen Saturation and Retention. Ecosystems 15: 175-187.

Christenson, L.M., G.M. Lovett, K.C. Weathers, and M. a. Arthur. 2009. The Influence of Tree Species, Nitrogen Fertilization, and Soil C to N ratio on Gross Soil Nitrogen Transformations. Soil Science Society of America Journal 73: 638

Chung, H., J.H. Grove, and J. Six. 2008. Indications for Soil Carbon Saturation in a Temperate Agroecosystem. Soil Science Society of America Journal 72: 1132

Currie, W.S. 1999. The responsive C and N biogeochemistry of the temperate forest floor. Trends in ecology & evolution 14: 316–320.

Davidson, E. a., and I.L. Ackerman. 1993. Changes in soil carbon inventories following cultivation of previously untilled soils. Biogeochemistry 20(3): 161–193

Davidson, E. a., J. Chorover, and D.B. Dail. 2003. A mechanism of abiotic immobilization of nitrate in forest ecosystems : the ferrous wheel hypothesis. Global Change Biology 9: 228–236.

Dittman, J. a, C.T. Driscoll, P.M. Groffman, and T.J. Fahey. 2007. Dynamics of nitrogen and dissolved organic carbon at the Hubbard brook experimental forest. Ecology 88(5): 1153–66.

Dungait, J. a. J., D.W. Hopkins, A.S. Gregory, and A.P. Whitmore. 2012. Soil organic matter turnover is governed by accessibility not recalcitrance. Global Change Biology 18(6): 1781–1796

Emmett, B.A. 2007. Nitrogen Saturation of Terrestrial Ecosystems: Some Recent Findings and Their Implications for Our Conceptual Framework. Water, Air, & Soil Pollution: Focus 7(1-3): 99–109

Emmett, B.A., D. Boxman, M. Bredemeier, P. Gundersen, O.J. Kjønaas, F. Moldan, P. Schleppi, A. Tietema, and R.F. Wright. 1998. Predicting the Effects of Atmospheric Nitrogen Deposition in Conifer Stands : Evidence from the NITREX Ecosystem-Scale Experiments. Ecosystems 1: 352–360.

Fenn, M.E., M. a. Poth, J.D. Aber, J.S. Baron, B.T. Bormann, D.W. Johnson, A.D. Lemly, S.G. McNulty, D.F. Ryan, and R.S. Stottlemeyer. 1998. Nitrogen excess in North American ecosystems: predisposing factors, ecosystem responses and management strategies. Ecological Applications 8: 706–733.

Fitzhugh, R.D., G.M. Lovett, and R.T. Venterea. 2003. Biotic and abiotic immobilization of ammonium , nitrite , and nitrate in soils developed under different tree species in the Catskill Mountains , New York , USA. Global Change Biology: 1591–1601.

Fricks, B., J. Kaye, and R. Seidel. 2009. Abiotic Nitrate Retention in Agroecosystems and a Forest Soil. Soil Science Society of America Journal 73: 1137

Gentile, R., B. Vanlauwe, P. Chivenge, and J. Six. 2008. Interactive effects from combining fertilizer and organic residue inputs on nitrogen transformations. Soil Biology and Biochemistry 40: 2375–2384

Gentry, L.F., M.L. Ruffo, and F.E. Below. 2013. Identifying Factors Controlling the Continuous Corn Yield Penalty. Agronomy Journal 105: 295

Grandy, a S., and J.C. Neff. 2008. Molecular C dynamics downstream: the biochemical decomposition sequence and its impact on soil organic matter structure and function. The Science of the total environment 404(2-3): 297–307

Gruber, N., and J.N. Galloway. 2008. An Earth-system perspective of the global nitrogen cycle. Nature 451: 293–296

Gulde, S., H. Chung, W. Amelung, C. Chang, and J. Six. 2008. Soil Carbon Saturation Controls Labile and Stable Carbon Pool Dynamics. Soil Science Society of America Journal 72(3): 605

Gundersen, P., B.A. Emmett, O.J. Kjgnaas, C.J. Koopmans, and A. Tietema. 1998. Impact of nitrogen deposition on nitrogen cycling in forests : a synthesis of NITREX data. Forest Ecology and Management 101: 37–55.

Gundersen, P., L. Sevel, J.R. Christiansen, L. Vesterdal, K. Hansen, and A. Bastrup-Birk. 2009. Do indicators of nitrogen retention and leaching differ between coniferous and broadleaved forests in Denmark? Forest Ecology and Management 258: 1137–1146

Gurmesa, G.A., I.K. Schmidt, P. Gundersen, and L. Vesterdal. 2013. Soil carbon accumulation and nitrogen retention traits of four tree species grown in common gardens. Forest Ecology and Management

Gärdenäs, A.I., G.I. Ågren, J. a. Bird, M. Clarholm, S. Hallin, P. Ineson, T. Kätterer, H. Knicker, S.I. Nilsson, T. Näsholm, S. Ogle, K. Paustian, T. Persson, and J. Stendahl. 2011. Knowledge gaps in soil carbon and nitrogen interactions – From molecular to global scale. Soil Biology and Biochemistry 43: 702–717

Hassink, J. 1997. The capacity of soils to preserve organic C and N by their association with clay and silt particles. Plant and Soil 191: 77–87.

Hassink, J., and A.P. Whitmore. 1997. A Model of the Physical Protection of Organic Matter in Soils. Soil Science Society of America Journal 61: 131–139.

Heitkamp, F., M. Wendland, K. Offenberger, and G. Gerold. 2012. Implications of input estimation, residue quality and carbon saturation on the predictive power of the Rothamsted Carbon Model. Geoderma 170: 168–175

Huggins, D., C. Clapp, R. Allmaras, J. Lamb, and M. Layese. 1998. Carbon Dynamics in Corn-Soybean Sequences as Estimated from Natural Carbon-13 Abundance. Soil Science Society of America Journal 62: 195–203.

Hättenschwiler, S., and P. Vitousek. 2000. The role of polyphenols in terrestrial ecosystem nutrient cycling. Trends in ecology & evolution 15: 238–243.

Idol, T.W., P.E. Pope, and F. Ponder. 2003. N mineralization , nitrification , and N uptake across a 100-year chronosequence of upland hardwood forests. Forest Ecology and Management 176: 509–518.

Jastrow, J.D., T.W. Boutton, and R.M. Miller. 1996. Carbon Dynamics of Aggregate-Associated Organic Matter Estimated by Carbon-13 Natural Abundance. Soil Science Society of America Journal 60: 801–807.

Johnson, D.W. 1992. Nitrogen Retention in Forest Soils. Journal of Environment Quality 21: 1–12.

Johnson, D.W., W. Cheng, and I.C. Burke. 2000. Biotic and Abiotic Nitrogen Retention in a Variety of Forest Soils. Soil Science Society of America Journal 64: 1503–1514.

Kaye, J., J. Barrett, and I. Burke. 2002. Stable Nitrogen and Carbon Pools in Grassland Soils of Variable Texture and Carbon Content. Ecosystems 5: 461–471.

Kaye, J.P., and S.C. Hart. 1997. Competition for nitrogen between plants and soil microorganisms. Trends in ecology & evolution 12: 139–143.

Kleber, M., and M.G. Johnson. 2010. Advances in Understanding the Molecular Structure of Soil Organic Matter : Implications for Interactions in the Environment. Advances in Agronomy 106(10): 77–142

Kong, A.Y.Y., J. Six, D.C. Bryant, R.F. Denison, and C. van Kessel. 2005. The Relationship between Carbon Input, Aggregation, and Soil Organic Carbon Stabilization in Sustainable Cropping Systems. Soil Science Society of America Journal 69(4): 1078–1085

Kool, D.M., H. Chung, K.R. Tate, D.J. Ross, P.C.D. Newton, and J. Six. 2007. Hierarchical saturation of soil carbon pools near a natural CO 2 spring. Global Change Biology 13(6): 1282–1293

Lal, R., R.F. Foiiett, B.A. Stewart, and J.M. Kimbie. 2007. Soil carbon sequestration to mitigate climate change and advance food security. Soil Science 172: 943–956.

Lewis, D.B., and J.P. Kaye. 2011. Inorganic nitrogen immobilization in live and sterile soil of old-growth conifer and hardwood forests: implications for ecosystem nitrogen retention. Biogeochemistry

Lovett, G.M., and C.L. Goodale. 2011. A New Conceptual Model of Nitrogen Saturation Based on Experimental Nitrogen Addition to an Oak Forest. Ecosystems 14: 615–631

Lovett, G.M., K.C. Weathers, and M. a. Arthur. 2002. Control of Nitrogen Loss from Forested Watersheds by Soil Carbon:Nitrogen Ratio andTree Species Composition. Ecosystems 5: 712–718

Lovett, G.M., K.C. Weathers, M.A. Arthur, and J.C. Schultz. 2004. Nitrogen cycling in a northern hardwood forest : Do species matter ? Biogeochemistry 67: 289–308.

McSwiney, C.P., S.S. Snapp, and L.E. Gentry. 2010. Use of N immobilization to tighten the N cycle in conventional agroecosystems. Ecological applications : a publication of the Ecological Society of America 20: 648–62

Mueller, K.E., S.E. Hobbie, J. Oleksyn, P.B. Reich, and D.M. Eissenstat. 2012. Do evergreen and deciduous trees have different effects on net N mineralization in soil? Ecology 93(6): 1463–72

Nadelhoffer, K.J., B.A. Emmett, P. Gundersen, O.J. Kjùnaas, C.J. Koopmansk, P. Schleppi, A. Tietemak, and R.F. Wright. 1999. Nitrogen deposition makes a minor contribution to carbon sequestration in temperate forests. Nature 398: 1997–2000.

Norton, M., and M.K. Firestone. 1996. N Dynamics in the rhizosphere of Pinus Ponderosa Seedlings. Soi Biology and Biochemistry 28(3): 351–362.

Olk, D.C., M.M. Anders, T.R. Filley, and C. Isbell. 2009. Crop Nitrogen Uptake and Soil Phenols Accumulation under Continuous Rice Cropping in Arkansas. Soil Science Society of America Journal 73(3): 952

Paustian, K, H.P. Collins, and E. A. Paul. Management controls on soil carbon. in: Soil organic matter in temperate agroecosystems CRC Press p. 15-42.

Palm, C. a, C.N. Gachengo, R.J. Delve, G. Cadisch, and K.E. Giller. 2001. Organic inputs for soil fertility management in tropical agroecosystems: application of an organic resource database. Agriculture, Ecosystems & Environment 83: 27–42

Plante, a. F., and W.B. McGill. 2002. Soil aggregate dynamics and the retention of organic matter in laboratory-incubated soil with differing simulated tillage frequencies. Soil and Tillage Research 66: 79–92

Raun, W., and G. Johnson. 1999. Improving Nitrogen Use Efficiency for Cereal Production. Agronomy Journal 91: 357–363.

Schimel, J.P., and S.M. Schaeffer. 2012. Microbial control over carbon cycling in soil. Frontiers in microbiology 3: 348

Schmidt, M.W.I., M.S. Torn, S. Abiven, T. Dittmar, G. Guggenberger, I. a. Janssens, M. Kleber, I. Kögel-Knabner, J. Lehmann, D. a. C. Manning, P. Nannipieri, D.P. Rasse, S. Weiner, and S.E. Trumbore. 2011. Persistence of soil organic matter as an ecosystem property. Nature 478: 49–56

Six, J., H. Bossuyt, S. Degryze, and K. Denef. 2004. A history of research on the link between (micro)aggregates, soil biota, and soil organic matter dynamics*1. Soil and Tillage Research 79: 7–31

Six, J., R.T. Conant, E.A. Paul, and K. Paustian. 2002. Stabilization mechanisms of soil organic matter : Implications for C-saturation of soils. Plant and Soil 241: 155–176.

Six, J., E.T. Elliott, and K. Paustian. 2000. Soil macroaggregate turnover and microaggregate formation : a mechanism for C sequestration under no-tillage agriculture. Soil Biology and Biochemistry 32: 2099–2103.

Sollins, P., P. Homann, and B.A. Caldwell. 1996. Stabilization and destabilization of soil organic matter : mechanisms and controls. Geoderma 74: 65–105.

Sollins, P., M.G. Kramer, C. Swanston, K. Lajtha, T. Filley, A.K. Aufdenkampe, R. Wagai, and R.D. Bowden. 2009. Sequential density fractionation across soils of contrasting mineralogy: evidence for both microbial- and mineral-controlled soil organic matter stabilization. Biogeochemistry 96: 209–231

Stevens, W.B., R.G. Hoeft, and R.L. Mulvaney. 2005. Fate of Nitrogen-15 in a Long-Term Nitrogen Rate Study. Agronomy Journal 97: 1046

Stewart, C.E., K. Paustian, R.T. Conant, A.F. Plante, and J. Six. 2007. Soil carbon saturation: concept, evidence and evaluation. Biogeochemistry 86: 19–31

Stewart, C., K. Paustian, R. Conant, a Plante, and J. Six. 2009. Soil carbon saturation: Implications for measurable carbon pool dynamics in long-term incubations. Soil Biology and Biochemistry 41: 357–366

Vance, G.F., and M.B. David. 1992. Dissolved organic carbon and sulfate sorption by spodosol mineral horixons. Soil Science 154:151-157.

Wright, R.F., and N. Van Breemen. 1995. The NITREX project : an introduction. Forest Ecology and Management 1: 3–7.

Zogg, G.P., D.R. Zak, K.S. Pregitzer, and A.J. Burton. 2000. Microbial immobilization and the retention of anthropogenic nitrate in a northern hardwood forest. Ecology 81: 1858–1866.

REAL TIME MONITORING OF N_2O EMISSIONS FROM AGRICULTURAL SOILS USING FTIR SPECTROSCOPY

Yael Dubowski[1], D. Harush[1], A. Shaviv[1], L. Stone[2] and R. Linker[1]

[1]Faculty of Civil and Environ. Eng. Technion– Israel Inst. of Technology Haifa, Israel

[2]Dep. of Civil and Environ. Eng. Massachusetts Institute of Technology. Cambridge, MA 02139

Abstract

Emissions of N_2O from agricultural soils are an important source for this greenhouse gas. The present work examines the potential of Fourier transformed infrared (FTIR) spectroscopy coupled with a long path (LP) infrared (IR) gas cell for on-line measurement of concentration and isotopic signature of N_2O emitted from soils. Nitrous Oxide was spectrally monitored during incubations of soil samples in a closed system under different conditions. Its emission from a Grumosol (Vertisol) was measured in presence and absence of acetylene, with various additions of nitrate and glucose, under aerobic and anaerobic conditions, and for two soil thickness layers. For comparison N_2O emissions from a Terra Rossa (Cambisol) and a Hamra (Luvisol) were measured in the presence and absence of acetylene. In an additional experimental set the isotopic signature of emitted N_2O was quantified after enrichment with $K^{15}NO_3$. Acetylene addition led to an increase in N_2O emissions in all three soils but at various extents. Under aerobic conditions, N_2O emission from the Grumosol became detectable only when running the experiments with a thicker soil layer (10 mm), suggesting the existence of coupled nitrification–denitrification. Nitrate addition to soils enhanced N_2O emissions especially when coupled with glucose addition. Addition of $^{15}NO_3^-$ to the Grumosol resulted in the emission of all four N_2O isotopologues: $^{14}N_2O$, $^{15}N_2O$, $^{14}N^{15}NO$, and $^{15}N^{14}NO$. The observed slight delay in appearance of the species containing ^{15}N and the relatively lower ^{15}N enrichment of the N_2O compared with the soil nitrate, indicate isotopic fractionation during denitrification. Yet, within the accuracy of our isotopic analysis, temporal emission patterns of $^{14}N^{15}NO$ and $^{15}N^{14}NO$ were similar indicating low possibility for "site preference" under the specific experimental conditions.

https://www.soils.org/publications/sssaj/articles/78/1/61?highlight=&search-result=1

Session 3: Microsensors for Investigating Soil Processes

In situ Measurements of Diffusion and Mass Flow of Nitrogen Compounds in Forest Soils Using Microdialysis

Torgny Näsholm, Olusegun Ayodeji Oyewole, Erich Inselsbacher

Department of Forest Ecology & Management, Swedish University of Agricultural Sciences, SE-901 83 Umeå, Sweden

Plant biomass production and species composition in terrestrial ecosystems is largely regulated by the availability of soil nitrogen (N). Since the discovery that plants take up organic N, thereby bypassing the bottleneck of N mineralization, the role of soil organic N for plant nutrition has received increased attention (Jämtgård et al., 2008; Kielland, 1994; Lipson and Näsholm, 2001; Näsholm et al., 1998; Paungfoo-Lonhienne et al., 2008; Persson and Näsholm, 2001). Detailed knowledge about the concentrations and composition of soil N pools are therefore crucial for studying and understanding plant N nutrition. Until now this remained a challenging task, due to the lack of adequate sampling techniques. The traditional and still most commonly used method for estimating soil N pools is the extraction of soil with water or salt solutions. However, the disruptive nature of this sampling method that commonly includes sieving, homogenizing, and the extraction processes, leads to a significant alteration of the natural equilibrium of the soil N composition as a consequence of microbially mediated transformations, losses and contaminations (Carrillo-Gonzales et al., 2013; Jones and Willett, 2006; Makarov et al., 2013; Miro and Hansen, 2006; Rousk and Jones, 2010; Warren and Taranto, 2010). Therefore, the results from the soil extraction method are poor indicators of *in situ* soil N concentrations (Inselsbacher and Näsholm, 2012; Miro and Frenzel, 2011).

Plant N acquisition is determined by the flux of nutrients from the soil to root surfaces rather than by the soil N concentrations (Clarkson and Hanson, 1980; Lambers et al., 2008; Leadley et al., 1997; Marschner, 1995; Tinker and Nye, 2000). The two main processes driving N fluxes towards roots are diffusion and mass flow, but the relative

importance of each processes to plant N acquisition remain controversial (e.g., Barber, 1995; Comerford, 2005). Until now the method for estimating the relative contributions of mass flow and diffusion to plant N acquisition was indirect and could not account for a range of uncertainties, such as spatial and temporal variations in soil water contents and N concentrations, N uptake by mycorrhizae and potential interactions between mass flow and diffusion (Chapin et al., 2011; Nye and Mariott, 1969; Oyewole et al., 2013). Obviously, a direct and more robust method for estimating diffusion and mass flow of N in soil is needed.

Recently, a novel in situ sampling technique based on passive microdialysis was introduced in environmental research (Öhlund, 2004; Inselsbacher et al., 2011; Miro and Hansen, 2006; Miro et al., 2010; Sulyok et al., 2005). Earlier, this technique has been extensively studied and applied in neurosciences and pharmacokinetic studies (e.g., Davies, 1999; Kehr, 1993; Korf et al., 2010), but it had hardly been used in other areas. Microdialysis is a passive sampling technique where the sole driving force for sampling the target compound is the concentration gradient across the microdialysis membrane induced by the solution (perfusate) pumped through the probes. We have evaluated and concluded that the microdialysis technique allows monitoring of soil N fluxes with minimal invasiveness. Unlike other soil sampling methods, the miniaturized design and the passive sampling approach of microdialysis allows for continuous monitoring of soil N fluxes at an unrivalled spatial and temporal resolution (Inselsbacher et al., 2011). We found that differences in soil N concentrations can be detected at small scales (< 1 cm) and within short time intervals (< 30 min). Microdialysis revealed that individual N compounds, especially amino acids, were distributed highly heterogeneously in soil, showing that this technique is suitable for studying N dynamics in soil microsites. Further, application of N compounds to soil led to an immediate peak of diffusive N flux over the membrane followed by a rapid decline. This indicates that microdialysis can be used to monitor the root capture of N pulses and formation of depletion zone similar to those obtained in the rhizosphere of active roots (Inselsbacher et al., 2011).

One of the significant advantages of microdialysis technique compared to other sampling techniques is that it allows monitoring soil N fluxes directly in the field with minimal disturbance to natural environment (Inselsbacher and Näsholm, 2012). To this end, studying diffusive fluxes of inorganic and organic N in soils of 15 different boreal

forests using the microdialysis method revealed that amino acids accounted for 80 % of total soil N supply. This result is in sharp contrast to the general notion that plant-available N in this ecosystem is dominated by ammonium. In addition, the majority of amino acids diffused freely through the soil when sampling with microdialysis unlike soil bound amino acids obtained in soil extractions techniques, suggesting that the full spectrum of amino acids is available for plant and mycorrhizal uptake.

Although these latter studies focused on diffusive fluxes only, their results are striking and have a significant impact on our current understanding of plant N acquisition.

As mentioned above, two processes govern plant N acquisition; diffusion and mass flow. The microdialysis technique, as described above and in the cited literature, was relying on induced diffusion to drive fluxes of N (or other) compounds into the microdialysis system as dialysate. We have, however, extended the microdialysis technique to also include monitoring of mass flow of soil N (Oyewole et al., 2013). We accomplished this by using a solution of macromolecules larger than the molecular-weight cut-off of the probe membrane as perfusate, thereby establishing a water potential gradient between the interior of the probe membrane and the external soil solution. This gradient in water potential then induces mass flow of water towards and over the probe membrane causing mass transfer of N compounds present in the soil water. Varying the osmotic potential of the perfusate a wide range of mass flow rates can be achieved. Application of this technique in solution and in soil suggests that mass flow may play a significant role in plant N acquisition. Total N fluxes were significantly higher when mass flow was induced, due to the inflow of N dissolved in the surrounding water, but especially due to a significant increase of diffusive fluxes indirectly by mass flow. The latter may be explained by mass flow causing a steeper N concentration gradient around the microdialysis membrane.

In conclusion, *in situ* monitoring reveals a dominance of amino acids in the total N flux of boreal forest soils. The contrast between this result and those of earlier studies may be ascribed to the low invasiveness of the applied microdialysis methodology in our studies. A further development of this technique now enables studies of both induced diffusion and induced mass flow as drivers of plant N acquisition. Preliminary results from our studies suggest mass flow may have a major effect on root N acquisition. Studies involving measurements of agricultural settings and further investigations of

the relationship between transpirationally induced mass flow and N acquisition are underway.

References

Barber, S.A. 1995. Nutrient uptake by plant roots growing in soil. In: Barber, S.A., editor, Soil nutrient bioavailability: a mechanistic approach. John Wiley & Sons Inc., New York, USA, p. 85-109.

Carrillo-Gonzalez, R., M.C.A. Gonzalez-Chavez, J.A. Aitkenhead-Peterson, F.M. Hons, and R.H. Loeppert. 2013. Extractable DOC and DON from a dry-land long-term rotation and cropping system in Texas, USA. Geoderma 197-198: 79-86.

Chapin, F.S., P.A. Matson, and P.M. Vitousek. 2011. Principles of terrestrial ecosystem ecology. Springer, New York, USA.

Clarkson, D.T., and J.B. Hanson. 1980. The mineral nutrition of higher plants. Annu. Rev. Plant Phys. 31: 239-298.

Comerford, N.B. 2005. Soil factors affecting nutrient bioavailability. In: BassiriRad, H., editor, Nutrient acquisition by plants an ecological perspective. Ecological Studies, Vol. 181. Springer, Berlin Heidelberg, Germany, p. 1-14.

Davies, M.I. 1999. A review of microdialysis sampling for pharmacokinetic applications. Anal. Chim. Acta 379: 227-249.

Inselsbacher, E., and T. Näsholm. 2012. The belowground perspective of forest plants – soil provides mainly organic N for plants and mycorrizal fungi. New Phytol. 195: 329-334 (Rapid report)

Inselsbacher, E., J. Öhlund, S. Jämtgård, K. Huss-Danell, and T. Näsholm. 2011. The potential of microdialysis to monitor organic and inorganic nitrogen compounds in soil. Soil Biol. Biochem. 43: 1321-1332.

Jämtgård, S., T. Näsholm, and K. Huss-Danell. 2008. Characteristics of amino acid uptake in barley. Plant Soil 302: 221-231.

Jones, D.L., and V.B. Willett. 2006. Experimental evaluation of methods to quantify dissolved organic nitrogen (DON) and dissolved organic carbon (DOC) in soil. Soil Biol. Biochem 38: 991-999.

Kehr, J. 1993. A survey on quantitative microdialysis – theoretical models and practical implications. J. Neurosci. Meth. 48: 251-261.

Kielland, K. 1994. Amino acid absorption by arctic plants: implications for plant nutrition and nitrogen cycling. Ecology 75: 2373-2383.

Lambers, H., F.S. Chapin, and T.L. Pons. 2008. Plant physiological ecology. Springer, New York, USA.

Leadley, P.W., J.F. Reynolds, and F.S.A. Chapin. 1997. A model of nitrogen uptake by Eriophorum vaginatum roots in the field: ecological implications. Ecol. Monogr. 67: 1-22.

Lipson, D., and T. Näsholm. 2001. The unexpected versatility of plants: organic nitrogen use and availability in terrestrial ecosystems. Oecologia 128: 305-316.

Makarov, M.I., M.S. Shuleva, T.I. Malysheva, and O.V. Manyailo. 2013. Solubility of the labile forms of soil carbon and nitrogen in K_2SO_4 of different concentrations. Eurasian Soil Sci. 46: 369-374.

Marschner, H. 1995. Mineral nutrition of higher plants. Academic Press Limited, London, UK.

Miro, M., W.J. Fitz, S. Swoboda, and W.W. Wenzel. 2010. In-situ sampling of soil pore water: evaluation of linear-type microdialysis probes and suction cups at varied moisture contents. Environ. Chem. 7: 123-131.

Miro, M., and W. Frenzel. 2011. Microdialysis in environmental monitoring. In: Tsai, T.H., editor. Applications of Microdialysis in Pharmaceutical Science. Wiley & Sons, Inc., Hoboken, New Jersey, USA, p. 509-530.

Miro, M., and E.H. Hansen. 2006. Recent advances and perspectives in analytical methodologies for monitoring the bioavailability of trace metals in environmental solid substrates. Microchim. Acta 154: 3-13.

Näsholm, T., A. Ekblad, A. Nordin, R. Giesler, M. Högberg, and P. Högberg. 1998. Boreal forest plants take up organic nitrogen. Nature 392: 1155-1161.

Nye, P.H., and F.H. Marriott. 1969. A theoretical study of distribution of substances around roots resulting from simultaneous diffusion and mass flow. Plant Soil 30: 459-472.

Öhlund, J. 2004. Organic and inorganic nitrogen sources for conifer seedlings. Diss. Acta Universitatis agriculturae Sueciae. Silvestria, 1401-6230; 312 ISBN 91-576-6546-X

Oyewole, O.A., E. Inselsbacher, and T. Näsholm. 2013. Direct estimation of mass flow and diffusion of nitrogen compounds in solution and soil. New Phytol. in press.

Paungfoo-Lonhienne, C., T.G.A. Lonhienne, D. Rentsch, N. Robinson, M. Christie, R.I. Webb, H.K. Gamage, B.J. Carroll, P.M. Schenk, and S. Schmidt. 2008. Plants can use protein as a nitrogen source without assistance from other organisms. P. Natl. Acad. Sci. USA 105: 4524-4529.

Persson, J., and T. Näsholm. 2001. Amino acid uptake: a widespread ability among boreal forest plants. Ecol. Lett. 4: 434-438.

Rousk, J., and D.L. Jones. 2010. Loss of low molecular weight dissolved organic carbon (DOC) and nitrogen (DON) in H_2O and 0.5 M K_2SO_4 soil extracts. Soil Biol. Biochem. 42: 2331-2335.

Sulyok, M., M. Miro, G. Stingeder, G. Koellensperger. 2005. The potential of flow-through microdialysis for probing low-molecular weight organic anions in rhizospere soil solution. Anal. Chim. Acta 546: 1-10.

Tinker, P.B., and P.H. Nye. 2000. Solute movement in the rhizosphere. Oxford University Press, Inc., New York, USA.

Warren, C.R., and M.T. Taranto. 2010. Temporal variation in pools of amino acids, inorganic and microbial N in a temperate grassland soil. Soil Biol. Biochem. 42: 353-359.

DISTRIBUTION OF EXTRACELLULAR ENZYMES IN SOILS: SPATIAL HETEROGENEITY AND DETERMINING FACTORS AT VARIOUS SCALES

Petr Baldrian

Laboratory of Environmental Microbiology, Institute of Microbiology of the ASCR, v.v.i., Vídeňská 1083, 14220 Praha 4, Czech Republic, E-mail: baldrian@biomed.cas.cz

Abstract

Decomposition of organic matter in soil is mediated by a complex set of extracellular enzymes that are produced by soil fungi and bacteria. Therefore, enzyme activity measurements can suitably represent the turnover of nutrients in soils and litter and can be widely used to explore soil functioning. Previous studies that have been performed at different scales indicate that enzyme distribution in space is highly inhomogeneous. This review summarizes the current knowledge regarding the extent of this spatial variability and the factors that contribute to its establishment. The distribution of enzymes is spatially heterogeneous at various scales. Spatial autocorrelation is recorded for activity of hydrolytic and oxidative enzyme in the range of tens of centimeters to a scale of meters, when considering areas ranging from square meters to hectares. However, enzyme molecules are unevenly distributed even over areas of several centimeters, exhibiting spatial autocorrelation in the range of tens of millimeters. At these scales, patches of nutrients and microbial biomass, plant roots or colonies of specific microorganisms seem to induce high enzyme activity. In such areas, activity of multiple enzymes is often increased. At larger scales, variation of microbial biomass, effect of individual trees and actual soil moisture may shape enzyme distribution. Additionally, when studying a range of several square kilometers, dominant vegetation, land use type and soil physicochemical properties affect enzyme distribution. Because the above factors change over time (the soil moisture content, in particular), the distribution of soil enzymes and the decomposition rates are likely highly dynamic.

https://www.soils.org/publications/sssaj/articles/78/1/11?highlight=&search-result=1

EFFECTS OF ORGANO-MODIFICATION ON THE INTERACTIONS BETWEEN SOIL PARTICLES AND INORGANIC CATIONS AS REVEALED BY WIEN EFFECT MEASUREMENTS

Yujun Wang[1], Chengbao Li[1*], Lingxiang Wang[1,2], Dongmei Zhou[1], Youbin Si[2], Shmulik P. Friedman[3]

[1]Key Laboratory of Soil Environment and Pollution Remediation, Institute of Soil Science, the Chinese Academy of Sciences, Nanjing 210008, China
[2]College of Resources and Environment, Anhui Agricultural University, Hefei 230036, China
[3]Institute of Soil, Water, and Environmental Sciences, Agricultural Research Organization, the Volcani Center, Bet Dagan 50250, Israel
*Corresponding author: E-mail address: chbli@issas.ac.cn, Fax: 086-025-86881000

Abstract

The behavior of soil and clay particles modified with organic cations and anions (surfactants) is of interest mostly in the context of the enhanced retentive properties of the modified particles to organic pollutants. However, the adsorption of organic ions on the surfaces of the soil particles has other consequences, and the present article addresses one of them, i.e., the effects of pre-adsorbed organic ions on the interactions between soil particles and inorganic cations. In order to characterize this effect we applied the previously established method of measuring the Wien effect, i.e., the increase in electrical conductivity of dilute suspensions with increasing applied electrical field. A paddy soil and a latosol were modified with two surfactants – cationic cetyl-trimethylammonium bromide (CTAB) and anionic sodium dodecyl-sulfonate (SDS) – and were used to study the effects of organo-modifiers on the interactions between counter ions and soil particles, by means of Wien effect measurements. The variations with field strength (E) of the electrical conductivities (EC) of the suspensions of the paddy soil were strongly related to the concentration of pre-adsorbed cetyl-trimethylammonium (CTA), whereas the EC vs. E curves of the organo-modified and natural latosol suspensions were almost flat. The mean free binding energies, ΔG_{bi} , of K^+ and Cd^{2+} to the paddy soil decreased with increasing concentration of CTA and the ΔG_{bi} of Cd^{2+} to the natural paddy soil was larger than that of K^+, but the ΔG_{bi} of Cd^{2+} to organo-modified paddy soils were lower than those of K^+. The stripping intensities

(*Is*) of K^+ and Cd^{2+} adsorbed on surfaces of natural paddy soil were 0.155 and 0.165 μS kV^{-1}, respectively; they rapidly decreased with increasing CTA concentration, and then decreased slowly toward zero. In the organo-modified paddy soil *Is* values of K^+ were always larger than those of Cd^{2+}. The *Is* values of inorganic cations adsorbed on surfaces of latosols were close to zero for both the natural and the SDS-modified soil particles.

Abbreviations: AEC, anion exchange capacity; CEC, cation exchange capacity; CTAB, cetyl-trimethylammonium bromide; EC, electrical conductivity; OM, organic matter; NCEC, net cation exchange capacity; NR, neutralization ratio; SDS, sodium dodecyl-sulfonate; SHP, Short high-voltage pulse.

Introduction

Since about 1980 numerous studies of organo-modification of soil (mineral/clay) particles have been reported, mainly in the context of removal of organic pollutants, because of the strong sorptive capabilities of these particles for organic molecules (Boyd et al., 1988; Redding et al., 2002; Ganigar et al., 2010; Radian et al., 2011). Boyd et al. (1988) were among the first to report that soil organo-modification could attenuate the mobility of organic contaminants. Redding et al. (2002), for example, studied the relationship between organo-clay sorption of benzene and total organic carbon content, and, recently, several organo-clay composites were developed for water treatment (Ganigar et al., 2010; Radian et al., 2012). Although several studies (e.g., Meng et al., 2008) characterized the surface properties of the organo-modified soils, the effects of the organo-modification on the interactions between counter ions and soil particles has not been given proper attention. Recently, Meng and Zhang (2005) investigated the Cd adsorption on organo-modified soils and how it was affected by temperature, and Meng et al. (2006) described the CrO_4^{2-} adsorption characteristics of organo-modified soils. It was found that the adsorption capacity for Cd^{2+} increased with temperature and that adsorption decreased, but did not vanish, on modified soils. The effect of temperature on Cd^{2+} adsorption was significantly higher in the tillage layer than in the clay layer of the Lou soil, indicating that chemical adsorption on the tillage layer soil particles is stronger than on the clay layer particles. The CrO_4^{2-} adsorption rate on modified soils did not vary much with increasing CrO_4^{2-} equilibrium concentration in the temperature range from 20°C to 40°C. Upon temperature increase CrO_4^{2-} adsorption on modified

tillage layer soil particles decreased, whereas that on modified clay layer particles depended on both modifier kind and modification rate.

An early study by Levy and Francis (1976) of Cd adsorption to humic acid-modified montmorillonite revealed lower adsorption than that to natural montomorillonite: their data indicated either that Cd and humic acid adsorption sites on A1- or Fe-coated clays were identical, or that prior adsorption of humic acid simply covered available Cd sites. Malakul et al. (1998) found that the maximum Cd-adsorption capacity of a montmorillonite-cetylbenzyldimethylammonium-palmitic acid (M-CBDA-PA) was about 40 mg per gram of clay, and that the affinity constant was about 3.0 mg/L. The metal adsorption has been shown to be mainly through chemical complexation rather than ion exchange, and to be pH dependent.

The present article describes an experimental study of the effects of the interactions between a few counter ions and natural and organo-modified soil particles. Four model inorganic cations – K^{+}, NH^{4+}, Ca^{2+} and Cd^{2+} – were chosen, as being chemically representative of monovalent and divalent cations and in their role as plant nutrients, and an environmental pollutant. The study of the sorptive interactions was based on a previously established method that used a custom-made apparatus (Li and Friedman, 2003) for exploring the interactions between suspended charged particles and counter ions via measurements of the Wien effect. Namely, cheking the increase of the suspension electrical conductivity with increase in the applied, strong – $O(10^7\ \mathrm{V\ m^{-1}})$ – electrical fields (Li et al., 2002, 2003, 2005; Wang et al., 2013).

Materials and Methods

Soil samples

The two model soils used in this study were a paddy soil derived from a yellow-brown soil collected at depths of 100 to 130 cm at Hefei, Anhui, China and a latosol collected at depths of 50 to 100 cm at Xuwen, Guangdong, China. The basic properties of the two natural soils are shown in Table 1. The principal clay fraction of the paddy soil consists of hydromuscovite, minor amounts of vermiculite and kaolinite, and a small percentage of quartz. That of the latosol consists mainly of poorly crystallized kaolinite, some gibbsite, and a small concentration of vermiculite. The clay fractions with particles less

than 2 μm in diameter were separated by sedimentation, dried, and ground. The positive and negative charge densities of the clay fractions of the two soils at various pH levels are presented in Fig. 1. The paddy soil particles carried no significant positive charge, but the latosol charge was variable (Qafoku and Sumner, 2002), and this soil carried both negative and positive charges. At a later stage of the study samples of the clay fractions of the two natural soils were modified with various organic surfactants, the paddy soil with the cationic CTAB and the latosol with the anionic SDS.

Procedures of organo-modification and inorganic cation saturation

The surface modification of soil particles was conducted under wet conditions. The paddy soil and latosol, respectively, were modified with the cationic modifier, cetyl-trimethylammonium bromide (CTAB), and the anionic modifier, sodium dodecyl-sulfonate (SDS), both in the form of analytical grade reagents. Appropriate amounts of the clay fraction of the paddy soil (CEC of 16.3 cmol kg^{-1}) and of CTAB (molecular weight of the 364.44 g mol^{-1}) were weighed to give concentrations of CTAB in soil particles of 0.0326, 0.0815, 0.1467, and 0.2445 mol kg^{-1}. Each required amount of CTAB was first poured into deionized water in a container, heated to 60^0C, and stirred until it dissolved. Note that at the two higher CTAB concentrations in soil particles – 0.1467 and 0.2445 mol kg^{-1} – their concentration in the prepared solutions exceeded the critical micelle concentration of 0.92 mM (the critical micelle concentration is the threshold concentration of dissolved surfactant molecules above which they coagulate to form larger groups called micelles). Then, the appropriate amount of paddy soil was added to the container under continuous stirring; the CTAB was allowed to react with the soil particles for 3 h at a constant temperature of 60^0C, after which the wet samples were filtered under vacuum and rinsed five times with deionized water in order to remove the bromide.

Each of the paddy soil samples, modified with its appropriate amount of CTAB, was divided into two equal parts, into which 0.5-mol L^{-1} solutions of KNO_3 and $Cd(NO_3)_2$, respectively, were added. The suspensions were stirred, shaken for 2 h at 25^0C and centrifuged. The supernatant was discarded, the same solution was added and the above procedure was repeated three times. Subsequently, the precipitate was rinsed repeatedly with deionized water until the electrical

conductivity of the supernatant did not change. The wet soil samples were dried at 60^0C, passed through a 1-mm nylon sieve, and stored for later use.

The SDS weights corresponded to 100% of the anion exchange capacity (AEC) of the natural latosol samples, i.e., a concentration of 0.04 cmol kg^{-1} (Fig. 1), corresponding to a pH value of 5.61 (Table 1), in order to saturate all of the positively charged sites with the dodecyl-sulfonate (DS). The concentration of SDS in the prepared solution was 0.004 mol L^{-1}, which is less than the critical micelle concentration of SDS in water, i.e., 0.0098 mol L^{-1}.

The modification procedure of the latosol was the same as that of the paddy soil: the organo-modified latosol samples were divided into four equal parts, to each of which the appropriate volume of a 0.5-mol.L^{-1} solution of KCl, NH_4Cl, $Ca(Cl)_2$, or $Cd(Cl)_2$, respectively, was added. The latosol samples were subsequently prepared for testing according to the same procedure as above.

Wien effect measurement

Soil suspensions were firstly prepared by adding deionized water to the soil samples in 50-mL plastic bottles to a solid concentration of 10 g L^{-1}. The plastic bottles were sealed and shaken for 30 min, and the suspensions were then dispersed ultrasonically for 45 min and shaken again for 1 h every day. The suspensions were allowed to stand for about 7 to 10 d to achieve sufficient equilibration of ion reactions in the suspensions before the Wien effect measurements were performed. The weak-field electrical conductivities of the soil suspensions were determined with a regular conductivity meter to ensure that they were well within the 500 Ω to 20 kΩ measurement range of the Short High-voltage Pulse (SHP) apparatus. The strong-field EC values of the suspensions were measured with the SHP-2 apparatus at various field strengths between 9 and 220 kV cm^{-1} at a constant temperature of 25°C. The SHP apparatus and its application to Wien effect measurement are described in detail by Li et al. (2002, 2003), Li and Friedman (2003) and Wang et al. (2008). Two cycles of measurements of the Wien effect were conducted, the first progressing from low to high field strengths and the second cycle in the reverse order, to eliminate possible effects of irreversible phenomena such as long-term heating.

Calculations of mean free binding and adsorption energies, and stripping intensity

Wien effect measurements yield the EC-E relationship, i.e., the EC of the suspension vs. the applied field strength (*E*).

After determination of the pH of the suspension, the cation exchange capacity (CEC) of the unmodified soil (Fig. 1) can be used for evaluating the net CEC (NCEC), according to the difference between the original CEC and the amount of CTA adsorbed. Then the following equation is used to evaluate the mean Gibbs free binding energies (Li et al., 2005):

$$\Delta G_{bi} = RT \ln \frac{2NCEC \times C_p \times \lambda}{EC_0} \qquad (1)$$

in which R is the universal gas constant (8.315 J mol^{-1} K^{-1}), T is the thermodynamic temperature (K), NCEC the net cation exchange capacity, C_p the solid concentration of the suspension (g L^{-1}), and λ the equivalent conductivity (mS cm^{-1} mol^{-1} L) of the cation and EC_0 is the weak-field electrical conductivity.

The mean Gibbs free binding energy (ΔG_{bi}), derived from the measured EC_0, is a mean value representing the whole spectrum of adsorption energies of the given counter ion. Wien effect measurements enable evaluation of the distribution of adsorption energies, i.e., the fraction of counter ions adsorbed at a given energy. The expression for evaluating the mean free adsorption energy, i.e., the mean adsorption energy of the population of counter ions stripped off the particle surfaces as the applied field strength was increased from zero to the given strong field strength (*E*), as derived from conservative thermodynamics is (Li et al., 2005)

$$\Delta G_{ad} = RT \ln (EC/EC_0) \qquad (2)$$

in which EC and EC_0 represent the electrical conductivities of the suspension under the strong and the weak electrical fields, respectively. Application of this expression to a series of Wien effect (EC-E) measurements can provide the spectrum of the counter ion adsorption energies.

On the basis of the analysis of polarization processes occurring in soil suspensions subjected to strong fields (Wang et al., 2009), it can be safely argued that beyond

(towards higher E values) the local minima of the EC-E curves, the process of stripping off of adsorbed counter ions dominates, and the stripping intensity, *Is*, can be characterized by the slope of the assumed linear *EC* vs. *E* relationship:

$$Is = \Delta EC/\Delta E \qquad (3)$$

in which ΔEC is the increment in the *EC* of the suspension as the field strength increases by ΔE, and $\Delta E = Eh - Em$, with *Eh* taken to be larger than *Em* by 30 to 100 kV cm^{-1}.

Zeta potential measurement

Samples of the suspensions used for the Wien effect measurements were diluted with deionized water to a solid concentration of 0.5 g L^{-1}. No supporting electrolytes were added, in order to ensure that the electrokinetic properties of the soil particles saturated with the various inorganic cations were evaluated in poorly conducting background solutions. After the suspensions had been dispersed ultrasonically for 45 min and shaken for 1 h they were equilibrated for one to two days, after which the zeta potentials, which are the potentials at the slipping planes of the double layers of the colloidal particles, were determined by electrophoretic mobility measurements with a JS94H Micro-Electrophoresis Meter (Powereach Digital-Technical Equipment Company, Shanghai, China) as follows. A 0.5-mL sample of the suspension was placed in the special electrophoresis cup, the electrode was inserted into the cup and the focus of the cup was adjusted so that the clear marker “+" was displayed on the computer screen. The zeta potentials of the soil particles were automatically calculated by the meter after the relevant parameters had been inserted, based on photographs of 20 tested particles. Twenty particles were sufficient to determine the electrophoretic velocities of the tested suspension with a coefficient of variation smaller than 5%. The zeta potential was evaluated by using the Helmholtz-Smoluchowski equation, derived for a spherical particle with relatively low surface charge density, and applicable to thin-double-layer conditions (Hunter, 1981).

Results and Discussion

EC-E curves of organo-soil suspensions

Figures 2 and 3, respectively, show the EC-E curves of organo-modified paddy soil saturated with K^+ and Cd^{2+}, and of organo-modified latosol saturated with various

chlorides; the curves presented in Figs 2 and 3 were derived from the Wien effect measurements. It is clear that the variations with field strength, in the EC values of the paddy soil suspensions, were related to the concentration of adsorbed quaternary amines (CTA) (Fig. 2). The EC-E curves for both inorganic cations and for adsorbed CTA concentrations in the range of 0.0815 to 0.2445 mol kg^{-1} are almost flat, but those for suspensions of paddy soil saturated with K^+ for CTA concentrations of 0 and 0.0326 mol kg^{-1} rise monotonically over the field strength ranges of 14 to 140 kV cm^{-1} and of 90 to 160 kV cm^{-1}, respectively, and there was no negative Wien effect in these ranges of field strength (Fig. 2a). The EC/-E curves of the suspensions of paddy soil saturated with Cd^{2+} for the CTA concentrations of 0 and 0.0326 mol kg^{-1} rise over the field strength ranges of 66 to 160 kV cm^{-1} and of 94 to160 kV cm^{-1}, respectively, and a significant negative Wien effect is evident at lower field strengths (Fig. 2b). In previous studies that addressed the Wien effects of mono- and divalent cations adsorbed on unmodified soil particles different forms of the EC-E curves were obtained at low to medium fields (Wang et al., 2009) – differences that reflect the differing binding strengths of mono- and divalent cations to soil particles, and the various different polarization mechanisms. In the present study the neutralization ratio (*NR*), which is the ratio between the amount of cationic modifier and the – pH-dependent – CEC of modifier-free paddy soil particles, was less than 0.97 (Table 2). Thus, it can be safely assumed that the added amounts of CTA were all adsorbed on the surfaces of the soil particles and that they neutralized increasing proportions of the particles' negative charge sites as the CTA amounts increased. Zhang et al. (1993), for example, showed that when various amounts of CTA (60-100% of the CEC) were added to Na- and K-montmorillonite particles, practically all of the CTA, i.e., 99.2-99.7% of the added amounts was adsorbed to the clay particles. The adsorption of the larger organic molecules to the surfaces of soil particles was much stronger than that of the inorganic cations, mostly because of hydrophobic interactions (Rytwo et al., 1996). Thus, it safely can be assumed that in the Wien effect measurements the inorganic cations were being stripped off whereas the organic ions remain adsorbed to the surfaces.

The data presented in both Fig. 2 and Table 2 reveal that when the *NR* was larger than 0.3 the EC-E curves were almost flat. This indicates that the pre-adsorbed oriented CTA molecules on the surfaces of the soil particles impeded the adsorption of the inorganic cations, that otherwise would have been stripped off from the particles at varying

electrical field strengths, on the unoccupied negative sites. This interference was slightly more significant for K^+ than for Cd^{2+}, as indicated by the contrasting trends of generally increasing EC_0 values of the Cd^{2+} suspensions with increasing concentrations of pre-adsorbed CTA, on the one hand, and of decreasing EC_0 values of the K^+ suspensions with increasing concentrations of CTA, on the other hand. However, the flat EC-E curves imply that the adsorbed oriented CTA molecules masked the applied electrical field, and thereby partly protected the counter ions against being stripped off the surfaces. The monovalent counter ion, K^+, was located further from the surfaces of the colloidal particles than the divalent counter ion, Cd^{2+}, as was manifested also in the higher ζ potentials of K^+-saturated soil particles than of Cd^{2+}-saturated ones. This is discussed below.

The EC-E curves of latosol suspensions that were modified with SDS and saturated with various inorganic cations, as well as those of the unmodified latosols saturated with various chlorides are almost flat lines (Fig. 3). Complex mechanisms stand behind this pattern. The positive charge densities of the latosol particles were 42-78% of the negative charge densities in the tested pH range of 4.4-4.8 (Zhu et al., 2009), and this would have reduced the probability of release of cations and anions under the influence of strong electrical fields, because of the mutual charge neutralization of the positive and negative sites (Qafoku and Sumner, 2002). In addition, the mutual masking of the positive and negative diffuse layers – located near the negatively and positively charged sites, respectively – on the surfaces of latosol particles reduced the effect of the external strong field, and thereby impeded the stripping off of the cations and anions from the surfaces of the latosol particles (Zhu et al., 2009).

Comparison between the weakest-field measurements of Fig. 3a and Fig. 3b – note the differing ordinate scales – reveals that the EC_0 values of the suspensions of DS-modified latosol particles were larger by 28 to 29 μS cm^{-1} than those of the suspensions of unmodified latosol particles saturated with the relevant chlorides (Table 3). From these results it can be deduced that the dodecyl-sulfonate did not truly neutralize the positive charge sites on the surfaces of the latosol particles, but only adhered to their surfaces, i.e., there was no electrical binding of the DS to the latosol particles, and the adsorption of the DS did not alter the mutual masking of the positive and negative diffuse layers on the surfaces of latosol particles. Thus, the EC values of the suspensions

of the DS-modified latosol did not change as the external field strength changed (Fig. 3a) – behavior similar to that of natural, unmodified latosol particles.

Mean free binding energy in relation to the concentration of organic modifier

The parameters required for calculating the mean free binding energy (ΔG_{bi}) from the EC_0 measurements by means of Eq. 1, and the mean free binding energies of K^+ and Cd^{2+} to the paddy soil are presented in Table 4. Since almost 100% of the added quaternary amine (cetyltrimethylammonium, CTA) was adsorbed on the clay particles (Zhang et al., 1993), the net cation exchange capacity (NCEC) at the prescribed pH can be considered as the CEC of CTA-free paddy soil minus the CTA concentration, as listed in Table 4. It can be seen that the mean free binding energies, ΔG_{bi} , of K^+ and Cd^{2+} to the paddy soils always decreased with increasing concentration of pre-adsorbed CTA, i.e., as the NCEC decreased. Interestingly, the ΔG_{bi} of Cd^{2+} to the original paddy soil particles was larger than that of K^+, but the ΔG_{bi} values of Cd^{2+} to the organo-modified paddy soils were lower than those of K^+ at similar CTA concentrations. These results suggest that there might have been complexation between the adsorbed inorganic cations and CTA, and that there was more complexation for Cd^{2+} than for K^+. Complexation would lead to larger fractions of ionized Cd^{2+} in the suspensions, and this, in turn, would enhance the electrical conductance of the Cd^{2+}. Previous studies (Meng and Zhang, 2005; Zhang et al. 2004) showed that the complexation between Cd^{2+} and organic matter could result in dissociation of Cd^{2+} adsorbed on surfaces of soil particles.

Mean free adsorption energy in relation to the concentration of organic modifier

The mean free adsorption energies of K^+ and Cd^{2+} on the surfaces of the paddy soil particles modified with various concentrations of CTA at measured field strengths, as evaluated from the corresponding EC-E curves (Fig. 2) by means of Eq. 2 are presented in Fig. 4. Sample evaluated ΔG_{ad} values for CTA concentrations of 0 and 0.03 mol kg^{-1} at four field strengths (50, 100, 130, and 160 kV cm^{-1}) are also listed in Table 5. For the two CTA concentrations of 0 and 0.03 mol kg^{-1} there was a range of positive adsorption energies at certain field strengths, whereas for the higher CTA concentrations the adsorption energies were all negative. At a field strength of 130 kV cm^{-1} the ΔG_{ad} values of K^+ and Cd^{2+} on unmodified paddy soil were similar, but the ΔG_{ad} values of K^+ and Cd^{2+} on the paddy soil modified with CTA at 0.03 mol kg^{-1} were

0.308 and 0.0510 kJ mol^{-1}, respectively. This was possibly because the Cd^{2+} and CTA formed a chelate, which would adhere tightly to the soil particles with almost none being released (Houghton. 1979), thus decreasing the fraction of the total adsorbed Cd^{2+} that was electro-adsorbed. Consequently, this would lead to an apparent reduction of the adsorption energy of Cd^{2+} on the surfaces of the soil particles, because the stripped-off, chelated Cd^{2+} would not increase the electrical conductivity of the suspension.

Stripping intensity of inorganic cations in relation to the concentration of organic modifier

The stripping intensities of inorganic cations adsorbed on surfaces of paddy soil particles in strong electrical fields, as calculated with Eq. 3, were closely related to the concentrations of adsorbed CTA (Fig. 5). Clearly, the stripping intensities of K^+ and Cd^{2+} adsorbed on the surfaces of the original paddy soil particles were much higher – 0.155 and 0.165 μS kV^{-1}, respectively – and they rapidly decreased exponentially at higher CTA concentrations. The stripping intensity of K^+ adsorbed on the surfaces of original paddy soil particles was lower than that of Cd^{2+} by 0.01 μS kV^{-1}, but for all concentrations of CTA the stripping intensities of K^+ were larger than those of Cd^{2+}, which was partly because of the differing equivalent conductivities of the K^+ and Cd^{2+}: 73.5 and 54 mS L cm^{-1} mol^{-1}, respectively

These results indicate that the organo-modifier neutralized the negative charge on the surfaces of the paddy soil particles, thus reducing the concentration of adsorbed inorganic cations that could be stripped off by high external fields. It also seems that complexation between the Cd^{2+} ions and the organic modifier resulted in lower stripping intensities of Cd^{2+} than of K^+ from the surfaces of CTA-modified paddy soil particles**.**

The stripping intensities of inorganic cations adsorbed on the surfaces of SDS-modified latosol particles were practically zero, as is evident from their flat EC-E curves (Fig. 3a).

Zeta potentials of organo-soil particles

The ζ potentials of particles of paddy soil modified with various concentrations of CTA and saturated with K^+ and Cd^{2+} are shown in Fig. 6. The ζ potential of the paddy soil particles saturated with both K^+ and Cd^{2+} cations increased, i.e., became less negative,

as the concentration of CTA increased up to 0.15 mol kg^{-1}. As the CTA concentration increased further, from 0.15 to 0.24 mol kg^{-1}, the ζ potential became more negative. In the CTA concentration range of 0 to 0.15 mol kg^{-1}, which was below 58% of the CEC of paddy soil (Table 2) and also below the critical micelle concentration of CTA, the ζ potentials gradually increased from -64 to -35 mV because of electrostatic adsorption of the CTA cations on the surfaces of the paddy soil particles, partly neutralizing their negative charges. Nevertheless, at a CTA concentration of 0.24 mol kg^{-1}, corresponding to about 95% of the paddy soil CEC (Table 2), the ζ potentials of the soil particles saturated with both K^+ and Cd^{2+} decreased to about -50 mV. The mechanism behind this phenomenon is unknown at present and should be further investigated; it might be associated with formation of micelles above the critical micelle concentration and looser, non-electrostatic adsorption of the micellized surfactant on the surfaces of the soil particles.

The zeta potentials of latosol particles modified with SDS at 0.0715 mol kg^{-1} (corresponding to 100% of its AEC), and saturated with K^+, NH_4^+, Ca^{2+}, and Cd^{2+} were -22, -39, -28, and -27 mV, respectively.

Conclusions

The effect of pre-adsorbed organic cation (CTAB) and anion (SDS) on the adsorption energy relationships between inorganic cations and particles of a paddy soil and a latosol were inferred from measurements of electrical conductivity under weak field conditions and from Wien effect measurements in dilute suspensions of soil particles. The mean free binding energies of K^+ and Cd^{2+} to the paddy soil decreased with increasing concentration of CTA and the mean free binding energy of Cd^{2+} to the natural paddy soil was larger than that of K^+, but the mean free binding energies of Cd^{2+} to organo-modified paddy soils were lower than those of K^+. The mean free adsorption energy of Cd^{2+} on the paddy soil modified with a small CTA concentration, inferred from the Wien effect measurements, was also lower than that of K^+. The effect of the pre-adsorbed CTA on the binding energies indicate that the organo-modifier neutralized the negative charge on the surfaces of the paddy soil particles, thus reducing the concentration of adsorbed inorganic cations that could be stripped off by high external fields. The flat EC-E curves exhibited with the SDS-modified latosol particles indicate

that the dodecyl-sulfonate did not truly neutralize the positive charge sites on the surfaces of the latosol particles, but only adhered to their surfaces, i.e., there was no electrical binding of the DS to the latosol particles.

The mean Gibbs free binding energies evaluated from measurements of electrical conductivity at weak fields were comparable with those evaluated from measurements of ion activity with selective electrodes (Zhou et al., 2010). Thus, it safely can be assumed that the mean Gibbs free adsorption energies evaluated from the Wien effect measurements are also plausible, and that this applies also to adsorption of inorganic cations on organo-modified and unmodified soil particles. The results and conclusions of the present study apply also to other inorganic cations, organic ions and soil types, and enhance our understanding of the effects of organic ions on adsorption of inorganic cations on soil particles. A better understanding of the effects of modification of soil particles with organic ions on their interactions with inorganic cations is essential for evaluating the fate of the inorganic ions always present in natural soils or in packed-bed reactors comprising organo-modified soil and clay particles.

Acknowledgement
We acknowledge the support of the National Natural Science Foundation of China, under Project no. 40871114.

Table 1. Basic properties of the tested soils

Soil	Place	Depth	pH	Organic matter	CEC	Fe_2O_3
		cm		g kg^{-1}	cmol kg^{-1}	g kg^{-1}
Paddy soil	Hefei, Anhui	100-130	6.69	5.2	16.3	97.5
Latosol	Xuwen,Guangdong	50-100	5.61	7.0	7.15	156.4

Table 2. Neutralization ratio (*NR*) of negative charge sites on the surfaces of the paddy soil particles modified with various concentrations of CTA, and saturated with K^+ and Cd^{2+}

Cation	K^+					Cd^{2+}				
CTA conc. mol kg^{-1}	0	0.0326	0.0815	0.1467	0.2445	0	0.0326	0.0815	0.1467	0.2445
NR	0	0.118	0.296	0.533	0.889	0	0.129	0.322	0.580	0.966

Table 3. Weak-field conductivity values ($EC_{0,}$ μS cm^{-1}) of the latosol suspensions (retrieved from Fig. 3)

Treatment	K^+	NH_4^+	Ca^{2+}	Cd^{2+}
I unmodified	15.2	19.2		11.2
II DS-modified	44.6	47.6	32.7	39.6
II – I	29.4	28.4		28.4

Table 4. The concentrations of CTA used for modification; weak-field (approximately 10 kV cm^{-1}) electrical conductivity (EC_0); pH of the tested paddy soil suspensions with solids concentration (C_p) of 10 g L^{-1}; net cation exchange capacity at prescribed pH (NCEC), equivalent conductance (λ) of adsorbed cations, fraction of ionized ions in low electrical fields ($f_0 = EC_0/(2\ \text{NCEC}\ C_p\ \lambda)$), and mean Gibbs free binding energy (ΔG_{bi}).

Cation	CTA conc.	pH	EC_0	Λ	NCEC	f_0	ΔG_{bi}
	mol kg^{-1}		μScm^{-1}	mS L cm^{-1} mol^{-1}	mol kg^{-1}		kJ mol^{-1}
K^+	0	5.89	20.0	73.52	0.275	0.0493	7.46
	0.0326	5.91	20.7	73.52	0.242	0.0580	7.06
	0.0815	6.05	18.2	73.52	0.194	0.0641	6.81
	0.1467	6.13	18.5	73.52	0.128	0.0982	5.75
	0.2445	5.63	12.1	73.52	0.0305	0.269	3.26
Cd^{2+}	0	4.89	10.4	54	0.253	0.0379	8.11
	0.0326	5.28	16.1	54	0.220	0.0675	6.69
	0.0815	5.35	14.5	54	0.172	0.0782	6.32
	0.1467	5.41	20.2	54	0.106	0.188	4.15
	0.2445	5.01	12.7	54	0.0085	0.906	0.245

Table 5. Mean Gibbs free adsorption energies (kJ mol^{-1}) of K^+ and Cd^{2+} adsorbed on the surfaces of the paddy soil modified with various concentrations of CTA at several field strengths

Field strength,	K^+		Cd^{2+}	
kV cm^{-1}	Concentration of CTA, mol kg^{-1}			
	0	0.03	0	0.03
50	0.208			
100	0.775	0.076	0.218	
160		0.514	1.993	0.392

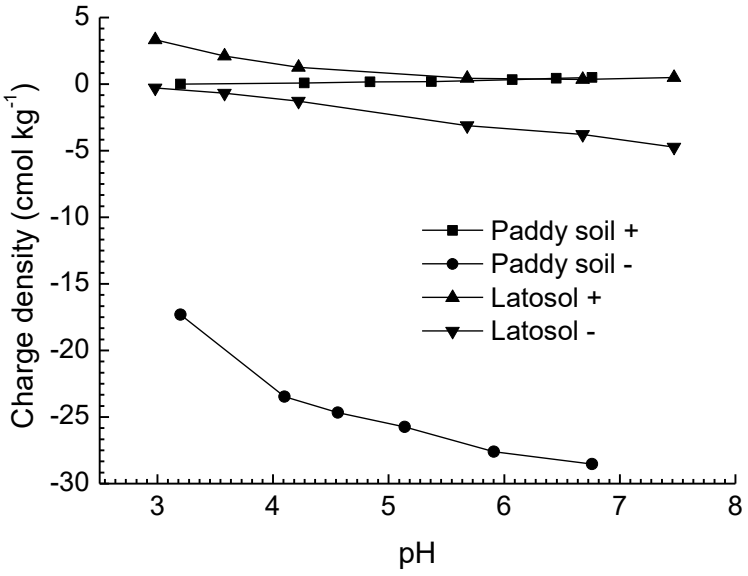

Fig. 1. Changes in positive and negative charge densities of the tested soils with changing pH

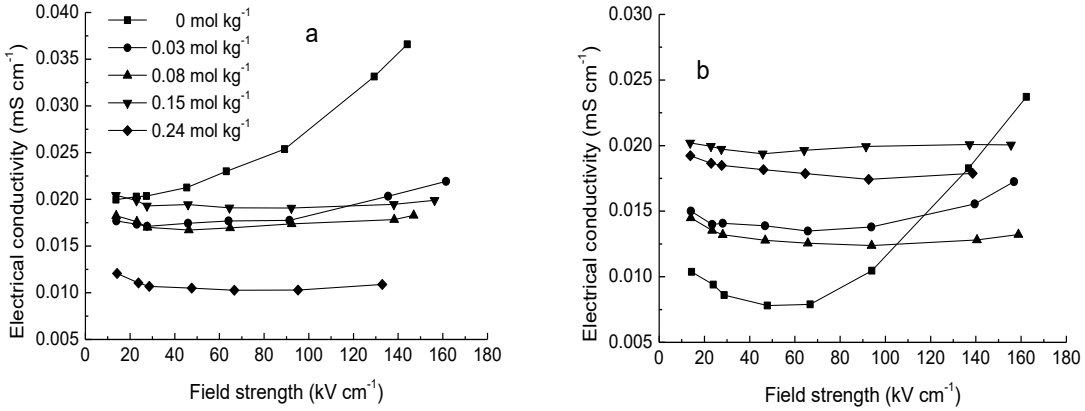

Fig. 2. Dependence on the field strength of the EC of suspensions (at 10 g L^{-1}) in deionized water, of the paddy soil modified with various concentrations of CTA, and saturated with K^+ (a), and Cd^{2+} (b)

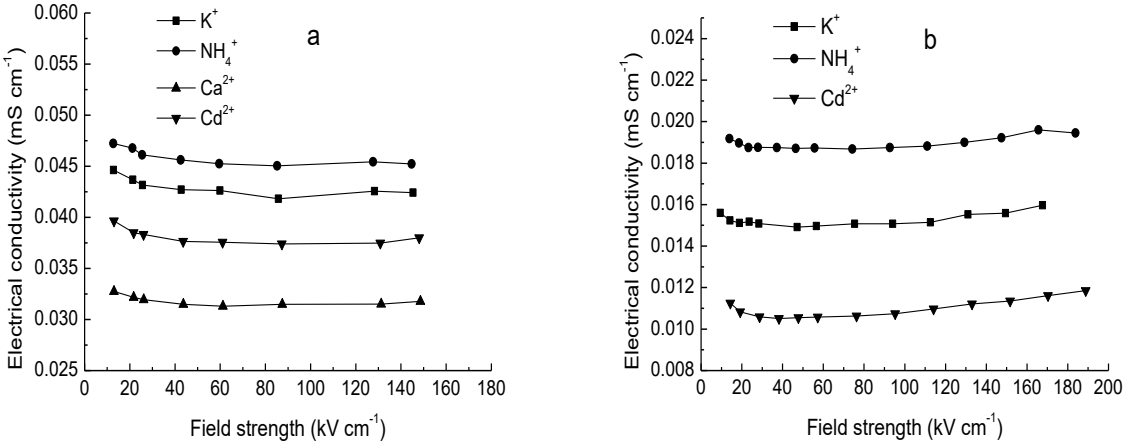

Fig. 3. Dependence on the field strength of the EC of suspensions (at 10 g L^{-1}) in deionized water, of SDS-modified (a) and unmodified (b) latosol saturated with various cations/chlorides

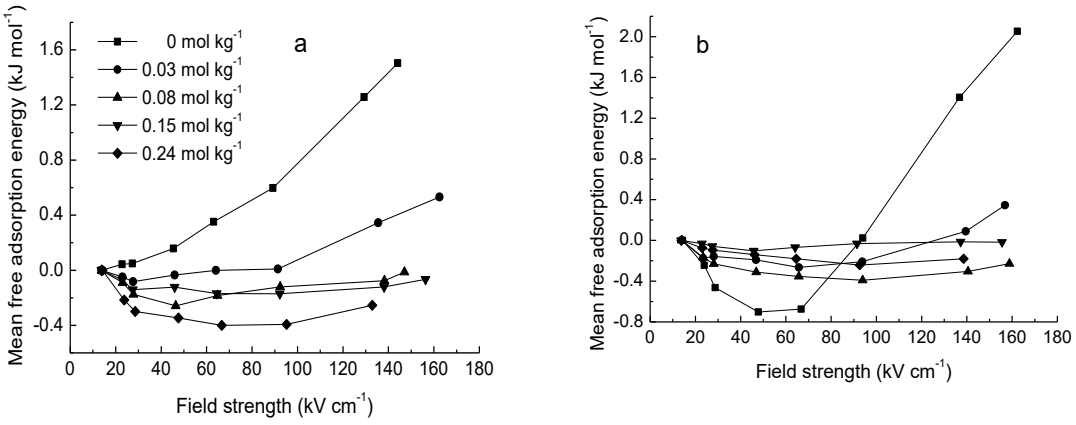

Fig. 4. Mean Gibbs free adsorption energies as a function of field strength for paddy soil suspended in deionized water (at 10 g L^{-1}), and modified with various concentrations of CTA and saturated with K^+ (a) and Cd^{2+} (b)

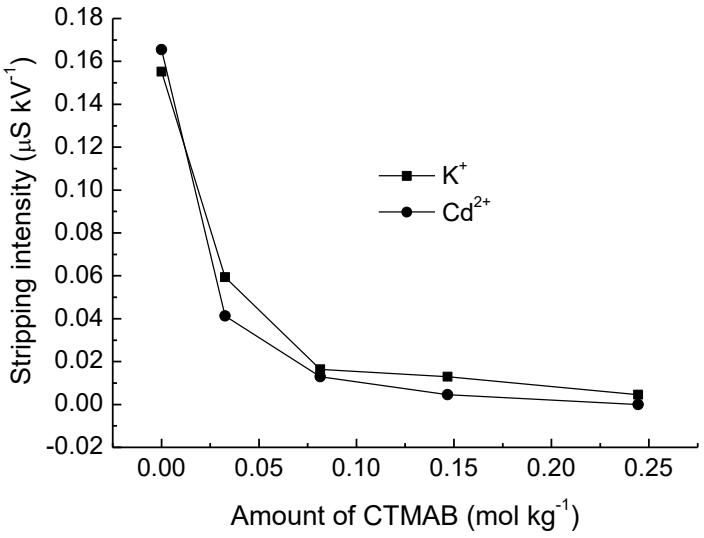

Fig. 5. Stripping intensities of adsorbed cations on the surfaces of the paddy soil particles modified with CTA, as a function of the CTA concentration.

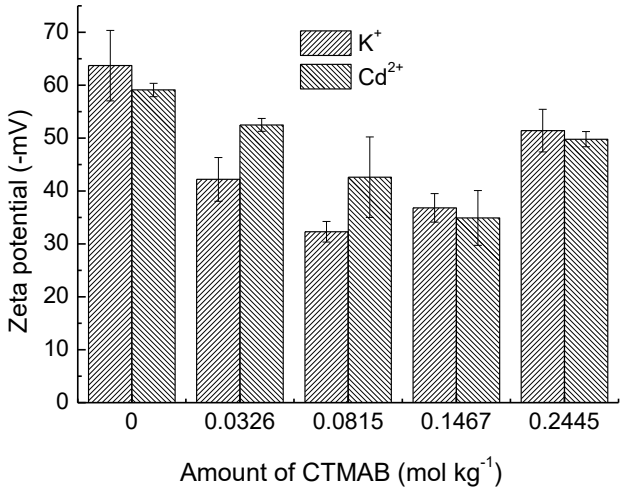

Fig. 6. Zeta potentials of paddy soil particles modified with various concentrations of CTA and saturated with K^+ and Cd^{2+} in deionized water.

References

Boyd, S. T., J. F. Lee and M. M. Mortland. 1988. Attenuating organic contaminant mobility by soil modification. Nature 333: 345-347.

Ganigar R., G. Rytwo, Y. Gonen, A. Radian and Y. G. Mishael. 2010. Developing polymer-clay nanocomposites for the removal of trichloro- and trinitro-phenol from water. Appl. Clay Sci. 49: 311-316.

Houghton, R. P. 1979. Metal Complexes in Organic Chemistry. Cambridge University Press, London.

Hunter, R. J. 1981. Zeta Potential in Colloid Science: Principles and Applications. Academic Press, London.

Levy, R. and C. W. Francis. 1976. Adsorption and desorption of cadmium by synthetic and natural organo-clay complexes. Geoderma 15: 361-370.

Li, C. B. and S. P. Friedman. 2003. An apparatus for measuring the Wien effect in suspensions. Colloid. Surf. A. 222: 133-140.

Li, C. B., S. P. Friedman and A. Z. Zhao. 2002. Wien effect in suspensions of electrodialyzed soil particles and its influencing factors. Pedosphere 12: 235–242.

Li, C. B., S. P. Friedman and A. Z. Zhao. 2003. Interactions of cations with electrodialyzed clay fraction of soils as inferred from Wien effect in soil suspensions. Pedosphere 13: 59–66.

Li, C. B., A. Z. Zhao and S. P. Friedman. 2005. A new method to estimate adsorption energies between cations and soil particles via Wien effect measurements in dilute suspensions and an approximate conductivity-activity analogy. Environ. Sci. Technol. 39: 6757-6764.

Malakul, P., K. R. Srinivasa and H. Y. Wang. 1998. Metal adsorption and desorption characteristics of surfactant modified clay complexes. Ind. Eng. Chem. Res. 37: 4296-4301.

Meng, Z. F. and Y. P. Zhang. 2005. Cd adsorption of organic modified soils and its temperature effect. Acta Pedol. Sin. 42: 238-246. (in Chinese)

Meng, Z. F., Y. P. Zhang and N. Gong. 2006. CrO42- adsorption characteristics of loess soils modified with organic substances. Acta Pedol. Sin. 43: 104-110. (in Chinese)

Meng, Z. F., Y. P. Zhang and Z. Y. Guo. 2008. Surface characteristics of organic modified soil I CEC and specific surface area. Acta Pedol. Sin. 45: 370-374. (In Chinese)

Qafoku, N. P. and M. E. Sumner. 2002. Adsorption and desorption of indifferent ions in variable charge subsoil: The possible effect of particle interactions on the counter-ion charge density. Soil Sci. Soc. Am. J. 66: 1231-1239.

Radian A., M. Carmeli, D. Zadaka-Amir, S. Nir, E. Wakshal and Y. G. Mishael.2011. Enhanced removal of humic acid from water by micelle-montmorillonite composites: Comparison to granulated activated carbon. Appl. Clay Sci. 54: 258-263.

Redding, A. Z., S. E. Burns, R. T. Upson and E. F. Anderson. 2002. Organoclay sorption of benzene as a function of total organic carbon content. J. Coll. Interface Sci. 250: 261-264.

Rytwo, G., S. Nir and L. Margulies. 1996. Adsorption and interactions of diquat and paraquat with montmorillonite. Soil Sci. Soc. Am. J. 60: 601-610.

Wang, Y. J., C. B. Li, W. Wang, D.M. Zhou, R. K. Xu and S. P. Friedman. 2008. Wien effect determination of adsorption energies between heavy metal ions and soil particles. Soil Sci. Soc. Am. J. 72: 56-62.

Wang, Y. J., C. B. Li, W. Wei, J. Jiang, D. M. Zhou, R. K. Xu and S. P. Friedman. 2009. Negative Wien effect measurements for exploring polarization processes of cations interacting with negatively charged soil particles. Soil Sci. Soc. Am. J. 73: 569-578.

Wang, Y.J, C.B. Li, D.M. Zhou, and S.P. Friedman, S. P. 2013. Wien effect in suspensions and its applications in soil science: A review. In Advances in Agronomy, Elsevier, The Netherlands, in press.

Zhang, G. Y., Y. Y. Dong, X. Y. Li, Y. Li and H. J. Li. 2004. Sorption-desorption of Cd2+ ion in several soil colloids in the presence of oxalic acid and citric acid. Acta Pedol. Sin. 41: 558-563. (In Chinese)

Zhang, Z. Z., D. L. Sparks and N. C. Scrivner. 1993. Sorption and desorption of quaternary amine cations on clays. Environ. Sci. Technol. 27: 1625-1631.

Zhou J, C. B. Li, C. Cheng, Y. J. Wang, D. M. Zhou and L. X. Zhou. 2010. Comparison between ion activity method and suspension Wien effect method in determining binding energy between soils and monovalent cations (in Chinese). Acta Pedologica Sinica 47:1151-1158.

Zhu, H. W., Y. J. Wang, Y. J., Zhou, J., Jiang, C. B. Li, D. M. Zhou and S. P. Friedman 2009. Wien effect characterization of the interactions between ions and charged sites on surfaces of variable-charge soils. Pedosphere 19: 545-553.

A Novel Method Combining FTIR-ATR Spectroscopy and Stable Isotopes to Investigate the Kinetics of Nitrogen Transformations in Soils

Oz Kira, Raphael Linker and Avi Shaviv

Faculty of Civil and Environ. Eng. Technion–Israel Institute of Technology Technion City Haifa 3200003 Israel

Abstract

Understanding and quantifying N transformations in soil is critical for sustainable use of this important plant nutrient and for understanding the mechanisms through which polluting N species are discharged to the environment. Advanced methods such as the "isotope dilution technique", which uses stable N-isotopes to estimate gross mineralization and nitrification rates, answer this need. In this study the use of Fourier transform infrared-attenuated total reflectance (FTIR-ATR) spectroscopy for measuring isotopic N species concentrations directly in soil pastes was tested as a complementary technique to the commonly used isotope ratio mass spectrometry (IRMS). It is shown that, with proper chemometric tools (e.g., partial least squares [PLS]), FTIR-ATR enables simple tracking of changes in the concentrations of the isotopic species of nitrate and ammonium and allows estimation of the gross reaction rates of N transformations in soil. Soil incubations were performed by adding either $^{15}NO_3^-$ or $^{15}NH_4^+$ to the soils. The incubations with added $^{15}NH_4^+$ yielded a gross mineralization rate of 6.1 mg N kg^{-1} dry soil d^{-1} compared with a net mineralization rate of 4.1 mg N kg^{-1} dry soil d^{-1} and a gross nitrification rate of 40.9 mg N kg^{-1} dry soil d^{-1} compared with a net nitrification rate of 29.5 to 25.3 mg N kg^{-1} dry soil d^{-1}. The incubations with added $^{15}NO_3^-$ yielded a gross nitrification rate of 18.6 mg N kg^{-1} dry soil d^{-1} compared with a net nitrification rate of 11.9 to 18.3 mg N kg^{-1} dry soil d^{-1}. The combined use of FTIR-ATR and $^{15}NO_3^-$ or $^{15}NH_4^+$ enrichment appears to provide an effective tool for almost real-time quantification of N-dynamics in soils with minimal interference.

https://www.soils.org/publications/sssaj/articles/78/1/54?highlight=&search-result=1

Session 4: Microbial Effects on Nitrogen Cycling

DISCRIMINATING SOIL NITRIFICATION CONTRIBUTIONS OF AMMONIA-OXIDIZING THAUMARCHAEA AND BACTERIA USING ALIPHATIC N-ALKYNES

Peter J. Bottomley[1,2*], Anne E. Taylor[1], Andrew T. Giguere[1], Alix I. Gitelman[3] and David D. Myrold[1]

[1]Department of Crop and Soil Science, 3017 Agricultural Life Science Building,
[2]Department of Microbiology, 220 Nash Hall,
[3]Department of Statistics, 48 Kidder Hall, Oregon State University, Corvallis, OR 97331
[*]Corresponding author: 541-737-1844 (phone) 541-737-0496 (fax)
peter.bottomley@oregonstate.edu

Abstract

Ammonia (NH_3)-oxidizing bacteria (AOB) and thaumarchaea (AOA) co-occupy most soils. We developed a short-term, growth-independent method to determine their relative contributions to nitrification in slurry and whole soil assays. Microbial monooxygenases differ in their vulnerability to inactivation by aliphatic n-alkynes, and evidence was obtained that NH_3 oxidation carried out by soil-borne AOA were insensitive to a C_8 alkyne, 1-octyne. In incubations (21 or 28 d) of two different whole soils, both acetylene and octyne effectively prevented NH_4^+-stimulated increases in AOB population densities, but octyne did not prevent increases in AOA population densities that were prevented by acetylene. Furthermore, octyne-resistant, NH_4^+-stimulated net nitrification rates of 2 and 7 µg N/g soil/d persisted throughout the incubation of the two soils. Other evidence that octyne-resistant nitrification was due to AOA included: 1) a positive correlation of octyne-resistant nitrification in soil slurries of cropped and noncropped soils with allyl-thiourea resistant activity (100 µM, r^2= 0.938), and 2), the fraction of octyne-resistant nitrification in soil slurries correlated with the fraction of nitrification that recovered from irreversible acetylene inactivation in the presence of bacterial protein synthesis inhibitors (r^2= 0.905), and with the octyne-resistant fraction of NH_4^+-saturated net nitrification measured in

whole soils (r^2= 0.884). Octyne can be useful in short-term assays to discriminate AOA and AOB contributions to soil nitrification.

Abbreviations: Ammonia oxidizing bacteria (AOB), Ammonia oxidizing thaumarchaea (AOA), Nitrification potential (NP), Recovered nitrification potential (RNP), Allyl-thiourea (ATU), Monooxygenase (MO), Aqueous phase concentrations (C_{aq}), Corvallis cropped (CC), Corvallis pasture (CP), Klamath cropped (KC), Klamath woodlot (KW), Pendleton, cropped (PC), Pendleton grassland (PG), Madras cropped (MC), Madras rangeland (MR), Octyne (oct), Bacterial antibiotics (ab), Whole soil (WS)

Introduction

For about a century most ammonia (NH_3) oxidation in soils was thought to be carried out by chemolithoautotrophic NH_3-oxidizing bacteria (AOB). In 2005, the nitrification paradigm changed with the discovery of another type of microorganism (Thaumarchaea) that performs NH_3-oxidation (Konneke et al., 2005). Molecular techniques have shown that NH_3-oxidizing Thaumarchaea (AOA) are widely distributed in soils throughout the world (Leininger et al., 2006; Pester et al., 2012). Because AOA are usually more numerous in soil than AOB, this led to speculation about the extent to which AOA contribute to soil nitrification (Hatzenpichler, 2012; Prosser and Nicol, 2012). The evidence for AOA contributing to soil nitrification has arisen from enrichment approaches involving long incubations (4 – 6 weeks) of soil in the laboratory where NH_3-oxidation was accompanied either by the incorporation of ^{13}C-CO_2 into thaumarchaeal DNA (Jia and Conrad, 2009; Pratscher et al., 2011; Xia et al., 2011; Zhang et al., 2010), or by acetylene preventing an increase in gene copies of the ammonia monooxygenase subunit A (*amo*A) of AOA (Offre et al., 2009; Verhamme et al., 2011) supported by either mineralization of soil organic N, or by repeated amendments of low amounts of NH_4^+.

Our goal has been to develop short-term assays (≤48 h) that are growth independent and directly measure the potential rates of soil nitrification attributable to either AOA or AOB. We have taken advantage of the fact that acetylene specifically and irreversibly inactivates AMO of both AOB and AOA (Hyman and Wood, 1985; Offre et al., 2009). After exposure and removal of acetylene (6 h), the recovery of NH_3-oxidizing activity in soil slurries was monitored ±antibiotics targeted at bacterial protein synthesis to discriminate between the relative contributions of AOA and AOB to the recovered nitrification potential activity (RNP). We showed that AOA dominate nitrification potentials (NP) of soil samples taken from pastures (Taylor et al., 2010), and that AOB

dominate NPs of soils cropped to wheat and recently fertilized with inorganic N. We showed that the relative contributions of AOA and AOB to NPs differed across the cropped and fallowed phases of a two-year winter wheat rotation, and were affected by the time since N fertilization and by seasonal soil conditions (Taylor et al., 2012). In the search for a strategy that would be more practical for unsaturated whole soils we reasoned that whereas monooxygenases (MO) generally have a broad substrate range, some are more restricted than others (Ensign, 2001; Keener et al., 1998; Rasche et al., 1990; van Ginkel et al., 1987). For example, AMO of *Nitrosomonas europaea* has a broad substrate range for n-alkanes (C_2 - C_8) and is inactivated by aliphatic n-alkynes of the same chain lengths (Hyman et al., 1988). In contrast, other Cu-containing membrane-bound monooxygenases, such as methane MO and the Cu-containing alkane MO of *Nocardioides* CF8, have a more restricted alkane substrate range ($\leq C_6$) (Burrows et al., 1984; Colby et al., 1977; Hamamura et al., 2001; Stirling and Dalton, 1979). Given that AOA AMO also falls into the Cu-containing AMO/PMO family (Sayavedra-Soto et al., 2011) we hypothesized that it might show different sensitivity than the bacterial AMO to the effects of aliphatic n-alkynes of different chain lengths (C_2 – C_9). Here we report on the results of studies carried out to assess the effects of n-alkynes on NH_3-oxidizing activity in soil slurries and whole soil incubations.

Materials and Methods

Chemicals. N-tris[hydroxymethyl]methyl-2-aminoethanesulfonic acid (TES) buffer, vanadium chloride, spectinomycin dihydrochloride, 1-allyl-2-thiourea (ATU), and NH_4Cl were obtained from Sigma-Aldrich (St. Louis , MO). Kanamycin sulfate was obtained from EMD Biosciences, Inc. (La Jolla, CA). Linear aliphatic 1-alkynes (C_3 – C_9) were obtained from Sigma-Aldrich, and acetylene (C_2) from Airgas (Radnor, PA).

Preparing n-alkyne stocks. Alkynes C_2 – C_4 exist in gaseous form at normal room temperature and pressure, and were diluted 10-fold (15 ml gas into a 155 ml bottle capped with a black phenolic cap fitted with a gray butyl stopper containing several 6 mm dia. glass beads). Alkynes C_5 – C_9 exist in neat liquid form at normal room temperature and pressure, and stocks were prepared by adding 40 µl neat liquid alkyne to a glass bottle (total volume 155 ml) containing several glass beads and quickly

capped with a black phenolic cap fitted with a gray butyl stopper. Bottles were over-pressured with 100 ml air and shaken briskly for 30 s to distribute the alkyne evenly through the airspace. The alkyne concentrations in bottles prepared this way were determined by gas chromatography. The volume of gas stock required to achieve specific aqueous phase concentrations (C_{aq}) under experimental conditions was calculated from the air/water phase partitioning Henry's constant (http://www.mpch-mainz.mpg.de/~sander/res/henry.html).

Selection of alkyne concentrations. Alkyne concentrations were chosen to be high enough to ensure inhibition but low enough to minimize time spent degassing to remove alkynes during inactivation and recovery experiments. In preliminary work, concentrations of acetylene as low as 0.01 kPa (0.01% vol/vol, or 4.3 μM in aqueous solution) completely inhibited nitrification in soil and pure culture, but to ensure inhibition 6 μM acetylene was routinely used in aqueous solution (C_{aq}). In the case of octyne, apparent concentrations from 0.1 to 10 μM C_{aq} completely inhibited AOB dominated nitrification in Corvallis Cropped soil. Octyne may bind to soil, so gas chromatography was used to check headspace concentrations in the presence and absence of soil once the decision was made to focus exclusively on this alkyne. Octyne binding varied with each soil, but when octyne was added to achieve 2 μM apparent C_{aq}, there was sufficient alkyne in the headspace to partition into the aqueous phase at >1 μM. Headspace analysis confirmed that when alkyne was added at an apparent C_{aq} > 2 μM that the percentage of alkyne bound to soil was insignificant and C_{aq} could be predicted by the Henry's constant.

Response of soil nitrification to alkynes. *(a) Soils.* Soil samples, representing different soil types from different regions of Oregon, were collected from cropped fields and noncropped locations (three replicates of each) at Oregon State University Agricultural Experimental Stations located in Corvallis, Pendleton, Madras, and Klamath Falls, Oregon (Table 1). Four to five soil samples were recovered to a depth of 10 cm from each replicate site via a random walk process. A composited sample was prepared for each replicate site and brought to the laboratory where they were sieved <4.75 mm. Soil samples (0.25 g) were stored at -80°C for future DNA extraction and quantification of AOA and AOB *amo*A gene copies by qPCR. The remaining soils were stored at 4°C prior to experimentation.

(b) Response of nitrification potentials to inhibitors. Nitrification potentials were determined on soil samples as described previously (Taylor et al., 2010). The NP treatments included ATU (100 μM) and C_2 – C_9 alkynes. The details of the RNP assay have been described in detail previously (Taylor et al., 2010; Taylor et al., 2012). In some treatments, the bacterial protein synthesis inhibitors kanamycin (800 μg/ml) plus spectinomycin (200 μg/ml) were added to prevent resynthesis of AMO by AOB. The fraction of RNP that recovers in the presence of bacterial protein synthesis inhibitors (RNP_{ab}) is considered to be due to AOA.

(c) Response of whole soil nitrification to octyne during 21 – 28 d incubations. Soils were collected from a pasture (CP) and a wheat cropped field (CC). Ten-gram portions of soil (a composite of three field replicates) were placed in 155 ml glass bottles with 0.5 ml dH_2O to achieve a moisture content approximating field capacity (0.42 and 0.33 g water/g oven dry soil for CP and CC, respectively). Bottles were capped with black phenolic caps and gray butyl stoppers, and three NH_4^+ levels were established by adding aliquots of anhydrous NH_3 gas to achieve 0, 2, and 20 μmol/g soil added NH_4^+. Three treatments were imposed at each NH_4^+level: (i) no alkyne amendment, (ii) plus acetylene (6 μM soil solution concentration, C_{aq}), and (iii) plus octyne (2 μM apparent C_{aq}), each in triplicate. Bottles were incubated in the dark at ~23ºC, and opened weekly to allow for gas exchange and sampling. Soil aliquots (0.25 g) were removed and stored at -80ºC for future DNA extraction. A second aliquot (1.5 g) was removed and added to 15 ml of water in a 155 ml bottle and shaken (200 rpm) for 15 min. Aliquots (1.8 ml) of soil slurry were removed to microcentrifuge tubes, centrifuged for 3 min at 13.4 $x10^3$ g, and NO_2^- +NO_3^- concentrations were determined immediately on the supernatants (Hood-Nowotny et al., 2010) and expressed on an oven-dried weight of soil basis. Initial concentrations of NO_2^-+NO_3^- were subtracted from all time points. After sampling, bottles were recapped, and acetylene and octyne applied at the same concentrations as when the incubation was established. NH_3 gas was added as needed to maintain the target NH_4^+ concentrations.

(d) Response of whole soil nitrification to octyne during short (2 d) incubations. Cropped and noncropped soils were incubated ±octyne, and ±NH_4^+. Portions (2.5 g) of soil (a composite of the three field replicates) were placed in 155 ml glass bottles with supplemental dH_2O to achieve a water content approximating 0.6 of maximum water holding capacity. Bottles were capped with black phenolic caps with gray butyl stoppers, and aliquots of anhydrous NH_3 gas were added sufficient to support the

maximum rate of nitrification. These NH_4^+ concentrations were determined in preliminary experiments, and ranged from 2 – 20 μmol/g soil (data not shown). Soils were incubated under three treatments: (i) no alkyne, (ii) plus acetylene (6 μM C_{aq} in soil solution), and (iii) plus octyne (2 μM apparent C_{aq} in soil solution). Bottles were incubated in the dark at ~23ºC for 2 d. At the end of the incubation 15 ml of water was added and bottles shaken (200 rpm) for 15 min. NO_2^-+NO_3^- concentrations were determined as described above.

Nucleic acid analysis. DNA was extracted from 0.25 g portions of soil using a MoBio PowerSoil (Carlsbad, CA) extraction kit, quantified using a NanoDrop ND-1000 UV-Vis Spectrophotometer (ThermoScientific, Rockwood, TN) and stored at -80ºC. QPCR of the AOA and AOB *amo*A genes was performed as described previously (Taylor et al., 2012).

Statistics. The experimental design of the 21- and 28-d incubations is characterized as a 3 x 3 factorial (inhibitor, NH_4^+ treatment, and sampling time) with repeated measurements and bi-variate response. The plus-acetylene treatments were run as biological controls; no effects were expected and none were observed, allowing the elimination of this treatment from further analysis. To determine whether the rate of NO_2^-+NO_3^- accumulation was different between treatment conditions, ANOVA was performed using the slopes from simple linear regressions of the repeated measurements versus time within each incubation replicate. AOA:AOB ratios of no alkyne and plus-octyne treatments were log transformed to simplify the analysis by reducing the bi-variate response to a univariate one, and by eliminating the substantial skewness in the distributions of the gene copy counts. Another simplification was to use the average of the three qPCR replicates as the response for each treatment combination, reducing the data to the three experimental replicates for each treatment combination. The data were fit with a linear mixed effects model in R (http://www.r-project.org/) with random effect for sample, and fixed effects for inhibitor, NH_4^+, and time of sampling, using additional R code, attributable to Christopher Moore (http://blog.lib.umn.edu/moor0554/canoemoore/2010/09/lmer_p-values_lrt.html), to calculate p-values. Other comparisons between ±octyne in the presence and absence of NH_4^+ were done with a two-tailed Student's t-test assuming equal variance.

Results

Effects of alkynes on nitrification potentials of soil slurries. The effects of C_2 – C_9 1-alkynes were evaluated on two soils that were shown previously with the RNP assay as having NPs dominated by either AOA (Corvallis Pasture, CP) or AOB (Corvallis Cropped, CC) (Taylor et al., 2010; Taylor et al., 2012). Samples of CC soil were incubated with 2 μM (apparent C_{aq}) of each alkyne, and CP soil with 4 μM (apparent C_{aq}) of each alkyne in the presence of 1 mM NH_4^+ in soil slurry NP assays (Fig. 1*A* and *B*). In the AOB-dominated CC soil there was no significant NO_2^-+NO_3^- production in treatments with alkynes ($p > 0.05$). However, in AOA-dominated CP soil, whereas C_2 completely inhibited NO_2^-+NO_3^- production, there was residual accumulation of NO_2^-+NO_3^- in the presence of alkynes C_3 – C_5, but no significant effect of alkynes C_6 – C_9 compared with the control ($p > 0.1$).

The effects of octyne on long-term (21 – 28 d) soil incubations. We evaluated the effects of octyne on NO_2^-+NO_3^- accumulation and changes in AOA and AOB *amo*A gene copies during long-term (21 – 28 d) whole soil (WS) incubations of both CC and CP soils amended with either: (i) no supplemental NH_4^+, (ii) low NH_4^+ (2 μmol/g soil), or (iii) high NH_4^+ additions (20 μmol/g soil).

After 21 d of incubation, microcosms of CC soil that received no or low NH_4^+ addition showed no significant difference in the rates of NO_2^-+NO_3^- accumulation ±2 μM apparent C_{aq} octyne ($p > 0.3$, Fig. 2*A* and *B*), suggesting that all nitrification in those NH_4^+ treatments was octyne-resistant (AOA). However, in the high NH_4^+ treatment, there was a significant difference in the rates of NO_2^-+NO_3^- accumulation between ±octyne treatments ($p < 0.001$, Fig. 2*C*) indicating an increased contribution to nitrification by AOB (octyne-sensitive). Although there was not a statistically significant response of octyne-resistant rates of nitrification to NH_4^+ treatments ($p > 0.4$), NO_2^-+NO_3^- accumulation in the no alkyne treatments (AOA+AOB) increased 6- and 14-fold over the unamended treatment in response to low and high NH_4^+, respectively ($p < 0.001$). The rate of NO_2^-+NO_3^- accumulation in the no alkyne, high NH_4^+ treatment was significantly greater than the rates of nitrification in the no and low NH_4^+ treatments ($p < 0.001$). Soil microcosms treated with acetylene did not accumulate NO_2^-+NO_3^- in response to any NH_4^+ treatment, and showed no increases in either AOA or AOB *amo*A gene copies. During the 21-d incubation of CC, there was convincing

evidence of differences between log(AOA:AOB) response to the octyne and no alkyne treatments ($p < 0.0001$). For example, AOA *amo*A gene copies increased in response to no added and low added NH_4^+ treatments ±octyne (Fig. 2*D* and *E*), whereas AOB *amo*A gene copies only increased in response to the high NH_4^+ treatment minus octyne (Fig. 2*F*). In ±octyne treatments there was also strong evidence of an interaction between NH_4^+ treatment and time on log(AOA:AOB). Specifically, there was convincing evidence of an increase in log(AOA:AOB) in response to the low NH_4^+ treatment from 0 to 21 d ($p < 0.0001$), and strong evidence of increases in log(AOA:AOB) from 7 to 21 d in both the no NH_4^+ and high NH_4^+ treatments ($p = 0.006$ and 0.01, respectively). In octyne-treated incubations with either low or high NH_4^+, ~3.3 µmol NH_4^+/g soil was oxidized and accompanied by an AOA *amo*A cell yield of 2.8 x 10^7 – 7.7 x 10^7cells/µmol NH_4^+. This yield compares favorably with the cell yields measured in cultures of *N. maritimus* (Konneke et al., 2005)*, Nitrosocaldus yellowstonii* (de la Torre et al., 2008)*,* and pyruvate assisted *N. viennensis* (1.6 x 10^7 – 4.7 x 10^7cells/µmol NH_4^+(Tourna et al., 2011)), and with the AOA yield measured in soil microcosms incubated with low additions of NH_4^+ (2.3 x 10^7 – 2.9 x 10^7cells/µmol NH_4^+ (Verhamme et al., 2011)).

During the 28-d incubation of CP soil, microcosms that received no NH_4^+ addition expressed the same rate of NO_2^-+NO_3^- accumulation ±octyne (Fig. 3*A*), whereas NO_2^- +NO_3^- accumulation in microcosms amended with low or high NH_4^+ were significantly greater in the no alkyne treatments than in the plus octyne treatments ($p < 0.001$, Fig. 3*B* and *C*). The octyne-resistant (AOA) rates of nitrification increased 5- and 6-fold in response to low and high NH_4^+, respectively ($p < 0.001$); whereas in the no alkyne treatment (AOA+AOB) rates of NO_2^-+NO_3^- accumulation increased significantly (6- and 14-fold) over the unamended rate in response to low and high NH_4^+, respectively ($p < 0.001$). Soil microcosms treated with acetylene did not accumulate NO_2^-+NO_3^-, and there were no increases in AOA and AOB *amo*A gene copies. During the 28 d incubation of CP there was strong evidence of a difference in the log(AOA:AOB) response between octyne and the no alkyne treatments ($p = 0.007$). In the no alkyne treatment, AOB *amo*A gene copies increased 10- and 100-fold in response to low and high NH_4^+ respectively (Fig. 3*E* and *F*), whereas AOA *amo*A did not change in either the no alkyne or octyne treatments. As a consequence, log(AOA:AOB) ratios were lower in the high NH_4^+ treatment compared with the no NH_4^+ treatment ($p = 0.03$, Fig. 3 *D*). Because there were no detectable AOA *amo*A gene copy increases in CP soil, an

alternate approach was taken to demonstrate that the AOA community of this soil could synthesize protein and express octyne-resistant NH_3-oxidizing activity. The CP soil was acetylene inactivated, and subjected to a RNP experiment where soil slurries were exposed to a combination of antibiotics targeted at bacterial protein synthesis (ab, kanamycin and spectinomycin, 800 and 200 μg/ml, respectively), octyne (oct, 2 μM apparent C_{aq}), or a combination of antibiotics and octyne. Rates of RNP_{ab}, RNP_{oct} and RNP_{ab+oct} were the same (0.36± 0.03 μmol $NO_2^-+NO_3^-$/g soil/d) demonstrating that AOA in CP soil were able to synthesize active AMO proteins and perform NH_3 oxidation in the combined presence of octyne and antibiotics. Considering the AOA yield observed in the cropped soil microcosms, it is unlikely that a statistically significant increase of this magnitude could be measured over the background AOA *amo*A gene copy abundance.

The fraction of octyne-sensitive soil nitrification correlates with the fraction sensitive to other AOB inhibitors. The effect of octyne on NH_3 oxidation was evaluated in cropped and noncropped soils collected from several agricultural research stations located across Oregon. These soils had a range of pH, total C and N, and population sizes of AOA and AOB (Table 1). The cropped soils were primarily cropped to winter wheat and had histories of being routinely fertilized with inorganic N fertilizers. Noncropped soils were sampled from under diverse native vegetation of either conifer, sage brush, or grasses, had no history of cultivation or N fertilization, and were close in proximity to the cropped soils. The effects of octyne on $NO_2^-+NO_3^-$ accumulation in NP slurries were compared with the effects of 100 μM allyl-thiourea (ATU) and also with the RNP response ±bacterial protein synthesis inhibitors. The sensitivities of NPs to octyne and ATU over the wide range of soils were strongly and positively correlated (Fig. 4*A*, $r^2 = 0.938$) showing a range from entirely sensitive to completely resistant. The fraction of RNP that was insensitive to antibiotics (RNP_{ab}/RNP) correlated positively and strongly ($r^2 = 0.905$) with the fraction of NP that was insensitive to octyne (NP_{oct}/NP, Fig. 4*B*). The cropped soils, which had the lowest AOA:AOB ratios (≤ 31), were more sensitive to antibiotics, ATU, and octyne than the noncropped soils, suggesting AOB had a greater potential to contribute to nitrification in these soils. Noncropped soils showed a wide range of responses, with two soils, CP and Madras rangeland (MR), expressing AOA-dominated nitrification (AOA:AOB ratios ≥ 396), and two noncropped soils, Klamath woodlot and Pendleton grassland

(KW and PG, respectively, with AOA:AOB ratios of 45 and 60), showing an intermediate effect of octyne, ATU, and RNP_{ab}, suggesting that both AOA and AOB populations were capable of contributing to NPs.

A comparison of the effects of octyne on nitrification in whole soil (WS) and soil slurry (NP) assays. The effects of octyne (2 μM apparent C_{aq}) on nitrification were compared between WS and NP assays (Fig. 4*C*). Unsaturated WS samples (soil water content ~ 0.6 of saturation) were incubated in sealed bottles supplemented with sufficient anhydrous NH_3 gas to support the maximum rate of nitrification (2 – 20 μmol NH_4^+/g soil). The fraction of the maximum WS rate of nitrification that was insensitive to octyne (WS_{oct}/WS) was strongly and positively correlated with the fraction of nitrification that was resistant to octyne in NP assays (NP_{oct}/NP, r^2 = 0.884). This confirmed that octyne has the potential to differentiate the contributions of AOA and AOB to soil nitrification in short-term (2 d) WS incubations.

Discussion

In this study we established that the octyne method could be used in relatively short assays (24 – 48 h) in both soils slurries and whole soils microcosms. The soils evaluated exhibited a range of nitrification rates that were completely inactivated by acetylene making it unlikely that heterotrophic nitrification accounted for the octyne-resistant activity. At least for this study, the fraction of nitrification that was octyne-resistant ranged widely and correlated well with other short-term methods used to assess the contributions of AOA activity, including ATU resistance and RNP plus antibiotics. Furthermore, in long-term soil incubations, octyne was as effective as acetylene in preventing AOB proliferation, but did not prevent NH_4^+-dependent, acetylene-sensitive AOA growth. There are some advantages of the octyne method over other published attempts to determine the relative contributions of AOA and AOB. First, in contrast to AOB, it has been reported previously that NH_3 oxidation by pure cultures and enrichments of AOA are partially insensitive to ATU (Hatzenpichler et al., 2008; Mosier et al., 2012). Interpretation of this ATU response by AOA is further complicated by the observation that NO_2^- production by the soil-borne AOA, *Nitrosotalea devanaterra*, is completely inhibited by ATU in culture (Lehtovirta-Morley et al., in press). Although we have had success in measuring the relative contributions of AOA

and AOB to NP in soil slurries by using the RNP ±antibiotics assay (Taylor et al., 2010), there are several challenges with extending this method into whole soil including: (i) difficulty in distributing aqueous solutions of antibiotics uniformly throughout an unsaturated soil, (ii) antibiotic effectiveness being negated by binding to soil particles (Subbiah et al., 2011; Sukul et al., 2008), (iii) variable antibiotic resistance among AOB (this study), and (d) incomplete removal of acetylene by degassing.

An observation with interesting implications was the detection in two noncropped soils (PG and KW) of both octyne-resistant and octyne-sensitive NH_3-oxidizing activities. This result indicates that in some noncropped soils active AOB co-exist in significant numbers alongside an active AOA population. In contrast, in another noncropped soil (CP), our previous RNP results (Taylor et al., 2010) and the results of the current octyne assay showed that AOB contributed very little to the short-term nitrification rate, which was explained by a low AOB abundance ($2.5\pm 0.4 \times 10^6$ *amo*A gene copies/g soil). A population of such magnitude could have accounted for ~10% of the observed rate of nitrification assuming a rate of 4×10^{-15} mol NH_4^+-N/cell/h (Belser and Schmidt, 1980), and two copies of *amo*A/cell (Chain et al., 2003; Norton et al., 2008). Nonetheless, in the long-term incubation of CP soil with NH_4^+ amendments, an NH_4^+-dependent octyne-sensitive increase in AOB *amo*A copies occurred, suggesting that the small AOB population was viable and proliferated in response to NH_4^+. By contrast, the short-term WS octyne assay showed that the majority of nitrification in the cropped soils was octyne-sensitive and presumably due to AOB. Yet, despite the short-term assays showing overwhelming dominance of AOB activity, after NH_4^+ amendment of cropped soils, an octyne-resistant and low NH_4^+-stimulated increase in AOA population density was detected after about 7 d of incubation. These results clearly emphasize that AOA in the cropped soil and AOB in the noncropped soil are capable of proliferating in response to supplemental NH_4^+ within a short period of time, and with the potential to change the relative contributions of AOA and AOB to soil nitrification. Further studies are needed to more accurately define the relationships between NH_4^+ availability and other factors that determine AOA and AOB population sizes, and control their activities and relative contributions to soil nitrification.

Acknowledgements. This research was supported by USDA NIFA Award No. 2012-67019-3028, an Oregon Agricultural Research Foundation competitive grant, and the Oregon State University Provost Distinguished Graduate Fellowship. Additional

support obtained from the Oregon State University community included: QPCR facilities at the Center for Genome Research and Biocomputing, field sites maintained by the Hyslop Field Research Laboratory, Columbia Basin Agricultural Research Center, Klamath Basin Research and Extension Center, and the Central Oregon Agricultural Research Center.

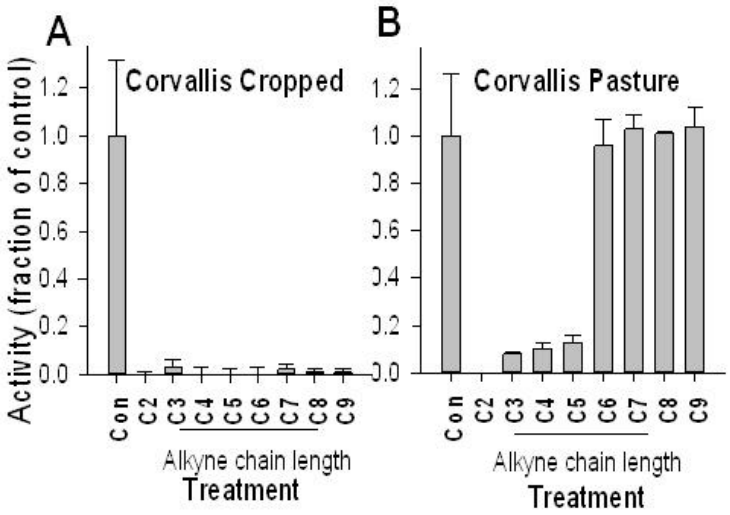

Fig. 1. The effect of C_2 - C_9 alkynes on NO_2^-+NO_3^- production by soil slurries of: *A*) Corvallis Cropped soil, and *B*) Corvallis Pasture soil incubated with 2 and 4 μM (apparent C_{aq}) respectively, of each alkyne in the presence of 1mM NH_4^+. See Materials and Methods for further experimental details. NO_2^-+NO_3^- production in the presence of each alkyne was compared with a no inhibitor control (Con). Error bars represent the SD of the mean (n = 3).

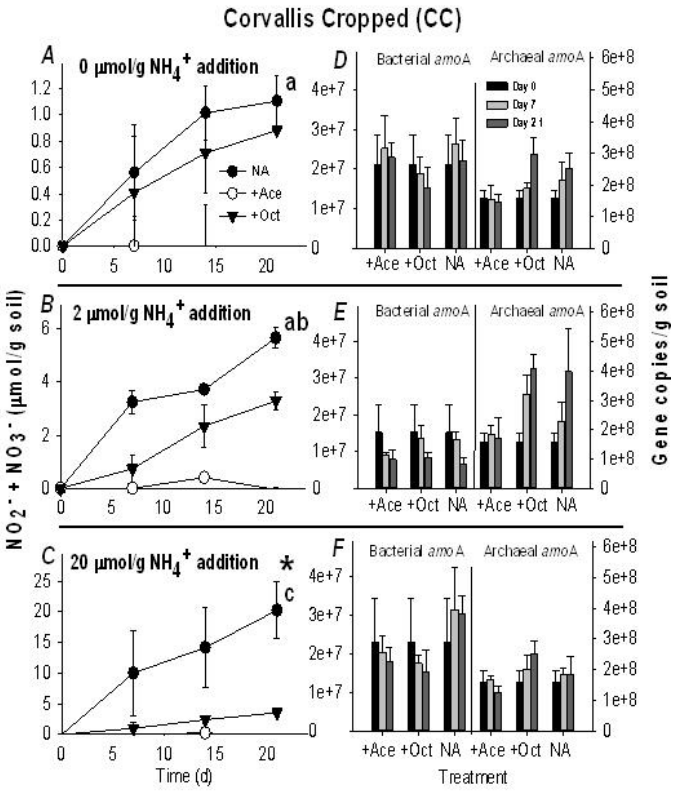

Fig. 2. A comparison of the effects of alkyne (acetylene, +Ace; octyne, +Oct) and no alkyne (NA) treatments on NO_2^-+NO_3^- accumulation and on AOA and AOB *amo*A gene copies during incubations of Corvallis Cropped (CC) soil amended with no (*A* and *D*), low (*B* and *E*), or high (*C* and *F*) NH_4^+ additions (0, 2, and 20 µmol NH_4^+/g soil, respectively). *A, B,* and *C* represent NO_2^-+NO_3^- accumulation over the time course of the experiment. Error bars represent the SD of the mean NO_2^-+NO_3^- concentration (n = 3). *D, E,* and *F* represent AOB and AOA *amo*A gene copies/g soil. Error bars represent the SD of the average *amo*A gene copies/g soil of triplicate qPCR reaction for each treatment (n = 3). The asterisk (*) indicates that NO_2^-+NO_3^- accumulation was significantly different in the NA and +Oct treatments within a NH_4^+ treatment ($p < 0.001$). Different lower case letters indicate that NO_2^-+NO_3^- accumulation was significantly different in the NA treatment between NH_4^+ levels ($p < 0.001$). There was no significant difference in the rate of NO_2^-+NO_3^- accumulation in +Oct treatment between NH_4^+ levels.

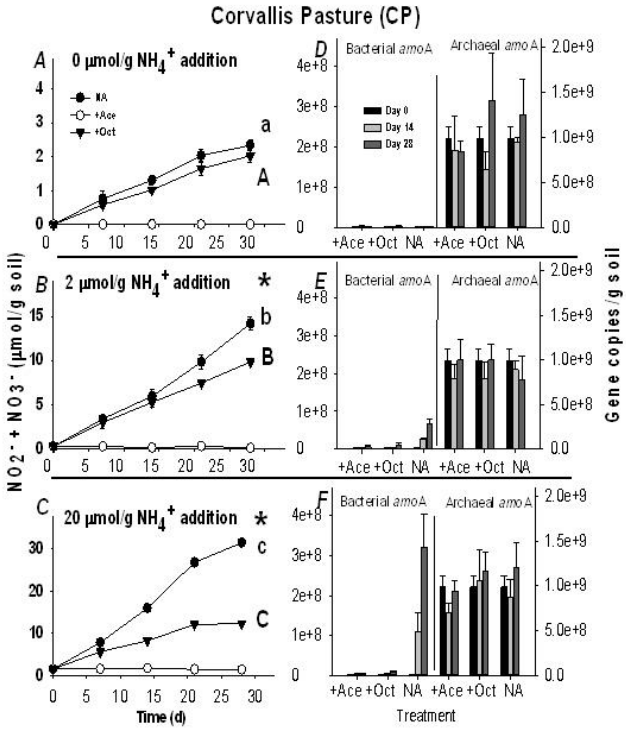

Fig. 3. A comparison of the effects of alkyne (acetylene, +Ace; octyne, +Oct) and no alkyne (NA) treatments on NO_2^-+NO_3^- accumulation and on AOA and AOB *amo*A gene copies during incubations of Corvallis Pasture (CP) soil amended with no (*A* and *D*), low (*B* and *E*), or high (*C* and *F*) NH_4^+ additions (0, 2, and 20 µmol NH_4^+/g soil, respectively). *A, B,* and *C* represent NO_2^-+NO_3^- accumulation over the time course of the experiment; error bars represent the SD of the mean NO_2^-+NO_3^- concentration (n = 3). *D, E,* and *F* represent changes in AOB and AOA *amo*A gene copies/g soil. Initial AOB *amo*A gene copies were 2.5 ± 0.4 x 10^6/g soil. See Materials and Methods for further experimental details. Error bars represent the SD of the average *amo*A gene copies/g soil of triplicate qPCR reaction for each treatment (n = 3). An asterisk (*) indicates that the rate of NO_2^-+NO_3^- accumulation was significantly different in the NA and +Oct treatments within a NH_4^+ level ($p < 0.001$). Different lower case letters indicate a significant difference between NH_4^+ treatments ($p < 0.001$) in the rate of NO_2^- +NO_3^- accumulation in the NA treatments. Different upper case letters indicate a significant difference between NH_4^+ treatments ($p < 0.001$) in the rate of NO_2^-+NO_3^- accumulation in the +Oct treatment.

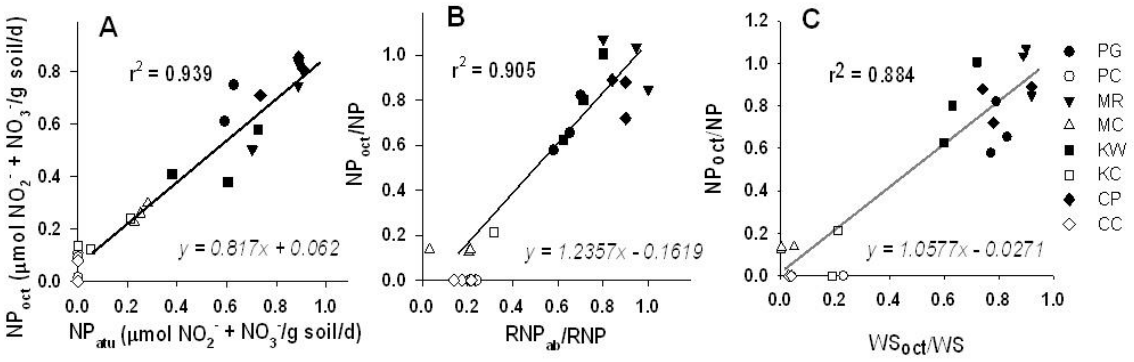

Fig. 4. Correlation among methods used to assess the relative contributions of AOA and AOB to nitrification of diverse Oregon soils. *A*) Correlation between the rates of NO_2^-+NO_3^- production that were resistant to octyne (NP_{oct}) versus resistant to 100 µM ATU (NP_{atu}). *B*) Correlation between the fractions of the recovered nitrification potentials (RNP) that were insensitive to bacterial protein synthesis inhibitors (RNP_{ab}/RNP) versus the fractions of activity resistant to octyne (NP_{oct}/NP). *C*) A comparison of the effects of octyne on the NH_4^+ saturated rate of NO_2^-+ NO_3^- accumulation by whole soils (WS) and soil slurries (NP) of diverse cropped and noncropped Oregon soils. Assays were performed as described in Materials and Methods; WS incubations were supplemented with sufficient anhydrous NH_3 gas to maximize the rate of nitrification and NP assays were supplemented with 1 mM NH_4^+. WS_{oct}/WS represents the fraction of NO_2^-+NO_3^- accumulation in WS incubations that was resistant to octyne. Open and closed symbols indicate cropped and noncropped soils, respectively. See Table 1 for site locations and soil characteristics.

Table 1. Selected characteristics of soils collected from the Oregon State University agricultural research stations used in this study. pH values are an average of the mean of the field replicates (n = 3), with the accompanying SD of the mean. Total C and N represent values obtained from a composite sample prepared by mixing individual samples from each of the field replicates. AOA and AOB *amo*A copies/g soil are the average of three technical replicates of each of three field replicates (n = 3), with the accompanying SD of the mean.

Agricultural Station	Pendleton		Madras		Klamath Falls		Corvallis	
	grassland (PG)/cropped (PC)		rangeland (MR)/cropped (MC)		woodlot (KW)/cropped (KC)		pasture (CP)	cropped (CC)
Lat/Long	45°43'14"/118°37'35"		44°38'12"/121°07'58"		42°10'52"/121°44'17"		44°40'44"/123°15'54"	44°38'03"/123°11'24"
Soil classification	Typic Haploxeroll		Dystric Cryochrept		Torripsammetic Haploxeroll		Vertic Haploxeroll	Aquultic Argixeroll
Soil Series	Walla Walla silt loam		Madras sandy loam		Forndey sandy loam		Witham clay loam	Woodburn silt loam
pH	7.5±0.1	6.2±0.8	7.5±0.1	7.0±0.7	7.3±0.2	6.8±0.1	6.3±0.3	5.7±0.1
Total C (g/kg)	20.7	10.6	8.7	8.7	13.4	6.6	53.1	12.9
Total N (g/kg)	1.8	0.9	0.9	0.8	1.1	0.6	3.9	0.6
AOA *amo*A*	352±197	123±73	474±47	283±244	419±228	307±48	990±130	160±24
AOB *amo*A*	5.9±2.6	5.6±0.9	0.5±0.2	15.6±15	9.4±8.7	9.8±2.1	2.5±0.9	21.0±7.4
AOA:AOB ratio	60	22	948	18	45	31	396	8

*x10^6 copies/g soil.

References

Belser, L.W., and E.L. Schmidt. 1980. Growth and oxidation-kinetics of 3 genera of ammonia oxidizing nitrifiers. (in English) FEMS Microbiol Lett 7:213-216.

Burrows, K.J., A. Cornish, D. Scott, and I.J. Higgins. 1984. Substrate specificities of the soluble and particulate methane mono-oxygenases of *Methylosinus-Trichosporium* OB3b. (in English) J Gen Microbiol 130:3327-3333.

Chain, P., J. Lamerdin, F. Larimer, W. Regala, V. Lao, M. Land, L. Hauser, A. Hooper, M. Klotz, J. Norton, L. Sayavedra-Soto, D. Arciero, N. Hommes, M. Whittaker, and D. Arp. 2003. Complete genome sequence of the ammonia-oxidizing bacterium and obligate chemolithoautotroph *Nitrosomonas europaea.* . (in English) J Bacteriol 185:6496-6496.

Colby, J., D.I. Stirling, and H. Dalton. 1977. Soluble methane mono-oxygenase of *Methylococcus-Capsulatus*-(Bath) - Ability to oxygenate normal-alkanes, normal-alkenes, ethers, and alicyclic, aromatic and heterocyclic compounds. (in English) Biochem J 165:395-402.

de la Torre, J.R., C.B. Walker, A.E. Ingalls, M. Konneke, and D.A. Stahl. 2008. Cultivation of a thermophilic ammonia oxidizing archaeon synthesizing crenarchaeol. (in eng) Environ Microbiol 10:810-818.

Ensign, S.A. 2001. Microbial metabolism of aliphatic alkenes. Biochem 40:5845-5853.

Hamamura, N., C.M. Yeager, and D.J. Arp. 2001. Two distinct monooxygenases for alkane oxidation in *Nocardioides* sp. strain CF8. (in eng) Appl Environ Microbiol 67:4992-4998.

Hatzenpichler, R. 2012. Diversity, physiology, and niche differentiation of ammonia-oxidizing archaea. (in English) Appl Environ Microbiol 78:7501-7510.

Hatzenpichler, R., E.V. Lebedeva, E. Spieck, K. Stoecker, A. Richter, H. Daims, and M. Wagner. 2008. A moderately thermophilic ammonia-oxidizing crenarchaeote from a hot spring. (in eng) Proc Natl Acad Sci USA 105:2134-2139.

Hood-Nowotny, R., N. Hinko-Najera Umana, E. Inselbacher, P. Oswald-Lachouani, and W. Wanek. 2010. Alternative methods for measuring inorganic, organic, and total dissolved nitrogen in soil. (in English) Soil Sci Soc Am J 74:1018-1027.

Hyman, M.R., and P.M. Wood. 1985. Suicidal inactivation and labeling of ammonia monooxygenase by acetylene. Biochem J 227:719-725.

Hyman, M.R., I.B. Murton, and D.J. Arp. 1988. Interaction of ammonia monooxygenase from *Nitrosomonas europaea* with alkanes, alkenes, and alkynes. (in English) Appl Environ Microbiol 54:3187-3190.

Jia, Z.J., and R. Conrad. 2009. *Bacteria* rather than *Archaea* dominate microbial ammonia oxidation in an agricultural soil. Environ Microbiol 11:1658-1671.

Keener, W.K., S.A. Russell, and D.J. Arp. 1998. Kinetic characterization of the inactivation of ammonia monooxygenase in *Nitrosomonas europaea* by alkyne, aniline, and cyclopropane derivatives. Biochim Biophys Acta 1388:373-385.

Konneke, M., A.E. Bernhard, J.R. de la Torre, C.B. Walker, J.B. Waterbury, and D.A. Stahl. 2005. Isolation of an autotrophic ammonia-oxidizing marine archaeon. Nature 437:543-546.

Lehtovirta-Morley, L.E., D.T. Verhamme, G.W. Nicol, and J.I. Prosser. in press. Effect of nitrification inhibitors on the growth and activity of *Nitrosotalea devanaterra* in culture and soil. Soil Biol Biochem.

Leininger, S., T. Urich, M. Schloter, L. Schwark, J. Qi, G.W. Nicol, J.I. Prosser, S.C. Schuster, and C. Schleper. 2006. Archaea predominate among ammonia-oxidizing prokaryotes in soils. Nature 442:806-809.

Mosier, A.C., M.B. Lund, and C.A. Francis. 2012. Ecophysiology of an ammonia-oxidizing Archaeon adapted to low-salinity habitats. (in English) Microb Ecol 64:955-963.

Norton, J.M., M.G. Klotz, L.Y. Stein, D.J. Arp, P.J. Bottomley, P.S. Chain, L.J. Hauser, M.L. Land, F.W. Larimer, M.W. Shin, and S.R. Starkenburg. 2008. Complete genome sequence of *Nitrosospira multiformis*, an ammonia-oxidizing bacterium from the soil environment. (in eng) Appl Environ Microbiol 74:3559-3572.

Offre, P., J.I. Prosser, and G.W. Nicol. 2009. Growth of ammonia-oxidizing archaea in soil microcosms is inhibited by acetylene. (in eng) FEMS Microbiol Ecol 70:99-108.

Pester, M., T. Rattei, S. Flechl, A. Grongroft, A. Richter, J. Overmann, B. Reinhold-Hurek, A. Loy, and M. Wagner. 2012. *amo*A-based consensus phylogeny of ammonia-oxidizing archaea and deep sequencing of *amo*A genes from soils of four different geographic regions. (in English) Environ Microbiol 14:525-539.

Pratscher, J., M.G. Dumont, and R. Conrad. 2011. Ammonia oxidation coupled to CO_2 fixation by archaea and bacteria in an agricultural soil. (in eng) Proc Natl Acad Sci U S A 108:4170-4175.

Prosser, J.I., and G.W. Nicol. 2012. Archaeal and bacterial ammonia-oxidisers in soil: the quest for niche specialisation and differentiation. (in English) Trends Microbiol 20:523-531.

Rasche, M.E., R.E. Hicks, M.R. Hyman, and D.J. Arp. 1990. Oxidation of monohalogenated ethanes and *n*-chlorinated alkanes by whole cells of *Nitrosomonas europaea*. (in English) J Bacteriol 172:5368-5373.

Sayavedra-Soto, L.A., N. Hamamura, C.W. Liu, J.A. Kimbrel, J.H. Chang, and D.J. Arp. 2011. The membrane-associated monooxygenase in the butane-oxidizing Gram-positive bacterium *Nocardioides* sp. strain CF8 is a novel member of the AMO/PMO family. (in English) Env Microbiol Rep 3:390-396.

Stirling, D.I., and H. Dalton. 1979. Properties of the methane mono-oxygenase from extracts of *Methylosinus-Trichosporium* OB3b and evidence for its similarity to the enzyme from *Methylococcus-Capsulatus* (Bath). (in English) Eur J Biochem 96:205-212.

Subbiah, M., S.M. Mitchell, J.L. Ullman, and D.R. Call. 2011. β-lactams and florfenicol antibiotics remain bioactive in soils while ciprofloxacin, neomycin, and tetracycline are neutralized. (in English) Appl Environ Microbiol 77:7255-7260.

Sukul, P., M. Lamshoft, S. Zuhlke, and M. Spiteller. 2008. Sorption and desorption of sulfadiazine in soil and soil-manure systems. (in English) Chemosphere 73:1344-1350.

Taylor, A.E., L.H. Zeglin, S. Dooley, D.D. Myrold, and P.J. Bottomley. 2010. Evidence for different contributions of archaea and bacteria to the ammonia-oxidizing potential of diverse Oregon soils. (in eng) Appl Environ Microbiol 76:7691-7698.

Taylor, A.E., L. Zeglin, T.A. Wanzek, D.D. Myrold, and P.J. Bottomley. 2012. Dynamics of ammonia oxidizing archaea and bacteria populations and contributions to soil nitrification potentials. ISME J 6:2024-2032.

Tourna, M., M. Stieglmeier, A. Spang, M. Konneke, A. Schintlmeister, T. Urich, M. Engel, M. Schloter, M. Wagner, A. Richter, and C. Schleper. 2011. *Nitrososphaera viennensis*, an ammonia oxidizing archaeon from soil. (in eng) Proc Natl Acad Sci U S A 108:8420-8425.

van Ginkel, C.G., H.G. Welten, and J.A. de Bont. 1987. Oxidation of gaseous and volatile hydrocarbons by selected alkene-utilizing bacteria. (in Eng) Appl Environ Microbiol 53:2903-2907.

Verhamme, D.T., J.I. Prosser, and G.W. Nicol. 2011. Ammonia concentration determines differential growth of ammonia-oxidising archaea and bacteria in soil microcosms. (in eng) ISME J 5:1067-1071.

Xia, W., C. Zhang, X. Zeng, Y. Feng, J. Weng, X. Lin, J. Zhu, Z. Xiong, J. Xu, Z. Cai, and Z. Jia. 2011. Autotrophic growth of nitrifying community in an agricultural soil. (in Eng) ISME J 5:1226-1236.

Zhang, L.M., P.R. Offre, J.Z. He, D.T. Verhamme, G.W. Nicol, and J.I. Prosser. 2010. Autotrophic ammonia oxidation by soil thaumarchaea. (in eng) Proc Natl Acad Sci USA 107:17240-17245.

DETERMINING THE CONTRIBUTION OF ARCHAEA TO NITRIFICATION IN ACIDIC SOILS

Graeme Nicol

Institute of Biological and Environmental Sciences, Cruickshank Building, University of Aberdeen, St Machar Drive, Aberdeen, Scotland, UK. AB24 3UU

Nitrification is a fundamental component of the global nitrogen cycle and leads to significant fertiliser loss and atmospheric and groundwater pollution. Since the late 19th century, ammonia oxidising bacteria were thought to be primarily responsible for the first step in nitrification. However, within the last decade, organisms belonging to the other prokaryotic domain, the Archaea, have been identified as contributing to this process in terrestrial and aquatic environments. A long-standing paradox in nitrification research has been the observation that rates of activity in acidic soils equal or exceed those of neutral soils. However, without exception, all ammonia oxidising bacteria grown in standard laboratory culture grow only at near-neutral pH. Using a combination of cultivation and culture-independent molecular methodologies, the presence and activity of ammonia oxidising archaea has now been identified as a previously unsuspected explanation for these observed high rates. This has included the cultivation of the world's first obligately acidophilic ammonia oxidiser, *Nitrosotalea devanaterra*, isolated from an acidic agricultural soil. Using a combination of genomic and physiological analyses, current research is trying to understand the specific adaptations that enables this organism to thrive in acidic environments.

ADVANCE IN UNDERSTANDING THE AMMONIA-OXIDIZING BACTERIA RESPONSE TO CHANGE IN ENVIRONMENTAL CONDITIONS

Sharon Avrahami

School of Marine Sciences, Michmoret Campus, Ruppin Academic Center, Michmoret, 40297, Israel

Abstract

The first step of nitrification, the oxidation of ammonia to nitrite, is of great importance in nitrogen recycling, loss of nitrogen from fertilized soils and reducing eutrophication in aquatic environments when coupled with anammox or denitrification. The effects of temperature, soil moisture and ammonium concentrations on nitrification activity and on microbial community structure of ammonia oxidizing bacteria (AOB) were observed separately in soils originated from various geographical regions (i.e. warm and moderate cold soils). However, change in nitrification activity was observed after few days, while the shift in community structure was only observed after a long period of incubation (i.e. at least 16 weeks). By a multifactorial laboratory experiment (manipulating temperature, soils moisture and fertilizer level) of a California meadow soil interactions between these factors in the way they affect community structure and function of AOB were observed. Thus, one cannot look at the effect of each factor alone. Furthermore, by using path analysis a link between activity rates and community structure (composition and abundance) was demonstrated after a long period of incubation (i.e. 16 weeks). By applying stable-isotope probing (SIP) a novel method, which can distinguish between active cells and non-active cells, further progress was achieved by overcoming bias of previous studies. A community shift of a biofilm-associated AOB, originating from two German stream water (683±550 and 16±7 μM NH_4^+, respectively) and developed in a flow-channel, was detected after relative short period of incubation (i.e. 6 weeks) under three temperature regimes. Although AOB composition in the ^{13}C-labeled DNA responded differently to temperature manipulation at two ammonium concentrations, activities has not been tested. In the future by applying SIP in multifactorial experiment one can get a better insight into the link between change in environmental conditions to any microbial community structure and its function in any environment.

Introduction

Two fundamental questions in microbial ecology are how change in environmental conditions influences the community structure of microorganisms and their function; and whether there is a link between these three parameters. The autotrophic ammonia oxidizing bacteria (AOB), which are responsible for the first and limiting step of nitrification, and oxidize ammonia to nitrite, were perfect candidates for testing these questions. Nitrification has an important role in the nitrogen cycle, but also emits a greenhouse gas as a by-product, nitrous oxide (N_2O) (Conrad, 1996), which plays a major role in global warming (Dickinson and Cicerone, 1986), as well as for the destruction of the stratospheric ozone layer (Crutzen, 1970). In the past most of our knowledge on ammonia oxidizing bacteria was based on controlled experiments studying the response of pure cultures to various environmental factors, and thus predicting their function and distribution under natural conditions. These studies demonstrated that pure cultures grow well in a liquid batch at moderate temperatures (25-30°C), at a narrow pH range from neutral to slightly alkaline and at low to moderate salt concentrations (Koops and Möller, 1992). Oren, (1999) explained these restrictions by the relatively low growth efficiency of nitrification reactions, which might not allow these bacteria to survive in energetically expensive extreme environments. However, ammonia oxidation have been reported in various environments including extreme habitats such as alkaline soda biotopes (Sorokin, 1998), Antarctic ice (Arrigo et al., 1995), hot springs (Golovatcheva, 1976) and in association with marine sponges (Diaz and Ward, 1997). Furthermore, an isolate from Mongolian alkaline soda lake, oxidizing ammonia at alkaline pH (values of up to 11.3, optimum at 9.5 to 10) and at high salinity (0.1 to 1.0 M of total Na^+, optimum 0.3 M), was found to be closely related to *Nitrosomonas halophila* (Sorokin et al., 2001).

Nitrification rates and N_2O emission rates in various environments were reported to respond to changes in environmental factors such as pH (reviewd by De Boer and Kowalchuk, 2001), ammonium concentration (reviewed by Kowalchuk and Stephen, 2001), temperature (Belser, 1979) soil moisture (Stark and Firestone, 1995) and salinity (Rysgaard et al., 1999). However, these shifts could be due to either a shift in the microbial community, or due to physiological changes of the same community. Most of ammonia-oxidizing bacteria cannot be cultured. Those that can be cultured are very slow growing, do not always remain active after cultivation, and in cases of successful

growth, the yield is often low. The poor culturability of many microbes has led to the development of culture-independent molecular tools for studying microbial communities. Thus, allowed to test the hypothesis that changes in environmental conditions result in shifts of AOB community structure, which impact the nitrification rate. In this review I will demonstrate the progress made in our understanding the effects of environmental conditions (in particular temperature, soil moisture and ammonium concentrations) on AOB community structure and on nitrification rates and N_2O emission rates. Furthermore, I will suggest an approach, which will result in a better insight into the link between environmental conditions, the community structure of AOB and their function, by detecting the active communities and by using statistical approach.

Temperature effect on nitrification

Temperature is one of the most important factors that influences the activity of nitrifiers populations (Belser, 1979). Several studies demonstrated that indigenous nitrifiers had temperature optima in correspondence to their climate region (Mahendrappa et al., 1966; Myers, 1975). Malhi and McGill, (1982) suggested that the optimum temperatures for nitrifiers communities from three soils was influenced by the mean annual temperature of the soils. In contrast, Stark and Firestone, (1996) suggested that optimum temperatures for nitrifiers communities appeared to be more related to differences in temperatures at particular times of the year than to differences in mean annual temperatures. Temperature had a positive correlation with N_2O emission rates as was observed in numerous studies (Conrad et al., 1983; Slemr et al., 1984; Williams and Fehsenfeld, 1991; Clayton et al., 1997; Macdonald et al., 1997; Mogge et al., 1998, 1999; Smith et al., 1998; Carnol and Ineson, 1999). Gödde and Conrad, (1999) studied the effect of temperature in the laboratory, and showed a monotonous increase of N_2O emission rates with increase in temperature. Soil samples, which were adapted to different temperatures for 5 days demonstrated similar trend with no AOB community shift after 4 weeks of incubation (Avrahami et al., 2002). However, in order to test indirect effects of temperature (through microbial community) on nitrification and on N_2O emission rates, further study was required.

Temperature effect on community structure of ammonia oxidizing bacteria (AOB)

Until recently we were only familiar with the ammonia oxidizing bacteria (AOB), which comprise two monophyletic groups base on the 16S rRNA: (1) the beta subdivision of the Proteobacteria, which includes two genera: *Nitrosomonas* and *Nitrosospira*, (2) the gamma subdivision of the Proteobacteria, which includes only two know pure cultures: *Nitrosococus oceani* and *Nitrosococus halophilus* (Purkhold et al., 2000). However, most of the studies on soils and aquatic environments focused on the beta-Proteobacteria (Kowalchuk and Stephen, 2001), while the gamma-Proteobacteria were studied in the marine environment (Ward and O'Mullan, 2002). Following the discovery of ammonia oxidizing archaea (AOA) both in metagenome (Treusch et al., 2005) and as a pure culture (Könneke et al., 2005) and considering their ubiquity (Francis et al., 2005) there has been enormous effort to determine their diversity in various environments and their contribution to activity. A pure culture study suggested niche differentiation of AOA and AOB (Martens-Habbena et al., 2009), which was supported by several environmental studies (Herrmann et al., 2011; Verhamme et al., 2011), and thus AOB outcompete AOA at high ammonium concentrations. The vast majority of the studies on the link between temperature, nitrification and ammonia oxidizing community were done in laboratory experiments applying high ammonium concentrations and thus focused on AOB community, excluding couple of studies (Urakawa et al., 2008; Tourna et al., 2008). The link between AOA to temperature and nitrification in oligotrophic environment should be study more thoroughly in the future. In this review I will focus on AOB community.

The effect of temperature on soil AOB community structure was examined by comparing soils from two climate regions, cold temperate soils and Mediterranean soil (i.e. warm region) (Avrahami et al., 2003; Avrahami and Conrad, 2003). The four soils were incubated in two set up; as moist soil incubation in high fertilizer (HF) concentration and buffered (pH 7) soil slurries. Two of these soils were additionally incubated in low fertilizer (LF) concentration. The soils in both set-ups were incubated at different temperatures (4- 37°C) for 20 weeks. AOB community structure was analyzed by denaturant gradient gel electrophoresis (DGGE) of the *amoA* gene, coding for the alpha-subunit of ammonia monooxigenase, followed by correspondence analyses, indicated that the effect of fertilizer treatment (HF, LF, slurry) masked that

of temperature (Fig. 1a). On the other hand, correspondence analysis for each treatment separately revealed the effect of temperature on community structure (Fig. 1b-d). In addition, slurry incubation, in which pH, ammonium and water activity were under control, showed a clear community shift that must result from a temperature effect (Fig. 1b) (Avrahami et al., 2003; Avrahami and Conrad, 2003). Cloning and sequencing of selected DGGE bands revealed two patterns of community shifts. One pattern was a community change between the different *Nitrosospira* clusters, which was observed in moist soil and slurry incubations of two soils, originated from cold regions. *Nitrosospira* AmoA cluster 1 was mainly detected below 30°C, while *Nitrosospira* cluster 4 was predominant at 25°C. *Nitrosopira* clusters 3a, 3b and 9 dominated at 30°C. The second pattern, observed in a soil originated from warm regions, showed a community shift predominantly within a single *Nitrosospira* cluster. The sequences of the individual DGGE bands that exhibited different trends with temperature almost exclusively belonged to *Nitrosospira* cluster 3a (Avrahami and Conrad, 2003). Evidence for a temperature effect on global distribution of *amoA* genes in warm and cold-temperate soils was reported by Avrahami and Conrad (2005). Based on the literature and unpublished data it was found that AmoA clusters 3a, 3b and 9-12 apparently exhibited no preference for either subtropical/tropical soils (i.e. warm regions) or temperate cold soils (Table1). However, AmoA clusters 1, and 4 (and perhaps cluster 2) seem to occur predominantly in soils from cold-temperate regions. Altogether these data indicated on AOB community composition that is depending on temperature, while during laboratory incubation the shifts as a response to temperature occurred only after relatively long period of incubation (i.e. 16 weeks). Thus, if community has changed in response to temperature the obvious question is how this affects the nitrification and N_2O emission rates due to nitrification.

Linking between AOB community structure to nitrification and N_2O emission rates

Most ecological studies on AOB have asked whether one environmental factor could influence their activity and/or community structure. However, since ecosystems are complex, one challenge is understanding the link between communities, activity, fluxes of greenhouse gases, and multiple biological, physical and chemical conditions. This is especially important given the possibility of interactions among environmental factors, resulting in different overall effects than those predicted from studies of each factor

alone. Therefore, the hypothesis, that changes in temperature interact with other environmental factors involved in global change (i.e., soil moisture and nitrogen inputs), and together will affect the AOB community and activity, was tested after 7 weeks of incubation of Jasper Ridge soil, California (Avrahami and Bohannan, 2007). Interactions among temperature, soil moisture and fertilizer level altered potential nitrification activity, with activity tending to be higher when soil moisture and temperature were increased. In parallel, increases in soil moisture, fertilizer level and temperature interacted to reduce the relative abundance of *Nitrosospira* sp. AF-like bacteria (i.e. AmoA cluster 10), although they remained numerically dominant. However, no significant relationship between potential nitrification activity and AOB community structure was observed after 7 weeks of environmental manipulation of this soil (Avrahami and Bohannan, 2007). Testing this hypothesis in the same soil after longer period of incubation (i.e. 16-20 weeks) resulted in interactions among the three environmental factors in the way it influenced the potential nitrification activity and N_2O emission rates due to nitrification ($NitN_2O$) (Avrahami and Bohannan, 2009). Although T-RFLP analysis revealed shifts in the community structure of AOB in all treatments, the shifts at high fertilizer concentrations were particularly striking, with dominance by three different phylogenetic groups under different combinations of the three environmental factors. Path analysis indicated that the major path by which ammonia influenced potential nitrification activity in this experiment was indirectly through its influence on the abundance of AmoA cluster 3a, which did not play a role in $NitN_2O$ emission rates (Figure 2). This group was increasing in relative abundance along with AmoA cluster 9 at the same treatment combination (i.e. 30°C and moderate/high soil moisture). In contrast, $NitN_2O$ rates revealed two patterns depending on fertilizer level: (1) In soils receiving low or moderate amounts of fertilizer the rates decreased sharply in response to increasing soil moisture and temperature. (2) In soils receiving high amounts of fertilizer, the rates were influenced by an interaction between soil moisture and temperature, such that at 20°C increasing soil moisture resulted in an increase in the rates, and at 30°C the highest rate was observed at moderate soil moisture. The inter-relationships that best explain these two patterns were revealed by path analysis. In the high fertilizer treatment the major path by which ammonia influenced $NitN_2O$ rates was indirect through an influence on the abundance of one particular phylogenetic group (AmoA cluster 10) (Figure 3a). In contrast, in the low and moderate fertilizer treatments soil moisture influenced the rates

both directly (the major path) and indirectly through AOB community structure (Figure 3b). Altogether, the complexity of the relationship between AOB community structure, their activity and fluxes of greenhouse gases, and environmental conditions had been demonstrated after a relatively long period of incubation (i.e. 16-20 weeks). The question, whether methodological biases did not mask these relationship after 7 weeks of incubation, remain unsolved.

Detection of the active biofilms-associated aerobic AOB at two ammonium concentrations respond to temperature manipulation by stable-isotope probing (SIP)

The failure to detect response of AOB to manipulation of environmental conditions after 4-7 weeks of incubation in previous laboratory studies (Avrahami et al., 2002, 2003; Szukics et al., 2010) raised the question whether the same AOB community is indeed active as a short term survival strategy, as suggested previously (Avrahami and Bohannan, 2007). Alternatively, these results could be interpreted as a bias of using a method detecting both active and resting (i.e. non active) AOB communities. By using $^{13}CO_2$ and stable-isotope probing (SIP) of nucleic acid (Friedrich, 2006) the active autotrophic ammonia oxidizing Prokaryotes could be determined, as was done previously for enrichment cultures of AOB from a lake sediment (Whitby et al., 2001), for AOB in estuary sediments (Freitag et al., 2006), and more recently for both AOB and AOA in soil microcosms (Jia and Conrad, 2009; Zhang et al., 2010). Nitrifying biofilms were developed in a flow-channel experiment with water originating from two German streams with two ammonium concentration (Ammerbach (AS) and Leutra South (LS); 683±550 and 16±7 μM NH_4^+, respectively) (Herrmann et al., 2011). The SIP method had been applied to these biofilms after incubation under three temperature regimes in order to resolve the uncertainties regarding the active autotrophic communities that are potentially oxidizing ammonia at different temperatures (Avrahami et al., 2011). The active biofilm-associated, aerobic ammonia-oxidizing communities detected by SIP were members of the *Bacteria* under all conditions tested (Avrahami et al., 2011). Copy numbers of bacterial *amoA* genes in ^{13}C-labeled DNA was lower at 30˚C than at 13˚C in both manipulated stream biofilms (Fig. 4), indicating that AOB responded to temperature manipulation. However, AOB composition in the ^{13}C-labeled DNA responded differently to temperature manipulation at two ammonium concentrations. In LS biofilm incubated at *in situ* temperature (13°C), *Nitrosomonas*

oligotropha-like sequences were retrieved with sequences from *Nitrosospira* AmoA cluster 4, while the proportion of *Nitrosospira* sequences increased at higher temperatures (Table 2). In AS biofilms incubated at 13°C and 20°C, AmoA cluster 4 sequences were dominant, and at 30°C *Nitrosomonas nitrosa*-like sequences were dominated. Avrahami et al., (2011) demonstrated changes in AOB community structure after a relative short period of 6 weeks. Members of AmoA cluster 4 were able to assimilate CO_2 and survive for a period of 6 weeks in LS biofilm enrichments at 30°C, a temperature that was reported as not suitable for their survival for a longer period (Avrahami et al., 2003; Avrahami and Conrad, 2003). However, AmoA cluster 4 were active only at 30°C and relatively low ammonium concentration and not at the same temperature and high ammonium concentrations (Avrahami et al., 2011). Similar response of AmoA cluster 10 to high temperature was observed, when this group outcompete other groups at 30°C and high ammonium concentrations after 7 weeks incubation, but not after 16 weeks of incubation (Avrahami and Bohannan, 2007). Avrahami and Bohannan (2007) suggested that being active under high temperatures might provide a short-term advantage through increased cell maintenance and survival, under high temperatures, a strategy that was not suitable for a long-term survival. Such a survival strategy has been proposed for *Nitrosospira briensis* under starvation conditions (Bollmann et al., 2005), but it has not previously been suggested for other stressful conditions or for other strains of *Nitrosospira*. Avrahami et al., (2011) findings are supporting this hypothesis for additional *Nitrosospira* (AmoA cluster 4) at high temperature (such as 30°C) but only at low ammonium concentration. In contrast, at 30°C and higher ammonium concentration member of AmoA cluster 9 (most closely related to *Nitrosospira* sp. Nsp.65) were dominating after 6 week of incubation in agreement with previous studies (Oved et al., 2001; Avrahami and Conrad, 2003; Avrahami and Bohannan, 2009), which reported on their presence in these condition but only after longer incubation (i.e. 16 weeks). Interestingly, member of AmoA cluster 9 increased in their relative abundance (to almost 30%) after 20 weeks of incubation at 30°C and lower (moderate) fertilizer (0.1%), but not at lowest (low) fertilizer tested (0.05%) (Avrahami and Bohannan, 2009). The shift in AOB community structure as a result of temperature manipulation after a relatively short period of incubation (6 weeks) (Avrahami et al., 2011) could not be detected in previous studies (Avrahami et al., 2002, 2003; Szukics et al., 2010). This is probably as it was masked by non-active DNA, and although some slow growing AOB groups were active and growing, these

groups were a minority among the non-active AOB, which were resting and waiting for better conditions. In conclusion, when looking for community shift in slow growing and resilient microorganisms such as ammonia oxidizing bacteria, it is required using methods that can distinguish between active and non-active cells. So far, no effort was done for linking between rates of nitrification and of N_2O emission due to the community structure (i.e. relative abundance and total abundance) of the active AOB cells. In the future by applying SIP in multifactorial experiment and analyzing it through path analysis one can get to a better insight into the link between change in environmental conditions to any resilient microbial community structure and its function in any environment.

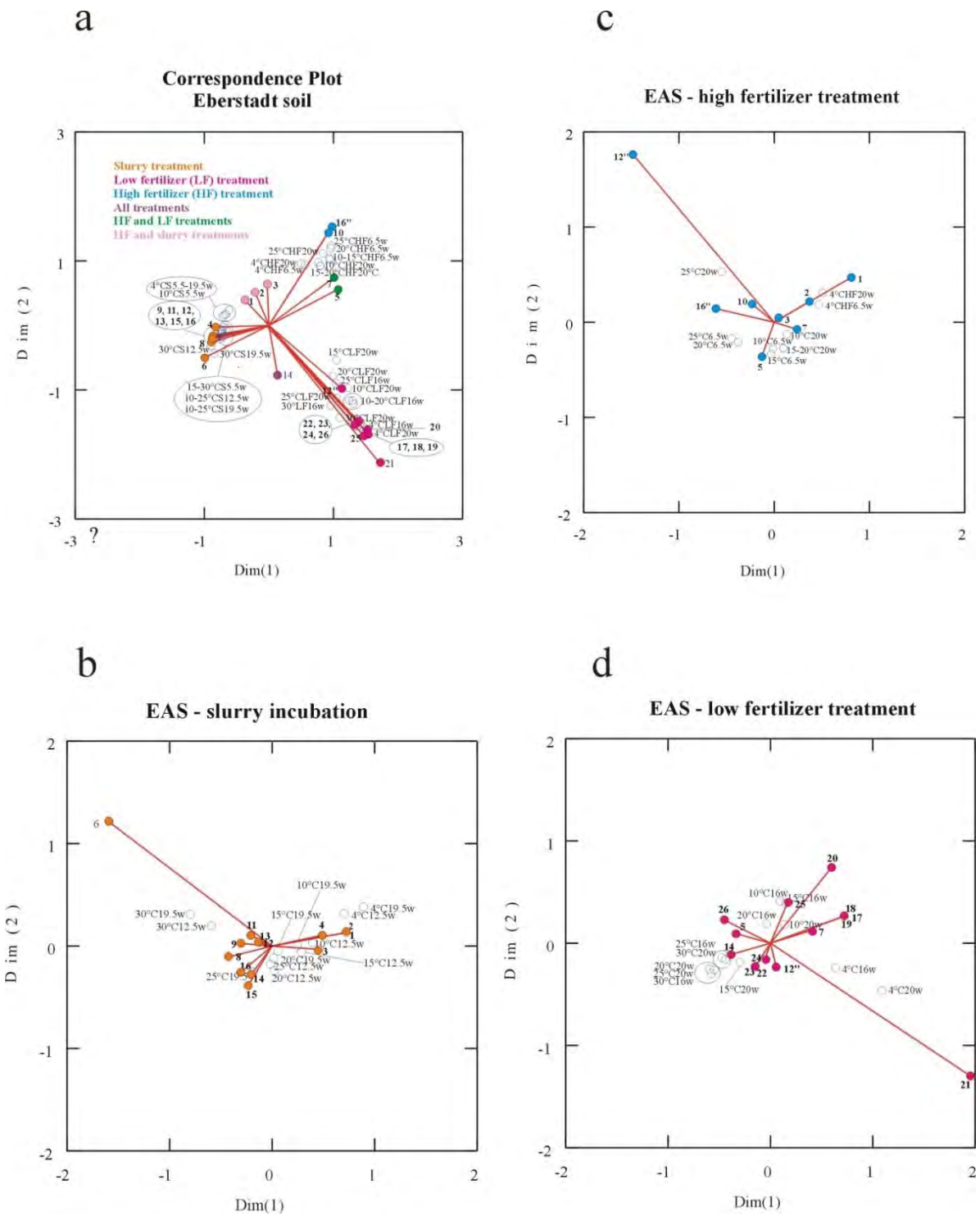

Fig. 1. Correspondence analysis comparing the differences in DGGE banding patterns by the program SYSTAT 9. Open circles represent different samples of Eberstadt Agriculture soil (EAS) soil, which were incubated at different temperatures (4 to 37°C) and/or in different ammonium treatments i.e. (a) all treatments, (b) only slurry treatments, (c) only HF treatments, and (d) only LF treatments. Name of samples composed of °C - temperature, S - slurry, LF - low fertilizer treatment, HF - high fertilizer treatment and w - period of incubation in weeks. Filled circles with a line represent bands with their numbers in bold (Avrahami et al., 2003).

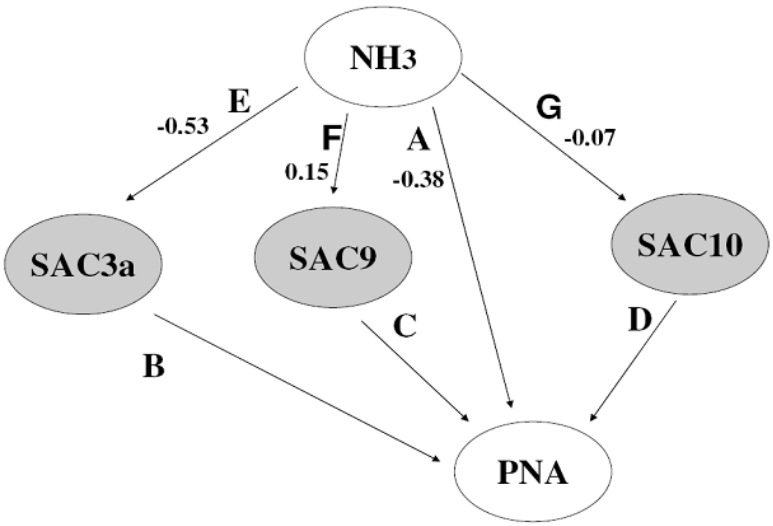

Fig. 2. Path diagram of the hypothesized models for potential nitrification activity in the high fertilizer treatment of Jasper Ridge soil incubation. Direct effects are designated as A, B, C and D, and indirect effects as E---B, F---C, G---D. Path coefficients for the latter are written on the first arrow and letter only, but represent the complete path. NH3=ammonia concentration, PNA= potential nitrification activity, SAC3a=scaled abundance of cluster 3a, SAC9=scaled abundance of cluster 9, SAC10=scaled abundance of cluster 10 (Avrahami and Bohannan, 2009).

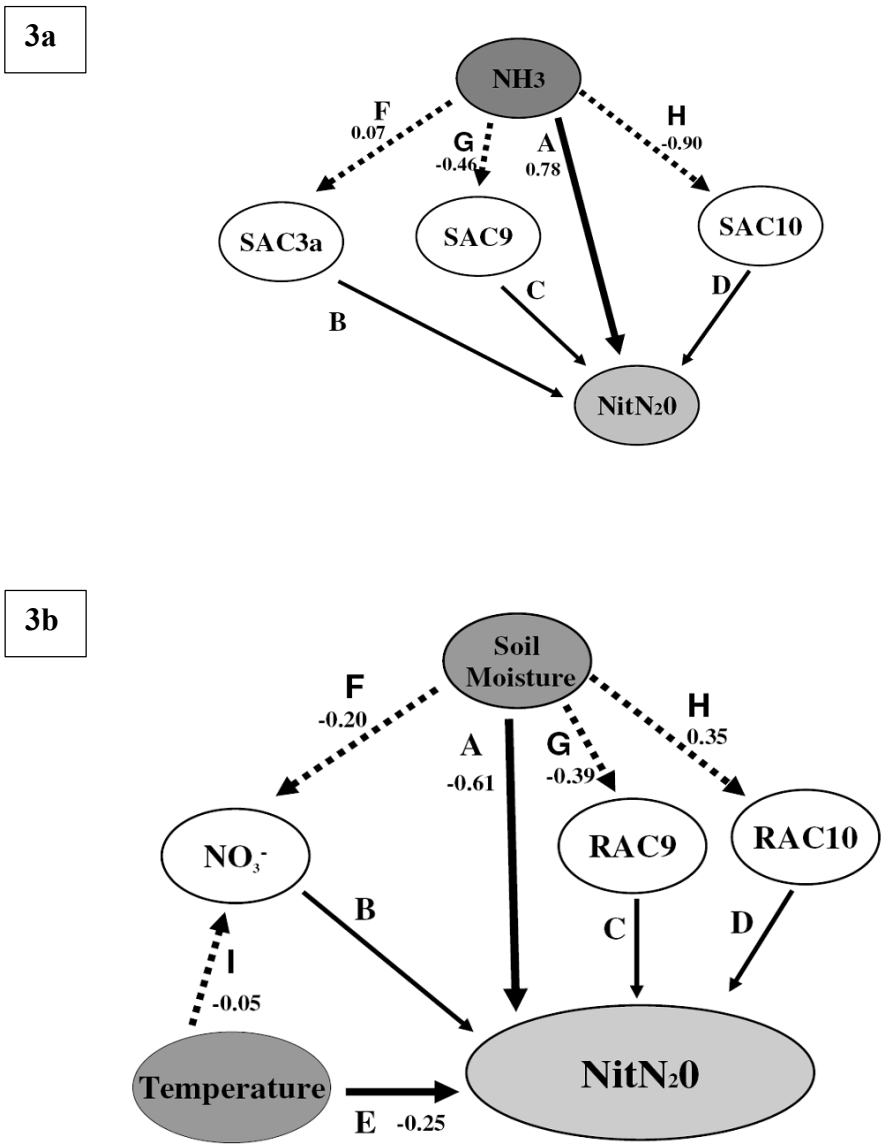

Fig. 3. Path diagram of the hypothesized models of nitrous oxide emission rates due to nitrification in (a) the high fertilizer treatment and (b) the low and moderate fertilizer treatments. Direct effects are designated as A, B, C, D and E, and indirect effects as F---B, G---C, H---D and H---B. Path coefficients for the latter are written on the first arrow and letter only, but represent the complete path. NH_3=ammonia concentration, $NitN_20$= nitrous oxide emission rates due to nitrification, SAC3a=scaled abundance of cluster 3a, SAC9=scaled abundance of cluster 9, SAC10=scaled abundance of cluster 10, NO_3^- =nitrate concentration, RAC9=relative abundance of cluster 9, RAC10=relative abundance of cluster 10 (Avrahami and Bohannan, 2009).

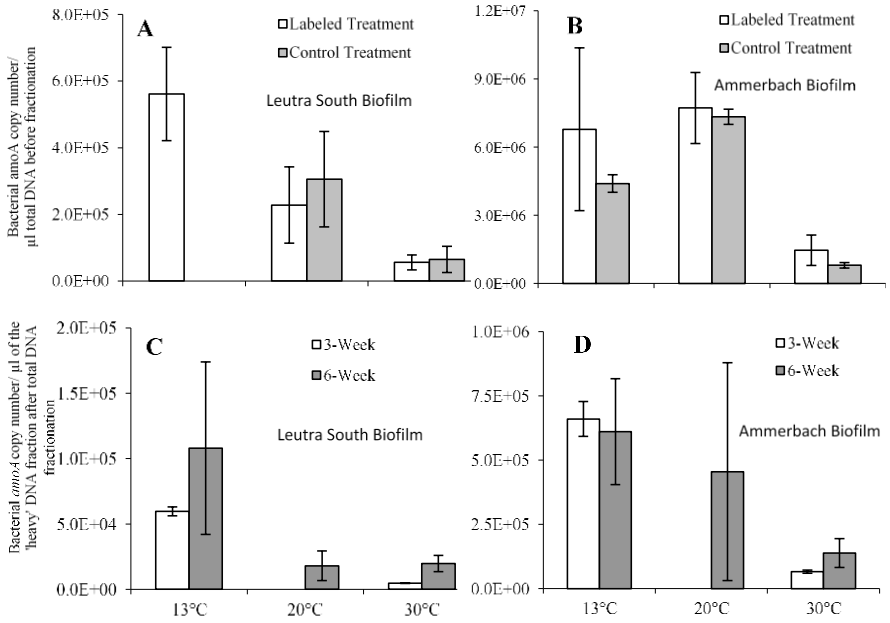

Fig. 4. The copy number of bacterial *amoA* gene in total DNA isolated from biofilm enrichments (A and B) and presumably labeled DNA after isopycnic centrifugation (C and D) of total DNA extracts. ^{13}C-$NaHCO_3$ and control referred to labeled and control treatments of stream biofilms for 6 weeks incubation in A and B, respectively. The ^{13}C-associated bacterial *amoA* copy number in C and D was the sum of those in the heavy DNA fractions-5, 6 and 7 of the labeled treatments for three and six weeks (Avrahami et al., 2011).

Table1. Distribution of the *Nitrosospira* AmoA clusters in various soils (Avrahami and Conrad, 2005)

Soil usage	Names and location of soil	AmoA Clu	1	2	3a	3b	4	9	10-12	*Nitroso-mo*	Reference
Subtropical [a]											
Grassland	KMS, Kahal, Israel	7.9			+						Avrahami and Conrad (2003)
Agriculture	VCAS, Vulcani, Israel	8.6			+	+					Own unpublished data [b]
Agriculture	Coastal Plain, Israel	6.6			+			+		+	Oved et al. (2001)
Grassland	JR, Jasper Ridge, California	6.3				+			+		Horz et al. (2004)
Cold-temperate [c]											
Grassland	GMS, Giessen, Germany	5.8	++ [d]		+	+	++				Avrahami and Conrad (2003)
Grassland	OKMS, Osterfelder, Germany	6.1	+				+				Own unpublished data [e]
Grassland	OMS, Oppenrod, Germany	5.0	+	(+)		+					Avrahami and Conrad (2003)
Grassland	Lookout, Oregon	5.6	++		+	+					Mintie et al. (2003)
Grassland	Carpenter, Oregon	5.8	++		+	+					Mintie et al. (2003)
Grassland	U4a, Scotland [f]	3.4			+	+	(+)			+ [g]	Webster et al. (2002)
Forest	Wekerom, The Netherlands [f]	3.3		+							Laverman et al. (2001)
Forest	Roggebotzand, The Netherlands [f]	4.7		+							Laverman et al. (2001)
Forest	Lookout, Oregon	5.6	++		+	+					Mintie et al. (2003)
Forest	Carpenter, Oregon	5.8	++		+	+					Mintie et al. (2003)
Forest	Harward Forest, Massachusetts	< 4.0		+		+					Compton et al. (2004)
Agriculture	EAS, Eberstadt, Germany	6.1	+		+	+	+	+		+	Avrahami et al. (2002)
Agriculture	MG6, Scotland [f]	5.4		+	++	++				+ [g]	Webster et al. (2002)
Agriculture	Alcoa, Tennessee	5.5							+		Stephen et al. (1999)
Agriculture	Knoxville, Tennessee	5.5							+		Chang et al. (2001)

[a] Including soils from Israel, California and Costa Rica.
[b] Accession No. AY256349 - AY256365
[c] Including soils from Germany, The Netherlands, Scotland, and USA
[d] ++ retrieved by high number of different sequences or dominating in T-RFLP; + frequently detected; (+) not found in all replicates
[e] Accession No. AY256366 - AY256379
[f] Analyzed by both *amoA* and 16S rRNA genes.
[g] 16S rRNA *Nitrosomonas* cluster 7

Table 2. Percentage of *amoA* gene clones within each phylogenetic group in clone libraries constructed from ^{13}C- enriched heavy DNA fractions from SIP experiments performed under different temperatures after 6 weeks incubation. In parentheses are the numbers of clones/total library clones (Avrahami et al., 2011).

Affiliation	Percentage of gene clones in					
	in Leutra South^{+} at			in Ammerbach^{++} at		
	13°C	20°C	30°C	13°C	20°C	30°C
Nitrosospira cluster 4	44% (22/50)	66% (33/50)	78% (38/49)	88% (44/50)	94% (47/50)	20% (10/50)
Nitrosomonas oligotropha – Cluster 6a	56% (28/50)	32% (16/50)	22% (11/49)	6% (3/50)	4% (2/50)	16% (8/50)
Nitrosomonasa communis – (*N. nitrosa*-like) Cluster 8	n.d.	n.d.	n.d.	n.d.	n.d.	60% (30/50)
Nitrosospira cluster 3a	n.d.	n.d.	n.d.	n.d.	2% (1/50)	4% (2/50)
Total abundance	1.08E+05 ± 6.6E+04	1.80E+04 ± 1.1E+04	1.97E+04 ± 6.2E+03	6.11E+05 ± 2.1E+05	4.55E+05 ±4.2E+05	1.39E+05 ±5.6E+04

$^{+}$ 100 μM NH_4Cl, $^{++}$ 1000 μM NH_4Cl, n.d. a not detected

Reference:

Arrigo, K.R., G. Dieckmann, M. Gosselin, D.H. Robinson, C.H. Fritsen, and C.W. Sullivan. 1995. High-resolution study of the platelet ice ecosystem in McMurdo sound, Antarctica - biomass, nutrient, and production profiles within a dense microalgal bloom. Marine Ecology-Progress Series 127: 255–268.

Avrahami, S., and B.J.M. Bohannan. 2007. Response of *Nitrosospira* sp. strain AF-like ammonia oxidizers to changes in temperature, soil moisture content, and fertilizer concentration. Applied and Environmental Microbiology 73(4): 1166–1173.

Avrahami, S., and B.J.M. Bohannan. 2009. N_2O emission rates in a California meadow soil are influenced by fertilizer level, soil moisture and the community structure of ammonia-oxidizing bacteria. Global Change Biology 15(3): 643–655.

Avrahami, S., and R. Conrad. 2003. Patterns of community change among ammonia oxidizers in meadow soils upon long-term incubation at different temperatures. Applied and Environmental Microbiology 69(10): 6152–6164.

Avrahami, S., and R. Conrad. 2005. Cold-temperate climate: a factor for selection of ammonia oxidizers in upland soil? Canadian Journal of Microbiology 51(8): 709–714.

Avrahami, S., R. Conrad, and G. Braker. 2002. Effect of soil ammonium concentration on N_2O release and on the community structure of ammonia oxidizers and denitrifiers. Applied and Environmental Microbiology 68(11): 5685–5692.

Avrahami, S., Z. Jia, J.D. Neufeld, J.C. Murrell, R. Conrad, and K. Küsel. 2011. Active autotrophic ammonia-oxidizing bacteria in biofilm enrichments from simulated creek ecosystems at two ammonium concentrations respond to temperature manipulation. Applied and Environmental Microbiology 77(20): 7329–7338.

Avrahami, S., W. Liesack, and R. Conrad. 2003. Effects of temperature and fertilizer on activity and community structure of soil ammonia oxidizers. Environmental Microbiology 5(8): 691–705.

Belser, L.W. 1979. Population ecology of nitrifying bacteria. Annual Review of Microbiology 33: 309–333.

De Boer, W., and G.A. Kowalchuk. 2001. Nitrification in acid soils: micro-organisms and mechanisms. Soil Biology and Biochemistry 33(7-8): 853–866.

Bollmann, A., I. Schmidt, A.M. Saunders, and M.H. Nicolaisen. 2005. Influence of starvation on potential ammonia-oxidizing activity and *amoA* mRNA levels of *Nitrosospira briensis*. Applied and Environmental Microbiology 71(3): 1276–1282.

Carnol, M., and P. Ineson. 1999. Environmental factors controlling NO_3^- leaching, N_2O emissions and numbers of NH_4^+ oxidisers in a coniferous forest soil. Soil Biology and Biochemistry 31(7): 979–990.

Clayton, H., I.P. McTaggart, J. Parker, L. Swan, and K.A. Smith. 1997. Nitrous oxide emissions from fertilised grassland: A 2-year study of the effects of N fertiliser form and environmental conditions. Biology and Fertility of Soils 25(3): 252–260.

Conrad, R. 1996. Soil microorganisms as controllers of atmospheric trace gases (H_2, CO, CH_4, OCS, N_2O, and NO). Microbiological Reviews 60(4): 609–640.

Conrad, R., W. Seiler, and R. Bunse, G. 1983. Factors influencing the loss of fertilizer nitrogen into the atmosphere as N_2O. Journal of Geophysical Research 88: 6709–6718.

Crutzen, P.J. 1970. Influence of nitrogen oxides on atmospheric ozone content. Quarterly Journal of the Royal Meteorological Society (96): 320.

Diaz, M.C., and B.. Ward. 1997. Sponge-mediated nitrification in tropical benthic communities. Marine Ecology-Progress Series 156: 97–107.

Dickinson, R.E., and R.J. Cicerone. 1986. Future global warming from atmospheric trace gases. Nature 319: 109–115.

Francis, C.A., K.J. Roberts, J.M. Beman, A.E. Santoro, and B.B. Oakley. 2005. Ubiquity and diversity of ammonia-oxidizing archaea in water columns and sediments of the ocean. Proceedings of the National Academy of Sciences of the United States of America 102(41): 14683–14688.

Freitag, T.E., L. Chang, and J.I. Prosser. 2006. Changes in the community structure and activity of betaproteobacterial ammonia-oxidizing sediment bacteria along a freshwater-marine gradient. Environmental Microbiology 8(4): 684–696.

Friedrich, M.W. 2006. Stable-isotope probing of DNA: insights into the function of uncultivated microorganisms from isotopically labeled metagenomes. Current Opinion in Biotechnology 17(1): 59–66.

Gödde and R. Conrad., M. 1999. Immediate and adaptational temperature effects on nitric oxide production and nitrous oxide release from nitrification and denitrification in two soils. Biology and Fertility of Soils 30: 33–40.

Golovatcheva, R.S. 1976. Thermophilic nitrifying bacteria from hot springs. Microbiology 45: 329–331.

Herrmann, M., A. Scheibe, S. Avrahami, and K. Küsel. 2011. Ammonium availability affects the ratio of ammonia-oxidizing bacteria to ammonia-oxidizing archaea in simulated creek ecosystems. Applied and Environmental Microbiology 77(5): 1896–1899.

Jia, Z., and R. Conrad. 2009. Bacteria rather than Archaea dominate microbial ammonia oxidation in an agricultural soil. Environmental Microbiology 11(7): 1658–1671.

Könneke, M., A.E. Bernhard, J.R. de la Torre, C.B. Walker, J.B. Waterbury, and D.A. Stahl. 2005. Isolation of an autotrophic ammonia-oxidizing marine archaeon. Nature 437(7058): 543–546.

Koops, H.P., and U.C. Möller. 1992. The lithotrophic ammonia-oxidizing bacteria . p. 2625–2637. *In* Balows, A.., Trüper, H.G.., Dwrkin, M.., Harder, W.., Schleifer, K.H. (eds.), The Porokaryotes. A Handbook on the Biology of Bacteria: Ecophysiology, Isolation, Identification, Applications. Springer-Varlag, New-York.

Kowalchuk, G.A., and J.R. Stephen. 2001. Ammonia-oxidizing bacteria: A model for molecular microbial ecology. Annual Review of Microbiology 55: 485–529.

Macdonald, J.A., U. Skiba, L.J. Sheppard, B. Ball, J.D. Roberts, K.A. Smith, and D. Fowler. 1997. The effect of nitrogen deposition and seasonal variability on methane oxidation and nitrous oxide emission rates in an upland spruce plantation and moorland. Atmospheric Environment 31: 3693–3706.

Mahendrappa, M.K., R.L. Smith, and A.T. Christiansen. 1966. Nitrifying organisms affected by climatic region in Western United States. Soil Science Society of America Journal 30(1): 60–62.

Malhi, S.S., and W.B. McGill. 1982. Nitrification in three Alberta soils: Effect of temperature, moisture and substrate concentration. Soil Biology and Biochemistry 14(4): 393–399.

Martens-Habbena, W., P.M. Berube, H. Urakawa, J.R. de la Torre, and D.A. Stahl. 2009. Ammonia oxidation kinetics determine niche separation of nitrifying Archaea and Bacteria. Nature 461(7266): 976–979.

Mogge, B., E.A. Kaiser, and J.C. Munch. 1998. Nitrous oxide emissions and denitrification N-losses from forest soils in the Bornhoved Lake Region (Northern Germany). Soil Biology and Biochemistry 30(6): 703–710.

Mogge, B., E., A. Kaiser, and J.C. Munch. 1999. Nitrous oxide emissions and denitrification N-losses from agricultural soils in the Bornhöved Lake region: influence of organic fertilizers and land-use. Soil Biology and Biochemistry 31(9): 1245–1252.

Myers, R.J.K. 1975. Temperature effects on ammonification and nitrification in a tropical soil. Soil Biology and Biochemistry 7(2): 83–86.

Oren, A. 1999. Bioenergetic aspects of halophilism. Microbiology and Molecular Biology Reviews 63(2): 334–348.

Oved, T., A. Shaviv, T. Goldrath, R.T. Mandelbaum, and D. Minz. 2001. Influence of effluent irrigation on community composition and function of ammonia-oxidizing bacteria in soil. Applied and Environmental Microbiology 67(8): 3426–3433.

Purkhold, U., A. Pommerening-Roser, S. Juretschko, M.C. Schmid, H.P. Koops, and M. Wagner. 2000. Phylogeny of all recognized species of ammonia oxidizers based on comparative 16S rRNA and *amoA* sequence analysis: Implications for molecular diversity surveys. Applied and Environmental Microbiology 66(12): 5368–5382.

Rysgaard, S., P. Thastum, T. Dalsgaard, P. Christensen, and N. Sloth. 1999. Effects of salinity on NH_4^+ adsorption capacity, nitrification, and denitrification in Danish estuarine sediments. Estuaries 22(1): 21–30.

Slemr, F., R. Conrad, and W. Seiler. 1984. Nitrous-oxide emissions from fertilized and unfertilized soils in a sub-tropical region (Andalusia, Spain). Journal of Atmospheric Chemistry 1: 159–169.

Smith, K.A., P.E. Thomson, H. Clayton, I.P. McTaggart, and F. Conen. 1998. Effects of temperature, water content and nitrogen fertilisation on emissions of nitrous oxide by soils. Atmospheric Environment 32: 3301–3309.

Sorokin, D.Y. 1998. On the possibility of nitrification in extremely alkaline soda biotopes. Microbiology 67(3): 335–339.

Sorokin, D., T. Tourova, M.C. Schmid, M. Wagner, H.P. Koops, J.G. Kuenen, and M. Jetten. 2001. Isolation and properties of obligately chemolithoautotrophic and extremely alkali-tolerant ammonia-oxidizing bacteria from Mongolian soda lakes. Archives of Microbiology 176(3): 170–177.

Stark, J.M., and M.K. Firestone. 1995. Mechanisms for soil-moisture effects on activity of nitrifying bacteria. Applied and Environmental Microbiology 61(1): 218–221.

Stark, J.M., and M.K. Firestone. 1996. Kinetic characteristics of ammonium-oxidizer communities in a California oak woodland-annual grassland. Soil Biology and Biochemistry 28(10–11): 1307–1317.

Szukics, U., G.C.J. Abell, V. Hödl, B. Mitter, A. Sessitsch, E. Hackl, and S. Zechmeister-Boltenstern. 2010. Nitrifiers and denitrifiers respond rapidly to changed moisture and increasing temperature in a pristine forest soil. FEMS Microbiology Ecology 72(3): 395–406.

Tourna, M., T.E. Freitag, G.W. Nicol, and J.I. Prosser. 2008. Growth, activity and temperature responses of ammonia-oxidizing archaea and bacteria in soil microcosms. Environmental Microbiology 10(5): 1357–1364.

Treusch, A.H., S. Leininger, A. Kletzin, S.C. Schuster, H.-P. Klenk, and C. Schleper. 2005. Novel genes for nitrite reductase and Amo-related proteins indicate a role of uncultivated mesophilic crenarchaeota in nitrogen cycling. Environmental Microbiology 7(12): 1985–1995.

Urakawa, H., Y. Tajima, Y. Numata, and S. Tsuneda. 2008. Low temperature decreases the phylogenetic diversity of ammonia-oxidizing archaea and bacteria in aquarium biofiltration systems. Applied and Environmental Microbiology 74(3): 894–900.

Verhamme, D.T., J.I. Prosser, and G.W. Nicol. 2011. Ammonia concentration determines differential growth of ammonia-oxidising archaea and bacteria in soil microcosms. The ISME Journal 5(6): 1067–1071.

Ward, B.B., and G.D. O'Mullan. 2002. Worldwide distribution of *Nitrosococcus oceani*, a marine ammonia-oxidizing - Proteobacterium, detected by PCR and sequencing of 16S rRNA and *amoA* Genes. Applied and Environmental Microbiology 68(8): 4153–4157.

Whitby, C.B., G. Hall, R. Pickup, J.R. Saunders, P. Ineson, N.R. Parekh, and A. McCarthy. 2001. ^{13}C incorporation into DNA as a means of identifying the active components of ammonia-oxidizer populations. Letters in Applied Microbiology 32(6): 398–401.

Williams, E.J., and F.C. Fehsenfeld. 1991. Measurement of soil nitrogen oxide emissions at three North American ecosystems. Journal of Geophysical Research 96(D1): 1033–1042.

Zhang, L.-M., P.R. Offre, J.-Z. He, D.T. Verhamme, G.W. Nicol, and J.I. Prosser. 2010. Autotrophic ammonia oxidation by soil thaumarchaea. Proceedings of the National Academy of Sciences of the United States of America 107(40): 17240–17245.

IMPACT OF SHORT-TERM ACIDIFICATION ON NITRIFICATION AND NITRIFYING BACTERIAL COMMUNITY DYNAMICS IN SOILLESS CULTIVATION MEDIA

Eddie Cytryn[1], Irit Levkovitch[1], Yael Negreanu[1,2], Scot Dowd[3], Sammy Frenk[1,2], and Avner Silber[1]

[1]Institute of Soil, Water and Environmental Sciences, The Volcani Center, Agricultural Research Organization, POB 6, Bet Dagan, 50250, Israel.

[2]Department of Plant Pathology and Microbiology, The Robert H. Smith Faculty of Agriculture, Food and Environment, The Hebrew University of Jerusalem, P.O. Box 12, Rehovot 76100, Israel.

[3]MR DNA Molecular Research LP, Shallowater, Texas USA

Running Title: Nitrification dynamics in soilless media

Abstract

Soilless media-based horticulture systems are becoming extremely prevalent worldwide due to their capacity to optimize growth of high-cash crops. However, the high fertilization loads and reduced buffer capacity of soilless media suggests that they may be more dynamic and more sensitive to physiochemical and pH perturbations than traditional agricultural soils. The objective of this study was to assess the impact of nitrification-generated acidification on ammonia-oxidation rates and nitrifying bacterial community dynamics in soilless growth media. To achieve this goal, perlite from a commercial bell pepper greenhouse was incubated with ammonium in bench-scale microcosm experiments. The β-proteobacterial ammonia-oxidizing bacteria (AOB) were found to be the dominant members of these systems and therefore research focused on this group. A highly comprehensive overview of β-proteobacterial AOB dynamics was achieved by applying a novel method based on pyrosequencing of *amoA* gene amplicons. Ammonia oxidation rates were highest between 0-9 days ($4.9 < pH < 7.4$), during which the R-strategist-like *Nitrosomonas* was the dominant ammonia-oxidizing bacterial genus. Reduction of pH to levels below 4.8 resulted in a significant decrease in both ammonia oxidation rates and the diversity of ammonia-oxidizing bacteria, with increased relative abundance of the r-strategist-like *Nitrosospira*.

Introduction

Greenhouse horiculture has expanded considerably over the past four decades due to increased global demand for high-value foods and ornamentals, and specifically, out-of-season high-quality produce (Lamont Jr, 2005; Pardossi et al., 2004; Von Elsner et al., 2000). In many cases, greenhouse cultivation has transformed from soil-based systems, to commercial-scale soilless media-based systems that enable increased crop productivity and efficiency with significant reduction of soil-associated plant pathogens (van Lenteren, 2000). Although medium-free hydroponic systems are sometimes used, most contemporary soilless culture is based on growth in artificial substrates such as sand, stone wool, polyurethane, vermiculite, perlite and scoria (tuff) (Silber and Bar-Tal, 2008). Growth in these media provide plants with physical support, a steady reservoir of nutrients, water and oxygen and simplifies the capacity to monitor and regulate key agronomic parameters such as electrical conductivity, pH and temperature (Sonneveld and Voogt, 2009). Although soilless media used in greenhouse horticulture initially contain very low levels of microbial communities, they are rapidly colonized, and develop complex communities of heterotrophic (Calvo-Bado et al., 2006; Ofek et al., 2009; Postma et al., 2005) and nitrifying (Lang and Elliott, 1997) bacteria within a few weeks after planting, and therefore artificial microbial inoculants are generally not introduced into these systems. The sources of the initial microbial inocula in these systems are believed to be the seedlings, the irrigation water and aerosols (Carlile and Wilson, 1990).

Fertigation (the application of fertilizers, soil amendments, or other water- soluble products through irrigation systems) is frequently applied in soilless greenhouse cultivation systems because it enables optimization of nutrient (most notably nitrogen, phosphorus and potassium) supply. Although urea is the cheapest and most concentrated nitrogen source fertilizer, it requires a hydrolysis to ammonium before it can be utilized by plants and therefore soilless culture systems more frequently apply ammonium and nitrate fertilizers (Silber and Bar-Tal, 2008). The ratio between ammonium and nitrate has great agricultural significance, and affects both plants and soil/growth medium. Different plant species require different ammonium/nitrate (RN) ratios for optimal growth, and the correct ratio to be applied also varies with temperature, growth stage, rhizosphere pH and soil properties (Silber and Bar-Tal, 2008).

Ammonium-based nutrition is generally more beneficial to plant growth than nitrate-based nutrition. In well buffered systems, moderate reductions in pH due to nitrification and root excretion of protons increase uptake of micronutrients, which prevent plant growth disorders induced by micronutrient deficiencies (Silber and Bar-Tal, 2008). However, application of ammonium-based fertilizer in low-buffered soils and soilless media may result in rapid nitrification-associated soil acidification, which can significantly modify the soil microbiome and have deleterious impact on crop growth. The depth and intensity of acidification is affected by a multitude of parameters including soil/media type, level of organic matter, rate and type of N fertilizer (Rasmussen, 1989) and the abundance and activity of nitrifying prokaryotes, and more specifically ammonia oxidizing prokaryotes, which lower medium pH (Arp et al., 2007).

The immense significance of nitrification to both soil ecology and to plant nutrition has generated a multitude of studies focused on elucidating the diversity, distribution and activity of ammonia oxidizing prokaryotes (AOP) in soils in general (Avrahami and Conrad, 2003; Boyle Yarwood et al., 2008; Jordan et al., 2005; Kowalchuk et al., 2000b; Morimoto et al., 2011; Nicol et al., 2008; Shah et al., 2011b); and specifically in agricultural soils (Gubry Rangin et al., 2010; Hastings et al., 1997; Jia and Conrad, 2009; Oved et al., 2001; Wang et al., 2009; Xia et al., 2011). In many cases the functional gene *amoA*, which encodes the subunit containing the putative ammonia oxygenase (AMO) enzyme active site, is used as a phylogenetic marker for characterization of ammonia-oxidizing bacteria and *Archaea* in environmental samples (Francis et al., 2005; Rotthauwe et al., 1997). Several recent studies have assessed how soil pH impacts AOP distribution and abundance, including a recent study that tested specialization of terrestrial archaeal ammonia oxidizers over a pH gradient (Gubry-Rangin et al., 2011). Nicol *et al.* (2008) found that both ammonia oxidizing bacteria (AOB) and ammonia oxidizing archaea (AOA) were characterized by distinct lineages in acid *vs.* neutral soils, but that archaeal *amoA* gene were by far the dominant group in acidic soils (Nicol et al., 2008). This was also supported by Yao *et al.* (Yao et al., 2011) who found that nitrification was mainly driven by AOA in acidic soils and that specific AOA and AOB populations dominated in these low pH soils. These studies provided substantial insight into the correlation between soil pH and AOP community structure

in different soils; however, they did not evaluate nitrification and AOP community dynamics under continued acidification.

The objective of this study was to assess the impact of short-term acidification due to nitrification, on nitrification rates and nitrifying bacterial community dynamics in soilless growth media. Microcosm experiments were conducted with perlite from an established commercial greenhouse horticulture system incubated in ammonia-amended non-buffered medium. Time-dependent pH-associated fluctuations in nitrogen species were measured concomitant to microbial community dynamics using molecular fingerprinting (DGGE) and pyrosequencing of bacterial *amoA* and 16s rRNA genes.

Materials and Methods

Experimental Setup

Two year-old perlite, that served as a soilless growth medium for sweet peppers in an experimental greenhouse (Bsor experimental station, Israel), was used as to assess nitrification and nitrifying microbial community dynamics in the bench-scale microcosm experiments described below.

Prior to the experiments, the perlite was irrigated (with water) daily to saturation in a greenhouse at 25ºC for a week, and then fertigated (irrigated with fertilizer) for an additional week, in order to enhance the relative abundance of nitrifying bacteria. The pH and EC of the fertigation solution were 6.5 ± 0.4 and 1.3 ± 0.1 dS m^{-1}, respectively. The N, P, K, Ca and Mg concentrations in the irrigation solution were 100, 25, 150, 80 and 25 mg L^{-1}, respectively. The nutrient solutions were prepared from commercial fertilizers – KNO_3, KCl, $Ca(NO_3)_2$, $Mg(NO_3)_2$, H_3PO_4, and tap water containing Ca, Mg, Na and Cl at 40, 5, 30 and 30 mg L-1, respectively. Micronutrients Zn, Fe, Cu, B, and Mo, all EDTA based, were applied at concentrations of 0.25, 1.0, 0.02, 0.2, and 0.02 mg L^{-1}, respectively. During this period ammonium was measured daily to verify AOP activity in the mature perlite.

Following the two weeks, 10 g perlite aliquots were transferred to 2 L Erlenmeyer flasks containing 500 ml of tap water supplemented with 1 mM of KH_2PO_4, and 1 mM of KCl. The bench-scale experiments were comprised of four initial solution pH values (4.5 ±

0.1, 5.5 ± 0.1, 6.2 ± 0.2 and 7.4 ± 0.3), in four replicates. The Erlenmeyer flasks were incubated at 30°C for a week (pre-equilibration period) in which the pH values were adjusted by adding appropriate amounts of 0.1 M HCI or NaOH as needed. At the end of this period 50 mg N l^{-1} as $(NH_4)_2SO_4$ was added and the Erlenmeyer flasks were incubated at 30°C without further intervention. Aqueous and perlite samples were taken for chemical and microbial analyses as described below.

Physiochemical Analyses

Physical and chemical parameters were measured at selected time points in 15 ml subsamples taken from the Erlenmeyer flasks. The pH and electrical conductivity (EC) were measured, and the samples were filtered through a 0.45-µm membrane (Millipore Corporation, Bedford, MA). To stop the nitrification activity, 100 µl 1% methiolate (ethylmercurithio-salicylic acid, sodium salt) was added to the subsamples and the solutions were frozen and kept for chemical analyses. NH_4^+, NO_3^-, and NO_2^- concentrations were later measured with a Lachat Autoanalyzer (Lachat Instruments, Milwaukee, WI).

DNA extraction, PCR and denaturing gradient gel electrophoresis (DGGE)

Perlite subsamples were periodically removed from the Erlenmeyer flasks using a long sterile spatula. DNA was extracted from 0.3 g of perlite using the PowerSoil® DNA Isolation Kit (MoBio, Carlsbad, CA). Extracted DNA was visualized by electrophoresis in 1% agarose gels and quantified spectrophotometrically by NanoDrop (NanoDrop Technologies, Wilmington, DE).

PCR amplification of partial bacterial *amoA* genes sequences for DGGE analysis, was performed on ~10 ng of extracted DNA template using the amoA1F/amoA2R primer set with a 40 bp GC-clamp attached to its 5' end (Oved et al., 2001; Rotthauwe et al., 1997). PCR reactions (final volume of 50 µL): 1.5 U Taq DNA polymerase (DreamTaq; Fermentas Life Science, Vilnius, Lithuania), Taq buffer containing a final magnesium concentration of 2.5 mM, dNTPs (20 nmol each), 12.5 µg bovine serum albumin and 25 pmol of each primer, were carried out as previously described (Oved et al., 2001). PCR amplification was verified by agarose gel electrophoresis (1%) and staining with ethidium bromide.

DGGE was performed in 6% (wt/vol) acrylamide gels containing a linear urea-formamide gradient ranging from 20 to 60% denaturant (with 100% defined as 7 M urea and 40% (vol/vol) formamide). Gels were run for 17 h at 100 V in the Dcode

Universal Mutation System (Bio-Rad Laboratories, Hercules, CA). DNA was visualized after staining with Gelstar (Invitrogen Corporation, Carlsbad, CA) by UV transillumination (302 nm) and photographed using a Kodak KDS digital camera (Kodak Co., New Haven, CT).

High throughput sequencing

454-Sequencing using tag-encoded FLX gene amplicon pyrosequencing (bTEFAP) was performed at the Research and Testing Laboratories (Lubbock, TX, USA). PCR targeting AOBs was carried out using the *amoA* primer pair amoA-1F and amoA-2R (Rotthauwe et al., 1997) using the previously defined bTEFAP protocol (Dowd et al., 2008). High throughput sequencing of perlite-extracted DNA from selected time points (0, 3, 6, 9, 27, 34, 48 and 0, 2, 3, 6, 9, 13, 27, 34, 48 days following ammonia amendment, for the *amoA* and 16S rRNA gene amplicons, respectively) yielded 35,949 raw *amoA* reads.

Bioinformatic and statistical analysis

Betaproteobacteria *amoA* amplicons from the different time points were trimmed, aligned, clustered and classified using the MOTHUR software package (Schloss et al., 2009). The *amoA* amplicons were aligned with 9,188 bacterial *amoA* genes from the FunGene, functional gene pipeline & repository database (http://fungene.cme.msu.edu/index.spr). The *amoA* downloaded reference sequences were aligned using MAFFT web-based multiple alignment program (MAFFT version 6, http://mafft.cbrc.jp/alignment/server/, FFT-NS-1-Progresive method). The 454-generated sequences were aligned to the reference sequences with the MOTHUR alignment tool using default settings. Following alignment, the sequences were cut to a defined length of 455 and 967 aligned characters (including gaps) resulting in a total of 15,642 sequences. A distance matrix was calculated for all sequences and operational taxonomic units (OTUs) were defined for 80% cutoff values as suggested by Purkhold et al. (Purkhold et al., 2000). Using a group annotation file a matrix of samples verses OTU was created and further analyzed using multivariate statistics.

Phylogenetic analysis

The phylogenetic affiliation of the bTEFAP-generated perlite-associated *amoA* sequences from the selected time points was determined using the Mega5 (Molecular Evolutionary Genetics Analysis phylogenetic package (Tamura et al., 2011). The evolutionary history was inferred using the Neighbor-Joining method (Saitou and Nei,

1987) using amino acid sequences generated from DNA sequences. The bootstrap consensus tree inferred from 1000 replicates is taken to represent the evolutionary history of the taxa analyzed (Felsenstein, 1985). Branches corresponding to partitions reproduced in less than 50% bootstrap replicates are collapsed. The evolutionary distances were computed using the Poisson correction method (Zuckerkandl and Pauling, 1965) and are in the units of the number of amino acid substitutions per site. The analysis involved 47 amino acid sequences. All positions containing gaps and missing data were eliminated. There were a total of 76 positions in the final dataset.

Statistical analysis

Clustering and ordination of the bacterial ammonia oxidizing community, based on *amoA* OTUs from the seven analyzed time points defined above, was accomplished using Non-metric multidimensional scaling (NMDS) followed by verification with the multiple response permutation procedure (MRPP) with a significance of $P<0.01$ using the PC-ord Multivariate Analysis of Ecological Data software package (MjM Software, Gleneden Beach, OR).

Results

Chemical parameters. Fluctuations in pH (Figure 1) ammonium (figure 2) were measured in all four initial pH profiles (4.5, 5.5, 6.2, and 7.4) of the soilless culture microcosm experiment over a period of 90 days subsequent to initial ammonium amendment. Nitrification (as visualized by ammonium oxidation- and corresponding nitrate formation) in the 5.5, 6.2, and 7.4 initial pH profiles was highest between days 0-9, when pH dropped from 7.4 to 4.9 (nitrification was not initially observed in the 4.5 initial pH profile). During this period nitrite did not accumulate in the vessels (except for day 3 of the initial pH 7.4 profile where a concentration of 0.04 mM was measured), indicating substantial activity of nitrite oxidizing bacteria. Ammonium concentration dynamics (Figures 1) indicated that nitrification continued at much lower rates, at pH values of 3-4.8.

DGGE. The community composition of β-proteobacterial ammonia oxidizing bacteria in the perlite of the 4 initial pH profiles at selected time points was visualized using DGGE targeting β-proteobacterial *amoA* amplicons (Figure 3). Three band clusters characterized by their migration distance in the acrylamide gel were detected. It has be

shown in previous studies (Briones et al., 2002; Oved et al., 2001) that all *amoA* bands migrating to the upper third of the gel (clusters 1 and 2 of Figure 3) are phylogenetically associated with *Nitrosomonas* strains, whereas *amoA* bands migrating to the lower third of the DGGE gel (cluster 3 of Figure 3) are phylogenetically related to *Nitrosospira* strains. Using this stipulation, *Nitrosomonas* strains were more abundant at pH levels above 4.8 and *Nitrosospira* strains were dominant at pH levels under 4.6 (Figure 2).

High throughput DNA pyrosequencing of bacterial amoA genes. Pyrosequencing of amplified β-proteobacterial partial *amoA* gene fragments was conducted at selected time points of the initial pH 7.4 profile in order to assess the diversity and relative abundance of ammonia oxidizing bacteria in the perlite at selected times. *AmoA* amplicons were grouped into 15 taxonomical groups using an 80% nucleotide sequence similarity cutoff criterion and phylogenetically characterized relative to known β-proteobacterial *amoA* sequences (Figure 4). The ammonia oxidizing community composition significantly shifted in response to ammonia oxidation-associated reductions in pH over the course of the incubation experiment. Cluster analysis of the *amoA* amplicons revealed three time/pH-associated clusters that were characterized by significant differences in AOB relative abundance (Figure 5). Days 0-9 (cluster I) were dominated by *Nitrosomonas communis*-associated lineages (sub-groups A and B), day 27 (cluster 2) was characterized by relatively equal abundances of *Nitrosomonas* and *Nitrosospira* strains, whereas days 34-48 were characterized by a significant reduction in the relative abundance of nitrosomonads, and a significant increase in the relative abundance of *Nitrosospira* cluster 3a-affiliated OTUs (Figure 5). These results strongly correlated with the DGGE analyses, where pH levels above 4.8 were characterized by higher levels of *Nitrosomonas*- and pH values below 4.6 were dominated by *Nitrosospira*-associated phylotypes.

Discussion

Preliminary qPCR and pyrosequencing of archaeal 16S rRNA gene amplicaon analyses indicated that bacteria and not archaea were the prominent AOPs in the soilless media microcosm experiments. The proportion of AOA to AOB in agricultural soils based on current literature is extremely ambiguous. While several recent studies have determined that AOA dominate the active ammonia oxidizing microbial community in some

agricultural soils (Gubry Rangin et al., 2010; Leininger et al., 2006; Nicol et al., 2008), other studies have shown that ammonia oxidation activity is primarily associated with AOB (Jia and Conrad, 2009). It has been suggested that the AOB/AOA ratio is directly correlated to inorganic nitrogen loads. For example, Fan *et al,* showed that increased inorganic fertilization led to a six- to 60-fold increase in the AOB/AOA ratio (Fan et al., 2011). Integration of our results with these previous studies suggests that ammonia oxidation in ammonium fertigated soilless culture systems, is primarily associated with AOB and not AOA.

Pyrosequencing of *amoA* and 16S rRNA gene amplicons, showed that the soilless media microcosm was initially dominated by members of the *Nitrosomonas communis* lineage (Figures 4 and 5), contrary to most molecular-based studies that have found *Nitrosospira* to be the major ammonium-oxidizing genera in agricultural soils (Avrahami et al., 2002; Avrahami et al., 2011; Kowalchuk et al., 2000a; Kowalchuk et al., 2000b; Mintie et al., 2003). Fierer *et al* hypothesized that N additions may result in a shift from a more oligotrophic bacterial community to one that is more copiotrophic, analogues to a shift from k- to r-selection often used to describe plant species ecology (Fierer et al., 2011). This is supported by a recent study targeting *amoA* gene fragments in rice paddy soils, which found that the AOB community was predominantly composed of members of the *Nitrosomonas communis* cluster, and that the relative abundance of *Nitrosomonas* increased relative to *Nitrosospira* with the increase of N fertilization, particularly in soils exposed to high oxygen concentrations (Wang et al., 2009). Ecological analyses of both soil (Hastings et al., 1997; Nicolaisen et al., 2004; Wang et al., 2009) and wastewater (Schramm et al., 2000) treatment environments have indeed supported the notion of *Nitrosomonas* strains as r strategists, with low substrate affinities and high maximum activity compared with the K strategist *Nitrosospira*.

The significant decline in *Nitrosomonas* abundance relative to *Nitrosospira* following media acidification to pH values below 4.4-4.8 (Figures 3 and 5) supports the notion that copiotrophic strains may be less resilient to environmental stress than oligotrophic ones.

Several cultivation-based and molecular methods studies have determined that *Nitrosospira* are indeed the dominant AOB genera in acidic soils, where clusters 2, 3 and 4 are generally most abundant (Burton and Prosser, 2001; Jordan et al., 2005; Kowalchuk et al., 2000b; Nugroho et al., 2005). Indeed, the dominat *Nitrosopira*-

associated OTU (NSP1) was shared high sequence similarity with an uncultured ammonia-oxidizing bacterium (GU048997) from Chinese polytunnel greenhouse vegetable soil that is generally characterized by pH values below 5.5 (Wang et al., 2009).

This study demonstrated that intensive ammonia-based fertilization in soilless culture media may result in significant difference in both nitrification dynamics and AOP community composition, relative to traditional soil-based agricultural systems. We show that under neutral and slightly acidic pH, "r-strategists"-like *Nitrosomonas* strains are the dominant AOB due to their low substrate affinity and high maximum activity, but that with increasing pH stress "k-strategists"-like *Nitrosospira* strains, characteristically dominant in soils, become more abundant. Intensive horticulture based on growth in soilless media is becoming increasingly popular and therefore, additional studies are required to enhance understanding of biogeochemical processes within them.

Acknowledgments
We thank Maya Ofek and Max Kolton for technical assistance.

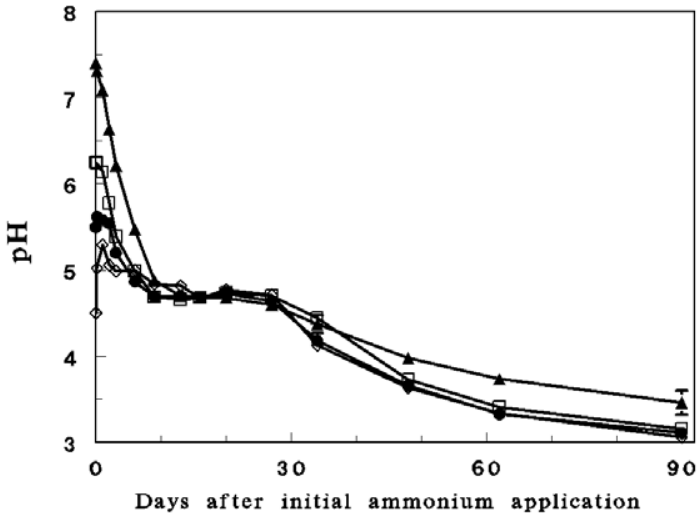

Fig. 1. Time-dependent fluctuations in pH in the different initial pH profiles of the microcosm experiment over a period of 90 days incubation. Initial pH: 7.4 (full triangles); pH 6.2 (open squares); 5.5 (full circles); and 4.5 (open diamonds).

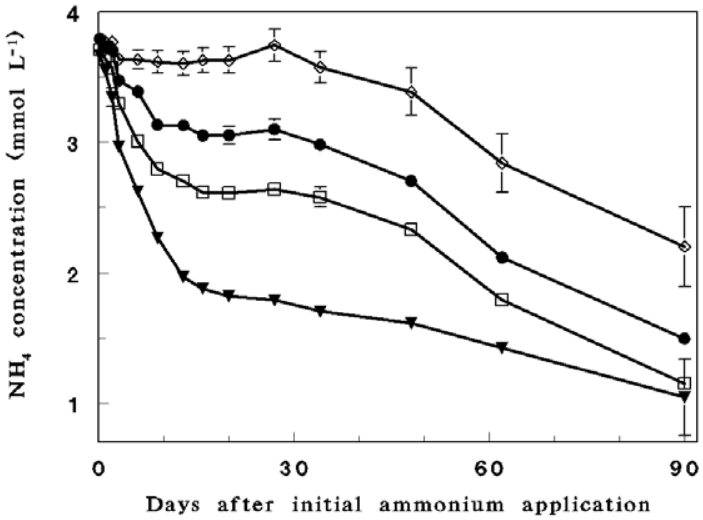

Fig. 2. Time-dependent fluctuations in ammonium concentration in the different initial pH profiles of the microcosm experiment over a period of 90 days incubation. Initial pH: 7.4 (full triangles); pH 6.2 (open squares); 5.5 (full circles); and 4.5 (open diamonds)

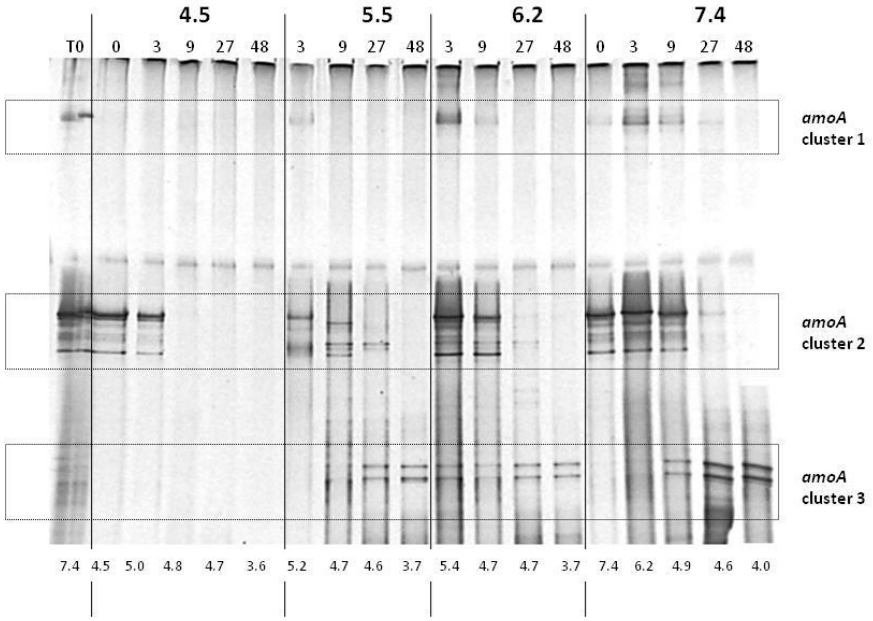

Fig. 3. AOB community dynamics depicted by DGGE of amplified β-proteobacterial *amoA* gene amplicons in the four initial pH profiles of the microcosm experiment: 4.5, 5.5, 6.2, 7.4. Bold numbers above the gel indicate the initial pH values. Labels above gel show the time (in days) following initial ammonia amendment (T0 is the initial pre-incubation perlite inoculant). Numbers below the gel indicate the actual pH values during the time of sampling. Arrows indicate the critical pH zone (4.6-4.8), where ammonium oxidation rates significant dropped and AOB community shifted from *Nitrosomonas-like* phylotypes (clusters 1 and 2) to *Nitrosospira-like* phylotypes (cluster 3).

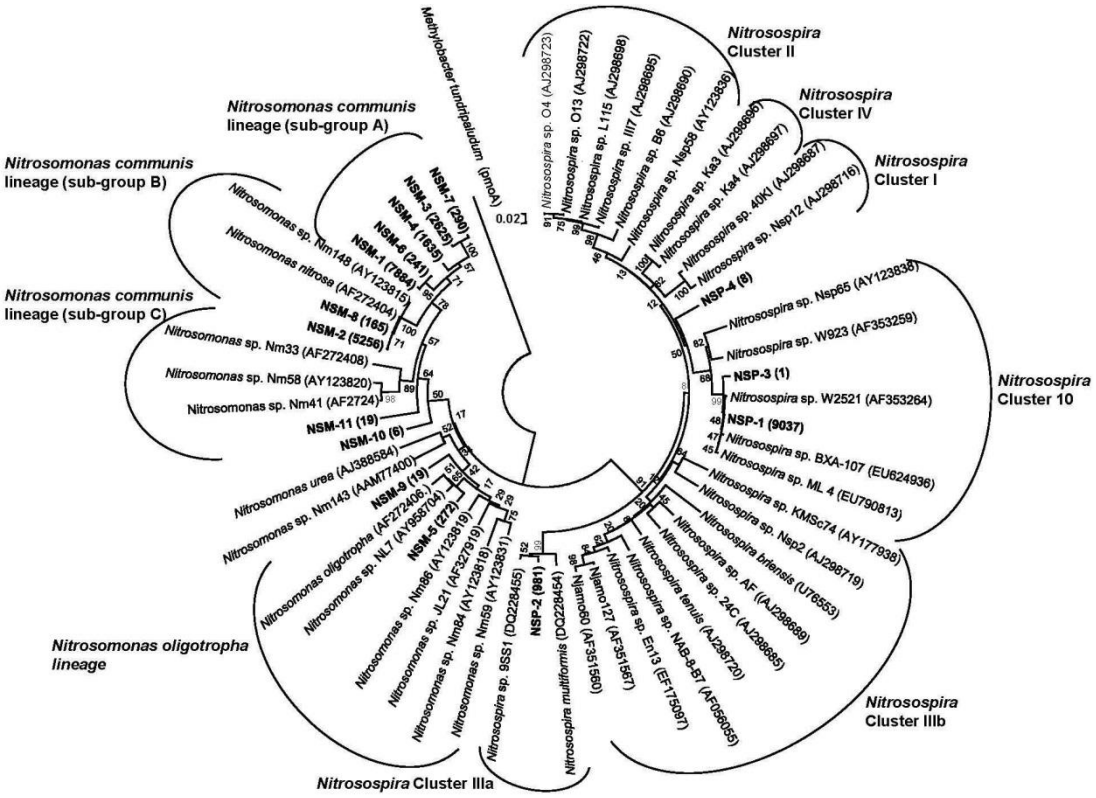

Fig. 4. Phylogenetic affiliation of the 15 generated *amo*A OTU clusters (bold) relative to closely related reference sequences. Numbers in bold parentheses represent the number of sequences generated in the pyrosequencing analysis for the designed OTU

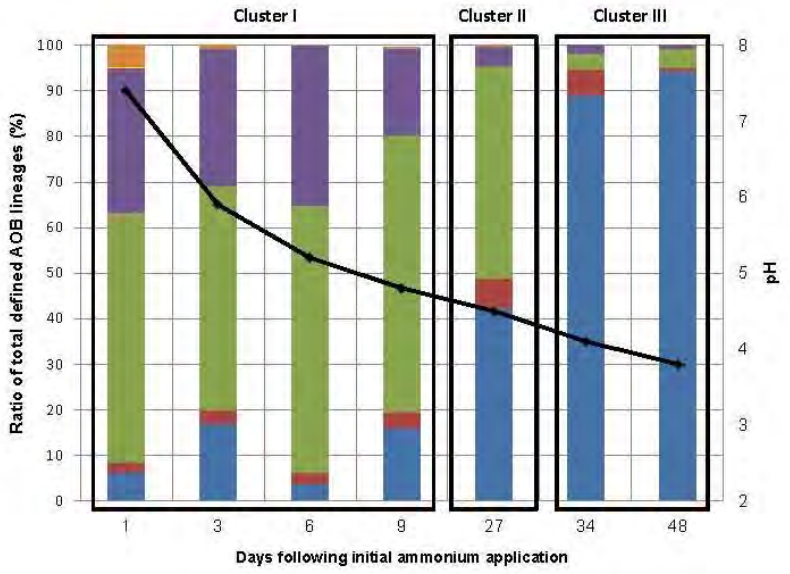

Fig. 5. Relative abundance of *amoA* defined AOB lineages in relation to time dependent pH vlues at seleced time points of the initial pH 7.4 profile of the microcosm experiment *Nitrosopira* cluster 1 (Blue), *Nitrosopira* cluster 3 (Red) *Nitrosomas* communis lineage sub-group A (Green), *Nitrosomas* communis lineage sub-group C (Yellow), *Nitrosomonas* oligotropha lineage (Orange). The black line shows time dependent pH fluctuations (right x-axis)

Reference:

Arp, D.J., P.S.G. Chain, and M.G. Klotz. 2007. The impact of genome analyses on our understanding of ammonia-oxidizing bacteria. (in English) Annu Rev Microbiol 61:503-528.

Avrahami, S., and R. Conrad. 2003. Patterns of community change among ammonia oxidizers in meadow soils upon long-term incubation at different temperatures. Appl Environ Microbiol 69:6152-6164.

Avrahami, S., R. Conrad, and G. Braker. 2002. Effect of soil ammonium concentration on N2O release and on the community structure of ammonia oxidizers and denitrifiers. Appl Environ Microbiol 68:5685-5692.

Avrahami, S., Z.J. Jia, J.D. Neufeld, J.C. Murrell, R. Conrad, and K. Kusel. 2011. Active Autotrophic Ammonia-Oxidizing Bacteria in Biofilm Enrichments from Simulated Creek Ecosystems at Two Ammonium Concentrations Respond to Temperature Manipulation. Applied and Environmental Microbiology 77:7329-7338.

Boyle Yarwood, S.A., P.J. Bottomley, and D.D. Myrold. 2008. Community composition of ammonia oxidizing bacteria and archaea in soils under stands of red alder and Douglas fir in Oregon. Environmental microbiology 10:2956-2965.

Briones, A.M., S. Okabe, Y. Umemiya, N.B. Ramsing, W. Reichardt, and H. Okuyama. 2002. Influence of different cultivars on populations of ammonia-oxidizing bacteria in the root environment of rice. (in eng) Appl Environ Microbiol 68:3067-3075.

Burton, S.A.Q., and J.I. Prosser. 2001. Autotrophic ammonia oxidation at low pH through urea hydrolysis. Appl Environ Microbiol 67:2952-2957.

Calvo-Bado, L.A., G. Petch, N.R. Parsons, J.A.W. Morgan, T.R. Pettitt, and J.M. Whipps. 2006. Microbial community responses associated with the development of oomycete plant pathogens on tomato roots in soilless growing systems. Journal of Applied Microbiology 100:1194-1207.(ed.)^(eds.). 1990.

Dowd, S.E., T.R. Callaway, R.D. Wolcott, Y. Sun, T. McKeehan, R.G. Hagevoort, and T.S. Edrington. 2008. Evaluation of the bacterial diversity in the feces of cattle using 16S rDNA bacterial tag-encoded FLX amplicon pyrosequencing (bTEFAP). (in English) BMC Microbiol 8.

Fan, F.L., Q.B. Yang, Z.J. Li, D. Wei, X. Cui, and Y.C. Liang. 2011. Impacts of organic and inorganic fertilizers on nitrification in a cold climate soil are linked to the bacterial ammonia oxidizer community. (in English) Microb Ecol 62:982-990.

Felsenstein, J. 1985. Confidence limits on phylogenies: an approach using the bootstrap. Evolution:783-791.

Fierer, N., C.L. Lauber, K.S. Ramirez, J. Zaneveld, M.A. Bradford, and R. Knight. 2011. Comparative metagenomic, phylogenetic and physiological analyses of soil microbial communities across nitrogen gradients. ISME J.

Francis, C.A., K.J. Roberts, J.M. Beman, A.E. Santoro, and B.B. Oakley. 2005. Ubiquity and diversity of ammonia-oxidizing archaea in water columns and sediments of the ocean. Proc Nat Acad Sci 102:14683.

Gubry-Rangin, C., B. Hai, C. Quince, M. Engel, B.C. Thomson, P. James, M. Schloter, R.I. Griffiths, J.I. Prosser, and G.W. Nicol. 2011. Niche specialization of terrestrial archaeal ammonia oxidizers. (in eng) Proc Natl Acad Sci 108:21206-21211.

Gubry Rangin, C., G.W. Nicol, and J.I. Prosser. 2010. Archaea rather than bacteria control nitrification in two agricultural acidic soils. FEMS Microb Ecol 74:566-574.

Hastings, R.C., M.T. Ceccherini, N. Miclaus, J.R. Saunders, M. Bazzicalupo, and A.J. McCarthy. 1997. Direct molecular biological analysis of ammonia oxidising bacteria populations in cultivated soil plots treated with swine manure. FEMS Microb Ecol 23:45-54.

Jia, Z.J., and R. Conrad. 2009. Bacteria rather than Archaea dominate microbial ammonia oxidation in an agricultural soil. Environ Microbiol 11:1658-1671.

Jordan, F.L., J.J.L. Cantera, M.E. Fenn, and L.Y. Stein. 2005. Autotrophic ammonia-oxidizing bacteria contribute minimally to nitrification in a nitrogen-impacted forested ecosystem. (in English) Appl Environ Microbiol 71:197-206.

Kowalchuk, G.A., A.W. Stienstra, G.H.J. Heilig, J.R. Stephen, and J.W. Woldendorp. 2000a. Molecular analysis of ammonia-oxidising bacteria in soil of successional grasslands of the Drentsche A (The Netherlands). FEMS Microbiol Ecol 31:207-215.

Kowalchuk, G.A., A.W. Stienstra, G.H.J. Heilig, J.R. Stephen, and J.W. Woldendorp. 2000b. Changes in the community structure of ammonia-oxidizing bacteria during secondary succession of calcareous grasslands. Environ Microbiol 2:99-110.

Lamont Jr, W.J. 2005. Plastics: Modifying the microclimate for the production of vegetable crops. Hort Technol 15:477-481.

Lang, H.J., and G.C. Elliott. 1997. Enumeration and inoculation of nitrifying bacteria in soilless potting media. J Am Soc Hortic Sci 122:709-714.

Leininger, S., T. Urich, M. Schloter, L. Schwark, J. Qi, G. Nicol, J. Prosser, S. Schuster, and C. Schleper. 2006. Archaea predominate among ammonia-oxidizing prokaryotes in soils. Nature 442:806-809.

Mintie, A.T., R.S. Heichen, K. Cromack, D.D. Myrold, and P.J. Bottomley. 2003. Ammonia-oxidizing bacteria along meadow-to-forest transects in the oregon cascade mountains. Appl Environ Microbiol 69:3129-3136.

Morimoto, S., M. Hayatsu, Y.T. Hoshino, K. Nagaoka, M. Yamazaki, T. Karasawa, M. Takenaka, and H. Akiyama. 2011. Quantitative analyses of ammonia-oxidizing Archaea (AOA) and ammonia-oxidizing Bacteria (AOB) in fields with different soil types. Microbes and Environments 26:248-253.

Nicol, G.W., S. Leininger, C. Schleper, and J.I. Prosser. 2008. The influence of soil pH on the diversity, abundance and transcriptional activity of ammonia oxidizing archaea and bacteria. Environ Microbiol 10:2966-2978.

Nicolaisen, M.H., N. Risgaard-Petersen, N.P. Revsbech, W. Reichardt, and N.B. Ramsing. 2004. Nitrification-denitrification dynamics and community structure of ammonia oxidizing bacteria in a high yield irrigated Philippine rice field. FEMS Microbiol Ecol 49:359-369.

Nugroho, R.A., W.F.M. Roling, A.M. Laverman, H.R. Zoomer, and H.A. Verhoef. 2005. Presence of *Nitrosospira* cluster 2 bacteria corresponds to N transformation rates in nine acid Scots pine forest soils. (in English) FEMS Microbiol Ecol 53:473-481.

Ofek, M., Y. Hadar, and D. Minz. 2009. Comparison of effects of compost amendment and of single-strain inoculation on root bacterial communities of young cucumber seedlings. Appl Enviro Microbiol 75:6441.

Oved, T., A. Shaviv, T. Goldrath, R.T. Mandelbaum, and D. Minz. 2001. Influence of effluent irrigation on community composition and function of ammonia-oxidizing bacteria in soil. Appl Enviro Microbiol 67:3426.

Pardossi, A., F. Tognoni, and L. Incrocci. 2004. Mediterranean greenhouse technology. Chronica Hort 44:28-34.

Postma, J., B.P. Geraats, R. Pastoor, and J.D. van Elsas. 2005. Characterization of the Microbial Community Involved in the Suppression of Pythium aphanidermatum in Cucumber Grown on Rockwool. (in eng) Phytopathology 95:808-818.

Purkhold, U., A. Pommerening-Roser, S. Juretschko, M.C. Schmid, H.P. Koops, and M. Wagner. 2000. Phylogeny of all recognized species of ammonia oxidizers based on comparative 16S rRNA and amoA sequence analysis: Implications for molecular diversity surveys. (in English) Appl Enviro Microbiol 66:5368-5382.

Rasmussen, P.E.R. 1989. Soil acidification from ammonium-nitrogen fertilization in moldboard plow and stubble-mulch wheat-fallow tillage. Soil Sci Soc Am 53:119.

Rotthauwe, J.H., K.P. Witzel, and W. Liesack. 1997. The ammonia monooxygenase structural gene amoA as a functional marker: molecular fine-scale analysis of natural ammonia-oxidizing populations. Appl Enviro Microbiol 63:4704.

Saitou, N., and M. Nei. 1987. The neighbor-joining method: a new method for reconstructing phylogenetic trees. Mol Biol Evol 4:406-425.

Schloss, P.D., S.L. Westcott, T. Ryabin, J.R. Hall, M. Hartmann, E.B. Hollister, R.A. Lesniewski, B.B. Oakley, D.H. Parks, C.J. Robinson, J.W. Sahl, B. Stres, G.G. Thallinger, D.J. Van Horn, and C.F. Weber. 2009. Introducing mothur: open-source, platform-independent, community-supported software for describing and comparing microbial communities. (in English) Appl Enviro Microbiol 75:7537-7541.

Schramm, A., D. De Beer, A. Gieseke, and R. Amann. 2000. Microenvironments and distribution of nitrifying bacteria in a membrane-bound biofilm. Environ Microbiol 2:680-686.

Shah, V., S. Shah, M.S. Kambhampati, J. Ambrose, N. Smith, S.E. Dowd, K.T. McDonnell, B. Panigrahi, and T. Green. 2011a. Bacterial and archaea community present in the Pine Barrens Forest of Long Island, NY: unusually high percentage of ammonia oxidizing bacteria. (in eng) PloS one 6:e26263.

Shah, V., S. Shah, M.S. Kambhampati, J. Ambrose, N. Smith, S.E. Dowd, K.T. McDonnell, B. Panigrahi, and T. Green. 2011b. Bacterial and Archaea community present in the pine varrens forest of Long Island, NY: Unusually high percentage of Ammonia Oxidizing Bacteria. PloS one 6:e26263.

Silber, A., and A. Bar-Tal. 2008. Nutrition of substrate-grown plants, p. 291-339, *In* M. Raviv and H. Lieth, (eds.) Soilless culture: Theory and practice. ed. Elsevier Science, London, UK.

Sonneveld, C., and W. Voogt. 2009. Plant nutrition of greenhouse crops. Springer Verlag, Dordrecht

Tamura, K., D. Peterson, N. Peterson, G. Stecher, M. Nei, and S. Kumar. 2011. MEGA5: Molecular evolutionary genetics analysis using maximum likelihood, evolutionary distance, and maximum parsimony methods. (in English) Mol Biol Evol 28:2731-2739.

van Lenteren, J.C. 2000. A greenhouse without pesticides: fact or fantasy? Crop prot 19:375-384.

Von Elsner, B., D. Briassoulis, D. Waaijenberg, A. Mistriotis, C. Von Zabeltitz, J. Gratraud, G. Russo, and R. Suay-Cortes. 2000. Review of structural and functional characteristics of greenhouses in European Union countries: Part I, Design requirements. J Agricul Eng Res 75:1-16.

Wang, Y., X. Ke, L. Wu, and Y. Lu. 2009. Community composition of ammonia-oxidizing bacteria and archaea in rice field soil as affected by nitrogen fertilization. Syst Appl Microbiol 32:27-36.

Xia, W.W., C.X. Zhang, X.W. Zeng, Y.Z. Feng, J.H. Weng, X.G. Lin, J.G. Zhu, Z.Q. Xiong, J. Xu, Z.C. Cai, and Z.J. Jia. 2011. Autotrophic growth of nitrifying community in an agricultural soil. ISME J 5:1226-1236.

Yao, H., Y. Gao, G.W. Nicol, C.D. Campbell, J.I. Prosser, L. Zhang, W. Han, and B.K. Singh. 2011. Links between ammonia oxidizer community structure, abundance, and nitrification potential in acidic soils. Appl Enviro Microbiol 77:4618.

Zuckerkandl, E., and L. Pauling. 1965. Evolutionary divergence and convergence in proteins. Evolv Gen Prot 97:166.

Session 5: Factors Affecting Soil Microbial Activity

PORE-SCALE HYDROLOGICAL CONTROLS OF MICROBIAL LIFE IN SOIL

Dani Or

Department of Environmental Sciences, ETH Zurich, Switzerland

By some accounts exploring microbial diversity found in soils represents a scientific frontier at the scope similar to that of space exploration. The immense diversity of microbial life is attributed to the complex and heterogeneous pore surfaces and spaces with highly dynamic aqueous and chemical microenvironments. In most unsaturated near-surface soils the aqueous network that defines nutrient diffusional pathways and shapes microbial dispersion patterns is in a constant state of change. We explore effects of microscale hydrological processes on biophysical interactions affecting microbial dispersion and controlling coexistence of competing bacterial species inhabiting unsaturated soil surfaces. A novel metric for hydration-controlled microbial diversity based on combining information on fragmentation of aquatic microhabitats, motion and dispersion distances in aqueous films, and diffusion-supported nutrient transport control cohabitation in soil pores. Experiments confirm a surprisingly narrow range of hydration-enabled motility and onset of limiting and heterogeneous diffusion fields that promote coexistence even under mild unsaturated conditions (only a few kPa matric potential values mark the transition in most soils). Spatial self- organization of trophically-interacting microbial populations and formation of consortia shaped by dynamic diffusion fields will be presented.

MICROBIAL COMMUNITIES SELECTED BY AGRICULTURAL MANAGEMENT AND THE ASSOCIATED FLUX OF GREENHOUSE GASES

Thomas M. Schmidt*, Vicente Gomez-Alvarez, Tracy Teal and Bjørn Østman

Department of Microbiology and Molecular Genetics, Michigan State University
*Current address: Departments of Internal Medicine; Ecology and Evolutionary Biology, University of Michigan

Increasing concentrations of carbon dioxide, methane and nitrous oxide have intensified the radiative forcing of Earth's atmosphere. The global cycles of each these gases is catalyzed in part by microbial communities in agricultural ecosystems. Microbes in agricultural soils contribute approximately half of the anthropogenically derived N_2O in the atmosphere. Methane-oxidizing bacteria in upland soils represent the largest known biological sink for atmospheric methane and all heterotrophic bacteria contribute to the flux of carbon dioxide. We used both targeted and shotgun metagnomes to better understand the effect of agriculture on the composition of microbial communities responsible for each of these ecosystem-level processes across a gradient of land uses in the upper Midwest United States.

Targeted metagenomes of 16S rRNA-encoding genes were used to test the neutral model in community ecology. The composition of bacterial communities in agricultural soils could not be explained solely as a consequence of dispersion from the adjacent deciduous forest soil, confirming that agricultural practices have indeed influenced microbial community composition.

The analysis of shotgun metagenomes revealed that an increased proportion of bacteria with the denitrification pathway distinguished microbial communities in agricultural soils from those in native soils. Among the dramatic diversity of denitrifiers identified in shotgun metagenomes, approximately 75% of the sequences annotated as nitrite reductase would not be captured in commonly used PCR-based gene surveys. The ratio of nonsynonymous to synonymous substitutions in targeted metagenomes of nitrite reductase (*nirK*), a pivotal gene in the denitrification pathway, confirmed that *nirK* from

heterotrophic bacteria was under increased purifying selection in agricultural soils compared to native deciduous forest soils.

We found that agricultural practices led to local extinctions of methanotrophs and a commensurate drop in methane consumption. As methanotroph diversity decreased, so did the rate and stability of methane oxidation. Conversely, neither the rate nor stability of CO_2 emissions from soil were related to total bacterial diversity.

Our results are consistent with a conceptual model in which microbial diversity is a strong predictor of the magnitude and stability of ecosystem processes when relatively few species are present that catalyze the process, e.g. methane oxidation by methanotrophs in soil, and a poor predictor of processes driven by metabolic processes that are widely distributed in an environment, including the production of nitrous oxide and carbon dioxide.

We also document the imprint of agriculture on the genetic diversity and taxonomic composition of terrestrial microbial communities for more than 20 years after the cessation of agriculture. Understanding shifts in the composition of microbial communities that underlie the flux of greenhouse gases is the first step towards managing microbial biodiversity in soil to mitigate the production of this potent greenhouse gas. These results also demonstrate how evolutionary methods can be used to identify selective pressures on specific genes in complex microbial communities.

TREATED WASTEWATER EFFECT ON SOIL MICROBIAL COMMUNITY ECOLOGY

Sammy Frenk[1,2] and Dror Minz[1]

[1]Institute for Soil, Water and Environmental Sciences, Agricultural Research Organization, Bet-Dagan, Israel,
[2]Robert H. Smith Faculty of Agriculture, Food and Environment, The Hebrew University of Jerusalem, Rehovot, Israel

Fresh water (FW) availability is declining in many parts of the world (Vörösmarty et al. 2010) and is expected to decline even further in coming years due to three main reasons; i) high consumption rate by the continuously growing world population and increase in standard of living, resulting in higher requirements for water, ii) Anthropogenic contamination of available resources, iii) global climate change leading to different precipitation regimes causing less rain fall in many Mediterranean and semi arid regions (Milly et al. 2005; Vörösmarty et al. 2010; World Health Organization 2006).

The use of treated wastewater (TWW) for agricultural practices is therefore an essential solution to the water shortage of many regions, as part of their water management program (Chen et al. 2008; Jueschke et al. 2008). Despite the importance of water reuse in irrigation, there are drawbacks concerning the environmental impact it might impose on the soil and its microbial ecology. Amongst these drawbacks are the introduction of dissolved minerals and organic matter (Lieth & Hamdy 1999; Meli et al. 2002), human associated pathogens (Estrada et al. 2004; Shuval 2010; World Health Organization 2006) and pharmaceutical and personal care products (PPCPs) (Kosma et al. 2014). These introduced materials range from potentially beneficial for plant and microbial growth, such as some dissolved minerals and organic matter, to pathogens and many of the PPCPs that may be hazardous to humans and soil organisms. All of the described materials have the potential to affect the soil microbiome. Since pathogen introduction to soils and the effects of PPCPs on bacterial communities following TWW irrigation were recently discussed (Forslund et al. 2010, 2012; Negreanu et al. 2012), this review focus on the effect of TWW related dissolved minerals and organic matter on soil microbial communities. The soil microbial communities are composed of different

populations of bacterial, archaeal and eukaryotic organisms, which differ in their responses to these compounds. TWW used for irrigation can origin from either municipal sewage or industrial operations (Iannelli & Giraldi 2010) and therefore vary greatly in quality. The quality of TWW used for irrigation is thus highly dependent on the origin of the wastewater (WW) and treatment used to create it. Due to high variation in water quality between various studies, there is a need for long term surveys in different sampling sites and using a variety of WW treated with different methods to fully understand TWW affect on soil biology.

The Soil microbiome, and particularly the bacterial fraction of it, is composed of a vast number of cells from many different populations. Bacteria in soil are abundant and extremely diverse, consisting $4.8 \cdot 10^9$ - $2.1 \cdot 10^{10}$ cells of hundreds to thousands of unique genomes/cm^{-3} of soil (Torsvik & Ovreås 2002; Torsvik et al. 2002). The environmental factors determining the soil bacterial community's composition include the texture of the soil they inhabit (Carson et al. 2010), pH level (Fierer & Jackson 2006; Lauber et al. 2009), nitrogen content (Wessén et al. 2010; Fierer et al. 2011) and moisture (Brockett et al. 2012). Further, a good predictor for the bacterial community size was found to be soil organic matter (SOM) content (Fierer et al. 2009). A stable, active and diverse soil bacterial community is important for plant growth (Van Bruggen & Semenov 2000), degradation of organic matter (Doran & Zeiss 2000) and various pollutants (Cea et al. 2010), and for the prevention of establishment of plant pathogenic organisms (van Elsas et al. 2012). However, the soil bacterial community, similarly to other microbial communities, maintains a cause and effect relationship between the management practice of a given environment and the presence of the microorganism in it. Thus, applying various materials to the soil leads to their consequential degradation/utilization by the microbial community, followed by community changes. This is true for degradable organic materials (Cleveland et al. 2007; Dungait et al. 2013; Jenkins et al. 2010) as well as nutrients introduced to soil (Enwall et al. 2007; Peacock et al. 2001). Irrigation with TWW is not different in this sense and recent publications demonstrating these principles will be further discussed here.

The utilization rate of many substrates can be evaluated using several enzymatic assays, CO_2 evolution (for the estimation of respiration) and measurements of biogeochemical end products. These methods were used in several studies of various soils irrigated with different water qualities, ranging from untreated WW to high quality TWW with

relatively low organic materials. The hypothesis driving these studies is that a recurring exposure to a specific material, abundant in TWW, will result in development of microbial community better acclimated to degrade that material. Thus, TWW irrigation will be considered sustainable if the biogeochemical processes related to the introduced substances in soil will be increased or unaffected (Chen et al. 2008). This hypothesis was proven to be correct for several tested minerals. For example, nitrogen cycling was studied by several enzymatic assays, including protease, amidohydrolases, urease, histidine ammonia-lyase, as well as ammonia oxidation (Brzezinska et al. 2006; Chen et al. 2008; del Mar Alguacil et al. 2012; Elifantz et al. 2011; Filip et al. 1999) that showed increased activity under TWW irrigation. An increase of phosphorus cycling examined using alkaline phosphatase, acid phosphatase, inorganic pyrophosphatase and phosphodiesterase assays was also demonstrated in TWW irrigated soils (del Mar Alguacil et al. 2012; Chen et al. 2008; Filip et al. 1999), although contradictory evidence for higher activity of phosphorus cycling in FW irrigated soils compared to TWW irrigated ones exist as well (Meli et al. 2002; Brzezinska et al. 2006). Carbon cycling assays using Cellulase, α-glucosidase, α-galactosidase, invertase and soil oxidative potential using dehydrogenase activity showed increased activities in TWW irrigated soils in most studies (del Mar Alguacil et al. 2012; Chen et al. 2008; Brzezińska et al. 2001; Elifantz et al. 2011; Filip et al. 1999). The response of soil microbial communities measured in these cases may result from two main changes; an increase in microbial community population size in soil, as a result of increased resource availability, and/or changes of the microbial community composition as some organisms gain selective advantage and thrive in the new conditions developed due to irrigation with TWW.

Increase of microbial biomass was recorded during long term irrigation with untreated WW (Hidri et al. 2010; Filip et al. 1999; Friedel et al. 2000). On the other hand, TWW irrigated soils showed very small and mostly insignificant differences in bacterial 16S rRNA gene copy counts compared to FW irrigated soils (Negreanu et al. 2012; Frenk et al. 2014), despite TWW bacterial abundance being significantly higher than that found in FW (Negreanu et al. 2012). This is mainly due to the inability of bacteria of TWW origin to establish in soil, as well as the relatively low organic input to soil by TWW, compared to untreated WW, insufficient for significant proliferation of soil bacteria. TWW organic matter content is mostly measured by biological and/or

chemical oxygen demands (BOD and COD, respectively). While BOD measurements in WW are usually between 110-350 mg/l O_2, values of TWW after an activated sludge bioreactor are around 5-25 mg/l O_2 (Chen et al. 2010). Usually, high levels of biodegradable organic matter (OM) input to the soil environment are necessary to increase the microbial biomass (Bastida et al. 2013; Fierer et al. 2009). For example, high levels of OM amendment, via WW irrigation or solid waste application have long term effects on microbial activity and biomass that last for as many as 20 years after application ended (Bastida et al. 2010, 2008; Filip et al. 1999).

In addition to OM, various minerals including nitrogen, phosphorus and sulfates are also introduced to the soil environment via TWW and may influence the soil microbial populations. As stated previously, based on published data, as well as in our studies, it is currently difficult to determine the contribution of each component of TWW. Therefore, we discuss here the effects of TWW mostly as reflected by its nitrogen and organic carbon content. Nitrogen, relatively abundant in TWW, is a limiting nutrient for plant growth (LeBauer & Treseder 2008) but may also affect soil microbial communities. Several forms of nitrogen can be found in TWW including nitrite, nitrate, ammonium and organic matter, the last two being the predominant in most cases. While nitrogen fertilization did not show significant increase in microbial biomass, both bacterial and fungal (Treseder 2008), significant changes to microbial community's composition were described (Fierer et al. 2011; Yuan et al. 2013). Changes in the composition of microbial communities were also described for soil under carbon amendments (Eilers et al. 2010; Jenkins et al. 2010; Monard et al. 2008) and microbial inoculation (Pettersson & Bååth 2013; Thion et al. 2013). As TWW includes all these components, a similar effect on microbial community composition compared to FW irrigation is to be expected.

Changes in soil bacterial as well as on fungal community composition and diversity were previously described following irrigation with TWW (Frenk et al. 2014) and WW (Hidri et al. 2010; del Mar Alguacil et al. 2012). The differences in community composition following TWW irrigation were characterized by a decrease in relative abundance of predominant soil members of bacteria and fungi. The bacterial community shift included decrease in the relative abundance of actinobacterial populations that typically characterize Mediterranean and arid soils and increased abundance of various Proteobacteria (Frenk et al. 2014). Furthermore, WW and TWW

had a significant effect on nitrifying bacterial communities (Ndour et al. 2008; Oved et al. 2001). Ammonia oxidation, the first step in the nitrification process is performed by a unique group of prokaryotes, both archaeal and bacterial, and is important for plant nutrition (Leininger et al. 2006; Koops et al. 2006). Ammonia oxidizing bacteria (AOB) that were described to-date are phylogenetically related to either Betaproteobacteria or Gammaproteobacteria classes (Koops et al. 2006). Soil AOB communities are mostly dominated by various species of the genus *Nitrosospira*, while other AOB genera are far less represented (Koops et al. 2006). However, during TWW irrigation an AOB from the genus *Nitrosomonas* related to *N. nitrosa* was found to increase in soils (Oved et al. 2001). Although *N. nitrosa* did not dominate the AOB community, it significantly changed its structure. As for fungal communities, decreases in diversity of Arbuscular mycorrhizal fungi (AMF) and increases in abundance of specific groups of uncultivable AMF was demonstrated (del Mar Alguacil et al. 2012). Thus, the overall services and functions that the microbial community provide to the environment were maintained, but by a different community of organisms. All the community changes described above are related in the sense that natural oligotrophic soil inhabitants are replaced with copiotrophic organisms, more adapted to high amounts of minerals and organic matter (Avrahami et al. 2011; Cytryn et al. 2012; Eilers et al. 2010; Fierer et al. 2011; Oved et al. 2001; Philippot et al. 2009).

These shifts in community composition are a response of the microbial community to changing environmental conditions that TWW imposed on the soil, and can be described as a disturbance (Frenk et al. 2014). A 'disturbance' is a biotic or abiotic cause which results in an effect on an ecological process (and described as a "perturbation") or on a physiological response of an individual or system (and described as a "stress") (Rykiel 1985; Griffiths & Philippot 2013). The two alternatives that dictate the responses of a community to a disturbance are; (i) resistance -the ability of a community to withstand the disturbance without changing, and (ii) resilience - the ability to return to a pre-disturbed steady-state (Allison & Martiny 2008). Allison & Martiny (2008) showed in their literature survey of disturbance patterns, mostly in the soil environment, that 83% of the studies reporting C amendments and 84% of the studies reporting N/P/K fertilization caused a disturbance to the microbial community. Furthermore, the recovery of the microbial community back to a steady state after the disturbance was shown to take at least a few days and in some cases resulted in a

permanent change defined as an alternative steady state (Allison & Martiny 2008; Griffiths & Philippot 2013). Soil community compositions were not resistant to the effect of irrigation with TWW and WW but their functionality was maintained, as activities stayed unchanged or higher than the reported controls. In the case of temporary TWW irrigation, as usually performed in the summer in Mediterranean and semi-arid regions, the community composition followed a seasonal trend. During the irrigation season, in several studies we performed there was a shift of community composition and activity with a return to the original community composition and activity levels, similar to the control, during the rainy season (Elifantz et al. 2011; Frenk et al. 2014). These results show that despite the low resistance to the disturbance caused by TWW, the soil community showed high resilience on an annual time scale.

Various agricultural managements were shown to disturb the soil microbial community and consequently lower the resistance of the community to a secondary disturbance (such as heat shock, pH differences and heavy metal contamination, see review by Griffiths & Philippot 2013). Since TWW irrigation changes the soil microbial community composition, if only temporarily, it may lead to the development of community less resistant to a secondary stress as well. These changes in the microbiome may lead, in some cases, to the loss of diversity, as reported for AMF communities (del Mar Alguacil et al. 2012). This may further lead to lower functional diversity, affecting services provided by soil microbiology. The loss of diversity may also make the soil more susceptible to the establishment of pathogens (van Elsas et al. 2012), which may lower production yields and quality of agricultural operations. Another possible consequence of diversity loss is lower functional redundancy in the community that is manifested by losing rare traits. In a dynamic environment such as soil, it is expected that the microbial community under TWW irrigation might be at higher risk of stress than soil irrigated with FW. Further research is needed to evaluate the effect of TWW irrigation, under variable disturbance scenarios, on the performance of soil microbial community.

In summary, TWW irrigation is a well established practice in many regions in the world and important for a responsible water management in a scenario of depleting water resources. This practice had been shown to change microbial community size composition and function even when applying TWW of relatively high qualities. However, changes in community size were diminished or reduced when TWW quality

improved. Some issues concerning TWW irrigation, such as possible change in a community's resistance to stresses and consequently compromising the microbial mediated services provided by soil needs to be further studied.

Reference:

Allison SD, Martiny JBH. (2008). Resistance, resilience, and redundancy in microbial communities. Proceedings of the National Academy of Sciences 105:11512–11519.

Avrahami S, Jia Z, Neufeld JD, Murrell JC, Conrad R, Küsel K. (2011). Active autotrophic ammonia-oxidizing bacteria in biofilm enrichments from simulated creek ecosystems at two ammonium concentrations respond to temperature manipulation. Applied and environmental microbiology 77:7329–7338.

Bastida F, Hernández T, Albaladejo J, Garcìa C. (2013). Phylogenetic and functional changes in the microbial community of long-term restored soils under semiarid climate. Soil Biology and Biochemistry 65:12–21.

Bastida F, Hernández T, Garcìa C. (2010). Soil degradation and rehabilitation: microorganisms and functionality. In:Microbes at Work, Insam, Heribert and Franke-Whittle, Ingrid and Goberna, Marta, (ed)., Springer Berlin Heidelberg, pp. 253–270.

Bastida F, Kandeler E, Hernández T, Garcìa C. (2008). Long-term effect of municipal solid waste amendment on microbial abundance and humus-associated enzyme activities under semiarid conditions. Microbial ecology 55:651–661.

Brockett BF, Prescott CE, Grayston SJ. (2012). Soil moisture is the major factor influencing microbial community structure and enzyme activities across seven biogeoclimatic zones in western Canada. Soil Biology and Biochemistry 44:9–20.

Van Bruggen A, Semenov A. (2000). In search of biological indicators for soil health and disease suppression. Applied Soil Ecology 15:13–24.

Brzezińska M, Stępniewska Z, Stępniewski W. (2001). Dehydrogenase and catalase activity of soil irrigated with municipal wastewater. Polish Journal of Environmental Studies 10:307–311.

Brzezińska M, Tiwari S, Stepniewska Z, Nosalewicz M, Bennicelli R, Samborska A. (2006). Variation of enzyme activities, CO 2 evolution and redox potential in an Eutric Histosol irrigated with wastewater and tap water. Biology and Fertility of Soils 43:131–135.

Carson JK, Gonzalez-Quiñones V, Murphy DV, Hinz C, Shaw JA, Gleeson DB. (2010). Low pore connectivity increases bacterial diversity in soil. Applied and environmental microbiology 76:3936–3942.

Cea M, Jorquera M, Rubilar O, Langer H, Tortella G, Diez M. (2010). Bioremediation of soil contaminated with pentachlorophenol by Anthracophyllum discolor and its effect on soil microbial community. Journal of hazardous materials 181:315–323.

Chen W, Wu L, Frankenberger WT, Chang AC. (2008). Soil enzyme activities of long-term reclaimed wastewater-irrigated soils. Journal of environmental quality 37:S–36.

Chen Y, Dosoretz CG, Katz I, Jüeschke E, Marschner B, Tarchitzky J. (2010). Organic Matter in Wastewater and Treated Wastewater-Irrigated Soils: Properties and Effects. In:Treated Wastewater in Agriculture: Use and Impacts on the Soil Environment and Crops, G. J. Levy, P. Fine and A. Bar-Tal, (ed)., Wiley Online Library: Oxford, UK, pp. 400–417.

Cleveland CC, Nemergut DR, Schmidt SK, Townsend AR. (2007). Increases in soil respiration following labile carbon additions linked to rapid shifts in soil microbial community composition. Biogeochemistry 82:229–240.

Cytryn E, Levkovitch I, Negreanu Y, Dowd S, Frenk S, Silber A. (2012). Impact of short-term acidification on nitrification and nitrifying bacterial community dynamics in soilless cultivation media. Applied and Environmental Microbiology 78:6576–6582.

Doran JW, Zeiss MR. (2000). Soil health and sustainability: managing the biotic component of soil quality. Applied Soil Ecology 15:3–11.

Dungait JA, Kemmitt SJ, Michallon L, Guo S, Wen Q, Brookes P, et al. (2013). The variable response of soil microorganisms to trace concentrations of low molecular weight organic substrates of increasing complexity. Soil Biology and Biochemistry 64:57–67.

Eilers KG, Lauber CL, Knight R, Fierer N. (2010). Shifts in bacterial community structure associated with inputs of low molecular weight carbon compounds to soil. Soil Biology and Biochemistry 42:896–903.

Elifantz H, Kautsky L, Mor-Yosef M, Tarchitzky J, Bar-Tal A, Chen Y, et al. (2011). Microbial activity and organic matter dynamics during 4 years of irrigation with treated wastewater. Microbial ecology 62:973–981.

van Elsas JD, Chiurazzi M, Mallon CA, Elhottov D, Krivstuufek V, Salles JF. (2012). Microbial diversity determines the invasion of soil by a bacterial pathogen. Proceedings of the National Academy of Sciences 109:1159–1164.

Enwall K, Nyberg K, Bertilsson S, Cederlund H, Stenström J, Hallin S. (2007). Long-term impact of fertilization on activity and composition of bacterial communities and metabolic guilds in agricultural soil. Soil Biology and Biochemistry 39:106–115.

Estrada IB, Aller A, Aller F, Gómez X, Morán A. (2004). The survival of Escherichia coli, faecal coliforms and enterobacteriaceae in general in soil treated with sludge from wastewater treatment plants. Bioresource technology 93:191–198.

Fierer N, Grandy AS, Six J, Paul EA. (2009). Searching for unifying principles in soil ecology. Soil Biology and Biochemistry 41:2249–2256.

Fierer N, Jackson RB. (2006). The diversity and biogeography of soil bacterial communities. Proceedings of the National Academy of Sciences of the United States of America 103:626–631.

Fierer N, Lauber CL, Ramirez KS, Zaneveld J, Bradford MA, Knight R. (2011). Comparative metagenomic, phylogenetic and physiological analyses of soil microbial communities across nitrogen gradients. The ISME Journal 6:1007–1017

Filip Z, Kanazawa S, Berthelin J. (1999). Characterization of effects of a long-term wastewater irrigation on soil quality by microbiological and biochemical parameters. Journal of Plant Nutrition and Soil Science 162:409–413.

Forslund A, Ensink J, Battilani A, Kljujev I, Gola S, Raicevic V, et al. (2010). Faecal contamination and hygiene aspect associated with the use of treated wastewater and canal water for irrigation of potatoes (Solanum tuberosum). Agricultural Water Management 98:440–450.

Forslund A, Ensink J, Markussen B, Battilani A, Psarras G, Gola S, et al. (2012). E. coli contamination and health aspects of soil and tomatoes (Solanum Lycopersicum) subsurface drip irrigated with on-site treated domestic wastewater. Water research 46:5917–5934.

Frenk S, Hadar Y, Minz D. (2014). Resilience of soil bacterial community to irrigation with water of different qualities under Mediterranean climate. Environmental Microbiology16:559–569.

Friedel JK, Langer T, Siebe C, Stahr K. (2000). Effects of long-term waste water irrigation on soil organic matter, soil microbial biomass and its activities in central Mexico. Biology and Fertility of Soils 31:414–421.

Griffiths BS, Philippot L. (2013). Insights into the resistance and resilience of the soil microbial community. FEMS Microbiology Reviews 37:112–29.

Hidri Y, Bouziri L, Maron PA, Anane M, Jedidi N, Hassan A, et al. (2010). Soil DNA evidence for altered microbial diversity after long-term application of municipal wastewater. Agronomy for Sustainable Development 30:423–431.

Iannelli R, Giraldi D. (2010). Sources and composition of sewage effluent; treatment systems and methods. In:Treated Wastewater in Agriculture: Use and Impacts on the Soil Environment and Crops, G. J. Levy, P. Fine and A. Bar-Tal, (ed)., Wiley Online Library: Oxford, UK, pp. 1–50.

Jenkins SN, Rushton SP, Lanyon CV, Whiteley AS, Waite IS, Brookes PC, et al. (2010). Taxon-specific responses of soil bacteria to the addition of low level C inputs. Soil Biology and Biochemistry 42:1624–1631.

Jueschke E, Marschner B, Tarchitzky J, Chen Y. (2008). Effects of treated wastewater irrigation on the dissolved and soil organic carbon in Israeli soils. Water science and technology 57:727–733.

Koops H-P, Purkhold U, Pommerening-Röser A, Timmermann G, Wagner M. (2006). The Lithoautotrophic Ammonia-Oxidizing Bacteria. In:The Prokaryotes, Dworkin M, Falkow S, Rosenberg E, Schleifer, K-H, Stackebrandt E. (ed)., Springer New York, pp. 778–811.

Kosma CI, Lambropoulou DA, Albanis TA. (2014). Investigation of PPCPs in wastewater treatment plants in Greece: Occurrence, removal and environmental risk assessment. Science of The Total Environment 466:421–438.

Lauber CL, Hamady M, Knight R, Fierer N. (2009). Pyrosequencing-based assessment of soil pH as a predictor of soil bacterial community structure at the continental scale. Applied and environmental microbiology 75:5111–5120.

LeBauer DS, Treseder KK. (2008). Nitrogen limitation of net primary productivity in terrestrial ecosystems is globally distributed. Ecology 89:371–379.

Leininger S, Urich T, Schloter M, Schwark L, Qi J, Nicol G, et al. (2006). Archaea predominate among ammonia-oxidizing prokaryotes in soils. Nature 442:806–809.

Lieth H, Hamdy A. (1999). Halophyte uses in different climates I: ecological and ecophysiological studies: proceedings of the 3rd seminar of the EU Concerted Action Group IC 18CT 96-0055, Florence, Italy, 20 July, 1998. Backhuys Publishers.

del Mar Alguacil M, Torrecillas E, Torres P, García-Orenes F, Roldán A. (2012). Long-Term Effects of Irrigation with Waste Water on Soil AM Fungi Diversity and Microbial Activities: The Implications for Agro-Ecosystem Resilience. PloS one 7:e47680.

Meli S, Porto M, Belligno A, Bufo SA, Mazzatura A, Scopa A. (2002). Influence of irrigation with lagooned urban wastewater on chemical and microbiological soil parameters in a citrus orchard under Mediterranean condition. Science of the total environment 285:69–77.

Milly PC, Dunne K, Vecchia AV. (2005). Global pattern of trends in streamflow and water availability in a changing climate. Nature 438:347–350.

Monard C, Binet F, Vandenkoornhuyse P. (2008). Short-term response of soil bacteria to carbon enrichment in different soil microsites. Applied and environmental microbiology 74:5589–5592.

Ndour NYB, Baudoin E, Guissé A, Seck M, Khouma M, Brauman A. (2008). Impact of irrigation water quality on soil nitrifying and total bacterial communities. Biology and Fertility of Soils 44:797–803.

Negreanu Y, Pasternak Z, Jurkevitch E, Cytryn E. (2012). Impact of treated wastewater irrigation on antibiotic resistance in agricultural soils. Environmental science & technology 46:4800–4808.

Oved T, Shaviv A, Goldrath T, Mandelbaum RT, Minz D. (2001). Influence of effluent irrigation on community composition and function of ammonia-oxidizing bacteria in soil. Applied and environmental microbiology 67:3426–3433.

Peacock AD, Mullen MD, Ringelberg DB, Tyler DD, Hedrick DB, Gale PM, et al. (2001). Soil microbial community responses to dairy manure or ammonium nitrate applications. Soil Biology and Biochemistry 33:1011–1019.

Pettersson M, Bååth E. (2013). Importance of Inoculum Properties on the Structure and Growth of Bacterial Communities during Recolonisation of Humus Soil with Different pH. Microbial ecology 66:416–426.

Philippot L, Bru D, Saby N, Čuhel J, Arrouays D, Šimek M, et al. (2009). Spatial patterns of bacterial taxa in nature reflect ecological traits of deep branches of the 16S rRNA bacterial tree. Environmental microbiology 11:3096–3104.

Rykiel EJ. (1985). Towards a definition of ecological disturbance. Australian Journal of Ecology 10:361–365.

Shuval H. (2010). Health considerations in the recycling of water and use of treated wastewater in agriculture and other non-potable purposes. In:Treated Wastewater in Agriculture: Use and Impacts on the Soil Env. and Crops, G. J. Levy, P. Fine and A. Bar-Tal, (ed)., Wiley Online Library: Oxford, UK, pp. 51–76.

Thion C, Cébron A, Beguiristain T, Leyval C. (2013). Inoculation of PAH-degrading strains of Fusarium solani and Arthrobacter oxydans in rhizospheric sand and soil microcosms: microbial interactions and PAH dissipation. Biodegradation 24:569–581.

Torsvik V, Ovreås L. (2002). Microbial diversity and function in soil: from genes to ecosystems. Current opinion in microbiology 5:240–245.

Torsvik V, Øvreås L, Thingstad TF. (2002). Prokaryotic Diversity-Magnitude, Dynamics, and Controlling Factors. Science 296:1064–1066.

Treseder KK. (2008). Nitrogen additions and microbial biomass: A meta-analysis of ecosystem studies. Ecology Letters 11:1111–1120.

Vörösmarty CJ, McIntyre PB, Gessner MO, Dudgeon D, Prusevich A, Green P, et al. (2010). Global threats to human water security and river biodiversity. Nature 467:555–561.

Wessén E, Hallin S, Philippot L. (2010). Differential responses of bacterial and archaeal groups at high taxonomical ranks to soil management. Soil Biology and Biochemistry 42:1759–1765.

World Health Organization. (2006). WHO Guidelines for the Safe Use of Wastewater. Excreta and Greywater 2.

Yuan H, Ge T, Zhou P, Liu S, Roberts P, Zhu H, et al. (2013). Soil microbial biomass and bacterial and fungal community structures responses to long-term fertilization in paddy soils. Journal of Soils and Sediments13:877–886.

Session 6: Tools to Investigate Phosphorus Reactions in Soils

SOLUTION ^{31}P-NMR SPECTROSCOPY OF SOILS FROM 2005-2013: A REVIEW OF SAMPLE PREPARATION AND EXPERIMENTAL PARAMETERS

Barbara Cade-Menun[1]* and Corey W. Liu[2]

[1]Agriculture and Agri-Food Canada, Swift Current, SK, S9H 3X2, Canada.
[2]Stanford Magnetic Resonance Laboratory, Stanford University, Stanford CA 94305-5126 USA.
*Corresponding author: Barbara.Cade-Menun@agr.gc.ca. Phone: 306-778-7245; Fax: 306-778-3188

Abstract

Phosphorus nuclear magnetic resonance (^{31}P NMR) spectroscopy is an important tool for the study of soil P and has significantly advanced our knowledge of soil P forms, particularly organic P; however, it must be used correctly to provide meaningful results. This review covers the ^{31}P NMR studies of soil published from 2005 to 2013. The first part discusses preparing samples for ^{31}P NMR, including extractants, pre- and post-extraction treatments, the physical state of the soil sample at the time of extraction, extraction length, the soil/extractant ratio, P recovery, P in residues, methods to concentrate extracts, redissolving samples for ^{31}P NMR experiments, the use of the internal standard methylene diphosphonic acid, and the potential for degradation with any of these steps. The second part of this review focuses on NMR experiment parameters, including delay times, proton decoupling, and experiment length. Potential concerns in these areas are noted, and suggestions are given for procedures to optimize the information obtained from a ^{31}P NMR experiment.

https://www.soils.org/publications/sssaj/articles/78/1/19?highlight=&search-result=1

Molecular Speciation of Phosphorus Present in Readily Dispersible Colloids from Agricultural Soils

Jin Liu[1], Jianjun Yang[2], Xinqiang Liang[2], Yue Zhao[2], Barbara J. Cade-Menun[3] and Yongfeng Hu[4]

[1]Dep. of Environmental Engineering Zhejiang Univ. Hangzhou 310058 China and Agriculture and Agri-Food Canada SPARC Box 1030 Swift Current, SK S9H 3X2 Canada

[2]Dep. of Environmental Engineering Zhejiang Univ. Hangzhou 310058 China

[3]Agriculture and Agri-Food Canada SPARC Box 1030 Swift Current, SK S9H 3X2 Canada

[4]Canadian Light Source Univ. of Saskatchewan Saskatoon, SK S7N 0X4 Canada

Abstract

Speciation of colloidal P (P_{coll}) is vital yet little known. For the first time ever, the P species in readily released colloids from agricultural soils were determined by P K-edge X-ray absorption near-edge structure (XANES) and solution ^{31}P nuclear magnetic resonance (P-NMR) spectroscopy. Water-dispersible P_{coll} was the dominant fraction of readily released P (<1 μm) from the studied soils cultivated with rice (*Oryza sativa* L.) (RS; 80.9%) and vegetables (VS; 55.1%). The P_{coll} in these samples was predominantly in inorganic form, which XANES showed to be moderately labile Fe- and Al-associated P (total 70.4–83.3%) and nonlabile hydroxyapatite (16.8–19.7%). The P-NMR analysis showed that the dominant organic P compound class in colloids from RS was orthophosphate monoesters, of which inositol hexakisphosphate was the largest component. These results strongly suggested that colloids are richer in stable P forms and poorer in labile and mineralizable P than the bulk soils.

https://www.soils.org/publications/sssaj/abstracts/78/1/47?search-result=1

PHOSPHORUS FORMS IN THE SOIL PROFILE DETERMINED BY ^{31}P-NMR SPECTROSCOPY AS INFLUENCED BY TILLAGE PRACTICES AND P FERTILIZATION

Dalel Abdi[1,3], Barbara J. Cade-Menun[2], Noura Ziadi[3] and Léon-Étienne Parent[1]

[1]Agriculture and Agri-Food Canada, Soils and Crops Research and Development Centre, 2560 Hochelaga Boulevard, Québec, QC, Canada G1V 2J3;
[2]Agriculture and Agri-Food Canada, Semiarid Prairie Agricultural Research Centre, P.O. Box 1030 Swift Current, SK, Canada, S9H 3X2;
[3]Department of Soils and Agri-Food Engineering, Université Laval, Québec, QC, Canada G1K 7P4.
Corresponding author: Phone number: 306-778-7245; Fax number: 306-778-3188; E-mail: barbara.cade-menun@agr.gc.ca

Abstract

A better understanding of organic phosphorus transformations is needed to improve management of phosphorus fertilization and tillage. Conservation tillage practices have become increasingly common in recent years to reduce soil erosion, improve water conservation, and increase soil organic matter. However, the effects on soil properties, especially phosphorus (P) forms, amounts and distribution in the soil profile remain largely unknown. This study was conducted to assess the long term effects of tillage practices (no till [NT] and mouldboard plowing to 20 cm depth, [MP]), and P fertilization on P composition and distribution in the soil profile. The long term corn-soybean rotation experiment was established in 1992 on a deep clay loam soil of the St-Blaise series (Dark Grey Gleysol) in Acadie, Canada. The experimental design is a split plot with NT and MP assigned to main plots and nine combinations of three P (0, [P_0], 17.5 [$P_{17.5}$], and 35 [P_{35}] kg P ha^{-1}) and three N (0, 80, and 160 kg N ha^{-1}) additions assigned to subplots. Only the plots with the P_0 and P_{35} treatment combined with 160 kg N ha^{-1} were considered in this study. We used 32 air-dried soil samples collected from three depths (0-5, 5-10, and 10-20 cm). These were analysed for Mehlich 3 P (PM3) and with solution phosphorus-31 nuclear magnetic resonance spectroscopy (^{31}P-NMR). Results showed a greater surface (0 – 5 cm) PM3 and inorganic orthophosphate concentration in NT-P_{35} soils, suggesting a greater potential for P loss from runoff. Two

inositol hexakisphosphate (IP_6) stereoisomers (*myo*- and *neo*-) were uniformly distributed in the soil profile under NT and MP systems, but were slightly higher in the P fertilized soils. In contrast, another stereoisomer (*scyllo*-IP_6) was accumulated in the deep layer of NT-P_{35} treatment presumably due to preferential movement.

Abbreviations: α-gly, α-glycerophosphate; β-glycerophosphate; chol-P, choline phosphate; *clr*, centered log ratio; IP_6, inositol hexakisphosphate; MP, mouldboard plow; NT, no-till; PM3, soil P content extracted using the Mehlich 3 method; P_0, soil treatment with 0 kg P ha^{-1}; P_{35}, soil treatment with 35 kg P ha^{-1}; TC, total carbon; TP, total P.

Introduction

Phosphorus (P) is one of the essential and common limiting macronutrients for plant growth, but it is a major cause of freshwater eutrophication. Conservation tillage practices (e.g. no-till, NT) have become increasingly used in recent years to reduce off-site losses of nutrient including P. Some benefits of NT over conventional tillage include reduced wind and water erosion (Dick, 1992; Olson and Ebelhar, 2009) and greater soil biological activity (Duiker and Beegle, 2006). Further advantage of NT on crop production (Lafond et al., 2011) and economic performance (Holm et al., 2006) are well recognized.

However, by maintaining of crop residues and fertilizers on the soil surface and reducing their mixing from the surface into the plow layer, the relatively immobile nutrients remain on or near the soil surface. Therefore, NT management system often result in P and other nutrient stratification or variation of nutrient concentrations with soil depth (Lupwayi et al., 2006).

Stratification of P is of particular concern because high concentrations at the soil surface increase the runoff of dissolved P (Kleinman et al., 2009) and low concentrations at depth may decrease P uptake by decreasing the P that is in the rooting zone (Lupwayi et al., 2006). Identifying specific P forms and determining their distribution patterns in the soil profile is important to determine the cause of stratification. The objectives of this study were: (i) to use ^{31}P-NMR spectroscopy to identify the soil P forms under a long-term tillage and P fertilized study in Québec, Canada, (ii) to examine the effect of tillage systems and P fertilization on their distribution patterns, and (iii) to determine the possible stratification causes of these P forms.

Materials and Methods

Experimental site

The long-term crop rotation experiment was established in 1992 at the l'Acadie Research Station (45°18'N; 73°21'W), Agriculture and Agri-Food Canada. The soil is a clay loam (Dark Grey Gleysoil) with 364 g kg^{-1} of clay and 204 g kg^{-1} of sand in the Ap horizon. This deep soil originates from a fluvial deposit and evolved from a fine-textured, greyish-to- brown parent material. The site is tile drained with slope less than 1% and was originally cropped with alfalfa (*Medicago sativa*) before 1992; it has been under an annual rotation of soybean (*Glycine max* L.) and maize (*Zea mays* L.) since1994.

The chemical characteristics of the topsoil when the experiment was established were, on average: soil organic matter (SOM) 38 g kg^{-1}, PM3 135 kg ha^{-1}, (P/Al) Mehlich-3 saturation ratio 4.3%, and pH 6.3 (1:2 soil/water) (Légère et al., 2008). The mean annual temperature in the area of the study is 6.3°C, and the mean total annual precipitation is 1100 mm (Poirier et al., 2009).

The experimental set-up was a split plot with two tillage practices (NT and MP) assigned to main plots and nine fertilization combinations consisting of three N (0, 80 and 160 kg N ha^{-1}) and three P (0, 17.5 and 35 kg P ha^{-1}) applications to subplots. Experimental treatments were replicated in four blocks, with individual plots measuring 25 m long and 4.5 m wide. The MP treatment consisted of one moldboard plowing operation in the fall after harvest to a depth of 20 cm, followed by disking and harrowing to 10 cm each spring before seeding. For the NT treatment, plots had previously been ridge-tilled from 1992 to 1997 and were flat direct-seeded from 1998 onward. For direct seeding, crop residues were left on the ground after harvest. There were six rows per sub plot unit, and maize and soybean were sown at rates of 74 x 10^3 and 45 x 10^4 plants ha^{-1}, respectively. Mineral fertilizers (N x P) were band-applied (5 cm from the seeding row) only during the maize phase of the rotation using a disk opener (3 – 4 cm deep), according to local recommendation. The P treatments were applied in a single application at planting as triple super-phosphate (0-46-0). Nitrogen treatments were first band-applied at seeding at rates of 0, 48 and 48 as urea, and completed at 0, 32, and 112 kg N ha^{-1} side-dressed as ammonium nitrate at approximately the eight-leaf stage.

Soil Sampling and Chemical Analysis

Although the experiment was conducted with four replicate blocks per treatment, only three blocks with sub-plots receiving 0 and 35 kg P ha^{-1} and 160 kg N ha^{-1} were selected for this study. Soil profiles were sampled to a depth of 0-5 cm, 5-10 cm and 10-20 cm during fall 2010 for a total of 36 samples (2 tillage x 2 P-fertilization x 3 replicates x 3 depths), air-dried and sieved to < 2 mm. Soil pH was measured in distilled water with 1:2 soil to solution ratio (Hendershot et al., 2007). Soils were extracted by shaking 2.5 g of soil with a 25 ml of Mehlich-3 solution (pH 2.3) for 5 min (Mehlich, 1984) and the concentrations of P, Al, Fe and Ca were determined with an Inductively Coupled Plasma Optical Emission Spectrometer (ICPOES; Model 4300DV, Perkins Elmer, Shelton, CT). Total soil P was determined as described in (Nelson, 1987). Briefly, 0.1 g of finely ground soil (0.2 mm) was mixed in a 50-mL boiling flask with 0.5 g $K_2S_2O_8$ and 10 mL 0.9 M H_2SO_4, digested at 121 ◦C in an autoclave for 90 min. The solution was analysed by the ammonium molybdate-ascorbic acid method (Murphy and Riley, 1962). Total C and N were determined by dry combustion on 0.20 mm ground soils with a LECO CNS-1000 analyzer (LECO Corp., St. Joseph, MI).

Solution ^{31}P-NMR Spectroscopy

Samples were analyzed by solution ^{31}P-NMR spectroscopy using a modified version of the Cade-Menun and Preston (1996) procedure. This involved shaking 2.5 g of soil with 25 ml of combined 0.25 mol L^{-1} NaOH and 0.05 mol L^{-1} Na_2EDTA for 6h, followed by centrifugation for 20 min at approximately 1500 x g. A 1 mL aliquot was removed and diluted to 10 ml with deionized water for determination of TP, Al, Fe, Ca, and Mn by ICP-OES. The remaining filtrates were then frozen and freeze-dried.

Freeze-dried filtrates were redissolved in 1.0 mL D_2O, 0.6 mL 10 mol L^{-1} NaOH, and 0.6 mL of the NaOH-EDTA extracting solution. The samples were then centrifuged (1500 x g) for 20 min to remove particles > 0.1 μm in diameter and transferred to 10 mm NMR tubes. Solution ^{31}P-NMR spectra were acquired on a 600-Mhz spectrometer (INOVA; Varian, Palo Alto, CA) equipped with a 10 mm broadband probe.

Chemical shifts of signals were determined in parts per million (ppm) relative to an external orthophosphoric acid standard (85%), and the orthophosphate peak was standardized to 6 ppm for each sample. Signals were assigned to P compounds based on the literature (Cade-Menun, 2005; Cade-Menun et al., 2010; Turner et al., 2012).

Peak areas were calculated by integration on spectra processed with 1 Hz and 7 Hz line broadening, using NMR Utility Transform Software (NUTS, Acorn NMR, Livermore CA, 2000 edition).

Statistical Analysis

Phosphorus compounds are compositional data since they represented proportions varying between 0 and 100%. To conduct linear statistical procedures, compositional data must be freed from their constrained space using centered log ratio (*clr*) transformation (Aitchison, 1986). Mathematical transformations (*clr*) and statistical analysis (ANOVA) were conducted in R (van den Boogaart et al., 2010) to compare the tillage and P fertilized treatments for the three depths.

Results

Chemical analysis

Total P was slightly higher in the NT treatment at 0 to 5 cm than 5 to 20 cm, while the opposite was true under MP where TP was accumulated in the deep soil layer. There were no significant differences between treatments at any depth for TP. In contrast, a significant tillage x P fertilization interaction ($p < 0.05$) was obtained for the PM3 at 0 to 5 cm and 10 to 20 cm. The highest results for PM3 were recorded under NT in P fertilized treatment at 0 to 5 cm. Soil pH was significantly higher in NT treatment at 0 to 5 cm than the MP. A significant total carbon (TC) difference between tillage treatments was detected at the 0 to 5 cm ($p < 0.001$), where it was higher under NT, and 5 to 10 cm ($p < 0.05$) depth where it was higher under MP treatment. None of the soils parameters tested, except PM3, showed any effect of P fertilization.

NMR-^{31}P Phosphorus Forms Identification and Distribution

The ^{31}P-NMR peaks for P compounds detected in this study fall between 25 and -25 ppm. Four groups of inorganic P forms were detected: orthophosphate at 6.00 ± 0.01 ppm chemical shift, pyrophosphate at -4.02 ± 0.02 ppm, polyphosphates between 4.23 and -24.76 ppm and the polyphosphate end group detected at -3.98 ± 0.05 ppm in fertilized soils in one replicate under NT and in two replicates under MP at different depth. Orthophosphate was the major fraction of extracted P in all analyzed soil samples. The highest relative percent of orthophosphate (49.7 %) was found in the NT-P_{35} treatment at 0 to 5 cm depth and was significantly different from the values at 5 to

10 cm ($p < 0.01$) and 10 to 20 cm ($p < 0.05$). In contrast, the lowest percent (34.8 %) was observed in the deep layer (10 – 20 cm) under NT-P_0.

Organic P compound classes detected by solution ^{31}P-NMR include phosphonates from 25 to 7.80 ppm, orthophosphates monoesters at 7.70 to 6.20 ppm and at 5.78 to 3.5 ppm, and orthophosphates diesters between 2.20 and -3.40 ppm (Cade-Menun et al., 2005; Cade-Menun et al., 2010). For all treatments and depths, the ^{31}P-NMR spectra indicated that orthophosphates monoesters were dominated by the stereoisomers of inositol hexakisphosphate (IP_6). Three of these (*myo*, *neo,* and *scyllo*) were detected in all treatments, whereas D-*chiro*-IP_6 was detected in NT-P_0 in one bloc at the 0 to 5 cm depth, and in NT-P_{35} at three depths. The most abundant stereoisomer of IP_6, *myo*-IP_6, , gave four characteristics signals in the ratio 1:2:2:1 at 5.48 (± 0.02), 4.51 (± 0.02), 4.11 (± 0.02), and 4.02 (± 0.02) ppm (Cade-Menun et al., 2005; Turner et al., 2003) . The identification of these peaks as *myo*-IP_6 was confirmed by rerunning two samples after spiking with phytic acid. Two signals at 6.41 (± 0.01) ppm and 4.27 (± 0.01) ppm in 1:4 ratio were assigned to the 4 equatorial/2-axial conformation of *neo*-IP_6 based on Turner et al. (2012). The peaks for D-*chiro* IP_6 were detected in 2:2:2 ratio in the 2-equatorial/4-axial conformation at 6.23 ppm, 4.75 (± 0.01) ppm, and 4.34 (± 0.03), ppm (Turner et al., 2012). The signal from *scyllo*-IP_6 occurred at 3.71 ± 0.02 ppm (Cade-Menun et al., 2005) and was significantly ($p < 0.01$) different between the depths 0 to 5 cm and 5 to 20 cm in NT-P_{35} treatment. Glucose 6-phosphate was detected at 5.12 ± 0.03 ppm, while the 4.93 ± 0.02 ppm and 4.55 ± 0.02 ppm peaks were assigned to α-glycerophosphate (α-glyc) and β-glycerophosphate (β-glyc), respectively. Choline phosphate (chol-P, 3.85 ± 0.03 ppm) and two signals of nucleotides (4.33 ± 0.01, 4.16 ± 0.02 ppm) were also detected in every soil sample. Peak locations for β-glyc and chol-P were confirmed by spiking samples with these two P forms. Unidentified groups of the orthophosphate monoesters were divided into three general groups based on their locations (Cade-Menun, 2005; Hill and Cade-Menun, 2009). The Monoester 1 group contained unidentified peaks between 6 and 7 ppm, and included a peak at 6.51± 0.04 ppm. Peaks in the Monoester 2 region were detected at 5.68 ± 0.02 ppm, 5.26 ± 0.01 ppm, and 4.75 ± 0.03 ppm. The Monoester 3 group included a peak at 3.79 ± 0.15 ppm observed in the soil samples containing D-*chiro* IP_6. The DNA peak was found in most samples at -0.75 ± 0.03 ppm. The remaining orthophosphate diesters were grouped into two groups. Peaks for “Other diester 1”, were detected between 3.34 and 0.41 ppm, and

may include intact phospholipids (Cade-Menun et al., 2010). The "Other diester 2" group was observed between 1.76 and -3.72 ppm. The unknown P component, P.E.G and D-chiro that were detected in a few soil samples were grouped as a residual fraction "R" of TP.

Discussion

The results clearly showed that TP and TC were higher in the upper layer (0 - 5 cm) of soils under NT (Table 1), but they were depleted with soil profile compared to MP, owing to the crop residues at the surface and the minimal soil disturbance. There was no evidence of TP stratification in these soils (Table 2). By contrast, a significant accumulation of PM3 was apparent in NT treatment in the top 5 cm layer and 5 to 10 cm with a rapid decline in the 10 - 20 cm when P fertilizer was added (Table 1), as reported elsewhere (Cade-Menun et al., 2010; Messiga et al., 2012). This might have resulted from a lack of mixing of fertilizer with soil. The depletion of soluble P in lower layers of NT can result in reduced P uptake by plants (Lupwayi et al., 2006). For the NT-P_0 treatment, PM3 was uniformly distributed in the soil profile. Likewise, the ^{31}P-NMR spectra showed concomitant stratification of inorganic orthophosphate in NT-P_{35} (Fig. 1). A significant correlation was found between the PM3 concentration and orthophosphate ($r = 0.79$, $p < 0.0001$). This suggests that they measure the same P form, with Mehlich 3 extracting a portion of inorganic orthophosphate.

Organic phosphorus stratification was shown with *scyllo*-IP_6 in NT-P_{35} (Fig. 2), where concentrations where low at 0 to 5 cm and then increased significantly in lower layers ($p < 0.01$) possibly due to preferential movement of this P compound through the soil column. Less is known about the source of this P form but it was thought to originate from epimerization of *myo*-IP_6 since they are stereoisomers.

For P_0 treatment, *myo*-IP_6 was lower under NT than MP in the upper soil layer (0 – 5 cm), suggesting that tillage may influence the degradation of crops residues resulting in the release of *myo*-IP_6. In contrast, the concentration of this inositol phosphate was higher in the deep layer of NT presumably due to preferential movement. For P_{35}, *myo*-IP_6 was higher under NT than MP at all depths (Fig. 2), which might have resulted from uptake of fertilizer and transformation by plants to of P fertilizer to *myo*-IP_6, which is an important plant P storage compound, which may have been restricted by tillage. The

neo-IP_6 stereoisomer was uniformly distributed in all soil treatment and slightly higher under NT P fertilized soil at all depth (Fig. 2). Further investigation is warranted into the possible interactions between the soluble P (inorganic orthophosphates) derived from P fertilizer and *myo*- and *neo*-IP_6.

Conclusions

In conclusion, long-term tillage system and P fertilization application have been shown to result in stratification of soluble inorganic P at the top 5 cm layer, presumably due to the lack of mixing of applied P fertilizer. This effect may increase the potential for P loss from runoff. Organic monoesters such as inositol hexakisphosphate were greater under NT-P_{35} than the other management system. Only the *scyllo*-IP_6 was accumulated in the deep layer and could be related to a microbial transformation of inorganic P. Further investigations are required to study the possible interaction between the P form to understanding detailed P changes derived from agricultural management practices.

Table 1. Total phosphorus, Mehlich-3 extractable phosphorus, total carbon, and pH for soils at various depths under tillage and P fertilization systems**.**

Soil treatment	TP (mg.kg^{-1})	PM3 (mg.kg^{-1})	TC (%)	pH
	0 - 5 cm			
†**NT-P$_0$**	1876 (65)	23.37 (7.66)	2.68 (0.33)	6.29 (0.37)
NT-P$_{35}$	1809 (202)	59.43 (2.77)	2.76 (0.13)	6.37 (0.41)
MP-P$_0$	1666 (81)	17.23 (5.77)	2.05 (0.15)	6.02 (0.39)
MP-P$_{35}$	1679 (242)	28.68 (8.00)	1.99 (0.24)	5.99 (0.53)
	5 – 10 cm			
NT-P$_0$	1755 (80)	18.25 (6.77)	2.10 (0.35)	6.14 (0.85)
NT-P$_{35}$	1740 (91)	37.09 (13.39)	2.08 (0.26)	6.17 (0.40)
MP-P$_0$	1914 (164)	14.88 (5.36)	2.39 (0.31)	5.61 (0.35)
MP-P$_{35}$	1873 (58)	28.26 (10.17)	2.31 (0.16)	5.97 (0.36)
	10 – 20 cm			
NT-P$_0$	1870 (350)	17.86 (7.47)	1.85 (0.43)	6.34 (0.98)
NT-P$_{35}$	1652 (289)	19.06 (5.76)	1.87 (0.34)	6.07 (0.67)
MP-P$_0$	1856 (135)	14.56 (4.25)	2.30 (0.15)	5.69 (0.36)
MP-P$_{35}$	2023 (76)	25.63 (8.66)	2.15 (0.11)	5.97 (0.24)

† NT, No-Till; MP, mouldboard plowing, P_0, soil treatment with 0 kg P ha^{-1}; P_{35}, soil treatment with 35 kg P ha^{-1}.

Table 2. Analysis of variance for the effects of tillage and P fertilization on total P, Mehlich-3 phosphorus, total carbon, and pH at various soil depths.

Source of variation	TP (mg.kg^{-1})	PM3 (mg.kg^{-1})	TC (%)	pH
	0 – 5 cm			
T (Tillage)	n.s	< 0.01	< 0.001	< 0.05
F (Fertilization)	n.s	< 0.01	n.s	n.s
T*F	n.s	< 0.05	n.s	n.s
	5 - 10 cm			
T	n.s	n.s	< 0.05	n.s
F	n.s	< 0.01	n.s	n.s
T*F	n.s	n.s	n.s	n.s
	10 – 20 cm			
T	n.s	n.s	n.s	n.s
F	n.s	< 0.05	n.s	n.s
T*F	n.s	< 0.05	n.s	n.s

n.s, not significant at $p = 0.05$

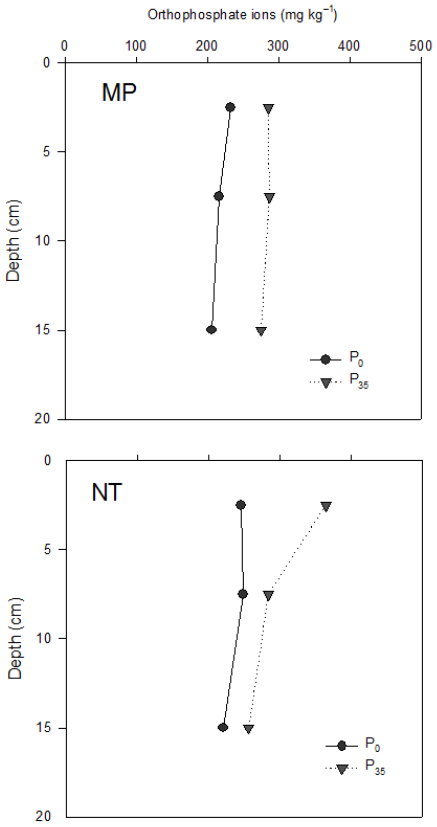

Fig. 1. Distribution of inorganic orthophosphate concentrations at various soil depths under (a) mouldboard plow (MP) and (b) no-till (NT). P_0 and P_{35} represent additions of 0 and 35 kg P ha^{-1}.

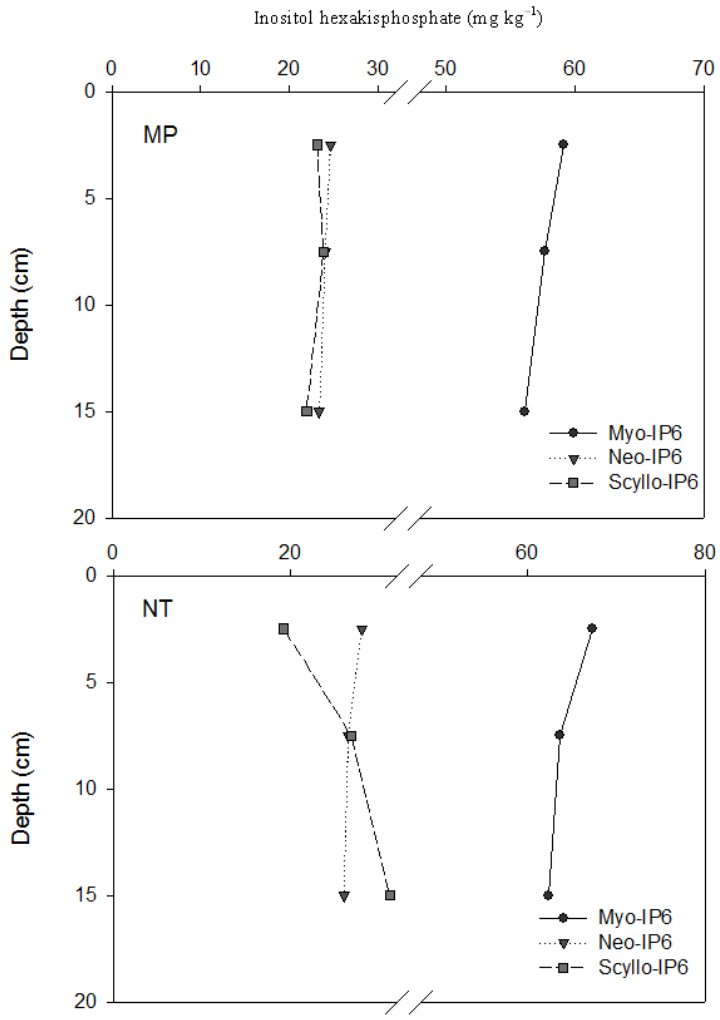

Fig. 2. Distribution of inositol hexakisphosphate (myo, neo, and scyllo) concentrations at various soil depths under (a) mouldboard plow (MP) and (b) no-till (NT). P_0 and P_{35} represent additions of 0 and 35 kg P ha^{-1}.

References

Aitchison, J. 1986. The Statistical Analysis of Compositional Data. Monographs on Statistics and Applied Probability. Chapman & Hall Ltd., London (UK). 416 p.

Cade-Menun, B.J. 2005. Characterizing phosphorus in environmental and agricultural samples by 31P nuclear magnetic resonance spectroscopy. Talanta 66:359-371.

Cade-Menun, B.J., and C.M. Preston. 1996. A comparison of soil extraction procedures for 31P NMR spectroscopy. Soil Sci. 161:770-785.

Cade-Menun, B.J., M.R. Carter, D.C. James, and C.W. Liu. 2010. Phosphorus forms and chemistry in the soil profile under long-term conservation tillage: A phosphorus-31 nuclear magnetic resonance study. J. Environ. Qual. 39:1647-1656.

Dick, R.P. 1992. A review: long-term effects of agricultural systems on soil biochemical and microbial parameters. Agric. Ecosyst. Environ. 40:25-36.

Duiker, S.W., and D.B. Beegle. 2006. Soil fertility distributions in long-term no-till, chisel/disk and moldboard plow/disk systems. Soil Tillage Res. 88:30-41.

Hendershot, WH., H . Lalande, and M. Duquette. 2007. Soil reaction and exchangeable acidity. In: Carter MR, Gregorich EG (Eds) Soil sampling and methods of analysis, 2nd ed. Can. Soc. Soil Sci, CRC Press Inc., Boca Raton, FL, pp 173‑178.

Hill, J.E., and B.J. Cade-Menun. 2009. Phosphorus-31 nuclear magnetic resonance spectroscopy transect study of poultry operations on the Delmarva Peninsula. J. Environ. Qual. 38:130-138.

Holm, F.A., R.P. Zentner, A.G. Thomas, K. Sapsford, A. Légère, B.D. Gossen, O. Olfert, and J.Y. Leeson. 2006. Agronomic and economic responses to integrated weed management systems and fungicide in a wheat-canola-barley-pea rotation. Can. J. Plant Sci. 86:1281-1295.

Kleinman, P.J.A., A.N. Sharpley, L.S. Saporito, A.R. Buda, and R.B. Bryant. 2009. Application of manure to no-till soils: Phosphorus losses by sub-surface and surface pathways. Nutr. Cycling Agroecosyst. 84:215-227.

Lafond, G.P., F. Walley, W.E. May, and C.B. Holzapfel. 2011. Long term impact of no-till on soil properties and crop productivity on the Canadian prairies. Soil Tillage Res.117:110-123.

Légère, A., F.C. Stevenson, and N. Ziadi. 2008. Contrasting responses of weed communities and crops to 12 years of tillage and fertilization treatments. Weed Technol. 22:309-317.

Lupwayi, N.Z., G.W. Clayton, J.T. O'Donovan, K.N. Harker, T.K. Turkington, and Y.K. Soon. 2006. Soil nutrient stratification and uptake by wheat after seven years of conventional and zero tillage in the Northern Grain belt of Canada. Can. J. Soil Sci. 86:767-778.

Mehlich, A. 1984. Mehlich 3 soil test extractant: A modification of Mehlich 2 extractant. Comm. Soil Sci. Plant Anal. 15:1409-1416.

Messiga, A.J., N. Ziadi, C. Morel, C. Grant, G. Tremblay, G. Lamarre, and L.E. Parent. 2012. Long term impact of tillage practices and biennial P and N fertilization on maize and soybean yields and soil P status. Field Crops Res. 133:10-22.

Murphy, J., and J.P. Riley. 1962. A modified single solution method for the determination of phosphrous in natural waters. Anal. Chim. Acta 27:31.

Nelson, N.S. 1987. An acid-persulfate digestion procedure for determination of phosphorus in sediments. Commun. Soil Sci. Plant Anal. 18:359-369.

Olson, K.R., and S.A. Ebelhar. 2009. Impacts of conservation tillage systems on long-term crop yields. J. Agron. 8:14-20.

Poirier, V., D.A. Angers, P. Rochette, M.H. Chantigny, N. Ziadi, G. Tremblay, and J. Fortin. 2009. Interactive effects of tillage and mineral fertilization on soil carbon profiles. Soil Sci. Soc. Am. J. 73:255-261.

Turner, B.L., Mahieu, N., Condron, L.M. 2003. Phosphorus-31 nuclear magnetic resonance spectral assignments of phosphorus compounds in soil NaOH-EDTA extracts. Soil Sci. Soc. Am. J. 67:497-510.

Turner, B.L., A.W. Cheesman, H.Y. Godage, A.M. Riley, and B.V.L. Potter. 2012. Determination of neo- and d-chiro-inositol hexakisphosphate in soils by solution 31P NMR spectroscopy. Environ. Sci. Technol. 46:4994-5002.

van den Boogaart, K. G, R. Tolosana, and M. Bren (2010) Compositions: Compositional Data Analysis. R package version 1.10-1. http://CRAN.R project.org/package=compositions.

PHOSPHORUS TRANSFORMATIONS FROM RECLAIMED WASTEWATER TO IRRIGATED SOIL: A ^{31}P NMR STUDY

Iris Zohar[1*], Barbara Cade-Menun[2], Adina Paytan[3] and Avi Shaviv[4]

[1]Department of Environmental, Water and Agricultural Engineering, Faculty of Civil and Environmental Engineering, The Technion - Israel Institute of Technology, Haifa, Israel 32000

[2]Agriculture & Agri-Food Canada, Semiarid Prairie Agricultural Research Centre, Box 1030, Gate 4,Airport Road, Swift Current, SK, Canada S9H 5E3

[3]Institute of Marine Sciences, Earth and Marine Science Building, Room C308, University of California, Santa Cruz. 1156 High Street, Santa Cruz, CA 95064

*Corresponding author: E-mail address: irisz2910@gmail.com

Abstract

Irrigation of soils with reclaimed wastewater (RW) is a common practice in arid regions, but may pose an environmental threat if labile phosphorus (P) forms accumulate at the soil surface. Soil P lability can be affected by P forms in the applied RW and by P composition and distribution in the soil. Solution 31P nuclear magnetic resonance (NMR) spectroscopy was employed to identify P forms in RW solutions, in whole soil extracts and in fractionated soil P pools in agricultural soils (maize crop, Acre, Israel) irrigated with the examined RW or with freshwater (FW) and a chemical fertilizer. The RW was rich with total P (PT) and molybdate-reactive P (MRP), consistent with high concentrations of MRP in the RW-irrigated-soil. Identified compounds and compound classes in the RW and in the soils include orthophosphate, polyphosphate, orthophosphate monoesters and orthophosphate diesters. However, there was a shift in P compound classes from the RW to the RW-irrigated-soil; although the water sources were different, P forms in the soils of the different treatments were similar. The possible factors that might control this change are discussed, including biological and geochemical P recycling and crop inputs.

(Under review of SSSAJ)

Oxygen Isotopes for Unraveling Phosphorus Transformations in the Soil–Plant System: A Review

Federica Tamburini[1*], Verena Pfahler[1], Christian von Sperber[1], Emmanuel Frossard[1] and Stefano M. Bernasconi[2]

[1]Institute of Agricultural Sciences ETH Zurich Research Station Eschikon 33 8315 Lindau, Switzerland

[2]Geological Institute ETH Zurich Sonneggstrasse 5 8092 Zurich, Switzerland

Abstract

Phosphorus is a major nutrient for all living organisms. In the terrestrial environment, P is considered a double-edged sword. In some areas, agricultural production is strongly limited by the low soil P availability, while in others, P inputs in excess of plant needs have resulted in pollution of water bodies. A better understanding of soil–plant P cycling is needed to provide agricultural and environmental managers with better concepts for P use. Together with the routine analysis of soil available P, the determination of P chemical forms, and the use of P radioisotopes, researchers have recently started using the ratio of stable oxygen isotopes in phosphate (δ^{18}O-P). The scientific community interested in using this isotopic tracer is slowly but steadily expanding because δ^{18}O-P has proven to provide important information on biological processes influencing the P cycle and it could be used to trace the origin and fate of P in soil–plant systems. This review examines the published results and compiles the available data relevant for soil–plant systems, pinpoints gaps in analytical techniques and knowledge, and suggests key questions and topics to be investigated.

https://www.soils.org/publications/sssaj/articles/78/1/38?highlight=&search-result=1

PHOSPHATE STABLE ISOTOPES IN SOILS

Alon Angert and Avner Gross

The Institute of Earth Sciences, The Hebrew University of Jerusalem

Abstract

The stable oxygen isotope compositions of soil phosphate (δ^{18}Op) were suggested recently to be a tracer of phosphorus cycling in soils and plants. Here we present a survey of bioavailable (resin-extractable or resin-P) inorganic phosphate δ^{18}Op across natural and experimental rainfall gradients, and across soil formed on sedimentary and igneous bedrock. In addition, we also analyzed the soil HCl-extractable inorganic δ^{18}Op, which mainly represents calcium-bound inorganic phosphate. The resin-P values were in the range of 14.5-21.2‰. A similar range, 15.6-21.3‰, was found at sedimentary bedrock soils for the HCl-extractable inorganic δ^{18}Op, in contrast to ~21‰ for sedimentary phosphate in the study area. For samples taken from a soil with igneous origin, we found lower values, 8.2-10.9‰, which indicate that a large fraction of the inorganic phosphate in this soil is still in the form of a primary mineral. The available-P δ^{18}Op values are considerably higher than the values we calculated for extracellular hydrolysis of organic phosphate, based on the known fractionation from lab experiments. However, these values are close to the values expected for enzymatic-mediated phosphate equilibration with soil water. We discuss here possible processes that can explain this observation, and present a set of lab incubation experiments to test which of explanation is correct. Based on our results, we suggest that δ^{18}Op can be used estimating microbial turnover rates, and for tracing P sources in dust.

Introduction

Phosphorus and soils

Phosphorus (P) is an important macro-nutrient which constituent of major bio-molecules such as ATP, RNA, DNA, and phospholipids. The main source of Phosphorus to terrestrial ecosystem is the soil parent material, although supply by dust can make significant contribution in some tropical ecosystems (Swap et al., 1992), and potentially also in semiarid ecosystems (Okin et al., 2004). A large fraction of an

ecosystem Phosphorus is recycled within it (Schlesinger, 1991), while the reminder is lost by leaching to groundwater or rivers.

Phosphorus is by far the least mobile macro-nutrient in most soil conditions (Hinsinger, 2001; Schlesinger, 1991). The poor mobility of soil phosphate is due to the retention of most of soil organic phosphate in stable compounds and strong retention of inorganic phosphate onto numerous soil constituents – mainly iron and aluminum oxides at highly weathered tropical soils (Ae et al., 1990; Batjes and Sombroek, 1997), and carbonates in Mediterranean soils (Schlesinger, 1991) . These retentions make most of the soil phosphate unavailable for plant use, and create P limitation to plant growth.

This P limitation was shown to increase over the long-term (>1000 years), in the absence of catastrophic disturbance, and cause a decline phase in ecosystem productivity ((Vitousek and Farrington, 1997; Walker and Syers, 1976; Wardle et al., 2004)). The decline in available phosphate is believed to be due to leaching of the primary mineral P in the soil, and P immobilization in organic fractions (organic P, (Stewart and Tiessen, 1987)). The P limitation to plant growth may also interact with other limiting factors. For example, it was shown (Grunzweig and Korner, 2003) that while the increase in atmospheric [CO_2] may boost plant productivity, as previous studies found (Ainsworth and Long, 2005), this increase in productivity is limited by P availability at semiarid soils. Another example of interaction was suggested by a recent study (Houlton et al., 2008) which argued that the high rates of (energy demanding) N_2 fixation in tropical forests and savannas, support the production of N rich extra-cellular phosphatase, which breakdown organic-P and make it available to plant uptake. Hence, according to that study, these globally important ecosystems are also strongly controlled by supply of phosphate from organic-P.

The transformations of organic-P in soils to the transformation of the organic carbon, and the P turnover by the microbial community strongly affect the P availability to plants. Indeed, some soil carbon models (Century, CASA-CNP) have included recently a P module, which feedback both to productivity and decomposition. In the next section we will discuss the carbon in soils, and its links to phosphorus.

Expected Oxygen Isotopic Effects in the Terrestrial Phosphate Cycle

The oxygen isotope composition of phosphate in soils ($\delta^{18}O_P$) is likely to be controlled by several processes. First, primary phosphate is supplied to soils by dissolution from minerals – mainly apatite – supplied by the bedrock and airborne dust. These sources have a range of $\delta^{18}O_P$ values, between ~5‰ for igneous rocks (Taylor and Forester, 1979) and 11–35‰ for marine phosphorites (Shemesh et al., 1983). There is no fractionation during the dissolution of apatite (Lecuyer et al., 1999).

In the second step, phosphate is assimilated into plants or soil microbial biomass. Fractionations involved in this step, if any, are unknown. Fractionation of –3‰ was observed for *Escherichia coli* under laboratory conditions (Blake et al., 2005). However, this effect may not represent the soil microbial population under natural conditions, and can be different from that of fungi and plants.

In the third step, we expect that intra-cellular enzymatic activity within plants will result in isotopic equilibrium between oxygen in phosphate and oxygen in water, as found for other organisms. The known equilibrium fractionation for this reaction is temperature dependent (Blake et al., 2005; Longinelli and Nuti, 1973):

$\delta^{18}O_p = \delta^{18}O_{water} + (111.4-T) / 4.3$ (where T is the temperature in °C) (Equation 1)

This equilibrium fractionation stems from a reaction catalyzed by the intracellular enzyme pyrophosphatase (Blake et al., 2005). This equilibration will take place in the microbial biomass and in the stems and roots of plants, with water with the same $\delta^{18}O$ as the soil water, and in the leaves with water that is isotopicall enriched (White, 1988). Fractionation and isotopic exchange are expected also to occur in the fourth step: mineralization. The biota releases organic P into the soil, where phosphate-scavenging enzymes break down large and complex organic molecules and release inorganic phosphate, which becomes available again for biological uptake (Blake et al., 2005; Liang and Blake, 2006b). For example, when phosphate is released from phosphomonoesters, which are the most common organic P compounds in soils (Turner et al., 2002), by the extra-cellular enzyme alkaline-phosphatase, one of the oxygen atoms is acquired from water, with a kinetic fractionation of –30(±8)‰ (Liang and Blake, 2006b). The other three oxygen atoms in the inorganic phosphate are then inherited from the original organic phosphate. A similar reaction is catalyzed by 5'-nucleotidase, but with a fractionation of -10(±1)‰ (although this enzyme is not

common in soils). For phosphodiesters (e.g. DNA, RNA, phospholipids), two C-P bonds must be broken, and two oxygen atoms are incorporated with associated isotopic fractionation into the liberated phosphate molecule. The fractionation associated with phosphodiester hydrolysis was reported to be substrate related (Liang and Blake, 2009). The isotopic exchange and fractionations associated with other common phosphatases in soils, such as phytase is currently unknown. Phosphate released from organic P re-enters the inorganic pool, and can be then assimilated by plants or by the soil microbial population, or be sorbed to soil and form secondary phosphate minerals. Lab experiments have shown that precipitation of apatite involves only very small isotopic fractionations of ~1‰ (Liang and Blake, 2007). A recent study (Jaisi et al., 2010) has found negligible fractionation between phosphate sorbed into iron oxides and the one in aqueous-phase at equilibrium, and only small fractionations (~2‰) in the early stages of phosphate sorption. Other sorbing reactions in soils might have different isotopic effect associated with them. Phosphate assimilated into microbial biomass is expected to reach isotopic equilibration with intra-cellular water that has $\delta^{18}O$ similar to that of soil water. This phosphate is then released into the organic and inorganic pools, upon microbial cells death or predation and subsequent digestion.

As discussed above, the understanding of phosphate isotopic effects involved with enzyme activity, and the phosphate cycling in aquatic systems, has improved in the last two decades. However, there is so far only limited use of the phosphate isotopes in soils. In the study, we test the use of $\delta^{18}O_P$ for studying the microbial turnover in soil incubation experiments. These experiments results will be evaluated in the framework of a SOM and P model that we will develop.

Analytical methods

The resin-extractable inorganic phosphate isotopic composition was measured by a method already developed and tested at the Angert lab (Angert et al., 2011; Weiner et al., 2011)(and partly supported by a Young-GIF grant that precede this proposal). Briefly: phosphate is extracted from the soil by an anion-exchange membrane, and SOM is removed from the extract by DAX-8 resin. The phosphate is then purified by a number of steps and then precipitated as silver phosphate. The HCl-extractable phosphate isotopic composition will be assessed following the method of Shemesh

(1983) and Tudge (1960) adopted for soils at ETH-Zurich, with assistant from the Angert lab (Tamburini et al., 2010). Using ^{18}O labeled water in both extractions helps to rule out or correct for the possible unwanted effects of isotopic exchange or organic-P hydrolysis.

For isotopic composition determinations, the silver phosphate is packed in silver capsules and introduced into a high temperature pyrolisys unit, where it is converted to CO in the presence of glassy carbon (Lecuyer et al., 2007; Vennemann et al., 2002). The CO gas is isolated by a GC and the oxygen isotope ratio is then measured by a continuous-flow isotope ratio mass spectrometer (IRMS). Concentrations of phosphate are determined by the standard method of complexing with molybdate and measuring the resulting blue color with a spectrophotometer.

The incubation experiments will be mostly conducted with a spike of organic P. In order to estimate the $\delta^{18}O$ of this phosphate which enters the soil pool, Phosphate is must to be released from the organic compound. This step may involve isotopic exchange of the oxygen. Indeed, a recent study showed that the treatment of organic phosphate with acid, or combustion, erases much of its original isotopic signal (Liang and Blake, 2006a). The same study has also shown that oxidation by UV radiation and H_2O_2 can be used to extract organic phosphate with only a small (and for some organic compound, no) modification of its isotopic composition from reactions with the solution water. Following these findings, we release the phosphate from the organics by irradiating with UV-C, in the presence of H_2O_2, in a specially designed UV-incubation chamber we built. The phosphate is then purified in the method described above for inorganic phosphate. The organic matter oxidation will take place in two batches of water with markedly different $\delta^{18}O$ values, which will be pre-determined. This will enable us to identify isotopic exchange with water, and to correct for these effects. The UV method is already established in our lab and used in the preliminary experiments, while elemental analyzer runs of the resulting AG_3PO_4 proved that it is free of residual carbon.

Results and Discussion

In the course of a previous research, we have developed and tested methods for determining the $\delta^{18}O$ of inorganic resin-extractable phosphate (Weiner et al., 2011) at

low available P soils (<2 μg/g soil). These methods were applied in a semi-arid site under natural vegetation where drought and irrigation experiment took place (Angert et al., 2011). The soil of this site, in which rainfall usually occurs only between October and April, was sampled at seasonal resolution (January, April, August, and October). The results provide the first evidence for seasonal variations in $\delta^{18}O$ of soil phosphate (Fig. 1). Full discussion of possible causes for these changes in the mean values and the variability between soil samples is already published (Angert et al., 2011).

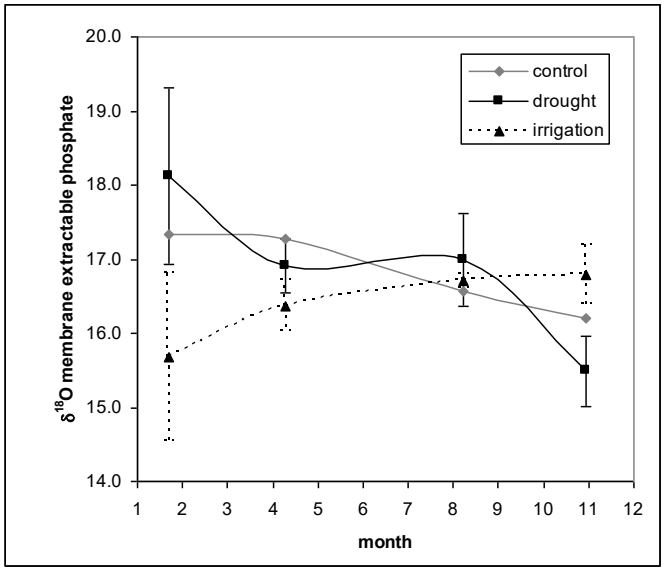

Fig. 1. Seasonal variations in $\delta^{18}O_P$ (versus VSMOW) of available (membrane extractable) inorganic soil phosphate, averaged over replicates from the same treatment and date. The error bars represent standard deviations.

These results hint that the $\delta^{18}O$ of soil phosphate can be used to trace P turnover in soils. However, in natural soils the signal is complex due to the contrasting effects of plants, soil micro-biota, and changes in soil water and temperature. These difficulties can be avoided in controlled lab incubations of soils. For example we have incubated soils to which we added either inorganic-P (Fig. 2) or organic-P (glycerol phosphate, Fig. 3). The addition of inorganic-P caused an increase in the microbial activity, which we monitored by the CO_2 respiratory efflux. This increase in the microbial activity went hand-in-hand with a decrease in the phosphate concentrations, and changes in the phosphate isotopic composition towards equilibrium with water. The addition of inorganic-P (Fig. 3) resulted in slower release of inorganic-P to the soil solution, as the glycerol phosphate was hydrolyzed, and the balance between the isotope kinetic effects involved in enzymatic hydrolyzation, and the equilibrium effects, is evident by the initial decrease, and the later increase in the phosphate isotopic composition.

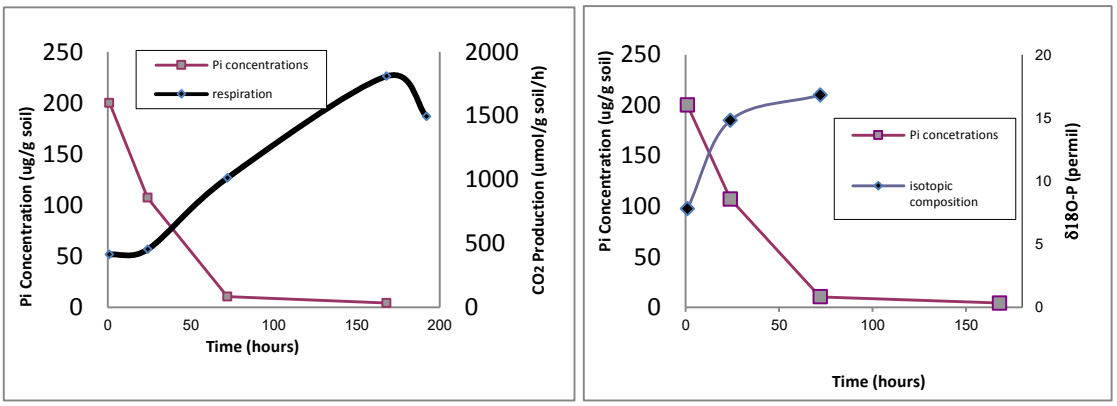

Fig. 2. Changes in the resin-extractable inorganic phosphate (Pi) concentrations, microbial respiration rates, and phosphate concentrations, in incubation experiment with added inorganic P.

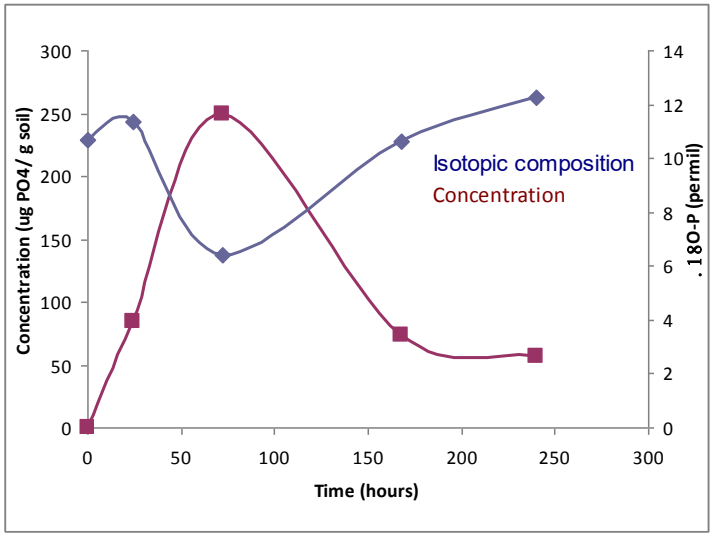

Fig. 3. Changes in the resin-extractable inorganic phosphate (Pi) concentrations, and phosphate concentrations, in incubation experiment which started with added organic-P (glycerol phosphate).

References

Ae, N., Arihara, J., Okada, K., Yoshihara, T. and Johansen, C., 1990. Phosphorus uptake by pigeon pea and its role in cropping systems of the Indian subcontinent. Science, 248(4954): 477-480.

Ainsworth, E.A. and Long, S.P., 2005. What have we learned from 15 years of free-air CO2 enrichment (FACE)? A meta-analytic review of the responses of photosynthesis, canopy. New Phytologist, 165(2): 351-371.

Angert, A., Barkan, E., Barnett, B., Brugnoli, E., Davidson, E.A., Fessenden, J., Maneepong, S., Panapitukkul, N., Randerson, J.T., Savage, K., Yakir, D. and Luz, B., 2003. Contribution of soil respiration in tropical, temperate, and boreal forests to the O-18 enrichment of atmospheric O-2. Global Biogeochemical Cycles, 17(3): doi:10.1029/2003GB002056.

Angert, A., Biraud, S., Bonfils, C., Buermann, W. and Fung, I., 2004. CO2 seasonality indicates origins of post-Pinatubo sink. Geophysical Research Letters, 31(11): doi:10.1029/2004GL019760.

Angert, A., Biraud, S., Bonfils, C., Henning, C.C., Buermann, W., Pinzon, J., Tucker, C.J. and Fung, I., 2005. Drier summers cancel out the CO2 uptake enhancement induced by warmer springs. Proceedings of the National Academy of Sciences of the United States of America, 102(31): 10823-10827.

Angert, A. and Luz, B., 2001. Fractionation of oxygen isotopes by root respiration: Implications for the isotopic composition of atmospheric O-2. Geochim. Cosmochim. Acta, 65(11): 1695-1701.

Angert, A., Luz, B. and Yakir, D., 2001. Fractionation of oxygen isotopes by respiration and diffusion in soils and its implications for the isotopic composition of atmospheric O-2. Global Biogeochemical Cycles, 15(4): 871-880.

Angert, A., Weiner, T., Mazeh, S., Tamburini, F., Frossard, E., Bernasconi, S.M. and Sternberg, M., 2011. Seasonal variability of soil phosphate stable oxygen isotopes in rainfall manipulation experiments. Geochimica et Cosmochimica Acta 75(15): 4216-4227.

Batjes, N.H. and Sombroek, W.G., 1997. Possibilities for carbon sequestration in tropical and subtropical soils. Global Change Biology, 3(2): 161-173.

Blake, R.E., O'Neil, J.R. and Surkov, A.V., 2005. Biogeochemical cycling of phosphorus: Insights from oxygen isotope effects of phosphoenzymes. American Journal of Science, 305(6-8): 596-620.

Bonan, G.B. and Levis, S., Quantifying carbon-nitrogen feedbacks in the Community Land Model (CLM4). Geophysical Research Letters, 37(7): L07401.

Dick, W.A. and Tabatabai, M.A., 1978. Inorganic Pyrophosphatase Activity of Soils. Soil Biology & Biochemistry, 10(1): 59-65.

Grunzweig, J. and Korner, C., 2003. Differential P and N effects drive species and community responses to elevated CO2 in semi-arid grassland. Functional Ecology, 17: 766-777.

Hinsinger, P., 2001. Bioavailability of soil inorganic P in the rhizosphere as affected by root-induced chemical changes: A review. Plant and Soil, 237(2): 173-195.

Houlton, B.Z., Wang, Y.P., Vitousek, P.M. and Field, C.B., 2008. A unifying framework for dinitrogen fixation in the terrestrial biosphere. Nature, 454(7202): 327-330.

Jaisi, D.P., Blake, R.E. and Kukkadapu, R.K., 2010. Fractionation of oxygen isotopes in phosphate during its interactions with iron oxides. Geochim. Cosmochim. Acta, 74(4): 1309-1319.

Lecuyer, C., Fourel, F., Martineau, F., Amiot, R., Bernard, A., Daux, V., Escarguel, G. and Morrison, J., 2007. High-precision determination of O-18/O-16 ratios of silver phosphate by EA-pyrolysis-IRMS continuous flow technique. Journal of Mass Spectrometry, 42(1): 36-41.

Lecuyer, C., Grandjean, P. and Sheppard, S.M.F., 1999. Oxygen isotope exchange between dissolved phosphate and water at temperatures <=135°C: Inorganic versus biological fractionations. Geochim. Cosmochim. Acta, 63(6): 855-862.

Liang, Y. and Blake, R.E., 2006a. Oxygen isotope composition of phosphate in organic compounds: Isotope effects of extraction methods. Organic Geochemistry, 37(10): 1263-1277.

Liang, Y. and Blake, R.E., 2006b. Oxygen isotope signature of P-i regeneration from organic compounds by phosphomonoesterases and photooxidation. Geochim. Cosmochim. Acta, 70(15): 3957-3969.

Liang, Y. and Blake, R.E., 2007. Oxygen isotope fractionation between apatite and aqueous-phase phosphate: 20-45 °C. Chemical Geology, 238(1-2): 121-133.

Liang, Y. and Blake, R.E., 2009. Compound- and enzyme-specific phosphodiester hydrolysis mechanisms revealed by [delta]18O of dissolved inorganic phosphate: Implications for marine P cycling. Geochim. Cosmochim. Acta, 73(13): 3782-3794.

Longinelli, A. and Nuti, S., 1973. Oxygen isotope measurements of phosphate from fish teeth and bones. Earth Planet. Sci. Lett., 20(3): 337-340.

Okin, G.S., Mahowald, N., Chadwick, O.A. and Artaxo, P., 2004. Impact of desert dust on the biogeochemistry of phosphorus in terrestrial ecosystems. Global Biogeochemical Cycles, 18(2): doi:10.1029/2003GB002145.

Reichstein, M. and Beer, C., 2008. Soil respiration across scales: the importance of a model-data integration framework for data interpretation. Journal of Plant Nutrition and Soil Science, 171: 344-354.

Reichstein, M., Ciais, P., Papale, D., Valentini, R., Running, S., Viovy, N., Cramer, W., Granier, A., Ogée, J., Allard, V., Aubinet, M., Bernhofer, C., Buchmann, N., Carrara, A., Grünwald, T., Heimann, M., Heinesch, B., Knohl, A., Kutsch, W., Loustau, D., Manca, G., Matteucci, G., Miglietta, F., Ourcival, J.M., Pilegaard, K., Pumpanen, J., Rambal, S., Schaphoff, S., Seufert, G., Soussana, J.-F., Sanz, M.-J., Vesala, T. and Zhao, M., 2007. Reduction of ecosystem productivity and respiration during the European summer 2003 climate anomaly: a joint flux tower, remote sensing and modelling analysis. Global Change Biology, 13: 634–651.

Reichstein, M., Falge, E., Baldocchi, D., Papale, D., Aubinet, M., Berbigier, P., Bernhofer, C., Buchmann, N., Gilmanov, T., Granier, A., Grünwald, T., Havránková, K., Ilvesniemi, H., Janous, D., Knohl, A., Laurela, T., Lohila, A., Loustau, D., Matteucci, G., Meyers, T., Miglietta, F., Ourcival, J.-M., Pumpanen, J., Rambal, S., Rotenberg, E., Sanz, M., Tenhunen, J., Seufert, G., Vaccari, F., Vesala, T., Yakir, D. and Valentini, R., 2005. On the separation of net ecosystem exchange into assimilation and ecosystem respiration: review and improved algorithm. Global Change Biology, 11: 1424-1439.

Reichstein, M., Rey, A., Freibauer, A., Tenhunen, J., Valentini, R., Banza, J., Casals, P., Cheng, Y., Grünzweig, J., Irvine, J., Joffre, R., Law, B., Loustau, D., Miglietta, F., Oechel, W., Ourcival, J.-M., Pereira, J., Peressotti, A., Ponti, F., Qi, Y., Rambal, S., Rayment, M., Romanya, J., Rossi, F., Tedeschi, V., Tirone, G., Xu, M. and Yakir, D., 2003a. Modelling temporal and large-scale spatial variability of soil respiration from soil water availability, temperature and vegetation productivity indices. Global Biogeochemical Cycles, 17(1104): doi:10.1029/2003GB002035.

Reichstein, M., Tenhunen, J., Ourcival, J.M., Rambal, S., Roupsard, O., Miglietta, F., Pecchiari, M., Peressotti, A., Tirone, G. and Valentini, R., 2003b. Inverse modelling of seasonal drought effects on canopy CO2/H2O exchange in three Mediterranean ecosystems. Journal of Geophysical Research, 108 (4726): doi:10.1029/2003JD003430.

Schlesinger, W.H., 1991. Biogeochemistry - An Analysis of Global Change Academic Press, San Diego, 588 pp.

Shemesh, A., Kolodny, Y. and Luz, B., 1983. Oxygen isotope variations in phosphate of biogenic apatites .2. Phosphorite rocks. Earth Planet. Sci. Lett., 64(3): 405-416.

Stewart, J.W.B. and Tiessen, H., 1987. Dynamics of soil organic phosphorus. Biogeochemistry, 4(1): 41-60.

Swap, R., Garstang, M., Greco, S., Talbot, R. and Kallberg, P., 1992. Saharan dust in the Amazon Basin. Tellus Series B-Chemical and Physical Meteorology, 44(2): 133-149.

Tabatabai, M.A. and Dick, W.A., 1979. Distribution and Stability of Pyrophosphatase in Soils. Soil Biology & Biochemistry, 11(6): 655-659.

Tamburini, F., Bernasconi, S.M., Angert, A., Weiner, T. and Frossard, E., 2010. A method for the analysis of the δ18O of inorganic phosphate in soils extracted with HCl. European Journal of Soil Science, 61(6): 1025–1032.

Taylor, H.P.J. and Forester, R.W., 1979. An oxygen and hydrogen isotope study of the Skaergaard Intrusion and its country rocks: A description of a 55 M.Y. old fossil hydrothermal system. J. Petrology, 20(3): 355-419.

Tudge, A.P., 1960. A method of analysis of oxygen isotopes in orthophosphate - its use in the measurement of paleotemperatures. Geochim. Cosmochim. Acta, 18(1-2): 81-93.

Turner, B.L., Paph¡zy, M.J., Haygarth, P.M. and McKelvie, I.D., 2002. Inositol phosphates in the environment. Philosophical Transactions of the Royal Society of London. Series B: Biological Sciences, 357(1420): 449-469.

Vennemann, T.W., Fricke, H.C., Blake, R.E., O'Neil, J.R. and Colman, A., 2002. Oxygen isotope analysis of phosphates: A comparison of techniques for analysis of Ag3PO4. Chemical Geology, 185(3-4): 321-336.

Vitousek, P.M. and Farrington, H., 1997. Nutrient limitation and soil development: Experimental test of a biogeochemical theory. Biogeochemistry, 37(1): 63-75.

Walker, T.W. and Syers, J.K., 1976. Fate of phosphorus during pedogenesis. Geoderma, 15(1): 1-19.

Wardle, D.A., Walker, L.R. and Bardgett, R.D., 2004. Ecosystem properties and forest decline in contrasting long-term chronosequences. Science, 305(5683): 509-513.

Weiner, T., Mazeh, S., Tamburini, F., Frossard, E., Bernasconi, S.M., Chiti, T. and Angert, A., 2011. A method for analyzing the δ18O of resin-extractable soil inorganic phosphate. Rapid Communications in Mass Spectrometry, 25(5): 624-628.

White, J.W.C., 1988. Stable hydrogen isotope ratios in plants: A review of current theory and some potential applications. In: P.W. Rundel, J.R. Ehleringer and K.A. Nagy (Editors), Stable Isotopes in Ecological Research. Springer-Verlag, Berlin, pp. 142-162.

Zaehle, S., Friend, A.D., Friedlingstein, P., Dentener, F., Peylin, P. and Schulz, M., 2010. Carbon and nitrogen cycle dynamics in the O-CN land surface model: 2. Role of the nitrogen cycle in the historical terrestrial carbon balance. Global Biogeochemical Cycles, 24(1): doi:10.1029/2009GB003522

Zohar, I., Shaviv, A., Young, M., Kendall, C., Silva, S. and Paytan, A., 2010. Phosphorus dynamics in soils irrigated with reclaimed waste water or fresh water - A study using oxygen isotopic composition of phosphate. Geoderma, 159(1-2): 109-121.

BACTERIALLY MEDIATED REMOVAL OF PHOSPHORUS IN A NON-POLLUTING INTENSIVE MARICULTURE SYSTEM

Michael Krom[1,4], Jaap van Rijn[2], Arad Ben David[2], Ellery Ingall[3], Liane G. Benning[4], Santiago Clerici[4] and Robert J.G. Mortimer[4]

[1]Charney School of Marine Sciences, Haifa University
[2]The Robert H. Smith Faculty of Agriculture, Food and Environment, The Hebrew University of Jerusalem, Rehovot
[3]School of Earth and Atmospheric Sciences, Georgia Tech. Atlanta, USA
[4]School of Earth and Environment, Leeds University, UK

Discharge of dissolved inorganic nitrogen (N) and phosphorus (P) is the major cause of environmental pollution from agriculture. Zero discharge systems (ZDS) are innovative intensive systems which produce marine fish with no pollutant discharge and minimal use of valuable freshwater. The systems are designed to use natural populations of aerobic bacteria to convert the (toxic) ammonia excreted by fish to nitrate and then to use other anaerobic bacteria, called denitrifying bacteria, to convert nitrate to nitrogen gas (Shnel et al., 2002; Gelfand et al., 2003; Neori et al., 2009). In this study, we used routine water quality measurements combined with intensive sampling of the sediment sludge in the anoxic sampling basin (SB) including the use of gel probes to understand the fate of N and P within the ZDS system.

Our data showed that during routine operation of the system nitrate built up as a result of nitrification in the trickling filter. After 70 days operation, denitrification in the SB increased to the point where any further nitrate produced in the system was reduced quantitatively to nitrogen gas. The nitrate content remained constant over time at ~15 mmoles/l. Such constant nitrate concentrations likely reflect limitation on the supply of readily reducible organic matter, which sustains the denitrification processes. Simultaneously, phosphate, which had been taken up in the oxic surface layers of the SB, was released to the overlying water column. By analogy with waste treatment systems, we speculate that phosphate was released from polyphosphate accumulating aerobic microbes.

Detailed sampling of the SB sludge was carried out after 217 days of ZDS operation. Nitrate and sulphate, circulating in the overlying water at constant concentrations (~15

mmoles/l), were rapidly consumed in the upper 10-15 cms of the sludge as a result mainly of heterotrophic bacterial nitrate and sulphate reduction.

While apatite was supplied to the fish in their food, our results showed that there was also major conversion of organic P to apatite within the sediment sludge. The evidence for this included observations on the pore water profiles in which the ammonium concentration increased with depth, while the phosphate concentration decreased. Since it is known that both ammonium and phosphate are produced by heterotrophic reduction of organic matter, their depth profiles requires that there is a process in the upper layers which actively removes phosphate. Thermodynamic calculations showed that the system was strongly oversaturated relative to both hydroxyapatite and calcite, consistent with analyses showing an accumulation with depth of solid phases containing calcium, inorganic carbon and phosphate. Furthermore our XRD data suggest that the apatite present in the sludge was different from that supplied in the fish feed. These data suggest that there was active precipitation of apatite in the surface layers of the sludge. We also calculated that the observed amount of inorganic P in the surface layer could only have been the result of active conversion of organic P to apatite and could not be attributed to the concentration increase associated with a loss of sediment mass through conversion of biomass to nitrogen and carbon dioxide/methane gases.

We tentatively conclude that the SB sludge is a location where organic P is created in the form of bacterial biomass, it is also the loci of bacterial respiration in which organic P is broken down to dissolved P, which is then precipitated as diagenetic apatite. It is possible that there may be a polyphosphate intermediate in this process as suggested in studies on a similar system in which denitrifying bacteria were found to accumulate polyphosphate (Barak and van Rijn, 2000; Barak et al., 2003). However, if there is such an intermediate, it appears to be transient. This conversion of organic P to apatite represents a shunt out from the bacteria into mineral apatite. This results in a final sink for P in the system, which could be used in the future as a source for P to be extracted a reused as a fertilizer.

References

Barak, Y., van Rijn, J. 2000. Atypical polyphosphate accumulation by the denitrifying bacterium *Paracoccus denitrificans*. Appl. Environ. Microbiol. 66: 1209-1212.

Barak, Y., Cytryn, E., Gelfand, I., Krom, M., van Rijn, J. 2003. Phosphate removal in a marine prototype recirculating aquaculture system. Aquaculture 220: 313-326.

Gelfand, I., Barak Y., Even-Chen, Z., Cytryn, E., Krom, M., Neori, A., van Rijn, J., 2003, A novel zero-discharge intensive seawater recirculating system for culture of marine fish, J. World Aquacult. Soc., 34: 344-358.

Neori, A., Krom, M.D., van Rijn, J., 2007, Biogeochemical processes in intensive zero effluent marine fish culture system with recirculating aerobic and anaerobic biofilters, Journal of Experimental Marine Biology and Ecology, 349: 235-247.

Shnel, N. , Barak, Y. , Ezer, T. , Dafni, Z. , van Rijn, J., 2002, Design and performance of a zero-discharge tilapia recirculating system. Aquacultural Engineering 26: 191-203.

Session 7: Micro and Nano Systems to Investigate Biogeochemical Processes

JOINING NANOSIMS AND STXM/NEXAFS TO VISUALIZE SOIL BIOTIC AND ABIOTIC PROCESSES AT THE NANO-SCALE

Jennifer Pett-Ridge[1]*, Marco Keiluweit[1, 3], Lydia H. Zeglin[3], Jeremy J. Bougoure[1], David D. Myrold[3], Markus Kleber[3], Peter K. Weber[3], and Peter S. Nico[2]

[1]Chemical Sciences Division, Physical and Life Sciences Directorate, Lawrence Livermore National Laboratory, Livermore, California, USA
[2]Earth Sciences Division, Lawrence Berkeley National Laboratory, Berkeley, California, USA
[3]Department of Crop and Soil Science, Soil Science Division, Oregon State University, Corvallis, Oregon, USA
*Corresponding author: Email: pettridge2@llnl.gov, Ph: +1 925-424-2882

Abstract

Understanding the fate and residence time of organic matter in soils is important to natural resource management, including strategies to mitigate climate change. Here we propose that a combination of stable isotope tracer experiments followed by high-resolution secondary ion mass spectroscopy (NanoSIMS) and Scanning Transmission X-ray Microscopy (STXM) coupled with Near Edge X-ray Absorption Fine Structure spectroscopy (NEXAFS) can be a profitable way to address critical characteristics of soil microscale processes, such as the time scales of carbon cycling, relative importance of biotic and abiotic processes in organic matter stabilization in soils, and spatial variance in these processes. When used in concert, these analytical techniques have the capacity to yield quantitative, *in situ* information on the source, molecular class, and elemental quantity of organic matter. We have described in detail the analytical methods for combining the two techniques, using a series of control experiments on pure mineral samples mixed with isotopically labeled yeast cells as well as tests of soil aggregates incubated with isotopically labeled plant or microbial tissues. STXM and NanoSIMS are used to correlate the chemical and isotopic heterogeneity of C and N

compounds in diverse samples ranging from field and controlled lab experiments, mineral and organic soil horizons, for both thin-sectioned and intact particles. Prescreening samples with SEM is particularly useful for selecting target locations and providing important visual clues and does not produce significant spectral artifacts via electron beam damage. In contrast, repeated STXM analysis of a particle both before and after NanoSIMS analysis showed that it is crucial to conduct STXM analysis prior to NanoSIMS imaging. Electrical changing was a persistent concern in combined mineral-organic phase samples, but using an electron flood gun during NanoSIMS analysis significantly eliminated charging artifacts and increased secondary ion signal intensity. Finally, our investigation of an artificial mixture of isotopically labeled yeast cultures with purified minerals demonstrated rapid association of microbially derived lipid materials with both phylosciliate and iron oxide mineral surfaces. Taken together, we suggest that combined isotope labeling, SEM, STXM/NEXAFS and NanoSIMS imaging can be used to infer the molecular and spatial fate of added labeled material in a mineral matrix, and this approach has great potential to contribute to a mechanistic understanding of sorption, occlusion, and decomposition processes that operate at fine spatial scales in natural environments.

Keywords: NanoSIMS; STXM; NEXAFS; SEM; isotope labeling; organic matter; soil carbon

Introduction

Soils house major transformations in the global cycles of C, N, S, and P, and are often described as one of the most complex media on earth. This complexity extends from the ecosystem scale to the habitat of individual microorganisms and microaggregates, where nanometer scale interactions between microbes, organic matter and mineral particles are thought to control the long-term fate of soil carbon (Lehmann et al., 2007; Schmidt et al., 2011). Soil organic matter (SOM) occlusion at the clay microstructure level has long been attributed to abiotic mechanisms (Duiker et al., 2003), but recent work indicates that soil biota are also strongly involved; microbial cells, secretions, root exudates and faunal mucus all act as cementing agents and are likely occluded within microaggregates (Lützow et al., 2006; Six et al., 2006). The characteristics of these various plant and microbially derived organic compounds (lipids, phenolics, lignin, amino acids, polysaccharides) are likely to interact differently with soils mineral phases in soils, and their persistence is tied to the reactivity of their component molecular

groups (carboxylic acids, amines, aromatic rings) (Kuzyakov, 2002). Advancing our understanding of these organic-mineral interactions requires an ability to disentangle the complex interactions between soil mineral surfaces, decomposed organic compounds and microbial catalysts. However, this research field has long lacked analytical methods to characterize organic-mineral interactions in a physically intact state at the micron or nanometer scale (Lehmann et al., 2009).

In order to study process dynamics as a function of location within aggregates and microaggregates, simultaneous information on (a) localization, (b) identification and (c) transformation of organic matter and mineral phases is required with high spatial resolution (nm to μm). Conventional electron microscopy can provide high spatial resolution imaging and major element composition (e.g. (Laird and Thompson, 2009)), but it cannot be used to chemically identify microbial residues and amorphous organic matter (OM). Although a number of techniques can yield data on OM composition (e.g. ion microprobe laser desorption approaches, laser ionization mass spectrometry, micro Raman spectroscopy, ^{13}C-NMR, FTIR (Lehmann et al., 2005; Lehmann et al., 2009)), few can provide molecular or elemental characterization with the sub-micron resolution necessary to study mechanisms of OM physio-chemical stabilization in microaggregates. An ideal methodology might allow *in situ* analysis of undisturbed soil particles, at the spatial scale of organic-mineral interactions (nm to μm), with the capacity to both chemically identify organic residues and simultaneously evaluate their source.

The combination of stable isotope tracer experiments followed by analysis by high-resolution secondary ion mass spectrometry (Pierzynski et al., 1994) and Scanning Transmission X-ray Microscopy, Near Edge X-ray Absorption Fine Structure (STXM/NEXAFS) has been proposed to bridge this analytical gap in soil science (Behrens et al., 2012; Keiluweit et al., 2012; Remusat et al., 2012b). Tracing stable isotope labeled natural materials (purified compounds or whole plant/microbial cells) should allow elements such as carbon and nitrogen to be traced from their sources into the soil matrix; NanoSIMS should allow the fate of these tracers to be imaged; STXM should allow the molecular composition of the traced material to be determined; and all should be possible at high resolution in a relatively undisturbed sample. In short, this approach could allow the imaging of organic C distribution, associations of organics

with specific mineral types, and trace organic matter of differing origins into the soil matrix (Lehmann et al., 2007; Wan et al., 2007b).

The Cameca NanoSIMS 50 series represents the state-of-the-art for *in situ* microanalysis by SIMS, combining unprecedented spatial resolution (better than 50 nm) with ultra-high sensitivity (<200 atom detection limit). The NanoSIMS couples a high transmission, high mass resolution mass spectrometer with an array of detectors, enabling simultaneous collection of as many as seven elements or isotopes originating from the same sputtered volume of a sample. The primary ion beam ($^{133}Cs^+$ or $^{16}O^-$) can be scanned across the sample to produce quantitative secondary ion images. This capability for multiple isotope imaging with permil precision and accuracy and nanometer scale spatial resolution is unique to the NanoSIMS and provides a novel new approach to the study of the isotope and trace element distributions. The NanoSIMS also provides an unprecedented ability for correlated analyses of morphological, structural, chemical and isotopic characteristics with nanometer resolution—particularly when used in concert with electron microscopy. The application of SIMS to soils and SOM is still relatively rare (Clode et al., 2009; Herrmann et al., 2007; Keiluweit et al., 2012; Mueller et al., 2012; Pumphrey et al., 2009; Remusat et al., 2012b) compared to work in geochemical, marine, and microbial systems (Dekas et al., 2009; Finzi-Hart J. & Pett-Ridge et al., 2009; Moreau et al., 2007; Musat et al., 2008; Woebken et al., 2012).

STXM/NEXAFS is a state-of-the-art technique for understanding the chemical form of organic material with the highest possible spatial resolution. STXM instruments provide a high brightness, monochromatic, X-ray spot of less than 50 nm, comparable to the NanoSIMS spot size. Using interferometer-based precise sample position control and high resolution monochromators, raster scan sample images can be obtained at energy spacings of ~0.1 eV across 100's of eV energy ranges, ~200-800eV for the Advanced Light Source (ALS) beamline 5.3.2.2 (Kilcoyne, 2003) at Lawrence Berkeley National Laboratory (LBNL). The spatially resolved NEXAFS spectra extracted from these image stacks reveal the bonding environment of the element of interest (e.g. C, N, O, or Fe), allowing for spatial interpretation of not only elemental concentrations but also organic matter or mineral chemical speciation. STXM/NEXAFS has been used successfully to describe spatial patterns and speciation

of soil organic matter associated carbon (Lehmann et al., 2007; Lehmann et al., 2008; Solomon et al., 2005; Wan et al., 2007a), and nitrogen (Gillespie et al., 2009; Leinweber et al., 2010; Leinweber et al., 2007) in a broader range of environments, including marine systems (Brandes et al., 2004).

Together, we think these two techniques have the potential to yield complementary data at similar resolution, documenting both molecular class and elemental concentration. Preliminary work has sought to combine them in meteoritic material (De Gregorio et al., 2010; Matrajt et al., 2008) and soil samples (Keiluweit et al., 2012; Remusat et al., 2012b), but the best method sequence, possible artifacts due to combined analysis, and ideal sample preparation approaches remain undescribed. Here we examine the analytical challenges of jointly applying NanoSIMS and STXM/NEXAFS to both whole and sectioned soil aggregates, using samples from incubation experiments with natural and artificial soils. Our goal is to document important aspects of both method development (analysis order, effect of one method on another, sample charging effects) and data interpretation. Test samples included a series of mineral and organic materials, of varying complexity: (1) a sterilized preparation of ^{13}C and ^{15}N enriched yeast/bacteria cell culture; (2) an artificial incubation comprised of ^{13}C and ^{15}N enriched yeast and bacteria cells mixed with montmorillonite minerals; (3) natural microaggregates separated from a forest soil (Hatton et al., 2012; Remusat et al., 2012b); (4) H.J. Andrews forest mineral soil exposed in a lab microcosm incubation to ^{13}C-glucose, and (5) H.J. Andrews organic horizon soil incubated with isotopically enriched fungal cell wall material (Keiluweit et al., 2012).

Materials and Methods

Sample specimens were prepared for image analysis by placing them directly onto silicon nitride (Si_3N_4) windows via wet or dry deposition without a chemical adhesive. Samples were coated with a < 10 nm conductive layer of gold (Au) or iridium (Ir) and imaged by scanning electron microscopy (SEM), STXM, and NanoSIMS. SEM mapping was performed on a JEOL 7401 SEM (Tokyo, Japan) at LLNL.

Forest soil microaggregates

Samples of A-horizon soils (Hatton et al., 2012) were sieved to pass 2 mm and density fractionated according to previously described methods (Sollins et al 2006). While particles from both the 2.2 and 2.4 g.cm^{-3} density fraction were deposited either as a dry powder or a deionized water slurry on individual Si_3N_4 windows and then imaged by SEM, STXM-NEXAFS and NanoSIMS. Additional characterization suggests these fractions are dominated by phylosillicates and microbially derived organic matter (Hatton et al., 2012).

Sterilized microbe-mineral incubations

Artificial associations of isotopically labeled bacteria and yeast residues mixed with montmorillonite or goethite minerals were obtained as follows: a bacteria and yeast (*Sachharomyces cerevisiae*) culture was grown in a fed batch reactor with sucrose, and 99.9 atm % ^{13}C-glucose/^{15}N-ammonium. Cultures were initially grown in yeast nitrogen base media (Sigma Y1251) with natural abundance ^{13}C and ^{15}N sucrose, ammonium sulfate and essential amino acids; then transferred to media enriched with additional ^{13}C-glucose (final δ^{13}C 200‰) and ^{15}N-NH_4SO_4 (final δ^{15}N 785‰). Final cell density was approximately 10 g (Welden et al.) / L. Cells were harvested in late exponential phase, washed 3x in DI water and pelleted. To create cell fragments that could react with a mineral phase without the added effects of biological activity, 10 mg of pelleted cell material was re-suspended in 100 ml 0.01 mM NaCl and autoclaved. Then, 5 ml of continuously stirred cell suspension was pipetted into 50 ml centrifuge tubes containing 10 mg Na-exchanged montmorillonite or goethite in 48 ml 0.01 mM NaCl. The suspension was adjusted to pH 7 using 0.1M HCl and NaOH. The tubes were sealed with Teflon-lined caps and the mixture was incubated for 8 hours on a rotary shaker, subsequently centrifuged and washed 3X with 0.01mM NaCl. The remaining particles were re-suspended in DI water, 2 µl transferred onto standard Si_3N_4 windows (Silson Ltd., England) for image analysis, and air-dried under a dust cover. On each Si_3N_4 window, several regions were imaged by both light microscopy and SEM at LLNL to determine surface morphology and ideal regions (< 10 µm thick) for STXM and NanoSIMS analysis.

Isotope incubations of forest soil

Incubations of forest soils and $^{13}C/^{15}N$ labeled fungal extracts are described in detail in Zeglin et al. (2011a) and Keiluweit et al (2012). Briefly, ^{15}N- and ^{13}C-labeled fungal cell wall material was generated by culturing yeast (*Saccharomyces cerevisiae*) with ^{13}C-glucose and $^{15}NH_4^+$, and then chemically extracting insoluble chitin-enriched cell wall material (Kirchman and Clarke, 1999; Roff et al., 1994). The resulting material, enriched to 501.2‰ $\delta^{15}N$ and 151.2‰ $\delta^{13}C$, was mixed at 1% w/w (dry mass basis) with 30 g field wet O-horizon soil (collected from the H.J. Andrews Experimental Forest, Oregon, USA) and incubated for 3 weeks. To ready the samples for STXM-NanoSIMS analysis, 40 mg of soil was gently dispersed in 2 ml 10mM NaCl for 1 minute. One μL of the supernatant (containing numerous hyphal fragments) was dried onto a silicon nitride (Si_3N_4) window (Silson Ltd, England), sputter-coated with 5 nm of iridium, and then mapped using the LLNL JEOL 7401 SEM with an accelerating voltage of 1 KV.

In a second experiment with soils from the H.J. Andrews Forest, mineral soils were incubated in lab microcosms and supplied with ^{13}C-glucose diluted to 20 atom% ^{13}C and supplied via a 'synthetic root' at 100 μm C d^{-1} ml^{-1}over a 40 day period. Aggregates were collected from the zone closest to the root (<5 mm) and prepared for image analysis by high pressure freezing (HPF) and sectioning. For HPF, aggregates < 300um were pipetted into Cu tubes (16mm long, internal diameter 300um) and allowed to absorb filtered deionized H_2O from the bottom for 1 hour to achieve maximum hydration. Tubes were frozen in liquid nitrogen with a Leica EM PACT2 (Leica Microsystems, Buffalo Grove, IL), trimmed, and 300 nm sections were cut with a Leica ultramicrotome using a 35 degree diamond knife at –150ºC. Sections were then transferred to a SiNi window and brought to room temp slowly in a pre-chilled (liquid N_2) metal sample holder.

Synchrotron near edge X-ray absorption fine structure (NEXAFS) spectroscopy

Synchrotron X-ray spectroscopy analysis for all samples was conducted on the Advanced Light Source (ALS) beamline 5.3.2 at the Lawrence Berkeley National Laboratory (Berkeley, California). Detailed operation principles of STXM/NEXAFS are published elsewhere (Braun et al., 2003; Hitchcock et al., 2006; Kilcoyne et al., 2003) and described here only briefly. Except where noted, we disregarded particles with optical density greater than 2.0 at any energy between 278 eV and 330 eV, i.e. the

energy range of our carbon K-edge spectra. This limited particle selection to those smaller than approximately 5 microns. We collected stacks in the region of 278 eV to 330 eV for carbon, 396 to 430 eV for nitrogen, and 705 to 730 for Fe NEXAFS. NEXAFS stack alignment and analyses, and alignment of background and edge maps of other elements were done using the Zimba alignment module of the software package aXis2000 (Hitchcock et al., 2006). NEXAFS spectra were extracted using the software package aXis2000 (Hitchcock et al., 2006). Color composite of quantitative component maps of proteins, amino sugars and phopholipids; obtained by spectral fitting of reference compounds to STXM/NEXAFS image sequences using a linear regression procedure (Koprinarov et al., 2002).

NanoSIMS

Isotopic and chemical images were acquired on the Cameca NanoSIMS 50 instrument (Gennevilliers, France) at LLNL. The NanoSIMS 50 allows the simultaneous collection of five isotopes with high spatial resolution (up to 50 nm) and high mass resolution. For our soil sample analyses, a focused 1.2 - 2.7 pA Cs^+ primary beam with a nominal spot size of 100-150 nm was stepped over the surface in a 256 x 256 pixel raster to generate secondary ions, collected by electron multipliers with a dead time of 44 ns, and secondary electrons, which were detected with a photomultiplier tube, except during the operation of the normal-incidence electron flood gun (e-gun). The e-gun was used for mineral samples to compensate for charging effects, which can be identified based on low secondary electron and ion transmission and sometimes streaking. Before using the e-gun, samples were first imaged by secondary electrons, yielding a reference image useful for comparison to the NanoSIMS secondary ion and SEM images. Raster size was either 10 x 10 μm or 20 x 20 μm. Carbon isotopic ratios were measured using $^{12}C^{12}C^-$ and $^{13}C^{-12}C^-$ or $^{12}C^-$ and $^{13}C^-$, and nitrogen isotopic ratios measured with $^{12}C^{14}N^-$ and $^{12}C^{15}N^-$. Other detected species included $^{32}S^-$, $^{56}Fe^{16}O^-$, and $^{16}O^-$. The secondary mass spectrometer was tuned for high mass resolving power (~7000) to resolve masses of interest and isobaric interferences, particularly $^{13}C^{12}C$ and $^{12}C_2{}^1H$ at mass 25, $^{12}C^{14}N$ and $^{13}C_2$ at mass 26, and $^{12}C^{15}N$ and $^{11}B^{16}O$ at mass 27.

Measurements were repeated on 10-12 individual cells for the yeast-bacteria culture alone, and three different locales in the mixed cell-mineral sample. In the natural soils samples, STXM and NanoSIMS images of the same spot were collected for 3-6 locations per sample. Each cell or mineral particle was defined as a region of interest

(ROI) based on associated SEM images or by encircling pixels where $^{12}C^{14}N^-$ counts > 30% of the maximum counts in the image. The isotopic composition of each ROI was calculated by averaging over all replicate layers where both C and N isotopes were at sputtering equilibrium. A *Bacillus subtilis* spore preparation was used as a reference standard for C and N isotopic measurements ($^{13}C/^{12}C$ = -23.75; $^{15}N/^{14}N$ = 7.85), and 12 regions of this standard (~28 individual spores) were also analyzed both with and without the e-gun on two separate analysis dates. Isotopic enrichment of standards was independently determined at the University of Utah (Finzi-Hart J. & Pett-Ridge et al., 2009). Data were processed as quantitative isotopic ratio images using LIMAGE software, developed by L. Nittler (Carnegie Institution of Washington), and were corrected for effects of quasi-simultaneous arrival (QSA), detector dead-time and image shift from layer to layer (due to drift in the location of the ion beam from frame to frame). Isotopic ratio data are presented using delta notation in parts per thousands (‰): $\delta = (R_m/R_{std} - 1)\cdot 1000‰$, where R_m and R_{std} are the measured ratios for the unknown and standard, respectively.

Results and Discussion

Correlated analysis

Using a preparation of natural microaggregates separated from a forest soil (Hatton et al., 2012), we made sure it was possible to identify soil particles in the SEM and relocate them for analysis in both the STXM and NanoSIMS instruments. Figure 1 shows a correlated suite of SEM, STXM and NanoSIMS images on a forest soil microaggregate. The SEM image (Fig. 1A) shows the physical structure of the soil microaggregate, and was used to identify particles of interest. While we found that the general location of most particles could be initially relocated using light microscopy, SEM mapping greatly facilitated precise relocating of individual particles in the STXM and NanoSIMS instruments for correlated analysis. In the STXM, particle identity was confirmed based on the morphology observed in raw absorption images. Particle identity in the NanoSIMS was confirmed based on secondary electron imaging. In the aggregate shown in Figure 1, the NanoSIMS-derived ^{16}O distribution (Fig. 1H) is well-correlated with what appear to be phyllosilicate minerals composing much of the aggregate's surface area. The STXM image shows the distribution of Fe and C within the particle.

The C and N NEXAFS spectra (Fig. 1I and 1J) are dominated by peaks at 288.3 eV and 401.6 eV, respectively, confirming the presence of a large fraction of amide functional groups and therefore an organic phase dominated by proteins or amino-sugars (e.g. chitin). There is little variability in the STXM C image (Fig. 1C), which suggests a fairly homogenous distribution of this organic matter 'glue' throughout the aggregate volume. This is in contrast to the NanoSIMS carbon and nitrogen images (Fig. 1E and 1G), which indicate a heterogeneous C and N distribution exists, at least at the surface. In the corresponding SEM image, these areas appear to have a more amorphous and possibly organic nature. The STXM Fe image shows that the particle is not homogenous with respect to Fe. These findings highlight an obvious difference between the capabilities of NanoSIMS analysis—which is inherently a surface sputtering approach (though it may be used to depth profile), and STXM/NEXAFS analysis—where data are collected via X-ray transmission and integrated through the entire particle volume. In the case of this aggregate, each approach adds nuance to our interpretation of its physical structure: a mineral-organic 'sandwich' consisting of proteinaceous organic matter and Fe and Si minerals.

Sequence of analysis

Using our preparations of natural soils, we also tested the effect of order of processing and analysis on subsequent analyses. Our presumed order was metal (Au or Ir) coating, low-voltage SEM imaging (< 2 kV), STXM analysis, and finally NanoSIMS analysis; based on the supposition that electron analysis would be inherent less destructive than ion analysis. First we considered the potential effect of Au or Ir or Au coating on STXM analyses using the LBNL Center for X-ray Optics web based calculator (Gullikson, 2012; Henke et al., 1993) to determined that the X-ray transmission of the thickest possible Ir coating we might want to use. Our calculations indicated that even with a 20 nm Ir coating (more than twice the typical amount), transmission would be greater than 47% and vary less than 2% over the C and N scan ranges of 280eV to 310eV, and 400eV to 430eV respectively. Based on these calculations and the fact that the calculated impact of Au was less than that of Ir, we concluded that metal coating should have a minimal impact on the X-ray absorption data collection. Second, we tested for effects of SEM imaging on subsequent STXM analyses, and observed no apparent damage from pre-STXM SEM scanning (e.g. no observable raster boxes or backgrounds of particularly high aromaticity) and conclude that as long as the SEM accelerating voltage

is kept low (<1-2 kV), there should be no negative effect. Finally, we tested whether samples could be returned to STXM after NanoSIMS analysis. After comparing a forest soil sample both pre- and post- NanoSIMS analysis by STXM-NEXAFS, it is clear that the post-NanoSIMS set of NEXAFS spectra are significantly different relative to initial measurements (Fig. 2B, C). From one location to another, significant redistribution of C had occurred; STXM images collected prior to NanoSIMS analysis are crisper with more clearly defined features regardless of the functional group type (Fig. 2). The chemistry of the C was also altered with increased signals of aromatic (285.0-285.3 eV) and phenolic (286.5 eV) and carbonate (292.5) functional groups.

Effects of Mineral Charging

Electrical charging effects are a particular concern during NanoSIMS analyses of soil particles (Cliff et al., 2002; Herrmann et al., 2007; Pett-Ridge and Weber, 2012; Remusat et al., 2012b) but can be sample-dependent and the effects on ion yield have not been well documented for heterogeneous samples. We tested the effect of mineral charging during NanoSIMS analyses both with and without the use of the electron e-gun. In our analyses of soil minerals and intact soil aggregates, even those initially coated with Au or Ir sometimes began to show evidence of sample charging under the Cs^+ primary ion beam after ~ 20 minutes of analysis. Figure 3 shows a soil particle that is charging, and the same particle subsequently imaged with charge compensation (e-gun). Charging can be identified based on areas of the NanoSIMS secondary electron image that are black, reflecting very low electron transmission (Fig. 3). It also results in reduced ion transmission, though this can be difficult to identify in ion images of heterogeneous samples. We performed systematic analyses of the same particles with and without the e-gun and found that the ion count rates were significantly lower in charging particles (mean +/- SE). With the e-gun, the ion count rates increased by as much as 10 X for C and similarly for N. To evaluate concerns that the e-gun might affect measured isotope ratios, we conducted additional tests on standard reference materials, and found that isotope ratios of organic standards (Finzi-Hart & J. Pett-Ridge et al., 2009) analyzed with the egun (-20.1 ± 0.91 and 33.8 ± 1.4 for $\delta^{13}C$ and $\delta^{15}N$ respectively) and without the e-gun (-22.8 ± 1.2 and 30.8 ± 2.0 for $\delta^{13}C$ and $\delta^{15}N$ respectively) were not significantly different ($p = 0.091$ and 0.223 respectively).

Across all the synthetic and natural soil materials we worked with, we frequently determined that the e-gun improved ion yield and reducing charging. Because secondary electron imaging in the NanoSIMS is not possible with the e-gun on, we initially determined the coordinates of particles of interest in the NanoSIMS with secondary electron imaging, and then turned on the e-gun for the NanoSIMS analyses. The e-gun is not likely to work with samples with significant topography and is not a solution in cases where topography is already causing charging and ion shadowing. While an alternative solution would be to simply avoid the use of charge compensation and blank out all regions on images where obvious charging occurs (Remusat et al., 2012a), we suggest that using the electron e-gun is preferable if both organic and mineral phases are to be simultaneously examined.

Control experiments

To assess the role of microbial cell components in the formation of mineral-organic associations, we applied SEM, STXM/NEXAFS and NanoSIMS to laboratory prepared samples with defined organic and minerals constituents. Figure 4 shows the results of this joined analysis of an artificial yeast-mineral preparation made from an autoclaved ^{13}C- and ^{15}N-labeled yeast culture combined with montmorillonite particles. In scanning electron micrographs of the mixture, cell components of two differing morphologies are clearly distinct from mineral particles (Figure 4A). The sample morphology is consistent with the treated yeast culture before creating the mixture. These components can be identified in the NanoSIMS $\delta^{13}C$ and $\delta^{15}N$ images (Figure 4C & D); the large particle at the center is enriched in ^{15}N (947 ± 12‰) and ^{13}C (54 ± 6‰), the three smaller particles in the image have $\delta^{15}N$ and $\delta^{13}C$ of 402 ± 26‰ and 102 ± 12‰ respectively. The starting enrichment for the treated yeast culture before making the mixture was ~700‰ $\delta^{15}N$ and ~250‰ $\delta^{13}C$ based on NanoSIMS analysis. The data for the mixture confirm that the identified components are from the yeast culture, though some alteration occurred.

By linear combination fitting to standard NEXAFS spectra (Fig 4E), the chemical differences between different microbial cell fragments and organic matter coatings were grouped into three broad chemical types: protein, amino-sugar, and phospholipid, evident in the false color image of Fig 4B. Cell component #1 appears to be comprised of a mixture of phospholipids and amino-sugars, whereas cell component #2 is

dominated by a proteinaceous signature. The spectra of mineral particles are fairly homogeneously coated by yeast culture-derived lipids.

With spectra extracted specifically from mineral particle regions of interest, the carbon NEXAFS spectrum associated with the mineral fraction of this yeast-mineral mixture shows a pronounced feature at 287.5 eV, indicative of saturated alkane C. However, detailed examination of this same spectrum reveals a noticeable 288.7 eV peak indicative of carboxyl C which is not found in the simple lipid standard spectra but is consistent with a lipopolysaccharide (LPS) complex of the type expected in cellular membranes (Parikh, Chorover, 2008). In a parallel experiment where we combined the yeast culture with a goethite mineral suspension (data not shown) the carbon spectra associated with the goethite fraction are similar to the result with monmorillinite. This suggests that LPS - type material from cell membranes has the ability to rapidly associate with mineral surfaces of both metal oxide and phyllosilicate clay surface types. Our observation of a concentration of lipid C near mineral surfaces is consistent with previous observations of lipid or alkane type C closely associated with and tightly bound to mineral surfaces (Baldock and Skjemstad, 2000; Kögel-Knabner, 2000; Mahieu et al., 1999; Song et al., 2008; Song et al., 2011). Multiple researchers have explored the role of LPS in bacterial cell adhesion to mineral surfaces and biofilm formation (Makin, Beverage 1996; Omoike and Chorover 2006), suggesting that microbes may have developed modes of attachment based on the ability of LPS - like materials to become quickly associated with mineral surfaces, regardless of mineral surface specifics. However, the observation that this association does indeed develop rapidly and spontaneously in the absence of metabolically viable organism and before the partitioning of other C types such as proteins and polysaccharides is novel.

The preferential association of LPS-type compounds with mineral surfaces can be justified in terms of three important binding mechanisms. First, the low water solubility of lipid C will drive reordering of LPS into either free floating micelles or onto surfaces. Surface binding is likely favored over micelle formation as a long-term stable state as mineral surfaces already represent a disruption in the water hydrogen bonding network and therefore a low energy location for low solubility material. For example, Hanczyc et al (2003) showed that in the presence of montomorillinite surfaces myristoleate micelles reordered within less than 20 minutes, to form surface coatings and

encapsulating the clay particles. In addition, the amphiphilic nature of LPS allows them to interact with both hydrophilic or hydrophobic surfaces or surface regions creating both electrostatic and entropy driven surface associations depending on surface charge characteristics. Second, previous work has shown that the phosphate groups of LPS can form strong associations with mineral surface and drive the attachment of LPS to those surfaces (Omoike and Chorover 2006, Parikh, Chorover, 2008).

Third, an additional, although speculative, possibility for the strong association between the clay and the LPS is the intercalation of amphiphilic molecules into the interlayer sites on montmorilinte and other clays (Boufatit, et al.), although this would not be true in the goethite case.

Comparing STXM and NanoSIMS

STXM is a transmission microscopy technique, and the collected image is a sum of contributions from the entire line of sight, included the top and the bottom of the sample. If there is only a very thin coating of organic matter on top and bottom of the particle, it could be eroded by NanoSIMS analysis, and only the sides of the particle will be seen. The second difference that arises from the close comparison NanoSIMS/ STXM is the gradient we sometimes observe for the C/N ratio towards the edge of the aggregate. Indeed, one possible analytical artifact with NanoSIMS imaging is the contribution of the Si_3N_4 window to the N signal. This can be overcome by considering the secondary electrons image; we can identify a region of interest (ROI) that includes only the aggregate particle free of any contamination by the Si_3N_4 window on the sides of the particle. N-NEXAFS is also useful as the N spectra for Si_3N_4 and organic matter are different. By combining the two techniques, we can then confirm that the N signal observed is indigenous to the organic coating the particle. Then, if we rule out the artifact explanation, we may observe an increasing contribution of a microbial component towards the edge.

The fact that STXM is a transmission method and NanoSIMS is a surface method poses some challenges. Particle components observed by STXM can be at any depth with in a particle, and therefore direct correlation is potentially open to interpretation in whole particles. Depth analysis can be performed by NanoSIMS to give a representation of the sample isotopic and elemental composition with depth (Ghosal et al., 2008), but

this approach still leaves some question regarding the relationship between the integrated and the depth-resolved data. To address this issue, sample sectioning can be performed to reduce the sample to ~100 nm thickness, thereby largely eliminating the depth issue.

Assessment of soil STXM data

The quality of STXM/NEXAFS data is such that clear peaks and shoulders that are discernible above the noise level can be seen in both the C and N spectra. The spectra had a maximum optical density of less than 1.5 making spectral artifacts from higher order X-rays or detector dark counts unlikely. This result shows that STXM/NEXAFS analysis of soil microagregates (Fig 1) with at least two dimensions in the low micron range (~3 x 5 microns) is possible. However, for thicker particles, sectioning is necessary.

Assessment of soil NS data

NanoSIMS analyses of soil samples for OM tracer studies are challenging. Soils are normally low in organic content (percent level), they have potentially complex topography, and they contain insulating minerals that can result in sample charging. With the proper methods and control analyses, measurement precision can be calculated to account for these issues.

Based on these results and previous results, C and N ion count rates in the NanoSIMS analyses are low in natural soils compared to fresh OM. This result is a direct consequence of the percentage of OM in soil. Because the number of ions detected directly determines the potential precision of a measurement, the precision of NanoSIMS C and N isotopic measurements in soils is likely to relatively poor (>1% or 10‰). As a result, to be able to detect and image the distribution of a tracer, the level of isotopic enrichment in a soil sample must be large relative to the level needed in an organic sample. IN the case of the natural forest soil in this study, the tracer was not detectable in individual particles, even though the tracer was still detectable in the bulk soil. Further work is necessary to provide a practical guideline for such studies.

Compared to count-rate limits on precision, the effect of sample topography is likely small. Deviations in isotopic ratios from true ratios on the order of ~1% (10‰) can be

observed with samples with >10 μm height variation (Carpenter et al.), but in the case of these soil particles, the height variation is significantly less, and the measurement precision is likely worse. Still, the irregular surfaces of soil samples could result in local distortions in the ion extraction electric field, compounding deviations from the true ratio. Analyses of controls can provide some guide these samples. Here, sectioned samples would eliminate this potential source of uncertainty.

In addition to these other issues, sample charging is a wild card. Silicates, clays, and Fe/Al oxide minerals make it challenging to conduct isotope tracing experiments in soil matrices because they make it difficult to embed and thin-section soil samples, and also cause electrical charging effects (Cliff *et al.*, 2002, Pett-Ridge and Weber, Hermann, Remusat et al 2012). Deviations from the true isotopic ratio on the order of 10% (100‰) can readily be observed in samples that are charging (Carpenter et al.). It is not yet clear if similar deviations from the true ratio occur, possibly when charging occurs at a small scale, and perhaps only in small regions of a NanoSIMS analysis. We believe that this does occur, because it is the trajectory and energy of the individual ions emanating from a given location that determine whether the mass spectrometer is out of tune for that location. Therefore, if a location on the sample is charging, the true ratio for that location can potentially be significantly different from the measured ratio. Because we cannot test the ion extraction conditions at each location in an analysis field, if we observe any indication of charging, we chose to use the e-gun to prevent charging.

Conclusions

To gain a better understanding of organic matter processing and storage in soil it is critical that we develop a robust mechanistic understanding of micron- and nanometer-scale subsurface C cycling processes. Here we present an analytical strategy that allows for *in situ* morphological, chemical and isotopic analysis of single particles, through combined SEM, STXM/NEXAFS and NanoSIMS analysis. To allow for high-resolution analysis of the same sample specimen, ideal samples should have limited topography, are able to withstand high vacuum, are dry, conductive, thin enough to allow photon transmission, and prepared without carbon-based reagents. To quantitatively map elemental, isotopic and OM molecular speciation in a single soil particle, the analysis sequence SEM→STXM/NEXAFS→SIMS provides a number of

clear benefits. SEM imaging is a relatively fast screening tool, and if done first, allows pre-identification of particles of appropriate size and morphology (e.g. hyphal vs. bacterial surfaces; amorphous vs. crystalline minerals). SEM images are very useful to guide post-STXM and SIMS data analysis, when regions with unique isotopic or molecular signatures have been identified. With accelerating voltages in the range of ~1 KV, we observed no evidence of SEM beam damage. NanoSIMS imaging is destructive and therefore should come last in this combined approach.

Combined STXM-SIMS data may be used to document the forms of C that become stored in subsoil aggregates, and illustrate how isotope tracer experiments can allow tracking of microbial debris and other organic polymers into the soil matrix. NanoSIMS compliments the STXM-NEXAFS microstructure chemical characterization with information on the distribution of isotopic labels (e.g., ^{13}C and ^{15}N). These data, when coupled to more bulk-scale characterization of a soil's chemical and physical context, have the potential to provide information about organic matter-mineral-microbial relationships in an unaltered state, free from the effects of chemical or physical fractionation. By characterizing the fate of microbial biomass constituents and determining which organic materials are associated with which mineral types over time, the combination of STXM and NanoSIMS could lead to mechanistic explanations for the long-term protection of soil C.

Acknowledgements

This research was supported by a Laboratory Directed Research and Development program (LDRD) grant to J.P.R., and the Lawrence Scholar Program (M.K.) at LLNL. We would like to acknowledge the helpful support and Dr. David Kilcoyne and that access to ALS beamline 5.3.2.2 was provided by the Office of Science, Office of Basic Energy Science. We thank Larry Nittler for software development, Christina Ramon for sample preparation and Kevin Carpenter for assistance with SEM imaging. This work was performed under the auspices of the U.S. Department of Energy by Lawrence Livermore National Laboratory under Contract DE-AC52-07NA27344, and OBER-SBR Sustainable Systems SFA at Lawrence Berkeley National Laboratory under Contract DE-AC02-05CH11231. Additional support was provided by the US DOE Office of Science, Climate and Environmental Science Division

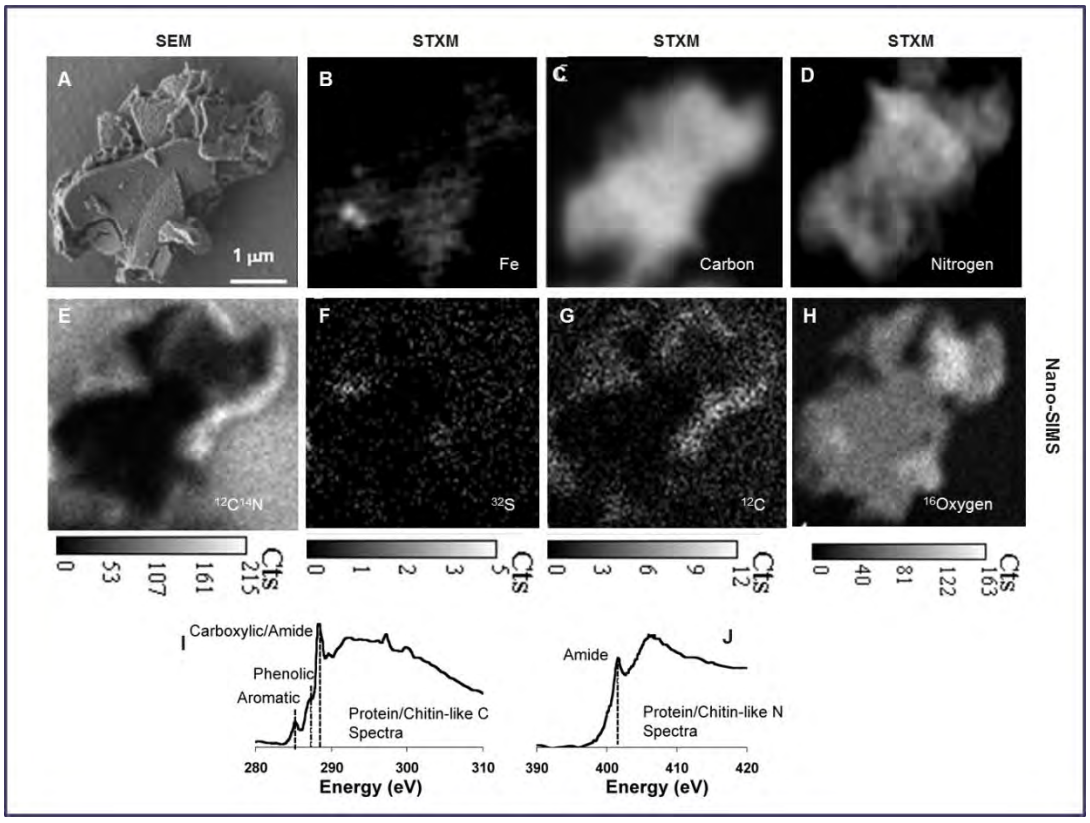

Fig. 1. Example of multimodal imaging of a single soil micro-aggregate using SEM, STXM, and NanoSIMS. TOP: Shown from left to right are: (a) the whole aggregate by SEM, (b) iron distribution as imaged by STXM, (c) STXM carbon distribution and (d) STXM nitrogen image. MIDDLE: NanoSIMS ion images of the same soil particle previously imaged by SEM and STXM (e) $^{12}C^{14}N$ (nitrogen) image; (f) ^{32}S (sulfur) image; (g) ^{12}C (carbon) image; (h) ^{16}O distribution.

BOTTOM: corresponding (i) carbon and (j) nitrogen NEXAFS spectra indicating the protein/amino-sugar (e.g. chitin)-like nature of the SOM within the aggregate.

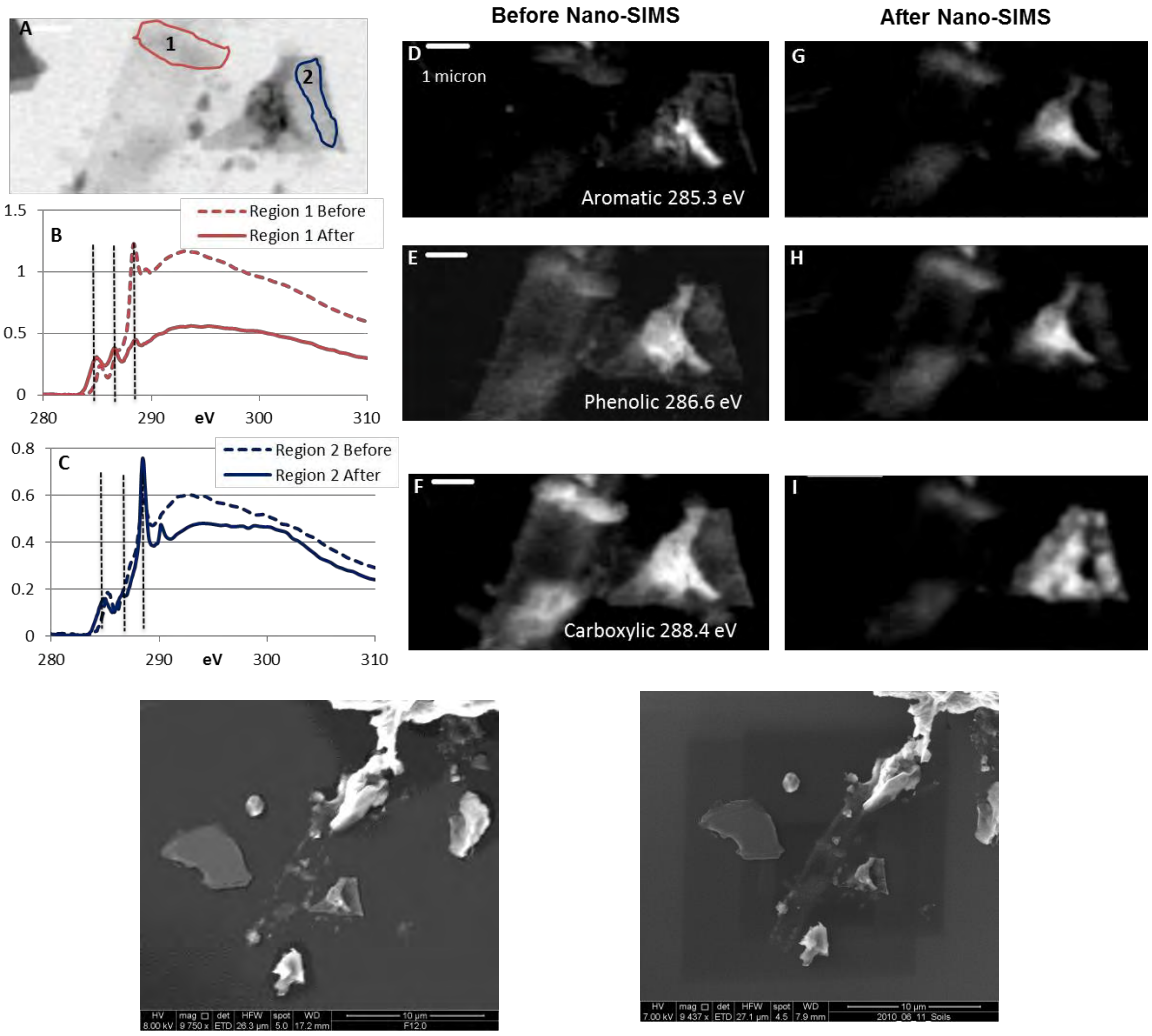

Fig. 2. Effects of NanoSIMS analysis on STXM/NEXAFS spectra. (a) Transmission image showing two regions from which spectra were extracted before and after NanoSIMS analysis, (b) region 1 spectra before and after NanoSIMS analysis showing relative increases in 284.6 eV (aromatic) and 286.4 eV (phenolic) and corresponding decrease in 288.3 eV (carboxylic) resonances, (c) region 2 spectra before and after NanoSIMS analysis showing increase in 288.5 eV (carboxylic) resonance, (d-e), and (h-i) Paired images showing relative redistribution of 285.3 (aromatic), 286.6 eV (phenolic), and 288.4 (carboxylic) resonances, respectively, (j,k) pre and post-NanoSIMS SEM micrographs, respectively.

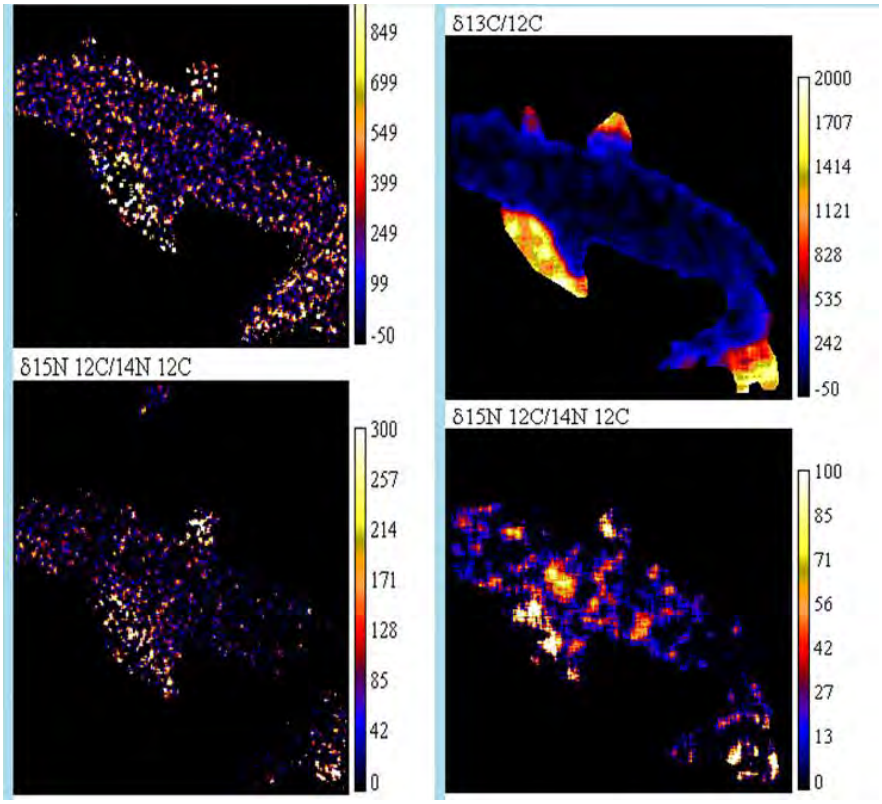

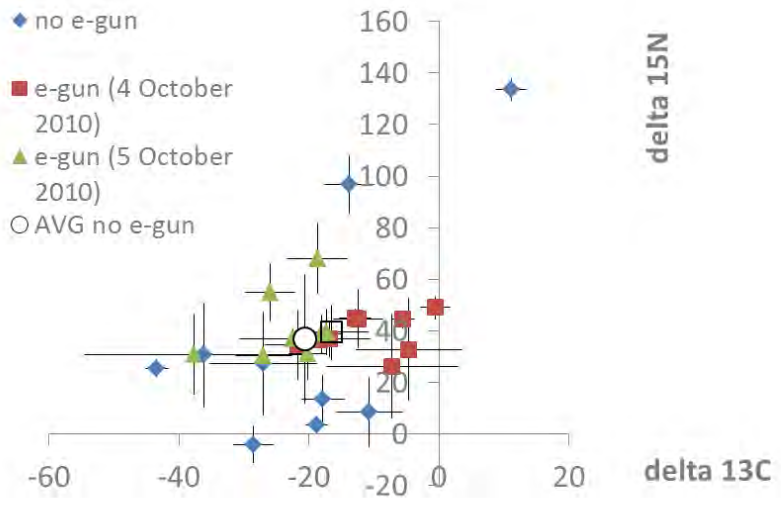

Fig. 3. (A). Comparison of NanoSIMS 13C and 15N ratio images (per mil units) of the same soil particles, with the use of the electron flood gun "e-gun" versus no e-gun use (B) NanoSIMS data from an analysis of a standard Bacillus subtilis spore preparation run with (two dates) and without the e-gun. Each point represents a single spore.

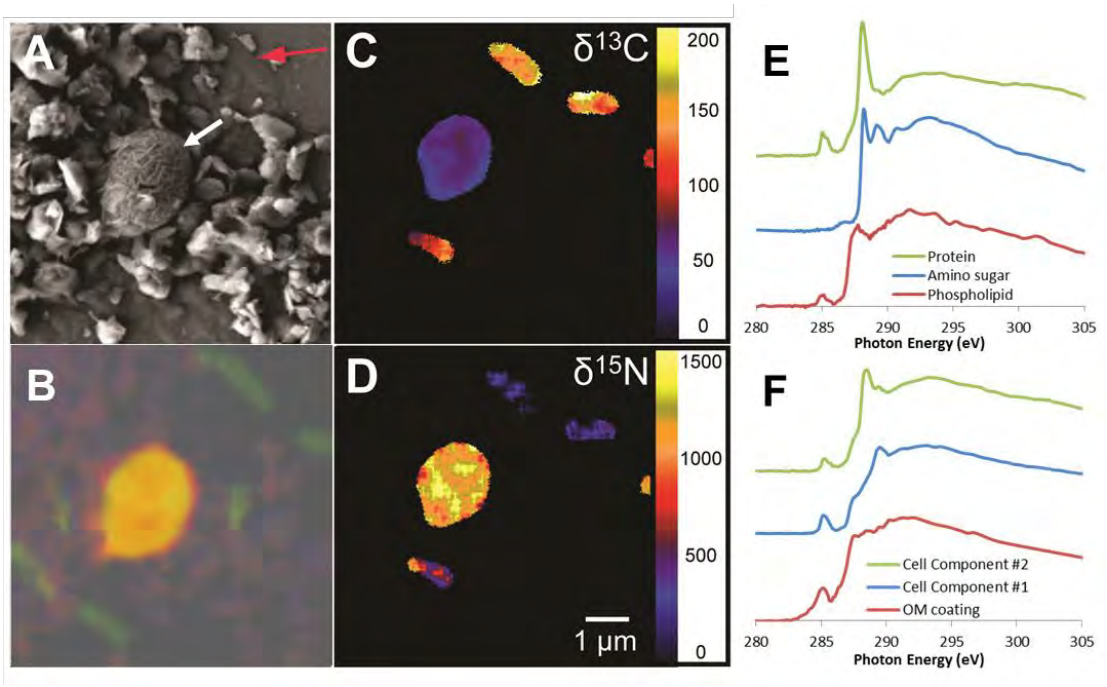

Fig. 4. Distribution of isotopically labeled microbial cell components after incubation with a common soil mineral (montmorillonite), imaged by a combination of SEM, STXM and NanoSIMS. (A) SEM of a region containing mineral particles along with detrital material from the added yeast culture (white arrow = cell component #1, red arrow = #2). (B) distribution of carbon chemical form as determined by STXM. The carbon was grouped into three broad chemical types: protein (red), amino-sugar (blue), and phospholipids (green), which are characterized by the standard carbon spectra shown in (E). In this image, lipids are associated with mineral particles, cell component #2 is dominated by a proteinaceous signature and cell component #1 is comprised of a mixture of phospholipids and amino-sugars. (C) and (D) NanoSIMS $\delta^{13}C$ and $\delta^{15}N$ isotope ratio images respectively, the scale bars for enrichment are in per mil (‰). (F) Spectra extracted from visually determined regions in image B.

Refernces

Baldock, J.A., Skjemstad, J.O., 2000. Role of the soil matrix and minerals in protecting natural organic materials against biological attack. Organic Geochemistry 31, 697-710.

Behrens, S., Kappler, A., Obst, M., 2012. Linking environmental processes to the in situ functioning of microorganisms by high-resolution secondary ion mass spectrometry (NanoSIMS) and scanning transmission X-ray microscopy (STXM). Environmental Microbiology, no-no.

Brandes, J.A., Lee, C., Wakeham, S., Peterson, M., Jacobson, C., Wirick, S., Cody, G., 2004. Examining marine particulate organic matter at sub-micron scales using scanning transmission X-ray microscopy and carbon X-ray absorption near edge structure spectroscopy. Marine Chemistry 92, 107-121.

Braun, A., Huggins, F., Shah, N., Chen, Y., Wirick, S., Mun, S., Jacobsen, C., Huffman, G., 2003. Advantages of soft X-ray absorption over TEM-EELS for solid carbon studies - a comparative study on diesel soot with EELS and NEXAFS. Carbon 43, 117-124.

Cliff, J.B., Bottomley, P.J., Haggerty, R., Myrold, D.D., 2002. Modeling the effects of diffusion limitations on nitrogen-15 isotope dilution experiments with soil aggregates. Soil Science Society of America Journal 66, 1868-1877.

Clode, P.L., Kilburn, M.R., Jones, D.L., Stockdale, E.A., Cliff, J.B., 3rd, Herrmann, A.M., Murphy, D.V., 2009. In situ mapping of nutrient uptake in the rhizosphere using nanoscale secondary ion mass spectrometry. Plant Physiol 151, 1751-1757.

De Gregorio, B.T., Stroud, R.M., Nittler, L.R., Alexander, C.M.O.D., Kilcoyne, A.L.D., Zega, T.J., 2010. Isotopic anomalies in organic nanoglobules from Comet 81P/Wild 2: Comparison to Murchison nanoglobules and isotopic anomalies induced in terrestrial organics by electron irradiation. Geochimica et Cosmochimica Acta 74, 4454-4470.

Dekas, A.E., Poretsky, R.S., Orphan, V.J., 2009. Deep-Sea Archaea Fix and Share Nitrogen in Methane-Consuming Microbial Consortia. Science 326, 422-426.

Duiker, S.W., Rhoton, F.E., Torrent, J., Smeck, N.E., Lal, R., 2003. Iron (Hydr)Oxide Crystallinity Effects on Soil Aggregation. Soil Sci Soc Am J 67, 606-611.

Finzi-Hart J. & Pett-Ridge, J., Weber, P., Popa, R., Fallon, S.J., Gunderson, T., Hutcheon, I., Nealson, K., Capone, D.G., 2009. Fixation and fate of carbon and nitrogen in Trichodesmium IMS101 using nanometer resolution secondary ion mass spectrometry (NanoSIMS). Proceedings of the National Academy of Sciences, USA 106, 6345-6350.

Ghosal, S., Fallon, S.J., Leighton, T., Wheeler, K.E., Hutcheon, I.D., Weber, P.K., 2008. Imaging and 3D elemental characterization of intact bacterial spores with high-resolution secondary ion mass spectrometry (NanoSIMS) depth profile analysis. Analytical Chemistry 80, 5986–5992.

Gillespie, A.W., Walley, F.L., Farrell, R.E., Leinweber, P., Schlichting, A., Eckhardt, K.U., Regier, T.Z., Blyth, R.I.R., 2009. Profiling Rhizosphere Chemistry: Evidence from Carbon and Nitrogen K-Edge XANES and Pyrolysis-FIMS. Soil Science Society of America Journal 73, 2002-2012.

Gullikson, E., 2012. X-ray Interactions with Matter, LBNL.

Hatton, P.-J., Kleber, M., Zeller, B., Moni, C., Plante, A., Townsend, K., Lajtha, K., Derrien, D., 2012. Transfer of a 15N litter label from the organic surface layer (O) to mineral-organic associations in the A-horizon: a decadal perspective. Organic Geochemistry 42, 1489-1501.

Henke, B.L., Gullikson, E.M., Davis, J.C., 1993. X-ray interactions: photoabsorption, scattering, transmission, and reflection at E=50-30000 eV, Z=1-92. Atomic Data and Nuclear Data Tables 54, 181-342.

Herrmann, A., Ritz, K., Nunan, N., Clode, P., Pett-Ridge, J., Kilburn, M., Murphy, D., O'Donnell, A., Stockdale, E., 2007. Nano-scale secondary ion mass spectrometry—A new analytical tool in biogeochemistry and soil ecology: A review article. Soil Biology and Biochemistry 39, 1835-1850.

Hitchcock, A.P., Morin, C., Zhang, X., Araki, T., Dynes, J.J., Stöver, H., Brash, J.L., Lawrence, J.R., Leppard, G.G., 2006. Soft X-ray spectromicroscopy of biological and synthetic polymer systems. Journal of Electron Spectroscopy 144-147, 259-269.

Keiluweit, M., Bougoure, J.J., Zeglin, L., Myrold, D., Kleber, M., Nico, P., Pett-Ridge, J., 2012. Rapid association of microbial amide N with iron (hydr)oxides in a forest soil O-horizon. Geochim. et Cosmochim. Acta. in press.

Kilcoyne, A.L.D., T. Tyliszczak, W. Steele, S. Fakra, P. Hitchcock, K. Franck, E.H. Anderson, B. Harteneck, E.G. Rightor, G.E. Mitchell, A.P. Hitchcock, L. Yang, T. Warwick and H. Ade, , 2003. Interferometer controlled scanning transmission x-ray microscopes at the Advanced Light Source. Journal of Synchrotron Radiation 10, 125-136.

Kilcoyne, A.L.D., Tyliszczak, T., Steele, W.F., Fakra, S., Hitchcock, P., Franck, K., Anderson, E., Harteneck, B., Rightor, E.G., Mitchell, G.E., Hitchcock, A.P., Yang, L., Warwick, T., Ade, H., 2003. Interferometer controlled scanning transmission X-ray microscopes at the Advanced Light Source. J. Synchrotron Rad. 10, LBNL-53202.

Kirchman, D., Clarke, A., 1999. Hydrolysis and mineralization of chitin in the Delaware Estuary. Aquatic Microbial Ecology 18, 187-196.

Kögel-Knabner, I., 2000. Analytical approaches for characterizing soil organic matter. Organic Geochemistry 31, 609-625.

Koprinarov, I.N., Hitchcock, A.P., McCrory, C.T., Childs, R.F., 2002. Quantitative Mapping of Structured Polymeric Systems Using Singular Value Decomposition Analysis of Soft X-ray Images. The Journal of Physical Chemistry B 106, 5358-5364.

Kuzyakov, Y., 2002. Review: Factors affecting rhizosphere priming effects. Journal of Plant Nutrition and Soil Science 165, 382-396.

Laird, D.A., Thompson, M., 2009. The Ultrastructure of Clay-Humic Complexes in an Iowa Mollisol, In: Laird, D.A., Cervini-Silva, J. (Ed.), Carbon Stabilization by Clays in the Environment: Process and Characterization Methods, CMS Workshop Lectures. Clay Minerals Society, Chantilly, VA, pp. 95-118.

Lehmann, J., Kinyangi, J., Solomon, D., 2007. Organic matter stabilization in soil microaggregates: implications from spatial heterogeneity of organic carbon contents and carbon forms. Biogeochemistry 85, 45-57.

Lehmann, J., Liang, B.Q., Solomon, D., Lerotic, M., Luiza˜ o, F., Kinyangi, J., Scha¨ fer, T., Wirick, S., Jacobsen, C., 2005. Near-edge X-ray absorption fine structure (NEXAFS) spectroscopy for mapping nano-scale distribution of organic carbon forms in soil: application to black carbon particles. Global Biogeochemical Cycles 29, Art. No. GB1013.

Lehmann, J., Solomon, D., Brandes, J., Fleckenstein, H., Jacobson, C., Thieme, J., 2009. Synchrotron-Based Near-Edge X-Ray Spectroscopy of Natural Organic Matter in Soils and Sediments, Biophysico-Chemical Processes Involving Natural Nonliving Organic Matter in Environmental Systems. John Wiley & Sons, Inc., pp. 729-781.

Lehmann, J., Solomon, D., Kinyangi, J., Dathe, L., Wirick, S., Jacobsen, C., 2008. Spatial complexity of soil organic matter forms at nanometre scales. Nature Geoscience 1, 238-242.

Leinweber, P., Jandl, G., Eckhardt, K.U., Kruse, J., Walley, F.L., Khan, M.J., Blyth, R.I.R., Regier, T., 2010. Nitrogen speciation in fine and coarse clay fractions of a Cryoboroll - new evidence from pyrolysis-mass spectrometry and nitrogen K-edge XANES. Canadian Journal of Soil Science 90, 309-318.

Leinweber, P., Kruse, J., Walley, F.L., Gillespie, A., Eckhardt, K.U., Blyth, R.I.R., Regier, T., 2007. Nitrogen K-edge XANES - An overview of reference compounds used to identify 'unknown' organic nitrogen in environmental samples. Journal of Synchrotron Radiation 14, 500-511.

Lützow, M.v., Kögel-Knabner, I., Ekschmitt, K., Matzner, E., Guggenberger, G., Marschner, B., Flessa, H., 2006. Stabilization of organic matter in temperate soils: mechanisms and their relevance under different soil conditions – a review. European Journal of Soil Science 57, 426-445.

Mahieu, N., Powlson, D.S., Randall, E.W., 1999. Statistical analysis of published carbon-13 CPMAS NMR spectra of soil organic matter. Soil Science Society of America Journal 63, 307-319.

Matrajt, G., Ito, M., Wirick, S., Messenger, S., Brownlee, D.E., Joswiak, D., Flynn, G., Sandford, S., Snead, C., Westphal, A., 2008. Carbon investigation of two Stardust particles: A TEM, NanoSIMS, and XANES study. Meteoritics & Planetary Science 43, 315-334.

Moreau, J.W., Weber, P.K., Martin, M.C., Gilbert, B., Hutcheon, I.D., Banfield, J.F., 2007. Extracellular proteins limit the dispersal of biogenic nanoparticles. Science 316, 1600-1603.

Mueller, C.W., Kölbl, A., Hoeschen, C., Hillion, F., Heister, K., Herrmann, A.M., Kögel-Knabner, I., 2012. Submicron scale imaging of soil organic matter dynamics using NanoSIMS – From single particles to intact aggregates. Organic Geochemistry 42, 1476-1488.

Musat, N., Halm, H., Winterholler, B., Hoppe, P., Peduzzi, S., Hillion, F., Horreard, F., Amann, R., Jørgensen, B.B., Kuypers, M.M.M., 2008. A single-cell view on the ecophysiology of anaerobic phototrophic bacteria. Proceedings of the National Academy of Sciences 105, 17861-17866.

Pett-Ridge, J., Weber, P.K., 2012. NanoSIP: NanoSIMS applications for microbial biology, In: Navid, A. (Ed.), Microbial Systems Biology: Methods and Protocols. Humana Press.

Pierzynski, G.M., Sims, J.T., Vance, G.F., 1994. Soil and Environmental Quality. Lewis Publishers, Ann Arbor, 313 pp.

Ploug, H., Adam, B., Musat, N., Kalvelage, T., Lavik, G., Wolf-Gladrow, D., Kuypers, M.M., 2011. Carbon, nitrogen and O(2) fluxes associated with the cyanobacterium Nodularia spumigena in the Baltic Sea. ISME J 5, 1549-1558.

Pumphrey, G.M., Hanson, B.T., Chandra, S., Madsen, E.L., 2009. Dynamic secondary ion mass spectrometry imaging of microbial populations utilizing 13C-labelled substrates in pure culture and in soil. Environmental Microbiology 11, 220-229.

Remusat, L., Hatton, P.-J., Nico, P.S., Zeller, B., Kleber, M., Derrien, D., 2012a. NanoSIMS Study of Organic Matter Associated with Soil Aggregates: Advantages, Limitations, and Combination with STXM. Environmental Science & Technology 46, 3943-3949.

Remusat, L., Hatton, P.J., Nico, P.S., Zeller, B., Kleber, M., Derrien, D., 2012b. NanoSIMS Study of Organic Matter Associated with Soil Aggregates: Advantages, Limitations, and Combination with STXM. Environmental Science & Technology 46, 3943-3949.

Roff, J., Kroetsch, J., Clarke, A., 1994. A radiochemical method for secondary production in planktonic custacea based on rate of chitin synthesis. Journal of Plankton Research 16, 961-976.

Schmidt, M.W.I., Torn, M.S., Abiven, S., Dittmar, T., Guggenberger, G., Janssens, I.A., Kleber, M., Kogel-Knabner, I., Lehmann, J., Manning, D.A.C., Nannipieri, P., Rasse, D.P., Weiner, S., Trumbore, S.E., 2011. Persistence of soil organic matter as an ecosystem property. Nature 478, 49-56.

Six, J., Frey, S.D., Thiet, R.K., Batten, K.M., 2006. Bacterial and Fungal Contributions to Carbon Sequestration in Agroecosystems. Soil Sci. Soc. Am. J. 70, 555-569.

Solomon, D., Lehmann, J., Kinyangi, J., Liang, B.Q., Schafer, T., 2005. Carbon K-edge NEXAFS and FTIR-ATR spectroscopic investigation of organic carbon speciation in soils. Soil Science Society of America Journal 69, 107-119.

Song, G., Novotny, E.H., Simpson, A.J., Clapp, C.E., Hayes, M.H.B., 2008. Sequential exhaustive extraction of a Mollisol soil, and characterizations of humic components, including humin, by solid and solution state NMR. European Journal of Soil Science 59, 505-516.

Song, G.X., Hayes, M.H.B., Novotny, E.H., Simpson, A.J., 2011. Isolation and fractionation of soil humin using alkaline urea and dimethylsulphoxide plus sulphuric acid. Naturwissenschaften 98, 7-13.

Wan, J., Tyliszczak, T., Tokunaga, T.K., 2007a. Organic carbon distribution, speciation, and elemental correlations within soil microaggregates: Applications of STXM and NEXAFS spectroscopy. Geochimica et Cosmochimica Acta 71, 5439-5449.

Wan, J., Tyliszczak, T., Tokunaga, T.K., 2007b. Organic carbon distribution, speciation, and elemental correlations within soil microaggregates: applications of STXM and NEXAFS spectroscopy.

Welden, C.W., Hewett, S.W., Hubbell, S.P., Foster, R.B., 1991. Sapling Survival, Growth, and Recruitment - Relationship to Canopy Height in a Neotropical Forest. Ecology 72, 35-50.

Woebken, D., Burow, L.C., Prufert-Bebout, L., Bebout, B.M., Hoehler, T.M., Pett-Ridge, J., Spormann, A.M., Weber, P.K., Singer, S.W., 2012. Identification of a novel cyanobacterial group as active diazotrophs in a coastal microbial mat using NanoSIMS analysis. The ISME Journal 6, 1427-1439.

Zeglin, L.H., Myrold, D.D., Kluber, L., 2011a. The importance of amino sugar turnover to C and N cycling in mycorrhizal and non-mycorrhizal old-growth Douglas-fir forest organic layer soils. In review.

ACCELERATED HYBRIDIZATION OF DNA USING ISOTACHOPHORESIS AND APPLICATION TO RAPID DETECTION OF BACTERIA

M. Bercovici[1,2*], C.M. Han[1], J.C. Liao[2], J.G. Santiago[1]

[1]Department of Mechanical Engineering, Stanford University, Stanford, CA 94305, USA

[2]Department of Urology, Stanford University, Stanford, CA 94305, USA

*Current Affiliation: Faculty of Mechanical Engineering, Technion, Haifa Israel 32000

Abstract

We use ITP to control and increase the rate of homogenous DNA hybridization reactions. We present a physical model, validation experiments, and demonstrations of this assay. We studied the coupled physics and chemistry of the dynamics of preconcentration, mixing, and chemical reaction kinetics under ITP. Our experimentally-validated model enables closed form solution for two-species hybridization reaction under ITP, and predicts 10,000 fold speed-up of chemical reaction rate at concentrations of order 10 pM, with greater enhancement of reaction rate at lower concentrations. We experimentally demonstrate 1000 fold speed-up using ITP compared to the standard case of reaction in a simple, well mixed reaction chamber. Finally, we demonstrate the applicability of the assay for amplification-free detection of bacteria. We use ITP to extract, focus, and detect 16S rRNA, a well-characterized bacterial-specific bio-signature, directly from bacterial lysate. Rapid hybridization enables the entire assay to be completed in under 15 min.

Introduction

Isotachophoresis (ITP) is an electrophoresis technique which uses two buffers consisting of a high mobility leading electrolyte (LE) and a low mobility trailing electrolyte (TE). [1] It focuses sample species whose mobility is bracketed by those of the LE and TE. We use so-called peak mode ITP to simultaneously preconcentrate, rapidly mix, and expedite reactions between target RNA or DNA species extracted from biological samples and molecular beacon probes.

Molecular beacons are partially self-hybridizing synthetic oligonucleiotides which use a fluorophore and a quencher to produce a sequence specific fluorescence signal. [2] We use ITP to focus target and molecular beacons into a sharp, order 10 micron, ITP interface which we use as a customizable, 10 pL reaction volume to achieve unprecedented speed up of reaction and sensitivity .

Theory

We denote the concentrations of free molecular beacons, free targets, and hybridized beacons-target complexes as B, T, and BT respectively. Following Tsourkas *et al.,* the hybridization of DNA and molecular beacons can be expressed as

$$B + T \underset{k_{off}}{\overset{k_{on}}{\rightleftharpoons}} BT \quad ,$$

where k_{on} and k_{off} are the on- and off-rate of the reaction, respectively. [3]

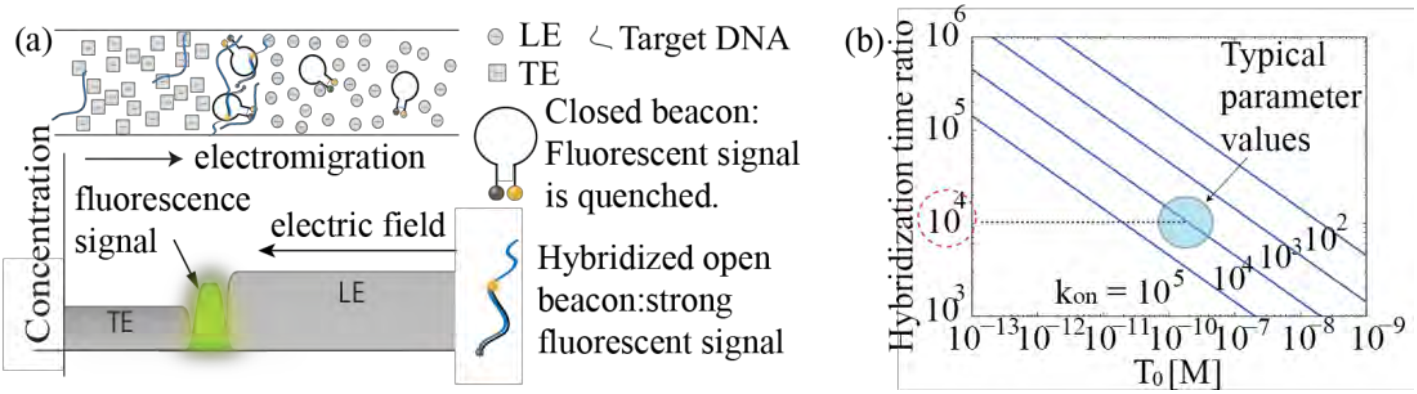

Fig. 1. (a) Schematic showing DNA hybridization at an 10 micron (10 picoliter) ITP interface, speeding up hybrid product rate by over 10,000 fold and increasing the absolute fluorescence signal intensity by 10^6 times at O(10 pM). **(b)** Ratio of characteristic hybridization time predicted by our model for various initial target concentration and on-rate constant values.

By considering the fluxes into the control volume surrounding the ITP interface, as well the reaction kinetics within the control volume, we derived a set of non-linear ODEs describing the average concentration of species at the interface over time. These

governing equations assume a constant interface width, δ, in which all species have an overlapping Gaussian distributions in space.

$$\begin{cases} \dfrac{d\overline{c_B}}{dt} = \dfrac{\eta_{LE} V_{ITP}}{\delta} B_0 - k_{on} \dfrac{3}{\sqrt{\pi}} \overline{c_B c_T} + k_{off} \overline{c_{BT}} \\ \dfrac{d\overline{c_T}}{dt} = \dfrac{\eta_{TE} V_{ITP}}{\delta} T_0 - k_{on} \dfrac{3}{\sqrt{\pi}} \overline{c_B c_T} + k_{off} \overline{c_{BT}} \\ \dfrac{d\overline{c_{BT}}}{dt} = k_{on} \dfrac{3}{\sqrt{\pi}} \overline{c_B c_T} - k_{off} \overline{c_{BT}} \end{cases} \quad (1)$$

where $\overline{c_i}$ with $i = B,\ T,$ and BT are defined as average concentration over the control volume, η_{LE} and η_{TE} denote ITP focusing rate coefficients in LE and TE zones respectively, B_0 and T_0 are initial beacons and target concentrations.

A closed form analytical model can be obtained by further assuming slow off-rate ($k_{off} \ll k_{on} T_0$) and one dominant reactant concentration at the ITP interface ($T_0 \ll B_0$). The solution of our analytical model is presented in Table 1, and is compared with the standard hybridization case of a simple reaction (*sans* ITP) in a well mixed reaction chamber.

Importantly, we find that the speed-up in reaction time is inversely proportional to the square root of the initial concentration of the abundant reactant. **This leads, for example, to 10,000 fold speed-up of chemical reaction rate at order 10 pM concentrations**. In Figure 1b, speed-up in rate of reaction via ITP is predicted from the model for various initial target concentrations and relevant kinetic rate constants of molecular beacons. Furthermore, while the maximum concentration of the hybrid in the standard case is limited by the initial concentration of molecular beacons, ITP focusing results in a continuosly increasing hybridization product concentration. This results in a 1,000,000-fold increase in the absolute concentration of the hybridized product. The assay yields a 1000-fold increase in signal enhancement over the control case (ITP of beacons without target).

Table 1. Analytical solution comparison of ITP hybridization and standard (reaction chamber) hybridization

	ITP-enhanced hybridization	Standard hybridization
Hybridization product concentration	$c_{BT} = \frac{\eta V_{ITP}}{\delta} B_0 t \left(1 - e^{-\frac{1}{2}\frac{3}{\sqrt{\pi}}\frac{\eta V_{ITP}}{\delta} k_{on} T_0 t^2}\right)$	$c_{BT} = B_0 \left(1 - e^{-k_{on} T_0 t}\right)$
Characteristic time scale	$t_{ITP} \sim \sqrt{\frac{1}{\frac{\eta_{TE} V_{ITP}}{\delta} k_{on} T_0}}$	$t_{st} \sim \frac{1}{k_{on} T_0}$

Experimental

We validated the model using a set of controlled experiments in which we hybridize DNA-based molecular beacons with synthetic complementary oligonucleotides. We mix target DNA with TE, and mix molecular beacons with LE. This ensures that the reactants remain separated until they simultaneously and progressively focus into the same 10 pL ITP reaction volume, at which point they begin to react and hybridize (c.f. Figure 1a). In order to monitor reaction rate, we recorded the fluorescence signal at seven locations along the length of the channel. We normalize the signal by the signal of beacons alone, to obtain the fraction of hybridized beacons.

For bacteria detection, we prepared pellets from *E. coli* by centrifuging 1 ml of sample at 10,000 rpm for 2 min, and then discarding the supernatant. The pellets were kept frozen at -80ºC. For each experiment, we resuspended the pellet in 100 μL of deionized (DI) water (UltraPure DNase/RNase free distilled water, GIBCO Invitrogen, Carlsbad, CA). Bacterial lysis was done with a buffer consisted of 10 μL 2 mM EDTA, 20 mM tris, 0.5% PVP and 5 mg/ml lysozyme for 5 minutes, followed by additional 5 minutes with 10 μL 400 mM NaOH. In the case of bacterial cultures, we used an initial concentration of 5E8 cfu/mL, and diluted it to the different concentrations tested. We then took 10 μL of the lysate and mixed it with 90 μL of 50 mM tricine, 100 mM bistris, 4 mM $MgCl_2$, and 5 nM of molecular beacons (Cy5-GCG AGC CAT CGT TTA CGG CGT GGA CTA CCA GGG GCT CGC-BHQ3, IDT, Coralville, Iowa).

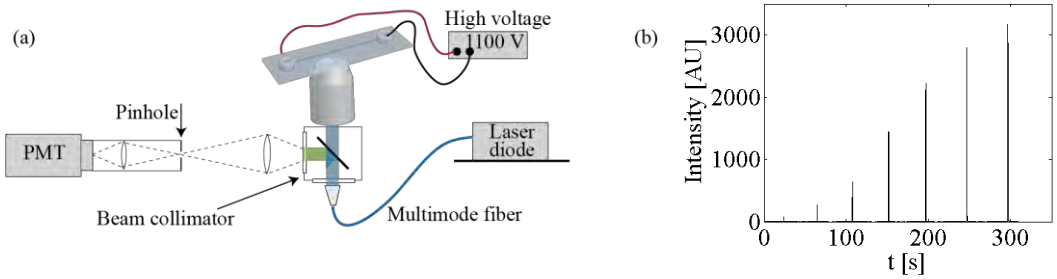

Fig. 2. (a) Schematic of the experimental setup used to study DNA hybridization under ITP. Our set-up consists of a straight 4 cm long microfluidic channel, laser excitation, high-voltage supply, and a custom point confocal fluorescence system. We use laser diode illumination and photomultiplier tube detection for rapid, sensitive detection of reactions. **(b)** An example raw data from the setup. These temporal fluorescence signals (isotachopherograms) are collected from our custom point detector and integrated in time. We use these signal integrals to quantify concentration of hybridization product.

Results and Discussion

In Figure 3a we summarize our model validation study by comparing between a direct numerical solution of the governing equations, our analytical model, and experimental results at various target concentrations. We see good agreement between the model and experimental data (inset of Figure 3a). We use our analytical model to propose a new time-scale normalization which completely collapses data across beacon concentrations, target concentrations, and ITP conditions. This collapse of data is shown in the main plot of Figure 3a.

Figure 3b presents an experimental comparison of ITP based DNA hybridization and standard hybridization using 10 nM of molecular beacons and 50 nM of complementary oligonucleotides. Standard (simple mixing-based reaction without ITP) hybridization required 50 min to complete 50 % of the reaction, while ITP-based hybridization required only 3.5 s. This experimental demonstration of 800 fold speed-up is in good agreement with the model prediction.

Fig. 3. (a) Analytical and numerical predictions vs. ITP-aided DNA hybridization data with no fitting parameters. (We quantify forward kinetic reaction rate in independent experiments.) Shown are normalized fluorescence signal over time. In the inset we show raw example experimental data at target concentrations of 1, 10, and 100 nM

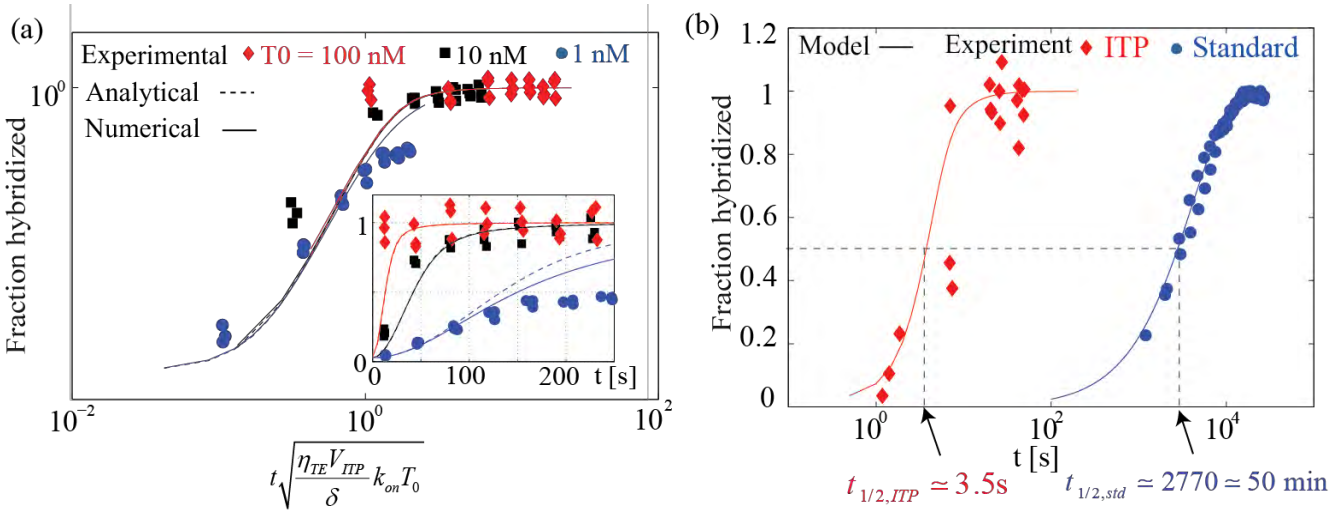

versus 10 nM concentration of molecular beacons (probe length 28-mer; stem length 7-mer). TE was 50 mM Tricine and 100 mM Bistris, and LE was 250 mM HCl, 500 mM Bistris, 2 mM $MgCl_2$, 0.1 % PVP. In the main plot, we show the same data plotted in log-log scale with the time axis normalized by the characteristic time scale predicted by the model. **(b)** Experimental demonstration of the predicted 800 fold hybridization speed-up for O(10 nM) DNA oligonucleotides. Fraction hybridized plotted in log-log scale for ITP and standard hybridization (without ITP preconcentration) cases as a direct demonstration of rapid hybridization by the assay. The experiment was conducted using 10 nM concentration of molecular beacons and 50 nM target concentration. For ITP, we used TE of 30 mM Tricine and 60 mM Bistris, and the same LE used for Figure 3a. The standard hybridization data were obtained from pressure-driven flow system where reactants were premixed in the LE buffer used in the ITP experiments. The model prediction solid lines are plotted based on independent kinetic rate measurement, interface width, and ITP speed values extracted from the experiment.

We have validated our bacterial detection assay by performing ITP on bacterial isolates grown in culture media. When no target is present (control case) the molecular beacons are closed, resulting in a relatively low fluorescent signal. When lysed sample is present, the beacons bind to their target resulting in an increased fluorescent signal. Since peak intensities are very sensitive to sampling rate and dispersion, we define

'total fluorescence' as the integral of the signal (or area under the curve). We then define the assay SNR as the ratio between the total fluorescence of the signal and that of the negative control. This normalized quantity allows to reduce the sensitivity of results to possible photobleaching of the molecular beacons. Fig. 4 presents the assay SNR versus bacteria concentration for a range of bacteria culture samples. As the bacteria concentration increases, a larger fraction of the molecular beacons is hybridized and the fluorescent signal (and assay SNR) increases. We chose a molecular beacons concentration which would enable quantitative detection across the range 1E6-1E8 cfu/ml. Lower molecular beacons concentrations would result in better SNR at low bacteria concentrations, but loss of quantitation at higher concentrations (since above a certain threshold, all beacons would essentially be hybridized). Similarly, higher molecular beacons concentrations would yield higher SNR at higher bacteria concentration, but would reduce the SNR at lower bacteria concentrations (since only a small fraction of the beacons would be hybridized).

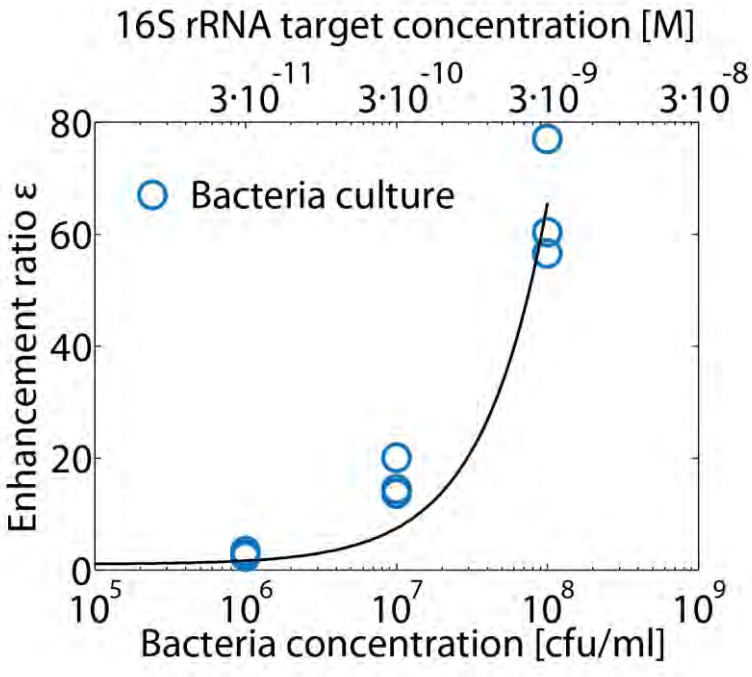

Fig. 4. Quantitative detection of E. coli 16S rRNA from bacterial culturs. 16S rRNA was extracted and focused with ITP, and detected using molecular beacons. We define total fluorescence as the as the integral of the detection signal (i.e. area under the curve). The enhancement ratio is then defined as the ratio between the total fluorescence of the signal and that of the negative control.

Conclusion

Our work confirms that on-chip ITP can be used to speed up chemical reactions by 10,000 fold by strongly preconcentrating reactant species in simple, straight microchannels. We use peak mode ITP to focus species by up to 50,000 fold into order 10 micron zone lengths; yielding order 10 picoliter volumes which incubate reactions. We have developed and experimentally validated the detailed reaction kinetics model coupled with ITP which can be used to design and optimize a wide range of reaction systems. Our method therefore provides a dramatic increase in sensitivity without sacrificing molecular beacons' specificity. The assay is a unique and highly precise method of studying a wide range of chemical reactions across broad ranges of timescales and reactant concentrations. Leveraging ITP-based rapid hybridization, we have demonstrated PCR-free quantitative detection of bacterial rRNA.

References

[1] F.M. Everaerts *et al*., Isotachophoresis: theory, instrumentation, and applications, Elsevier Scientific Publishing Company, 1976.

[2] S. Tyagi and F. Kramer, Nature Biotechnology, Vol. 14, 1996, pp. 303-308.

[3] A. Tsourkas *et al*., Nucleic Acids Research, Vol. 31, No. 4, 2003, pp. 1319-1330

[4] M. Bercovici *et.al.*, *Anal. Chem.* Vol. 83, 2011, 4110–4117.

[5] M. Bercovici *et.al.*, *PNAS* Vol. 109, 2012, 11127–11132.

EVALUATING NUTRIENT DYNAMICS IN STREAMS USING A COMBINATION OF MICROELECTRODES AND AN ONLINE UV-VIS SPECTROPHOTOMETER

Shai Arnon[1*], Arie Fox[1], Natalie de Falco[1], and Fulvio Boano[2]

[1]Zuckerberg Institute for Water Research, J. Blaustein Institutes for Desert Research, Ben-Gurion University of the Negev, Israel

[2]Department of Environment, Land and Infrastructure Engineering, Politecnico di Torino, Italy

[*]Corresponding author: sarnon@bgu.ac.il

Abstract

The exchange of water between the surface and subsurface environments plays a crucial role in hydrological and biogeochemical. The exchange of water is driven by the local morphology of the streambed (hyporheic exchange) and the regional forcing of a large-scale hydraulic gradient, which results in losing or gaining flow conditions. We measured the effects of flow conditions on dissolved organic carbon (DOC) uptake in a recirculating flume using an online UV-Vis spectrophotometer and microelectrodes. DOC uptake was increased as overlying velocity increases due to enhanced solute exchange between the bulk water and the streambed. DOC exchange and uptake was further enhanced under losing conditions, but was sustained under gaining conditions, as observed by the oxygen profiles in the streambed. This type of interaction between overlying velocities and subsurface flow pattern is expected to regulate nutrient transformation by microbial activity in streambeds and should be incorporated into modeling frameworks that describe solute transport in streams.

Introduction

Interactions between streams and groundwater systems play a fundamental role in contaminant transport and remediation, in the functioning of aquatic ecosystems, and in water resources management (Findlay, 1995; Krause et al., 2009a; Hester and Gooseff, 2010). Further, the interactions between the stream and the streambed induce a water flux into and out of the channel bed and banks, i.e., the hyporheic zone; these interactions are commonly termed hyporheic exchange processes (Bencala and Walters, 1983; Thibodeaux and Boyle, 1987). The intensity and the direction of the exchange

between streams and subsurface water may follow complex patterns that depend on the hydrologic conditions in both the stream and the groundwater (e.g., water levels) and the composition and morphology of the sediment surrounding the stream channel (Dent et al., 2007; Ruehl et al., 2007; Cardenas and Wilson, 2007). These water fluxes allow the nutrients carried by the stream to reach the subsurface environment; they thus control the growth of microorganisms and the biotic processes in the subsurface (Boulton et al., 1998; Hester and Gooseff, 2010). The location of the hyporheic zone at the interface between the groundwater and the stream confers on the zone unique hydrodynamic, physiochemical, and biotic characteristics that are different from those of both the stream and the subsurface environments (Brunke and Gonser, 1997).

A prominent feature of hyporheic zones is the presence of steep chemical gradients, which are often associated with microbial activity; for example, elevated oxygen concentrations delivered from stream water to the hyporheic zone support extensive microbial activity close to the water-sediment interface, with oxygen becoming depleted as the water moves into the sediment (Boulton, 1993; Arnon et al., 2007a). The role of the hyporheic zone becomes critical in contaminated streams, since it acts as a hub for natural attenuation or degradation activities due to its high potential for intensive biogeochemical activity (e.g., continuous oxygen supply from stream water, high microbial density, etc.), despite its relatively small volume vis-à-vis the subsurface environment (Dent et al., 2007; Hester and Gooseff, 2010). The spatial and temporal distribution of oxygen in the hyporheic zone leads to the formation of biogeochemical "hot spots" (Arnon et al., 2007b; Lautz and Fanelli, 2008; Wilson and Dodds, 2009), i.e., aerobic-anaerobic zones that control the fate of nutrients.

Despite the large number of research studies on hyporheic exchange, relatively little attention has been given to the coupling between the hydrodynamic properties of the exchange and the biochemical reactions that occur in the hyporheic zone (Rutherford et al., 1995; Cardenas, 2009; Boano et al., 2010). The major drawback of previous attempts – mostly using laboratory flumes – to understand the fundamental relationships between overlying flow conditions and nutrient dynamics was that those experiments used simple set-ups of neutral flow conditions and thus did not include critical factors imposed by losing or gaining stream conditions that play a major role in redox-related transformation processes in natural systems (Krause et al., 2008, 2009b). In this study we evaluated the effect of subsurface flow patterns resulting from neutral,

losing and gaining stream conditions on oxygen, and carbon transformations by a combination of online spectrophotometer and microelectrodes.

Materials and Methods

Experimental system

The effect of flow conditions on redox zonation and dissolved organic carbon (DOC) uptake by benthic biofilm was studied in a recirculating flume, 260 cm long and 29 cm wide (Fig. 1). The flume is packed with natural silica sand (328μm average diameter and hydraulic conductivity of 0.0278 cm s^{-1}) to form an average 7 cm deep sand bed with stationary bedforms. The bedform wavelength was 19.6 cm ±2 long.

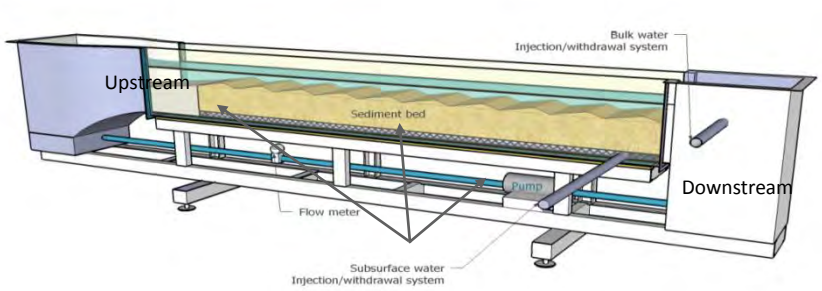

Fig. 1. Schematic illustration of the experimental system

The flow in the main channel was driven by a variable-speed pump that recirculates the water in the flume, and creates a purely gravity-driven open channel flow. At the bottom of the channel, the flume has a novel perforated structure equipped with a drainage system that enabled the operation of the flume under neutral, losing and gaining flow conditions. Losing and gaining stream conditions are achieved by injecting water into, or pumping water out from the bottom of the sediment bed, respectively. Under gaining conditions, the same volume of water that was added along the bottom of the bed, was pumped out from the main channel to maintain a constant volume of water in the system. For losing conditions, the same water that is pumped out, was re-injected into

the main channel to compensate for the withdrawal of water along the bottom of the sediment bed.

Hyporheic exchange

Hyporheic exchange flux was measured with tracer experiments under various combinations of two overlying water velocities and six subsurface flow rates. Tracer experiments were conducted by introducing a tracer solution to the recirculating water, and then monitoring the reduction in the in-stream tracer concentration over time (Packman et al., 2004). Dissolved NaCl was used as a conservative tracer, and its concentration was measured as EC using an LR 925/01 electrode connected to a multi 3430 logger (WTW). The background EC in the flume before the injection was approximately 90 and 160 µS cm-1, before and after the tracer addition, respectively. The resolution of the sensor was 0.1 µS cm^{-1}. Water temperature was maintained at 25 ± 1 ºC.

Biofilm growth

The initial benthic microbial seed was obtained in July 2012 from the Yarqon Stream, Israel. The biofilm was scraped off the stream pebbles, mixed it into 3l of mineral nutrient solution, filtered through a 75 µm mesh to remove grazers and particles and spread evenly over the flume. The microbial solution was inoculated into the channel and then allowed to settle in the water column under no-flow conditions for 24 hours. Thereafter the flow initiated, a growth medium (Aakra et al., 1999) has been used to promote biofilm development following procedures that were developed in previous studies (Arnon et al., 2007a, 2013). Biofilm was cultivated in the flume under the maximum velocity to be used in all the experiments (~8 cm s^{-1}). This velocity is well below the levels that could produce sediment transport but sufficiently high to produce turbulent conditions. The photoautotrophic community can be supported by supplying light via fluorescent lamps (40 µmol m^{-2} s^{-1}) for 12 h each day for 3 months.

DOC uptake

DOC uptake from the water column was measured under overlying velocities of 0.6 and 6 cm s^{-1}. In addition, DOC uptake under losing and gaining flow conditions was measured under overlying velocity of 6 cm s^{-1} and losing and gaining flux per unit bed area of 0.76 cm s^{-1}. To ensure similar initial conditions in the uptake experiments, the flume was spiked benzoic acid as a carbon source to a starting DOC concentration of

15 mg l^{-1}. The reduction of the in-stream DOC concentrations was monitored until the DOC levels were back to the background concentrations. During the DOC uptake experiments, oxygen profiles were measured at the upper section of the bedform from the bulk water into the streambed.

Analytical techniques

DOC concentration in the bulk water is measured using an online UV/Vis spectrophotometer (spectro::lyzer model, S::can Messtechnik, Vienna, Austria). The instrument is a 2-beam, 256 pixel, UV/Vis spectrophotometer, with a Xenon lamp as a light source. The spectro::lyzer records light absorption in the wavelength region between 200nm and 750nm. By recording the light absorption between 200-750 nm, the probe is capable to determine the fingerprint spectrum and specific concentrations of carbon and nitrate using algorithms provided by S::CAN.

Oxygen concentrations in the streambed were measured using a Clark-type oxygen electrode mounted on micromanipulator with computerized depth control and data acquisition (Unisense). The microelectrode had a tip diameter of 50 mm, a stirring sensitivity, 2%, and a 90% response time 5 s.

Results and Discussion

Rates of DOC uptake were evaluated by monitoring DOC concentration in the bulk water under different overlying water velocities (Fig. 2). The linear regressions of DOC concentrations versus time were used to evaluate the uptake rates. DOC uptake under 6 cm s^{-1} (turbulent conditions) was three times faster than at a non-turbulent conditions 0.6 cm s^{-1} ($P < 0.05$). The main reason for the enhanced uptake under faster overlying velocity is due to the increase in solute exchange rate which was 25 times higher under 6 versus 0.6 cm s^{-1} (data not shown).

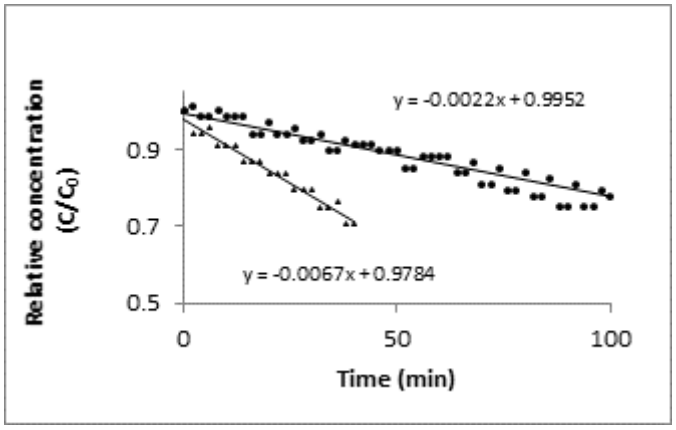

Fig. 2. DOC uptake under 0.6 (●) and 6 (▲) cm s^{-1}.

The biogeochemical active zone was strongly influenced by the hyporheic exchange and subsurface flow patterns. Oxygen profiles revealed that before adding DOC to the channel, oxygen was at saturation in the bulk water and in the streambed. Oxygen concentrations in the streambed were influenced by DOC uptake soon after DOC was added to the channel (data not shown), and were stabilized after 90 min. as shown in Fig. 2. Under losing conditions, oxygen was consumed as DOC penetrated into the sediments, until anaerobic conditions were evident at a depth of 3300 µm. DOC penetration was driven by hyporheic exchange and the imposed losing flux. Under gaining conditions, oxygen increased from the concentrations in the bulk water to saturation at a depth of 2800 µm. It seems that hyporheic exchange under gaining conditions had little impact on DOC penetration into the sediment, which was prevented by the upwelling flow due to the imposed gaining flux. The impact of losing and gaining flow conditions on DOC uptake was masked by high DOC uptake rates in the bulk water, but was evident by the microelectrode measurements.

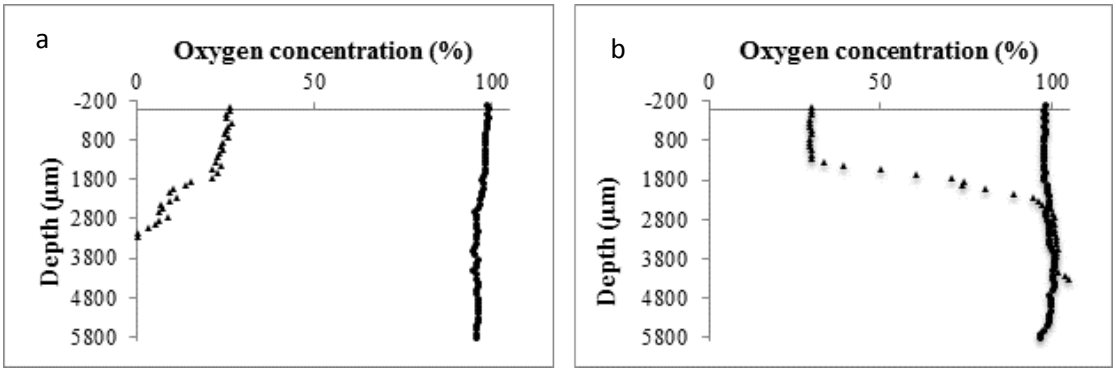

Fig. 3. Oxygen profile under losing (a) and gaining (b) flow conditions, before addition DOC (●) and 90 min. after DOC addition (▲). Depth of zero represents the interface between the bulk water (negative depth values) and the streambed (positive depth values).

Conclusions

Hyporheic exchange flux is driven by local and regional scale geomorphological structures and hydraulic gradients in a complex manner. In this study, we evaluated how losing and gaining stream flow conditions influence hyporheic exchange fluxes of water and solutes using a novel laboratory flume set-up. It was found that increasing overlying velocities leads to increased hyporheic exchange and higher DOC uptake. When losing and gaining flow conditions were applied, they become the dominant mechanisms of water exchange and DOC uptake. While losing conditions increased the supply of the DOC to the benthic biofilm, gaining conditions prevented DOC uptake by constraining the DOC in the main channel due to the upwelling water. This study showed that the combination of an online UV-Vis spectrophotometer and microelectrodes holds a great potential for the acquisition of unique sets of data, which can be used to improve the current understanding the effect of the coupling between stream velocity and losing /gaining flow conditions on nutrient dynamics in streams.

Acknowledgments.

This research was supported by the Israel Science Foundation (Grant No. 694/11) to S. Arnon, and by a grant (Israel-Italy Joint Innovation Program for Scientific and Technological Cooperation in R&D) from the Israeli Ministry of Science, Technology and Space and the Italian Ministry of Foreign Affairs, Directorate General for Political and Security Affairs to S. Arnon and F. Boano.

References

Aakra, A., J.B. Utaker, I.F. Nes, and L.R. Bakken. 1999. An evaluated improvement of the extinction dilution method for isolation of ammonia-oxidizing bacteria. J. Microbiol. Methods. 39(1): 23–31.

Arnon, S., K.A. Gray, and A.I. Packman. 2007a. Biophysicochemical process coupling controls nitrate use by benthic biofilms. Limnol. Oceanogr. 52(4): 1665–1671.

Arnon, S., A.I. Packman, C.G. Peterson, and K. a. Gray. 2007b. Effects of overlying velocity on periphyton structure and denitrification. J. Geophys. Res. 112(G1): 1–10.

Arnon, S., K. Yanuka, and A. Nejidat. 2013. Impact of overlying water velocity on ammonium uptake by benthic biofilms. Hydrol. Process. 27(4): 570–578.

Bencala, K.E., and R.A. Walters. 1983. Simulation of solute transport in a mountain pool-and-riffle stream: a transient storage model. Water. Resour. Res. 19(3): 718–724.

Boano, F., A. Demaria, R. Revelli, and L. Ridolfi. 2010. Biogeochemical zonation due to intrameander hyporheic flow. Water. Resour. Res. 46(2): 1–13.

Boulton, A.J. 1993. Stream ecology and surface hyporheic hydrologic exchange - implications, techniques and limitations. Aust. J. Mar. Freshe. Res. 44(4): 553–564.

Boulton, A.J., S. Findlay, P. Marmonier, E.H. Stanley, and H.M. Valett. 1998. The functional significance of the hyporheic zone in streams and rivers. Annu. Rev. Ecol. Syst. 29(1): 59–81.

Brunke, M., and T. Gonser. 1997. The ecological significance of exchange processes between rivers and groundwater. Freshwater Biol. 37(1): 1–33.

Cardenas, M.B. 2009. A model for lateral hyporheic flow based on valley slope and channel sinuosity. Water. Resour. Res. 45.

Cardenas, M.B., and J.L. Wilson. 2007. Thermal regime of dune-covered sediments under gaining and losing water bodies. J. Geophys. Res. 112(G4): G04013.

Dent, C.L., N.B. Grimm, E. Marti, J.W. Edmonds, J.C. Henry, and J.R. Welter. 2007. Variability in surface-subsurface hydrologic interactions and implications for nutrient retention in an arid-land stream. J. Geophys. Res. 112.

Findlay, S. 1995. Importance of surface-subsurface exchange in stream ecosystems - The hyporheic zone. Limnol. Oceanogr. 40(1): 159–164.

Hester, E.T., and M.N. Gooseff. 2010. Moving beyond the banks: Hyporheic restoration is fundamental to restoring ecological services and functions of streams. Environ. Sci. Technol. 44(5): 1521–1525.

Krause, S., D.M. Hannah, and J.H. Fleckenstein. 2009a. Hyporheic hydrology: interactions at the groundwater-surface water interface. Hydrol. Process. 23(15): 2103–2107.

Krause, S., J. Jacobs, A. Voss, A. Bronstert, and E. Zehe. 2008. Assessing the impact of changes in landuse and management practices on the diffuse pollution and retention of nitrate in a riparian floodplain. Sci. Total. Environ. 389(1): 149–164.

Krause, S., H. Louise, B. Andrew, K. Patrick, L. Heathwaite, A. Binley, and P. Keenan. 2009b. Nitrate concentration changes at the groundwater-surface water interface of a small Cumbrian river. Hydrol. Process. 23(15): 2195–2211.

Lautz, L.K., and R.M. Fanelli. 2008. Seasonal biogeochemical hotspots in the streambed around restoration structures. Biogeochemistry. 91(1): 85–104.

Packman, A., M. Salehin, and M. Zaramella. 2004. Hyporheic exchange with gravel beds: Basic hydrodynamic interactions and bedform-induced advective flows. J. Hydraul. Eng. 130(7): 647–656.

Ruehl, C.R., A.T. Fisher, M. Los Huertos, S.D. Wankel, C.G. Wheat, C. Kendall, C.E. Hatch, and C. Shennan. 2007. Nitrate dynamics within the Pajaro River, a nutrient-rich, losing stream. J. N. Am. Benthol. Soc. 26(2): 191–206.

Rutherford, J.C., J.D. Boyle, A.H. Elliott, T.V.J. Hatherell, and T.W. Chiu. 1995. Modeling Benthic Oxygen-Uptake by Pumping. J. Environ. Eng. 121(1): 84–95.

Thibodeaux, L.J., and J.D. Boyle. 1987. Bedform-generated convective transport in bottom sediment. Nature. 325: 341–343.

Wilson, K.C., and W.K. Dodds. 2009. Centimeter-scale stream substratum heterogeneity and metabolic rates. Hydrobiologia. 623(1): 53–62.

SENSOR-BASED PRECISION FERTILIZATION FOR FIELD CROPS

Kenneth A. Sudduth[1*], Hak-Jin Kim[2]

[1]Cropping Systems and Water Quality Research Unit, USDA Agricultural Research Service, Columbia, Missouri, USA

[2]Department of Biosystems Engineering and Biomaterials Scien, Seoul National University, Seoul, South Korea

[*]Corresponding author: phone +1(573)882-1114, Email ken.sudduth@ars.usda.gov

Abstract

From the development of the first viable variable-rate fertilizer systems in the upper Midwest USA, precision agriculture is now approaching three decades old. Early precision fertilization practice relied on laboratory analysis of soil samples collected on a spatial pattern to define the nutrient-supplying capacity of the soil, which was then used in map-based control of variable-rate applicators. This practice is still common today, but issues of cost and practicality limit the intensity of sample collection and therefore the accuracy of the resulting precision application. A mobile soil sensing system that could be linked to a variable-rate applicator and guide fertilizer application in real time could overcome these issues. Research to develop proximal sensors for soil variables important in precision fertilization decisions began almost three decades ago and efforts to develop sensors for soil variables such as pH, plant-available phosphorus and potassium, and soil nitrate have continued to the current day. Most soil nutrient sensors developed to date have been based on either diffuse reflectance spectroscopy or electrochemical methods. While both of these approaches have advantages, they also have drawbacks which have precluded the development of a commercially viable system. An understanding of the different sensing approaches and their associated issues is an important step toward an improved system. To that end, this paper reviews the history of proximal soil nutrient sensing and describes the current state of the technology, with a focus on describing different sensor designs and applications. Future directions and considerations for soil nutrient sensing are also discussed.

Introduction

The soil macronutrients, nitrogen (N), phosphorus (P), and potassium (K), are essential for crop growth, and the use of commercial N, P, and K fertilizers has contributed greatly to the increased yield of agricultural crops. However, excessive fertilizer applications can lead to environmental contamination, primarily of surface and ground waters (Vadas et al., 2004). Ideally, fertilizer application should be adjusted to match the requirements for optimum crop production at each within-field location because there can be high spatial variability in the N, P, and K levels found within fields (Page et al., 2005; Ruffo et al., 2005).

Site-specific crop management (SSCM), also called precision agriculture, is a soil and crop management system that assesses variability in soil properties (e.g., pH, organic matter, and soil nutrient levels), field (e.g., slope and elevation) and crop parameters (e.g., yield and biomass), to optimize inputs such as fertilizers and herbicides based on information obtained at within-field locations (Sudduth et al., 1997). SSCM aims to improve profitability and to better protect soil and water resources as compared to conventional management practices (Kitchen et al., 2005). Most commercial precision fertilization services in the United States use nutrient variability mapping by means of point-by-point grid soil sampling (e.g., Carr et al., 1991). Fields are then divided into manageable units based on the spatial pattern of nutrient variability. The optimum grid size for use in soil nutrient mapping is dependent on the level of spatial variability present and the cost of soil sampling and analysis. In a field where previous nutrient maps have been obtained, it may be possible to infer the grid size needed to adequately characterize spatial variability. However, for newly mapped fields, initial sampling should be at a small grid size, so that all significant patterns can be represented. Bullock et al. (1994) studied the effect of grid size on soil fertility maps obtained at eight sites. In comparing 0.25 ha grids to 1 ha grids (a standard size for commercial SSCM implementation in the US), they sometimes found significant differences, leading to over-fertilizing or under-fertilizing of large areas of fields when using 1 ha grids.

Conventional soil analysis methods, based on manual or mechanical soil sampling and laboratory-based colorimetric or atomic emission spectroscopy, are costly and time consuming. This limits the number of samples that can be practically analyzed for a given field, making it difficult to accurately characterize within-field spatial variability

in soil nutrient levels (Schepers and Schlemmer, 1998, Artigas et al., 2001). Most notably, soil nitrate monitoring has been limited by the relatively long turn-around time of laboratory analysis, because soil nitrate can be easily lost by leaching and denitrification between the time of testing and plant uptake (Blackmer et al., 1989). Therefore, quantifying soil nitrate variability requires a fast on-site measurement at a high sampling intensity to deal with both spatial and temporal variability (Sudduth et al., 1997; Wollenhaupt et al., 1997).

To quantify soil nutrient levels at the spatial scale needed in SSCM, on-the-go real-time sensors present an attractive alternative to current manual and/or laboratory methods (Sibley et al., 2009, Schirrmann et al., 2011). These automated sensors could provide measurements at a high spatial density and relatively low cost (Adamchuk et al., 2004), and with an overall accuracy potentially higher than that of conventional soil testing. This occurs because there are two sources of error in soil testing -- analysis error due to sub-sampling and analytical determination, and sampling error due to point-to-point variation in soils. With traditional soil testing, analysis error is relatively low; however, sampling error can be substantial since cost limits the sampling intensity. Real-time sensors can provide a sampling intensity several orders of magnitude greater than traditional methods. Therefore, a real-time soil sensor can tolerate much higher analysis errors while providing greater overall accuracy in mapping soil variability.

The goals of this paper are to provide a review of nutrient sensing research from the basics of sensing to the implementation of field-ready systems, and to discuss directions and considerations for the application of nutrient sensing to field crop fertilization.

Nutrient Sensing Methods

Broad reviews of various types of sensors to measure mechanical, physical and chemical soil properties were given by Sudduth et al. (1997) and Adamchuk et al. (2004). More recently there have been reviews focused specifically on soil nutrient sensing (Kim et al., 2009; Sinfield et al., 2010).

Here we discuss approaches and results associated with sensors for measuring macronutrients (N, P, and K) and pH levels in soils. Although other sensing techniques are available, we focus on two widely-used measurement methods:

- optical sensing that uses reflectance spectroscopy to detect the level of energy absorbed/reflected by soil particles and nutrient ions, and
- electrochemical sensing that uses ion-selective electrodes or ion-selective field effect transistors, which generate a voltage or current output in response to the activity of selected ions.

Spectroscopy

Optical diffuse reflectance spectroscopy in visible and near-infrared (NIR) wavelength ranges is one approach to rapidly quantify soil properties for SSCM. Optical methods have several advantages over electrochemical technology, including non-destructive (and often non-contact) measurement and no need to take a soil sample (Chang et al., 2001; Viscarra Rossel et al., 2006). The principle of diffuse reflectance spectroscopy is based on the interaction between incident light and soil surface properties, such that the characteristics of the reflected light vary due to the soil physical and chemical properties (Mouazen et al., 2005).

Many researchers have investigated optical soil N sensing. Upadhyaya et al. (1994) used NIR absorbance data in conjunction with FFT (fast Fourier transform) and PLSR (partial least squares regression) analyses to determine soil NO_3-N over a concentration range of 0 to 300 mg kg^{-1}. The linear relationship between the NIR and standard methods was high ($r^2 > 0.9$). However, the standard error of prediction (SEP) was also fairly high (6 ~ 38 mg kg^{-1} NO_3-N). Ehsani et al. (1999) determined an optimal NIR wavelength range (1800 ~ 2300 nm) for measuring soil nitrate, but a soil-specific calibration was needed to map nitrate variation over a large area due to the effect of soil type.

Linker et al. (2004; 2005; 2006) used Fourier transform infrared (FTIR) attenuated total reflectance (ATR) spectroscopy in the mid-infrared range to measure nitrate content in soil solutions and pastes. They proposed a two-step approach, consisting of soil identification and a soil-dependent model, to improve accuracy. The soil identification was performed by comparing the so-called 'fingerprint' region of the spectrum (6,400 ~12,500 nm) to a reference spectral library, in conjunction with PCA (principal component analysis) decomposition and NN (neural network) classification techniques. Nitrate determination was achieved using PLSR models. Resulting errors ranged from

6.2 to 13.5 mg kg^{-1} N, smaller than the error obtained with a model for all soil types combined (19.1 mg kg^{-1} N).

Jahn et al. (2005) used wavelet spectral analysis for the determination of soil nitrate based on mid-infrared FTIR-ATR spectroscopy. They tested a loam and a clay soil treated with nitrate fertilizers by adding interfering compounds such as carbonate and humic acid. In the concentration range of 0 to 140 mg L^{-1} NO_3-N, they obtained r^2 = 0.43 for nitrate concentration. However, the results were not satisfactory when attempting to measure low concentrations of soil nitrate or to obtain consistent predictive capabilities across a range of soils due to relatively high SEP (about 9.5 mg L^{-1} NO_3-N) and a significant effect of soil type. To investigate the feasibility of using wavelet analysis for nitrate determination in various soil types, Jahn et al. (2006) applied wavelet analysis to soil FTIR-ATR spectra collected by Linker et al. (2004). Coefficients of determination (r^2) as high as 0.96 ~ 0.99 and standard errors as low as 5 ~ 24 mg kg^{-1} NO_3-N were obtained in laboratory and field experiments when building site-specific calibration models for calcareous and non-calcareous soils. In addition, it was possible to use a single calibration equation and obtain standard errors as low as 3.6 mg kg^{-1} NO_3-N for 10 different soils using absorbance data in the 6,500 ~ 7,500 nm range.

Lee et al. (2003) related spectral characteristics to chemical properties, including P and K, of soil samples from major soil orders in Florida, USA, developing models to estimate pH, organic matter, P, K, Ca, and Mg concentrations. Their models accounted for more than 72% of the variation observed in the validation set for soil pH, P, Ca, and Mg, but less than 50% of the variation in K and soil organic matter. Bogrekci and Lee (2005) focused on soil and vegetation P sensing using ultraviolet-visible-NIR spectroscopy. Strong relationships (r^2 = 0.78 ~ 0.92) between absorbance and P concentration in soils were obtained with PLSR whereas a weak relationship (r^2 = 0.42) existed for vegetation samples. Follow-up studies investigated the effects of soil moisture content on the absorbance spectra of sandy soils with different P concentrations (Bogrecki and Lee, 2006) and compared the prediction capabilities of three different spectral regions, i.e., ultraviolet (UV), visible and NIR in determining P contents in soil (Bogrecki and Lee, 2007). Removing the moisture effect by spectral signal processing improved P prediction in soils considerably, reducing root mean

square error (RMSE) from 151 to 62 mg kg^{-1}. The NIR region produced better estimates than did the UV and visible regions, with a strong relationship (r^2 = 0.95) between reflectance and Mehlich I P concentration. Maleki et al. (2006) used 204 soil samples from fields in Belgium to estimate P using reflectance data from 305 to 1710 nm and PLSR analysis. They concluded that a model with multiplicative scatter correction (MSC) pretreatment performed best in the calibration stage but a model without MSC predicted P better in the two field datasets.

Other studies have simultaneously determined multiple soil properties using optical methods. Dalal and Henry (1986) used NIR reflectance spectroscopy to simultaneously estimate water content, total organic carbon, and total N in air-dried soils by multiple linear regression. They reported r > 0.87 for each of three wavelengths selected for the three measurement parameters. However, there was a significant difference in SEP between coarsely ground (< 2 mm) and finely ground (< 0.25 mm) soils. Chang et al. (2001) applied principal component regression (PCR) to relate 33 soil chemical, physical, and biochemical properties to NIR data obtained from 802 soil samples. They demonstrated the possibility of measuring diverse soil properties such as total C, total N, moisture content, cation exchange capacity (CEC), and extractable Ca with acceptable accuracy. Similarly, He et al. (2005) used NIR spectroscopy to estimate nitrogen and organic matter in soils of a province in China using a total of 125 soil samples. They reported that the correlation coefficients between measured and predicted soil nitrogen and organic matter were 0.92 and 0.93, respectively. More recently, the same authors applied NIR spectroscopy in conjunction with PLSR to the determination of P, K, and pH for 165 soil samples with a loamy mixed soil type (He et al., 2007). Good estimates were obtained for soil pH (r = 0.91, SEP = 0.07). However, the results were not satisfactory for soil P and K, with correlation coefficients of 0.47 and 0.68, and SEP of 33.7 and 26.5 mg kg^{-1}, respectively.

Daniel et al. (2003) used VNIR spectroscopy (400 - 1100 nm) and neural network analysis to investigate P and K of 41 soils from Thailand, obtaining satisfactory results. Udelhoven et al. (2003) analyzed 114 soil samples from a 13 ha area in southwest Germany, finding that the accuracy of estimation for multiple soil properties, including P and K, depended on pretreatment and spectral resolution. Ge et al. (2007) examined visible and NIR spectroscopy applied to 273 soil samples from an agricultural field.

Although some soil properties were well-estimated, results for P and K were poor. La et al. (2008) obtained good estimates of texture fractions, organic matter and CEC (r^2 = 0.83 to 0.92) for Missouri and Illinois surface soils whereas estimates of P and K were not as good ($r^2 < 0.7$). Similar estimates of P and K (r^2 = 0.72 and 0.74, respectively) were obtained for 14 distinct soil series of 42 Korean paddy fields (Lee et al., 2008). Sudduth et al. (2009) analyzed 104 surface soil samples from a 35 ha field, obtaining poor results for soil carbon, P, and K. Mouazen et al. (2010) compared three calibration methods (PCR, PLSR, and back propagation neural network – BPNN) for estimating soil properties including organic carbon, K, and P for 168 soil samples. They recommended the BPNN-latent variables (LVs) modeling technique for higher accuracy estimates.

In summary, many authors have reported high correlations with standard methods when using diffuse reflectance spectroscopy in conjunction with various calibration and signal processing methods (i.e., PLSR, PCR, and FFT wavelet analysis) to estimate soil physical properties. However, results have most often not been satisfactory for soil macronutrients in those ranges where fertilizer application decisions must be made, i.e., 10 ~ 30 mg kg^{-1}, 10 ~ 27.5 mg kg^{-1}, and 50 ~ 150 mg kg^{-1} for N, P, and K, respectively (Buchholz et al., 1983). Although reflectance spectroscopy can respond to total nutrient concentrations in soil, calibration of the reflectance signal to the plant-available portion of the nutrient pool measured by standard soil tests is a considerable challenge. This challenge has contributed to the inability to obtain consistently good estimates across a range of soils, relatively high standard errors and significant effects of soil type.

Electrochemical Sensing

Most of the electrochemical methods used to determine soil nutrient levels are based on the use of an ion-selective electrode (ISE), with glass or a polymer membrane, or an ion-selective field effect transistor (ISFET). The ISFET has the same theoretical basis as the ISE, i.e., both ISEs and ISFETs respond selectively to a particular ion in solution according to a logarithmic relationship between the ionic activity and electric potential (Birrell and Hummel, 2000).

The ISEs and ISFETs require recognition elements, i.e., ion-selective membranes, which are integrated with a reference electrode and enable the chemical response (ion

concentration) to be converted into an electrical potential signal (Eggins, 2002). Due to an increased demand for the measurement of new ions, and tremendous advances in the electronic technology required for producing multiple channel ISFETs, numerous ion-selective membranes have been developed in many areas of applied analytical chemistry, e.g., in the analysis of clinical or environmental samples (Bakker, 2004).

Nitrate ion-selective membranes and electrodes

Numerous nitrate ion-selective membranes have been described for various applications, such as food, plants, fertilizer, soil, and wastewater. Nielson and Hansen (1976) developed nitrate ISEs using various quaternary ammonium compounds and plasticizers in non-porous PVC-based membranes. A combination of tetradodecylammonium nitrate (TDDA) and dibutylphthalate (DBP) as the ligand and plasticizer, respectively, was found to show the best response to nitrate.

Birrell and Hummel (2000) evaluated various PVC matrix membranes prepared with different combinations of ligand and plasticizer materials. Membranes prepared with methyltridodecylammonium chloride (MTDA) or TDDA displayed an approximately Nernstian response to nitrates. The membranes based on the MTDA ligand showed slightly greater sensitivity to nitrate than did the TDDA membranes while the TDDA ligand gave superior selectivity for the nitrate ion. For best results in the presence of other interfering ions in soils, they developed multi-ISFET nitrate sensors using the TDDA-based nitrate membranes. The nitrate ISFETs effectively determined concentrations over a range of nitrates in soil with acceptable selectivity levels that were at least 40 times greater for nitrate than for chloride and bicarbonate.

Gallardo et al. (2004) used an artificial neural network to extract nitrate information from the cross-term responses to nitrate and chloride ions for quantifying nitrate in complex samples containing variable amounts of chloride. Three nitrate electrodes with different ionophores (i.e. tetraoctylammonium nitrate (TOAN), tridodecylmethylammonium nitrate (TDMAN), and tris (4,7-diphenyl-l, 10-phenantroline nickel(II) nitrate (TDPNN)) and one chloride electrode were used in conjunction with a flow-injection system. This approach improved the accuracy of nitrate concentration estimates over a range from 0.1 to 100 mg L^{-1} NO_3 without the

need to eliminate chloride. However, they mentioned as a drawback that a large number of known samples were needed for training the system.

More recently, Kim et al. (2006) investigated the responses of PVC membranes with TDDA or MTDA to nitrate ions in the Kelowna (Van Lierop, 1986; 1988) extracting solution. The TDDA-based nitrate membrane showed greater sensitivity and better selectivity for nitrate over interfering ions that may be present in soil than did the MTDA-based membrane. The TDDA-based membrane was capable of detecting soil concentrations as low as 10 mg kg^{-1} NO_3 with a 1:10 soil-to-solution ratio.

In a review of past research, Kim et al. (2009) found that the best overall results were obtained with PVC ion-selective membranes prepared with quaternary ammonium compounds, such as TDDA or MTDA as the sensing element for nitrate. These membranes were able to determine nitrate across the concentration range important for N fertilizer application management, i.e., 10~30 mg kg^{-1} NO_3. These membranes also maintained acceptable selectivity levels in mixed solutions, being at least 40 times more sensitive to nitrate than to chloride and bicarbonate.

Potassium ion-selective membranes and electrodes

Historically, a major interest for K analysis came from clinical chemistry because changes in K concentration in human serum bring about the risk of acute cardiac arrhythmia. Therefore, the majority of the research on the use of K ion-selective membranes has been focused on continuous monitoring of the human body during periods of rapidly changing K concentrations, such as during or after surgery.

Expanding on the medical findings, researchers have applied valinomycin-based K membranes to monitoring of environmental samples, such as food, water and soil. In addition, most of these studies also included research on the adhesion of the PVC membrane to the gate region of ISFETs. The efforts were directed toward extending the consistent sensitivity period, and thus, the lifetime of the electrode. Results demonstrated that valinomycin-based K membranes were useful in measuring K in environmental samples containing various interfering ions. From the results of numerous studies on ionophores for sensing K in analytical chemistry, it is clear that

valinomycin has been the most successful ionophore for sensing the ion because of its strong K selectivity (Kim et al., 2009).

Artigas et al. (2001) reported on the fabrication of pH, Ca, NO_3, and K ISFETs with photo-curable polymeric membranes and their evaluation in aqueous soil solutions. The photo-curable polymeric membrane adhered better and had a longer life than PVC-based membranes. Sensor response characteristics were stable for two months. During that time no membrane damage occurred and no peel-off was observed.

Kim et al. (2006) tested ion-selective membranes prepared with valinomycin as an ionophore and three different plasticizers (2-nitrophenyl octyl ether (NPOE), bis(2-ethylhexyl) sebacate (DOS), and bis(2-ethylhexyl) adipate (DOA)) for sensing Kelowna-extractable K. The DOS and DOA membranes showed satisfactory selectivity for measuring K in the presence of interfering cations such as Na, Mg, Ca, Al, and Li, and provided repeatable sensitivity slopes to different concentrations in the range of 10^{-4} to 10^{-1} M K. The sensitivity of these membranes to K in the Kelowna solution was high enough to measure the typical range in soil potassium at which additional K fertilizer is recommended.

Phosphate ion-selective membranes and electrodes

Due to the importance of real-time monitoring of P in biological systems and living organisms, many researchers have tried to develop phosphate sensors in the form of ion-selective electrodes and biosensors. However, the design of an ionophore for selective recognition of phosphate is especially challenging for several reasons. Due to the very high hydration energy of phosphate, ion selective membranes have a very poor selectivity for phosphate. The free energy of the phosphate species is very small and the large size of orthophosphate ions prohibits the use of size-exclusion principles for increased selectivity. Reviews (Buhlmann et al., 1998; Engblom, 1998; Kim et al., 2009) report work on various phosphate sensors, including polymer membranes based on organotin, cyclic polyamine, or uranyl salophene derivatives; protein-based biosensors; and cobalt-based electrodes.

The use of organotin compounds was initiated by Glazier and Arnold (1988, 1991). They prepared various dibenzyltin dichloride derivatives, such as bis(p-

chlorobenzyl)tin dichloride, dibenzyltin dichloride, and bis(p-methylbenzyl)tin dichloride. The bis(p-chlorobenzyl)tin dichloride showed the best selectivity for dibasic orthophosphate (HPO_4^{2-}) against various anions, such as nitrate, bromide, chloride, and acetate. The sensitivity was satisfactory, yielding a detection limit of 3.2×10^{-5} M and a linear range of response from 2.2×10^{-4} to 1.2×10^{-2} M for dibasic phosphate activity, when tested in standard solutions at pH 7. Others have developed new ionophores based on tin compounds that have been reported to enhance selectivity and durability (Liu et al., 1997; Sasaki et al., 2004).

Carey and Riggan (1994) tested four types of cyclic polyamines as ionophores for sensing dibasic phosphate ions. The electrodes were tested in phosphate solutions at pH 7.2. The best alternative achieved a linear calibration curve between 10^{-6} and 10^{-1} M, and had a lifetime of about nine months. Wroblewski et al. (2000, 2001) developed a different type of PVC membrane based on uranyl salophene derivatives as ionophores. Their membrane had a sensitivity slope of -59 mV/decade and a maximum lifetime of two months. Kubo (2002) developed a biosensor based on phosphate-bind protein from Escherichia coli. The response time was about 5 min in the concentration range of $10^{-4} \sim 1.5 \times 10^{-3}$ M and there was no change in electric potential when other anions such as sulfate, nitrate, and bromide were added at a concentration of 5×10^{-4} M.

Xiao et al. (1995) first used cobalt metal as a phosphate ion-selective electrode material. They reported that oxidized cobalt electrodes showed potentiometric sensitivity to phosphate in the concentration range of $10^{-5} \sim 10^{-2}$ M in 0.025 M potassium hydrogen phthalate (KHP) solution at pH 4.0 and good selectivity for $H_2PO_4^-$ over other anions. In a follow-up study, Chen et al. (1997) used cobalt wire as a phosphate electrode in FIA. The electrode showed a linear response with a slope of about -38 mV/decade change in phosphate. The system was applied for the direct determination of phosphate in soil extract samples by spiking and diluting the soil samples with standard phosphate solutions. Spiked soil extracts showed good recoveries for phosphate in the concentration range of $10^{-4} \sim 10^{-3}$ M (Chen et al., 1998). Engblom (1999) studied the applicability of a cobalt rod electrode to the measurement of phosphate in soil extracts. Ammonium lactate-acetic acid (AL), commonly used in Sweden, was chosen as a soil extracting solution. The cobalt electrode was linearly sensitive to phosphate ranging

from 10^{-4} to 10^{-3} M in the AL soil extractant with a sensitivity slope of -30 mV/decade.

Similarly, Kim et al. (2007a) evaluated cobalt rod-based electrodes for sensing phosphorus extracted from soils using the Kelowna soil extracting solution. The cobalt rod-based electrodes exhibited sensitive responses to $H_2PO_4^-$ over a range from 10^{-5} to 10^{-1} M total phosphate concentration with a detection limit of 10^{-5} M in the Kelowna solution at a pH of 3.2. It was expected that this detection range would encompass the typical range of soil phosphorus concentrations measured in agricultural fields (Buchholz et al., 1983). The selectivity of the cobalt electrodes was also satisfactory for measuring phosphates in the presence of each of six interfering ions, i.e., HCO_3^-, Cl^-, Br^-, NO_3^-, Ac^-, and F^-.

In contrast to the nitrate and potassium membrane studies previously mentioned, a wider range of compositions has been considered for phosphate-sensitive ionophores. However, despite this broad range of investigation and the technical progress made so far, a clearly superior P-sensitive ionophore has not been found. A key impediment remaining is the low selectivity response of such membranes toward many anions. At present, the best alternative appears to be the solid cobalt electrode, which has exhibited sufficient sensitivity, selectivity and durability to provide a quantitative measure of phosphates in soil extracts.

Application of ISEs and ISFETs in laboratory tests

Ion selective electrodes have historically been used in soil testing laboratories to conduct standard chemical soil tests, especially soil pH measurement. Many researchers in the 1970's and 1980's concentrated on the suitability of ISEs as an alternative to routine soil nitrate testing. More recently, researchers whose end goal was a mobile macronutrient sensing system have reported on laboratory tests of components of such systems (Kim et al., 2009).

Adamchuk (2002) tested nitrate and potassium ion-selective electrodes in moistened soils as opposed to soil extracts. The laboratory test showed that it was feasible to determine soluble nitrate and K content of moist soil samples (r^2 = 0.56 ~ 0.94) if several limitations such as inconsistent contact between soil and electrode and potential

drift due to continuous measurements were addressed. Brouder et al. (2003) correlated plant-available K of 32 agricultural soils as determined by two ISEs (glass and PVC-based) and by AAS analysis. Results showed that the ISE-K readings in soil slurries were highly correlated with AAS-K values in filtrates when using DI water at a 1:1 soil:solution ratio for extraction (slope = 0.93, r^2 = 0.76). However, the PVC-based ISE was not usable for measurement in soil slurries due to durability problems. Also, results obtained using DI water for extracting K were not well correlated with those obtained with standard methods.

An ISFET chip combined with FIA has been used by several researchers for soil nitrate analysis. According to the literature, ISFET technology offers inherent features such as fast response, small dimensions, low output impedance, high signal-to-noise ratio, low sample volumes, and the ability to integrate several sensors on a single electronic chip -- all of which are desirable for a real-time sensor (Price et al., 2003).

Birrell and Hummel (2000; 2001) investigated the use of a multi-ISFET sensor chip to measure soil nitrate in a FIA system using low flow rates, short injection times, and rapid rinsing (Fig. 1). The multi-ISFET/FIA system successfully estimated soil nitrate-N content in manually prepared soil extracts (r^2 > 0.90). The rapid response of the system allowed samples to be analyzed within 1.25 s with sample flow rates less than 0.2 mL s^{-1}. However, the prototype automated soil extraction system did not consistently provide soil extracts that could be analyzed by the ISFET/FIA, due to blockages in the filtration process. Price et al. (2003) developed a rapid extraction system designed to be used in the field for real-time measurement of soil nitrates using the ISFETs developed by Birrell and Hummel (2001). Several design parameters affecting nitrate extraction were studied. Nitrate concentration could be determined 2 to 5 s after injection of the extracting solution when using data descriptors based on the peak and slope of the ISFET nitrate response curve.

Kim et al. (2007b) evaluated a sensor array including three different ISEs based on TDDA-NPOE and valinomycin-DOS membranes and cobalt rod using an automated test stand (Fig. 2), to simultaneously determine NO_3-N, available K, and available P in Kelowna-soil extracts. The nitrate ISE in conjunction with the Kelowna extractant provided results in close agreement with the standard method (Lachat analyzer and 1M KCl extractant). However, the Kelowna-K ISE concentrations were about 50% lower

than those obtained with the standard method (Mehlich III extractant and ICP spectrophotometer) due to decreased K extraction by the Kelowna solution. Soil P concentrations obtained with the Kelowna extractant and cobalt P ISEs were about 64% lower than those obtained by the standard method (Mehlich III extractant and ICP spectrophotometer) due both to a lower P extraction by the Kelowna solution, and to lower estimates of P concentrations in the extract by the cobalt P ISEs. Although P and K concentrations were low in comparison to standard laboratory procedures, a calibration factor could address this issue because there was a strong linear relationship between ISE and standard methods ($r^2 = 0.81$ and 0.82 for P and K, respectively).

More recently, Kim et al. (2013) evaluated the ability of the system developed by Kim et al. (2007b) to estimate variations in soil NO_3-N, P, and K within a single test site. The results showed that it was possible to transfer existing calibration equations to new membranes and electrodes. The ISEs measured N, P, and K ions in Kelowna-based soil extracts independently with approximately 1:1 relationships between the concentrations determined by ISEs and by standard laboratory instruments. An adjustment for the difference in extraction efficiency between Kelowna and standard extractants yielded linear relationships with near 1:1 slopes between estimates and actual N and K values. However, a relatively large offset between calibrated ISE and standard method concentrations for P was said to require further investigation.

On-the-Go Soil Macronutrient Sensing

Several researchers, beginning in the early 1990s, have reported on real-time on-the-go soil nutrient sensing using custom-designed soil samplers and commercially available ion-selective electrodes for sensing nitrate and pH in soils. Adsett et al. (1999) designed a prototype tractor-mounted field monitoring system to measure soil nitrate levels in fields using ISEs because they found a nitrate ion-selective electrode gave reliable sensor readings and acceptable response times of less than 20 s (Thottan et al., 1994). Results from laboratory testing indicated that nitrate level could be estimated with 95% accuracy after 6 s of measurement. However, several mechanical and electrical problems were found during field testing, e.g., clogging of the extractor outlet with plant residue, which resulted in unacceptable levels of noise in the electrode signal. The functionality of the automated soil sampler was later improved and evaluated with comprehensive performance testing conducted in five fields. Soil samples with uniform

bulk density were collected in a device of fixed volume, thereby providing precise estimates of the sample mass, as needed for accurate calculation of nitrate concentration (Sibley et al., 2008). Additional field-scale validation tests documented agreement between measurements of the soil nitrate by the extraction system and by standard laboratory instruments (slope = 1.0, $r^2 = 0.94$) (Sibley et al., 2009).

Viscarra Rossel and Walter (2004) built a soil analysis system comprising a batch-type mixing chamber with two inlets for 0.01M CaCl2 solution and water. In the mixing chamber, there was a flat spinning disc ensuring efficient mixing of the solution and the soil. A pH ISFET was used to determine soil pH and estimate lime requirements. The system was tested in the laboratory using soil solutions of 91 Australian soils obtained by mixing 3 g of sieved soil and 15 ml of 0.01M $CaCl_2$ and tested in a 17-ha agricultural field to estimate lime requirements. The system produced an RMSE of 0.2 pH_{Ca} (r^2 = 0.66). However, the coefficient of determination for buffer pH estimates was not high ($r^2 = 0.49$).

Adamchuk et al. (1999) developed an automated sampling system for soil pH based on direct soil measurement (DSM) by placing a flat-surface combination pH electrode in direct contact with moist soil collected by the sampling system. Tests showed a high correlation between the electrode voltage output and soil pH in the laboratory and field (r^2 = 0.92 and 0.83, respectively). The system could measure pH while taking soil samples at a pre-selected depth between 0 and 20 cm every 8 s. Based on the results reported by Adamchuk et al. (1999), a commercial soil pH mapping system was developed by Veris Technologies, Salina, Kansas, USA (Collings et al., 2003). The accuracy of the system was evaluated by comparing collected pH data to laboratory analysis, with r = 0.79 between sensor and laboratory measurements. When using the soil pH mapping system for the establishment of site-specific lime recommendations, Lund et al. (2004) reported that on-the-go mapping of soil pH provided improved accuracy of lime prescription maps, showing a smaller lime estimation error of 1,340 kg ha^{-1} than that obtained using 1 ha grid sampling (2,109 kg ha^{-1}) when lime recommendations were calculated based on buffer pH laboratory tests. Feasibility was further studied by Adamchuk et al. (2007), who used the soil pH mapping system to plan variable-rate liming for eight production fields in six of the United States. The pH maps developed were compared with corresponding maps generated using conventional

grid sampling. They reported that a field-specific bias in overall error estimates of 0.4 pH units or greater could be reduced to less than 0.3 pH units through site-specific calibration. Additionally, Staggenborg et al. (2007) tested the feasibility of using the commercial mobile soil pH system on two fields in Kansas, one with a uniform soil and the other with six different soil types. Results showed that the real-time system provided more accurate estimates at the 0 to 7.5 cm depth (r^2 = 0.75 to 0.83) than at the 7.5 to 15 cm depth (r^2 = 0.53 to 0.79). In addition, the inclusion of soil electrical conductivity (EC) as a covariable improved pH estimates in the field with six different soil types, but not the uniform field.

Adamchuk et al. (2005) investigated the suitability of the DSM approach for soil K, NO_3, and Na as well as pH. The r^2 of regressions between values determined by ISE and corresponding reference methods were 0.93~0.96, 0.61~0.62, 0.41~0.51, and 0.1 for soil pH, K, NO_3-N, and Na, respectively. They stated that the reason for decreased accuracy for K, NO_3-N and Na was a lower level of variability of the sensed property in the soil samples tested. Sethuramasamyraja et al. (2007; 2008) developed an agitated soil measurement (ASM)-based integrated system that placed ISEs into a suspension of soil and water. They investigated the effects of various measurement parameters, such as soil-water ratio and quality of water for electrode rinsing, on sensor performance and evaluated the system for on-the-go mapping of soil pH, soluble potassium and residual nitrate contents in 15 Nebraska soils under laboratory conditions. They reported that a 1:1 soil:water ratio and tap water for electrode rinsing were usable for simultaneous measurement of pH, K, and NO_3 with ion-selective electrodes. Calibration parameters were stable during each test for pH and K electrodes. However, significant drift was observed for the NO_3 electrode. Both accuracy and precision errors were low with good correlations to the reference measurements (r^2 = 0.67~0.98 for means).

Several researchers have used mobilized reflectance spectroscopy for in-situ monitoring of soil chemical properties in fields. Mouazen et al. (2007) developed a soil sensing system consisting of a soil penetration unit and an optical probe to measure soil carbon, moisture content, pH and P. Two different sets of VIS-NIR spectral data were collected in the laboratory and field. Calibration models were developed using the laboratory data, and the developed models were validated using the field measurement spectra. Estimation of moisture content was satisfactory (r^2 = 0.89) whereas the

estimates of C, pH and P were not as well matched to the corresponding reference values (r^2 = 0.73, 0.71, and 0.69, respectively). Christy (2008) evaluated NIR spectroscopy (920 to 1,718 nm) for real-time, on-the-go measurement of soil chemical properties. The system was evaluated in eight fields in central Kansas where spectral data were collected on transects and calibration soil samples were obtained at multiple locations in each field. Of the soil properties evaluated, best estimates were obtained for organic matter (OM), with a RMSE of 0.52% and an r^2 of 0.67 between the laboratory measurements and NIR estimates. Soil P estimates were also fairly good (RMSE = 41 mg kg^{-1}, r^2 = 0.65), while K estimates were poor (RMSE = 146 mg kg^{-1}, r^2 = 0.26).

Overall, there has been much progress in on-the-go soil nutrient sensing based on ion-selective electrode technology. Notably, a soil pH mapping system is now commercially available after a sequence of research studies. Also, an automated field monitoring system with potential as a real-time soil NO_3-N analyzer has recently been improved with an automated sampler that provides precise estimates of the sample mass. On the other hand, on-the-go sensing of soil chemical properties using reflectance spectroscopy is somewhat less promising. Although good results have been reported in some cases, a number of calibration and accuracy issues remain to be addressed.

Directions and Considerations in Nutrient Sensing

Sensor Fusion

As noted above, there are several limitations to current on-the-go nutrient sensing systems. Although electrochemical systems can directly measure soil nutrient levels, there are implementation issues. Direct electrochemical measurement of moist soil, while shown to be viable for pH and perhaps nitrate, seems to be less feasible for the other soil macronutrients. Thus, a complex set of steps is generally needed to acquire a sample from the field, create a soil slurry or extract, and then complete the measurement. Spectroscopic sensing, while less invasive, generally measures soil nutrients indirectly, through correlations with other soil properties. Thus, local calibrations are generally necessary and results have been of variable accuracy.

One potential approach for improved accuracy is sensor fusion, whereby readings from multiple, functionally different sensors are combined to estimate the soil properties of

interest. For example, Christy et al. (2004) reported on a mobile sensor platform (Fig. 3) that combined the soil pH sensing system described by Collings et al. (2003) with soil apparent electrical conductivity (EC) sensing. As EC provides a strong indication of soil texture variations (Sudduth et al., 2005), the combination of the pH and EC data was useful for establishing lime requirements. An NIR reflectance sensor was later added to this multi-sensor platform (Christy, 2008).

In a laboratory-based example of sensor fusion, La et al. (2008) collected both ISE and spectral reflectance data on 37 surface soil samples from the US states of Missouri and Illinois. Although ISE estimates of P and K were of good accuracy ($r^2 \geq 0.87$), they were further improved ($r^2 \geq 0.95$) by including both ISE and spectral data in the PLSR calibration model. The authors attributed the increased accuracy to the ability of the spectral data to provide an estimate of soil texture.

Sensor Calibration

Widespread adoption of on-the-go soil nutrient sensing may be somewhat limited by the degree to which precise sampling and rapid extraction of the macronutrients in the sample can be achieved in a real-time system. Because extraction efficiency is strongly affected by the extraction time and because the time required for complete extraction may not be feasible in a real-time system, this approach may provide different results as compared to traditional soil testing methods. In this regard, research will be needed to calibrate sensor-based nutrient measurements against plant nutrient response, so that agronomists and growers gain confidence in the applicability of the new methods. Such a calibration might be implemented in the same way that past calibrations to standard laboratory measurements were developed. However, this process would require numerous field experiments with different crops and soil types. An alternative method, whereby sensor measurements were directly calibrated to laboratory nutrient measurements across a broad range of conditions, might be preferable. Although the calibration to plant response would be an indirect one with this approach, it would be considerably less costly and time-consuming.

Integration with Fertilizer Application Equipment

Control decisions for variable rate application can be implemented either on-line or off-line. In the on-line, or sensor-based approach, the controlled equipment incorporates onboard sensors and the sensor data are used immediately for automatic control. In the off-line, or map-based approach, data are collected and stored in one operation, and the controlled equipment uses the information in a separate field operation. The map-based approach allows more flexibility in data manipulation and preprocessing but requires multiple field operations. Most systems currently available are map-based, but more on-line systems will likely become available as real-time sensing technologies become more mature. Hybrid systems which rely on a combination of both mapped and real-time data may also come into more widespread use.

Development and implementation of a variable-rate application system presents a number of engineering challenges. Physical connectivity and data flow in such a system can be quite complex (Fig. 4). The general system consists of both office tasks and vehicle tasks. Office tasks include interpreting input data, developing management plans, and determining application rate maps. Vehicle tasks include using these application rate maps in conjunction with onboard sensors and actuators to apply fertilizer, chemicals or inputs in the field, along with any real-time sensing that may be employed. In any given system, the elements shown in this general schematic (Fig. 4) may not be present. For example, a system may or may not include on-line sensors and may or may not generate an actual application rate map. It is worth noting that the information to drive a map-based system could also come from on-the-go sensor measurements. Decoupling the sensing and application operations might make sense if sensor operating requirements, such as a long delay time for sensing nutrient levels in a soil extract, precluded sensing and application in the same operation.

Summary

Traditionally, soil nutrient measurements have been carried out in a central laboratory, involving time-consuming sampling, transportation and storage steps. Within-field monitoring of N, P, and K nutrients is preferable due to the potential for a higher density of measurements at a relatively low cost, allowing more efficient mapping of soil nutrient variability for variable-rate nutrient management. Optical diffuse reflectance in visible and near-infrared wavelength ranges has been used as a non-destructive

method to rapidly quantify soil properties for site-specific management. However, application of optical sensor technology for on-site measurements of soil nutrients has been limited, primarily due to relatively poor estimates at critical macronutrient levels for soil fertility management, as well as strong effects of soil type. In principle, electrochemical sensing with ion-selective electrodes or ion-selective field effect transistors is a promising approach for real-time analysis because of rapid response, direct measurement of the analyte with a wide range of sensitivity, simplicity and portability. The disadvantage of on-the-go sensors based on ion-selective technology is that soil sampling and nutrient extraction are required, increasing the complexity of the system and the time required for a measurement.

Commercialization of on-the-go soil macronutrient sensing will require additional research and development efforts to integrate soil sample collection, automated sample preparation, and nutrient analysis. Furthermore, use of a sensor array capable of simultaneously determining several analytes, such as soil macronutrients and pH, would reduce sample processing time, sample volume and reagent consumption. Sensor fusion using the multiple data streams available from such a sensor array, perhaps along with data from optical or other auxiliary sensors, should be considered as a potential way of improving measurement accuracy.

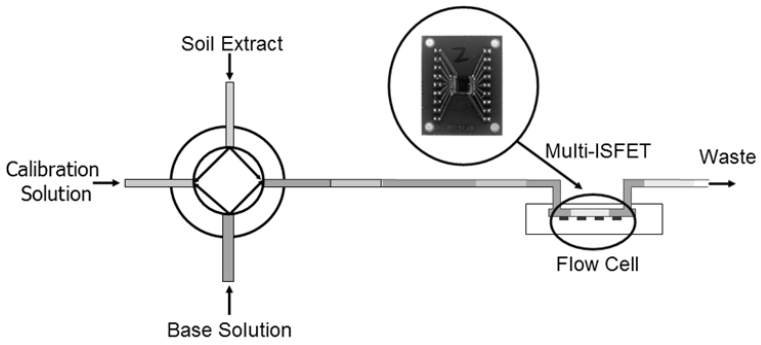

Fig. 1. Schematic of an ion-selective field effect transistor (ISFET) – flow injection analysis (FIA) system. The soil extract sample, calibration and base solutions are sequentially introduced through a flow injection line system with multiple inlets, and are transported to a multi-ISFET chip with outputs that continuously change due to the passage of the sample through the flow cell.

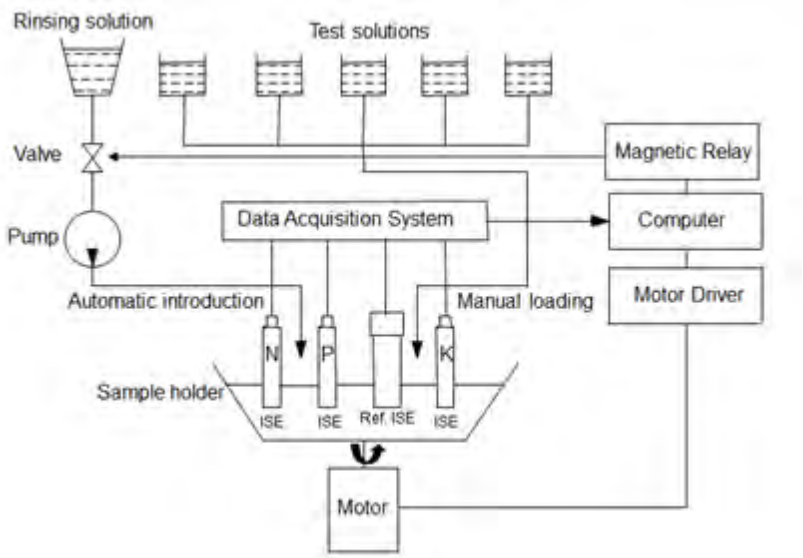

Fig. 2. Schematic diagram of a test stand for multiple electrode tests (from Kim et al., 2013).

Fig. 3. Commercial sensor system integrating soil electrical conductivity and pH mapping (Veris pH manager, Veris Technologies, Salina, Kansas, USA).

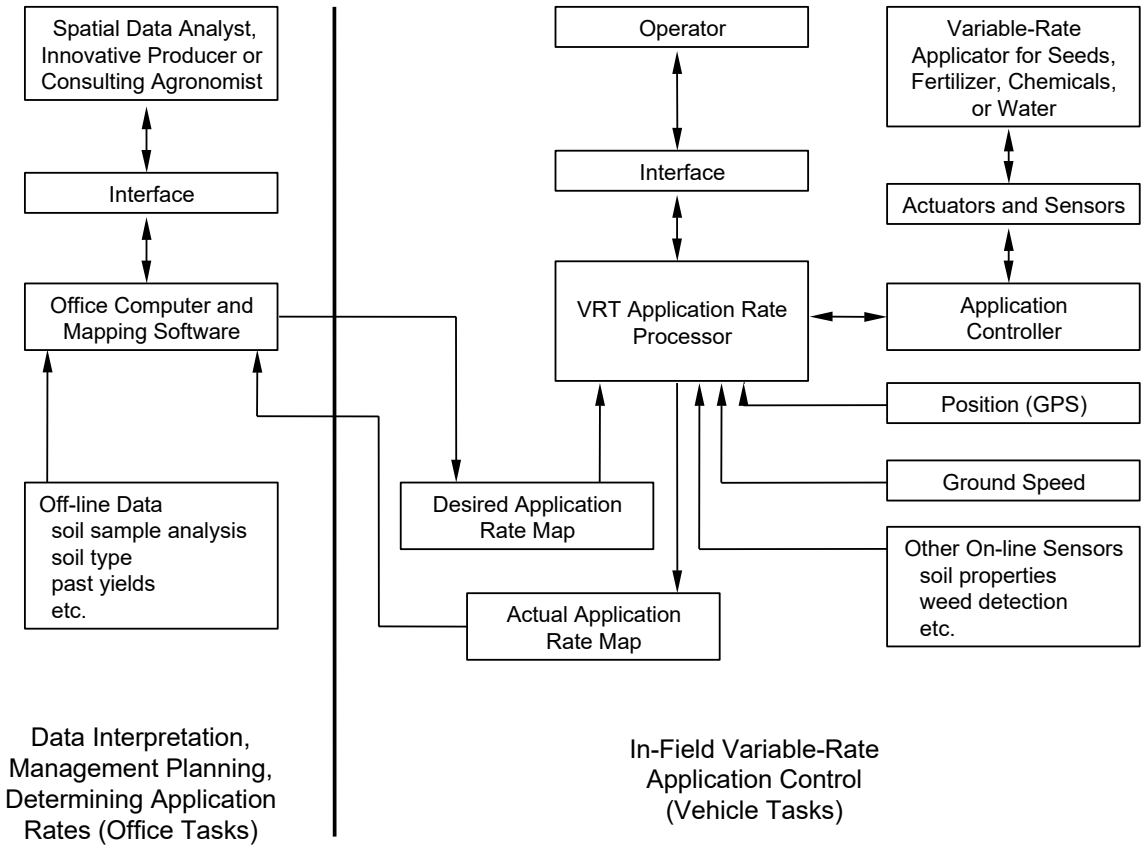

Fig. 4. Generalized schematic of data flow in a variable-rate application system.

References

Adamchuk, V.I. 2002. Feasibility of on-the-go mapping of soil nitrate and potassium using ion-selective electrodes. ASAE Paper No. 02-1183. ASAE, St. Joseph, MI.

Adamchuk ,V.I., J.W. Hummel, M.T. Morgan, and S.K. Upadhyaya. 2004. On-the-go soil sensors for precision agriculture. Comp. Electron. Agric. 44:71-91.

Adamchuk, V.I., E.D. Lund, T.M. Reed, and R.B. Ferguson. 2007. Evaluation of an on-the-go technology for soil pH mapping. Precision Agric. 8:139-149.

Adamchuk, V.I., E.D. Lund, B. Sethuramasamyraja, M.T. Morgan, A. Dobermann, and D.B. Marx. 2005. Direct measurement of soil chemical properties on-the-go using ion-selective electrodes. Comput. Electron. Agric. 48:272-294.

Adamchuk, V.I., M.T. Morgan, and D.R. Ess. 1999. An automated sampling system for measuring soil pH. Trans. ASAE 42:885-891.

Adsett, J.F., J.A. Thottan, and K.J. Sibley. 1999. Development of an automatic on-the-go soil nitrate monitoring system. Appl. Eng. Agric. 15: 351-356.

Artigas, J., A. Beltran, C. Jimenez, A. Baldi, R. Mas, C. Dominguez, and J. Alonso. 2001. Application of ion selective field effect transistor based sensors to soil analysis. Comp. Electron. Agric. 31:281-293.

Bakker , E. 2004. Electrochemical sensors. Anal. Chem. 76:3285-3298.

Birrell, S.J., and J.W. Hummel. 2000. Membrane selection and ISFET configuration evaluation for soil nitrate sensing. Trans. ASAE 43:197-206.

Birrell, S.J., and J.W Hummel. 2001 Real-time multi ISFET/FIA soil analysis system with automatic sample extraction. Comput. Electron. Agric. 32:45-67.

Blackmer, A.M., D. Pottker, M.E. Cerrato, and J. Webb. 1989. Correlations between soil nitrate concentrations in late spring and corn yields in Iowa. J. Prod. Agric. 2:103-109.

Bogrekci, I. and W.S. Lee. 2005. Spectral soil signatures and sensing phosphorus. Biosyst. Eng. 92:527-533.

Bogrekci, I., and W.S. Lee. 2006. Effects of soil moisture content on absorbance spectra of sandy soils in sensing phosphorus concentrations using UV-VIS-NIR spectroscopy. Trans. ASABE 49:1175-1180.

Bogrekci, I., and W.S. Lee. 2007. Comparison of ultraviolet, visible, and near infrared sensing for soil phosphorus. Biosyst. Eng. 96:293-299.

Brouder, S.M., M. Thom, V.I. Adamchuk, and M.T. Morgan. 2003. Potential uses of ion-selective potassium electrodes in soil fertility management. Commun. Soil Sci. Plant Anal. 34: 2699-2726.

Buchholz, D.D., J.R. Brown, J.D. Garret, R.G. Hanson, and H.N. Wheaton. 1983. Soil Test Interpretations and Recommendations Handbook. University of Missouri, Department of Agronomy, Revised 12/92 edition. Columbia, MO.

Buhlmann, P., E. Pretsch, and E. Bakker. 1998. Carrier-based ion-selective electrodes and bulk optodes. 2. Ionophores for potentiometric and optical sensors. Chem. Rev. 98: 1593-1687.

Bullock, D.G., R.G. Hoeft, P. Dorman, T. Macy, and R. Olson. 1994. Nutrient management with intensive soil sampling and differential fertilizer spreading. Better Crops 78:10-12.

Carey, C.M., and W.B. Riggan. 1994. Cyclic polyamine ionophores for use in a dibasic-phosphate-selective electrode. Anal. Chem. 66:3587-3591.

Carr, P.M., G.R. Carlson, J.S. Jacobsen, G.A. Nielsen, and E.O. Skogley. 1991. Farming soils, not fields: a strategy for increasing fertilizer profitability. J. Prod. Agric. 4:57-61.

Chang, C.W., D.A. Laird, M.J. Mausbach, and C.R. Hurburgh Jr. 2001. Near-infrared reflectance spectroscopy- principal component regression analysis of soil properties. Soil Sci. Soc. Am. J. 65:480-490.

Chen, Z.L., R. De Marco, and P.W. Alexander. 1997. Flow-injection potentiometric detection of phosphates using a metallic cobalt wire ion-selective electrode. Anal. Commun. 34:93-95.

Chen, Z.L., P. Grierson, and M.A. Adams. 1998. Direct determination of phosphate in soil extracts by potentiometric flow injection using a cobalt wire electrode. Anal. Chim. Acta 363:191-197.

Christy, C.D. 2008. Real-time measurement of soil attributes using on-the-go near-infrared reflectance spectroscopy. Comput. Electron. Agric. 61:10-19.

Christy, C.D., K. Collings, P. Drummond, and E. Lund. 2004. A mobile sensor platform for measurement of soil pH and buffering. ASAE Paper No. 041042. ASAE, St. Joseph, MI.

Collings, K., C. Christy, E. Lund, and P. Drummond. 2003 Developing an automated soil pH mapping system. ASAE Paper No. MC03-205. ASAE, St. Joseph, MI.

Dalal, R.C., and R.J. Henry. 1986. Simultaneous determination of moisture, organic carbon, and total nitrogen by near infrared reflectance spectrophotometry. Soil Sci. Soc. Am. J. 50:120-123.

Daniel, K.W., N.K. Tripathi, and K. Honda. 2003. Artificial neural network analysis of laboratory and in situ spectra for the estimation of macronutrients in soils of Lop Buri (Thailand). Aust. J. Soil Res. 41:47-59.

Eggins, B.R. 2002. Chemical Sensors and Biosensors. John Wiley and Sons, West Sussex, U.K.

Ehsani, M.R., S.K. Upadhyaya, D. Slaughter, L.V. Protsailo, and W.R. Fawcett. 1999. A NIR technique for rapid determination of soil mineral nitrogen. Precis. Agric. 1:217-234.

Engblom, S.O. 1998. The phosphate sensor. Biosens. Bioelectron. 13:981-994.

Engblom, S.O. 1999. Determination of inorganic phosphate in a soil extract using a cobalt electrode. Plant Soil 206:173-179.

Gallardo, J., S. Alegret, and M.D. Valle. 2004. A flow-injection electronic tongue based on potentiometric sensors for the determination of nitrate in the presence of chloride. Sensors Actuators B 101:72-80.

Ge, Y., J.A. Thomasson, C.L. Morgan, and S.W. Searcy. 2007. VNIR diffuse reflectance spectroscopy for agricultural soil property determination based on regression-kriging. Trans. ASABE 50:1081-1092.

Glazier, S.A., and M.A. Arnold. 1988. Phosphate-selective polymer membrane electrode. Anal. Chem. 60:2540-2542.

Glazier, S.A., and M.A. Arnold. 1991. Selectivity of membrane electrodes based on derivatives of dibenzyltin dichloride. Anal. Chem. 63:754-759.

He, Y., M. Huang, A. Garcia, A. Hernandez, and H. Song. 2007. Prediction of soil macronutrients content using near-infrared spectroscopy. Comput. Electron. Agric. 58:144-153.

He, Y., H.Y. Song, A.G. Pereira, and A.H. Gomez. 2005. Measurement and analysis of soil nitrogen and organic matter content using near-infrared spectroscopy techniques. J. Zhejiang Univ. Sci. B 6:1081-1086.

Jahn, B.R., P.A. Brooksby and S.K. Upadhyaya. 2005. Wavelet-based spectral analysis for soil nitrate content measurement. Trans. ASAE 48:2065-2071.

Jahn, B.R., R. Linker, S.K. Upadhyaya, A. Shaviv, D.C. Slaughter, and I. Shmulevich, I. 2006. Mid-infrared spectroscopic determination of soil nitrate content. Biosyst. Eng. 94:505-515.

Kim, H.J., J.W. Hummel, and S.J. Birrell. 2006. Evaluation of nitrate and potassium ion-selective membranes for soil macronutrient sensing. Trans. ASABE 49:597-606.

Kim, H.J., J.W. Hummel, K.A. Sudduth, and S.J. Birrell. 2007a. Evaluation of phosphate ion-selective membranes and cobalt-based electrodes for soil nutrient sensing. Trans. ASABE 50:215-225.

Kim, H.J., J.W. Hummel, K.A. Sudduth, and P.P. Motavalli. 2007b. Simultaneous analysis of soil macronutrients using ion-selective electrodes. Soil Sci. Soc. Am. J. 71:1867-1877.

Kim, H.J., K.A. Sudduth, and J.W. Hummel. 2009. Soil macronutrient sensing for precision agriculture. J. Environ. Monit. 11:1810-1824.

Kim, H.J., K.A. Sudduth, J.W. Hummel, and S.T. Drummond. 2013. Validation testing of a soil macronutrient sensing system. Trans. ASABE 56:23-31.

Kitchen, N.R., K.A. Sudduth, D.B. Myers, R.E. Massey, E.J. Sadler, R.N. Lerch, J.W. Hummel, and H.L. Palm. 2005. Development of a conservation-oriented precision agriculture system: Crop production assessment and plan implementation. J. Soil Water Conserv. 60:421-430.

Kubo, I. 2002. Potentiometric phosphate-sensing system utilizing phosphate-binding protein. Anal. Bioanal. Chem. 372:273-275.

La, W.J., K.A. Sudduth, S.O. Chung, and H.J. Kim. 2008. Spectral reflectance estimates of surface soil physical and chemical properties. ASABE Paper No. 084242. ASABE, St. Joseph, MI.

Lee, K.S., D.H. Lee, I.K. Jung, S.O. Chung, and K.A. Sudduth. 2008. Sampling and calibration requirements for optical reflectance soil property sensors for Korean paddy soils. J. Biosyst. Eng. 33:260-268.

Lee, W.S., J.F. Sanchez, R.S. Mylavarapu, and J.S. Choe. 2003. Estimating chemical properties of Florida soils using spectral reflectance. Trans. ASAE 46:1443-1453.

Linker, R., A. Kenny, A. Shaviv, L. Singher, and I. Shmulevich. 2004. Fourier transform infrared-attenuated total reflection nitrate determination of soil pastes using principal component regression, partial least squares, and cross-correlation. Appl. Spectrosc.58:516-520.

Linker, R., I. Shmulevich, A. Kenny, and A. Shaviv. 2005. Soil identification and chemometrics for direct determination of nitrate in soils using FTIR-ATR mid-infrared spectroscopy. Chemosphere 61:652-658.

Linker, R., M. Weiner, I. Shmulevich, and A. Shaviv. 2006. Nitrate determination in soil pastes using attenuated total reflectance mid-infrared spectroscopy: Improved accuracy via soil identification. Biosyst. Eng. 94:111-118.

Liu, D., W.C. Chen, R.H. Yang, G.L. Shen and R.Q. Yu. 1997. Polymeric membrane phosphate sensitive electrode based on binuclear organotin compound. Anal. Chim. Acta 338: 209-214.

Lund, E.D., K.L. Collings, P.E. Drummond, C.D. Christy and V.I. Adamchuck. 2004. Managing pH variability with on-the-go pH mapping. In: Proc. Seventh Intl. Conf. on Precision Agriculture. ASA, CSSA, and SSSA, Madison, WI. p. 120-132.

Maleki, M.R., L.Van Holm, H. Ramon, R. Merckx, J.De Baerdemaeker, and A.M. Mouazen. 2006. Phosphorus sensing for fresh soils using visible and near infrared spectroscopy. Biosyst. Eng. 95:425-436.

Mouazen, A.M., J. De Baerdemaeker, and H. Ramon. 2005. Towards development of on-line soil moisture content sensor using a fibre-type NIR spectrophotometer. Soil Till. Res. 80:171-183.

Mouazen, A.M., B. Kuang, J. De Baerdemaeker, and H. Ramon. 2010. Comparison among principal component, partial least squares and back propagation neural network analyses for accuracy of measurement of selected soil properties with visible and near infrared spectroscopy. Geoderma 158:23-31.

Mouazen, A.M., M.R. Maleki, J. De Baerdemaeker, and H. Ramon. 2007. On-line measurement of some selected soil properties using a VIS-NIR sensor. Soil Till. Res. 93:13-27.

Nielson, H.J., and E.H. Hansen. 1976. New nitrate ion-selective electrodes based on quaternary ammonium compounds in nonporous polymer membranes. Anal. Chim. Acta 85:1-16.

Page, T., P.M. Haygarth, K.J. Beven, A. Joynes, T. Butler, C. Keeler, J. Freer, P.N. Owens, and G.A. Wood. 2005. Spatial variability of soil phosphorus in relation to the topographic index and critical source areas: sampling for assessing risk to water quality. J. Environ. Qual. 34: 2263-2277.

Price, R.R., J.W. Hummel, S.J. Birrell, and I.S. Ahmad. 2003. Rapid nitrate analysis of soil cores using ISFETs. Trans. ASAE 46:601-610.

Ruffo, M.L., G.A. Bollero, R.G. Hoeft, and D.G. Bullock. 2005. Spatial variability of the Illinois soil nitrogen test: implications for soil sampling. Agron. J. 97:1485-1492.

Sasaki, S., S. Ozawa, D. Citterio, K. Yamada, and K. Suzuki. 2004. Organic tin compounds combined with anionic additives- an ionophore system leading to a phosphate ion-selective electrode. Talanta 63:131-134.

Schepers, J.S., and M.R. Schlemmer 1998. Influence of grid sampling points on fertilizer recommendations p. ii117-ii121, In: Proc. First Intl. Conf. on Geospatial Information in Agriculture and Forestry. Lake Buena Vista, FL. 1-3 June, 1998. ERIM International Inc, Ann Arbor, MI.

Schirrmann, M., R. Gebbers, E. Kramer, and J. Seidel. 2011. Soil pH mapping with an on-the-go sensor. Sensors 11:573-598.

Sethuramasamyraja, B., V.I. Adamchuk, A. Dobermann, D.B. Marx, D.D. Jones, and G.E. Meyer. 2008. Agitated soil measurement method for integrated on-the-go mapping of soil pH, potassium and nitrate contents. Comput. Electron. Agric. 60:212-225.

Sethuramasamyraja, B., V.I. Adamchuk, D.B. Marx, A. Dobermann, G.E. Meyer, and D.D. Jones. 2007. Analysis of an ion-selective electrode based methodology for integrated on-the-go mapping of soil pH, potassium, and nitrate contents. Trans. ASABE 50:1927-1935.

Sibley, K.J., J.F. Adsett, and P.C. Struik. 2008. An on-the-go soil sampler for an automated soil nitrate mapping system. Trans. ASABE 51:1895-1904.

Sibley, K.J., T. Astatkie, G. Brewster, P.C. Struik, J.F. Adsett, and K. Pruski. 2009. Field-scale validation of an automated soil nitrate extraction and measurement system. Precis. Agric. 10:162-174.

Sinfield, J.V., D. Fagerman, and O. Colic. 2010. Evaluation of sensing technologies for on-the-go detection of macro-nutrients in cultivated soils. Comput. Electron. Agric. 70:1-18.

Staggenborg, S.A., M. Carignano, and L. Haag. 2007. Predicting soil pH and buffer pH in situ with a real-time sensor. Agron. J. 99:854-861.

Sudduth, K.A., J.W. Hummel and S.J. Birrell. 1997. Sensors for site-specific management. In: F. J. Pierce and E. J. Sadler, editors, The state of site-specific management for agriculture. ASA, CSSA, and SSSA, Madison, WI. p. 183-210.

Sudduth, K.A., N.R. Kitchen, and R.J. Kremer. 2009. VNIR spectroscopy estimation of soil quality indicators. ASABE Paper No. 097019. ASABE, St. Joseph, MI.

Sudduth, K.A., N.R. Kitchen, W.J. Wiebold, W.D. Batchelor, G.A. Bollero, D.G. Bullock, D.E. Clay, H.L. Palm, F.J. Pierce, R.T. Schuler, and K.D. Thelen. 2005. Relating apparent electrical conductivity to soil properties across the north-central USA. Comput. Electron. Agric. 46:263-283.

Thottan, J., J.F. Adsett, K.J. Sibley, and C.M. MacLeod. 1994. Laboratory evaluation of the ion selective electrode for use in an automated soil nitrate monitoring system. Commun. Soil Sci. Plant Anal. 25:3025-3034.

Udelhoven, T., C. Emmerling, and T. Jarmer. 2003. Quantitative analysis of soil chemical properties with diffuse reflectance spectrometry and partial least-square regression: A feasibility study. Plant Soil 251:319-329.

Upadhyaya, S.K., S. Shafii, and D. Slaughter. 1994. Sensing soil nitrogen for site specific crop management (SSCM). ASAE Paper No. 941055. ASAE, St. Joseph, MI.

Vadas, P.A., P.J.A. Kleinman, and A.N. Sharpley. 2004. A simple method to predict dissolved phosphorus in runoff from surface-applied manures. J. Environ. Qual. 33:749-756.

Van Lierop, W. 1986. Soil nitrate determination using the Kelowna multiple element extractant. Commun. Soil Sci. Plant Anal. 17:1311-1329.

Van Lierop, W. 1988. Determination of available phosphorus in acid and calcareous soils with the Kelowna multiple-element extractant. Soil Sci. 146:284-291.

Viscarra Rossel, R.A., and C. Walter. 2004. Rapid, quantitative and spatial field measurements of soil pH using an ion sensitive field effect transistor. Geoderma 119:9-20.

Viscarra Rossel, R.A., D.J.J. Walvoort, A.B. McBratney, L.J. Janik, and J.O. Skjemstad. 2006. Visible, near infrared, mid infrared or combined diffuse reflectance spectroscopy for simultaneous assessment of various soil properties. Geoderma 131:59-75.

Wollenhaupt, N.C., D.J. Mulla and C.A.G. Crawford. 1997. Soil sampling and interpolation techniques for mapping spatial variability of soil properties. In: F. J. Pierce and E. J. Sadler, editors, The state of site-specific management for agriculture. ASA, CSSA, and SSSA, Madison, WI. p. 19-53.

Wroblewski, W., K. Wojciechowski, A. Dybko, Z. Brzozka, R.J.M. Egberink, B.H.M. Snellink-Ruel, and D.N. Reinhoudt. 2000. Uranyl salophenes as ionophores for phosphate-selective electrodes. Sens. Actuators B 68:313-318.

Wroblewski, W., K. Wojciechowski, A. Dybko, Z. Brzozka, R.J.M. Egberink, B.H.M. Snellink-Ruel, and D.N. Reinhoudt. 2001. Durable phosphate-selective electrodes based on uranyl salophenes. Anal. Chim. Acta 432:79-88.

Xiao, D., H.Y. Yuan, J. Li, and R.Q. Yu. 1995. Surface-modified cobalt-based sensor as a phosphate-sensitive electrode. Anal. Chem. 67:288-291.

REMOTE ESTIMATION OF NITROGEN AND CHLOROPHYLL CONTENTS IN MAIZE AT LEAF AND CANOPY LEVELS

M. Schlemmer[1,2], A. Gitelson[3*], J. Schepers[1], R. Ferguson[1], Y. Peng[3], J. Shanahan[1,4], D. Rundquist[3]

[1]Department of Agronomy and Horticulture, University of Nebraska-Lincoln, Lincoln, NE 68583, USA.
[2]Currently with Bayer CropScience, Lincoln, NE 68583, USA
[3]CALMIT, School of Natural Resources, University of Nebraska-Lincoln, Lincoln, NE 68583, USA.
[4]Currently with Pioneer Hi-Bred International, Johnston, IA 50131, USA.
*Corresponding author: agitelson2@unl.edu.

Abstract

Leaf and canopy nitrogen (N) status relates strongly to leaf and canopy chlorophyll (Chl) content. Remote sensing is a tool that has the potential to assess N content at leaf, plant, field, regional and global scales. In this study, remote sensing techniques were applied to estimate N and Chl contents of irrigated maize (*Zea mays* L.) fertilized at five N rates. Leaf N and Chl contents were determined using the red-edge chlorophyll index with R^2 of 0.74 and 0.94, respectively. Results showed that at the canopy level, Chl and N contents can be accurately retrieved using green and red edge Chl indices using near infrared (780-800 nm) and either green (540-560 nm) or red-edge (730-750 nm) spectral bands. Spectral bands that were found optimal for Chl and N estimations coincide well with the red-edge band of the MSI sensor onboard the near future Sentinel-2 satellite. The coefficient of determination for the relationship between the red-edge chlorophyll index, simulated in Sentinel-2 bands, and Chl and N content was 0.90 and 0.87, respectively.

Keywords*:* Chlorophyll, nitrogen, reflectance, remote sensing, vegetation indices.

Abbreviations: Chl – chlorophyll; N – nitrogen; NDVI – Normalized Difference Vegetation Index; EVI – Enhanced Vegetation Index, MTCI - MERIS terrestrial chlorophyll index, CI – chlorophyll index.

Introduction

Numerous leaf-level studies have demonstrated a strong link between nitrogen (N) content and photosynthetic activity (Field and Mooney, 1986; Wullschleger, 1993). Kergoat et al. (2008) analyzed the relationship between leaf N content and the eddy covariance CO_2 flux measurements obtained at a range of diverse sites located in mid to high latitudes, encompassing managed and unmanaged stands, mono- and pluri-specific canopies. They concluded that leaf N content was a strong factor influencing both optimum canopy light use efficiency and canopy photosynthesis rate. Gitelson et al. (2003a, 2006a) found a close, consistent relationship between gross primary productivity (GPP) and total plant Chl content in maize (*Zea mays* L.) and soybean (*Glycine max* (L.) Merr.). Moreover, it was shown that despite great differences in leaf structure and canopy architecture in the C_3 and C_4 crops studied, the relationship between GPP and Chl content was not species specific. Thus, monitoring of N and Chl content provides important information about crop photosynthetic status.

Evans (1983, 1989) demonstrated the partitioning of N between protein fractions of soluble and thylakoid proteins remained unaltered with increasing N content. Therefore, changes in leaf N content will result in similar changes to the thylakoid pigment protein complex, that consists primarily of Chl, and the carbon fixing soluble protein enzyme activity of ribulose 1,5-bisphosphate (RuBP). An accurate measure of one component can provide estimates of the other two. Walters (2003) found a very close relationship between leaf Chl and N contents in maize, and also between leaf N content and crop yields. Baret et al. (2007) found that canopy Chl content was well suited for quantifying canopy-level N content. They concluded that canopy Chl content was a physically sound quantity that represents the optical path in the canopy where absorption by Chl dominates the radiometric signal. Thus, absorption by Chl provides the necessary link between remote sensing observations and canopy-state variables that are used as indicators of N status and photosynthetic capacity.

Reflectance in the green and red-edge spectral regions was shown to be optimal for non-destructive estimation of leaf Chl content in a wide range of its variation (Blackburn, 2006; Gitelson, 2011a; Hatfield et al., 2008; le Maire et al., 2004; Richardson et al., 2002; Ustin et al., 2009). Féret et al. (2011), using a large set of leaf data collected from all over the world, showed that the Prospect 5 radiative transfer

model provided an accurate estimation of leaf Chl content using reflectance in the red-edge and near infrared spectral regions.

However, at canopy level the estimation of Chl and N content is much more problematic and only a few papers have demonstrated a way to estimate them (Gitelson et al, 2005; Gitelson, 2011b; Lee et al., 2008; Sripada et al., 2008; Takahashi et al., 2000; Tian et al., 2011; Xue et al., 2004; Zhu et al., 2008;). Among recently published results, it is worthy to note technique for the accurate assessment of N content in rice using hyperspectral measurements (Inoue et al., 2012). They found that the combination of reflectance values at two wavebands (near infrared at 825 nm and red-edge around 735 nm) has a significant and consistent role in the assessment of rice N content. High predictive accuracy was achieved when using models involving the normalized difference or the ratio of reflectance at these wavebands. Clevers and Kooistra (2012), using PROSAIL simulations, showed that the red-edge chlorophyll index ($CI_{red\text{-}edge}$, Table 1) with a wide red-edge band (700-730 nm) was linearly related to the canopy Chl content over the full range of potential Chl values. At their study sites, the $CI_{red\text{-}edge}$ was also found to be a good and linear estimator of canopy N content in both grassland and potato cropping systems.

Clevers and Gitelson (2012) focused on the potential of Sentinel-2 (http://www.esa.int/Our_Activities/Observing_the_Earth/GMES/Sentinel-2) and Sentinel-3 (http://www.esa.int/Our_Activities/Observing_the_Earth/GMES/Sentinel-3) satellites for estimating total crop and grassland Chl and N contents. The Multi Spectral Instrument (MSI) on the Sentinel-2 satellite system has bands centered at 560 nm (green), 665 nm (red), 705 and 740 nm (red edge) and 783 nm (NIR). The Ocean and Land Colour Instrument (OLCI) on the Sentinel-3 satellite system has one spectral band in red edge region centered at 709 nm. Clevers and Gitelson (2012) found that the $CI_{red\text{-}edge}$, the green chlorophyll index, CI_{green}, and the MERIS terrestrial chlorophyll index, MTCI (Table 1) were accurate and linear estimators of canopy Chl and N contents. Bands of MSI in the green and red edge are well positioned for deriving these indices. Results confirm the particular importance of the Sentinel-2 sensor for agricultural applications because it provides access to green and red-edge waveband data with high spatial resolution of 20 m.

Importantly, papers describing non-destructive N and Chl content retrieval employed spectral bands located far from the main red absorption band of Chl where absorption saturates at low-to-moderate Chl values. Use of either green or red-edge spectral regions makes it possible to avoid this saturation, retaining a high sensitivity to changes in Chl content (Gitelson, 2011a, 2011b; Hatfield et al., 2008; Ustin et al., 2009).

Collectively, the previously mentioned studies indicate that the use of remote sensing techniques may provide accurate measures of N content. This paradigm suggests that absorption by Chl provides the necessary link between remote sensing observations and canopy-state variables that are used as indicators of N status (Baret et al., 2007). However, previous studies dealt separately with N or Chl content estimation and, thus, cannot test the concept. To prove this concept, performance of remote sensing techniques to estimate *both Chl and N* contents in leaf and canopy should be investigated. This study evaluates performance of remote sensing techniques to estimate both N and Chl leaf and canopy contents in maize and, specifically, accuracy of N and Chl estimation using near future satellites Sentinel-2 and Sentinel-3. Firstly, we established relationships between N and Chl contents at the leaf and canopy levels and then tested the performance of Chl-related vegetation indices to retrieve N and Chl contents in both leaf and canopy scenarios. Secondly, we identified optimal spectral ranges in the green and the red-edge regions allowing accurate estimation of N and Chl contents in maize over a wide range of leaf area index values. Finally, we assessed accuracy of suggested technique using spectral bands of Sentinel-2, which allows monitoring of Chl and N contents in crops with high spatial and temporal resolutions.

Materials and Methods

Field plots used to address the study objectives were grown in 2006 on a Hord silt loam, a fine-silty textured mollic soil with a 0-1% slope near Shelton, Nebraska, USA (40º45’01” N, 98º46’01” W, elevation of 620-m above sea level). These plots were part of a long term cropping system and N management study established in 1991. The maize crop was seeded on 9 May 2006 at a target density of 78,500 seeds ha^{-1} using conventional tillage methods. To satisfy P requirement at this site, liquid ammonium phosphate fertilizer was applied at the rate of 94 L ha^{-1} beneath the seed at planting, providing approximately 12 kg N ha^{-1} and 18 kg P ha^{-1}. All other plant nutrients were

determined, by annual soil test results, to be adequate. The crop received irrigation throughout the growing season according to established sprinkler irrigation scheduling principles; no additional N was supplied to the study through irrigation water. Weed control was accomplished through a combination of cultivation and herbicide application.

Using monoculture maize as a subset of the original long term N management study provided conditions with the greatest range in N availability. Crop physiological data and canopy reflectance were collected from two architecturally contrasting Pioneer brand hybrids (Pioneer Brand 31N28 and 33V16) and five N treatments (0, 50, 100, 150, and 200 kg N ha^{-1}). The five N rates were applied shortly after emergence using a solution of urea ammonium nitrate (UAN) containing 28% N. It was our intention to use hybrids with the greatest architectural diversity available (erectophile vs. planophile) providing dramatically different light environments. Data were analyzed as a split-plot treatment design within a randomized complete block experiment with four replications. Maize hybrid was assigned as the main plot with N treatments as the subplots. Individual plot dimensions were 7.3 by 15.2-m, consisting of eight 0.91-m rows planted in an east-west direction.

Data collected throughout the growing season were referenced by thermal time (Growing Degree Days, GDD) and calculated from the acquisition of climatological data recorded using an automated weather station (High Plains Regional Climate Center Network, University of Nebraska) located on site. The GDD were logged and accumulated beginning from the planting date. Computations were made using Method II of McMaster and Wilhelm (1997) with a temperature base of 10ºC, and a temperature threshold of 30ºC.

Data acquisition occurred on six occasions between GDD 554 and 918. This span in thermal time covered plant development from approximately six fully expanded leaves during the vegetative stage through the early reproductive stage when pollination begins and ear silks beginning to emerge. For each acquisition event, three separate canopy reflectance measurements were acquired within a one-square meter sampling area of each plot. The three readings were averaged to produce one spectral signature representative of each plot. Canopy spectral reflectance was measured using dual Ocean Optics USB2000 spectroradiometers (Ocean Optics, Dunedin, Florida, USA) in the range from 350 nm to 1024 nm in 0.37 nm increments. This dual sensor system allows for simultaneous measurements of target radiance and available incoming irradiance.

The fiber-optic for the radiance sensor was fitted with a 20° full field of view optical restrictor and placed 1-m above the canopy in a nadir position directly over the row of plants. This orientation provided a circular field of view with a 0.35-m dia. footprint at the top of the canopy. The fiber optic for the irradiance sensor was mounted to a cosine corrected irradiance probe and placed directly above the radiance sensor. A white reference panel, utilizing the Spectralon diffuse reflectance material (Labsphere, Inc., North Sutton, New Hampshire, USA), was used for calibration. Calibration scans are necessary to adjust one sensor to the other and were acquired before and after each data collection event. The reference panel was placed beneath the radiance sensor to collect simultaneous measurements with the irradiance sensor. With the sensors matched, canopy reflectance can then be calculated as the ratio of the simultaneously measured radiance sensor value to the irradiance sensor value.

Plants from the same one-square meter of plot were harvested and the leaves removed. Leaves were grouped into upper and lower canopy zones for each plot providing a better, more homogenous, representation of the Chl and N distributions throughout the canopy. Zones were defined differently for the vegetative and reproductive growth stages. The two zones were separated into mature and elongating leaves for the vegetative growth stages while for the reproductive stages the zones were defined relative to the ear leaf position. Four specific sample locations were identified on leaves representative of each canopy zone. Leaf reflectance was measured using the Ocean Optics USB2000 spectroradiometer connected to a Li-Cor 1800IS integrating sphere (Li-Cor Inc., Lincoln, Nebraska, USA). Measurements were then averaged, resulting in a single reflectance spectrum representing the plot and leaf zone.

Tissue sampling was then accomplished by excising 1-cm dia. leaf disks collected at the same location, halfway from the leaf base to the tip and half way from the midrib to the leaf margin. Leaf Chl concentration was determined using photometric methods as described by Wellburn (1994), Richardson et al. (2002). The solvent dimethyl sulfoxide (DMSO) was selected for its ability to stabilize Chl molecules for periods longer than the more commonly used acetone and eliminate material maceration and centrifuging. The four disks were held in a solution of 10 ml DMSO and placed in a 65°C water bath for 20-30 minutes. The extract was then passed through a spectrophotometer to acquire the absorption (A_λ) measurements necessary to calculate Chl concentration. Equations for Chl *a* and Chl *b* are provided by Wellburn (1994):

Chl_a, μg $ml^{-1} = 12.19A_{665} - 3.45A_{649}$

Chl_b, μg $ml^{-1} = 21.99A_{649} - 5.32A_{665}$

$Chl_{total} = Chl_a + Chl_b$;

Leaf Chl content was derived as a function of Chl concentration, the volume of DMSO ($DMSO_{vol}$) used in the extraction, and the leaf disk area (LDA) sampled.

The remaining leaf tissue from each leaf zone for each plot was measured to calculate total leaf area (LA), and total dry matter (DM) on an oven dried basis. To determine N concentrations of plant materials, dried samples were first processed with a Wiley mill (20-mesh sieve). A sub-sample of approximately 0.3 g of the plant material was further ground on a roller-mill, as per Arnold and Schepers (2004). Approximately 5.5 mg of the sub-samples were used to determine N concentration using a flash combustion N analyzer following Schepers et al., (1989). The analyzer was calibrated periodically using standards with known N concentration. Chl and total N content for each leaf zone were summed for each plot and divided by the soil surface area (SA) from which they were harvested, resulting in total Chl and N contents per meter squared of surface area:

N, g m^{-2}, = $\Sigma(DM \times \%N)/SA$

Chl, mg $m^{-2} = \Sigma(((Chl_{total} \times DMSO_{vol})/LDA) \times LA)/SA$

Leaf level analysis was performed on a leaf area basis:

N, g $m^{-2} = \Sigma((DM \times \%N)/LA)$

Chl, mg $m^{-2} = \Sigma((Chl_{total} \times DMSO_{vol})/LDA)$

The best-fit relationships for Chl and N contents versus vegetation indices (VI) were determined. Then, the leave-one-out technique (Stone, 1974) was used to define root mean square error (RMSE) of N and Chl estimations and coefficients of determination (R^2).

It is important to note that R^2 represents the dispersion of the points from the best-fit regression lines. It constitutes a measure of how good the regression model (best-fit function) is in capturing the relationship between N or Chl and VI. However, when the best-fit function is nonlinear, the R^2 might be misleading. To determine the accuracy of N estimation, the noise equivalent (NE) of N was employed (Viña and Gitelson, 2005; Viña et al., 2011):

$NE\Delta N = RMSE(VI \text{ vs. } N)/[d(VI)/d(N)]$

Where d(VI)/d(N) is the first derivative of VI with respect to N and RMSE(VI vs. N) is the root mean square error of the VI vs. N relationship. The NEΔN provides a measure

of how well the VI responds to N across its entire range of N variation. NEΔN takes into account not only RMSE of N estimation but also accounts for sensitivity of the VI to N, thus providing a metric accounting for both scattering of the points from the best fit function and the slope of the best fit function.

Results and Discussion

Leaf Chl and N contents estimations

Linear relationships were found between leaf N content and leaf Chl content across all sampling dates in this study (Fig. 1), however, these relationships varied somewhat through the growing season (Table 2). For early stages of growth (when GDD was around 550), N uptake outpaced the production of Chl. At this point the plant had approximately six fully expanded leaves producing an LAI between 0.50 and 0.75. Plant material, at this stage of development, contained higher N content with respect to Chl content and the slope of the relationship N vs. Chl was the highest. As plant growth accelerated and reached an LAI of nearly 3.0 (GDD of 660) at the 10-11 fully elongated leaf stage, a dip in the N vs. Chl relationship occurred. Available N was being used by the biochemical reactions within the plant faster than its ability to uptake the additional N required to maintain the pace. This was short lived as growth rates became more linear. With linear growth, the relationship between leaf N and Chl contents stabilized and the slope varied slightly between 2.2 and 2.9 resulting in a season average of 2.5. Variations in plant growth and N uptake experienced early in the growing season accounts for a large portion of the scatter observed in Fig. 1. The coefficients of determination (R^2) for N vs. Chl relations were the lowest in the beginning of the growing season (GDD 554 through 660) and then increased significantly to well above 0.8. Even with the observed scattering of points at the beginning of the growing season, the N vs. Chl relationship for the combined dataset was very close with $R^2 = 0.73$ (Table 2). Additional contributions to the scatter observed can be the result of tissue age and irradiance as a function of the leaf position within the architecture of the canopy. Evans (1989) indicates slight variations in the relationship between total leaf N and Chl can exist as influenced by N nutrition and irradiance during plant growth. The result is an increased scatter and a y-intercept deviating from zero, as observed in Fig. 1.

Estimation of leaf Chl content was accomplished by calculating $CI_{red\ edge} = (\rho_{NIR}/\rho_{red\ edge}) - 1$ (Ciganda et al., 2009; Gitelson et al., 2003b; 2006b) where ρ_{NIR} is reflectance in the range 770-800 nm and $\rho_{red\ edge}$ is reflectance in the range 720-730 nm. The relationship between Chl content and $CI_{red\ edge}$ was very close with R^2 above 0.94 (Fig. 2). In Fig. 2, the relationship established by Ciganda et al. (2009) for maize is also presented. Importantly, best fit functions of both relationships have quite close parameters: difference in slope was less than 4%, and relationship offset for our data set was -23 mg m^{-2} while -8 mg m^{-2} for the Ciganda et al. (2009) relationship. This difference in offsets is probably due to very different geometry of measurements in these studies: integrating sphere in our study and leaf clip in Ciganda et al. (2009). Taking into account these factors, close relationships obtained in two independent studies is remarkable.

Leaf N content estimation was accomplished using $CI_{red\ edge}$. When considering the strong relationship between leaf N and Chl contents (Fig. 1), an equally strong relationship between leaf N content and $CI_{red\ edge}$ was expected; it was achieved with $R^2 = 0.74$ and RMSE of N estimation of 0.18 g m^{-2} (Fig. 3). This is in accord with Baret et al. (2007) who concluded that N status could be accurately assessed through Chl estimates. The scatter observed between $CI_{red\ edge}$ and N content is expected to be similar to that observed between measured leaf N and Chl contents (Fig. 1). Thus, obtained results show a strong potential for reflectance-based techniques to non-destructively estimate leaf N content.

Total canopy Chl and N contents estimation

Temporal behavior of total canopy N and Chl contents is presented in Fig. 4. With increase in N content, Chl content increased nearly synchronously. Moving away from the leaf level perspective toward the integration of the full canopy within a specified surface area acted as a normalization factor, improving the N vs. Chl relationship. A very strong linear relationship was established between N and Chl contents at the canopy level (Fig. 5). The strong canopy level N vs. Chl relationship was the basis for using Chl-related vegetation indices to estimate canopy N content.

Reflectance spectra of maize canopy varied significantly during the growing season as total canopy N and Chl contents increased. The NIR reflectance increased with increasing green LAI and biomass, while reflectance in the red region (maximum Chl absorption around 670 nm) decreased (Fig. 6). When Chl content approached 0.8 g m^{-2} with an N content of 4 g m^{-2}, this occurring at LAI values as low as 2.0, red reflectance stopped changing due to saturation of absorption in the red range at these moderate LAI values. In contrast to red reflectance, green reflectance (around 550 nm) and red edge reflectance (from 710 to 750 nm) continued to decrease following increases in Chl and N contents (Fig. 6).

Several Chl-related vegetation indices were selected to evaluate the estimation of N content at the canopy level (Table 1): NDVI (Rouse et al., 1974) and EVI2 (Huete et al.,1997; Jiang et al., 2008) that employ NIR and red spectral bands only, as well as indices that use green and red edge bands: MERIS terrestrial chlorophyll index (MTCI; Dash and Curren, 2004), red edge position (REP; Guyot and Baret, 1988), and green an red edge chlorophyll indices (CI_{green}, $CI_{red\ edge}$; Gitelson et al., 2003b; 2005; 2006b). The NDVI and EVI2 indices were simulated with reflectance in spectral bands of Landsat and MODIS; CI_{green} was simulated for green spectral bands of MERIS/OLCI and Landsat; and MTCI, REP and $CI_{red\ edge}$ were simulated using spectral bands of MERIS/OLCI centered at 754 nm (NIR), 709 nm (red edge) and 665 nm (red).
The NDVI was sensitive to N below 4 g m^{-2}, but did not change thereafter (Fig. 7A). The EVI2 and REP showed almost the same pattern as NDVI but reached saturation at a higher N content, above 6 g m^{-2} (Figs. 7B and 7C). Yet, MTCI and $CI_{red\ edge}$ showed much higher sensitivity to N content over the entire range of its variation (Figs. 7D and 7E). However, when N exceeded 10 g m^{-2}, the sensitivity of MTCI decreased more than two fold (Fig. 7D), while the sensitivity of $CI_{red\ edge}$ only decreased about 60% (Fig. 7E). The best fit for the CI_{green} vs. N relationship was the power function $N = 1.23 \times CI_{green}^{0.97}$ ($R^2 = 0.79$) and was quite close to linear with $R^2 = 0.73$ (Fig. 7F).

Noise equivalent of N estimation (NEΔN) using VIs, is presented in Fig. 8 versus canopy N content. This parameter facilitated understanding how well the VIs responded to N across the entire range of N variation. Both NDVI and EVI had quite small NEΔN and, thus, high sensitivity to N content below 2-3 g m^{-2}. This sensitivity decreased

drastically with increasing N content beyond 3 g m^{-2} (Fig. 7a, 7b) resulting in NEΔN increasing exponentially (insert to Fig. 8). For REP, $CI_{red\ edge}$, and MTCI, NEΔN was below 2 g m^{-2} for N < 9 g m^{-2}, and then increased reaching values above 4 g m^{-2} for N content around 14 g m^{-2}. The behavior of NEΔN for CI_{green} was quite different. It was nearly invariant over the entire range of N variation. For N content below 6 mg m^{-2}, to estimate N content the use of either REP, $CI_{red\text{-}edge}$, or MTCI is recommended, while for higher N content CI_{green} is more accurate.

The next step was to explore the potential of the MultiSpectral imager (MSI) sensor onboard Sentinel-2 to estimate total maize N and Chl contents. This sensor has narrow spectral bands (15-nm width) centered at 705 nm and 740 nm, providing outstanding potential for retrieving canopy Chl and N contents. In combination with the high spatial resolution (20 m) and short revisit time (near weekly with a constellation of two identical satellites), it offers improved applications in fields like precision agriculture.
To find an optimal band in the red-edge spectral region for estimating Chl content, we calculated RMSE of the total Chl estimation using the red-edge chlorophyll index, $CI_{red\ edge} = (\rho_{NIR}/\rho_{red\ edge}) - 1$ with ρ_{NIR} at 780-800 nm and variable red-edge spectral bands from 680 to 760 nm. The minimal RMSE and the highest accuracy of Chl estimation by means of $CI_{red\ edge}$ was found in the red-edge range 735 to 745 nm (Fig. 9). This optimal spectral range is positioned more than 60 nm away from the position of in-situ red absorption band of Chl. In this spectral region, the absorption coefficient of Chl is very low (Lichtenthaler, 1987), however, light penetration inside the leaf and canopy is much deeper than in the red and shortwave red-edge region (Ciganda et al., 2012; Merzlyak and Gitelson, 1995). Thus, absorption by the canopy around 740 nm (i.e., product of light pathway and absorption coefficient) is enough to provide high sensitivity of reflectance to Chl content.

The $CI_{red\ edge}$ shown in Fig. 10 was simulated using the red-edge band of the MSI sensor onboard Sentinel-2 centered at 740 nm (width 15 nm). Both N vs. $CI_{red\ edge}$ and Chl vs. $CI_{red\ edge}$ relationships were very close and nearly linear (linear approximations result in $R^2 = 0.84$ for Chl and 0.82 for N). Noise equivalent of $CI_{red\ edge}$ with 740 nm band was even lower than that of CI_{green} allowing very accurate N estimation (Fig. 11).

Previous studies showed that CI_{green} and $CI_{red\text{-}edge}$ are robust for estimating canopy N content (Clevers and Kooistra, 2012; Clevers and Gitelson, 2012). However, it was found that the precise position of the spectral bands in the $CI_{red\text{-}edge}$ is not very critical. This study with maize illustrated that for crops with very high Chl and N contents the precise position of the spectral bands in the $CI_{red\text{-}edge}$ is quite critical. The RMSE of Chl and N estimations using $CI_{red\text{-}edge}$ with the long-wave 740 nm band of Sentinel-2 was 50% smaller when using the short-wave 705 nm band. Different climates and irrigation regimes (and perhaps varieties) will result in variable quantities of N and Chl, and thus require both Sentinel-2 bands, centered at 705 nm for lower Chl and 740 nm for higher Chl. Importantly, the optimal spectral bands, as well as techniques to estimate Chl and N contents demonstrated in this maize study, are in accord with findings for rice (Inoue et al., 2012; Lee et al., 2008; Takahashi et al., 2000), wheat (Wu et al., 2009; Zhu et al., 2008), and maize (Gitelson et al., 2005; Wu et al., 2010).

Conclusions

The paper showed that chlorophyll and nitrogen content in maize can be estimated by the same remote sensing techniques and confirmed a paradigm, suggesting that absorption by Chl provides the necessary link between remote sensing observations and canopy-state variables that are used as indicators of N status. This study presents the significance of the green and long wave red-edge bands of the MSI sensor on Sentinel-2 for estimating Chl and N contents in maize. This study confirms that green chlorophyll index CI_{green} accurately estimates N content, which is consistent with findings for both crops and grassland systems (Clevers and Gitelson, 2012). Also notably, $CI_{red\text{-}edge}$ with quite a wide spectral band around 740 nm was optimal for N and Chl estimation. $CI_{red\text{-}edge}$ with red edge band 720-730 nm allowed accurate non-species specific estimation of gross primary production in maize and soybean (Peng and Gitelson, 2011) and the same range was found to be optimal for N estimation in rice (Inoue et al., 2012). Thus, it is likely that presented techniques for N and Chl estimation in maize could accurately estimate the same characteristics in other crops. This study offers possible options for users to collect the appropriate data from proximal sensors to space-borne platforms that will provide measures of such important physiological variables as Chl and N from the plant to the global scale.

Table 1: Vegetation indices examined.

Index	Equation	Reference
Normalized Difference Vegetation Index (NDVI)	(NIR - Red)/(NIR + Red)	Rouse et al. (1974)
Enhanced Vegetation Index 2 (EVI2)	2.5×(NIR - Red)/(NIR + 2.4×Red + 1)	Jiang et al. (2008)
Red Edge Inflection Point (REP)	$708.75 + 45\times[(\rho_{665}+\rho_{778.75})/2)-\rho_{708.75})/(\rho_{753.75}-\rho_{708.75})]$	Guyot & Baret (1988), Clevers et al. (2000)
MERIS Terrestrial Chlorophyll Index (MTCI)	(NIR - Red Edge)/ (Red Edge + Red)	Dash & Curran (2004)
Green Chlorophyll Index (CI_{green})	(NIR/Green) - 1	Gitelson et al. (2003a; 2005)
Red Edge Chlorophyll Index ($CI_{red\ edge}$)	(NIR/Red Edge) - 1	Gitelson et al. (2003a; 2005)

Table 2. Relationships leaf nitrogen (N) content versus leaf chlorophyll (Chl) content by growing degree days (GDD) for irrigated maize. Coefficient of determination (R^2) and standard error of the relationships are indicated. N and Chl contents are in g/m^2.

GDD	N/Chl relationship	R^2	Std Err N content
554	N=4.1×Chl-0.30	0.73	0.156
660	N=1.9×Chl+0.41	0.64	0.131
738	N=2.7×Chl+0.03	0.85	0.145
809	N=2.9×Chl+0.14	0.89	0.136
918	N=2.2×Chl+0.21	0.83	0.148
Combined	N=2.5×Chl+0.21	0.73	0.180

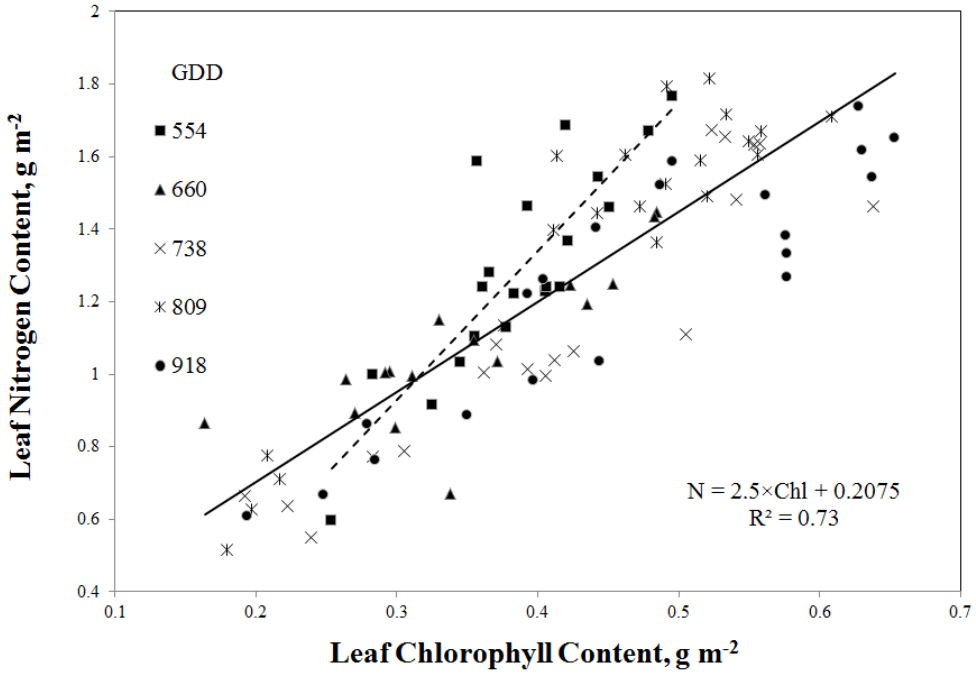

Fig. 1. Relationship between leaf nitrogen and leaf chlorophyll contents for maize at five growth stages. Solid line is best fit function for whole growing season N vs. Chl relationship. Dashed line is best fit function for early stage with GDD = 554. The close leaf-level relationship was the basis for using Chl-related vegetation indices to estimate N content.

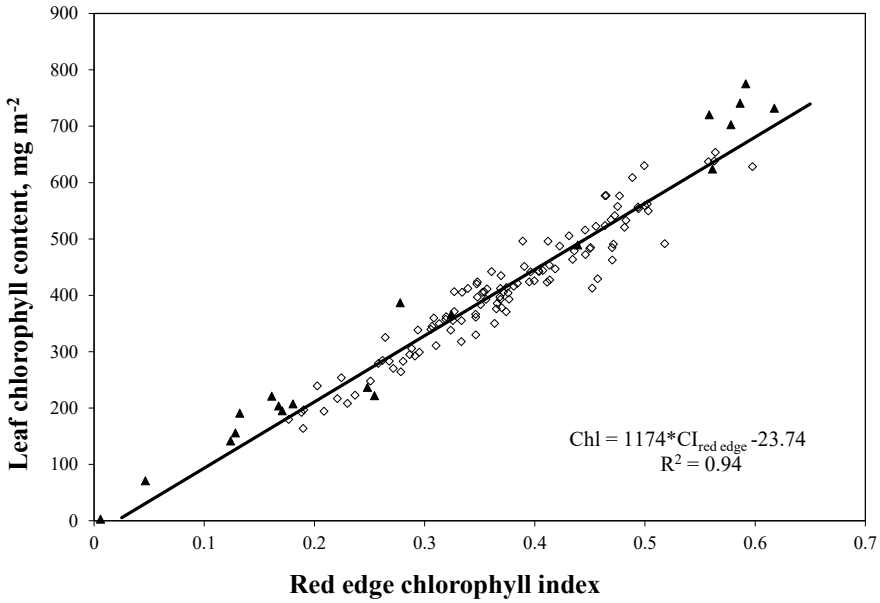

Fig. 2. Maize leaf chlorophyll content versus red-edge chlorophyll index. Squares represent data taken in this study; triangles are from Ciganda et al., 2009.

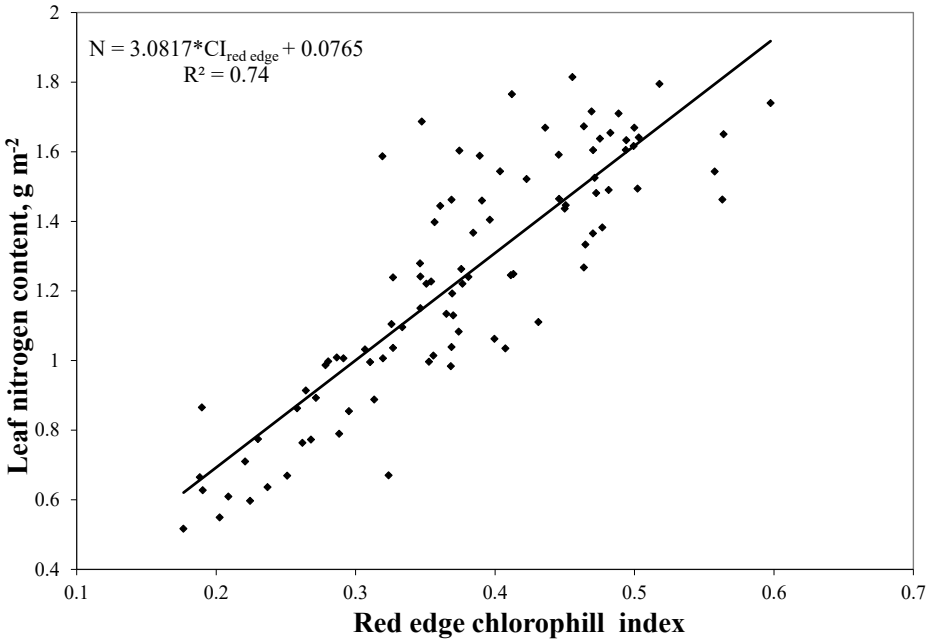

Fig. 3. Maize leaf nitrogen content versus red-edge chlorophyll index.

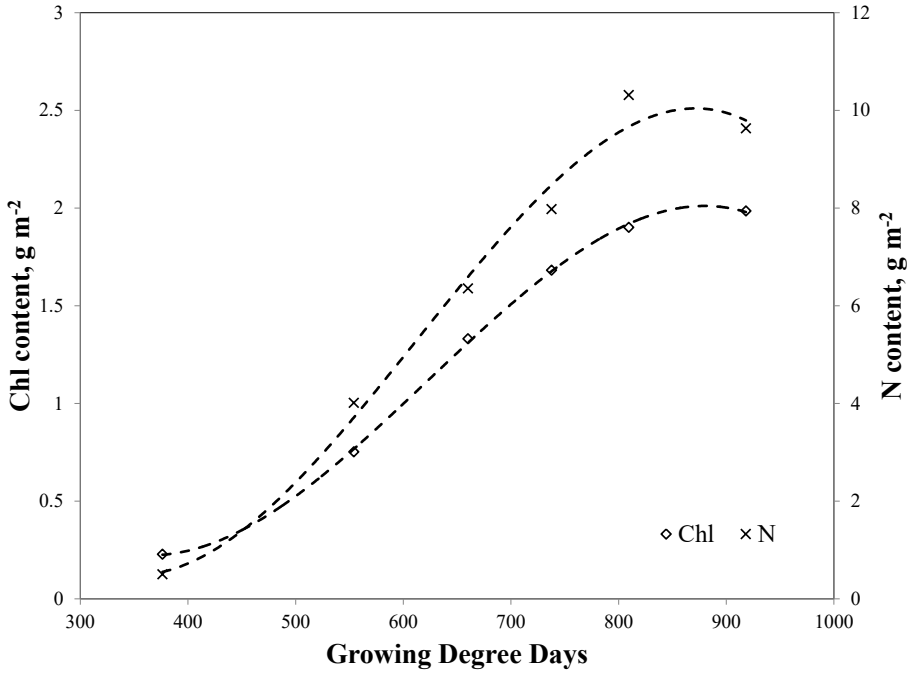

Fig. 4. Total canopy chlorophyll and nitrogen contents versus growing degree days. Lines are second order polynomial best fit functions with coefficients of determination for both N and Chl approximations above 0.94.

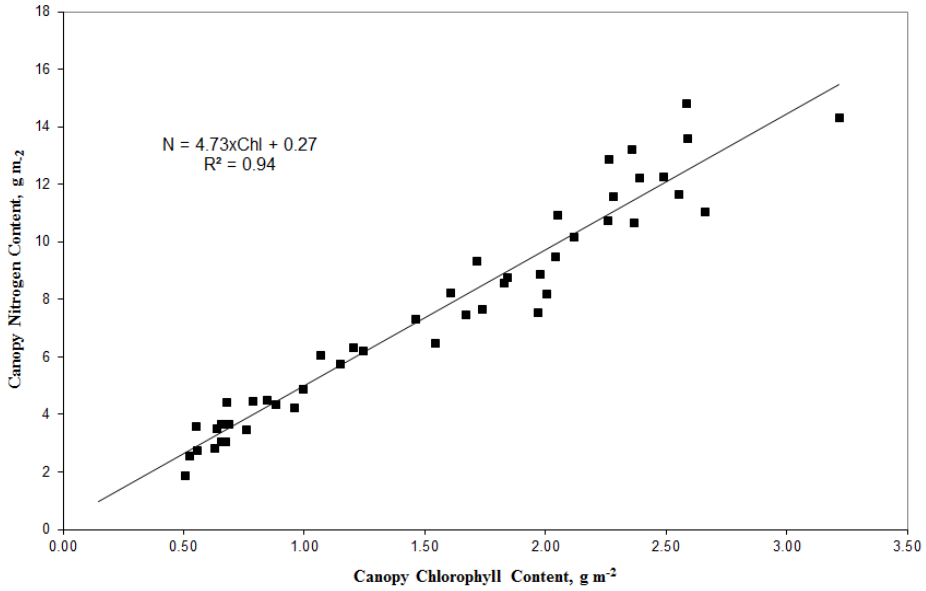

Fig. 5. Relationship between canopy nitrogen and chlorophyll contents for maize. Canopy chlorophyll content was calculated as a product of leaf chlorophyll content and leaf area index normalized to area covered by plant.

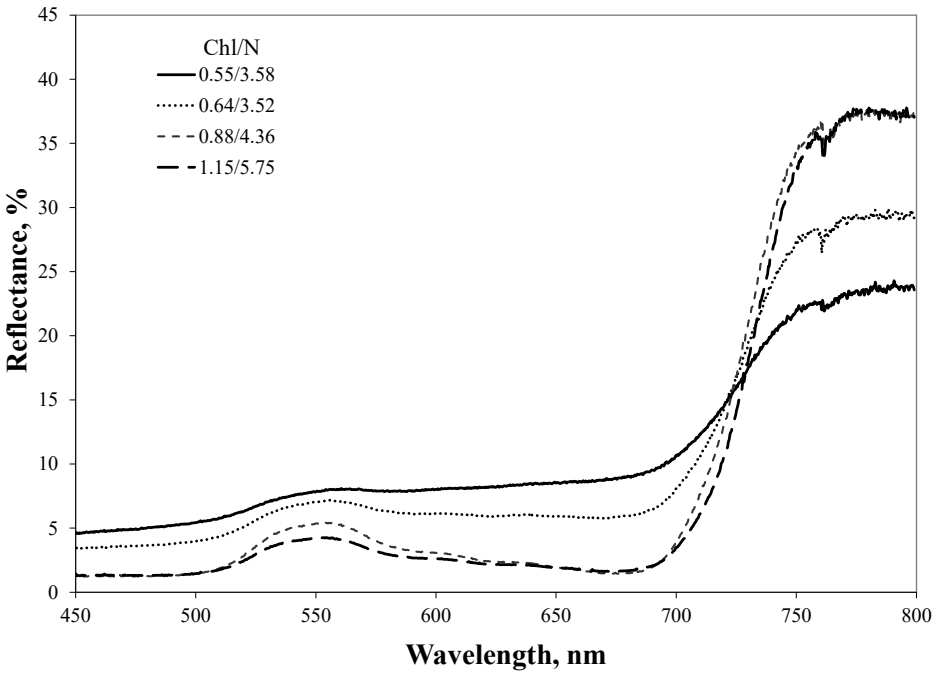

Fig. 6. Reflectance spectra of maize canopy with different chlorophyll and nitrogen contents. Chlorophyll and nitrogen contents (in g/m^2), Chl/N, are shown.

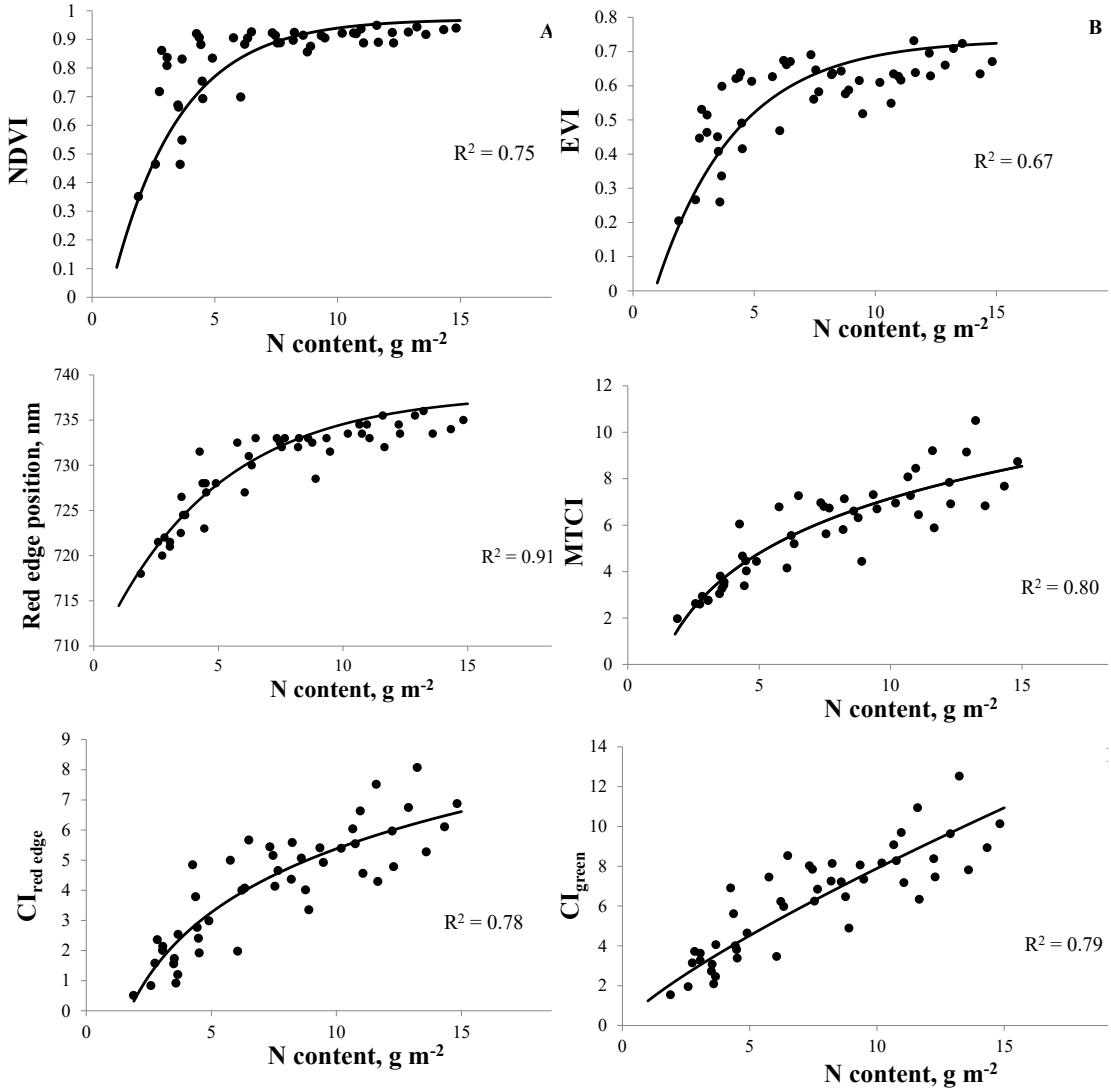

Fig. 7. Canopy nitrogen content versus (a) NDVI; (b) EVI2; (c) MTCI; (d) red-edge position (REP); (e) red-edge chlorophyll index, $CI_{red\ edge}$ and (f) green chlorophyll index, CI_{green}. NDVI, EVI and CI_{green} were calculated using spectral bands of MODIS. MTCI, REP and $CI_{red\ edge}$ were calculated with spectral bands of OLCI sensor onboard Sentinel-3.

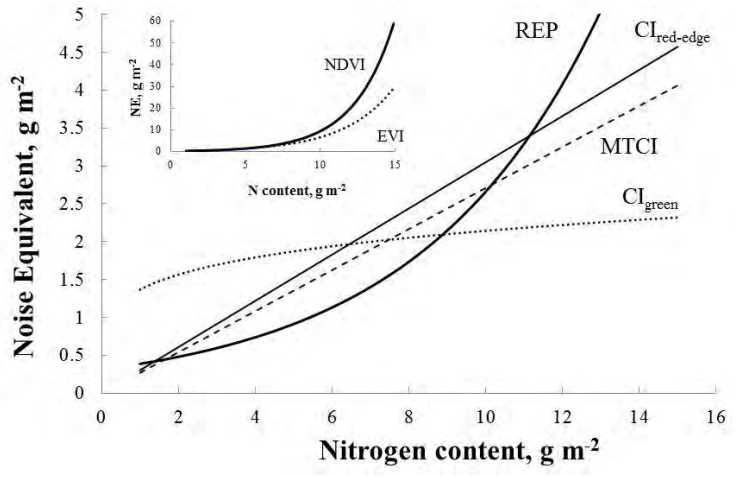

Fig. 8. Noise equivalent of total nitrogen estimation by vegetation indices red-edge position (REP), MTCI (dashed line), CI_{green}, and $CI_{red\ edge}$. Insert illustrates noise equivalents of NDVI and EVI. NDVI, EVI and CI_{green} were calculated using spectral bands of MODIS/OLCI. MTCI, REP and $CI_{red\text{-}edge}$ were calculated with spectral bands of OLCI sensor onboard Sentinel-3.

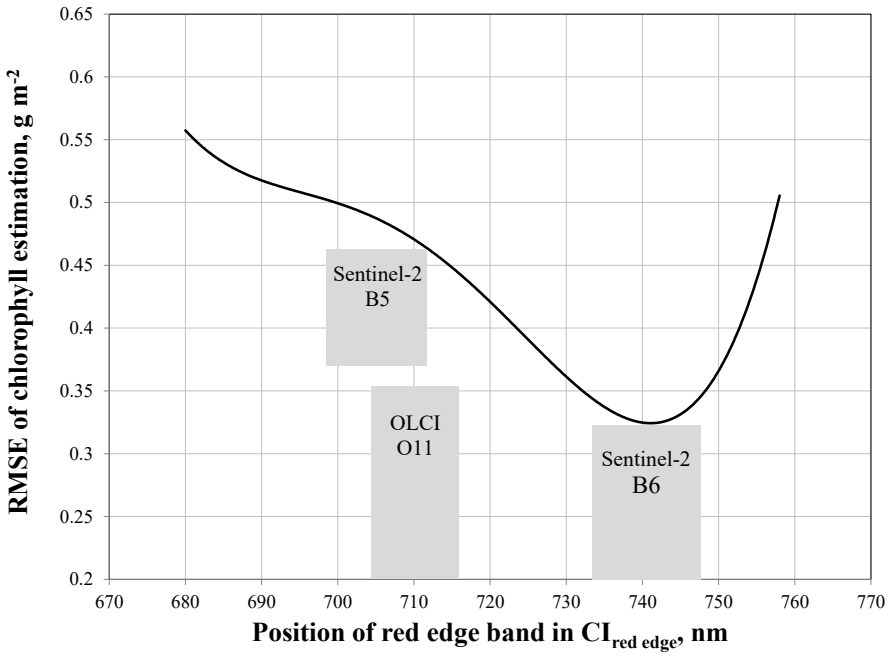

Fig. 9. RMSE of total chlorophyll estimation by red edge chlorophyll index, $CI_{red\ edge} = (\rho_{NIR}/\rho_{red\ edge})\text{-}1$ with ρ_{NIR} = 780-800 nm and variable red edge spectral band from 680 to 760 nm. In the range 735 to 745 nm, the $CI_{red\ edge}$ had minimal RMSE and the highest accuracy of chlorophyll estimation.

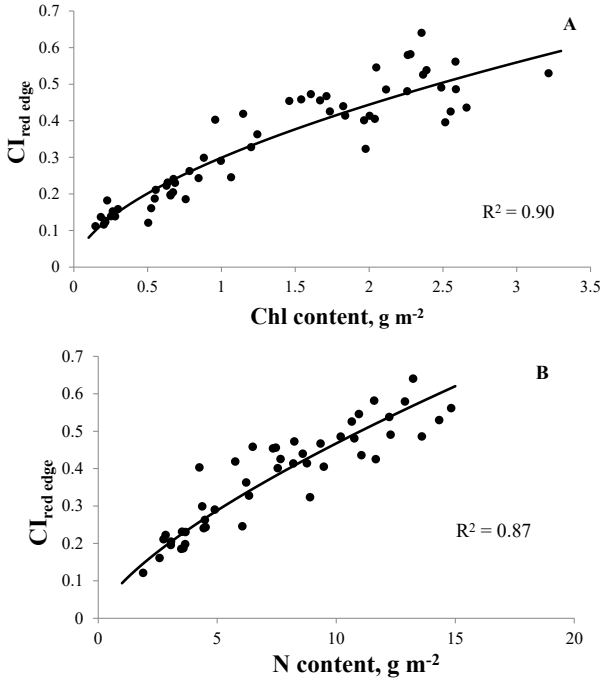

Fig. 10. Relationships between canopy chlorophyll content (a) and canopy nitrogen content (b) and red-edge chlorophyll index with simulated B6 spectral band at 740 nm (width 15 nm) of MSI sensor onboard Sentinel-2.

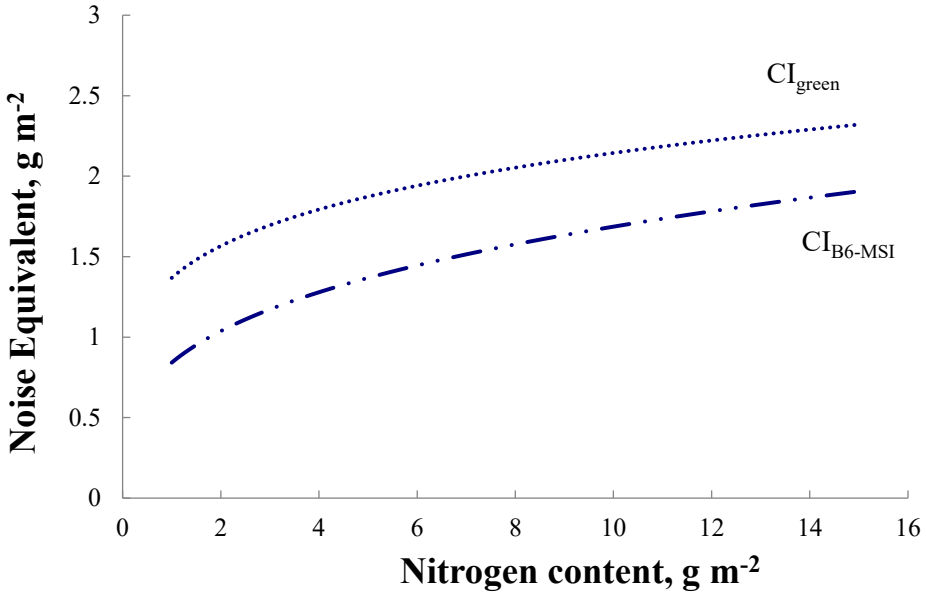

Fig. 11. Noise equivalent of total nitrogen content estimation by green and red edge chlorophyll indices (CI_{green} and $CI_{red\ edge}$), calculated using green spectral band of MODIS/OLCI and red-edge band B6 (732-747 nm) of MSI sensor onboard Sentinel-2.

References

Arnold, S.L., Schepers, J.S., 2004. A simple roller-miller grinding procedure for plant and soil samples. Communications in Soil Science and Plant Analysis 35, 537-545.

Baret, F., Houlès, V., Guérif, M., 2007. Quantification of plant stress using remote sensing observations and crop models: the case of nitrogen management. Journal of Experimental Botany 58, 869–880.

Blackburn, G. A., 2006. Hyperspectral remote sensing of plant pigments. Journal of Experimental Botany 58, 855-867.

Ciganda, V., Gitelson, A., Schepers J., 2009. Non-destructive determination of maize leaf and canopy chlorophyll content. Journal Plant Physiology 166, 157-167.

Ciganda, V. S., Gitelson, A. A., Schepers, J., 2012. How deep does a remote sensor sense? Expression of chlorophyll content in a maize canopy. Remote Sensing of Environment 126, 240-247.

Clevers, J.G.P.W., de Jong, S.M., Epema, G.F., van der Meer, F., Bakker, W.H., Skidmore, A.K., Addink, E.A., 2001. MERIS and the red-edge position. International Journal of Applied Earth Observation and Geoinformation, 3, 313–320.

Clevers, J.G.P.W., Gitelson, A.A., 2013. Remote estimation of crop and grass chlorophyll and nitrogen content using red-edge bands on Sentinel-2 and -3, International Journal of Applied Earth Observation and Geoinformation, 23, 344-351.

Clevers, J.G.P.W., Kooistra, L., 2012. Using hyperspectral remote sensing data for retrieving canopy chlorophyll and nitrogen content. IEEE Journal of Selected Topics in Applied Earth Observations and Remote Sensing 5, 574–583.

Dash, J., Curran, P.J., 2004. The MERIS terrestrial chlorophyll index. International Journal of Remote Sensing 25, 5403–5413.

Evans, J.R., 1983. Nitrogen and photosynthesis in the flag leaf of wheat (*Triticum aestivum* L.). Plant Physiology 72, 297-302.

Evans, J.R., 1989. Photosynthesis and nitrogen relationships in leaves of C_3 plants. Oecologia 78, 9-19.

Féret, J-B., François, C., Gitelson, A.A., Barry, K.M., Panigada, C., Richardson, A.D., and Jacquemoud, S., 2011. Optimizing spectral indices and chemometric analysis of leaf chemical properties using radiative transfer modeling, Remote Sensing of Environment, 115: 2742-2750.

Field C. B., Mooney, H. A., 1986. The photosynthesis-nitrogen relationship in wild plants. In T. J. Givnish [ed.], On the economy of plant form and function, 25–55.

Gitelson, A. A., S. B. Verma, A. Vina, D. C. Rundquist, G. Keydan, B. Leavitt, T. J. Arkebauer, G. G. Burba, and Suyker, A. E., 2003a. Novel technique for remote estimation of CO_2 flux in maize, Geophys. Res. Lett., 30(9), 1486, doi:10.1029/2002GL016543.

Gitelson, A.A., Gritz, Y., Merzlyak, M.N., 2003b. Relationships between leaf chlorophyll content and spectral reflectance and algorithms for non-destructive chlorophyll assessment in higher plant leaves. Journal Plant Physiology 160, 271-282.

Gitelson, A.A., Viña, A., Ciganda, V., Rundquist, D.C., Arkebauer, T.J., 2005. Remote estimation of canopy chlorophyll content in crops. Geophysical Research Letters 32, L08403, doi:10.1029/2005GL022688.

Gitelson, A. A., A. Viña, S. B. Verma, D. C. Rundquist, T. J. Arkebauer, G. Keydan, B. Leavitt, V. Ciganda, G. G. Burba, and Suyker, A. E., 2006a. Relationship between gross primary production and chlorophyll content in crops: Implications for the synoptic monitoring of vegetation productivity, J. Geophys. Res., 111, D08S11, doi:10.1029/2005JD006017.

Gitelson, A.A., Keydan, G.P., Merzlyak, M.N., 2006b. Three-band model for noninvasive estimation of chlorophyll, carotenoids, and anthocyanin contents in higher plant leaves. Geophysical Research Letters 33, L11402, doi:10.1029/2006GL026457.

Gitelson, A.A., 2011a. Non-destructive estimation of foliar pigment (chlorophylls, carotenoids and anthocyanins) contents: espousing a semi-analytical three-band model. Chapter 6 in Hyperspectral Remote Sensing of Vegetation (Thenkabail, P.S., Lyon, J.G., Huete, A., Eds), pp. 141-165, Taylor and Francis.

Gitelson, A.A., 2011b. Remote Sensing estimation of crop biophysical characteristics at various scales. Chapter 15 in Hyperspectral Remote Sensing of Vegetation (Thenkabail, P.S., Lyon, J.G., Huete, A., Eds), pp. 329-358, Taylor and Francis.

Guyot, G., Baret, F., 1988. Utilisation de la haute resolution spectrale pour suivre l'etat des couverts vegetaux. In: Proceedings 4th International Colloquium 'Spectral Signatures of Objects in Remote Sensing', Aussois, France, pp. 279–286 (ESA, Paris).

Hatfield, J.L., Gitelson, A.A., Schepers, J.S., and Walthall, C.L., 2008. Application of spectral remote sensing for agronomic decisions. Agronomy Journal 100, S-117–S-131.

Huete, A. R., Liu, H. Q., Batchily, K., van Leeuwen, W., 1997. A comparison of vegetation indices global set of TM images for EOS-MODIS. Remote Sensing of Environment 59, 440–451.

Inoue, Y., Sakaiy, E., Zhu, Y., Takahashi, W., 2012. Diagnostic mapping of canopy nitrogen content in rice based on hyperspectral measurements. Remote Sensing of Environment 126, 210–221.

Jiang, Z., Huete, A.R., Didan, K., Miura, T., 2008. Development of a two-band enhanced vegetation index without a blue band. Remote Sensing of Environment 112, 3833-3845.

Kergoat, L., Lafont, S., Arneth, A., Le Dantec, V., Saugier, B., 2008. Nitrogen controls plant canopy Light-Use-Efficiency in temperate and boreal ecosystems. Journal of Geophysical Research 113, G04017, 1-19, DOI: 10.1029/2007JG000676.

le Maire, G., François, C., Dufréne, E., 2004. Towards universal broad leaf chlorophyll indices using PROSPECT simulated database and hyperspectral reflectance measurements. Remote Sensing of Environment 89, 1-28.

Lichtenthaler H.K., 1987. Chlorophyll and carotenoids: Pigments of photosynthetic biomembranes. Methods in Enzymology 148, 331–382.

Lee, Y., Yang, C., Chang, K., Shen, Y., 2008. A simple spectral index using reflectance of 735 nm to assess nitrogen status of rice canopy. Agronomy Journal 100, 205–212.

McMaster, G.S., Wilhelm, W.W., 1997. Growing degree-days: one equation, two 6 interpretations. Agricultural and Forest Meteorology 87, 291-300.

Merzlyak, M., Gitelson, A., 1995. Why and what for the leaves are yellow in autumn? On the interpretation of optical spectra of senescing leaves (Acer platanoides L.) Journal Plant Physiology 145(3), 315-320.

Peng, Y., Gitelson, A.A., 2011. Remote estimation of gross primary productivity in soybean and maize based on total crop chlorophyll content. Remote Sensing of Environment 117, 440-448.

Richardson, A.D., Duigan, S.P., Berlyn, G.P., 2002. An evaluation of noninvasive methods to estimate foliar chlorophyll content. New Phytologist 153, 185-194.

Rouse, J. W., Haas, R. H., Jr., Schell, J. A., Deering, D. W., 1974. Monitoring vegetation systems in the Great Plains with ERTS. Third ERTS-1 Symposium (pp. 309–317). Washington, DC: NASA.

Schepers, J.S., Francis, D.D., Thompson, M.T., 1989. Simultaneous determination of total C, total N, and 15N on soil and plant material. Communications in Soil Science and Plant Analysis 20, 949-959.

Sripada, R.P., Schmidt, J.P., Dellinger, A.E., Beegle, D.B., 2008. Evaluating multiple indices from a canopy reflectance sensor to estimate corn N requirements. Agronomy Journal 100, 1553–1561.

Stone, M., 1974. Cross-validatory choice and assessment of statistical predictions. Journal of the Royal Statistical Society. Series B., 36, 2, 111-147.

Takahashi, W., Nguyen-Cong, V., Kawaguchi, S., Minamiyama, M., 2000. Statistical models for prediction of dry weight and nitrogen accumulation based on visible and near-infrared hyper-spectral reflectance of rice canopies. Plant Production Science 3, 377–386.

Tian, Y.C., Yao, X., Yang, J., Cao, W.X., Hannaway, D.B., Y. Zhu., 2011. Assessing newly developed and published vegetation indices for estimating rice leaf nitrogen concentration with ground- and space-based hyperspectral reflectance. Field Crops Research 120, 299–310.

Ustin, S. L., Gitelson, A.A., Jacquemoud, S., Schaepman, M., Asner, G.P., Gamon, J.A., Zarco-Tejada, P., 2009. Retrieval of foliar information about plant pigment systems from high resolution spectroscopy. Remote Sensing of Environment 113, S67–S77.

Viña, A., Gitelson, A.A., 2005. New developments in the remote estimation of the fraction of absorbed photosynthetically active radiation in crops, Geophysical Research Letters 32, L17403, doi:10.1029/2005GL023647.

Viña, A., Gitelson, A.A., Nguy-Robertson A.L., Peng, Y., 2011. Comparison of different vegetation indices for the remote assessment of green leaf area index of crops, Remote Sensing of Environment 115, 3468–3478, doi:10.1016/j.rse.2011.08.010.

Walters, D.T., 2003. Diagnosis of nitrogen deficiency in maize and the influence of hybrid and plant density, North central Extension-Industry soil Fertility Conference, 2003. Vol. 19, Des Moines, IA.

Wellburn, A.R., 1994. The spectral determination of chlorophylls a and b, as well as total carotenoids, using various solvents with spectrophotometers of different resolution. Journal Plant Physiology 144, 307-313.

Wullschleger, S. D., 1993. Biochemical limitations to carbon assimilation in C3 plants—a retrospective analysis of the A/Ci curves from 109 species. Journal of Experimental Botany 44, 907–920.

Wu, C., Niu, Z., Gao, S., 2010. Gross primary production estimation from MODIS data with vegetation index and photosynthetically active radiation in maize. Journal of Geophysical Research 115, D12127, http://dx.doi.org/10.1029/2009JD013023

Wu, C., Niu, Z., Tang, Q., Huang, W., Rivard, B., Feng, J., 2009. Remote estimation of gross primary production in wheat using chlorophyll-related vegetation indices. Agricultural and Forest Meteorology 149, 1015–1021.

Xue, L., Cao, W., Luo, W., Dai, T., Zhu, Y., 2004. Monitoring Leaf Nitrogen Status in Rice with Canopy Spectral Reflectance, Agronomy Journal 96, 135–142.

Zhu, Y., Yao, X., Tian, Y., Liu, X., Cao, W., 2008. Analysis of common canopy vegetation indices for indicating leaf nitrogen accumulations in wheat and rice. International Journal of Applied Earth Observation and Geoinformation, 10, 1–10.

REMOTE SENSING FOR FERTILIZATION MANAGEMENT IN IRRIGATED CROPS

Victor Alchanatis

Institute of Agricultural Engineering, Agricultural Research Organization, The Volcani Center, Bet Dagan, Israel 50250

Nitrogen deficiency is one of the most important conditions to be detected, since it affects directly the productivity of the crop. An major reason that makes the detection of nitrogen deficiency very important is the fact that nitrogen leaches under the root zone when irrigation or water management is not appropriate, creating conditions that are sub-optimal for the crop growth. The relatively shallow root system of irrigated crops, coupled with its large nitrogen (N) requirement and sensitivity to water stress on coarse textured soil increases the risk of nitrate (NO_3-N) leaching. Therefore, precise N management is important, both for maximizing production and for minimizing N loss to groundwater.

Remote sensing provides information to compute spectral indices that are correlated with nitrogen deficiency. They can be divided to indices that are based on wavelengths in the visible and the near infra red region, and indices that include specific nitrogen absorption wavelengths in the SWIR (short wave infra red spectral region). The additional value of using SWIR based indices has been shown in studies on wheat and potato leaves.

Hyperspectral vegetation indices (VIs) have also been developed to estimate crop nitrogen (N) status at leaf and canopy levels. They have been evaluated for different growth stages and years using data from both N experiments and farmers' fields. The results indicated that best performing VIs included simple ratios in the red-edge region and in the blue regio. Red-edge and near infrared (NIR) bands were more effective for nitrogen estimation at early growing stage, but visible bands, especially ultraviolet, violet and blue bands, were more sensitive at later growing stage.

Potatoes (cv. Desiree) were grown in the spring seasons of 2007 and 2008 at two commercial potato fields in Kibbutz Ruhama, Israel (31.38ºN, 34.59ºE). This agricultural land is on the southern part of Israel's coastal plain, on the boundary between Mediterranean and semi-arid climates. The soil texture of both fields was sandy loam.

Each year, ground and aerial spectral data were acquired. Together with the spectal acquisition, vegetation data were acquired, consisting of the petiole NO_3-N and leaf N of the leaves, was quantified. Vegetation data were sampled at 10 plots in 2007, and at 26 plots in 2008.

Ground based reflectance of leaves in the field was measured with an HR2000 mini-spectrometer (OceanOptics Inc., Dunedin, FL, USA) with a spectral range of 400-900 nm. Airborne hyperspectral images were acquired with a custom hyperspectral system, consisting of camera coupled with a dispersing prism (Spectral Image, Spectral Imaging Ltd., Oulu, Finland). One imaging campaign was performed in 2007 and three campaigns in 2008. It has a 800 pixel swath width and was configured to capture imagery in 420 narrow bands (2 nm spectral resolution) covering the visible and near-infrared portions of the solar spectrum from 398 to 1000nm; The images were taken at an altitude of approximately 1000 m. The ground spatial resolution at that time was 0.5 m perpendicular to the flight direction and 1.5m parallel to the flight direction.

Vegetation indices and multivariate methods were used to estimate leaf nitrogen content based on narrow-band spectral data. With the data acquired with the ground system, PLSR analysis resulted to stronger correlation between predicted and measured leaf nitrogen content ($R^2 = 0.95$) (Figure 1), than the nitrogen specific index TCARI ($R^2 = 0.81$) (Figure 2), even though in both models, data from narrow-bands was used.

Using the aerial data, leaf nitrogen prediction models were constructed with TCARI/OSAVE vegetation index (Figure 3) and PLSR model.

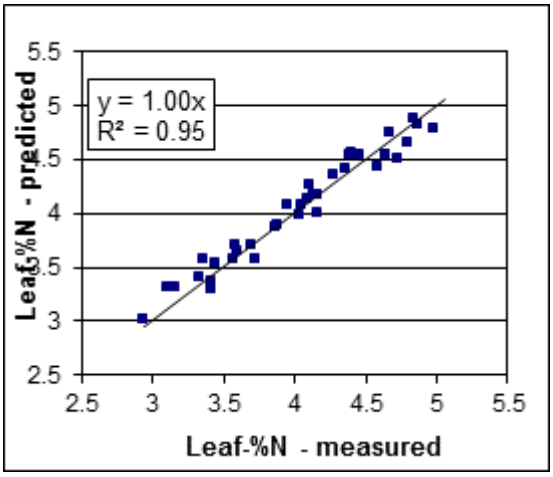

Fig. 1. Leaf nitrogen prediction using PLSR regression from ground data

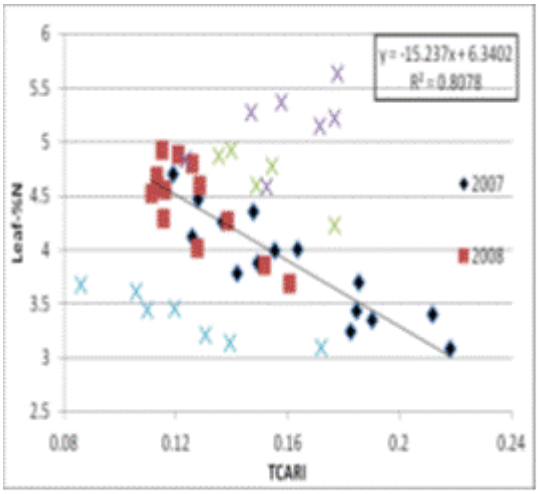

Fig. 2. Leaf nitrogen prediction using vegetation index TCARI from ground data

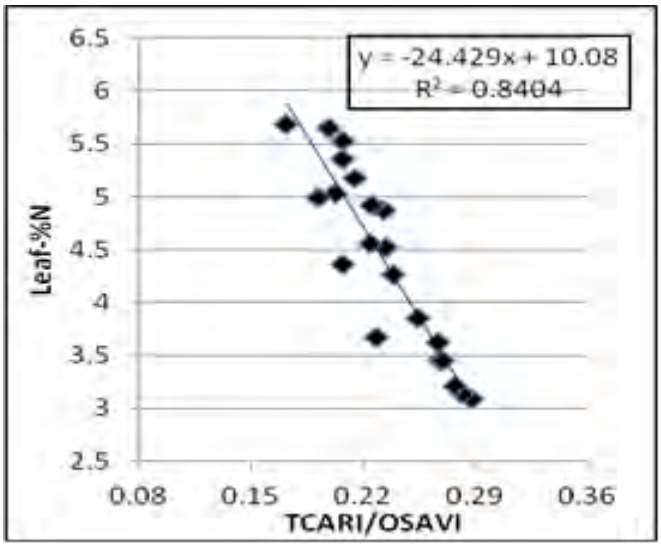

Fig. 3. Leaf nitrogen prediction using vegetation index TCARI from aerial data

Session 8: Carbon and C-N Interactions in Soils

New Insights on C Cycling in Soils: Do Microbial Residues from Diverse Groups Contribute Differently to Stable Soil Carbon Maintenance and Accumulation?

William R. Horwath[1*], H. M. Throckmorton[2], J. A. Bird[4], L. Dane,[3] M. K. Firestone[3]

[1]University of California, (UCD), Davis, US
[2]Los Alamos National Laboratory, Los Alamos, NM, US
[3]University of California, (UCB), Berkeley, US
[4]Queens College, City University of New York (CUNY), The CUNY Graduate Center, NY, US
*Corresponding author: wrhorwath@ucdavis.edu

Abstract

The observation that fungal residues contribute more to stable soil organic than other microbial groups has become the dominant thinking of soil scientists. This conclusion has been derived from a handful of laboratory studies with field studies distinctly lacking. This study assessed the contribution of residues from different microbial groups (fungi, actinobacteria, Gram-positive bacteria, and Gram-negative bacteria) to stable soil C in a temperate and tropical forest. Microorganisms were isolated from both sites, cultured in 99.9% atom enriched ^{13}C media and applied to soils in a reciprocal design. We hypothesized that distinct biochemistry of the microbial groups would lead to different turnover rates. Mean residence times (MRTs) ranged from 3.8- 7.1 yrs within California and 1.3- 3.8 yrs within Puerto Rico. Results showed that the residues from the different microbial groups had similar turnover rates though some groups had slightly slower turnover rates. The results suggest that the diverse biochemistry of different microbial groups had little impact on the maintenance of soil organic matter (OM). This simplifies are understanding of the roles of microbial inputs to OM maintenance and shows that the size and turnover rate of the entire microbial

community is likely more important than its composition in controlling soil C maintenance and stabilization.

Keywords: Bacteria, , fungi, decomposition, microbial, mineralization, carbon stabilization, soil, soil organic matter.

Introduction

The chemical composition of C inputs and decomposition products has been assumed to control the stability of soil C. The source of C to produce soil organic matter (OM) in soils comes from plants, the primary producers capturing light energy and converting it to organic compounds. Formally it was assumed plants contributed a great deal of substrates to OM formation. However, upon plants senesce, consortia of organisms, mainly microorganisms convert much of plant biomass (net primary production) into secondary decomposer production. Current thinking of the source of soil organic matter suggests that decomposer turnover is the primary source of stabilized OM (Liang and Balser 2010).

Organic matter consists of unrecognizable partially decayed plant residues, soil microorganisms, soil fauna and the byproducts of decomposition that serve as precursors for humic substances. The preservation of these fractions is controlled through three primary mechanisms: 1.) the physical occlusion of materials within soil aggregates, 2.) decomposition products are protected physically through the association with secondary minerals and 3.) metabolized products that are chemically recalcitrant state (humic substances) difficult to degrade further especially following association with mineral surfaces. The formation of humic substances results from many events of oxidation and reduction that create materials with increased C and H and lower O content compared to the original animal, microbial, and plant tissues (Stevenson 1994; Horwath 2007). During decomposition, N compounds react through radical coupling and increase the N content of humic substances, especially those protected through their association with minerals lowering the mineral C associated C to N ratio (Schnitzer 1978).

Recent studies show that microbial biomass provides a significant source of C to maintain and build OM (Kindler et al., 2006; Simpson et al., 2007). Microbial inputs to

soil reflect both the dominant groups of organisms present in a soil and their turnover rates. Voroney et al., (1989) showed the importance of microbial products for maintaining OM following the addition of ^{14}C-glucose to soil to label the microbial community, which produced products that were as or more stable than those derived from wheat residues. Martin and Haider (1979), using laboratory incubations suggested that fungi contributed more C to OM than other microbial groups due to their complex cell walls and pigments. Fungi and bacteria comprise approximately 90% of total soil biomass (Rinaan and Bath 2009) and the turnover is estimated to contribute as much as 80% to the maintenance of OM (Liang and Balser 2010). Microbial products such as phenols, amino sugars and fungal melanins likely contribute to the recalcitrant pool of OM precursors.

It has been hypothesized that microbial cellular biochemistry determines the amount and form of C stabilizing in OM, which could dictate difference across microbial groups in contributing to stable soil C. Higher carbon use efficiency, particularly those associated with fungi could suggest they contribute more to OM (Rinaan and Baath 2009). Diverse bacterial cell wall structures (e.g., Gram-stain classification) likely influence decomposition. For example, Gram-positive bacteria contain a greater amount of peptidoglycan in their cell walls than Gram-negative bacteria. Greater peptidoglycan content is often associated with slower decomposition, as these compounds have been shown to accumulate in soil (Vollmer et al., 2008). The limited number studies comparing fungal to bacterial turnover have not produced definitive conclusions of whether diverse microbial groups contribute differentially to stable soil C under field conditions field (Strickland and Rousk 2010).

The objective of this research was to compare the decomposition rates of microbial isolates from fungi, Gram-positive bacteria, actinobacteria, and Gram-negative bacteria under field conditions. Microbial isolates from a temperate and tropical forest were chosen to contrast turnover rates in diverse climates. Our main hypothesis was that the decomposition of microbial group isolates would differ due to biochemical differences, contributing different amount of carbon for OM maintenance.

Materials and Methods

Field sites

The study sites were forests in California (38° 53' N, 120° 39' W) at an elevation of 1315 m and Puerto Rico (18° 41' N, 65° 47' W) at an elevation of 780 m. The California forest temperate with a Mediterranean climate with mean annual precipitation of 177 cm and mean annual temperature of 14-27°C in the summer, and 0-9°C in the winter. The 20 year old forest is composed of *Pinus ponderosa (*ponderosa pine), *Pinus lambertiana* (sugar pine), *Abies concolor* (white fir), *Pseudotsuga menziesii* (douglas fir), and *Calocedrus decurrens* (incense cedar). The soil is a fine-loamy mixed mesic, ultic Haploxeralf with a mixed andesitic lahar/granitic parent material, with less than 20% clay content with a pH of 5.8, microbial biomass of 432 ug C g^{-1} soil and a fungal to bacterial ratio of 0.28 (see Throckmorton et al., 2012 for more details).

The tropical forest in Puerto Rico is > 40 years old with mean annual precipitation of 450 cm and mean annual temperature is 18.5° C. The dominant trees species is *Cyrilla racemiflora* (myrtle). The soils are derived from volcanoclastic sediments with quartz diorite intrusions (Ultisols), with high clay content (up to 70%) with a pH of 4.5, microbial biomass of 1,512 ug C g^{-1} soil and a fungal to bacterial ratio of 0.2 (see Throckmorton et al., 2012 for more details).

Microbial isolation and culture

Microbial isolation, selection, and production are described in Fan et al., (2009). A group of 2 to 4 distinct isolates within each group (fungi, actinomycetes, gram – and gram +) was selected for ^{13}C enrichment. The isolates were grown in liquid media amended with 20% glucose (99.9% - atom enriched with ^{13}C), yeast extract (10%) with M9 salts at pH 5.5 and grown to late stationary phase. Whole cells and extracellular polysaccharides (EPS) products were sterilized by autoclaving for two 30-minute cycles at 121° C. After autoclaving, cells and EPS were lyophilized. ^{13}C enriched microbial isolates contained 101.1 ± 2.5 atom% ^{13}C determined on a PDZ Europa ANCA-GSL elemental analyzer interfaced to a PDZ Europa 20-20 isotope ratio mass spectrometer (Sercon Ltd., Cheshire, UK). Total microbial isolate C and N elemental analyses as determined by dry combustion (Costech Analytical Technologies Inc., Lake Zurich, IL, USA). In particular, temperate and tropical fungi, and tropical bacteria

differed notably from other groups: exhibiting a greater lipid content, and lower abundance of benzene, phenol, and N-compounds (data not presented).

^{13}C- labeled microbial field study

Soil mesocosms (PVC), 10-cm diameter and 20 cm in depth, were installed to a depth of 18 cm 1 year prior to addition of microbial residues. Mesocosms were screened with 450-µm mesh (2.5-cm diameter) at 3, 8 and 13 cm depths to allow fungal hyphae and fine root access. The experiment was a split-plot design, with three replicate blocks (~10-20m diameter) at each site. Each of the 8 microbial treatments and unamended controls were randomly assigned to previously installed mesocosms within each block. Five mesocosms sets each with 3 replicates were installed per treatment, and were excavated on five separate sampling dates. The forest litter layer was removed and a total of 80 mg of ^{13}C- labeled microbial residues and EPS in 30 mL of deionized water was injected into top 1-3 cm of the soil using a syringe. Control mesocosms were unamended, but received the same amount of water. In California, treatments were applied on 21 June 2006 and soil cores were excavated at 33, 163, 370, 763, and 1133 days after application. In Puerto Rico, treatments were applied on 6 Oct. 2006 and soils were excavated 17, 114, 249, 480, and 886 days after application.

Soil processing

The litter layer was removed and the soils separated into 2 depths of 0-7.5 and 7.5-15cm. Soils were stored at 4°C prior immediately and during transport to UC Davis. Soil moisture content was determined after drying at 105° C. Organic C content was determined by dry combustion (Costech Analytical Technologies Inc., Valencia, CA, USA).

Soil and microbial ^{13}C isotope analyses

Soil and microbial ^{13}C was measured on a PDZ Europa ANCA-GSL elemental analyzer interfaced to a PDZ Europa 20-20 isotope ratio mass spectrometer (IRMS; Sercon Ltd., Cheshire, UK) and reported relative to a standards calibrated against NIST Standard Reference Materials (National Institute of Standards and Technology, Gaithersburg, MD, USA). Recovery of ^{13}C in soils was calculated using equation 1 (Balesdent and Mariotti 1996),

Equation 1. $C_M = (\delta_{MS} - \delta_C) / (\delta_{MI} - \delta_{NU})$

where C_M is the contribution of labeled C at time T, δ_{MS} is the $^{13}C/^{12}C$ ratio for microbial- treated soils at time T; δ_C is the $^{13}C/^{12}C$ ratio for unamended soils (ie. control soils); δ_{MI} is the $^{13}C/^{12}C$ input C; and δ_{NU} represents the $^{13}C/^{12}C$ of natural inputs. Recovery of ^{13}C at various time points was calculated as the percentage of labeled C remaining relative to initial inputs.

The turnover of ^{13}C, the amount of ^{13}C recovered in soil (%) were summarized empirically for best fit by fitting one compartment exponential decay models to each of the two observable phases of elimination. The phases were determined after graphing ^{13}C recovery curves across treatments and time. This yielded an initial ($k_{initial}$) and a terminal ($k_{terminal}$) rate constant for ^{13}C loss. Rate constants were determined using simple linear regression on the natural log transformation of ^{13}C recovery values (Weisenberg et al., 2004).

Statistical analyses

Sites were separately assessed for differences in ^{13}C recovery using linear mixed effects models. Separate models for sites were necessary since time increments between sampling points differed, resulting in ^{13}C recoveries that were not directly comparable across sites. MRT values for ^{13}C turnover at both sites were assessed together with a full linear mixed effects model. Statistical analyses were performed using SAS for Windows Version 9.1 (SAS institute, Cary, NC).

Results

Microbial Group Recoveries

The recovery of the ^{13}C labeled microbial treatments in California did not significantly differ after 1,133 d (Microbial treatment*Origin*Time, $P = 0.5307$; Origin*microbial treatment, $P = 0.4178$) (see Throckmorton et al., 2012 for more details). However, results show differences in ^{13}C recovery in microbial groups earlier at day 163 and 763 (Figure 1; microbial group*time $P = 0.0463$). This suggests a slower initial decay of Gram-positive bacteria and fungi in intermediate stages of decay. The differences are not substantial and disappeared as the field incubation continued.

The ^{13}C recoveries from microbial treatments in Puerto Rico were significantly different from 249 d and to 886 d (microbial treatment*group*time, $P = 0.0264$) (see

Throckmorton et al., 2012 for more details). The results suggest relatively lower stability of temperate Gram-negative bacteria compared to temperate fungi, temperate Gram-positive bacteria, tropical actinobacteria, and tropical Gram-negative bacteria. The ^{13}C recovery of temperate Gram-negative bacteria was consistently lower than most treatments throughout the course of the study, particularly after 249 d. Unlike California; in Puerto Rico there was no significant group effect (data not shown; microbial treatment*Time, $P = 0.4743$; Group, $P = 0.1406$).

Microbial treatment Turnover

Both $k_{initial}$ and $k_{terminal}$ were lower in California than Puerto Rico, corresponding to MRTs in California of 3.77 ± 1.33 to 7.08 ± 1.39 years compared to Puerto Rico of 1.31 ± 0.64 to 3.76 ± 1.15 years (Table 1). Significant differences in MRTs occurred only in Puerto Rico (site*origin*microbial treatment effect, $P = 0.0119$) in the temperate Gram-negative bacteria and tropical fungi treatments, which exhibited a significantly slower turnover compared to temperate fungi, temperate Gram-positive bacteria, and tropical actinobacteria. This supports microbial group recovery results and suggests faster turnover of temperate Gram-negative bacteria and highlight a slightly faster turnover of tropical fungi in later stages of decay (Fig. 2). No differences in MRT were found in California (Fig. 1).

Discussion

The mechanisms leading to the stabilization of OM in soils and sediments are continuously debated (Schimdt et al., 2011). A persistent view of OM formation has focused on molecular components of inputs such as lignin or indices of chemical quality, such as C to N ratio. The approach has described successfully the kinetics of OM turnover. The stabilization of OM with dense secondary minerals such as clay and amorphous oxides, notably iron oxides, was observed earlier and continues to be used as the basis to describe stabilization mechanisms (Allison et al., 1949; Theng 1982; Hayes and Clapp 2001). Notably lacking in these interpretations of OM stabilization is the source of inputs, whether of plant or microbial origin.

This study addresses the source of stable OM by determining the turnover of diverse microbial inputs to soil under field conditions. Our results show the source and diversity of microbial groups had minor influence on their turnover. In California our results

suggested a slightly greater stability of Gram-positive bacteria and fungi in early stages of decay; however, the effect was ephemeral. In addition, no difference in MRT of the microbial groups confirming the labeled microbial recovery results. Conversely, in Puerto Rico slightly lower turnover rates were observed in the temperate Gram-negative bacteria and to a lesser extent tropical fungi treatments. However, the effect were minor and in general findings do not strongly support the hypothesis that biochemically differences among microbial groups would lead to varied and distinct turnover rates. Most importantly our results do not support the widely held view that fungal inputs are more stable than bacterial inputs (Martin and Haider, 1979; Bailey et al., 2002).

The turnover of the microbial treatments may have been done by diverse microbial decomposers that specialize in degrading the unique biochemistry of the microbial treatments. This suggests that the consumption of the microbial inputs likely resulted in creating secondary biomass within different microbial groups. This could explain the differences in the timing of turnover for several groups in California and Puerto Rico. The differences in California disappeared while they persisted longer in Puerto Rico. This implies the turnover of the microbial inputs likely resulted in growing or maintaining at least one generation of decomposers before they themselves turned over and contributed to stable OM. Considering the the vast range and overlap of microbial communities that exist in soil, unique substrate utilization patterns could lead to different stabilization rates (Balser and Wixon, 2009; Rinaan and Baath, Singh, 2010; Bailey et al., 2002; Strickland and Rousk, 2010; Jastro et al., 2007; Holland and Coleman, 1987). Others have demonstrated that distinct microbial communities exhibit unique substrate utilization preferences (Waldrop and Firestone, 2004; Rannan and Baath, 2009). This could have broader implications for interpreting soil C sequestration associated with microbial contributions to stable soil C. However, our data do not strongly support that unique substrate utilization patterns are strong controllers of turnover of diverse microbial inputs.

Unlike plant litter quality effects on decomposition, our results suggest that microbial biochemistry is not a strong determinant of turnover rates. Plant litter decay rates correspond to a number of measurable properties including: solubility, lignin content, and C to N ratio (Paterson, 2009; Aerts, 1997). Plant litters have a vast range of nutrient C to N ratios (<19 to >300) in comparison to microbial inputs (5 to 15), respectively,

which could partly explain the lack of difference in the decomposition of diverse microorganisms.

This study provides an assessment of the stability of diverse microbial substrates in soil and their contribution to soil OM stabilization. We did not test physical and metabolic factors associated with the consumption of these microbial groups by the decomposer community, which could influence microbial C turnover. For example, fungal hyphae may be preferentially stabilized in aggregates. The metabolic effect, such as C use efficiency of decomposers was also not addressed. However, as mentioned above, these factors had little influence on the long-term stability of OM from different microbial inputs. The present study solves one piece of the puzzle in an effort to understand how microorganisms from diverse groups may influence soil C storage. We conclude that there are minor differences in the turnover of diverse microbial inputs. This simplifies our understanding of the roles of microbial inputs to OM maintenance and shows that the size and turnover rate of the entire microbial community is more important than its composition in assessing factors responsible for soil C stabilization.

Acknowledgements

This research was funded by a research award by the National Science Foundation's Division of Environmental Biology, Ecosystem Science Cluster (award nos. 0324002) and The Kearney Foundation of Soil Science (award no. 2008.031). We are grateful for the contributions by researchers E. Brodie, J. Braun, T. Doane, E. Dubinsky, J. Fortney, D. Herman, E. Long, N. Monte, J. Pett-Ridge, W. Silver, T. Shimada and K. Trihn. In addition, we thank the research staff of the UC Blodgett Forest Research Station and the Luquillo Experimental Forest

Table 1. $k_{initial}$ and $k_{terminal}$ (y^{-1}) for ^{13}C addition in California and Puerto Rico. Mean shown; n = 3. Mean residence time (MRT) estimates (years) for. Mean and standard errors shown (n = 3). LSD letter-group superscript. Treatments sharing a letter are not significantly different.

		$K_{initial}$		$K_{terminal}$		Mean Residence Times (MRTs)[1]	
		CA	PR	CA	PR	CA	PR
Temperate	***Actino***	7.16	29.20	0.19	0.61	^{AB}5.51	^{DEF}1.67
	Fungi	7.25	20.72	0.09	0.31	^{AB}5.86	^{BCD}3.19
	Gram+	4.83	22.68	0.26	0.43	^{AB}4.97	^{CD}2.41
	Gram-	9.27	23.78	0.15	1.46	^{A}7.08	^{F}1.31
Tropical	***Actino***	8.99	22.22	0.19	0.30	^{ABCD}3.77	^{ABCD}3.76
	Fungi	5.92	22.52	0.16	0.96	^{AB}5.99	^{EF}1.49
	Gram+	4.63	23.11	0.25	0.60	^{ABC}4.12	^{DEF}1.85
	Gram-	8.87	22.84	0.26	0.47	^{ABC}4.16	^{CDEF}2.08

[1]Site*Origin*Group (P = 0.0119)
CA (California); PR (Puerto Rico)

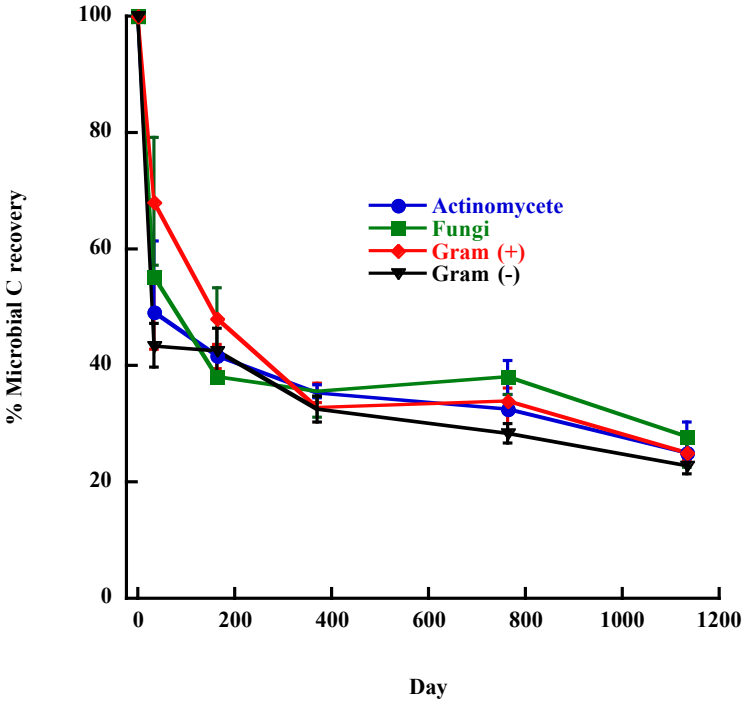

Fig. 1. Recovery of labeled ^{13}C- microbial treatment over time in California over time. Standard error of the mean shown as line bars (n = 3).

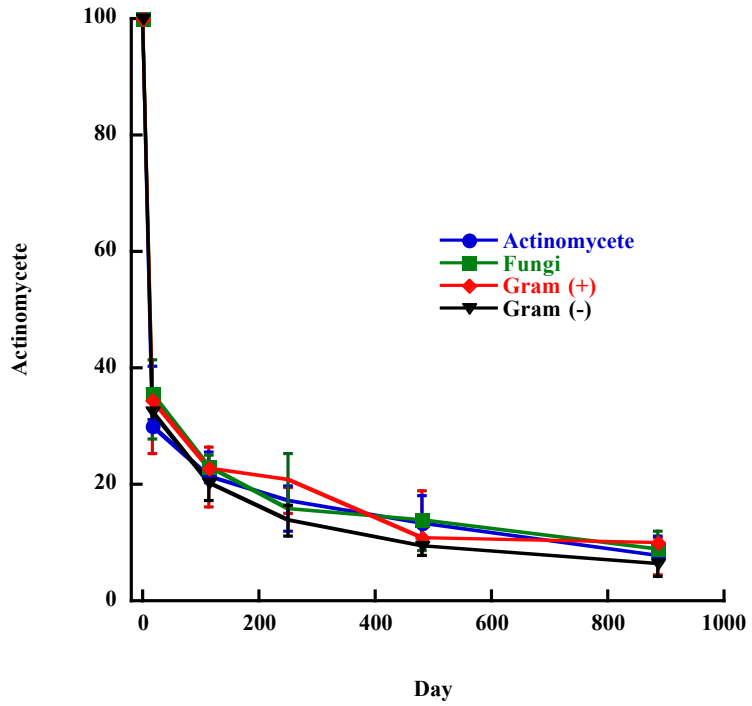

Fig. 2. Recovery of labeled ^{13}C- microbial treatment over time in Puerto Rico over time. Standard error of the mean shown as line bars (n = 3).

References

Aerts, R. 1997. Climate, leaf litter chemistry and leaf litter decomposition in terrestrial ecosystems: a triangular relationship. Oikos 79:439–449.

Allison F. E., M. S. Sherman and L. A. Pinck. 1949. Maintenance of soil organic matter: I. Inorganic soil colloid as a factor in retention of carbon during formation of humus. Soil Sci. 68:463-478.

Bailey, V., J. L. Smith and H. Bolton, Jr. 2002. Fungal-to-bacterial ratios in soils investigated for enhanced C sequestration. Soil Biol. Biochem. 34:997–1007.

Balser, T. and D. Wixon. 2009. Investigating biological control over soil carbon temperature sensitivity. Glob. Chang. Biol. 15:2935–2949.

Fan, T.W.M., J. A. Bird, E. L. Brodie and A. N. Lane. 2009. ^{13}C-Isotopomer-based metabolomics of microbial groups isolated from two forest soils. Metabolomics 5:108–122.

Hayes, M. H. B., and C. E. Clapp. 2001. Humic substances: Considerations of compositions, aspects of structure, and environmental influences. Soil Sci. 166:723-737.

Holland, E.A. and D. C. Coleman. 1987. Litter placement effects on microbial and organic matter dynamics in an agroecosystem. Ecology 68:425–433.

Horwath, WR. 2007. Carbon Cycling and Formation of Soil Organic Matter. E.A. Paul, Ed. In: Soil Microbiology, Ecology and Biochemistry. Academic Press, New York, pp. 303-339.

Jastrow, J.D., J. E. Amonette and V. L. Bailey. 2007. Mechanisms controlling soil carbon turnover and their potential application for enhancing carbon sequestration. Clim. Change 80:5–23.

Kindler, R., A. Miltner, H. Richnow and M. Kastner. 2006. Fate of gramnegative bacterial biomass in soil – mineralization and contribution to SOM. Soil Biol. Biochem., 38:2860–2870.

Liang, C. and T. C. Balser. 2010. Microbial production of recalcitrant organic matter in global soils: implications for productivity and climate policy. Nature Rev. Microbiol., DOI: 10.1038/nrmicro2386 cl.

Martin, J.P. and K. Haider. 1979. Biodegradation of ^{14}C-labeled model and cornstalk lignins, phenols, model phenolase humic polymers, and fungal melanins as influenced by a readily available carbon source and soil. Appl. Environ. Microbiol., 38:91–110.

Paterson, E., A. J. Midwood and P. Millard. 2009. Through the eye of the needle: a review of isotope approaches to quantify microbial processes mediating soil carbon balance. New Phytol., 184:19–33.

Rinnan, R. and E. Baath, E. 2009. Differential utilization of carbon substrates by bacteria and fungi in tundra soil. Appl. Environ. Microbiol., 75:3611–3620.

Rinnan, R. and E. Baath. 2009. Differential utilization of carbon substrates by bacteria and fungi in tundra soil. Appl. Environ. Microbiol., 75:3611–3620.

Schmidt, M. W. I., M. S. Torn, S. Abiven, T. Dittmar, G. Guggenberger, I. A. Janssens, M. Kleber, I. Kogel-Knabner, J. Lehmann, D. A. C. Manning, P. Nannipieri, D. P. Rasse, S. Weiner and S. E. Trumbore. 2011. Persistence of soil organic matter as an ecosystem property. Nature 478:49-56.

Schnitzer, M. 1978. Humic substances: Chemistry and reactions. *In* "Soil Organic Matter" (M. Schnitzer and S. U. Khan, eds.), Vol. 8, pp. 1-64. Elsevier Scientific Pub. Co., New York.

Simpson, A.J., M.S. Simpson, E. Smith and B.P. Kelleher. 2007. Microbially derived inputs to soil organic matter: are current estimates too low? Environ. Sci. Technol., 41:8070–8076.

Stevenson, F. J. 1994. "Humus Chemistry: Genesis, composition, reactions," John Wiley & Sons, Inc., New York.

Strickland, M.S. and J. Rousk. 2010. Considering fungal:bacterial dominance in soil – methods, controls, and ecosystem implications. Soil Biol. Biochem., 42:1385–1395.

Throckmorton, H. M., J. A. Bird, L. Dane, M. K. Firestone and W. R. Horwath. 2012. The source of microbial C has little impact on soil organic matter stabilization in forest ecosystems. Ecology Lett. 15:1257–1265.

Vollmer, W., D. Blanot, D. and M. A. de Pedro. 2008. Peptidoglycan structure and architecture. FEMS Microbiol. Rev., 32:149–167.

Voroney, R.P., E.A. Paul and D.W. Anderson. 1989. Decomposition of wheat straw and stabilization of microbial products. Can. J. Soil Sci., 69:63–77.

Waldrop, M.P. and M. K. Firestone. 2004. Microbial community utilization of recalcitrant and simple carbon compounds: impact of oak-woodland plant communities. Oecologia 138:275–284.

Wiesenberg, G.L.B., J. Schwarzbauer, M. W. I. Schmidt and L. Schwark. 2004. Source and turnover of organic matter in agricultural soils derived from n- alkane/n-carboxylic acid compositions and C-isotope signatures. Org. Geochem., 35:1371–1393.

RELATIONSHIPS BETWEEN CARBON SEQUESTRATION AND NITROGEN CYCLING IN A SEMI-ARID PINE FOREST

Dan Yakir, Ilya Gelfand, Eyal Rotenberg

Environmental Sciences and Energy Research, Weizmann Institute of Science, Rehovot 76100, Israel

Afforestation of semi-arid shrubland

Humans have continuous impact on the surrounding environment. Nowadays is commonly accepted by scientific community that human-induced changes such as atmospheric composition alternation and land-use change alert global as well local climatic conditions. Dry land ecosystems cover significant area of Earth's land surface and expected to increase in area due to desertification. Recently, global scale desertification of dry lands drew attention of the United Nations.

While in dryland ecosystems human impact expressed in accelerating land degradation (http://lada.virtualcentre.org/), on the more global scale, increase of the carbon dioxide concentration in the atmosphere, since end of 19th century have pronounced effects on the global climate. Forest planting or afforestation of the dry land ecosystems can be used as both carbon sequestration and land restoration/desertification combat tool.

The main consequences of afforestation include increase in ecosystem carbon storage and change of biomass distribution in the ecosystem, which may also extend to biological activity. Planting forests on "native" shrubland in a semi-arid climate possibly have affects upon nitrogen (N) cycle and turnover. These effects to date, however, have been insufficiently investigated. The expansion of the vegetation covered area, or the plant area index (the ratio of plant to land surface area) may change overall nutrient distribution. The afforestation may have an effect upon enlargement of "islands of fertility"; concept developed for shrubs in arid ecosystems by, or conversely may reduce the N availability by inhibition of the soil microbial processes and increasing the uptake of the N from the soil pools.

Increase in N demand of the ecosystem following the increase of carbon pools may enhance rates of N cycling in order to meet the trees' requirements. The soil N cycle is driven by microbial activities, which controlled partly by carbon and water availability,

and partly by abiotic factors. Understanding of interplay between biotic and abiotic factors as controllers of N cycling in semi-arid ecosystem is crucial for an understanding of the N flow through such system.

In Israel, since the beginning of the 20th century ongoing process of afforestation take place. This days more than 90000 ha of planted forest in Israel, being nearly 70% of the total (132000 ha) forested area. The common tree species used for planting in Israel is Aleppo pine (*Pinus halepensis* Mill.), this species was chosen for afforestation because its drought tolerance and Mediterranean origin.

Nitrogen cycle in semi-arid ecosystems and afforestation

Interplay between N and water limitation commonly occurs in semi-arid ecosystems. This reflected in low productivity and ecosystem plant community structure of the dry lands. The afforestation of the dry lands by pine species can significantly increase the water use efficiency and carbon sequestration potential of those ecosystems. The change in land cover, and following afforestation biomass increase and consequently N demand may have influence on the N cycle in newly created ecosystem.

Firstly, the ecosystem N input and output may change. Increase in N inputs can come from additional N deposited on the leaves and than washed out to the soil by rain or by direct uptake of N by foliage. The N inputs through biological N fixation, oppositely to the deposition, may decrease as result of biological soil crust destruction during afforestation process. The afforestation may change the amount and patterns of gaseous N emission from the soil as well, for an example the woody vegetation encroachment has resulted in increase of the nitric oxide emissions in Texas, while afforestation caused reduction of the soil emissions in Costa Rica.

Secondly, the internal cycle of N in the ecosystem and soil-plant interactions can be influenced. The changes in the amount and quality of the litterfall with change of dominant plant type shown to have influence on litter decomposition rates and mechanisms of the N return to the soil pool. Pine leaf litter usually has higher C/N ratios and slower decomposition rates, compared to the shrub and annuals litter. The afforestation has an influence on soil N processes as well. Although, effects on the specific N-cycle processes depends on the plant type and time scale of the land-use

change. For example, soils from young pine plantation in central Oregon exhibited similar N mineralization rates in mineral soil and higher in the litter layer than those of old plantation.

Finally, the main mechanism of the inorganic N removal from the soil, microbial and plant uptake is influenced by plant type change upon afforestation and exchange of the shrubs by trees. Overall, the land-use change induces the changes in the N cycle rates, influencing ecosystem productivity and N use efficiency.

Results and conclusions

Nitrogen cycle is closely connected to the carbon and water biogeochemical cycles and has grate importance for the Earth ecosystems functioning. In terrestrial ecosystems nitrogen usually limiting the productivity, but nowadays due to increasing of pollution and use of fossil fuels, N saturation is observed. The dry lands, although covering almost 17% of total land surface of the Earth receiving relatively low scientific attention, mostly due to remote location from the main research centers. The dry land experiencing desertification processes and with global warming tendencies likely that desertification processes will accelerate. Moreover, the increase of carbon dioxide concentration in the atmosphere due to fossil fuel and biomass burning have positive feedback on global warming and desertification.

The afforestation of dry lands can be used as both combat tool against desertification and tool for carbon sequestration from the atmosphere. Recent studies showed that afforestation significantly increases carbon sequestration capacity of semi-arid, north Negev desert. However, the influence of afforestation on N cycle is not clear.

In the research here we made the first attempt to understand afforestation driven changes in ecosystem N cycle. We compared N balances of the Yatir forest and surrounding shrubland ecosystems (Figure 1). The forest showed slower N cycling with increasing of the N input during the season of activity. The forest ecosystem showed sharp increase in NUE, N MRT, and N productivity, both at aboveground and belowground components of the ecosystem (Figure 2). Our results explain how by small “adjustments” of the ecosystem N cycle the almost 2.5 fold increase in the carbon stock of the ecosystem can be supported without any additional fertilization.

We investigated in depth controls on nitrification process and gaseous nitrogen oxides emissions from the ecosystems since those components of the N cycle play an important role in regulation of the N availability for plants.

We observed unexpected fast nitrite accumulation in the soil of semi-arid pine afforestation. Laboratory incubations indicate that the nitrite accumulation reflected a temporal delay between the oxidation of ammonium and nitrite, probably due to differences in drought tolerance and recovery rates of AOB versus NOB microbial populations. These effects resulted with a delay in the onset of nitrate accumulation at the beginning of the wet season in the soils of a semi-arid afforestation. We hypothesize that such delay may improve the synchronization of N availability with peak plant activity, and contribute to high ecosystem NUE and N productivity, such as observed in this semi-arid afforestation. We also note that the presence of nitrite in the soil may have inhibitory effects on microbial immobilization of inorganic N due to nitrite toxicity even at low concentrations, an effect that requires further study. As the Mediterranean region is expected to experience decreasing precipitation trends with future global warming, the effects observed in the semi-arid afforestation will be applicable to increasingly larger areas.

We measured potential nitrogen oxide emission from the soils of shrubland and Yatir forest ecosystems and upscaled results from those measurements to the ecosystem level. Our results showed that: NO emissions from this semi-arid ecosystem have very high spatial and seasonal variability; afforestation of semi-arid shrubland reduce NO emission by 35% on an annual basis; for upscaling and modelling approaches there is clear need to include spatial and temporal variability in the sampling design.

In summary, it was observed that afforestation in the semi-arid region could greatly increase carbon sequestration, with significant accumulation of soil organic matter. This led to the question; to what extent such increase carbon uptake depends on increased nitrogen availability. Construction of ecosystem nitrogen budget in the afforested area and the non-forested background shrubland indicated some compensating changes in nitrogen input/output, but no significant change in the net nitrogen budget between the two ecosystems. However, afforestation did result in significant changes in the characteristics of nitrogen cycling associated with afforestation. This included changes such as increased C/N ratios in biomass, increased

N remobilization, and reduced litter 'quality'. The overall effect was a marked slow-down in ecosystem N cycling, and large increase in ecosystem nitrogen use efficiency. These results support the notion of significant potential for carbon sequestration in the semi-arid regions, but some caveats must also be considered.

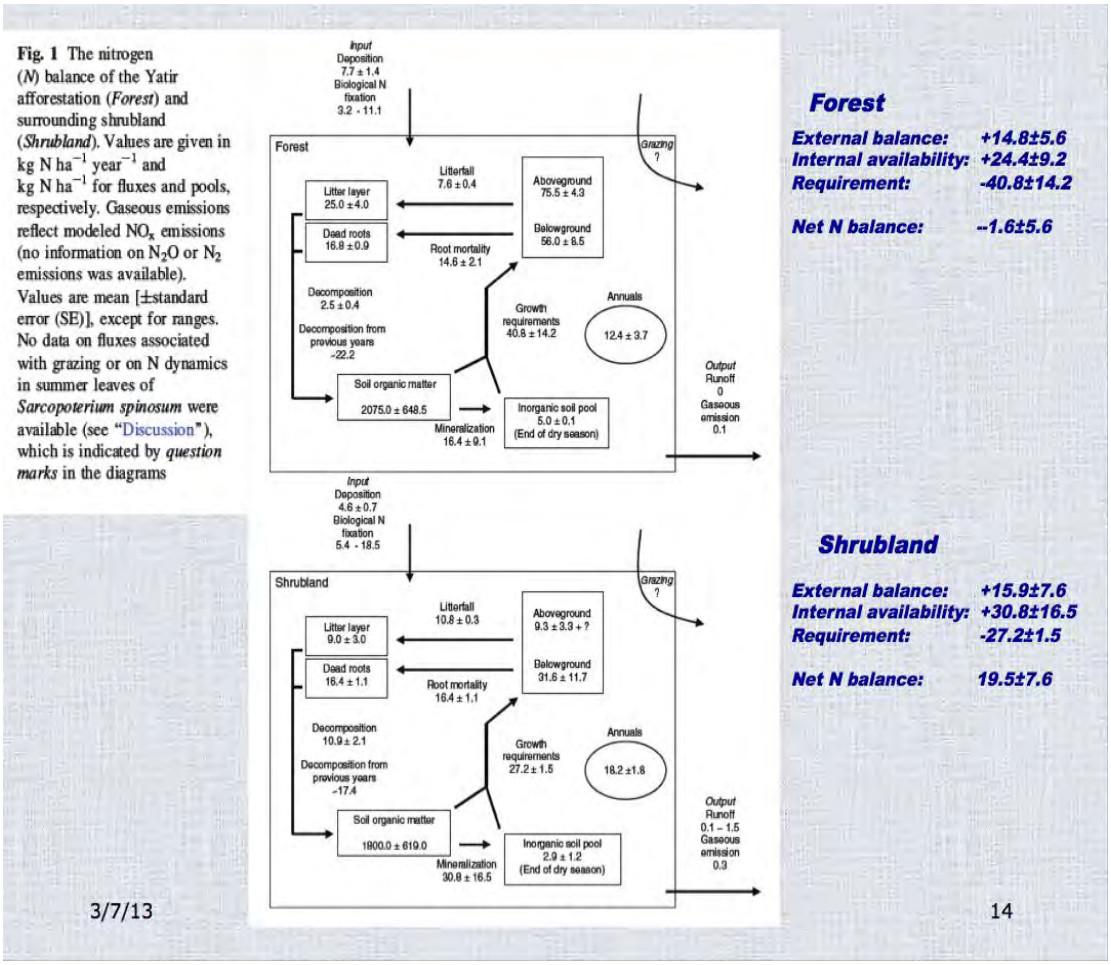

Figure 2. Nitrogen Use Efficiency up x4 compared to background shrubland

	Yatir forest		Shrubland	
	Aboveground	Belowground	Aboveground	Belowground
NPP (kg dw $ha^{-1}y^{-1}$)	3868	4773.2	1027	1437.8
A (N productivity) (kg dw $kg^{-1}N\ y^{-1}$)	51.2	85.5	41.8	43.8
MRT (y)	8.4	3.9	2.1	2
C/N	156		39	
NUE*	430	329	86.9	87.7

*Method of Berendse 1987; Using Vitousek 1982: 235 vs 83 for above ground.
(Units: Kg dw $kg^{-1}N$)

3/7/13 Greidinger 2013 15

References

Grunzweig JM, Gelfand I and Yakir D (2007) Biogeochemical factors contributing to enhanced carbon storage following afforestation of semi-arid shrubland. ***Biogeochemistry 4***, 891-904.

Gelfand I and Yakir D (2008) Influence of nitrite accumulation in association with seasonal patterns and mineralization of soil nitrogen in a semi-arid pine forest. ***Soil Biology Biochemi***, **40, 415-424**.

Gelfand, I, Feig, G, Meixner FX, Yakir D (2008) Effects of semi-arid shrubland afforestation on biogenic NO emission from soil. ***Soil Biology Biochemi***, 41, 1561-1570.

Gelfand I, Grunzweig JM and Yakir D (2012) Slowing of nitrogen cycling and increasing nitrogen use efficiency following afforestation of semi-arid shrubland. Oecologia, 168, 563-575. DOI 10.1007/s00442-011-2111-0

USING FOOD-WEB DYNAMICS TO EXPLAIN VARIATION IN CARBON AND NITROGEN CYCLING

Dror Hawlena

Department of Ecology, Evolution & Behavior The Hebrew University of JerusalemGivat-Ram, Jerusalem 91904, Israel.

Ecological science has largely treated the study of the organismal and biogeochemical aspects of ecosystems as separate scientific enterprises. This is in spite of growing evidence that species interactions in food-webs can determine the nature of elemental flux and cycling. To begin bridging this gap, we have developed a new conceptual framework that uses prey physiological responses to predation risk to explain context dependent variation in biogeochemical processes. Prey physiological reaction to the risk of predation involves allocation of resources from growth and reproduction to support emergency functions; e.g., an increase in maintenance respiration concomitant with higher carbohydrate and lower N demand. Such changes in energy and elemental budgets should alter the regulatory role prey species play in conveying energy and elements from plants to higher levels in the food-web, and in regulating quantity and quality of detritus available for decomposers. Elemental-nutrient content of detrital inputs (e.g., plant litter, carcasses, feces) to soils is an important determinant of the way belowground communities regulate ecosystem processes. Thus, physiological stress provides a general way to start linking plasticity in trait expression and biogeochemistry to produce an integrative theory for context-dependent variation in ecosystem functioning. First empirical examination using an old-field model food-chain of an herbivore grasshopper (prey) and a predatory spider, thus far, support this new conceptual framework. Grasshoppers stressed by spider predators prefer to eat more carbohydrates and have a higher body carbon-to-nitrogen ratio than do grasshoppers raised without spiders (1). This change in elemental content does not slow grasshopper decomposition but perturbs belowground community function, decelerating the subsequent decomposition of plant litter. This legacy effect of predation on soil community function appears to be regulated by the amount of herbivore protein entering the soil (2). Using a ^{13}C pulse-chase experiment in the same model system, we found

that carnivore presence enhanced initial carbon fixation by plants and slowed the relative rate of carbon loss via ecosystem respiration. These changes in carbon cycling led to 1.4-times more carbon storage in above-ground and below-ground plant biomass when carnivores were present compared to conditions with just herbivores.

[1]Hawlena D, Schmitz O. J, 2010. Herbivore physiological response to fear of predation alters ecosystem nutrient dynamics. Proceedings of the National Academy of Sciences. 107: 15503-15507.

[2]Hawlena, D, Strickland, M.S., Bradford, M.A., Schmitz, O.J, 2012. Fear of predation slows plant-litter decomposition. Science.336: 1434-1438.

HUMIC-LIKE AND PROTEINACEOUS COMPONENTS OF ORGANIC MATTER IN AQUATIC AND SOIL ENVIRONMENTS: THREE CASE STUDIES ANALYZED WITH EEM+PARAFAC METHODOLOGY

Mikhail Borisover[1*], Yael Laor[2], Guy J. Levy[1]

[1]Institute of Soil, Water and Environmental Sciences, Agricultural Research Organization (ARO), The Volcani Center, Bet Dagan, Israel;

[2]Institute of Soil, Water and Environmental Sciences, Agricultural Research Organization (ARO), Newe Ya'ar Research Center, Ramat Yishay, Israel;

*Corresponding author: vwmichel@volcani.agri.gov.il

Abstract

Excitation-emission matrix (EEM) fluorescence spectroscopy combined with parallel factor analysis (PARAFAC) has become a widely used tool for characterizing organic matter (OM) in multiple natural and engineered environments. This combination provides a relatively simple and fast methodology to relate changes in EEMs to changes in OM composition. The current contribution presents three case studies based on earlier EEM+PARAFAC analyses of OM in water samples obtained from lacustrine, riverine and soil environments: (i) Lake Kinneret (Sea of Galilee) and its catchment basin, (ii) the heavily polluted Lower Kishon river water, (iii) soils irrigated with treated wastewater vs. fresh water. In all these systems, aqueous samples containing either suspended or dissolved OM were characterized for humic-like and proteinaceous (or protein-like) OM fluorescent components, and their contents were expressed in terms of PARAFAC-based concentration scores. The concentration scores (or their ratios and/or mutual relationships) of these components allow to quantify changes in the proportions between concentrations of different types of fluorescent OM. A specific advantage of the EEM+PARAFAC technique, as compared with some traditional methods of OM characterization, is that it becomes even more effective with the increase in the number of samples studied. Moreover, due to the increase of the number of samples, the EEMs interpretation of already analyzed samples is improved.

Introduction

Organic matter (OM) present in soils, sediments and various aquatic systems (e.g., surface- and ground-water) is a complex mixture of multiple components differing in their structure, origin, capability to undergo chemical transformation, bio- and photo-degradation as well as in their multiple impacts on the environment. Certain OM components (such as humic substances, proteinaceous matter, pigments, some anthropogenic chemicals and microorganisms) are fluorescent, and therefore, their spatial and temporal variability can be studied by fluorescence spectroscopy. Specifically, excitation-emission matrix (EEM) fluorescence spectroscopy has been widely used as a tool for characterizing OM present in various aquatic systems or soil extracts (e.g., Chen et al., 2003; Alberts and Takács, 2004; Corvasce et al., 2006; Hudson et al., 2007).

Combining the EEM fluorescence spectroscopy with parallel factor analysis (PARAFAC) opened new perspectives in using fluorescence measurements and the interpretation of the EEMs data. PARAFAC is a decomposition method of multi-way data which can be considered as a restricted version of the two-way principal component analysis (Bro, 1997). The interest in its use for fluorescence analysis started relatively recently (Ross et al., 1991; Bro, 1997; Andersen and Bro, 2003; Stedmon et al., 2003, 2008) although the PARAFAC method originated earlier in psychometric studies (Bro, 1997; Andersen and Bro, 2003, and citations therein). This interest was caused by the capability of PARAFAC to extract from the EEMs the spectral images and concentration characteristics of chemically meaningful fluorescent components and to reveal the constituents that could be masked by the background of a strong emission and overlapping of fluorescence peaks. Furthermore, knowledge of the types of fluorescent OM components and of the changes in their concentrations may shed light on the formation of natural OM, OM degradation and reactivity in various environments. The increasing interest in combining the PARAFAC technique with the EEM fluorescence is illustrated in Fig. 1 where the trend in the number of publications in this topic is shown from 1996 to date and seems to be far from saturation.

The current review presents selected results of three case studies based on our earlier EEM+PARAFAC analyses of OM in water samples obtained from lacustrine, riverine and soil environments: (i) Lake Kinneret (Sea of Galilee) and its catchment basin (Borisover et al., 2009), (ii) the heavily polluted Lower Kishon river water (Borisover

et al., 2011), (iii) soils irrigated with treated wastewater vs. fresh water (Borisover et al., 2012). In all these systems, aqueous samples containing either suspended or dissolved OM were characterized, and the content and variability therein of humic-like and proteinaceous (tryptophan-containing) OM components were quantified in terms of the PARAFAC-based concentration scores. The objective of this communication is to share our own experience and to outline opportunities in characterizing OM, as provided by the EEM+PARAFAC methodology.

Experimental Details and Methodologies

Fluorescence spectra of water samples were measured in a 1.0 cm quartz cell with Shimadzu spectrofluorometer (RF-5301PC), equipped with 150WXenon lamp (Ushio Inc., Japan). Typically, every sample was characterized by a EEM obtained in the range of the excitation wavelengths from 220 nm to 590 nm, varied with 5 nm steps, and in the range of the emission wavelengths from 220 nm to 600 nm, varied with 2 nm steps, at excitation and emission slit widths of 5.0 nm band pass. Details on water sampling, sample characterization, experimental protocols and procedures of the PARAFAC analyses can be found for each specific dataset in the relevant reference (Borisover et al., 2009, 2011, 2012). Finally, based on the PARAFAC analysis, all the EEMs from a given dataset were characterized by a number of fluorescent components with their excitation and emission spectra, and component's concentration scores varying among individual EEMs. The concentration score of each component in a given EEM is proportional to its concentration in the sample analyzed. The coefficient of the above proportionality is specific for a given component and typically unknown. Therefore, the concentration scores of the fluorescent components can be used as a tool for quantitative examination of changes in the concentrations of the PARAFAC-derived components among samples.

Results and Discussion

Fluorescent OM in Lake Kinneret (Sea of Galilee) and its catchment basin

Analysis of fluorescent OM in water samples from Lake Kinneret and its catchment basin was carried out by Borisover et al. (2009) and involved collecting 167 water samples, over 20 months of sampling in the lake itself (at different depths and locations) and in the tributaries. Based on PARAFAC analysis, three major fluorescent

components were determined and characterized by maximal emission at the following combinations of excitation/emission wavelengths: 240&310/396; 260&355/460; <240&280/338 nm (where two excitation wavelength values indicate the presence of two excitation peaks). These fluorescent components were denoted as marine humic-like, terrestrial humic-like and proteinaceous (tryptophan-containing) matters, respectively. It should be emphasized that all three fluorescent components were obtained both from the PARAFAC analysis of the whole dataset and from analyzing separately the lacustrian and riverine samples, thus indicating that the same major components are responsible for OM fluorescence in water of the lake and its catchment basin and tributaries.

However, the composition of humic-like matter was found to differ between the lacustrine and the riverine OMs (Borisover et al., 2009). This difference was revealed by plotting the concentration scores of the terrestrial humic-like matter against concentration scores of the marine humic-like matter in all the samples studied (Fig. 2). It is clear from Fig. 2 that for a given concentration score of marine humic-like matter, samples from the lake (including all the sampling dates, depths and locations) were characterized by a smaller concentration score of terrestrial humic-like matter compared with the riverine samples. Therefore, the fraction of terrestrial humic-like OM (of the overall humic-like OM) in the riverine samples is greater than in the lacustrian samples. This difference between the OM from the lake and from the rivers makes sense since water from tributaries is expected to be relatively enriched by soil/sediment organic matter as compared with the lake water.

Characterizing OM in terms of fluorescent components may reveal also the changes that could not be identified from measuring concentrations of total (dissolved) organic matter (carbon). For example, Fig. 3 demonstrates the vertical distribution of concentration scores of the three fluorescent components in water sampled during the long-term monitoring of the center of Lake Kinneret. It is evident from Fig. 3 that the concentrations of the two humic-like components showed a stratification in the May-December samples, when this monomictic lake was also thermally stratified (Borisover et al., 2009). On the other hand, there was no stratification in the vertical distribution of concentrations of humic-like components in the January - April samples; most of this time period, i.e., from January to March, water in the lake was intermixed. However, dissolved organic carbon (DOC) concentration was found in this work (and in agreement with findings of earlier studies, i.e., by Parparov et al., 1998; Berman et al.,

2004) to be relatively insensitive to thermal stratification of the lake. In addition, the decrease in the concentrations of the humic-like substances in the upper lake layer compared with the concentrations in the deeper layers, during the May to December period, was suggested to reflect, at least in part, photo-degradation of the humic substances (Borisover et al., 2009). Unlike the humic-like matter, the vertical distribution of the proteinaceous (tryptophan-like) organic matter did not show any clear correlation with the lake stratification. Thus, spatial and temporal variations in proteinaceous organic matter in the lake, compared with those in the humic-like components, could be quantified.

Fluorescent components in the Lower Kishon River water

In another study by Borisover et al. (2011), PARAFAC analysis of EEM fluorescence of water from the heavily polluted Lower Kishon river (near the Haifa Bay) revealed only two fluorescent components. The analysis included 61 EEMs of water samples collected along the Lower Kishon river during 11 months. In addition, 58 samples of the riverine water from different locations were incubated under lab conditions in the presence of river inoculum. The observed fluorescent components represent humic-like organic matter and the "protein-like" component associated with biological activity. The components are characterized by maximal emission at the following excitation/ emission wavelengths: <250&345/438 and 280/364 nm, respectively. The presence of only two dominant fluorescent components was somewhat surprising in light of the expectation to observe a larger number of components in the heavily polluted river water, especially when compared with the relatively clean Lake Kinneret and its tributaries where three fluorescent components were identified.

Based on its emission spectrum, the second component associated with biological activity was red-shifted in comparison to the proteinaceous tryptophan-like component reported earlier in the literature (and linked to river contamination by treated sewage, Baker and Inverarity, 2004; Hudson et al., 2007). In the study by Borisover et al. (2011), this red-shifted protein-like component was found to be linked to the river region where the major input of industrial effluents occurred. When the spatial distribution of the concentration scores of the fluorescent components was examined along Lower Kishon river (Fig. 4), the location of the major input of industrial effluents into the river

correlated well with the appearance of the highest concentration of protein-like OM. Moving downstream from location 7 to location 6 (in direction to the seaside), there was a consistent increase in the concentration scores of this fluorescent OM component (Fig. 4). This section of the river was known to contribute about 85% of the total discharge of the industrial effluents in Lower Kishon river (Borisover et al., 2011).

No distinct and consistent indications concerning this effluent input could be derived from changes in DOC concentration, absorbance at 254 nm, EC of the water samples or the concentration scores of humic-like matter along the river (Fig. 4). The spatial correlation between the increase in the concentration of protein-like OM and the input of industrial effluents was ascribed to development of biological activity due to the supply of effluent-related nutrients (Borisover et al., 2011). Interestingly, this biological activity-related fluorescent OM component was found to be relatively stable, at least, for 10 days, against biodegradation by river microorganisms under lab conditions which might indicate its possible protection by interactions with other OM components.

Fluorescent components in soil environment: water-extractable soil organic matter

Using the EEM+PARAFAC technique, Borisover et al. (2012) examined the fluorescent components of water-extractable organic matter (WEOM) from four different soil types (loamy sand, sandy loam, sandy clay and clay) that had been irrigated for at least five years with fresh water (FW) or domestic secondary treated wastewater (TWW; with biochemical oxygen demand and total suspended solid concentration not exceeding 20 and 30 mg/L, respectively). The PARAFAC analysis involved 144 samples including original (filtered) aqueous soil extracts, the extract fraction not precipitating at pH=1.5 and the fraction that precipitated at acidic pH and was re-dissolved at basic pH. Three determined major fluorescent components were characterized by maximal emission at the following combinations of excitation/emission wavelengths: <254&320/432, 270&365/480, and 285/354 nm thus representing two humic-like and one proteinaceous (tryptophan-like) fluorescent components, respectively.

Both the concentrations of the fluorescent components and the proportions among them in aqueous extracts varied among the different soil types studied. For example, the

concentration scores of both humic-like components in the aqueous extracts from FW-irrigated clay soil (for the two soil depths studied) were distinctly lower compared with the concentration scores of these components in the FW-irrigated loamy sand extracts (Fig. 5). However, an opposite trend was observed for the concentrations of the proteinaceous matter demonstrating tryptophan-like fluorescence. In addition, soil type affected the impact of TWW irrigation on the concentrations of WEOM fluorescent components. For example, in the loamy sand at both the soil depths the concentration scores for all three fluorescent WEOM components from the TWW-irrigated samples were higher than those from the soil samples irrigated with FW. In the clay soil extracts no change or an opposite trend to that noted in the loamy sand was observed with respect to the TWW vs. FW effect on the concentrations of the fluorescent components (Fig. 5).

Notably, the composition of humic-like fluorescent WEOM expressed as a ratio of the concentration scores of the two humic-like components demonstrated a statistically significant linear dependence on soil clay content. This linear dependence is shown in Fig. 6 for the acid-soluble fraction of WEOM (which contains the major portion, i.e., 70-80%, of the humic-like WEOM in the soil systems studied; Borisover et al., 2012). One possible explanation for the trend shown in Fig. 6 is the selective interaction of humic components with clay, i.e., the weaker interaction between the negatively charged clay surfaces and humic-like component 1 as compared with component 2. Component 1 was characterized by shorter-wavelength emission maximum as compared with component 2 and was, therefore, supposed to have a smaller size. Hence, the weaker interaction of component 1 with clay may probably be due to its greater negative charge density, compared with that of the larger-size and more conjugated component 2.

Concluding Remarks

Based on the EEM-PARAFAC analysis, the composition of fluorescent OM can be described in terms of concentration scores of the identified fluorescent components. The concentration scores cannot be used for a quantitative comparison between concentrations of different components. However, PARAFAC-based concentration scores can be converted to the contributions of the separated components into the total

measured fluorescence. Use of this approach for comparing between the concentrations of different fluorescent components would also be misleading since different molecules differ in their capability to emit light.

However, the concentration scores of the fluorescent components (or their ratios and/or relationships among them) suggest an effective tool for quantifying the changes in the proportions between concentrations of different components, i.e., changes in the composition of the fluorescent OM. This possibility to quantitatively represent the changes in the fluorescent OM composition is an important advantage of using PARAFAC for analysis of EEMs. Traditionally, the changes in fluorescence spectra of OM could be described by applying various indices based on (i) the emission intensities at certain excitation/emission wavelengths, or (ii) integration of the intensities over a range of wavelengths. However, with PARAFAC, instead of this empirical analysis, the changes in fluorescence spectra may be expressed in terms of concentration changes of certain components. The latter could be further characterized by using their specific excitation and emission spectra and linked to those already presented in the literature.

Another feature of the EEM+PARAFAC analysis is that it becomes more effective with the increase in the number of samples, due to the increased ability of the PARAFAC to determine a greater number of fluorescent components from EEMs (Stedmon and Markager, 2005), and, therefore, the fluorescent OM composition may be characterized in greater detail. Moreover, due to the increase of the number of samples, the EEMs interpretation of already analyzed samples is improved. These features seem to be advantageous when comparing the EEM+PARAFAC technique with some traditional (and also time- and cost-consuming) methodologies for OM characterization (e.g., fractionation techniques).

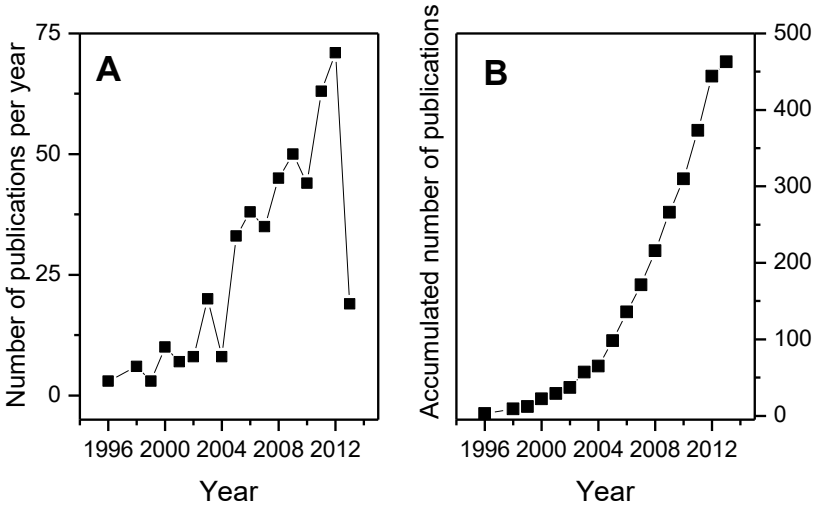

Fig. 1. Trend in publications combining fluorescence and PARAFAC analysis (based on the Web of Science examination; April, 2013): A – publications released per year, from 1996 to April, 2013. B – accumulated number of publications from 1996 to April, 2013.

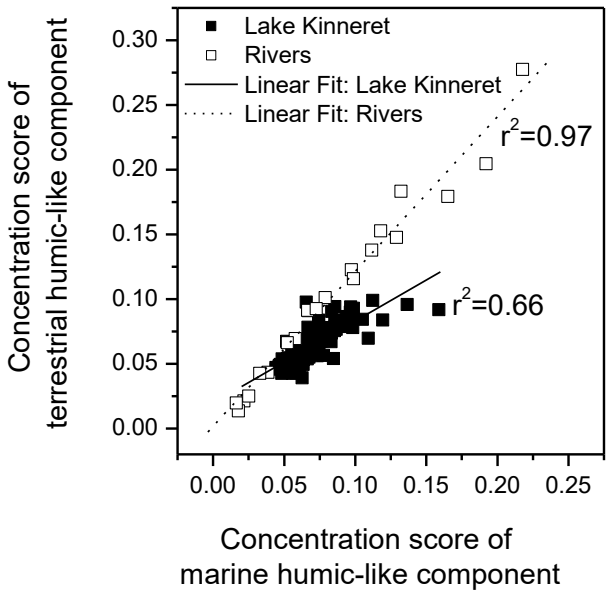

Fig. 2. Concentration scores of terrestrial humic-like component plotted against concentration scores of marine humic-like component for water sampled from Lake Kinneret (black squares) and rivers (open squares) for all the sampling dates, locations and depths (where applicable). Adapted from Borisover et al. (2009), with the permission.

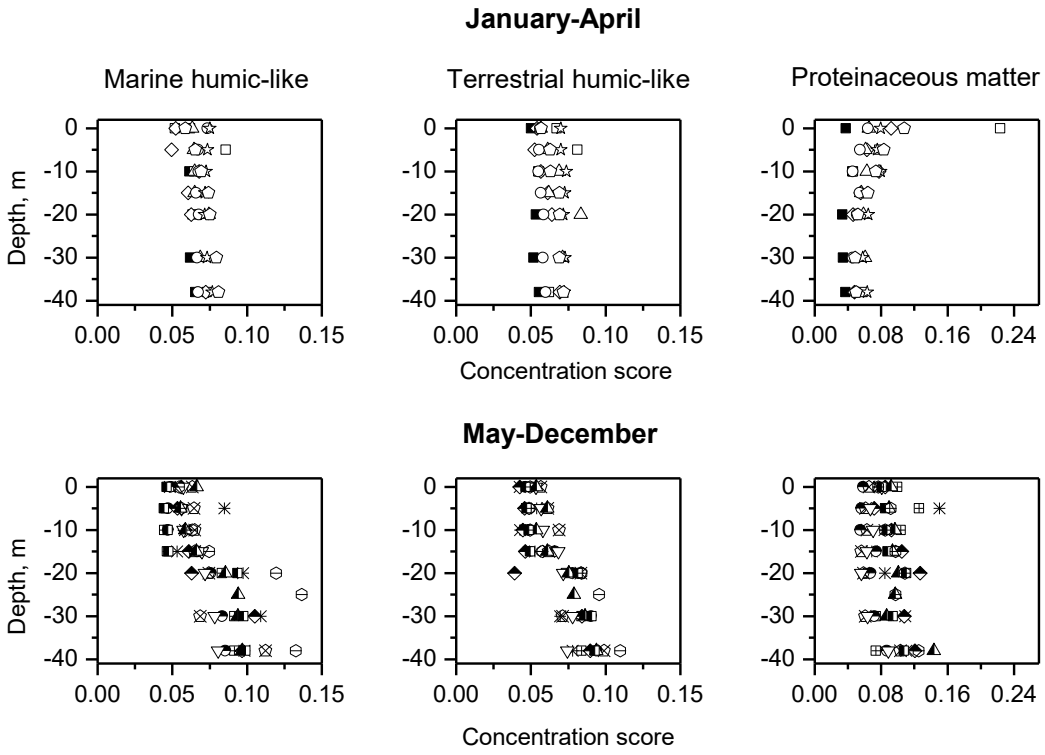

Fig. 3. Vertical distribution of concentration scores of three fluorescent components (marine humic-like matter, terrestrial humic-like matter, proteinaceous matter) in water sampled during the 20- months monitoring at Station A in the center of Lake Kinneret. First row represents sampling events (denoted with different symbols) from January to April; second row represents sampling events from May to December (Adapted from Borisover et al. 2009, with the permission).

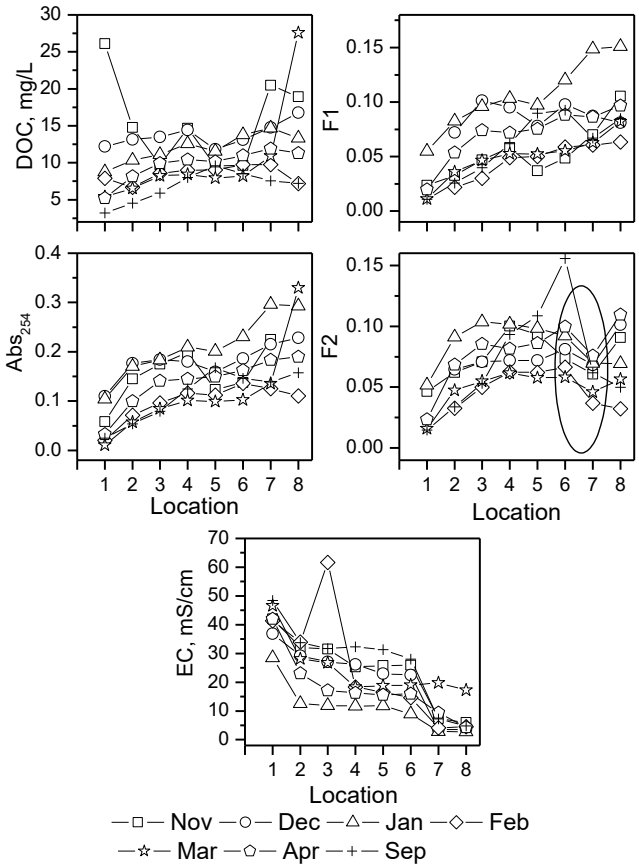

Fig. 4. Spatial distribution of DOC concentrations, absorbance measured at 254 nm, concentration scores, F1 and F2, of two fluorescent components (humic-like and protein-like matter, respectively) and electric conductivity (EC) along Lower Kishon river where the numbers on the X axis correspond to the monitoring stations of Kishon Authority (1 is the closest to Haifa Bay, and 8 is situated at the longest studied distance from the sea). Different symbols represent different sampling dates. The concentration scores F2 consistently increased from location 7 to location 6 (marked by the ellipse). Reproduced with permission from Borisover et al. (2011).

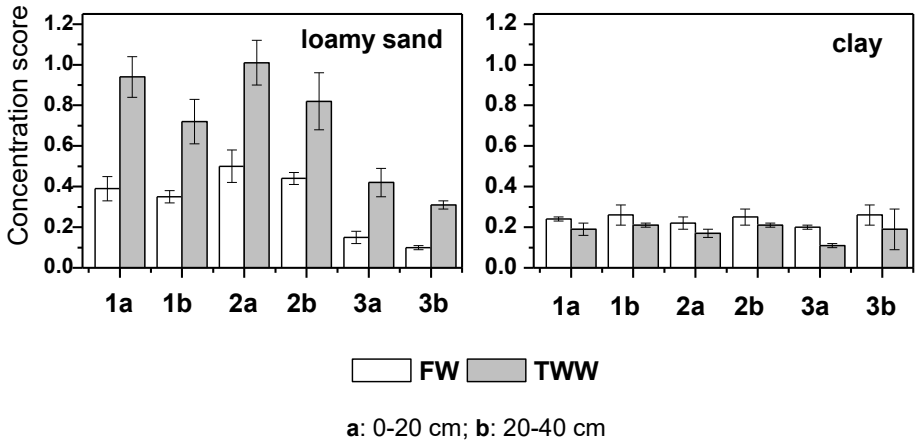

Fig. 5. Concentration scores of three fluorescent components where 1 and 2 denote humic-like components (with maxima at excitation/emission wavelengths <254&320/432 and 270&365/480 nm, respectively) and 3 denotes proteinaceous tryptophan-like component in aqueous extracts from loamy sand and clay soils. Letters "a" and "b" denote different depths of soil sampling (i.e., 0-20 and 20-40 cm, respectively). FW and TWW correspond to fresh water and treated water irrigation. Adapted from Borisover et al. (2012), with the permission.

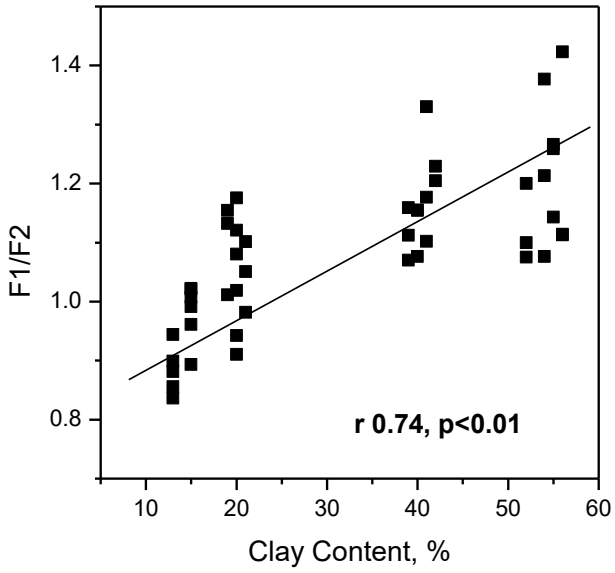

Fig. 6. Composition of humic-like matter in acid-soluble fraction of WEOM: ratio of concentration scores (F1/F2) of two humic-like components, 1 and 2 (with maxima at excitation/emission wavelengths <254&320/432 and 270&365/480 nm, respectively) plotted against clay content of soil samples. Reproduced with permission from Borisover et al. (2012).

References

Alberts, J. J., Takács, M. 2004. Total luminescence spectra of IHSS standard and reference fulvic acids, humic acids and natural organic matter: comparison of aquatic and terrestrial source terms. Organic Geochemistry 35: 243–256.

Andersen, C. M., Bro, R. 2003. Practical aspects of PARAFAC modeling of fluorescence excitation-emission data. Journal of Chemometrics 17: 200–215.

Baker, A., Inverarity, R. 2004. Protein-like fluorescence intensity as a possible tool for determining river water quality. Hydrological Processes 18: 2927–2945.

Berman, T., Parparov, A., Yacobi, Y.-Z. 2004. Planktonic community production and respiration and the impact of bacteria on carbon cycling in the photic zone of Lake Kinneret. Aquatic Microbial Ecology 34: 43–55.

Borisover, M., Laor, Y., Parparov, A., Bukhanovsky, N., Lado, M. 2009. Spatial and seasonal patterns of fluorescent organic matter in Lake Kinneret (Sea of Galilee) and its catchment basin. Water Research 43: 3104–3116.

Borisover, M., Laor, Y., Saadi, I, Lado, M., Bukhanovsky, N. 2011. Tracing organic footprints from industrial effluent discharge in recalcitrant riverine chromophoric dissolved organic matter. Water, Air & Soil Pollution 222(1-4): 255-269.

Borisover, M., Lordian, A., Levy, G. J. 2012. Water-extractable soil organic matter characterization by chromophoric indicators: Effects of soil type and irrigation water quality. Geoderma 179–180: 28–37.

Bro, R. 1997. PARAFAC: tutorial and applications. Chemometrics and Intelligent Laboratory Systems 38: 149–171.

Chen, W., Westerhoff, P., Leenheer, J. A., Booksh, K. 2003. Fluorescence excitation−emission matrix regional integration to quantify spectra for dissolved organic matter. Environ. Sci. Technol. 37: 5701–5710.

Corvasce, M., Zsolnay. A., D'Orazioa, V., Lopeza, R., Miano, T. M. 2006. Characterization of water extractable organic matter in a deep soil profile. Chemosphere 62: 1583–1590.

Hudson, N., Baker, A., Reynolds, D. 2007. Fluorescence analysis of dissolved organic matter in natural, waste and polluted waters: A review. River Research and Applications, 23: 631–649.

Parparov, A. S., Berman, T., Grossart, H.-P., Simon, M. 1998. The metabolic activity associated with seston in Lake Kinneret. Aquatic Microbial Ecology 98: 77–87.

Ross, R. T., Lee, C., Davis, C. M., Ezzeddine, B. M., Fayyad, E. A., Leurgans, S. E. 1991. Resolution of the fluorescence spectra of plant pigment complexes using trilinear models. Biochimica et Biophysica Acta. 1056: 317– 320.

Stedmon, C. A., Markager, S., Bro, R. 2003. Tracing dissolved organic matter in aquatic environments using a new approach to fluorescence spectroscopy. Marine Chemistry 82: 239–254.

Stedmon, C. A., Markager, S. 2005. Resolving the variability in dissolved organic matter fluorescence in a temperate estuary and its catchment using PARAFAC analysis. Limnology and Oceanography 50: 686–697.

Stedmon, C., Bro, R. 2008. Characterizing dissolved organic matter fluorescence with parallel factor analysis: tutorial. Limnology and Oceanography, Methods 6: 572–579.

Session 9: Soil Organic Matter and Environmental Aspects

CONTRIBUTION OF CARBONATE DISSOLUTION TO CO_2 EMISSION FROM SOILS WITH ADDITION OF ORGANIC N

Guy Tamir[1,2], Moshe Shenker[2], Hadar Heller[1], Paul Bloom[3], Pinchas Fine[1], Lilach Barsheshet[1], Guy Levy[1], Asher Bar-Tal[1]

[1]Institute of Soil, Water and Environmental Sciences, Agricultural Research Organization, Bet Dagan, Israel
[2]Department of Soil and Water Sciences, Robert H. Smith Faculty of Agriculture, Food and Environment, Hebrew University of Jerusalem, Rehovot, Israel
[3]Department of Soil, Water and Climate, University of Minnesota, St Paul, MN, USA

Root and microbial respiration is considered to be the main source of CO_2 production in soil. Carbonates are an important component of soils from arid and semi-arid regions, therefore calcite dissolution could also contribute to the emitted CO_2 from these soils. Several studies in the last decade showed that 10 to 80% of emitted CO_2-C from calcareous soils and from limed soils is due to acid dissolution of $CaCO_3$ (Bertrand et al., 2007; Buysse et al., 2012; Dong et al., 2013; Stevenson and Verburg, 2006). This information indicates that measurement of CO_2 emission may lead to overestimation of soil organic matter (SOM) turnover in arid and semiarid soils. Dissolution of $CaCO_3$ can be enhanced by decomposition of SOM and applied organic residues (OR) to soil, both generating acidity through the following processes: 1. Nitrification of the mineralized nitrogen (Conyers et al., 1995; Liu et al., 2008); 2. Oxidation of reduced S (De Vries and Breeuwsma, 1987) and 3. Production of organic acids (Lindsay, 1979).

There is a lack of information in the literature on the effects of OR application to calcareous soils on CO_2 evolution due to calcium carbonate dissolution and how this process is affected by temperature. Hence, our main objective was to quantify the contribution of $CaCO_3$ dissolution to CO_2 emission from soils with and without the addition of an organic residue (Tamir et al. 2011). A secondary objective was to investigate the effects of temperature on CO_2 emissions from SOM and $CaCO_3$.

The emissions of CO_2 and CO_2-$\delta^{13}C$ from two incubated soils (non-calcareous (Golan Heights [GH], −26.23‰) and calcareous (Bet She'an [BS], −11.47‰) soils, Table 1) with and without the addition of a pasteurized chicken manure (PCM, −23.2‰) were determined. During 56 d of incubation, 445 and 1804 mg kg^{-1} CO_2–C were emitted from BS and GH soils, and PCM application caused an additional emission of 2430 and 1884 mg kg^{-1} CO_2–C, respectively. The emitted CO_2–$\delta^{13}C$ from BS and GH soils were −20.0±0.2‰ and −27.2±0.09‰ and application of PCM changed it to −20.6±0.42‰ and −23.7±0.16‰, respectively (Table 2). The calculated contribution of the inorganic carbonates to CO_2–C emission from the BS soil without and with PCM and from GH with PCM were 113.4, 417.5, and 176 mg kg^{-1} (26.5, 14.5, and 5% of the total), respectively.

The effects of temperature on CO_2 emissions from the calcareous soil BS were investigated in incubation study with and without compost application. Elevating temperature from 18 ^{O}C to 30^{O}C enhanced CO_2 fluxes in the first days of the incubation, and this effect declined with incubation time (data no shown). Application of compost also increased CO_2 fluxes during the first days of the incubation and the difference between the control and the compost treatment decreased with time and no difference was observed at the end of the incubation (60 days). Isotopic measurement of the carbon in CO_2 fluxes from the control soil, as expressed by $\delta^{13}C$, indicated that both SOM and carbonates dissolution contributed to the emitted CO_2. The quantitative contribution of each pool was calculated according to the accumulative emitted CO2 and the isotopic signature of the carbon in it. Significant contribution to the CO_2 emission was measured from the soil carbonates (20-30%), but the highest contribution was from the SOM (Fig. 1). At 30°C in both compost and control samples the accumulative flux and the partial contribution of SOM was higher than at 18°C. Elevating temperature from suboptimal to optimal temperature (18°C to 30°C) enhanced CO2 emission from the organic sources (SOM and compost) as well as the inorganic source (carbonate), however the impact on organic matter decomposition was stronger than on carbonate dissolution (Fig. 1).

We evaluated the role of PCM on carbonate dissolution as related to nitrification and pH change in a range of soil types (Tamir et al. 2013). In this presentation only the results of the GH and BS soils (presenting non-calcareous and calcareous soils) are shown. The NO_3^-–N concentrations in the control BS and GH soils were 46 and 133

mg kg^{-1} and PCM application increased it to 508 and 577 mg kg^{-1}, respectively. To discriminate the effects of organic C mineralization from nitrification we added a nitrification inhibitor, dicyandiamide (DCD), which slows NH_4^+ oxidation without interfering with soil C respiration. PCM application without DCD resulted in a pH increase in the first few days of the incubation followed by a pH decrease (Fig. 1). DCD application effectively inhibited the nitrification process (Fig. 2) and the reduction in soil pH (Fig. 1). Application of DCD to PCM treatment inhibited nitrification, pH reduction (protons production) and reduced CO_2 emission in PCM amended soils, especially in the earlier part of the incubation of calcareous soils. The high correlation between nitrification and the reduction in pH and the effects of DCD application on nitrification and pH indicated that the nitrification process was the main source of protons released, which led to carbonate dissolution and CO_2 emission from $CaCO_3$.

Conclusions

Nitrification is the main process that leads to enhanced chemical dissolution of calcite and CO_2 emission when SOM and OR decompose in soil.

Temperature influences carbonate dissolution but to lower effect than SOM.

Ignoring calcite dissolution will result in the overestimation of respired C.

Table 1. Some properties of the Golan Heights and Bet She'an soils (SE in parentheses).

Variable	Golan Heights	Bet She'an
pH	6.8 (0.02)	7.7 (0.07)
$CaCO_3$, g kg^{-1}	2.0 (0.03)	628 (15)
$\delta^{13}C$ whole soil, ‰	−26.23 (0.3)	−11.47 (0.2)
$\delta^{13}C$ carbonate fraction, ‰	UDL†	−7.05 (0.04)
$\delta^{13}C$ soil organic matter, ‰	−26.73 (0.4)	−24.6 (0.1)

† Under detection limits.

Table 2. The $\delta^{13}C$ composition of CO_2 emitted throughout the incubation experiment in Golan Heights (GH) and Bet She'an (BS) soils with and without pasteurized chicken manure (PCM).

		Incubation time (days)			
		1	7	21	56
		$\delta^{13}C$ (‰)			
Soil	Treatment				
GH	Control	26.5	27.0	27.0	27.0
GH	PCM	24.2	23.2	23.6	23.6
BS	Control	20.5	19.0	19.5	20.5
BS	PCM	23.2	18.5	21.0	21.0

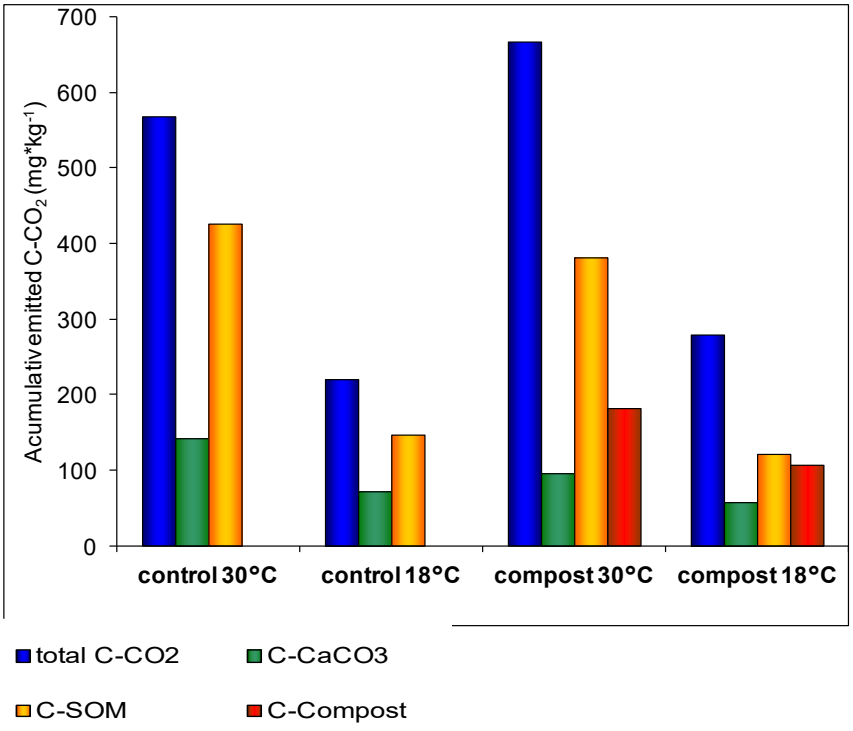

60 days of incubation from carbon soil and applied compost) as affected by

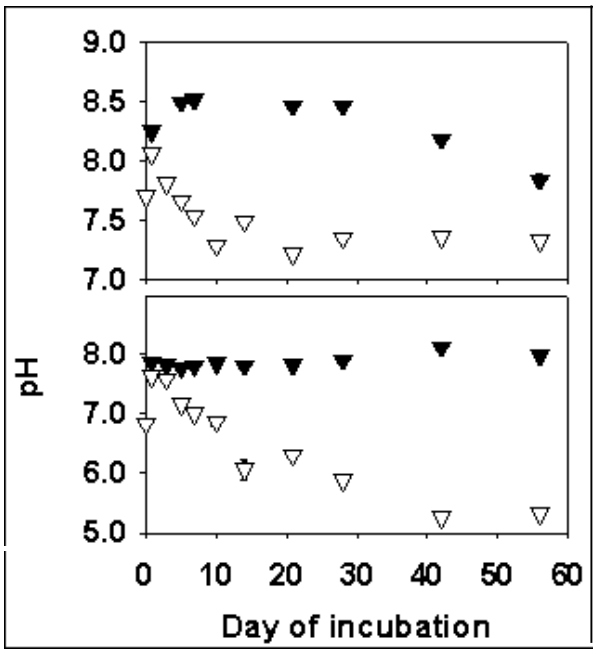

Fig. 2. The pH of soil solution extracts during the incubation of the soils with the PCM (∇) and the PCM+DCD (▼) treatments. The bars represent two standard error (SE) values for the mean of samples for each treatment at specific time (the bars arehidden when they are smaller than the symbols).

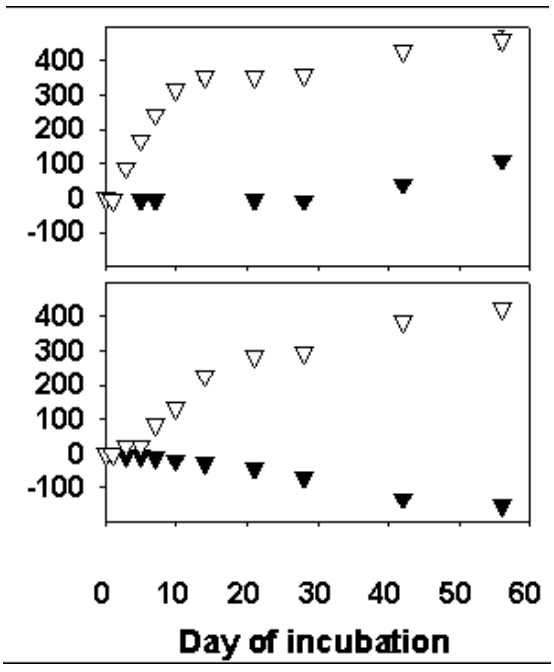

Fig. 3. Measured of NO_3^--N concentrations during the incubation of soils (∇) with the PCM (after subtracting the measured NO_3^--N concentrations in the Control treatment), and (▼) PCM+DCD (after subtracting the measured NO_3^--N concentrations in the DCD treatment) treatments. The bars represent two standard error (SE) values for the mean of samples for each treatment at specific times (the bars are hidden when they are smaller than the symbols).

References

Bertrand, I., O. Delfosse, and B. Mary. 2007. Carbon and nitrogen mineralization in acidic, limed and calcareous agricultural soils: Apparent and actual effects. Soil Biol. Biochem. 39:276-288.

Buysse, P., Goffin, S., Carnol, M., Malchair, S., Debacq, A., Longdoz, B., Aubinet, M. 2013. Short-term temperature impact on soil heterotrophic respiration in limed agricultural soil samples. Biogeochemistry. 112:441-455.

Conyers, M.M., Uren, N.C. and Helyar, K.R. 1995. Causes of changes in pH in acidic mineral soils. Soil Biol. Biochem. 27:1383–1392.

De Vries, W. and Breeuwsma, A. 1987. The relation between soil acidification and element cycling. Water Air Soil Pollut. 35:293–310.

Dong, Y-J., Cai, M., Liang, B., Zhou, J-B. 2013. Effect of additional carbonates on CO_2 emission from calcareous soil during the closed-jar incubation. Pedosphere 23, 137-142

Lindsay, W.L. 1979. Chemical equilibria in soils. John Wiley & Sons, New York.

Stevenson, B.A., and P.S.J. Verburg. 2006. Effluxed CO_2-^{13}C from sterilized and unsterilized treatments of a calcareous soil. Soil Biol. Biochem. 38:1727-1733.

Tamir, G., Shenker, M., Heller, H., Bloom, P.R., Fine, P. and Bar-Tal, A. 2011. Can soil carbonate dissolution lead to overestimation of soil respiration? Soil Sci. Soc. Am. J. (75: 1414-1422)

Tamir, G., Shenker, M., Heller, H., Bloom, P.R., Fine, P. and Bar-Tal, A. 2013. Organic N mineralization and transformations in soils treated with an animal waste in relation to carbonates dissolution and precipitation. Geoderma 209-210:50-56

NEW TECHNIQUES FOR NITROUS OXIDE FLUXES RESEARCH, INTER-COMPARISON, VALIDATION, AND MEASUREMENTS OF NITROUS OXIDE EMISSIONS FROM AGRICULTURAL SOILS: THE ROLE OF SOIL CARBON, NITROGEN, AND WATER AVAILABILITY

Ilya Gelfand[1,2]*, Mengdi Cui[3,4], Lei Tao[5], Kang Sun[5], Terenzio Zenone[2,6], Jim Tang[3,4,7], Jiquan Chen[2,6], Mark A. Zondlo[5] and G. Philip Robertson[1,2,8]

[1]W.K. Kellogg Biological Station, Michigan State University, Hickory Corners, MI 49060

[2]Great Lakes Bioenergy Research Center, Michigan State University, East Lansing, MI 48824

[3]Department of Ecology & Evolutionary Biology, Brown University, Providence, RI 02912

[4]Marine Biological Laboratory (MBL), Woods Hole, MA 02543

[5]Department of Civil and Environmental Engineering, Princeton University, Princeton, **NJ 08540**

[6]Department of Environmental Sciences, University of Toledo, Toledo, OH 43606

[7]Department of Geological Sciences, Brown University, Providence, RI 02912

[8] Department of Plant, Soil, and Microbial Sciences, Michigan State University, East Lansing, MI 48824

*Corresponding author: The publication is a proceedings version of the manuscript under review (Gelfand et al.).

Abstract

Agricultural soils significantly contribute to increasing atmospheric concentration of N_2O and dominate anthropogenic sources of this important greenhouse gas. The current "state of the art" method for measuring soil N_2O emissions is the static chamber method. There are two well known drawbacks with this method: static chambers cover only small percent of soil area and they cannot be sampled continuously. This means that measurements of soil N_2O emissions are usually performed with very low temporal and spatial resolution. The soil N_2O emissions, on the other hand, have very high spatial and temporal variability and are characterized by high episodic fluxes. This mismatch between our ability to capture flux variability and the nature of N_2O fluxes themselves is a major knowledge gap. We compared three techniques for measurements of soil N_2O

emissions, two techniques based on static chambers method — gas sampling and laboratory analysis using gas chromatography versus *in situ* analysis using a quantum cascade laser; and one based on a prototype of an open-path quantum-cascade laser sensor, capable to measure atmospheric concentrations of N_2O with 10 Hz temporal resolution, mounted on eddy-covariance tower. Both static chamber based measurement techniques provided highly correlated N_2O flux values. The open-path sensor showed promising potential for ecosystem-scale measurements and successfully measured the flux more than 40% of time. Tower based estimation was only slightly correlated to ground based estimation mostly due to drought conditions during field deployment and overall very low soil fluxes. Under drought conditions, average soil N_2O-N fluxes were up to 12 g ha^{-1} d^{-1} and were not affected by nitrogen fertilization. After an artificial rain event of 50 mm, soil N_2O fluxes increased ~34 fold with the magnitude of the response controlled by soil carbon levels.

Keywords: corn, drought, grassland, nitrous oxide, agriculture, static chambers, eddy-covariance

Introduction

Nitrous oxide (N_2O) is the third most important greenhouse gas with an atmospheric lifetime of ~114 years and a global warming impact ~300 times greater than CO_2. Anthropogenic emissions are the main cause of N_2O's atmospheric increase (IPCC, 2007). Over 80% of anthropogenic N_2O emissions are from the agricultural sector; most of these (~50% of the total anthropogenic flux) are soil emissions (Robertson et al., 2012). And given current trends in land-use change and agricultural intensification (in particular fertilizers use), we could expect an even greater increase in N_2O emissions around the globe in the near future (Vitousek et al., 2009). An accurate assessment of N_2O emissions from agriculture, therefore, is vital for our understanding of the global N_2O balance and its impact on climate as well as for the design of cropping systems with lower emissions. The current "state of the art" method for measuring soil N_2O emissions is the static chamber method, which was developed few decades ago and is still exclusively used by scientists around the world (Holland et al., 1999; Butterbach-Bahl et al., 2013). There are two well known drawbacks with this method: static chambers cover only small percent of soil area and they cannot be sampled continuously. This means that measurements of soil N_2O emissions are usually

performed with very low temporal and spatial resolution. The soil N_2O emissions, on the other hand, have very high spatial and temporal variability and are characterized by high episodic fluxes (e.g. Ruan and Robertson, 2013). This mismatch between our ability to capture flux variability and the nature of N_2O fluxes themselves is a major knowledge gap.

The shortcomings of static chamber methodologies are driving continuous development of new methods for field-level measurements of N_2O fluxes. The most promising direction for new development is the eddy-covariance (EC) approach; developed a few decades ago, today the EC approach is used to estimate CO_2, water, and energy fluxes around the world (http://fluxnet.ornl.gov/). The development of EC based measurements has significantly improved our understanding of the CO_2 cycle, resulting in the development of precise biogeochemical models (e.g. Migliavacca et al., 2011). Currently, the most advanced sensors for ecosystem-level N_2O measurements that can be integrated with the EC approach require closed-path analyzers, which consume large amounts of power (500-1000 W; Neftel et al., 2010; Zona et al., 2012). Although the EC approach coupled with this analyzer has produced interesting and promising data (Zona et al., 2012, 2013), the applicability of this technique to the field is limited due to the need for grid power.

Future climate change is predicted to have large effects on water cycling and availability, with overall intensification of both rainfall and droughts (Betts et al., 2007; Durack et al., 2012). Rewetting of soils after droughts and especially the "first" rain event after droughts can have a large effect on soil greenhouse gases emissions (e.g. Bergsma et al., 2002; Xu et al., 2004; Kim et al., 2012). Rewetting of dry soils typically induces large fluxes of N_2O during laboratory incubations of soils from seasonally-dry, semi-arid, and some temperate climates (Birch, 1958; Beare et al., 2009; Borken and Matzner, 2009; Prieme and Christensen, 2001; Mikha et al., 2005). Results from field studies, especially those in mesic climates, are not as conclusive as in the laboratory work.

Most field studies of GHG fluxes associated with soil rewetting have been performed in semi-arid or seasonally dry soils and show a strong overall increase in soil GHG emissions after rewetting of soils subjected to prolonged droughts (reviewed by Austin et al., 2004; Kim et al., 2012). The few studies in mesic climates show mixed results with an increase due to rewetting of dry sandy-loam arable soils (Jørgensen et al., 1998),

and no effect or a decrease in GHG fluxes due to drought in Danish heathland (e.g. Larsen et al., 2011).

Here we taking an advantage of a naturally occurring drought to investigate the effect of rewetting on *in situ* soil N_2O emissions in an agricultural soil in a mesic climate and compare three different methods to measure soil N_2O emissions. The research performed in a fertilized no-till continuous corn (*Zea mays*) cropping system, converted from a USDA Conservation Reserve Program (CRP; www. fsa.usda.go v/FSA/) grassland in 2009. We used newly developed open-path quantum cascade laser sensor mounted on eddy-covariance micrometeorological tower and compared results obtained from ecosystem-level measurements with two techniques for measurements with the static chamber method: a quantum cascade laser technique for measuring *in situ* N_2O fluxes and the standard off-site gas-chromatography method.

Methods

Study site

The experiment was conducted at the Great Lakes Bioenergy Research Center (GLBRC; http://glbrc.org/) Michigan field site, part of the Kellogg Biological Station Long-term Ecological Research (LTER) site (KBS; lter.kbs.msu.edu) in southwest Michigan USA (42° 24' N, 85° 24' W, 288 m asl). Mean annual air temperature at KBS is 9.2±0.9°C and annual precipitation is 891±151 mm (mean ± s.d. n = 25 years), generally distributed evenly throughout the year. Sandy loam soils are well-drained Typic Hapludalfs developed on glacial outwash. The experiment conducted on no-till corn field, the Corn (area of 19.5 ha) which was converted from CRP grassland in 2009 and managed under continuous no-till corn since 2010. The Corn site has soil C and N concentrations of 30 g kg^{-1} and 3 g kg^{-1}, respectively and productivity of 1970±174 g m^{-2} yr^{-1}. Soil temperature at three depths (-2, -5, and -10 cm) and volumetric water content (VWC, 0-30 cm) were measured continuously by CS 107 and CS 616 sensors, respectively (CSI, UT, USA).

Soil N_2O emission measurements and flux calculations

To measure soil N_2O fluxes we used the static chamber method described elsewhere (Holland et al., 1999). In May 2012, eight pairs of stainless steel cylindrical chambers (28.5 cm I.D. and 25 cm high) equipped with a vent for pressure equilibration were installed in the field along 50 meter transect, at least 5 meters apart, and inserted to a 5 cm soil depth between the adjacent corn rows. There was no vegetation inside chambers at the site.

Soil N_2O fluxes were measured from each pair of chambers using two measurement techniques. The first technique, hereafter denoted as "GC off site", is based on taking head space gas samples over a 40-60 minute incubation period while chambers are covered with gas-tight lids, storing the over-pressurized samples in glass vials, and analyzing the contents for N_2O in the laboratory using a gas chromatograph (7890A Agilent Technologies Inc. DE, USA) equipped with an ECD sensor (http://lter.kbs.msu.edu/protocols/113). The second technique, hereafter denoted as "QCL in situ", is based on field analysis using a closed-path quantum cascade laser (QCL) analyzer (N_2O/CO-23d; Los Gatos Research Inc., CA, USA) for measurements of N_2O concentrations. During QCL in situ measurements the head space atmosphere was circulated throughout the chamber for ~5 minutes and gas concentrations were analyzed at 2 second intervals and stored in a data logger.

Soil N_2O fluxes were calculated as the change in concentration in the chamber headspace over the incubation period corrected for air temperature. For direct comparison of these two techniques, we performed incubations using the same chamber at the same time. Average soil N_2O fluxes and cumulative emissions were calculated using a linear interpolation of measured individual fluxes.

Soil N_2O emissions were measured between June 4 and June 28, 2012 (Day of Year 156 and 180). During this time, chambers were removed from the field and reinstalled two times: on June 13-16 (DOY 165 - 168) for fertilization and herbicide application and on June 21-22 (DOY 173 - 174) for side-dress fertilization. In both cases at least 12 hours elapsed between chamber installation and measurements.

Eddy-Covariance measurements and data processing.

For eddy-covariance (EC) measurements we used an open-path, QCL sensor for measurements of atmospheric concentrations of N_2O (OP-QCL; Tao et al., 2012). The specific details of the technique, spectroscopy, and analyses are described in Tao et al., (2012). In short, sensing technique is optically based through wavelength modulation spectroscopy (WMS). WMS is used to simultaneously detect the second and fourth harmonic spectra of N_2O and C_2H_2 with a software-based lock-in amplifier. The detector signal is fitted in real-time (10 Hz) by a computationally fast numerical model for WMS to retrieve the N_2O concentrations from the known concentration of C_2H_2 in the reference cell. The sensor system has a mass of ~15 kg, electrical power consumption of ~ 50 W, and a size of 50 cm × 18 cm × 15 cm. The sensor was powered by batteries or solar panels.

The sensor was mounted on an EC tower (Gelfand et al., 2011; Zenone et al., 2011; 2013). In short, EC tower, of ~4 m height was erected in the middle of the Corn field. The tower was equipped accordingly to standard FLAXNET protocol (http://fluxnet.ornl.gov/), including full array of sensors for measurements of energy, water, and CO_2 fluxes with an open-path LI7500A analyzer (LiCor, NB, USA) and sonic anemometer for measurements of 3D wind direction.

The data of ecosystem-level N_2O exchange was analyzed accordingly to standard FLUXNET procedure using the EC processor software (Noormets *et al*., 2008; http://research.eeescience.utoledo.edu/lees/ECP/ECP.html; Zenone at al., 2013) and presented as half-hour averages.

Agricultural management, productivity, and water addition experiment

The Corn field was managed according to normal farming practices in the area. Nitrogen fertilizer was applied as 28% UAN (Urea-Ammonium-Nitrate solution) with ~40% ammonium nitrate and ~30% urea at rates of 35 kg N ha^{-1} at planting (~DOY 121), 135 kg N ha^{-1} on DOY 166, and 48 kg N ha^{-1} on DOY 174, overall ~217 kg N ha^{-1}.

To examine the effect of a rain event on soil GHG emissions, we added 50 mm (50 L m^{-2}) of water to all chambers at night between DOY 171 and 172. Water was added by sprinkling a total area of 0.5 m^2 that covers each chamber location and surrounding area

of totally 8 pairs of chambers. Rain events of 50 mm are heavy, but not uncommon in the region: during the past 25 years, rain events of similar magnitude occurred at least once in more than half of the years, and more than once in a third of the years (http://lter.kbs.msu.edu/datatables/7).

Measurements of soil GHG emissions were taken during the two days following wetting. Soil volumetric water content (VWC) before and after the wetting events was measured by a CS HS2 portable sensor in the 0-12 cm soil layer (SCI, USA). Aboveground net photosynthetic productivity (ANPP) was measured by manual harvest of whole plants in 1 m^{-2} quadrates at 10 stations across field during peak standing biomass (August) in 2010 and 2011.

Results and Discussion

Weather

During the study period the weather was extremely hot and dry, with only three rain events, each less than 1 mm (<1L m^{-2}), on DOY 168, 169, and 170. During these events the rain did not penetrate the soil surface more than 1 mm and had no effect on VWC (Fig. 1). Soil temperature continuously increased over the study period, reaching more than 30 °C at 2 cm depth (Fig. 1) in the second half of June.

Comparison of in situ and off site techniques for measurements with the static chambers.

For direct comparison of the "GC off site" and "QCL in situ" techniques, a total of 48 individual field incubations were conducted across a variety of soil temperature and moisture conditions. Overall, the two techniques exhibited very high correlations, with an R^2 of 0.96 (Fig. 2).

Soil GHG emissions

Soil emissions of N_2O during the rainless dry period (DOY 154 – DOY 170) at Corn site were 11.6±1.3 g N_2O-N ha^{-1} d^{-1}. Fertilization of at a rate of ~135 kg N ha^{-1} with 28% UAN solution had no effect on soil N_2O emissions during this time (Fig. 3).

Observed soil N_2O emissions during the dry period of our study, despite fertilization, can be explained by the lack of available water, as has been observed in seasonally dry

environments (Davidson et al., 1993). The flux, however, while was low relatively to post-wetting fluxes (see below) was much higher than nearby agricultural fields (Gelfand et al., in review) which exhibited five folds lower flux of 2.6±0.3 g N_2O-N ha^{-1} d^{-1}. Such large difference could be explained by relatively high soil organic C concentrations (30.9±7.7 g kg^{-1}), which are estimated carbon saturation level for this soils (Gelfand et al., 2011).

The study site exhibited response of 34 folds increase in soil N_2O emissions after wetting with average soil N_2O fluxes of 398.0±91.2 g N_2O-N ha^{-1} d^{-1} (Table 1). Jørgensen et al. (1998) showed a similar ~40 fold increase of soil N_2O emissions after rewetting of a dry hay field after harvest.

After rewetted soils dried to pre-wetting water content (DOY 175), soil N_2O emissions at the Corn site returned to pre-wetting levels of 11.5±3.1 g N ha^{-1} d^{-1} despite additional fertilization with 48 kg N ha^{-1} on June 22 and higher soil temperatures than earlier (Table 1, Fig. 1, 3).

Eddy-Covariance measurements of ecosystem level N_2O exchange.

The fluxes measured by the sensor were low and exhibited strong diurnal pattern (Fig. 4). Low fluxes can be explained by drought during June 2012, similarly to the fluxes measured by static chambers. The fluxes measured by EC-OP-QCL technique were non comparable to the fluxes measured by static chambers, probably due to differences in flux integration area, the footprint of the EC tower is ~600×10^3 m^2 (Zenone et al., 2013) while chambers covering 697 cm^2. Another potential reason of such mismatch is technical difficulties of the prototype sensor. While overall OP-QCL sensor exhibited promising ability to measure ecosystem level of soil N_2O flux, seems that the very high temperatures during deployment and very low soil N_2O fluxes affected estimation.

Our results demonstrate that the coupling between water, carbon, and nitrogen cycles is controlling soil N_2O emissions from crop ecosystem in a mesic climate.

We conclude that both techniques for measuring soil GHG emissions using static chamber method — laboratory GC analysis of GHG concentrations and the newly developed quantum cascade laser coupled with infra-red gas analyzer for simultaneous *in situ* measurements — were highly correlated and could be used interchangeably using the static chamber method. The eddy-covariance technique exhibited very

intriguing and promising results, but still need to be thoroughly checked during non-drought conditions.

Acknowledgments

We thank J. Bronson for field assistance. We thank J. Schuette for helpful comments on an early version of the manuscript. Financial support for this work was provided by the DOE Office of Science (DE-FC02-07ER64494, KP1601050) and Office of Energy Efficiency and Renewable Energy (DE-AC05-76RL01830, OBP 20469-19145), the US National Science Foundation LTER program (DEB 1027253), and MSU AgBioResearch.

Table 1. Average soil fluxes of N_2O-N (g ha^{-1} d^{-1}) before the wetting event (Dry, DOY 154 – DOY 170), immediately after the wetting effect (Wet, DOY 171 – DOY 174), and after complete drying of the soils (Post-Wet, DOY 177 – DOY 179) (mean ± S.E., n = 16 chambers).

Period	N_2O-N (g $ha^{-1}d^{-1}$)	VWC* m^3 m^{-3}
Dry	11.6 (1.3)	0.12 (0.01)
Wet	398.0 (91.2)	0.19 (0.02)
Post-Wet	11.5 (3.1)	0.10 (0.01)

* "Dry" values represent volumetric water content of the experimental field. "Wet" values represent volumetric water content of soil within wetted area of 0.5 m^2. Volumetric water contents of wetted areas at the second day after artificial rain application (DOY 173) was 14±1 m^3 m^{-3}. For continues volumetric water content, see Figure 1. Adopted from Gelfand et al., in review.

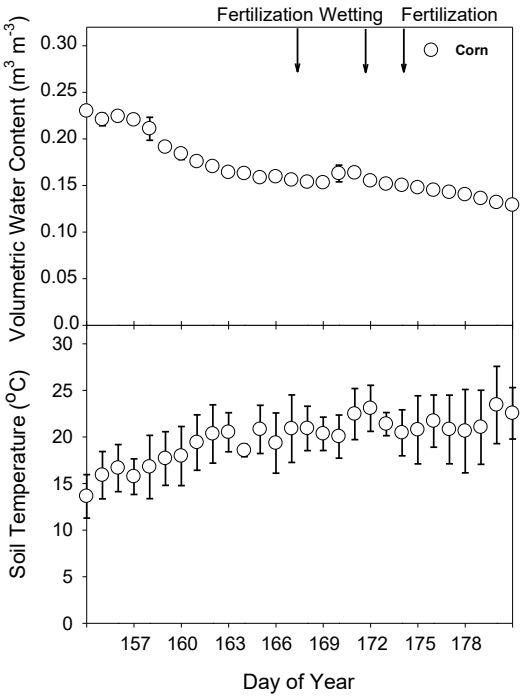

Fig. 1. Daily averages of soil volumetric water content (0-30 cm layer) and soil temperature (0-20 cm layer) measured by EC tower sensors. Arrows indicate timing of management and application of artificial rain. Adopted from Gelfand et al., in review.

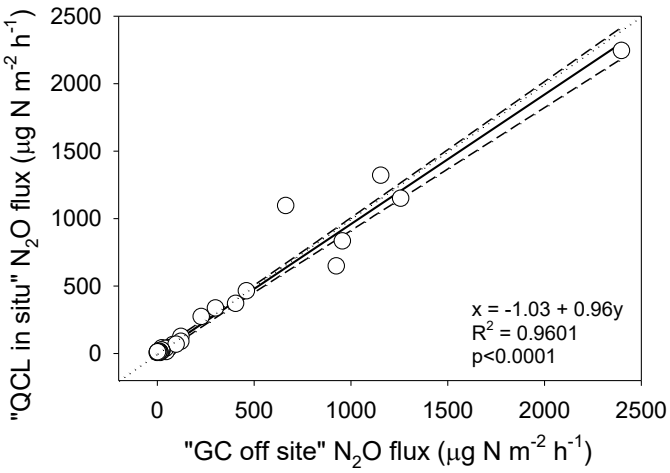

Fig. 2. Comparison of N_2O (μg N m^{-2} h^{-1}) fluxes measured from the same chambers by "QCL in situ" and "GC off site" techniques (solid line; 54 individual chamber/incubations) during field incubations. Dotted line represents 1:1 relationship; dashed line represents the 95% confidence interval. Adopted from Gelfand et al., in review.

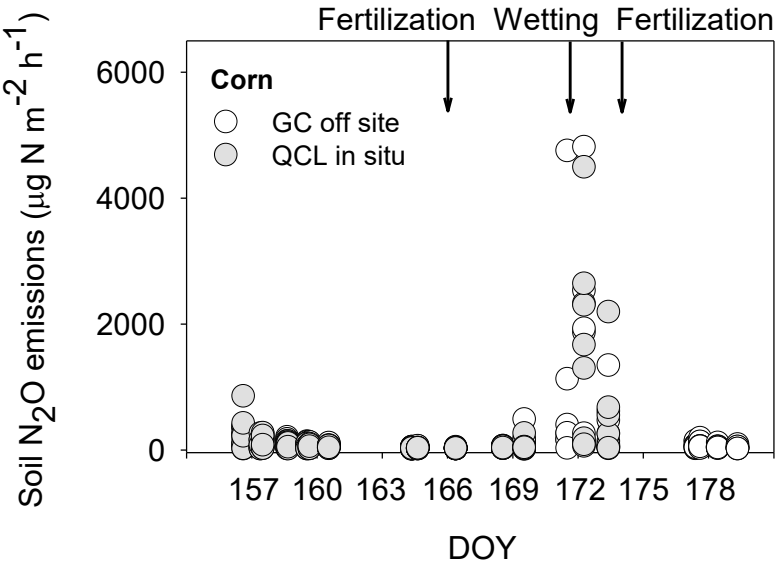

Fig. 3. Soil N_2O (µg N m^{-2} h^{-1}) fluxes over studied period. Arrows indicate timing of management and application of artificial rain. Adopted from Gelfand et al., in review.

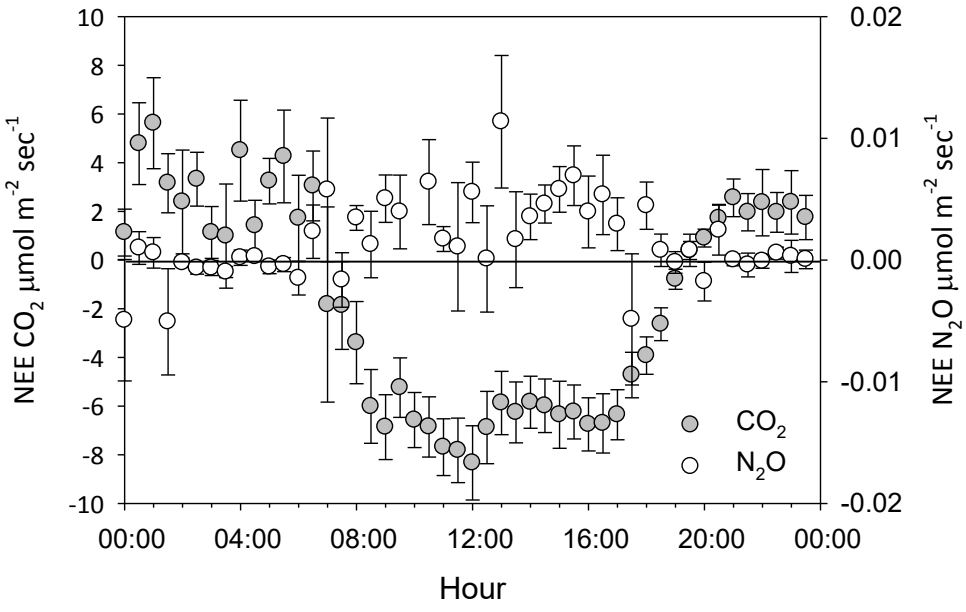

Fig. 4. Diurnal pattern of Net Ecosystem Exchange of CO_2 and N_2O, measured by eddy-covariance tower equipped with a prototype QCL N_2O sensor and standard LI-7500A CO_2 sensor.

References

Austin, A.L., Yahdjian, J. Stark, J. Belnap, A. Porporato, U. Norton, et al. 2004. Water pulses and biogeochemical cycles in arid and semiarid ecosystems. Oecologia 141:221-235.

Beare, M.H., Gregorich, E.G., and P. St-Georges. 2009. Compaction effects on CO_2 and N_2O production during drying and rewetting of soil. Soil Biol. Biochem. 41:611-621.

Bergsma, T. T., Robertson, G. P., and N. E. Ostrom. (2002), Influence of soil moisture and land use history on denitrification end-products. J. Environ. Qual. 31:711-717.

Betts, R.A., Boucher, O., Collins, M., Cox, P.M., Falloon, P.D., N. Gedney, et al. 2007. Projected increase in continental runoff due to plant responses to increasing carbon dioxide. Nature 448:1037-1041.

Birch, H.F. 1958. The effect of soil drying on humus decomposition and nitrogen availability. Plant Soil 10:9-31

Borken, W., and E. Matzner. 2009. Reappraisal of drying and wetting effects on C and N mineralization and fluxes in soils. Global Change Biol., 15:808-824.

Butterbach-Bahl, K., Baggs, E.M., Dannenmann, M., Kiese, R., and S. Zechmeister-Boltenstern. 2013. Nitrous oxide emissions from soils: how well do we understand the processes and their controls? Philosoph. Transac. Royal Soc. B: Biol. Sci. *In press.*

Davidson, E.A., Matson, P.A., Vitousek, P.M., Riley, R., Dunkin, K., Garsia-Mendez, G., et al. 1993. Processes regulating soil emissions of NO and N_2O in a seasonally dry tropical forest. Ecology 74:130-139.

Durack, P.J., Wijffels, S.E., and R.J. Matear. 2012. Ocean Salinities Reveal Strong Global Water Cycle Intensification During 1950 to 2000. Science 336:455-458.

Gelfand, I., Cui, M., Tang, J., Robertson, G.P. In review. N_2O and CO_2 fluxes from an agricultural site in the upper Midwest U.S. during 2012 drought: dependence on land-use history. JGR-Biogeosciences.

Holland, E.A., Robertson, G.P., Greenberg, J., Groffman, P.M., Boone, R.D., and J.R. Gosz. 1999. Soil CO_2, N_2O, and CH_4 exchange, p. 185-201, *In* G. P. Robertson, et al., eds. Standard soil methods for long-term ecological research. Oxford University Press, Oxford, UK.

IPCC. 2007. Contribution of Working Group I to the Fourth Assessment Report of the Intergovernmental Panel on Climate Change "The Physical Science Basis", *In* S. Solomon, D. Qin, M. Manning, Z. Chen, M. Marquis, K.B. Averyt, M. Tignor and H.L. Miller (eds.), ed. Intergovernmental Panel on Climate Change, Vol. IV. Cambridge University Press, Cambridge, United Kingdom and New York, NY, USA.

Jørgensen, R.N., Jørgensen, B.J., and N.E. Nielsen. 1998. N_2O emission immediately after rainfall in a dry stubble field. Soil Biol. Biochem. 30:545-546.

Kim, D.-G., Vargas, R., Bond-Lamberty, B., and M.R. Turetsky. 2012. Effects of soil rewetting and thawing on soil gas lfuxes: a review of current literature and suggestions for future research. Biogeosciences 9:2459 2483

Larsen, K.S., L.C. Andresen, C. Beier, S. Jonasson, K.R. Albert, P.E.R. Ambus, et al. 2011. Reduced N cycling in response to elevated CO_2, warming, and drought in a Danish heathland: Synthesizing results of the CLIMAITE project after two years of treatments. Global Change Biol. 17:1884-1899.

Migliavacca, M., Reichstein, M., Richardson, A.D., Colombo, R., Sutton, M.A., Lasslop, G., et al. 2011. Semiempirical modeling of abiotic and biotic factors controlling ecosystem respiration across eddy covariance sites. Global Change Biol. 17:390-409.

Mikha, M.M., Rice, C.W., and G.A. Milliken. 2005. Carbon and nitrogen mineralization as affected by drying and wetting cycles. Soil Biol. Biochem. 37:339-347.

Neftel, A.C. Ammann, C. Fischer, C. Spirig, F. Conen, L. B., Emmenegger, et al. 2012. N_2O exchange over managed grassland: application of a quantum cascade laser spectrometer for micrometeorological flux measurements. Ag. For. Meteor. 150, 775-785, doi:10.1016/j.agrformet.2009.07.013.

Noormets, A., McNulty, S.G., De Forest, J.L., Sun, G., Li, Q., Chen, J., 2008. Drought during canopy development has lasting effect on annual carbon balance in a deciduous temperate forest. New Phytologist 179: 818–828.

Prieme, A., and S. Christensen. 2001. Natural perturbations, drying-wetting and freezing-thawing cycles, and the emission of nitrous oxide, carbon dioxide and methane from farmed organic soils. Soil Biol. Biochem. 33:2083-2091.

Robertson, G., Bruulsema, T., Gehl, R., Kanter, D. Mauzerall, D., C. Rotz, et al. 2012. Nitrogen–climate interactions in US agriculture. Biogeochemistry: DOI:10.1007/s10533-012-9802-4.

Ruan, L., and G. P. Robertson. 2013. Initial nitrous oxide, carbon dioxide, and methane costs of converting conservation reserve program grassland to row crops under no-till vs. conventional tillage. Global Change Biol. 19:2478-2489.

Tao, L., Sun, K., Khan, M.A., Miller, D.J., and M.A. Zondlo. 2012. Compact and portable open-path sensor for simultaneous measurements of atmospheric N_2O and CO using a quantum cascade laser. Opt. Express, 20, 28106–28118, doi: 10.1364/OE.20.028106.

Vitousek, P.M., Naylor, R., Crews, T., David, M.B., Drinkwater, L.E., E. Holland, et al. 2009. Nutrient Imbalances in Agricultural Development. Science 324:1519-1520.

Xu, L. K., D. D. Baldocchi, and J. W. Tang. 2004. How soil moisture, rain pulses, and growth alter the response of ecosystem respiration to temperature. Global Biogeochem. Cycles 18:GB4002, doi:4010.1029/2004GB002281.

Zenone, T., J. Chen, M.W. Deal, B. Wilske, P. Jasrotia, J. Xu et al. 2011. CO_2 fluxes of transitional bioenergy crops: effect of land conversion during the first year of cultivation. GCB Bioenergy 3:401-412.

Zenone, T., Gelfand, I., Chen, J., Hamilton, S.K., Robertson, G.P. 2013. Carbon balances during land conversion in early bioenergy systems. Ag. For. Meteor. 182-183:1-12.

Zona, D., Janssens, I.A., Gioli, B., Jungkunst, H.F., Serrano, M.C., and R. Ceulemans. 2012. N_2O fluxes of a bio-energy poplar plantation during a two years rotation period. GCB Bioenergy.

Zona, D., Janssens, I.A., Aubinet, M., Gioli, B., Vicca, S., R. Fichot et al. 2013. Fluxes of the greenhouse gases (CO_2, CH_4, and N_2O) above a short-rotation poplar plantation after conversion from agricultural land. Ag. For. Meteorol. 169, 100-110, doi:10.1016/j.agrformet.2012.10.008

CONTAMINANTS OF EMERGING CONCERN IN THE AGRO-ENVIRONMENTS: FATE AND PROCESSES

Benny Chefetz, Rotem Navon, Adi Maoz, Daniella Harush, Tamar Mualem, Myah Goldstein and Moshe Shenker

Department of Soil and Water Sciences, Faculty of Agriculture, Food and Environment, The Hebrew University of Jerusalem, P.O. Box 12, Rehovot 76100, Israel

Pharmaceutical compounds (PCs) and dissolved organic matter (DOM) are co-introduced into soils by irrigation with reclaimed wastewater and sludge application. Various pharmaceuticals have been detected in different environmental compartments such as lakes, rivers and groundwater (Kolpin et al., 2002; Ternes et al., 2007; Calderón-Preciado et al., 2011). PCs were also detected in treated wastewater (Ternes et al., 2007). The use of treated wastewater for crop irrigation may lead to the introduction of PCs to agricultural fields. Once in the soil, PCs can accumulate in the top-soil layer, leach through the soil into the groundwater or surface water, or may enter the food-chain due to plant uptake.

We investigated the behavior (transport, sorption-desorption and plant uptake) of carbamazepine, naproxen and diclofenac in agro-ecosystem. All the studied compounds were detected in reclaimed wastewater used for crop irrigation. Transport and sorption experiments were performed with soil layers sampled from a citrus orchard which has been irrigated with reclaimed wastewater for more than 25 years. Carbamazepine and diclofenac were significantly retarded in the 0-5 cm soil sample rich in soil organic matter (SOM): carbamazepine was not affected by the water quality (freshwater vs. reclaimed wastewater), whereas diclofenac exhibited a higher retardation factor (RF) in the freshwater system. Naproxen exhibited significantly lower RFs than diclofenac but with a similar trend—higher retardation in the freshwater versus reclaimed wastewater system. In the 5-15 cm soil sample containing low SOM, naproxen was highly mobile while carbamazepine and diclofenac were still retarded. In the 15-25 cm sample, all compounds exhibited their lowest RFs. Our data suggest that carbamazepine and diclofenac can be classified as slow-mobile compounds in SOM-rich soil layers.

When these compounds pass this layer and/or introduced into SOM-poor soils, their mobility increases significantly.

Sorption data suggested that SOM governs the studied PCs' interactions with the soil samples. However higher C-normalized sorption coefficients (Koc) were measured for the PCs in the 15-25 cm sample, suggesting that both quantity and the physicochemical nature of SOM affect sorption interactions. While both naproxen and carbamazepine exhibited reversible sorption isotherms, diclofenac exhibited pronounced sorption-desorption hysteresis (Chefetz et al., 2008). Following this, we targeted carbamazepine as a model compound to study the tertiary interactions between relatively polar pharmaceutical compounds, DOM and soil.

Sorption-desorption behavior of carbamazepine was studied with bulk clay soil and the corresponding clay size fraction in the following systems: (i) without DOM, (ii) co-introduced with DOM, and (iii) pre-adsorption of DOM before CBZ introduction (Navon et al., 2011). Sorption of the DOM to both sorbents was irreversible and exhibited pronounced sorption-desorption hysteresis. Carbamazepine exhibited higher sorption affinity and nonlinearity, and a higher degree of desorption hysteresis with the bulk soil as compared to the corresponding clay size fraction. This was probably due to specific interactions with polar soil organic matter fractions that are more common in the bulk soil. Co-introduction of carbamazepine and DOM to the soil did not significantly affect the sorption behavior of carbamazepine; however, following pre-adsorption of DOM by the bulk soil, an increase in sorption affinity and decrease in sorption linearity were observed. In this latter treatment, desorption hysteresis of carbamazepine was significantly increased for both sorbents. We hypothesize that this was due to either strong chemical interactions of carbamazepine with the adsorbed DOM or physical encapsulation of carbamazepine in DOM-clay complexes.

Binding of carbamazepine by DOM fractions exhibited strong pH-dependence; the highest binding coefficients were at pH 4 (Maoz and Chefetz, 2010). Among the hydrophilic DOM fractions, the hydrophilic acid fraction exhibited the highest binding to carbamazepine, probably due to its bipolar character. Another interesting finding was that the binding coefficient value of carbamazepine with the bulk DOM sample was higher than the value calculated based on binding by the individual isolated fractions. Based on this study, we suggest that DOM facilitates stronger interactions of polar

pharmaceutical compounds with the solid surface. This mechanism can reduce pharmaceutical compounds desorption ability in soils (Navon et al., 2011).

Due to these results, the uptake potential of carbamazepine by cucumber plants and its fractionation into edible and other plant organs was evaluated (Shenker et al., 2011). Carbamazepine concentration in cucumber fruits and leaves was negatively correlated with the level of organic matter in the growing medium. The concentrations of carbamazepine in the roots and stems of cucumber plants were relatively low; most of it (76-84% of total uptake) was detected in the leaves. A greenhouse experiment using fresh water and reclaimed wastewater spiked, or not, with carbamazepine at $1 g \cdot L^{-1}$ (typical concentration in effluents) revealed that it can be taken up and bio-accumulated from its indigenous concentration in reclaimed wastewater. Our experimental data in hydroponic culture suggest that the uptake of carbamazepine can be considered passive and unrestricted and the translocation is governed by water mass flow; therefore, in the greenhouse experiments, the bioaccumulation factor for the fruits was significantly lower than the value calculated for the leaves (Shenker et al., 2011).

Conclusions

Our data suggest that carbamazepine and diclofenac can be classified as slow-mobile compounds in soil organic matter-rich soil layers. When these compounds pass this layer and/or introduced into soil organic matter-poor soils, their mobility increases significantly (Chefetz et al., 2008). Other compounds based on their physico-chemical properties can be considered as highly mobile in soils. This study emphasizes the potential uptake of active pharmaceutical compounds by crops in organic-matter-poor soils irrigated with reclaimed wastewater and highlights the potential risks associated with this agricultural practice (Shenker et al., 2011).

References

Calderón-Preciado, D., C. Jiménez-Cartagena, V. Matamoros, and J.M. Bayona. 2011. Screening of 47 organic microcontaminants in agricultural irrigation waters and their soil loading. Water research 45(1): 221–231.

Chefetz, B., T. Mualem, and J. Ben-Ari. 2008. Sorption and mobility of pharmaceutical compounds in soil irrigated with reclaimed wastewater. Chemosphere 73(8): 1335–1343.

Kolpin, D.W., E.T. Furlong, M.T. Meyer, E.M. Thurman, S.D. Zaugg, L.B. Barber, and H.T. Buxton. 2002. Pharmaceuticals, hormones, and other organic wastewater contaminants in U.S. streams, 1999-2000: a national reconnaissance. Environmental science & technology 36(6): 1202–1211.

Maoz, A., and B. Chefetz. 2010. Sorption of the pharmaceuticals carbamazepine and naproxen to dissolved organic matter: role of structural fractions. Water research 44(3): 981–989.

Navon, R., S. Hernandez-Ruiz, J. Chorover, and B. Chefetz. 2011. Interactions of carbamazepine in soil: effects of dissolved organic matter. Journal of environmental quality 40(3): 942–948.

Shenker, M., D. Harush, J. Ben-Ari, and B. Chefetz. 2011. Uptake of carbamazepine by cucumber plants--a case study related to irrigation with reclaimed wastewater. Chemosphere 82(6): 905–910.

Ternes, T.A., M. Bonerz, N. Herrmann, B. Teiser, and H.R. Andersen. 2007. Irrigation of treated wastewater in Braunschweig, Germany: an option to remove pharmaceuticals and musk fragrances. Chemosphere 66(5): 894–904.

USE OF STABLE ISOTOPES TO STUDY THE FATE OF ORGANIC POLLUTANTS IN SOILS

Anat Bernstein[1,3], Faina Gelman[2], Eilon Adar[3], Harald Lowag[4], Willibald Stichler[4], Rainer U. Meckenstock[4], Sharon Sagi-Ben Moshe[5], Ofer Dahan[3], Noam Weisbrod[3], and Zeev Ronen[3]

[1]Institute of Soil, Water and Environmental Sciences, Agricultural Research Organization, Volcani Center
[2]Geological Survey of Israel, 30 Malkhey Israel, Jerusalem 95501, Israel
[3]Dept. of Environmental Hydrology and Microbiology, Zuckerberg Institute for Water Research, Ben-Gurion University of the Negev, Sede Boqer 84990, Israel
[4]Helmholtz Zentrum München, German Research Center for Environmental Health, Institute of Groundwater Ecology, Ingolstädter Landstr. 1, 85764 Neuherberg, Germany
[5]Dept. of Soil and Water Sciences, The Hebrew University of Jerusalem, P.O. Box 12, Rehovot 76100, Israel

Introduction

Quantifying degradation extents of contaminants in the subsurface is a desired goal for management of water resources. Nevertheless, this task is often difficult, since observed decrease in a contaminant's concentration may not only be related to biodegradation, but also to other natural attenuating processes such as dispersion, sorption or volatilization. Under such circumstances, the sensitivity in quantifying biodegradation rates of an investigated contaminant based on shifts in its concentration may be low. Alternatively, analysis of the degradation products may as well not always be conclusive, as products may not be detectable or can originate from different parent compounds. Monitoring the concentration of the investigated contaminant and of its degradation products is, therefore, not always sufficient for dealing with the challenges of quantifying degradation rates in a complex environments.

In the last 15 years, compound specific isotope analyses (CSIA) was introduced as complementary approach that can overcome the above difficulties. This methodology is not based on monitoring the shifts in concentrations, but rather on shifts in isotope compositions. These shifts are mostly affected by bond cleavage/formation within the molecule, whereas dilution causes no isotope shifts and sorption and volatilization show normally negligible influence on the isotopic composition of the compound (Braeckevelt et al., 2012; Meckenstock et al., 2004).

By CSIA the shifts of stable isotope ratios in chemical compounds (most frequently $^{13}C/^{12}C$, $^{2}H/^{1}H$, and $^{15}N/^{14}N$) are measured along natural transformation reactions. Owing to the kinetic isotope effect of the reaction, isotope fractionation commonly occurs in the atoms that are directly involved in the biochemical bond-cleavage (Aelion, 2009). This means that the isotope composition of the residual compound that has not yet been degraded becomes enriched in the heavy isotopes along the degradation process. This enrichment is typical of the degradation pathway and is characterized by an enrichment factor (ε) which is specific for the compound under investigation. Thus, enrichment in the isotope composition of a pollutant at a contaminated field site can be used to verify the occurrence of degradation in the subsurface and, by correlation with an experimentally determined enrichment factor, may further allow to quantitatively assess its extent of transformation. Furthermore, it may assist in getting insight on the degradation mechanism.

Hereby we demonstrate the use of CSIA to study the fate of hexahydro-1,3,5-trinitro-1,3,5-triazine (RDX) in the sub-surface, and get insight on the degradation mechanism. RDX is an explosive that has been used extensively over the years, resulting in significant contamination of soils and groundwater, especially adjacent to explosives-manufacturing plants and in military training areas (Pennington and Brannon, 2002). Due to its toxicity, the fate of this compound in natural environments and water resources is of great interest.

Case Studies

Degradation mechanism

In recent years, considerable effort has been made to elucidate the aerobic biochemical pathway of RDX. Studies have shown that denitration is a key step in the process and that it is followed by ring cleavage (Fournier et al., 2002). The denitration process was found to be catalyzed by *Rhodococcus* strains, isolated from contaminated habitats worldwide, among them strains isolated from contaminated sediments in Australia, (Coleman et al., 2002), in England (Seth-Smith et al., 2002) and in Israel (Bernstein et al., 2011; Brenner et al., 2000). This global distribution may indicate that the denitration mechanism is probably a fundamental degradation pathway for the compound under aerobic conditions.

Although the denitration pathway has been thoroughly studied, the exact denitration mechanism was questioned. Specifically, there was no consensus on which bond is actually being initially cleaved during the enzymatic reaction. Since the triazinic RDX ring lacks stability, it was suggested that any theoretical attack of either an N-NO_2 or C-H bond will result in ring cleavage (Hawari et al., 2000). Therefore, the observation of denitration alone does not necessarily provide sufficient knowledge about the first mechanistic step.

Two different denitration mechanisms were postulated for the reaction: (1) The first suggested that cytochrome P450 catalyzes two sequential single electron transfers from NADPH, each resulting in denitration. The remaining unstable RDX product, having only one nitro group, spontaneously decomposes to the ring-cleavage product 4-nitro-2,4-diazabutanal (NDAB; Fig. 1) (Bhushan et al., 2003). (2) A C-H bond cleavage is initiated by superoxide radicals that are formed from O_2 by cytochrome P450, resulting in a $H^{\bullet}$ abstraction as the first catalytic step followed by subsequent denitration. Then, the reaction normally proceeds to the second denitration step (yet, to some extent, only one denitration step occurs) (Halasz et al., 2010).

A different, abiotic mechanism of alkaline hydrolysis can be seen with some analogy to the denitration of RDX, in which a nucleophilic attack results in the C-H bond cleavage as the initial step. This C-H cleavage is accompanied by denitration and the spontaneous formation of NDAB (Balakrishnan et al., 2003) (Fig. 1). Although this latter mechanism does not involve the formation of a radical intermediate, it shows that when degradation is initiated by a C-H bond cleavage, subsequent denitration and the formation of NDAB is indeed possible.

Compound-specific isotope analysis (CSIA) was applied as a tool for distinguishing between the different postulated degradation mechanisms. Since atoms within bonds that are cleaved during the reaction's rate limiting step frequently record observable isotope enrichment ("primary isotope effect"), whereas adjacent atoms typically show only slight, or undistinguished, enrichment ("secondary isotope effect") (Elsner et al., 2005), dual-isotope analysis of ^{13}C and ^{15}N in RDX may potentially shed light on the denitration mechanism. (1) If the enzymatic attack focuses on the nitro group and the N-N bond cleavage occurs directly without any involvement of a C-H bond, nitrogen is expected to present primary isotope effects, whereas carbon is expected to present

secondary isotope effects only. (2) Alternatively, if hydrogen abstraction by a radical reaction takes place, and cleavage of a C-H bond occurs during the reaction's rate limiting step, one would expect to observe a primary carbon isotope effect (as shown to occur in radical reactions during C-H bond cleavage of aromatic compounds (Morasch et al., 2001; Morasch et al., 2004)), whereas nitrogen is expected to present secondary isotope effects only. (3) If the microbial enzymatic reaction proceeds in a similar manner as alkaline hydrolysis, with the simultaneous loosening of the C-H and N-NO_2 bonds at the transition state, both primary carbon and nitrogen isotope effects can be expected (Fig. 1).

A primary ^{15}N enrichment was detected during the enzymatic denitration by three distinct *Rhodococcus* strains, whereas a^{13}C enrichment was almost in the range of the analytical method uncertainty (ε=-0.86±0.84‰ for strain YH1). This low, almost undistinguishable carbon isotope enrichment reflects secondary isotope effects. Combining both elements from biodegraded samples by the tested strains in a dual-isotope plot ($\delta^{13}C$ vs. $\delta^{15}N$; Fig. 2), shows a slope which is significantly different from the slope of the alkaline hydrolysis. This led to the conclusion that denitration of RDX by *Rhodococcus* species is initiated by N-N bond cleavage, rather than by a C-H bond cleavage or by a simultaneous loosening of both C-H and N-N bonds. This typical enrichment is shown for all three strains tested (Fig. 2).

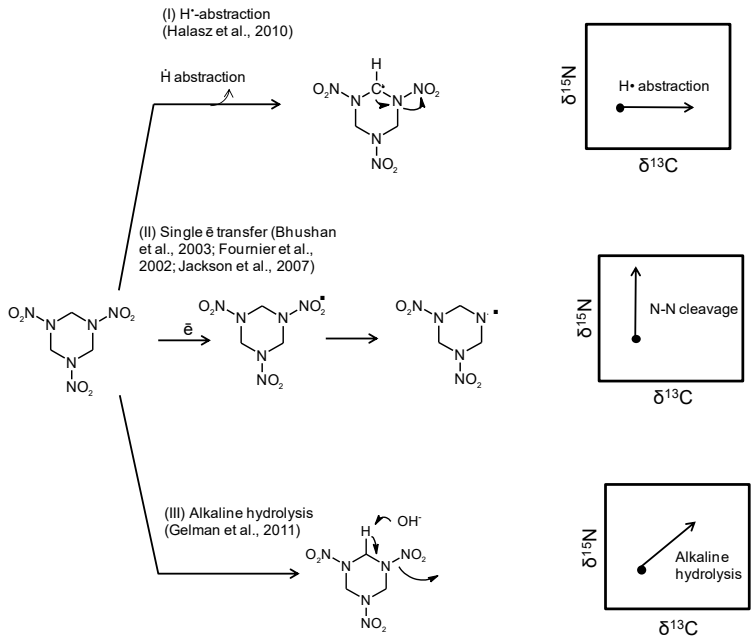

Fig. 1. Expected isotope enrichment following different degradation mechanisms. Adapted from (Bernstein et al., 2013)

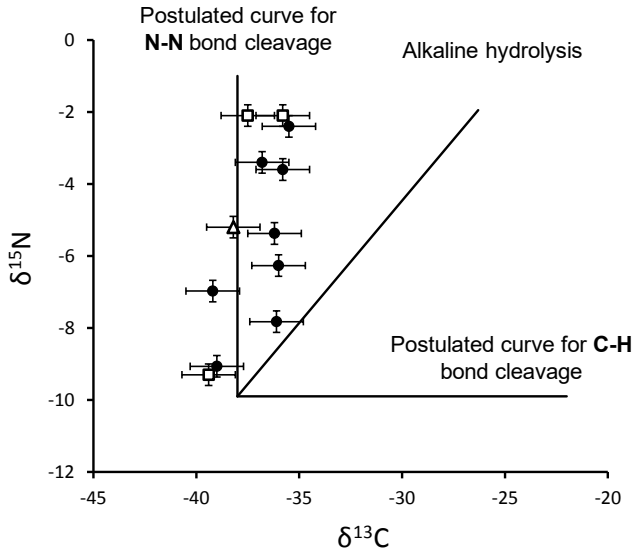

Fig. 2. Isotope enrichment in biodegraded RDX samples. Adapted from (Bernstein et al., 2013)

In-situ degradation

RDX contamination plume was detected in the Israeli Coastal Aquifer underneath its manufacturing site, near the city of Ramat Hasharon. The Israeli Coastal Aquifer is one of the major water-supply sources for the country. The aquifer produces an average 300 x 10^6 m^3 of water annually, ~15% of the yearly national water consumption. Stratigraphically, this aquifer consists of sedimentary rocks of the Pleistocene Kurkar Group. This group is underlain by the low-permeability shale and marls of the Saqiye Group (Gvirtzman and Reiss, 1965). The contaminated site is located adjacent to an explosives-manufacturing plant. From 1964 to 1982, and then to a much lesser extent until the year 2000, untreated industrial wastewater characterized by relatively high concentrations of RDX were disposed of in unlined wastewater ponds and nearby creeks as part of manufacturing operations. Since then, the effluent ponds have not received any industrial discharge. Nevertheless, the ponds have been subjected to rain water and local runoff accumulation during the winter rainy seasons (average of ≈ 500 mm y^{-1}), which could promote further transport of RDX along the soil profile. Large-scale site characterization and monitoring operations at the site revealed high concentrations of RDX, octahydro-1,3,5,7-tetranitro-1,3,5,7-tetrazocine (HMX), 2,4,6-trinitrotoluene (TNT) and their degradation products underneath these effluent ponds, mainly in the upper soil layer (up to 2 m below the surface). However, the contamination by these compounds was not unique to the upper layers, and lower concentrations, mainly of RDX were found along the ca. 45-m thick vadose zone in this area (Nativ and Adar, 2005). Moreover, high concentrations of RDX were found in the underlying groundwater in an ~1.35-km long contamination plume with peak concentrations of up to 2,100 μg l^{-1} (Nativ and Adar, 2005)

Although the potential for RDX biodegradation in soils has been detected (Nejidat et al., 2008; Ronen et al., 2008; Sagi-Ben Moshe et al., 2009), evidence for *in-situ* occurrence in the field was lacking and its extent was unknown. It was suggested to apply CSIA for elucidating the magnitude of biodegradation along the soil profile and contaminated groundwater.

Unsaturated zone

Along the soil profile, $\delta^{15}N$ values of RDX were measured in order to acquire evidence for in-situ biodegradation in the unsaturated zone (Fig. 3). RDX produced at this industrial site was used as a reference, having a $\delta^{15}N$ composition between -9.9 and -10.8‰. The $\delta^{15}N$ values of RDX along the entire unsaturated zone were enriched relative to $\delta^{15}N$ values of the reference RDX produced at the industrial site. One single exception was detected in the sample taken 2 m below ground surface, in which the $\delta^{15}N$ measured value, -10.4‰, was not different from the value of the RDX produced at the site. The most enriched value of $\delta^{15}N$ in RDX, corresponding to the highest fraction of biodegraded RDX, was detected in the upper soil layer ($\delta^{15}N$ = +0.2‰). The $\delta^{15}N$ values along the rest of the profile were more depleted, ranging between -1.9‰ and -9.4‰. Similar patterns were observed in the trends of RDX degradation products (MNX, DNX and TNX) and the $\delta^{15}N$ composition of RDX along the unsaturated profile (Fig. 3): A high fraction of degradation products was found concurrently in the profile sections in which $\delta^{15}N$-enriched RDX was observed.

This work led to the conclusion that biodegradation of RDX indeed takes place along the unsaturated zone, and is enhanced especially in the uppermost part of the profile, in which high content of organic matter exist.

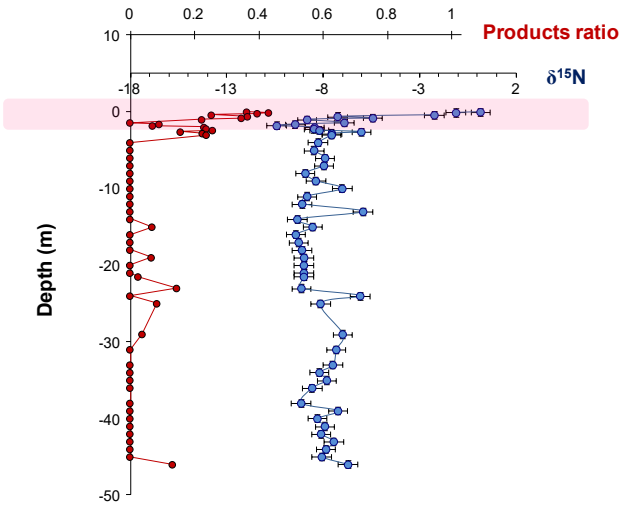

Fig. 3. Vertical distribution of $\delta^{15}N$ in RDX (red) and the ratio odegradation products (blue) along a contaminated thick soil profile. Adapted from (Sagi-Ben Moshe et al., 2010)

Groundwater

Groundwater contamination by RDX underneath the contaminated site was primarily related to methods of wastewater handling. Three sources of groundwater pollution by RDX have been identified at the site: (1) Contamination by effluents that drain directly from the production plant and contaminate groundwater adjacent to this plant. These effluents are characterized by relatively high RDX concentrations. As the production line involves the use of nitric acid, these effluents were also expected to exhibit relatively high nitrate (NO_3) concentrations. (2) Infiltration from infiltration ponds. In the past, effluents from the RDX production plant, as well as from other plants at the site, were discharged into unlined ponds. From these ponds, infiltration to groundwater occurred through 35 to 50 m of vadose zone. As these ponds were used to collect effluents from different sources, their RDX concentration was expected to be more dilute than that in the effluents that are released directly from the production plant. (3) Infiltration of effluents that were drained to a natural channel which conducts water drainage in the rainy season but was also used to conduct overflows from the effluent ponds.

Monitoring of RDX concentrations at the research site began in 2004. The length of the RDX contamination plume was found to be ~1.35 km. RDX concentrations measured in each monitoring well varied during the monitoring period. The maximal concentration detected in the monitoring period reached up to 2,100 μg/L (in a monitoring well adjacent to the production plant, March 2006). The shape of the contamination plume was determined by the historical flow regime. Currently the natural flow direction is perpendicular to the coastline, yet during certain periods in the past, flow lines were oriented to the north following intensive pumping for water supply.

The isotope analysis of RDX in the groundwater samples revealed a clear variation in $\delta^{15}N$ (Fig. 4), with an apparent enrichment further away from the contamination sources. In three of the four RDX contamination sources, values were the most depleted at the site (ranging between -7.0‰ and -8.1). Away from the sources, gradually enriched values of $\delta^{15}N$ are observed, with a spatial trend that reaches a maximal $\delta^{15}N$ value of +2.7‰ at a borehole located 1.15 to 1.35 km away from the different sources. An exception to the spatial enrichment trend is a borehole which, although located furthest from the RDX sources, presents relatively depleted $\delta^{15}N$ values. This well is

the deepest penetrating one of a three-well cluster.

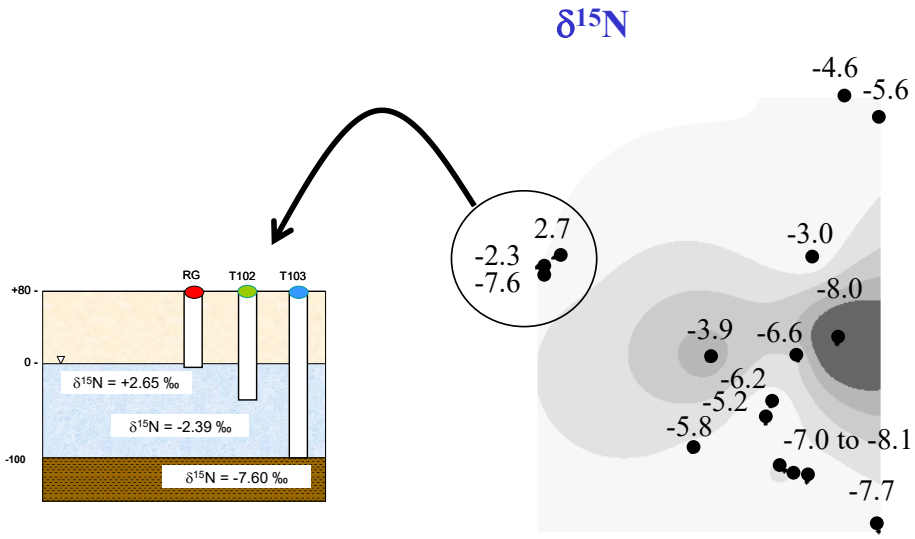

Fig. 4. $\delta^{15}N$ of RDX along the contamination plume and a vertical view on its distribution with depth. Adapted from (Bernstein et al., 2010)

The results revealed clear $\delta^{15}N$ enrichment in RDX downstream to the contamination sources, indicating the occurrence of biodegradation. The shift in isotope composition of RDX along the contamination plume enabled to quantify the extent of RDX degradation downstream and calculate the first-order kinetics constants for this process. Biodegradation rates were shown to decrease with depth (Bernstein et al., 2010).

Reference

Aelion, C.M. 2009. Environmental isotopes in biodegradation and bioremediation CRC.

Balakrishnan, V.K., A. Halasz, and J. Hawari. 2003. Alkaline Hydrolysis of the Cyclic Nitramine Explosives RDX, HMX, and CL-20: New Insights into Degradation Pathways Obtained by the Observation of Novel Intermediates. Environmental Science & Technology 37:1838-1843.

Bernstein, A., Z. Ronen, and F. Gelman. 2013. Insight on RDX Degradation Mechanism by Rhodococcus Strains Using 13C and 15N Kinetic Isotope Effects. Environmental Science & Technology 47:479-484.

Bernstein, A., E. Adar, A. Nejidat, and Z. Ronen. 2011. Isolation and characterization of RDX-degrading <i>Rhodococcus</i> species from a contaminated aquifer. Biodegradation 22:997-1005.

Bernstein, A., E. Adar, Z. Ronen, H. Lowag, W. Stichler, and R.U. Meckenstock. 2010. Quantifying RDX biodegradation in groundwater using δ15N isotope analysis. Journal of Contaminant Hydrology 111:25-35.

Bhushan, B., S. Trott, J.C. Spain, A. Halasz, L. Paquet, and J. Hawari. 2003. Biotransformation of Hexahydro-1,3,5-Trinitro-1,3,5-Triazine (RDX) by a Rabbit Liver Cytochrome P450: Insight into the Mechanism of RDX Biodegradation by Rhodococcus sp. Strain DN22. Applied and Environmental Microbiology 69:1347-1351.

Braeckevelt, M., A. Fischer, and M. Kästner. 2012. Field applicability of Compound-Specific Isotope Analysis (CSIA) for characterization and quantification of in situ contaminant degradation in aquifers. Applied Microbiology and Biotechnology 94:1401-1421.

Brenner, A., Z. Ronen, Y. Harel, and A. Abeliovich. 2000. Use of Hexahydro-1,3,5-trinitro-1,3,5-triazine as a Nitrogen Source in Biological Treatment of Munitions Wastes. Water Environment Research 72:469-475.

Coleman, N.V., J.C. Spain, and T. Duxbury. 2002. Evidence that RDX biodegradation by Rhodococcus strain DN22 is plasmid-borne and involves a cytochrome p-450. Journal of Applied Microbiology 93:463-472.

Elsner, M., L. Zwank, D. Hunkeler, and R.P. Schwarzenbach. 2005. A New Concept Linking Observable Stable Isotope Fractionation to Transformation Pathways of Organic Pollutants. Environmental Science & Technology 39:6896-6916.

Fournier, D., A. Halasz, J. Spain, P. Fiurasek, and J. Hawari. 2002. Determination of Key Metabolites during Biodegradation of Hexahydro-1,3,5-Trinitro-1,3,5-Triazine with Rhodococcus sp. Strain DN22. Applied and Environmental Microbiology 68:166-172.

Gvirtzman, G., and Z. Reiss. 1965. Stratigraphic nomenclature in the Coastal Plain and Hashephela regions. Israel Geological Survey Report OD/6/67 and Inst Petrol Res Geophys 1023:12.

Halasz, A., D. Manno, S.E. Strand, N.C. Bruce, and J. Hawari. 2010. Biodegradation of RDX and MNX with Rhodococcus sp. Strain DN22: New Insights into the Degradation Pathway. Environmental Science & Technology 44:9330-9336.

Hawari, J., S. Beaudet, A. Halasz, S. Thiboutot, and G. Ampleman. 2000. Microbial degradation of explosives: biotransformation versus mineralization. Applied Microbiology and Biotechnology 54:605-618.

Meckenstock, R.U., B. Morasch, C. Griebler, and H.H. Richnow. 2004. Stable isotope fractionation analysis as a tool to monitor biodegradation in contaminated acquifers. Journal of Contaminant Hydrology 75:215-255.

Morasch, B., H.H. Richnow, B. Schink, and R.U. Meckenstock. 2001. Stable Hydrogen and Carbon Isotope Fractionation during Microbial Toluene Degradation: Mechanistic and Environmental Aspects. Applied and Environmental Microbiology 67:4842-4849.

Morasch, B., H.H. Richnow, A. Vieth, B. Schink, and R.U. Meckenstock. 2004. Stable Isotope Fractionation Caused by Glycyl Radical Enzymes during Bacterial Degradation of Aromatic Compounds. Applied and Environmental Microbiology 70:2935-2940.

Nativ, R., and E.M. Adar. 2005. Soil and groundwater contamination in the Ramat Hasharon area. Annual scientific report submitted to the Water Authority. Ministry of national infrastructures, Tel Aviv.

Nejidat, A., L. Kafka, Y. Tekoah, and Z. Ronen. 2008. Effect of organic and inorganic nitrogenous compounds on RDX degradation and cytochrome P-450 expression in Rhodococcus strain YH1. Biodegradation 19:313-320.

Pennington, J.C., and J.M. Brannon. 2002. Environmetal Fate of explosives. Thermochimica Acta 384:163-172.

Ronen, Z., Y. Yanovich, R. Goldin, and E. Adar. 2008. Metabolism of the explosive hexahydro-1,3,5-trinitro-1,3,5-triazine (RDX) in a contaminated vadose zone. Chemosphere 73:1492-1498.

Sagi-Ben Moshe, S., Z. Ronen, O. Dahan, N. Weisbrod, L. Groisman, E. Adar, and R. Nativ. 2009. Sequential biodegradation of TNT, RDX and HMX in a mixture. Environ Pollut 157:2231-2238.

Sagi-Ben Moshe, S., Z. Ronen, O. Dahan, A. Bernstein, N. Weisbrod, F. Gelman, and E. Adar. 2010. Isotopic evidence and quantification assessment of in situ RDX biodegradation in the deep unsaturated zone. Soil Biology and Biochemistry 42:1253-1262.

Seth-Smith, H.M.B., S.J. Rosser, A. Basran, E.R. Travis, E.R. Dabbs, S. Nicklin, and N.C. Bruce. 2002. Cloning, Sequencing, and Characterization of the Hexahydro-1,3,5-Trinitro-1,3,5-Triazine Degradation Gene Cluster from Rhodococcus rhodochrous. Applied and Environmental Microbiology 68:4764-4771.

IRREVERSIBLE IMPACTS OF MICRO-POLLUTANTS ON NATURAL SOILS

Ishai Dror, Bruno Yaron, Brian Berkowitz

Dept. of Environmental Sciences and Energy Research, Weizmann Institute of Science, Rehovot 76100, Israel

Abstract

Changes induced to the natural soil matrix and its properties at the molecular level following irreversible interactions with anthropogenic micro-pollutants are identified and discussed. For example, the effect of exposure of clays and humic substances to pollutants such as engineered nanomaterials and their induced changes in the soil properties are explored. This group of contaminants induces structural modifications of clay minerals and organic matter, observed by spectroscopic and electron microscopy analyses. Additional examples of changes in soil surface composition, as identified by chromatography and elemental analysis, with consequences for soil water transmission are discussed. Finally, the implications of contamination on soil microbiological activity are shown. Based on these measurements we argue that chemical pollution leads to irreversible changes in soils. These changes may cause the formation of contemporary soils characterized by regimes different than those of natural soils. Under these conditions, natural soils become parent materials for contemporary, Anthropocene soils. Unlike the natural soil genesis process that is measured in geological time scales, the chemically-induced formation of the contemporary soil occurs within a much shorter “life time” scale.

Introduction:

Current studies on contaminant interactions with the subsurface focus mainly on contaminant retention, persistence and transport, and on potential remediation of polluted geological media. It should be further noted that properties altered by human intervention are usually looked upon as deviations from a normal geochemical environment, which will disappear under natural process or due to specific remediation procedures. We further note that beside their environmental toxic effects, contaminants may lead, under specific conditions, to irreversible changes of the subsurface properties.

We have demonstrated this idea in a number of publications in the last years (Yaron et al, 2008, 2009, 2010, 2012).

By contaminants of anthropogenic origin we consider the inorganic and organic chemicals that are reaching the subsurface during agricultural and soil remediation management or industrial and municipal residues accidentally released or deliberately disposed on land surface. In the literature we can find a very broad spectrum of research results on the contaminants- subsurface interaction. Current approach discusses mainly the contaminants fate as affected by the solid and the water phases of the vadose zone. There are however specific anthropogenic contamination impacts, which may lead to long-term changes in the natural properties of the subsurface geochemical system. These changes are often resistant to remediation procedure and natural attenuation and are thus irreversible on a human life scale. While in the natural process of subsurface genesis the formation factors act slowly over a prolonged "geological" time scale, the chemical contaminant may rapidly and irreversibly change the natural soil and the subsurface. For this reason chemical contamination may be considered an additional factor of contemporary soil formation. A recent paper by Ehlers and Kavanaugh (2013) stated that most of the contaminated sites that are considered large and complex to remediate (for example ~ 80% of the EPA superfund sites) remain polluted after many years of treatment. The number of these sites is estimated to be well over 100,000 in the USA alone and the total price of their remediation is estimated to exceed 100 billion $US. Ehlers and Kavanaugh (2013) further mention that there are significant technical limitations that will prevent complete cleanup of these sites. It therefore suggested that some achievable level of cleanup will be set as the target of remediation and a new level of contamination will be considered as a new baseline i.e. that the soil and subsurface that were contaminated and changed will be considered at some limitations as irreversibly changed.

An example for such effects can be found in the behavior of engineered nano materials (ENMs) in the environment. Considerable interest in recent years was attracted to ENMs due to the dramatic increase in production and consumer use, which resulted in increasing exposure and release to the environment. Transport, retention and mobility in saturated porous media were investigated for different types of nanoparticles including fullerenes, carbon nanotubes and metal oxides (Cheng et al. 2005; Dunphy et al. 2006; Espinasse et al. 2007; Lecoanet and Wiesner 2004; Lecoanet et al. 2004; Wang

and Pennell 2008; Wang et al. 2008). In general, the behavior of ENMs was shown to be strongly dependent on environmental conditions such as dissolved organic matter, pH and ionic strength. For example, soil organic matter was demonstrated to adsorb readily to nanoparticles, significantly enhancing their suspension stability in aqueous solution and increasing their mobility in porous media (Hyung et al. 2006; Johnson et al. 2009; Terashima and Nagao 2007; Xie et al. 2008).

Few studies have investigated the opposite phenomenon, namely, the effects of ENMs on the environment in general, and on soil properties in particular. Elliot and Zhang (2001) injected bimetallic (Fe/Pd) nanoparticles to a test area to demonstrate the reduction of trichloroethene and other chlorinated aliphatic hydrocarbons. The porosity of the soil was not affected by the ENMs, and clogging was shown to be minimal. A few studies investigated the effects of ENMs on soil microbiology. Fullerene nanoparticles were found to have little impact on soil microbial communities and microbial processes (Nyberg et al. 2008; Tong et al. 2007). Multi-walled carbon nanotubes were shown to reduce enzymatic activity in the soil as well as microbial biomass C and N (Chung et al. 2011). Metal oxide nanoparticles were also investigated; Ge et al. (2011) studied the impact of TiO_2 and ZnO on soil microbial communities and demonstrated that both ENMs reduced microbial mass and diversity. Pradhan et al. (2011) investigated the effects of copper oxide and silver nanoparticles on leaf microbial decomposition showing that exposure to these ENMs led to a decrease in leaf decomposition rate. Furthermore, the decrease in decomposition was accompanied by changes in the structure of the microbial communities.

Study of the interactions between ENMs and soil is complicated by the high variability in properties, caused by differences in environmental conditions and soil composition, as well as by the large number of types of available ENMs. In this study, two types of metal oxide ENMs were chosen, copper oxide (CuO) and magnetite (Fe_3O_4). These types of ENMs have wide, potential application: as gas sensors, magnetic phase transitions, catalysts and superconductors for copper oxide (Zhu et al. 2004), and in magnetic recording, magnetic data storage devices, toners and inks for xerography, and magnetic resonance imaging, wastewater treatment, bioseparation, and medicine for iron oxide (Mohapatra and Anand 2010). Both ENMs have low stability in aqueous suspension and tend to aggregate rapidly. They were shown previously to have limited mobility in saturated porous media (Ben-Moshe et al. 2010). Because of their low

mobility, large quantities of the ENMs are retained in the soil upon release to the environment.

In support of the conceptual approach, we will illustrate selected aspects of contaminant-induced, irreversible changes in the subsurface solid and aqueous phases based on research results meanly with ENMs.

Results and Discussion

Characterization of soil macroscopic properties:

The morphology of the soil aggregate surface is important both for the interactions between solute component and the solid matrix and for soil solution flow patterns. If the surface of the aggregate is coated by other materials like nanoparticles or other contaminants (organic or inorganic) it will affect the sorption capacity of the soil, the type of interaction with other compounds and if the particles change the roughness of the surface it will consequently change the flow of fluids near the surface. In many cases contaminants may also penetrate into clay layers and expend the interlayer spacing or interact with organic material and cause changes to its conformations or even composition. Here we give an example of two soils that are allowed to mix with copper oxide Nanoparticles. The SEM images of Bet Dagan and Yatir soil samples are presented in Figure 1. The nanoparticles clearly change the surface of the soil grains. For Bet Dagan soil, with 1% loading (Fig. 1B), the nanoparticles form large aggregates (hundreds of nm and larger) on the surface of the grains. EDS measurements confirmed that the aggregates are composed of the nanoparticles (results not shown). For 5% loading (Fig. 1C) the coverage is much more substantial with some of the grains being covered completely by the nanoparticles. Although the grains appear completely covered in the images, the coverage is not uniform and the majority of the soil grain surfaces are not covered with nanoparticles. For Yatir soil, large aggregates are also observed for the 1% loading (Fig. 1E). For the 5% loading (Fig 1F), both the number and the average size of these aggregates increase; however, areas of complete coverage are not observed.

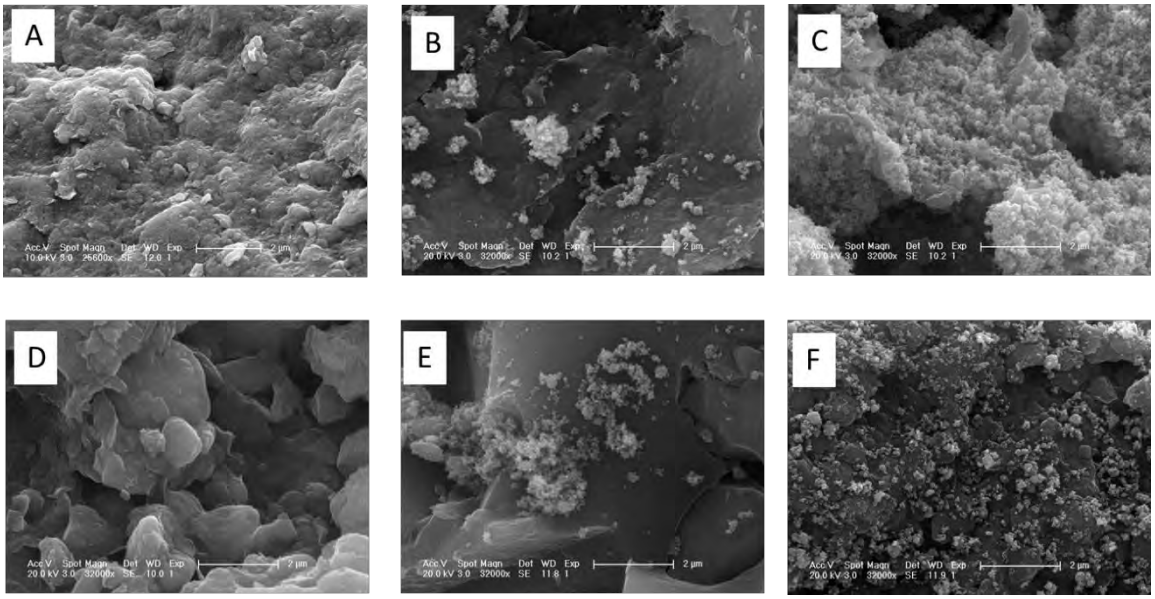

Fig. 1. SEM image of Bet Dagan (A-C) and Yatir (D-F) soil after mixing with copper oxide (cuO) Nanoparticles; A - Bet Dagan and D – Yatir – untreated ("clean") soils, B and D are a mixture of each soil with 1% CuO, C and F are a mixture of each soil with 5% CuO (modified after Ben Moshe et al 2012).

As shown by the SEM images upon mixing with the CuO Nanoparticles the surface of the soil aggregates is changed and particles are accumulating on the soil surface this changes the composition of the surface and thus its chemical and physical properties.

Changes to the dissolved organic matter in soil solution.

Fluorescence is a powerful technique for the characterization of organic material in the soil. Fluorescence emission spectra of the soil extracts were measured at multiple excitation wavelengths, and 3-D contour plots were generated, presenting the differences between samples with and without ENMs. These plots are presented Figures 2. Based on these maps, the main peaks were identified. For both soils and

ENMs there is one negative peak in each plot. The location of the peak is different for each type of nanoparticles and each soil; however in all cases the peaks are typical of humic-like substances (Hudson et al. 2007; Saadi et al. 2006; Stedmon et al. 2003). The nanoparticle concentration contributes to the peak formation as is evident by the increase in peak absolute value for the higher concentration. The peak is negative, indicating the concentration of fluorescent organic material in the soil extract is lower upon addition of nanoparticles. This may be due to quenching of the fluorescence by

the nanoparticles. This can occur either by absorption by the nanoparticles at excitation wavelength or by sorption of the organic material onto the surface of the nanoparticles (Manciulea et al. 2009). The samples were filtered before the measurements; however, it is possible that some nanoparticles remained in the solution. UV absorption at 254 nm was high for CuO samples, suggesting the presence of nanoparticles in the solution. The metal concentration was measured by ICP-MS. Iron was not visible, however copper was detected. Another possible explanation for the lower fluorescence upon nanoparticle addition is quenching of the fluorescent signal by metal ions. The ions can create non-fluorescent complexes with organic material and reduce the signal (Esteves et al. 1998; Ryan and Weber 1982; Waite and Morel 1984). This is more likely for CuO as copper was measured by ICP-MS. It is not possible to distinguish among the possible different sources of copper (nanoparticles or ions) in the ICP-MS. Another possible explanation is that extraction of the fluorescent organic material from the soil to the liquid was reduced. This could be caused by increased sorption of organic material to the nanoparticles, making extraction more difficult and less efficient. However, this explanation is unlikely as no change was observed in DOC upon addition of nanoparticles to the soil. Another possibility is transformation of fluorescent material to smaller, non-fluorescent molecules. This will not change the TOC but will reduce the fluorescence. Although complete degradation was shown not to take place, such transformation is still a possibility.

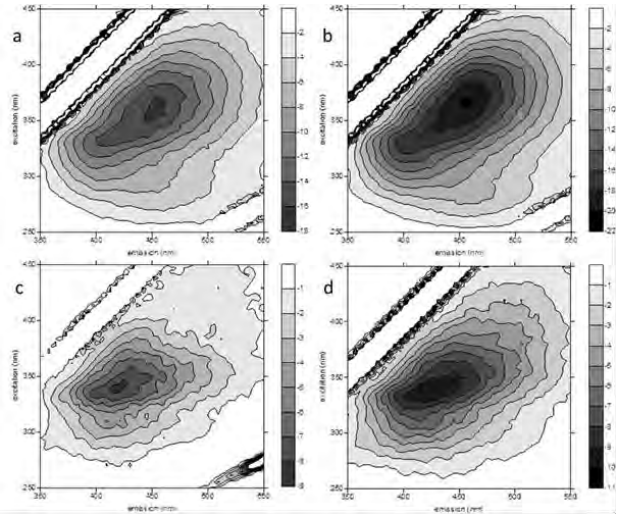

Fig. 2. Changes in EEM of Beit Dagan soil extracts after addition of (a) 1% CuO, (b) 5% CuO, (c) 1% Fe_3O_4 and (d) 5% Fe_3O_4. (after Ben Moshe et al 2012)

The measurements were repeated with samples that were treated with hydrogen peroxide prior to extraction to simulate strong oxidation process or induced oxidation. Results for the Yatir soil are presented in the Figure 3. For Bet Dagan soil, the results are similar to the results of the samples without the oxidant. In all cases, a single peak is observed at about the same wavelengths; the absolute values of the peaks are higher. These results suggest a decrease in fluorescent organic material concentrations, possibly due to partial degradation of the DOM. For Yatir soil, several peaks appear in the spectra at different locations. There are both negative and positive peaks and their absolute values do not increase with increased concentrations. The enhanced fluorescence further supports partial transformation, in this case of non-fluorescent species to smaller, fluorescent molecules. These results indicates that the Nanoparticles may interact with the dissolved organic mater and change its composition moreover we can see that the change is relatively fast (few days) even without inducing strong oxidation conditions and become much stronger when strong oxidation conditions are being induced. Since organic matter is very important for soil properties even at relatively small concentration any changes that are induced by contaminants (in this case) nanoparticles may have a substantial effect on soil properties.

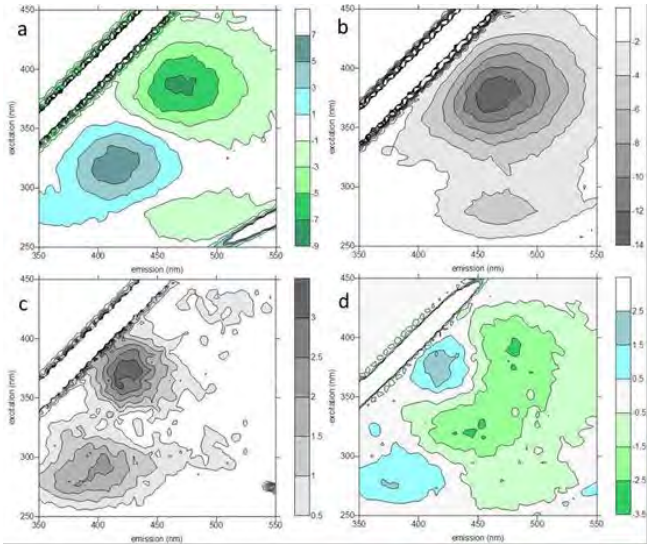

Fig. 3. Changes in EEM of Beit Dagan soil extract after treatment with H_2O_2 and addition of (a) 1% CuO, (b) 5% CuO, (c) 1% Fe_3O_4 and (d) 5% Fe_3O_4. (after Ben Moshe et al 2012)

Changes to soil microbial population following NPs application.

The influence of Cu and ZnO NPs on the soil microbial community was discussed recently by Collins et al. (2013). Cu and ZnO NPs were deposited on the soil surface and allowed to freely migrate through the soil while exposed to environmental conditions over 160 days. The addition of NP was found to have an immediate impact on the culturable microorganisms. Substrate richness - a good indicator of the functional diversity within soil in the top horizon changed from 22 for the control soil to 2 right after the addition of Cu NPs. Similarly, addition of ZnO NPs to the soil caused a dropped to 11 immediately following applications of the NPs. Based on the results Collins et al. (2013) suggested that direct contact between NPs and microbes, such that is achieved in the in vitro physiological assays, may be necessary for acute bacterial toxicity. While physiological profiles clearly showed microbial toxicity, likely due to the direct contact.

Despite the natural heterogeneity of soil and the intrinsic complication of comparing population within these soil samples, an overall impact of the microbial community by the introduced NPs was evident as is shown in figure 4.

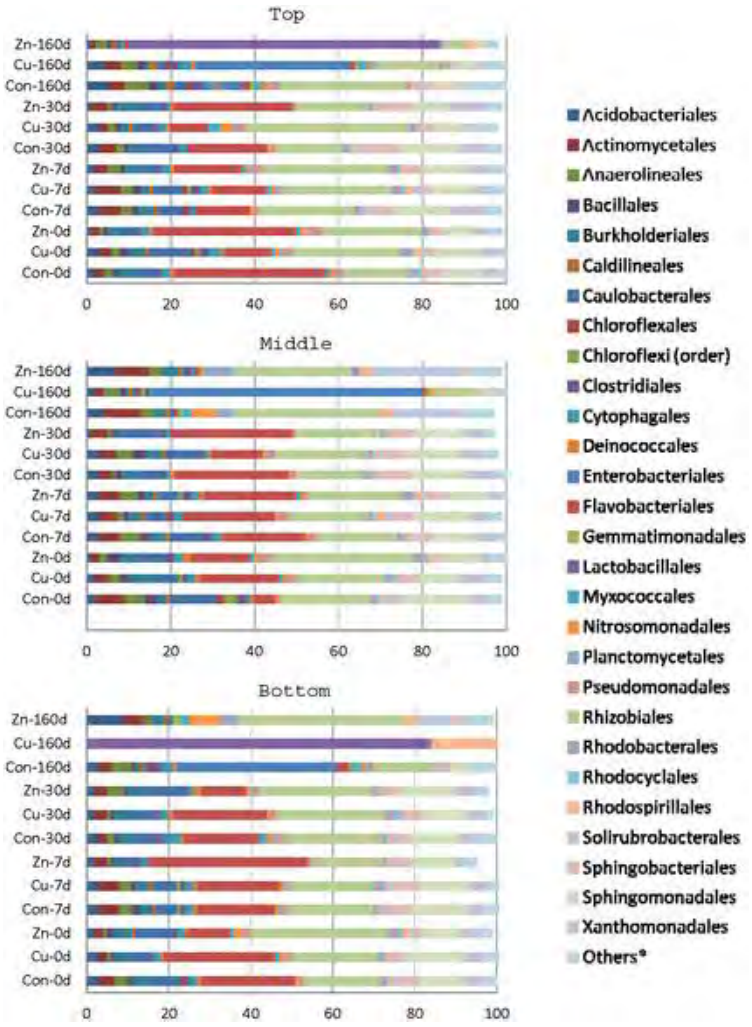

Fig. 4. Relative abundance of bacterial orders (%) determined by pyrosequencing in the top, middle and bottom horizons of unexposed and nanoparticle-exposed soils. (After Collins et al 2012)

Conclusions

Several changes to soil properties were demonstrated to occur upon exposure to NPs. These changes are an example to the many different possible effects of contamination on soil and subsurface properties. These changes are happening on relatively fast rate of days or months of contamination and then alter the soil irreversibly. Both direct impact on soil matrix and soil solution were demonstrated as well as indirect effect through changes to the microbial concentration which in turn has an effect on soil properties were shown. It should further be noted that as NPs become abundant in many commercial products and industrial process their release to the environment is expected to raise and one set of consequences of these contaminations may be fast change of soil

properties. It is therefore important to understand these effects and consider their implication.

References

Ben-Moshe, T., Dror, I., Berkowitz, B., 2010. Transport of metal oxide nanoparticles in saturated porous media, Chemosphere 81, 387-39

Ben-Moshe, T., Frenk, S., Dror, I., Minz, D. and Berkowitz, B. (2012). Effects of metal oxide nanoparticles on soil properties, Chemosphere 90, 640-646, doi: 10.1016/j.chemosphere.2012.09.018.

Cheng, X., Kan, A.T., Tomson, M.B., 2005. Study of C_{60} transport in porous media and the effect of sorbed C_{60} on naphthalene transport. J. Mater. Res. 20, 3244-3254.

Chung, H., Son, Y., Yoon, T.K., Kim, S., Kim, W., 2011. The effect of multi-walled carbon nanotubes on soil microbial activity. Ecotox. Environ. Safe. 74, 569-575.

Collins D, Luxton T, Kumar N, Shah S, et al. (2012) Assessing the Impact of Copper and Zinc Oxide Nanoparticles on Soil: A Field Study. PLoS ONE 7(8): e42663. doi:10.1371/journal.pone.0042663

Collins D, Luxton T, Kumar N, Shah S, et al. (2012) Assessing the Impact of Copper and Zinc Oxide Nanoparticles on Soil: A Field Study. PLoS ONE 7(8): e42663. doi:10.1371/journal.pone.0042663

Dunphy Guzman, K.A., Finnegan, M.P., Banfield, J.F., 2006. Influence of surface potential on aggregation and transport of titania nanoparticles. Environ. Sci. Technol. 40, 7688-7693.

Ehlers, l.J., Kavanaugh M. C., (2013) Redifining the end game for groundwater remediation. Groundwater 51:170-174

Ehlers, l.J., Kavanaugh M. C., (2013) Redifining the end game for groundwater remediation. Groundwater 51:170-174

Elliot, D.W., Zhang, W.X., 2001. Field Assessment of Nanoscale Bimetallic Particles for Groundwater Treatment. Environ. Sci. Technol. 35, 4922-4926.

Espinasse, B., Hotze, E.M., Wiesner, M.R., 2007. Transport and retention of colloidal aggregates of C_{60} in porous media: effects of organic macromolecules, ionic composition, and preparation method. Environ. Sci. Technol. 41, 7396-7402.

Esteves da Silva, J.C.G., Machado, A.A.S.C., Oliveira, C.J.S., Pinto, M.S.S.D.S., 1998. Fluorescence quenching of anthropogenic fulvic acids by Cu(II), Fe(III) and UO_2^{2+}, Talanta 45, 1155-1165.

Ge, Y., Schimel, J.P., Holden, P.A., 2011. Evidence for negative effects of TiO_2 and ZnO nanoparticles on soil bacterial communities. Environ. Sci. Technol. 45, 1659-1664.

Hudson, N., Baker, A., Reynolds, D., 2007. Fluorescence analysis of dissolved organic matter in natural, waste and polluted waters – A review. River. Res. Applic., 23, 631-649.

Hyung, H., Fortner, J.D., Hughes, J.B., Kim, J.H., 2007. Natural organic matter stabilizes carbon nanotubes in the aqueous phase. Environ. Sci. Technol. 41, 179–184.

Johnson, R.L., O'Brien Johnson, G., Nurmi, J.T., Tratnyek, P.G., 2009. Natural organic matter enhanced mobility of nano zerovalent iron. Environ.Sci. Technol. 43, 5455-5460.

Lecoanet, H.F., Bottero, J.Y., Weisner, M.R., 2004. Laboratory assessment of the mobility of nanomaterials in porous media. Environ. Sci. Technol. 38, 5164-5169.

Lecoanet, H.F., Weisner, M.R., 2004. Velocity effects on fullerene and oxide nanoparticle deposition in porous media. Environ. Sci. Technol. 38, 4377-4383.

Manciulea, A., Baker, A., Lead, J.R., 2009. A fluorescence quenching study of the interaction of Suwannee River fulvic acid with iron oxide nanoparticles. Chemosphere 76, 1023-1027.

Mohapatra, M., Anand, S., 2010. Synthesis and applications of nano-structured iron oxides/ hydroxides – a review. Inter. J. Eng. Sci. Technol. 2, 127-146.

Nyberg, L., Turco, R.F., Nies, L., 2008. Assessing the Impact of Nanomaterials on Anaerobic Microbial Communities. Environ. Sci. Technol. 42, 1938-1943.

Pradhan, A., Seena, S., Pascoal, C., Cassio, F., 2011. Can metal nanoparticles be a threat to microbial decomposers of plant litter in streams?, Microb. Ecol. 62, 58-68.

Ryan, D.K., Weber, J.H., 1982. Copper(II) complexing capacities of natural waters by fluorescence quenching. Environ. Sci. Tech. 16, 866-872.

Saadi, I., Borisover, M., Armon, R., Laor, Y., 2006. Monitoring of effluent DOM biodegradation using fluorescence, UV and DOC measurements. Chemosphere 63, 530-539.

Stedmon, C.A., Markager, S., Bro, R., 2003. Tracing dissolved organic matter in aquatic environments using a new approach to fluorescence spectroscopy. Mar. Chem., 82, 239-254.

Terashima, M., Nagao, S., 2007. Solubilization of [60]fullerene in water by aquatic humic substances. Chem. Lett., 36, 302–303.

Tong, Z., Bischoff, M., Nies, L., Applegate, B., Turco, R.F., 2007. Impact of Fullerene (C60) on a Soil Microbial Community. Environ. Sci. Technol. 41, 2985-2991.

Waite, T.D., Morel, F.M.M., 1984. Ligand exchange and fluorescence quenching studies of the fulvic acid-iron interaction. Anal. Chim. Acta 162, 263-274.

Wang, Y., Li, Y., Fortner, J.D., Hughes, J.B., Abriola, L.M., Pennell, K.D., 2008. Transport and retention of nanoscale C_{60} aggregates in water-saturated porous media. Environ. Sci. Technol. 42, 3588-3594.

Wang, Y., Li, Y., Pennell, K.D., 2008. Influence of electrolyte species and concentration on the aggregation and transport of fullerene nanoparticles in quartz sands. Environ. Toxicol. Chem. 27, 2860-1867.

Xie, B., Xu, Z., Guo, W., Li, Q., 2008. Impact of natural organic matter on the physicochemical properties of aqueous C_{60} nanoparticles. Environ. Sci. Technol. 42, 2853-2859.

Yaron B., Dror I., Berkowitz B. (2008) Contaminant induced irreversible changes in properties of the soil-vadose-aquifer zone: an overview, Chemosphere 71:1409-1321

Yaron B., Dror I., Berkowitz B. (2009) Chemical contaminants as factor of soil-subsurface metapedogenesis IUSS Bulletin 115:11-12

Yaron B., Dror I., Berkowitz B. (2010) Contaminant geochemistry - a new perspective, Naturwiessenschaften 97:1-17

Yaron B., Dror I.,Berkowitz B. (2012) "Soil Subsurface Change-Chemical Pollutant Impact", Springer-Verlag, Heidelberg,

Zhu, J., Li, D., Chen H., Yang X., Lu L., Wang X., 2004. Highly dispersed CuO nanoparticles prepared by a novel quick-precipitation method. Mater. Lett. 58, 3324-3327.

SUMMARY OF PANEL DISCUSSION

The final session of the symposium was devoted to a panel discussion led by Alchanatis, Cade-Menun, Horwath, Myrold, and Schmidt. This discussion was free-ranging rather than directed with specific questions. The goal was to capture the highlights of the symposium and to identify emergent themes.

Theme 1: Translation of research into practice

Discussion on this topic began with a question posed by Will Horwath: "We may be able to feed the world with what we now know, but what can we do to do it in a better, more sustainable way?"

Scientists have several potential roles to play, including: (1) generation of knowledge, (2) development of practical tools, and (3) communication with policy makers and end users. As scientists we are all comfortable with asking questions of scientific interest and creating knowledge; our inclination towards disseminating and translating that knowledge into useable information is more variable.

Several ideas were presented as means of improving our ability to make the connection from theory to application:
Will Horwath and Barbara Cade-Menun mentioned the traditional approach of goal-oriented work through agricultural experiment stations and agricultural extension activities.
Ways of improving the effectiveness of communicating scientific information included by Ilya Gelfand to establish collaborations with social scientists and by Achim Dobermann of utilizing new tools of social media, such as blogs and tweets.
Will Horwath mentioned that some funding agencies are requiring or encouraging such interactions.
Avi Shaviv reminded everyone that education and training is important in the transition of science to application.

Asher Bar-Tal noted that several examples were presented at the symposium of technology that was able to monitor variables in real-time, which hold promise for incorporation into practical tools for management.
Hillel Magen floated the idea of a field-deployable box that could collect data that would then be used to provide a customized solution to the farmer using decision support tools such as those described by Victor Alchanatis.

Theme 2: Incorporation microbiology information into management

Tom Schmidt began a discussion on this topic by asking the question: "Can managing microbial communities prevent losses of carbon and nitrogen?" which was broadened by Achim Dobermann who asked: "What can one do with a better understanding of microbial diversity?"

Jennifer Pett-Ridge noted that to date the emphasis has been on counting and taxonomy and that practical application of microbial information would likely benefit from moving to an emphasis on function, that perhaps the approaches of metatranscriptomics and proteomics would be more useful.
Graeme Nicol offered that the enormous diversity of soil is still a challenge with so much still to be understood. These two opinions seem to capture the conundrum related to soil biology, what might be done to move forward even with incomplete knowledge.
Dave Myrold wondered if the approach of soil testing and calibration might be applied to soil microbial properties or perhaps modeling would be an alternative.
Ken Sudduth thought that calibration and validation are still important but noted the challenges of scaling from plots to the landscape will still exist as it does for soil fertility. He suggested that perhaps there were opportunities to partner with agribusiness as they are trying to do similar scaling with plant genetics.
Michael Castellano bought up the idea of engineering the rhizosphere and that existing crop rotation and other experiments could be used as template for validation and calibration, although solutions will likely be site-specific.
Achim Dobermann agreed that calibration was essential and noted a plant breeding analogy where SNPs have taken over from morphological characteristics, which might be an example of how genomic information about soil communities might supersede activity assays.

Will Horwath raised the analogy with human health and wondered whether appropriate microbial metrics could be identified.

Peter Bottomley and Tim Cough brought up examples of the potential for managing the specific microbial process of nitrification, which has implications related to nitrate leaching and trace gas production. The ideas generated including developing inhibitors that might be specific for ammonia-oxidizing bacteria and archaea for use on sites where one or the other group dominates and using field-based sensors of N_2O to determine timing of inhibitor use.

Tom Schmidt suggested that perhaps a more ecological approach would be to manage nitrogen fertilizer applications in such a way as to regulate the populations, and perhaps composition, of ammonia-oxidizers to minimize nitrogen losses.

The discussion on this topic ended with a cautionary note by Barbara Cade-Menun about unintended consequences, pointing out that although a switch to no-tillage management was a boon for carbon storage it generated problems with phosphorus availability.

Theme 3: Methods with potential for application

The final topic was a call for identifying techniques that might hold particular promise for application development.

Jennifer Pett-Ridge offered that much soils research and methods have focused on spatial variability, but it is also important to capture and understand temporal variability, something that should be kept in mind when identifying application potential.

Two methods generated the most interest with respect to potential applications: spectroscopic methods, which were featured in several presentations, and microdialysis, which was presented by Torgny Näsholm. Dan Yakir noted that spectroscopic methods have advanced significantly, including laser-based methods. Avi Shaviv pointed out that an important component of the practical application of new measurement techniques is the need to integrate the data they collect with the knowledge we have about how agricultural ecosystems work and to provide decision support tools for the end users. This brought up again the importance of training and education.

The discussion finished with a question:

What aspects might not have been addressed in the symposium?

Those gaps included:

Plant physiology (Tim Clough), mycorrhizae and micronutrients (Barbara Cade-Menun), soil fauna (Jennifer Pett-Ridge), and a stronger modeling emphasis (Dan Yakir).

The multidisciplinary nature of the meeting (Asher Bar-Tal) and intimate setting of a small conference (Tim Clough) were mentioned as features that helped to make the symposium successful.

SUMMARY OF THE COLLECTION OF PAPERS IN SOIL SCIENCE SOCIETY OF AMERICA JOURNAL

doi:10.2136/sssaj2013.dgsintro
Soil Science Society of America Journal 2014 78:1-2

A Collection of Papers from "Advanced Methods for Investigating Nutrient Dynamics in Soils and Ecosystems"

David D. Myrold[1] and Avi Shaviv[2]

[1]Dept. of Crop and Soil Science Oregon State University Corvallis, OR 97331
[2] Dept. of Environmental, Water, and Agricultural Eng. Technion-IIT, Haifa Israel

The 11th Dahlia Greidinger Memorial Symposium on Advanced Methods for Investigating Nutrient Dynamics in Soils and Ecosystems was held from 4–7 Mar. 2013 at the Technion in Haifa, Israel, with the generous support of the Dahlia Greidinger fund and BARD (Binational US-Israeli fund for Agricultural R&D). Approximately 100 scientists from around the world gathered to address knowledge gaps and priorities for research and development related to the need to quantify nutrient dynamics and reaction mechanisms, particularly those of nitrogen (N) and phosphorus (P) in crop/food production systems. There was a focus on advanced and novel tools and approaches (including those developed in other disciplines) that enable real time/online investigation and quantification of processes and on options to observe and model changes at various scales (from microscopic up to field scales). Sessions were devoted to new approaches for understanding N and P cycling in soils, organic matter and interactions between carbon (C) and N, and advances in measurement methods at multiple scales. Manuscript based on symposium presentations were solicited, of which seven are published in this issue of the *Soil Science Society of America Journal*. The full proceedings of the symposium are available at: http://dgsymp13.technion.ac.il/.

Two papers emphasize recent developments in measuring microbial taxonomic and functional diversity. Rapid advances in DNA sequencing technology now makes it possible to sequence entire communities of microorganisms, or at least their collective genes.Myrold et al. (2014) review the status of the application of metagenomics, and related approaches, to determine the genetic potential of soil microbial communities. Microbial activities are the realization of this genetic potential and have often been

measured as enzyme activities. Baldrian (2014) focuses on how these enzyme activities vary in soils, with an emphasis on variation across spatial scales.

Soil P was the focus of three papers (Cade-Menum and Liu, 2014; Tamburnini et al., 2014;Liu et al., 2014). Cade-Menun and Liu (2014) review recent advances in the use of ^{31}P-NMR. Tamburini et al. (2014) review the application of ^{18}O for understanding P transformations in soil and its effectiveness in providing information on biological processes influencing the P cycle and for tracing the origin and fate of P in soil–plant systems. These approaches are yielding new insights into the forms and cycling of P in soils, as illustrated by the final paper by Liu et al. (2014), which explores molecular speciation of P associated with soil colloids.

The applications of different operating modes of FTIR spectroscopy to study N cycling were highlighted in two papers. Kira et al. (2014) found that FTIR-ATR (attenuated total reflectance) can be used with minimal disturbance to determine the ^{15}N abundance of inorganic N in soil pastes, which may pave the way to real-time measurements of N dynamics in incubated soils. Dubowski et al. (2014) demonstrate that the FTIR can be used to measure on-line gaseous emissions of N_2O from incubated soils under various conditions. Combing the FTIR technique with ^{15}N labeled mineral N allows direct determination of N_2O isotopologues and isotopomers released from the soil.

Collectively, this set of papers documents the interplay between methods development and experimental work necessary to enhance our understanding of soil processes

References

P Baldrian. 2014. Distribution of extracellular enzymes in soils: spatial heterogeneity and determining factors at various scales. Soil Sci. Soc. Am. J. 78:10..2136/sssaj2013.04.0155dgs.

Cade-Menun, B., and C.W. Liu. 2014. Solution phosphorus-31 nuclear magnetic resonance spectroscopy of soils from 2005 to 2013: A review of sample preparation and experimental parameters. Soil Sci. Soc. Am. J. 78: 10..2136/sssaj2013.05.0187dgs.

Dubowski, Y., D. Harush, A. Shaviv, L. Stone, and R. Linker. 2014. Real time monitoring of N2O emissions from agricultural soils using FTIR spectroscopy. Soil Sci. Soc. Am. J. 78: 10..2136/sssaj2013.09.0390dgs.

Kira, O., R. Linker, and A. Shaviv. 2014. A novel method combining FTIR-ATR spectroscopy and stable isotopes to investigate the kinetics of nitrogen transformations in soils. Soil Sci. Soc. Am. J. 78: 10..2136/sssaj.2013.08.0358dgs.

Liu, J., J. Yang, X. Liang, Y. Zhao, B.J. Cade-Menun, and Y. Hu. 2014. Molecular speciation of phosphorus present in readily dispersible colloids from agricultural soils.Soil Sci. Soc. Am. J. 78: 10..2136/sssaj2013.05.0159.

Myrold, D.D., L.H. Zeglin, and J K. Jansson. 2014. The potential of metagenomic approaches for understanding soil microbial processes. Soil Sci. Soc. Am. J.10.2136/sssaj2013.07.0287dgs.

Tamburini, F., V. Pfahler, C. von Sperber, E. Frossard, and S.M. Bernascon. 2014.Oxygen isotopes for unraveling phosphorus transformations in the soil–plant system: A review. Soil Sci. Soc. Am. J. 78: 10..2136/sssaj2013.05.0186dgs. Footnotes